Related titles

Eco-efficient masonry bricks and blocks: Design, properties and durability
(ISBN 978-1-78242-305-8)
Handbook of alkali-activated cements, mortars and concretes
(ISBN 978-1-78242-276-1)
Understanding the tensile properties of concrete
(ISBN 978-0-85709-045-4)

Woodhead Publishing Series in Civil and Structural Engineering: Number 63

Biopolymers and Biotech Admixtures for Eco-Efficient Construction Materials

Edited by

Fernando Pacheco-Torgal,
Volodymyr Ivanov, Niranjan Karak
and Henk Jonkers

ELSEVIER

AMSTERDAM • BOSTON • CAMBRIDGE • HEIDELBERG
LONDON • NEW YORK • OXFORD • PARIS • SAN DIEGO
SAN FRANCISCO • SINGAPORE • SYDNEY • TOKYO
Woodhead Publishing is an imprint of Elsevier

WP
WOODHEAD
PUBLISHING

Woodhead Publishing is an imprint of Elsevier
The Officers' Mess Business Centre, Royston Road, Duxford, CB22 4QH, UK
225 Wyman Street, Waltham, MA 02451, USA
Langford Lane, Kidlington, OX5 1GB, UK

Copyright © 2016 Elsevier Ltd. All rights reserved.

No part of this publication may be reproduced or transmitted in any form or by any means, electronic or mechanical, including photocopying, recording, or any information storage and retrieval system, without permission in writing from the publisher. Details on how to seek permission, further information about the Publisher's permissions policies and our arrangements with organizations such as the Copyright Clearance Center and the Copyright Licensing Agency, can be found at our website: www.elsevier.com/permissions.

This book and the individual contributions contained in it are protected under copyright by the Publisher (other than as may be noted herein).

Notices
Knowledge and best practice in this field are constantly changing. As new research and experience broaden our understanding, changes in research methods, professional practices, or medical treatment may become necessary.

Practitioners and researchers must always rely on their own experience and knowledge in evaluating and using any information, methods, compounds, or experiments described herein. In using such information or methods they should be mindful of their own safety and the safety of others, including parties for whom they have a professional responsibility.

To the fullest extent of the law, neither the Publisher nor the authors, contributors, or editors, assume any liability for any injury and/or damage to persons or property as a matter of products liability, negligence or otherwise, or from any use or operation of any methods, products, instructions, or ideas contained in the material herein.

ISBN: 978-0-08-100214-8 (print)
ISBN: 978-0-08-100209-4 (online)

British Library Cataloguing-in-Publication Data
A catalogue record for this book is available from the British Library

Library of Congress Cataloging-in-Publication Data
A catalog record for this book is available from the Library of Congress

For information on all Woodhead Publishing publications visit our website at http://store.elsevier.com/

ELSEVIER
Book Aid International
Working together
to grow libraries in
developing countries
www.elsevier.com • www.bookaid.org

List of contributors

M. Ahmad Quaid-i-Azam University, Islamabad, Pakistan

Y. Alvarado-Capó Instituto de Biotecnología de las Plantas, Universidad Central "Marta Abreu" de Las Villas, Santa Clara, Cuba

M.A. Ashraf University of Malaya, Kuala Lumpur, Malaysia; Centre for Research in Biotechnology for Agriculture (CEBAR), University of Malaya, Kuala Lumpur, Malaysia; Universiti Malaysia Sabah, Kota Kinabalu, Sabah, Malaysia

S. Batool University of Malaya, Kuala Lumpur, Malaysia

U.T. Bezerra Federal Institute of Paraíba, João Pessoa-PB, Brazil

G. Bracho Institute "Carlos J. Finlay", Habana, Cuba

A. Callico Institute "Carlos J. Finlay", Habana, Cuba

P.F. de J. Cano-Barrita Instituto Politécnico Nacional/CIIDIR Unidad Oaxaca, Oaxaca, México

V. Chevali University of Southern Queensland, Toowoomba, QLD, Australia

C. Croitoru Transilvania University of Brasov, Brasov, Romania

H.H.M. Darweesh National Research Center, Cairo, Egypt

Y. Diaz Universidad Central de las Villas, Carretera de Camajuani, Santa Clara, CP, Cuba

M. Grédiac Institut Pascal, Clermont Université, Université Blaise Pascal, Clermont-Ferrand, France; CNRS, UMR, Institut Pascal, Aubière, France

J.O. Guerra de Leon Faculty of Chemistry and Pharmacy, Universidad Central "Marta Abreu" de Las Villas, Santa Clara, Cuba

A. Hereira Faculty of Chemistry and Pharmacy, Universidad Central "Marta Abreu" de Las Villas, Santa Clara, Cuba

V. Ivanov Nanyang Technological University, Singapore

H.M. Jonkers Faculty of Civil Engineering and Geosciences, Materials and Environment Section, Delft University of Technology, Stevinweg, Delft, The Netherlands

E. Kandare RMIT University, Melbourne, VIC, Australia

N. Karak Tezpur University, Napaam, Tezpur, Assam, India

A.D. La Rosa University of Catania, Catania, Italy

F.M. León-Martínez Instituto Politécnico Nacional/CIIDIR Unidad Oaxaca, Oaxaca, México

Z. Li University of Arizona, Tucson, AZ, USA

S.H. Lv College of Resource and Environment, Shaanxi University of Science & Technology, Xi'an, China

F. Martirena Universidad Central de las Villas, Carretera de Camajuani, Santa Clara, CP, Cuba

J.-D. Mathias IRSTEA, Laboratoire d'Ingénierie pour les Systèmes Complexes, Aubière, France

P. Michaud Institut Pascal, Clermont Université, Université Blaise Pascal, Clermont-Ferrand, France; CNRS, UMR, Institut Pascal, Aubière, France

R.M. Mors Faculty of Civil Engineering and Geosciences, Materials and Environment Section, Delft University of Technology, Stevinweg, Delft, The Netherlands

W.S.A.W.M. Noor School of Biosciences and Biotechnology, Faculty of Science and Technology, National University Malaysia (UKM), Bangi, Selangor, Malaysia

F. Pacheco-Torgal University of Minho, Guimarães, Portugal

S. Patachia Transilvania University of Brasov, Brasov, Romania

T.M. Pique Instituto de Tecnología en Polímeros y Nanotecnología UBA/CONICET (ITPN), Buenos Aires, Argentina; Facultad de Ingeniería, Universidad de Buenos Aires, Buenos Aires, Argentina

Y. Rodriguez-Rodriguez Centro de Bioactivos Químicos (CBQ), Universidad Central "Marta Abreu" de Las Villas, Santa Clara, Cuba

A.Z.M. Rus University Tun Hussein Onn Malaysia (UTHM), Batu Pahat, Johor, Malaysia

M. Sarfraz Institute of Pharmacy, Physiology & Pharmacology, University of Agriculture, Faisalabad, Pakistan

M.G. Sierra-Beltran Faculty of Civil Engineering and Geosciences, Materials and Environment Section, Delft University of Technology, Stevinweg, Delft, The Netherlands

L. Sorelli Université Laval, Département de Génie Civil, Québec, QC, Canada

V. Stabnikov Nanyang Technological University, Singapore; National University of Food Technologies, Kiev, Ukraine

A. Vazquez Instituto de Tecnología en Polímeros y Nanotecnología UBA/CONICET (ITPN), Buenos Aires, Argentina; Facultad de Ingeniería, Universidad de Buenos Aires, Buenos Aires, Argentina

V. Wiktor Faculty of Civil Engineering and Geosciences, Materials and Environment Section, Delft University of Technology, Stevinweg, Delft, The Netherlands

L. Zhang University of Arizona, Tucson, AZ, USA

Woodhead Publishing Series in Civil and Structural Engineering

1 **Finite element techniques in structural mechanics**
C. T. F. Ross
2 **Finite element programs in structural engineering and continuum mechanics**
C. T. F. Ross
3 **Macro-engineering**
F. P. Davidson, E. G. Frankl and C. L. Meador
4 **Macro-engineering and the earth**
U. W. Kitzinger and E. G. Frankel
5 **Strengthening of reinforced concrete structures**
Edited by L. C. Hollaway and M. Leeming
6 **Analysis of engineering structures**
B. Bedenik and C. B. Besant
7 **Mechanics of solids**
C. T. F. Ross
8 **Plasticity for engineers**
C. R. Calladine
9 **Elastic beams and frames**
J. D. Renton
10 **Introduction to structures**
W. R. Spillers
11 **Applied elasticity**
J. D. Renton
12 **Durability of engineering structures**
J. Bijen
13 **Advanced polymer composites for structural applications in construction**
Edited by L. C. Hollaway
14 **Corrosion in reinforced concrete structures**
Edited by H. Böhni
15 **The deformation and processing of structural materials**
Edited by Z. X. Guo
16 **Inspection and monitoring techniques for bridges and civil structures**
Edited by G. Fu
17 **Advanced civil infrastructure materials**
Edited by H. Wu
18 **Analysis and design of plated structures Volume 1: Stability**
Edited by E. Shanmugam and C. M. Wang
19 **Analysis and design of plated structures Volume 2: Dynamics**
Edited by E. Shanmugam and C. M. Wang

20 **Multiscale materials modelling**
Edited by Z. X. Guo
21 **Durability of concrete and cement composites**
Edited by C. L. Page and M. M. Page
22 **Durability of composites for civil structural applications**
Edited by V. M. Karbhari
23 **Design and optimization of metal structures**
J. Farkas and K. Jarmai
24 **Developments in the formulation and reinforcement of concrete**
Edited by S. Mindess
25 **Strengthening and rehabilitation of civil infrastructures using fibre-reinforced polymer (FRP) composites**
Edited by L. C. Hollaway and J. C. Teng
26 **Condition assessment of aged structures**
Edited by J. K. Paik and R. M. Melchers
27 **Sustainability of construction materials**
J. Khatib
28 **Structural dynamics of earthquake engineering**
S. Rajasekaran
29 **Geopolymers: Structures, processing, properties and industrial applications**
Edited by J. L. Provis and J. S. J. van Deventer
30 **Structural health monitoring of civil infrastructure systems**
Edited by V. M. Karbhari and F. Ansari
31 **Architectural glass to resist seismic and extreme climatic events**
Edited by R. A. Behr
32 **Failure, distress and repair of concrete structures**
Edited by N. Delatte
33 **Blast protection of civil infrastructures and vehicles using composites**
Edited by N. Uddin
34 **Non-destructive evaluation of reinforced concrete structures Volume 1: Deterioration processes**
Edited by C. Maierhofer, H.-W. Reinhardt and G. Dobmann
35 **Non-destructive evaluation of reinforced concrete structures Volume 2: Non-destructive testing methods**
Edited by C. Maierhofer, H.-W. Reinhardt and G. Dobmann
36 **Service life estimation and extension of civil engineering structures**
Edited by V. M. Karbhari and L. S. Lee
37 **Building decorative materials**
Edited by Y. Li and S. Ren
38 **Building materials in civil engineering**
Edited by H. Zhang
39 **Polymer modified bitumen**
Edited by T. McNally
40 **Understanding the rheology of concrete**
Edited by N. Roussel
41 **Toxicity of building materials**
Edited by F. Pacheco-Torgal, S. Jalali and A. Fucic
42 **Eco-efficient concrete**
Edited by F. Pacheco-Torgal, S. Jalali, J. Labrincha and V. M. John

43 **Nanotechnology in eco-efficient construction**
Edited by F. Pacheco-Torgal, M. V. Diamanti, A. Nazari and C. Goran-Granqvist
44 **Handbook of seismic risk analysis and management of civil infrastructure systems**
Edited by F. Tesfamariam and K. Goda
45 **Developments in fiber-reinforced polymer (FRP) composites for civil engineering**
Edited by N. Uddin
46 **Advanced fibre-reinforced polymer (FRP) composites for structural applications**
Edited by J. Bai
47 **Handbook of recycled concrete and demolition waste**
Edited by F. Pacheco-Torgal, V. W. Y. Tam, J. A. Labrincha, Y. Ding and J. de Brito
48 **Understanding the tensile properties of concrete**
Edited by J. Weerheijm
49 **Eco-efficient construction and building materials: Life cycle assessment (LCA), eco-labelling and case studies**
Edited by F. Pacheco-Torgal, L. F. Cabeza, J. Labrincha and A. de Magalhães
50 **Advanced composites in bridge construction and repair**
Edited by Y. J. Kim
51 **Rehabilitation of metallic civil infrastructure using fiber-reinforced polymer (FRP) composites**
Edited by V. Karbhari
52 **Rehabilitation of pipelines using fiber-reinforced polymer (FRP) composites**
Edited by V. Karbhari
53 **Transport properties of concrete: Measurement and applications**
P. A. Claisse
54 **Handbook of alkali-activated cements, mortars and concretes**
F. Pacheco-Torgal, J. A. Labrincha, C. Leonelli, A. Palomo and P. Chindaprasirt
55 **Eco-efficient masonry bricks and blocks: Design, properties and durability**
F. Pacheco-Torgal, P. B. Lourenço, J. A. Labrincha, S. Kumar and P. Chindaprasirt
56 **Advances in asphalt materials: Road and pavement construction**
Edited by S.-C. Huang and H. Di Benedetto
57 **Acoustic emission (AE) and related non-destructive evaluation (NDE) techniques in the fracture mechanics of concrete: Fundamentals and applications**
Edited by M. Ohtsu
58 **Nonconventional and vernacular construction materials: Characterisation, properties and applications**
Edited by K. A. Harries and B. Sharma
59 **Science and technology of concrete admixtures**
Edited by P.-C. Aïtcin and R. J. Flatt
60 **Textile fibre composites in civil engineering**
Edited by T. Triantafillou
61 **Corrosion of steel in concrete structures**
Edited by A. Poursaee
62 **Innovative developments of advanced multifunctional nanocomposites in civil and structural engineering**
Edited by K. J. Loh and S. Nagarajaiah
63 **Biopolymers and biotech admixtures for eco-efficient construction materials**
Edited by F. Pacheco-Torgal, V. Ivanov, N. Karak and H. Jonkers

Foreword

The cliché, *never judge a book by its cover,* this time seems especially untrue. The very informative title on the familiar cover of Woodhead Publishing Series in Civil and Structural Engineering inspires confidence and interest.

Key words in the title of the book define its goal: *Ecoefficient Construction Materials*, and simultaneously show the means by which to do that: *biopolymers* and *biotech admixtures.* These characteristics could reduce to the common denominator: *biotech toward sustainable construction.* There is a yardstick of target and the grand scale of engineering ambitions and challenges claimed in this work.

Every material thing comes from something else, and every structure is of construction materials, now mainly from concrete. The construction industry consumes more than 40% of produced energy and about 50% mass of materials the building industry also emits 35% of greenhouse gases. There is no doubt that sustainable development is the fundamental requirement for construction. The notion of sustainable development aspires to the role of a high civilizational ideal. Sustainable development "implies meeting the needs of the present without compromising the ability of future generations to meet their own needs" (Brundtland, 1987). However, a softer definition exists close to the people. Antoine de Saint-Exupery in *The Little Prince* said: *we do not inherit the Earth from our parents; we borrow it from our children.* On first impression, this second definition is a *leitmotif* or underlying theme of the book. Annually over six billion m^3 of concrete is produced around the world. It is unrealistic or even impossible to substitute other materials for this concrete. Nevertheless, it is possible or even necessary to modify concrete to use an adequate admixture (see the book title) to make concrete and construction materials ecoefficient, more environmentally friendly. The book provides basic concepts, production aspects, and environmental impact assessments on the use of biopolymers and biotech admixtures for cement mortar and concrete, as well as for soil stability, wood preservation, and coatings in construction applications including bioadhesives, biofilters, and biobarriers. This knowledge is new but well structured, up-to-date, with an enormous number of references. What is more, on each page a reader feels the need for progress in the face of complexity by making sense of every piece of information. The book is rare that is both scholarly and engaging. It is a great work—a magnum opus: 450 pages and 40 contributors. Contrary to that diversity, from a reader′s point of view it makes the impression of an integral continuity. We can see here the merit of four experienced editors: V. Ivanov (Singapore), W. Karak (India), and H. Jonkers (The Netherlands) under the guideline of Fernando Pacheco-Torgal (Portugal). It is an excellent example of how to make order in informational chaos. Altogether, the contributors could be called the sense makers in the biotech construction material engineering field. The words that were chosen matter to the contributors. They suggest the ideas that the contributors want to bring into the world. The words and sentences can further our plans, fulfill our inspirations. Authors arrange lots of facts, reports, and discoveries in a way that makes it understandable and of value in the engineering field marked by the topical pillars: biotechnology—construction materials—ecology. Readers will feel a familiarity with the architecture of the presented information. What is more, readers feel the right to rely on those information sources and to be professionally active on this area. One of the reasons is a conviction that the authors know their topic and recognize their responsibility, clearly conveyed by the text. Implementing new or even modified construction materials means that we are able to assure durability (often more than 50 years), safety of use, health, and user comfort.

Each chapter shines light on the selected issue: scientific approach for construction biotechnology; biotechnological production; life cycle of biopolymers; biotech admixtures as modifiers for fresh concrete mixture and hardened concrete; microorganism-based bioplasticizers for concrete; fly ash materials; biopolymers for wood preservation; biopolymer coatings, including photocatalytic ones; bioadhesives; biofilters, and biobarriers. Thus, one can outline its edges and depths. The book touches the key problem of how, through experimentation techniques and tests, trials and failures, observations, and theories of construction, researchers have managed to unravel nature’s secrets and transform them into technology to achieve progress. Perhaps, the economic aspect is not accented enough.

It is true that biobased admixtures have been used in construction materials for centuries much earlier than the Roman Empire. However, it is also true that contemporary knowledge of this subject is arising almost simultaneously with the appearance of this book. Topicality is one of the extra values of the book.

How we do manage with construction materials in the twenty-first century?—It is one of the basic questions of civilization. Expectations include:

- a new arrangement of the research results,
- a new understanding of the nature of materials,
- a thrust for further development in theory and in application.

The new knowledge will help us to change our activity in our world.

Knowing is not enough, the book also encourages us. It seems that now is the right time. We can lessen our anxiety and follow the book to make progress.

The book appears as the 63rd entry on the list of the Woodhead Publishing Series in Civil and Structural Engineering. Five books published during the last three years have highlighted the significant adjective: *Ecoefficient*. It is not by accident that it exposes the development trend as a megatrend. The book makes a brilliant trace along this way. We have the essential reading.

Lech Czarnecki
Building Research Institute (ITB)
Warsaw, Poland.

Introduction to biopolymers and biotech admixtures for eco-efficient construction materials

1

F. Pacheco-Torgal
University of Minho, Guimarães, Portugal

1.1 Introduction

For more than half a century the fossil fuel industry has provided the resources for the polymer industry. Independently of the "Peak Oil" never ending discussion (Chapman, 2014), the future scarcity of petroleum resources (Sorrell et al., 2012) is a fact that must be faced sooner or later. Moreover, it does not matter very much that the shale oil euphoria could turn the USA into the world's largest oil producer (Morse, 2014).

Granting the fact, one believes that oil scarcity is not the major issue to be addressed concerning this nonrenewable resource. In the short term, interstate wars and environmental disaster are the major issues. Never before has a commodity triggered so many armed conflicts (Black, 2012). Moreover, since 1973, at least one-quarter of all interstate wars were connected to oil (Verbruggen and van de Graaf, 2013).

States with large oil reserves and unstable political governments tend to instigate conflicts at a rate three and a half times that of comparable states with stable governments and without oil (Colgan, 2013, 2014).

Most importantly, environmental disasters are caused by oil spills like the 1979 *Ixtoc 1* off-shore oil rig blowout, which during nine months released 530 million liters of crude oil into the Gulf of Mexico (Jernelov and Linden, 1981; Patton et al., 1980) causing massive damage to maritime ecosystems (Soto et al., 2014). Add to that the 1989 *Exxon Valdez* oil tanker "small" episode (41 million liters of crude oil) in Alaska that killed hundreds of thousands of seabirds, billions of fish eggs, and many whales and seals (Alford et al., 2014; Malakoff, 2014), and the 2010 British Petroleum (BP)-owned Deep Water Horizon oil spill, which released approximately 780 million liters of crude oil into the Gulf of Mexico (Atlas, 2011). These represent the dark side of crude oil production for which no life-cycle analysis can account.

The latter was considered the worst environmental disaster to have occurred in the USA. According to Costanza et al. (2010), this environmental tragedy was responsible for an almost complete shutdown of the $2.5 billion per year Louisiana fishing industry and was also responsible for a $34−$760 billion loss of ecosystem services in the Mississippi River delta alone. This value exceeds even BP total market value and still

Biopolymers and Biotech Admixtures for Eco-Efficient Construction Materials. http://dx.doi.org/10.1016/B978-0-08-100214-8.00001-4
Copyright © 2016 Elsevier Ltd. All rights reserved.

raises environmental and public health concerns (Ortmann et al., 2012; Wise et al., 2014; Drescher et al., 2014; Gill et al., 2012).

The chronology of other crude oil-related disasters can be seen at Infoplease (2014). In addition, the increase in crude oil transport by oil tankers has led to an increase in collision risk (Morgan et al., 2014).

Because oil exploration is moving into ever-deeper water and into stormier and icier seas, it means increased risks (Jernelov, 2010).

According to Sällh et al. (2015), the share of offshore oil production is expected to increase from 33% to 48% by 2030. This means that the risk of new environmental disasters related to oil production will also increase.

All of the foregoing clearly justifies the search for new and biodegradable polymers based on renewable feedstock.

Recent years have seen a tremendous increase in the number of publication citations on biobased polymers (around 1000% in the last 10 years). However, the fact is that these materials still constitute only a very small fraction of the polymer industry (Babu et al., 2013).

Biopolymers include polymers from agro-resources (polysaccharides, cellulose, starch, chitin, chitosan, and alginates), from microorganisms by fermentation (polyhydroxyalkanoates, such as polyhydroxybutyrate) and from biotechnology via conventional synthesis (polylactides (PLA), polybutadiene succinate, biopolyethylene (PE), polytrimethylene terephthalate, poly-*p*-phenylene) (Avérous and Pollet, 2012). Although some are biodegradable, that is not always the case, like, for instance, PE.

It is clear that the farming practices used to grow biobased feedstock including the fuel required for plowing, harvesting, manufacture, and transport, and the use of herbicides and pesticides, can also have environmental impacts as high as those of petrochemical-based polymers (Yates and Barlow, 2013). However, biopolymers are not associated with armed conflicts, nor are they responsible for large environmental disasters that so often occur in crude oil extraction and transportation. Besides, the reuse of agricultural and biomass waste will contribute to the environmental advantages of biopolymers over traditional petroleum-based polymers (Gopalakrishnan et al., 2012, 2013; Hottle et al., 2013).

1.2 Biopolymers and biotech admixtures for eco-efficient construction materials

Bio-based admixtures have been used in construction materials for centuries. The use of air lime mortars with the addition of vegetable fat goes back to Vitruvius of the Roman Empire (Albert, 1995).

The Romans also had recognized the role of bio-admixtures to improve their building materials; for example, dried blood was used as an air-entraining agent, whereas biopolymers such as proteins served as set retarders for gypsum (Plank, 2003).

The Chinese already have used egg white, fish oil, and blood-based mortars during the construction of the Great Wall due to their imperviousness (Yang, 2012).

In 1507, mortars based on lime mixed with small amounts of vegetable oil added during the slaking process were used in the construction of the Portuguese fortress, “Nossa Senhora da Conceição,” located on Gerum Island, Ormuz, Persian Gulf (Pacheco-Torgal and Jalali, 2011). More than 300 years after the fortress construction, A. W. Stiffe, a Lieutenant of the British Navy, visited the interior of the fortress and made a description of its conservation status for *Geographical Magazine*. He stated that “The mortar used was excellent, and much more durable than the stones” (Rowland, 2006).

The twentieth century became the age of admixtures, the history of which started in the 1920s with the introduction of lignosulfonate, a biopolymer, for Ordinary Portland Cement (OPC) concrete plasticization, the first functional polymer used in construction on a large scale (Plank, 2004).

OPC concrete, a typical civil engineering construction material, is the most used material on Planet Earth. Its production reaches 10,000 million tons/year and in the next 40 years will increase around 100% (Pacheco-Torgal et al., 2013b).

Currently, around 15% of the total OPC concrete production contains chemical admixtures to modify their properties, either in fresh or hardened state. Concrete super plasticizers based on synthetic polymers include melamine, naphthalene condensates, or polycarboxylate copolymers to improve their workability, strength, and durability. Examples of biopolymers used in concrete include lignosulfonate, starch, chitosan, pine root extract, protein hydrolysates, or even vegetable oils. Bioresins based on polyfurfuryl alcohol and produced from agricultural wastes have recently been used with interesting results in engineering structures (Gkaidatzis, 2014).

Biotech admixtures made in fermentation processes by employing bacteria (Pei et al., 2015) or fungi seem to have received an increased attention, because their biosynthesis rate is about two to four times higher than that of plant-based biopolymer (Ivanov et al., 2014). These admixtures include sodium gluconate, xanthan gum, curdlan, or gellan gum. Nevertheless, investigations on the use of biopolymers in OPC are still residual. Of the 8159 Scopus-referenced journal papers published since 2000 and related to OPC, fewer than 1% are related to the use of biopolymers.

The construction industry has become a major field of use for biopolymers. In 2000, an estimated $2 billion in sales was made at the manufacturer’s level, and this growth is expected to continue. Although OPC and dry-mix mortars consume the majority of biopolymers, a great diversity of bio-admixtures with well over 500 different products is now used by other building materials industries (Plank, 2004).

In the next few years, the construction industry will keep on growing at a fast pace just to accommodate urban population increase that will almost double, increasing from approximately 3.4 billion in 2009 to 6.4 billion in 2050 (World Health Organization (WHO, 2014)). Recent estimates on urban expansion suggest that until 2030 urban land cover will increase by 1.2 million km^2 (Seto et al., 2012). Therefore, demand for biopolymer-based construction materials will also increase (Ashby, 2015).

The nanotech advancements that have recently occurred will allow for the development of new and improved biopolymer-based materials. Investigations on cellulose nanocrystals (cellulose elements having at least one dimension in the 1−100 nm range) constitute an important and recent nanotechnology field that will enable the development of eco-efficient high-performance materials (Charreau et al., 2013; Chirayil et al., 2014).

The potential of nanocellulose materials can be perceived from the increase in the number of papers published involving keywords like nanocellulose, cellulose nanocrystals, or cellulose nanocomposites (Figure 1.1).

According to Mariano et al. (2014), the number of papers in this area is expected to increase by a further 500% by at least 2017, leading to an increase in perspective production in the range of 1000% in the following two years. However, the transition from advanced research to practical applications for the built environment is likely to take several years.

Cellulose, being the most abundant organic polymer on Earth and representing about 1.5 trillion tons of the total annual biomass production (Kim et al., 2015), is renewable, biodegradable, and carbon neutral. It has the potential to be processed at industrial-scale quantities and at low cost compared to other materials. The cellulose nanocrystals represent a potential green alternative to carbon nanotubes for reinforcing materials such as polymers and concrete.

Dri et al. (2013) used models based on the atomic structure of cellulose showing that these crystals have a stiffness of 206 GPa, which is comparable to that of steel.

Other authors (Dufresne, 2013) showed that the specific Young's modulus of cellulose nanocrystals, which is the ratio between the Young's modulus and the density of cellulose crystal, is around 85 Jg^{-1}, in comparison to around 25 Jg^{-1} for steel.

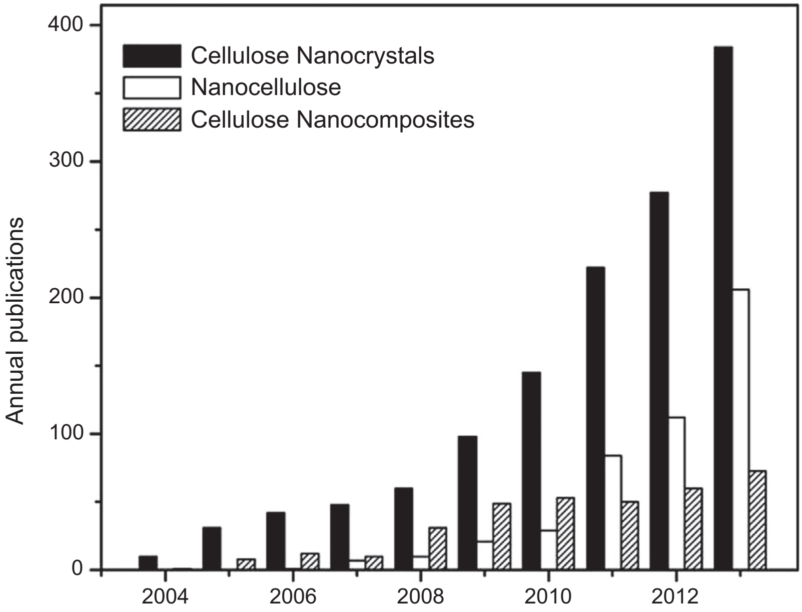

Figure 1.1 Number of publications related with nanocellulose terms during the last decade. Data from main scientific databases. Reprinted from Mariano et al. (2014). Copyright © 2012, with permission from Elsevier.

So far, some uses of nanocrystalline cellulose to improve the modulus of elasticity of cement boards have already been patented (Thomson et al., 2010). The cement industry has a potential nanocellulose market of over 4 million metric tons (Cowie et al., 2014).

Because biopolymers like chitosan, PLA, or starch have poor mechanical performance when compared to synthetic polymers, the use of cellulose nanofibers as reinforcing nanomaterials can help turn those biopolymers into biocomposites with high mechanical strength (Kim et al., 2015).

Cellulose aerogel is another promising application concerning the development of high-performance thermal-insulator building materials (Gavillon and Budtova, 2008; Chen et al., 2014; Nguyen et al., 2014).

Promising results on high-performance nanocellulose-based thermal insulators with fire retardant properties were recently disclosed (Wicklein et al., 2015).

High-performance thermal insulators are materials with a thermal conductivity lower than 0.020 W/m K, whereas current (petroleum-based) insulator materials like expanded polystyrene (EPS) and extruded polystyrene (XPS) have values around 0.03−0.06 W/m K. This is a very important application because the use of thermal insulation materials constitutes the most effective way of reducing heat losses in buildings, thus increasing their energy efficiency. It is worth remembering that the building sector is the largest energy user, responsible for about 40% of the European Union (EU)'s total final energy consumption (Lechtenbohmer and Schuring, 2011). According to the *Energy Road Map 2050* (European Commission, 2011), higher energy efficiency in new and existing buildings is key for the transformation of the EU's energy system. The European Energy Performance of Buildings Directive (EPBD) 2002/91/EC has been recast in the form of Directive 2010/31/EU by the European Parliament on May 19, 2010. One of the new aspects of the EPBD is the introduction of the concept of nearly zero-energy building (Pacheco-Torgal et al., 2013a). Building energy efficiency merits special funding under the HORIZON 2020 EU framework program (Pacheco-Torgal, 2014). In addition, the European market for building energy products and services will reach 80 billion euro by 2023 (Navigant Research, 2014).

Besides, because aerogels are nonflammable, they do not release toxic fumes upon burning as do current insulation materials like EPS or XPS (Pacheco-Torgal et al., 2012), which constitutes an extra advantage.

Some books have already been published concerning biopolymers and biotech admixtures. However, some have absolutely nothing on construction materials, whereas others have just one or two chapters on biobased admixtures for cement and plasters. To the best of my knowledge, none has ever been published that provides a wide view on the subject as does this one. Assembled by a team of leading international expert contributors, this book constitutes an innovative approach on biopolymers and biotech admixtures for eco-efficient construction materials.

1.3 Outline of the book

This book provides an updated state-of-the-art review on the eco-efficiency of biopolymers and biotech admixtures for construction materials. It includes basic concepts, production aspects, environmental impact assessment, the use of biopolymers and biotech admixtures for cement, mortar, and concrete, and covers other construction applications like biobased paintings and coatings, bioadhesives, biofilters, and biobarriers.

The first part of the book encompasses the production of biopolymers for eco-efficient construction materials (Chapters 2—4).

In Chapter 2, basic concepts on biopolymers and biotech admixtures for eco-efficient construction materials are introduced. The different types of biopolymers are reviewed. The case of polysaccharides and their applications in civil engineering are described. Microbial-based bioplastics are covered. Biocements and biogrouts are also covered.

Chapter 3 addresses production aspects of biopolymers and biotech admixtures for eco-efficient construction materials. The following approaches are reviewed: (1) solid or liquid organic wastes, such as food processing, municipal, or mining wastes, used as base materials; (2) aseptic cultivation of microorganisms without sterilization of medium and equipment; and (3) reducing or eliminating the stage of product concentration and purification.

Chapter 4 discusses the life-cycle analysis of biopolymers. The chapter first introduces the concept of biopolymers and the main advantages of shifting from traditional petroleum-derived polymers to biomass-derived polymers. Case studies are reported on the life-cycle assessment of biopolymers used in several sectors with a major focus on the building sector.

Biopolymers and biotech admixtures in cement and mortars are the subject of Part II (Chapters 5—9).

Chapter 5 is concerned with biotech admixtures for enhancing Portland cement hydration. The influence of different polymers including cellulose ethers, hydroxypropylmethyl cellulose, hydroxyethylmethyl cellulose, hydroxyethyl cellulose, chitosan, Diutan gum, gellan gum, xanthan, lignosulfonates, starch, and microcellulose are reviewed.

Chapter 6 covers the utilization of pulp black-liquor waste, a by-product from the papermaking industry as a cement admixture. Its influence on the physical and mechanical properties of cement pastes is analyzed. Infrared spectra and microstructure analysis are included. The optimum pulp black-liquor waste percentage is determined.

Chapter 7 analyzes the use of biopolymer chitosan-based high-performance superplasticizer. The preparation principles and major influence factors as well as the relationship of structure and properties are included. The application properties of the chitosan superplasticizer, such as fluidity, adsorption behavior, and impact on mechanical strength and microstructure of concrete, are studied.

Chapter 8 addresses the case of a new bioproduct produced through fermentation of a mixed culture of microorganisms as a plasticizer in concrete. The bio-admixture has a broad impact on cement and concrete properties probably caused by the various compounds present, and thus the various mechanisms of influence act in a synergetic way. Applications such as plasticizers and viscosity-controlling agents in concrete are discussed. Practical examples of self-compacting and normal concrete are also discussed.

Chapter 9 addresses the performance of fly ash-based geopolymer with kappa-carrageenan biopolymer (KC), a seaweed extract. Mechanical tests are conducted to study the improvement of strength and prepeak toughness, and scanning electron microscopy and Fourier transform infrared are employed to study the microstructural and chemical evolution when different amounts of KC are incorporated in the fly ash-based geopolymer paste specimens.

Part III (Chapters 10−13) deals with biopolymers and biotech admixtures in concrete.

Chapter 10 reviews biopolymers with superplasticizer properties for both fresh and hardened states of concrete. It includes aspects on concrete microstructure and concrete modeling.

Chapter 11 discusses biopolymers with viscosity-enhancing properties for concrete. The chemical structure, modes of action, rheological properties, and impact on cement hydration of commonly used viscosity-enhancing admixtures derived from biological sources are analyzed.

Chapter 12 looks at biotech solutions for concrete repair with enhanced durability. Two different specific systems for biotechnological repair of concrete structures are discussed. The first one covers liquid biobased repair systems for durable repair of cracked and porous concrete surfaces, and the second one addresses biobased mortar systems for repair of larger defects of concrete structures.

Finally, Part IV concerns other biopolymer applications (Chapters 13−18).

Chapter 13 is concerned with biofoam composites. Suggestions for damage prevention including utilization of additives and reinforcements in obtaining multifunctionalities are reported. Common design methodologies used in construction materials are presented.

Chapter 14 addresses the use of biopolymers for wood preservation. It reviews wood-degradative factors, their mechanism of action, and the method for diminishing them.

Chapter 15 is concerned with biopolymers for paintings and coatings. It covers the case of biobased polymers like polyester, poly(ester amide), epoxy, and polyurethane. It presents a typical preparative method for industrial painting based on biopolyester.

Chapter 16 reviews biobased adhesives covering the different existing families of adhesives.

Chapter 17 reviews biopolymers as biofilters and biobarriers. Mechanisms of biofiltration are reviewed. The performance of biopolymer-based barriers is included. The use of biobarriers for the removal of inorganic contaminants from wastewater is also covered.

Chapter 18 closes Part IV with a case study on biopolymers for superhydrophobic photocatalysis coatings, which prevent algae or moss deposits on façade or building roofs.

References

Ashby, F., 2015. Materials and Sustainable Development, first ed. Butterworth-Heinemann, Elsevier, Oxford, UK.

Albert, L.B., 1995. Ten Books on Architecture. Oxford University Press, London.

Alford, J., Peterson, M., Green, C., 2014. Impacts of Oil Spill Disasters on Marine Habitats and Fisheries in North America. In: CRC Marine Biology Series. CRC Press, 340 pp.

Atlas, R., 2011. Oil biodegradation and bioremediation: a tale of the two worst spills in U.S. history. Environmental Science and Technology 45, 6709−6767.

Babu, R., O'Connor, K., Seeram, R., 2013. Current progress on bio-based polymers and their future trends. Progress in Biomaterials 2 (8).

Black, B., 2012. Crude Reality: Petroleum in World History. Rowman & Littlefield Publishers, 288 pp.

Chapman, I., 2014. The end of peak oil? Why this topic is still relevant despite recent denials. Energy Policy 64, 93−101.

Charreau, H., Foresti, M., Vazquez, A., 2013. Nanocellulose patents trends: a comprehensive review on patents on cellulose nanocrystals, microfibrillated and bacterial cellulose. Recent Patents on Nanotechnology 7, 56−80.

Chen, W., Li, Q., Wang, Y., Yi, X., Zheng, J., Yu, H., Liu, Y., Li, J., 2014. Comparative study of aerogels obtained from differently prepared nanocellulose fibres. ChemSusChem 7, 154−161.

Chirayil, C., Mathew, L., Thomas, S., 2014. Review of recent research in nanocellulose preparation from different lignocellulosic fibers. Reviews on Advanced Materials Science 37, 20−28.

Colgan, J., 2014. Oil, domestic politics, and international conflict. Energy Research & Social Science 1, 198−205.

Colgan, J., 2013. Fueling the Fire: The Pathways from Oil to War. International Security MIT Press.

Costanza, R., Batker, D., Day Jr., J.W., Feagin, R.A., Martinez, M., Roman, J., 2010. The perfect spill: solutions for averting the next deepwater horizon. Solutions: For A Sustainable & Desirable Future 1 (5), 17−20.

Cowie, J., Bilek, E., Wegner, T., Shatkin, J., 2014. Market projections of cellulose nanomaterial-enabled products − part 2: volume estimates. Tappi Journal 13, 57−69.

Drescher, C., Schulenberg, S., Smith, E., Veronica, C., March 2014. The Deepwater horizon oil spill and the Mississippi Gulf Coast: mental health in the context of a technological disaster. American Journal of Orthopsychiatry 84 (2), 142−151.

Dri, F., Hector, L., Moon, R., Zavattieri, P., 2013. Anisotropy of the elastic properties of crystalline cellulose Iβ from first principles density functional theory with Van der Waals interactions. Cellulose 20, 2703−2718.

Dufresne, A., 2013. Nanocellulose: a new ageless bionanomaterial. Materials Today 16, 220−227.

European Commission, 2011. Energy Roadmap 2050. COM(2011) 885/.EC, Brussels.

Gavillon, R., Budtova, T., 2008. Aerocellulose: new highly porous cellulose prepared from cellulose-NaOH aqueous solution. Biomacromolecules 9, 269−277.

Gkaidatzis, R., 2014. Bio-based FRP Structures: A Pedestrian Bridge in Schiphol Logistics Park (Master thesis). TU Delft.

Gill, D., Ritchie, L., Picou, J., Langhinrichsen-Rohling, M., Shenesey, J., January 2012. The *Exxon Valdez* and BP oil spills: a comparison of psychosocial impacts. Natural Hazards, American Behavioral Scientist 56 (1), 3−23.

Gopalakrishnan, H., Ceylan, H., Kim, S., 2013. Renewable biomass-derived lignin in transportation infrastructure strengthening applications. International Journal of Sustainable Engineering 6, 316−325.

Gopalakrishnan, H., van Leeuwen, J., Brown, R., 2012. Sustainable Bioenergy and Bioproducts. Value added Engineering and Applications. Springer.

Hottle, T., Bilec, M., Landis, A., 2013. Sustainability assessments of bio-based polymers. Polymer Degradation and Stability 98 (2013), 1898−1907.

Infoplease, 2014. Oil spills and disasters. http://www.infoplease.com/ipa/A0001451.html. Accessed December 2014.

Ivanov, V., Chu, J., Stabnikov, V., 2014. Basics of construction microbial biotechnology. In: Pacheco-Torgal, F., Labrincha, J., Diamanti, M., Yu, C.-P., Lee, H. (Eds.), Biotechnologies and Biomimetics for Civil Engineering. Springer Verlag, London.

Jernelov, A., 2010. The threats from oil spills: now, then and in the future. Ambio 39, 353−366.

Jernelov, A., Linden, O., 1981. Ixtoc I: a case study of the world's largest oil spill. Ambio 10 (6), 299−306.

Kim, J.-H., Shim, B., Kim, H., Lee, Y.-J., Min, S.-K., Jang, D., Abas, B., Kim, J., 2015. Review of nanocellulose for sustainable future materials. International Journal of Precision Engineering and Manufacturing Green Technology 2 (2), 197−213.

Lechtenbohmer, S., Schuring, A., 2011. The potential for large-scale savings from insulating residential buildings in the EU. Energy Efficiency 4, 257−270.

Avérous, L., Pollet, E., 2012. Biodegradable polymers. In: Environmental Silicate Nano-biocomposites. Green Energy and Technology. Springer, Hiedelberg, pp. 13−39.

Malakoff, D., 2014. 25 years after the *Exxon Valdez*, where are the herring? Science 28 (6178), 1416.

Mariano, M., El Kissi, N., Dufresne, A., 2014. Cellulose nanocrystals and related nanocomposites: review of some properties and challenges. Journal of Polymer Science 52 (12), 791−806.

Morgan, A., Shaw-Brown, K., Bellingham, I., Lewis, A., Pearce, M., Pendoley, K., 2014. Global oil spills and oiled wildlife response effort: implications for oil spill contingency planning. In: International Oil Spill Conference Proceedings: May 2014, vol. 2014 (1), pp. 1524−1544.

Morse, E., 2014. Welcome to the revolution. Why shale is the next shale. Foreign Affair 93 (3).

Navigant Research, 2014. Energy Efficient Buildings: Europe. http://www.navigantresearch.com/research/energy-efficient-buildings-europe.

Nguyen, T., Feng, J., Ng, S., Wong, J., Tan, V., Duong, H., 2014. Advanced thermal insulation and absorption properties of recycled cellulose aerogels. Colloids and Surfaces A: Physicochemical and Engineering Aspects 445, 128−134.

Ortmann, A.C., Anders, J., Shelton, N., Gong, L., Moss, A.G., et al., 2012. Dispersed oil disrupts microbial pathways in pelagic food webs. PLoS One 7 (7), e42548.

Pacheco-Torgal, F., 2014. Eco-efficient construction and building materials research under the EU framework programme horizon 2020. Construction and Building Materials 51, 151−162.

Pacheco-Torgal, F., Labrincha, J.A., Jalali, S., John, V.M., 2013a. Eco-efficient Concrete. Woodhead Publishing Limited Abington Hall, Cambridge, UK.

Pacheco-Torgal, F., Cabeza, L., Mistretta, M., Kaklauskas, A., Granqvist, C.G., 2013b. Nearly Zero Energy Building Refurbishment. A Multidisciplinary Approach. Springer Verlag, London.

Pacheco-Torgal, F., Fucic, A., Jalali, S., 2012. Toxicity of Building Materials. Woodhead Publishing Limited Abington Hall, Cambridge, UK.

Pacheco-Torgal, F., Jalali, S., 2011. Eco-efficient Construction and Building Materials. Springer Verlag, London, UK.

Pei, R., Liu, J., Wang, S., 2015. Use of bacteria cell walls as a viscosity-modifying admixture of concrete. Cement and Concrete Composites 55, 186−195.

Plank, J., 2004. Application of biopolymers and other biotechnological products in building material. Applied Microbiology and Biotechnology 66, 1−9.

Plank, J., 2003. Applications of biopolymers in construction engineering. Biopolymers Online 29−39.

Patton, J., Rigler, M., Boehm, P., Fiest, D., 1980. Ixtoc 1 oil spill: flaking of surface mousse in the Gulf of Mexico. Nature 290, 235−238.

Rowland, P.B., 2006. Essays on Hormuz. http://www.dataxinfo.com/hormuz/essays/3.6.pdf.

Sällh, D., Wachtmeister, H., Tang, X., Höök, M., 2015. Offshore oil: Investigating production parameters of fields of varying size, location and water depth. Fuel 139, 430−440.

Seto, K.C., Buneralp, B., Hutyra, L.R., 2012. Global forecasts of urban expansion to 2030 and impacts on biodiversity and carbon pools. PNAS 17−21.

Sorrell, S., Speirs, J., Bentley, R., Miller, R., Thompson, E., 2012. Shaping the global oil peak: a review of the evidence on field sizes, reserves growth, decline rates and depletion rates. Energy 37, 709−724.

Soto, L., Botello, A., Licea-Duran, S., Lizarra-Partida, M., Yanez-Arancibia, A., 2014. The environmental legacy of the Ixtoc 1 oil spill in Campeche Sound, southwestern Gulf of Mexico. Frontiers in Marine Science 1, 57. http://dx.doi.org/10.3389/fmars.2014.00057.

Thomson, S.L., O'Callaghan, D.J., Westland, J.A., Su, B., 2010. Method of Making a Fiber Cement Board with Improved Properties and the Product US20100162926A1. http://www.google.com/patents/US20100162926.

Verbruggen, A., van de Graaf, V., 2013. Peak oil supply or oil not for sale? Futures 53, 74−85.

WHO, 2014. Urban population growth. Global health observatory.

Wicklein, B., Kocjan, A., Salazar-Alvarez, G., Carosio, F., Camino, G., Antonietti, M., Bergstrom, L., 2015. Thermally insulating and fire retardant lightweight anisotropic foams based on nanocellulose and graphene oxide. Nature Nanotechnology 10, 277−283.

Wise, J.P., Wise, J.T.F., Wise, C.F., Wise, S.S., Gianios, C., Xie, H., Thompson, W., Perkins, C., Falank, C., 2014. Concentrations of the genotoxic metals, chromium and nickel, in whales, tar balls, oil slicks, and released oil from the Gulf of Mexico in the immediate aftermath of the deepwater horizon oil crisis: is genotoxic metal exposure part of the Deepwater Horizon legacy? Environmental Science and Technology 48 (5), 2997−3006.

Yang, J., 2012. Intelligent Systems Analyzing Sections of the Great Wall of China for Ming and Pre-Ming Dynasty Construction (Electronic thesis or dissertation). Retrieved from: https://etd.ohiolink.edu/.

Yates, M., Barlow, C., 2013. Life cycle assessments of biodegradable, commercial biopolymers-A critical review. Resources, Conservation and Recycling 78, 54−66.

Basic concepts on biopolymers and biotechnological admixtures for eco-efficient construction materials

2

V. Ivanov[1], *V. Stabnikov*[1,2]
[1]Nanyang Technological University, Singapore; [2]National University of Food Technologies, Kiev, Ukraine

2.1 Construction biotechnology

The discipline of microbial biotechnology includes a scientific and practical knowledge of using microorganisms and their products. We differentiate the areas of biotechnological applications into such subdisciplines as medical, pharmaceutical, industrial, agricultural, and environmental biotechnology. Currently, the new subdiscipline of construction microbial biotechnology can be differentiated. This new scientific discipline has developed just in the last decade.

Construction microbial biotechnology takes two major directions:

1. the microbial production of construction materials; and
2. the applications of microorganisms in construction processes.

Different biotechnological products and biotechnologies for civil engineering are developing within these directions (Figure 2.1).

Production of cement, a major construction material, is energy consuming and environmentally unfriendly. Energy represents 20–40% of the total cost of cement production because temperatures above 950 °C are needed for transformation of limestone to cement clinker. New construction materials, microbial biocements, can be produced from limestone, dolomite, or iron ore at temperatures 20–60 °C with less than 10% of energy used for the manufacturing of conventional cement. Microbially based biocementing or bioclogging materials have advantages over conventional cements and grouts, for example, sustainability due to their production from organic matter, low viscosity, and low risk of negative environmental consequences.

Other types of biomaterials used in the construction industry include industrially produced microbial polysaccharides, such as xanthan, welan, succinoglucan, curdlan, and chitosan. They are used in dry-mix mortars, wall plasters, self-leveling underlayers, or injection grouts to improve viscosity, water retention, set retardation, and flowability (Plank, 2004). Other biopolymers, for example, proteins can also be used if the cost is acceptable. Sewage sludge of municipal wastewater treatment plants,

Biopolymers and Biotech Admixtures for Eco-Efficient Construction Materials. http://dx.doi.org/10.1016/B978-0-08-100214-8.00002-6
Copyright © 2016 Elsevier Ltd. All rights reserved.

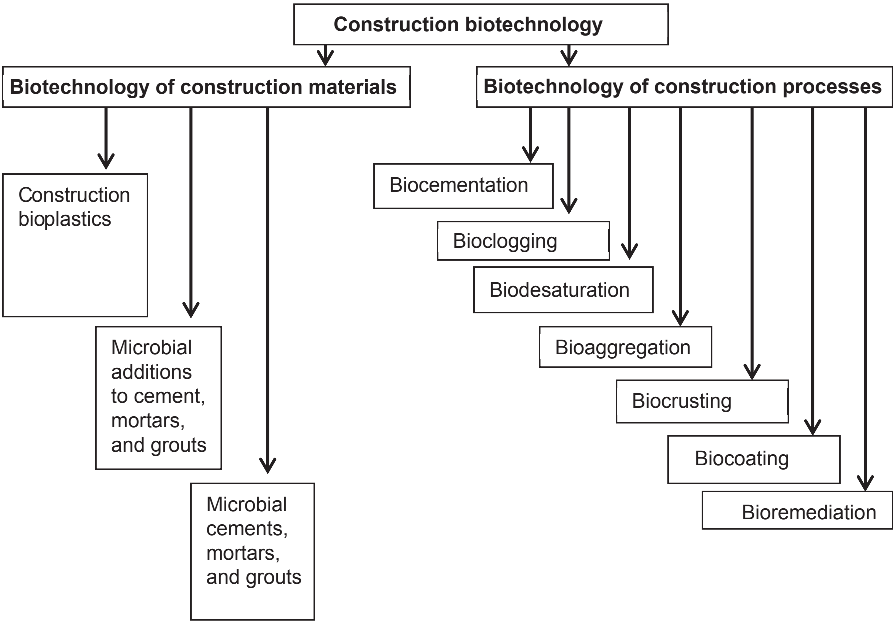

Figure 2.1 The applications of microorganisms in construction processes.

which is a waste microbial biomass produced in quantities of several million tons a year, could also be used as a source of cheap microbial polymers.

The production of bacterial polysaccharides in soil after addition of bacterial cells and necessary nutrients in situ is also used to modify soil properties. This approach could be used for such geotechnical applications as dam control, wind soil-erosion control, earthquake liquefaction mitigation, construction of reactive barriers, and long-term stabilization of contaminated soils. Different kinds of organic wastes can be used as sources of organic matter for polysaccharide-producing microorganisms in large-scale geotechnical applications to diminish the cost of soil clogging. Surface growth of exopolysaccharide-producing photosynthetic microorganisms in irrigation channels or aquaculture ponds is an effective way to control seepage.

The biotechnological production of construction biomaterials is a sustainable process because renewable agricultural and biotechnological biomass residues are used as organic raw materials and as the components of composite biocement.

In some geotechnical processes, microorganisms themselves are performing useful functions. There are at least eight types of construction-related biotechnological processes classified by the results of the microbial treatment of soil:

1. *Bioaggregation* of soil or particles is a process to increase the size of fine particles to reduce soil erosion by water and wind, sand movement, as well as dust emission (Bang et al., 2011; Stabnikov et al., 2013a).
2. *Biocrusting* is a process to form mineral or organic crusts on the soil surface to reduce erosion, dust emission, and water infiltration (Stabnikov et al., 2011; Chu et al., 2012).

3. *Biocoating* of solid surfaces is a process to form a solid surface layer to enhance aesthetics or the colonization of the surface (De Muynk et al., 2008a,b; 2010).
4. *Bioclogging* of soil or porous matrix is a process to fill in the pores and channels in soil/matrix to significantly reduce the hydraulic conductivity of soil or porous matrix (Ivanov et al., 2014a).
5. *Biocementation* of soil or particles is a process to significantly increase the strength of soil or particles (Ghosh et al., 2005; Mitchell and Santamarina, 2005; Whiffin et al., 2007; Ivanov and Chu, 2008; De Muynck et al., 2012; Sarda et al., 2009; van der Ruyt and van der Zon, 2009; Achal et al., 2010; Ivanov, 2010; Van Tittelboom et al., 2010; van Paassen et al., 2010; Harkes et al., 2010; Chu et al., 2012; Dhami et al., 2012; Li and Qu, 2012; DeJong et al., 2010, 2013; Dosier, 2013; Raut et al., 2014).
6. *Biodesaturation* of soil is a process to decrease saturation and liquefaction potential of soil through in situ biogas production (Chu et al., 2009; Rebata-Landa and Santamarina, 2012; Chu et al., 2013b; He et al., 2013).
7. *Bioencapsulation* of clay/soil/particles is a process to increase the strength of soft clayey soil through the formation of a strong shell around pieces of soft material (Ivanov et al., 2012).
8. *Bioremediation* of soil is a process to remove pollutants from soil or immobilize pollutants in the soil before construction (Warren et al., 2001; Fujita et al., 2004; Mitchell and Ferris, 2005).

The principles of the construction-related biotechnological processes are shown in Figure 2.2.

2.2 The types of biopolymers

Biopolymers are the major components of the cell, typically consisting of 90% dry cell matter. The major cell monomers are monosaccharides, amino acids, and nucleotides, which form such polymers as polysaccharides, proteins, and ribonucleic and deoxyribonucleic acids. Lipids also could be considered as physicochemical polymers due to aggregation of lipid molecules by hydrophobic forces.

Biopolymers perform different functions in a cell:

1. Cell metabolism due to enzymatic activity of proteins synthesized by ribosomal ribonucleic acids using the information in the messenger ribonucleic acids that is transcribed from the deoxyribonucleic acid of a chromosome. These compounds are arranged as solutions or suspensions inside cells.
2. Store of materials and energy in cells, for example, intracellular glycogen and polyhydroxybutyrate (PHB) in prokaryotes, starch and lipids in plants, and polyphosphates in bacteria. The storage compounds are usually arranged as slow soluble granules inside a cell. However, extracellular polysaccharides of bacteria just attach to cells or concentrate in the areas close to cells, and their main function is to protect the cells from drying and toxic compounds, as well as attachment of the cells to surfaces and to other cells. Storage biopolymers are easily and rapidly biodegradable substances, with the exception of PHB and lipids.
3. Structural components: rigid peptidoglycan of the bacterial cell wall, chitin of the fungal cell wall, cellulose and hemicellulose of plant and fungal cell walls, and the intercellular pectin of plants. Structural biopolymers are slow biodegradable substances, which are relatively stable when used as construction materials.

Type of biotreatment process	Soil particles or construction material (dark color) after biotreatment forming binding material/biocement (gray color)
Bioaggregation of soil: increase of soil particles size so that soil erosion and dust emission will be reduced	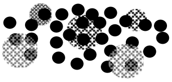
Biocrusting: formation of crust on soil surface so that wind and water erosions, dust emission, and water infiltration will be reduced	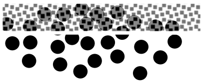
Biocoating: formation of a layer on the solid surface so that colonization or aesthetics, or corrosion protection of surface will be enhanced	
Bioclogging: filling the pores and channels in soil of fissured rock so that hydraulic conductivity of soil or fissured rock will be significantly reduced	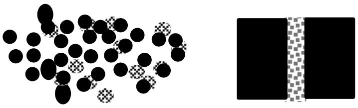
Biocementation: binding of the soil particles that significantly increase strength of soil	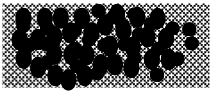
Partial biodesaturation of saturated soil: production of biogas bubbles in situ to reduce saturation and liquefaction potential of soil	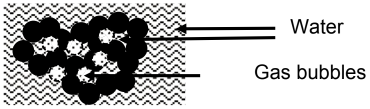
Bioencapsulation: increase of the strength of soft clayey soil, saturated loose soil, quick sand, muck soil of the drained swampland	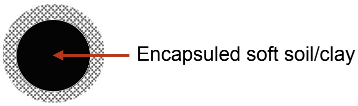
Bioremediation: biodegradation or bioimmobilization of the soil pollutants before construction process	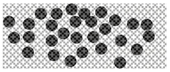

Figure 2.2 The types of construction-related biotechnological processes.

All biopolymers, but especially the cell storage and structural biopolymers, can be used in different areas of construction.

Animal biomaterials such as blood, urine, eggs, milk, lard, and plant biopolymers such as wood, straw, bark, cactus juice, flour have been used as admixtures from ancient times to improve the properties of mortars and plasters. Straw and cattle dung were used and are used even today in rural construction as composite biomaterials to improve the construction properties of clay. Probably, the Aztecs used the fermented juice of nopal cactus (*Opuntia ficus indica*) to improve plasticity and the water-absorption capacity of lime mortar and earthen plasters due to the presence of cellulose fibers, gel polysaccharides, and fermentation products. Extracts of nopal cactus and water hyacinth are proposed even today to enhance the viscosity of cement-based materials (Leon-Martinez et al., 2014; Sathya et al., 2013). The chemical derivates of plant biopolymers, for example, carboxymethylcellulose, carboxymethylcellulose sulfate, or such industrial waste as lignosulfonates are often used as cement and mortar admixtures for set retardation and increase of the plasticity of self-consolidated concrete (Plank, 2004; Yuan et al., 2013).

2.3 Microbial polysaccharides and their applications in civil engineering

Chemical and biological admixtures, mainly microbial extracellular polysaccharides, are using in cement- and gypsum-based materials for dispersing/thickening effects, viscosity enhancement, water retention, set acceleration and retardation, air entrainment, defoaming, hydrophobization, adhesion, and film forming (Plank, 2003) to improve such properties of the material as plasticity, water retention, adhesion, shrinkage reduction, flowability, and stability. The global market of admixtures is estimated at the level of US$15 billion with the share of more than 500 different biological and biodegradable admixtures about 13% (Plank, 2004).

The advantage of microbial admixtures is that the biosynthesis rate of the microbial biopolymers is significantly higher, by two to four orders of magnitude, than that of plants, and these substances can be produced at industrial scale in biotechnological factories. The major application of microbial biopolymers in the construction industry is an addition to concrete and dry-mix mortars. The examples of microbial admixtures that are used in concrete are protein hydrolyzates and welan gum; and in the case of dry-mix mortar these admixtures are succinoglycan and xanthan gum. The market share of microbial biopolymers is expected to increase because of technological advances and the growing trend to use naturally based or biodegradable products in building materials (Plank, 2004; Ramesh et al., 2010). These microbial products of the biotechnological industry are mainly viscosity-enhancing admixtures used to achieve high resistance to segregation of concrete. These biotechnological admixtures are usually microbial polysaccharides as shown in Table 2.1.

Table 2.1 Microbial polysaccharides as the major biotechnological admixtures used in building materials

Admixture	Function, applications, and dosage	Estimated price, US$
Xanthan gum	Viscosifier (thickener), set retarder for self-consolidated concrete, floor screeds, paints, 0.2–0.5%	2000–5000
Welan gum	Viscosifier (thickener), set retarder for self-consolidated concrete, floor screeds, paints, 0.1–0.5%	2000–5000
Scleroglucan	Thermostable viscosifier (no loss of viscosity at 90 °C for 500 days), similar to xanthan gum	2000–5000
Succinoglycan	High shear-thinning behavior with temperature-induced viscosity breakback for self-leveling compounds, soil stabilization, 1–15 g/L of water	2000–5000
Curdlan gum	Viscosifier (thickener), set retarder for self-consolidated concrete, up to 10 g/L of water; can absorb water about 100 times	1000–10,000
Polyaspartic acid	Biodegradable dispersant, inhibitor of corrosion in concrete, air-entraining agent for concrete or mortar, set retarder for gypsum	1000–10,000
Sodium alginate	Stabilizer, thickener, and emulsifier	2000–10,000
Carrageenan	Foam for protecting freshly poured concrete from premature drying during highway construction	2000–10,000
Dextran	Admixture to Portland cement, self-leveling grouts, fresh- or saltwater oil well cement slurries, microfine cements improving flow resistance (rheology-modified additive)	3000–9000
Pullulan	Viscosifier (thickener), set retarder for self-consolidated concrete	5000–20,000
Sewage sludge	Viscosifier (thickener), set retarder for self-consolidated concrete Production of sintered light-weight aggregated for nonstructural concrete (clay: Sewage sludge ratio is from 1:1 to 1:3 by mass) Co-combustion of sewage sludge in cement manufacturing (5% of the clinker production capacity)	0
Bacterial cell walls	Microstructured filler for concrete increasing compressive strengths of concrete by 15% and decreasing its porosity; 0.03–3.3% by mass	2000–10,000

Based on Plank (2003, 2004); Mun (2007); Fytili and Zabaniotou (2008); Pacheco-Torgal and Jalali (2011); Pei et al. (2013), and other sources.

2.4 Bioclogging of soil using in situ production of microbial polysaccharides

Another important application of microbial biopolymers is in situ production of microbial polysaccharides in porous soil to modify its geotechnical properties (Stewart and Fogler, 2001). Very often, microorganisms grow in soil as a biofilm being attached to solid surfaces and embedded in slimy exopolysaccharides produced by the cells (Flemming et al., 2007). This slime reduces the soil permeability. The effect of microbial biomass growth on the reduction of porosity, permeability, and hydraulic conductivity due to bioclogging of the porous media has been shown in many studies (Seifert and Engesgaard, 2007, 2012; Seki et al., 1998; Ross et al., 2001; Ross and Bickerton, 2002; Wu et al., 1997). Comparative study of four bacterial strains, used for inoculation of quartz sand packed in columns with a continuous supply of a medium, showed that only slime producers greatly reduced the saturated hydraulic conductivity of sand (Vandevivere and Baveye, 1992b).

It is well known that almost all bacteria produce exopolysaccharides under an excess of carbohydrates or other water-soluble sources of carbon over a source of nitrogen. Therefore, such food-processing wastes or subproducts as corn glucose syrup, cassava glucose syrup, and molasses with C:N ratio >20 are used for industrial production of bacterial water-insoluble polysaccharides (Portilho et al., 2006). After growth of exopolysaccharide-producing bacteria in soil in a medium with this C:N ratio, its permeability for water is greatly reduced. Growth of exopolysaccharide-producing bacteria in soil can be used for different geotechnical applications, such as selective zonal bioremediation, harbor and dam control, erosion potential minimization, earthquake liquefaction mitigation, construction of reactive barriers, and long-term stabilization of contaminated soils (Yang et al., 1993). The most suitable groups of microorganisms that produce insoluble extracellular polysaccharides to bind soil particles and fill in soil pores are the following: (1) oligotrophic bacteria from the genus *Caulobacter* (Tsang et al., 2006); (2) aerobic Gram-negative bacteria from the genera *Acinetobacter*, *Agrobacterium*, *Alcaligenes*, *Arcobacter*, *Cytophaga*, *Flavobacterium*, *Pseudomonas*, and *Rhizobium* (Portilho et al., 2006; Ross et al., 2001); (3) species of Gram-positive facultative anaerobic and aerobic bacteria, such as *Leuconostoc mesenteroides* producing water-insoluble exopolymer dextran (Stewart and Fogler, 2001) and *Cellulomonas flavigena* producing a curdlan-type (beta-1,3-glucan) exopolysaccharide from cellulose (Kenyon et al., 2005); and (4) the representatives of genus *Paracoccus* are often found in microbial biofilms (Bertin et al., 2006; Lee et al., 2003; Neef et al., 1996), especially *P. denitrificans*. The latter is able to produce exopolysaccharides under anaerobic conditions in the medium with organic compounds and nitrate (Rezic et al., 2006; Babenko et al., 2008). However, the list of bacteria that can be used for the in situ bioclogging of soil is much longer. For example, inoculation of soil by *Azotobacter chroococcum* clogged the soil pores and decreased hydraulic conductivity of soil to 1/8000 of initial value (Kim et al., 2006). Application of strictly aerobic bacteria *Arthrobacter* sp. to reduce permeability of the sand column showed that rapid reduction of saturated hydraulic conductivity up to four orders of magnitude was due to the formation of a bacterial mat at the inlet boundary of the sand column (Vandevivere and Baveye, 1992c). *Microbacterium arborescens*, a facultative alkaliphile with optimum growth at pH 10.5, isolated from coastal sand dunes, was able to grow in 12% sodium chloride solution and produce large amounts of partially soluble exopolysaccharide that was able to aggregate sand (Godinho and Bhosle, 2009). The authors supposed that exopolysaccharides play an important role in cell protection for dehydration and in the stabilization of sand dunes.

Development of a plugging biofilm by exopolysaccharide-producing bacteria feeding with nutrient solution in a compacted silty sand led to the decrease of hydraulic conductivity from 10^{-7}–10^{-8} m/s to 10^{-10} m/s (Dennis and Turner, 1998). Synthetic leachate containing acetic, propionic, and butyric volatile fatty acids in the ratio 7:5:1 was used as a medium to continuously feed the sand columns during 45 days inoculated with mixed microbial cultures, which were isolated from leachate collected from an open dumping site (Subramaniam et al., 2014). Initial hydraulic conductivity of the sand was 2.0×10^{-4} m/s and it was decreased for 2.3×10^{-6} m/s after 45 days of operation. This microbial bioclogging of soil may be used for protection of the environment from contamination of the dumping-site leachate. However, for practical use, the final hydraulic conductivity must be less than or equal to 1×10^{-9} m/s as is recommended for soil liners and covers that are used to contain hazardous, industrial, and municipal waste (Daniel and Benson, 1990).

Many microbial exopolysaccharides such as xanthan, hyaluronan, alginate, diutan, gellan, and succinoglycan are water soluble. Meanwhile, there are also water-insoluble exopolysaccharides, such as curdlan and glucan. Insoluble exopolysaccharides, which are most useful for bioclogging because of their longer stability, are often synthesized by *Streptococcus*. However, bacteria of this species can participate in the formation of pathogenic biofilms, for example, excreting glucan on the tooth surface (Koo et al., 2010).

Most of the bacterial strains used for bioclogging of the porous medium are aerobic microorganisms. However, inside the porous medium, anaerobic conditions are developed and facultative anaerobic bacteria become the preferable choice for microbial bioclogging of the media. Among the facultative anaerobic bacteria, which can produce exopolysaccharides, application of *Paracoccus denitrificans* may be the most attractive choice for bioclogging of the porous medium because these bacteria can produce exopolysaccharides and able to reduce nitrate to nitrogen gas under anaerobic conditions, and are not pathogenic ones for plants, animals, or humans.

Biofilm formation can be intensified by stimulation of indigenous microorganisms (biostimulation) or by injection of selected bacterial cultures (bioaugmentation). Growth of biofilms and the clogging of wells is a serious problem in the production of drinking water because it diminishes the quality and quantity of groundwater (Vandevivere and Baveye, 1992a,b,c). The development of a biofilm on the walls of a rock fracture may constrict flow through the fracture to prevent the diffusion of pollutants from the rocks and the migration of contaminants off site (Charbonneau et al., 2006). The biofilm plugs the rock matrix in these cases and diminishes its porosity (Charbonneau et al., 2006). The creation of biobarriers in fractured-limestone rock aquifers by stimulation of indigenous microbes to clog the fractures and to reduce the hydraulic conductivity was demonstrated by Ross et al. (2001). Long-term biofilm activity was shown even in the absence of nutrient additions (Castegnier et al., 2006). For example, the biofilm developed during 46 days in a limestone fracture sustained without feeding for another 179 days. The hydraulic conductivity diminished by three orders of magnitude for the 222 days of experiment.

So, bioclogging of soil or fissured rocks in situ can diminish their hydraulic conductivity and could be used to reduce drain-channel erosion, form grout curtains to reduce the migration of heavy metals and organic pollutants, and prevent piping of earth dams and dikes, as well as seepage in the tunnels. However, there are no data showing a decrease of porous soil permeability with exopolysaccharide production in situ below 1×10^{-6} m/s, which could be insufficient for many applications. There are also some doubts on the stability of this type of bioclogging because all microbial exopolysaccharides are at least partially soluble in water and can be extracted from soil by groundwater flow. Another reason for instability can be microbial degradation of soil exopolysaccharides by actinomycetes, fungi, or protozoa.

2.5 Microbial plastics for civil engineering

There is clear trend in the construction industry for the use of biodegradable materials and biopolymers (Plank, 2004; Ramesh et al., 2010). The use of bioplastics in construction will reduce the land area required for disposal of construction wastes. It will increase the environmental and economic sustainability of construction industry because the bioplastics are produced from renewable sources.

Most available types of bioplastics for the construction industry are polyhydroxyalkanoates (PHAs), especially poly-hydroxybutyrate (PHB) with monomer formula ($-OCH(CH_3)-CH_2-C(O)-$) and polyhydroxyvalerate with monomer formula ($-OCH(CH_2CH_3)-CH_2-C(O)-$). PHAs can be used in practice as bioplastics with melting temperature 160−180 °C, tensile strength 24−40 MPa, and elongation at break 3−142%. Chemical and physical properties of PHAs can be found in numerous reviews (Lowell and Rohwedder, 1974; Braunegg et al., 1998; Sudesh et al., 2000; Volova, 2004; DeMarco, 2005; Khanna and Srivastava, 2005; Lenz and Marchessault, 2005; Castilho et al., 2009; Sudesh and Abe, 2010). The applications of PHA bioplastics from bacterial biomass could be the production and use of biodegradable construction materials, which can diminish the area of land used for landfilling, because they are degraded very quickly in soil or in the landfill. For example, biodegradable bioplastic foam can be used for insulation of the walls and partitions in temporary construction. Bioplastics can be used also as the sealants and insulants replacing petrochemical plastics in the construction industry (Willke and Vorlop, 2004). Other examples of the potential application of crude nanocomposites from bacterial biomass containing PHAs are silt and dust fences that can be landfilled for fast biodegradation or even left in construction ground for degradation. There could be a big market for biodegradable bioplastic foam construction material, which does not require incineration after demolition.

The available bioplastics for the construction industry are not only PHAs, but also polylactic acid/poly-L-lactide (PLA or PLLA), which is produced by chemical polymerization of lactic acid that is synthesized by anaerobic lactic acid bacteria from any source of saccharides. PLA is applicable in many industries and medicine (Ebnesajjad, 2012). However, PLA is a pure biotechnological/chemical product, so it is more expensive material than crude PHAs and polypropylene or polyvinylchloride, but cheaper than pure PHAs.

Synthetic fibers are widely used to reinforce plaster or concrete (Balaguru, 1994; Zeiml et al., 2006; Suchomel and Marsche, 2013), because natural plant fibers have variable and changeable mechanical properties (Suchomel and Marsche, 2013). Bioplastics can be used as the fiber-reinforced polymer composites consisting of reinforcing fibers embedded in a bioplastic matrix.

PLA can be used for the manufacturing of composite biodegradable fibers for the reinforcement of construction materials (Huda et al., 2006; John and Thomas, 2008; Sin et al., 2012; Bajpai et al., 2013; Faludi et al., 2013; Saba et al., 2015), biocomposite sheets for construction and packaging, biodegradable resin composition for construction molds (Tokiwa and Tsuchiya, 2003), and for production of environmentally friendly flooring material, which can be recycled or rapidly decomposed upon discard (Ko et al., 2014). PLA can also be used for the manufacturing of bionanocomposites with significantly improved and new value-added properties in comparison with conventional PLA composites. For example, addition of 5% (v/v) clay to PLA improved tensile strength, break elongation, scratch resistance, and other mechanical properties (Ray, 2012). PLA nanocomposite containing 0.15% (w/w) multiwalled carbon nanotubes and 6% (w/w) of the plasticizer polyethylene glycol have tensile and flexural strengths up to 43.8 and 81.4 MPa, respectively, that are suitable levels for many industrial applications including the construction industry (Maizatulnisa et al., 2013).

2.6 Biocements and biogrouts

Different types of biocementation are possible based on diverse biogeochemical reactions performed by microorganisms (Ivanov and Chu, 2008; Ivanov, 2010).

2.6.1 Calcium- and urea-dependent biocementation

The most popular type of biocementation is based on so-called microbially induced calcium carbonate precipitation (MICCP), which is the formation of calcium carbonate minerals such as calcite, vaterite, or aragonite on the surface of soil particles due to

1. adhesion of cells of urease-producing bacteria (UPB) on the surface of particles;
2. creation of a microgradient of concentration of carbonate and pH at the site of cell attachment due to the hydrolysis of urea—$(NH_2)_2CO$—by the urease of UPB:

$$(NH_2)_2CO + 2\,H_2O + CaCl_2 \rightarrow CaCO_3\downarrow + 2\,NH_4Cl \qquad (2.1)$$

MICCP is being developed and field-tested for numerous geotechnical and civil engineering applications (DeJong et al., 2010, 2013). These include

- enhancement of slope and dam stability (Harkes et al., 2010; van Paassen et al., 2010);
- road construction and soil-erosion prevention (Mitchell and Santamarina, 2005; Whiffin et al., 2007; Ivanov and Chu, 2008; Ivanov, 2010);
- construction in sandy soil of channels, aquaculture ponds, or reservoirs (Stabnikov et al., 2011; Chu et al., 2013a,b);
- sand immobilization and dust suppression (Bang et al., 2011; Stabnikov et al., 2013a);
- sand reinforcement in near-shore areas (van der Ruyt and van der Zon, 2009).
- brick production (Sarda et al., 2009; Dhami et al., 2012; Raut et al., 2014);
- crack remediation in concrete and rock and increase in durability of concrete structures (Ghosh et al., 2005; De Muynck et al., 2008a,b, 2010; Achal et al., 2010; Van Tittelboom et al., 2010; Li and Qu, 2012);
- concrete improvement (Pacheco-Torgal and Labrincha, 2013a,b; Pacheco-Torgal and Jalali, 2013);
- concrete self-remediation (Jonkers, 2007; Jonkers et al., 2010; Siddique and Chahal, 2011; Wiktor and Jonkers, 2011; Wang et al., 2012);
- mortar modification (Ghosh et al., 2009; Vempada et al., 2011);
- consolidation of porous stone (Jimenez-Lopez et al., 2008);
- bioremediation of weathered building-stone surfaces (Fernandes, 2006; Webster and May, 2006; Achal et al., 2011);
- fractured-rock permeability reduction (Cuthbert et al., 2013);
- mitigation of earthquake-caused soil liquefaction (DeJong et al., 2006, 2013; Chu et al., 2009; Montoya et al., 2012; Weil et al., 2012); and
- encapsulation of soft marine clay to produce solid fill material (Ivanov et al., 2014b).

Biocementation can be performed in bulk through the supply of bacterial suspension altogether or separately with the solutions of calcium and urea by injection, surface percolation (Stabnikov et al., 2011; Cheng and Cord-Ruwisch, 2012), or surface spraying (Stabnikov et al., 2011, 2013a,b; Chu et al., 2012). Different technologies of the biotreatment are needed to form crusts on soil surfaces (Figure 2.3(a)), biocemented layers of defined thickness (Figure 2.3(b)), or even biocemented monoliths.

It was shown in our experiments that it is possible to form the layer of calcium carbonate minerals attached to surface of construction materials for their decoration or protection (Figure 2.4). This biocoating can be used also for the manufacturing of artificial coral reefs with the shapes of natural corals (Figure 2.5). It could be essential for the restoration of coral reefs because the formation of calcium carbonate frame of the natural coral reef required many years, sometimes almost a century to be formed, due to low concentration of calcium in sea water. Such artificial coral reefs can be used for recreational marine parks and in aquaculture.

An advantage of MICCP biogrouting/biocementation is low viscosity of solution permitting its injection through the small pores of soil for relatively long distance. However, there are many drawbacks of conventional MICCP which include (1) ammonium ion and ammonia gas, that are by-products of urea hydrolysis, are toxic substances for workers, are harmful for the aquatic environment and atmosphere,

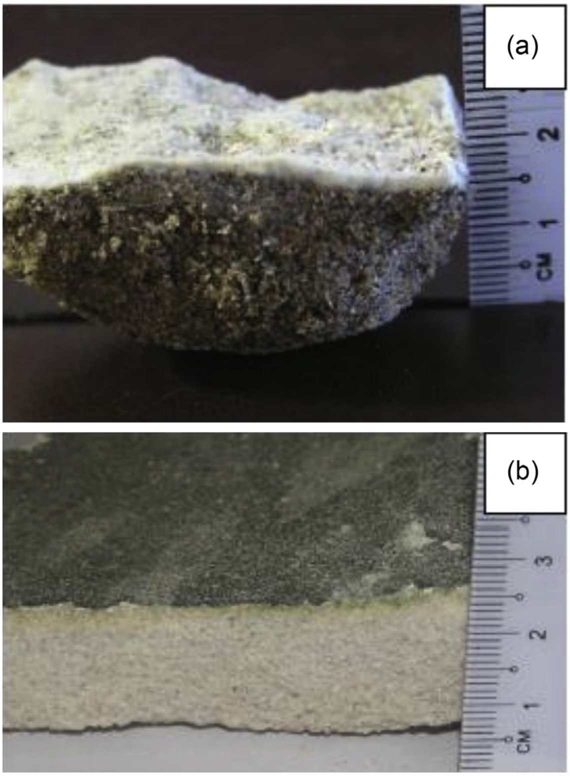

Figure 2.3 Spatial types of biocementation: (a) formation of the crust on surface of sand, (b) formation of the biocemented layer of the defined thickness.

and increase corrosion risk because of high pH (Pacheco-Torgal and Labrincha, 2013a); (2) the brittleness of calcite crystals bonding the soil particles; and (3) the cost of calcium salt and urea are higher than the cost of conventional cement. Therefore, MICCP must be improved or new types of biocementation have to be developed to overcome these disadvantages of conventional MICCP.

MICCP has been proposed for self-repair of concrete (Ramachandran et al., 2001; Jonkers, 2007; Jonkers et al., 2010). However, the volume of calcium carbonate produced from a solution of calcium salt will be always significantly smaller than the volume of the crack to be filled and sealed from the penetration of external water. Normally, the maximum volume of $CaCO_3$ precipitated from 1 M solution of $CaCl_2$ will be just 34.5 mL/L (3.5% v/v) of the pores to be filled in. So, MICCP in this case should be used together with some reagents that expand the volume of the filling material and immobilize the gas microbubbles inside the microcracks of the concrete but in every case the strength of the concrete will be decreased after this type of self-repair.

Figure 2.4 Concrete and brick biocoated with calcite.

2.6.2 Biocementation based on production of carbonates by heterotrophic bacteria during aerobic or anaerobic oxidation of organics

Precipitation of calcium carbonate can be due to increase of pH and the production of carbon dioxide by heterotrophic bacteria during aerobic or anaerobic oxidation of organics (Ehrlich, 1999; Wright and Oren, 2005; Rodriguez-Navarro et al., 2003; Jimenez-Lopez et al., 2008; Hamdan et al., 2011), for example, in the following biogeochemical reactions:

$$(CH_3COO)_2Ca + 4\,O_2 \rightarrow CaCO_3\downarrow + 3\,CO_2\uparrow + 3\,H_2O \tag{2.2}$$

$$\begin{aligned}(CH_3COO)_2Ca + 8/5\,NO_3^- \rightarrow \mathrm{CaCO3}\downarrow + 4/5\,N_2\uparrow \\ + 3\,CO_2\uparrow + 3\,H_2O + 8/5\,OH^-\end{aligned} \tag{2.3}$$

Calcium carbonate precipitation due to nitrate bioreduction of organics is useful for the combination of biocementation with nitrogen gas production in situ during partial desaturation of sandy soil, which is an effective method for the mitigation of earthquake-caused soil liquefaction (Chu et al., 2009; Rebata-Landa and Santamarina, 2012; He et al., 2013). Bioreduction of nitrate (bacterial denitrification process) can

Figure 2.5 Artificial corals biocoated with calcium carbonate minerals.

also increase pH and initiate precipitation of $CaCO_3$ without pH buffering (Hamdan et al., 2011). However, our experiments showed that the growth of denitrifiers and denitrification process are inhibited and finally terminated by Ca^{2+} ions, probably due to Ca-mediated precipitation of phosphorus of phosphate and sulfur of sulfate that are essential elements for bacterial growth.

2.6.3 Biogas production in situ for mitigation of soil liquefaction

Much of the damage during earthquakes is related to soil liquefaction. It is a phenomenon whereby soil substantially loses strength and stiffness. Conventional ground improvement for mitigating liquefaction-induced geotechnical hazards are vibroreplacement, compaction grouting, and deep dynamic compaction methods. However, these methods consume energy and not always can be used in urban areas.

Recent studies showed that inclusion of gas bubbles in saturated sand even for a few percent can substantially reduce its susceptibility to liquefaction (Xia and Hu, 1991; Yang et al., 2004; Yegian et al., 2007; Eseller-Bayat et al., 2012). The sand can be partially desaturated through the production of nitrogen gas by denitrifying bacteria in situ (Chu et al., 2009; 2013b; Rebata-Landa and Santamarina, 2012; He et al., 2013). Ethanol (C_2H_5OH), acetic acid (CH_3COOH), and glucose ($C_6H_{12}O_6$) are the most suitable electron donors to reduce nitrate to nitrogen gas because of their low cost, availability, and high solubility in water. For these electron donors, consumption is about 3.4 kg/m^3 of N_2, and consumption of sodium nitrate (electron acceptor) is about 7.6 kg/m^3 of N_2. The production of CO_2 was not considered in the desaturation of soil because the solubility of CO_2 in water at 10 °C is 2500 g/m^3. The estimated cost of electron donors and acceptors for 10% desaturation of soil with porosity 50% is about 0.25−0.31 US$/m^3 of N_2. However, even the stoichiometrical and economic parameters of the electron donors are similar, ethanol could be the more preferable electron donor than acetic acid or glucose syrup for geotechnical applications, because it is a liquid with neutral pH, noncorrosive, and has low viscosity.

Biocementation of loose sand using an MICCP process to increase the liquefaction resistance of sand has also been reported by DeJong et al. (2006) and Montoya et al. (2012). It was shown (Montoya et al., 2012) that the resistance of sand to liquefaction, as measured by a decrease in the excess pore-water pressure ratio, was significantly increased after MICCP. However, sufficiently strong biocementation of saturated sand, at the level of unconfined compressive strength of 250−500 kPa, could be at the content of precipitated calcium carbonate of 75−100 g/kg of sand (Ivanov et al., 2012a; Cheng et al., 2013). In other words, it could be a material-consuming process requiring about 88 kg $CaCl_2$ and 96 kg of urea per 1 m^3 of sand, which will cost at least \$41/m^3 of saturated soil. This value is about 140 times higher than 10% desaturation of soil using biogas production in situ. Therefore, biocementation of soil to mitigate liquefaction could be too expensive to be applicable for large-scale geotechnical practice.

2.6.4 Calcium-phosphate biocementation

Calcium phosphate precipitation from calcium phytate (*myo*-inositol hexakisphosphate, calcium salt) solution (the main storage form of phosphorus in plant seeds) using the phytase activity of microorganisms (Roeselers and Van Loosdrecht, 2010) produces a mixture of the crystal forms such as monetite ($CaHPO_4$), whitlockite $Ca_9Mg(PO_4)_6(HPO_4)$, and hydroxyapatite ($Ca_5(PO_4)_3OH$) with the Ca-to-P molar ratio 1.55. The problem of this type of biocementation is the low solubility of calcium phytate (in the described study the concentration was 5.6 mM), so large volumes of solution must be pumped through the soil.

2.6.5 Calcium bicarbonate biocementation

Important biocementation technology could be the precipitation of calcite using the removal of CO_2 from solution of calcium bicarbonate (Ehrlich, 1999):

$$Ca(HCO_3)_2 \rightarrow CaCO_3\downarrow + CO_2 + H_2O \tag{2.4}$$

The solubility of calcium bicarbonate is relatively high, about 1 M, to perform practically feasible bioclogging and biocementation. However, production of calcium bicarbonate by dissolution of calcium carbonate during the treatment with CO_2 gives only low-concentration solution, about 10 mM, due to increase of pH that inhibits dissolution of calcium carbonate:

$$CaCO_3 + H_2CO_3 \leftrightarrow Ca(HCO_3)_2 \leftrightarrow Ca^{2+} + 2\,CO_2 + 2\,OH^- \tag{2.5}$$

Low concentration of calcium bicarbonate is not an obstacle for the bioclogging/biosealing of the rocks with fine fissures but biocementation of sand and the rocks with thick fissures has to be performed at higher concentration of calcium bicarbonate. The rate of precipitation of calcium carbonate from calcium bicarbonate in nature is determined by the removal rate of CO_2 from the reaction 2.4. The problem of bicarbonate biocement is its instability, so the solution must be produced and stored at elevated pressure of CO_2.

2.6.6 Iron-based bioclogging and biocementation

Iron-based biocementation could be performed with soluble chelates of ferrous or ferric iron precipitating to ferrous/ferric hydroxides:

$$\begin{aligned} &Fe^{2+} + 1.5\,(NH_2)_2CO + 0.25\,O_2 + 5.5\,H_2O + UPB \rightarrow \\ &\quad Fe(OH)_3\downarrow + 1.5\,(NH_4)_2CO_3 + 2\,H^+ \end{aligned} \tag{2.6}$$

UPB and urea are used to maintain the pH above the neutral value because the oxidation of ferrous ions and the hydrolysis of ferric ions are accompanied by acidification of the solution. The advantages of using iron hydroxide as the clogging compound are that the soil treated by iron minerals is more ductile and able to resist low pH conditions. The soil treated using iron-based biocement is not as strong as that treated using calcium-based biocement (Ivanov et al., 2014a), but the clogging effect of precipitated iron hydroxide is higher than that of calcium carbonate.

2.7 Conclusions

Construction biotechnologies are based on the activity of urease-producing, acidogenic, halophilic, alkaliphilic, denitrifying, iron- and sulfate-reducing bacteria, cyanobacteria, algae, and microscopic fungi. The biorelated materials and processes can be used for particle aggregation, soil grouting and clogging, cementation of particles, desaturation of soil, encapsulation of soft clay, and coating of solid surfaces. The construction biotechnologies have many advantages in comparison with conventional construction processes, so practical implementations of construction biotechnologies could give significant economic and environmental benefits.

References

Achal, V., Mukherjee, A., Reddy, M.S., 2010. Microbial concrete: way to enhance the durability of building structures. Journal of Materials in Civil Engineering 23, 730−734.

Achal, V., Mukherjee, A., Reddy, M.S., 2011. Effect of calcifying bacteria on permeation properties of concrete structures. Journal of Industrial Microbiology and Biotechnology 38, 1229−1234.

Babenko, V.F., Golubera, L.A., Pirog, T.P., Grinberg, T.A., Barkov, A.V., Vinokurov, V.A., 2008. Microorganism Strain *Paracoccus denitrificans* as Producer of Exopolysaccharide. Patent of Russia 2322493.

Bajpai, P.K., Meena, D., Vatsa, S., Singh, I., 2013. Tensile behavior of nettle fiber composites exposed to various environments. Jounal of Natural Fibers 10, 244−256.

Balaguru, P., 1994. Contribution of fibers to crack reduction of cement composites during the initial and final settling period. ACI Material Journal 91, 280−288.

Bang, S., Min, S.H., Bang, S.S., 2011. Application of microbiologically induced soil stabilization technique for dust suppression. International Journal of Geo-Engineering 3, 27−37.

Bertin, L., Colao, M.C., Ruzzi, M., Marchetti, L., Fava, F., 2006. Performances and microbial features of an aerobic packed-bed biofilm reactor developed to post-treat an olive mill effluent from an anaerobic GAC reactor. Microbial Cell Factories 5, 16.

Braunegg, G., Lefebvre, G., Genser, K.F., 1998. Polyhydroxyalkanoates, biopolyesters from renewable resources: physiological and engineering aspects. Journal of Biotechnology 65, 127−161.

Castegnier, F., Ross, N., Chapuis, R.P., Deschenes, L., Samson, R., 2006. Long-term persistence of a nutrient-starved biofilm in a limestone fracture. Water Research 40, 925−934.

Castilho, L.R., Mitchell, D.A., Freire, D.M.G., 2009. Production of polyhydroxyalkanoates (PHAs) from waste materials and by-products by submerged and solid-state fermentation. Bioresource Technology 100, 5996−6009.

Charbonneau, A., Novakowski, K., Ross, N., 2006. The effect of a biofilm on solute diffusion in fractured porous media. Journal of Contaminant Hydrology 85, 212−228.

Cheng, L., Cord-Ruwisch, R., 2012. In situ soil cementation with ureolytic bacteria by surface percolation. Ecological Engineering 42, 64−72.

Cheng, L., Cord-Ruwisch, R., Shahin, M.A., 2013. Cementation of sand soil by microbially induced calcite precipitation at various degrees of saturation. Canadian Geotechnical Journal 50, 1−10.

Chu, J., Ivanov, V., Jia, H., Chenghong, G., Naeimi, M., Tkalich, P., 2009. Microbial geotechnical engineering for disaster mitigation and coastal management. In: Proceedings of WCCE − ECCE − TCCE Joint Conference: Earthquake and Tsunami, Istanbul, Turkey.

Chu, J., Stabnikov, V., Ivanov, V., 2012. Microbially induced calcium carbonate precipitation on surface or in the bulk of soil. Geomicrobiology Journal 29, 1−6.

Chu, J., Ivanov, V., Stabnikov, V., 2013a. Microbial method for construction of aquaculture pond in sand. Géotechnique 63, 871−875.

Chu, J., He, J., Ivanov, V., 2013b. Mitigation of liquefaction of saturated sand using biogas. Géotechnique 63, 267−275.

Cuthbert, M.O., McMillan, L.A., Handley-Sidhu, S., Riley, M.S., Tobler, D.J., Phoenix, V.R., 2013. A field and modeling study of fractured rock permeability reduction using microbially induced calcite precipitation. Environmental Science and Technology 47, 13637−13643.

Daniel, D.E., Benson, C.H., 1990. Water content-density criteria for compacted soil liners. Journal of Geotechnical Engineering 116, 1811−1830.

Dennis, M., Turner, J., 1998. Hydraulic conductivity of compacted soil treated with biofilm. Journal of Geotechnical and Geoenvironmental Engineering 124, 120−127.

DeJong, J., Fritzges, M., Nusstein, K., 2006. Microbially induced cementation to control sand response to undrained shear. Journal of Geotechnical and Geoenvironmental Engineering 32, 1381−1392.

DeJong, J.T., Mortensen, B.M., Martinez, B.C., Nelson, D.C., 2010. Bio-mediated soil improvement. Ecological Engineering 36, 197−210.

DeJong, J.T., Soga, K., Kavazanjian, E., et al., 2013. Biogeochemical processes and geotechnical applications: progress, opportunities and challenges. Géotechnique 63, 287−301.

DeMarco, S., 2005. Advances in polyhydroxyalkanoate production in bacteria for biodegradable plastics. Basic Biotechnology eJournal 1, 1−4.

De Muynck, W., Cox, K., Verstraete, W., De Belie, N., 2008a. Bacterial carbonate precipitation as an alternative surface treatment for concrete. Construction and Building Materials 22, 875−885.

De Muynck, W.D., Debrouwer, D., De Belie, N.D., Verstraete, W., 2008b. Bacterial carbonate precipitation improves the durability of cementitious materials. Cement and Concrete Research 38, 1005−1014.

De Muynck, W., De Belie, N., Verstraete, W., 2010. Microbial carbonate precipitation in construction materials: a review. Ecological Engineering 36, 118−136.

Dhami, N.K., Reddy, M.S., Mukherjee, A., 2012. Improvement in strength properties of ash bricks by bacterial calcite. Ecological Engineering 39, 31−35.

Dosier, G.K., 2013. Methods for Making Construction Material Using Enzyme Producing Bacteria. US Patent App. 13/093,335, 2011.

Ebnesajjad, S. (Ed.), 2012. Handbook of Biopolymers and Biodegradable Plastics: Properties, Processing and Applications. Elsevier, 447 pp.

Ehrlich, H.L., 1999. Microbes as geologic agents: their role in mineral formation. Geomicrobiology Journal 16, 135−153.

Eseller-Bayat, E., Yegian, M.K., Alshawabkeh, A., Gokyer, S., 2012. Prevention of liquefaction during earthquakes through induced partial saturation in sands. In: Geotechnical Engineering: New Horizons. IOS Press, Amsterdam, pp. 188−194.

Faludi, G., Dora, G., Renner, K., Móczó, J., Pukánszky, B., 2013. Biocomposite from polylactic acid and lignocellulosic fibers: structure−property correlations. Carbohydrate Polymers 92, 1767−1775.

Fernandes, P., 2006. Applied microbiology and biotechnology in the conservation of stone culture heritage materials. Applied Microbiology and Biotechnology 73, 291−296.

Flemming, H.C., Neu, T.R., Wozniak, D.J., 2007. The EPS matrix: the “house of biofilm cells”. Journal of Bacteriology 189, 7945−7947.

Fujita, F., Redden, G.D., Ingram, J.C., Cortez, M.M., Ferris, F.G., Smith, R.W., 2004. Strontium incorporation into calcite generated by bacterial ureolysis. Geochimica et Cosmochimica Acta 68, 3261−3270.

Fytili, D., Zabaniotou, A., 2008. Utilization of sewage sludge in EU application of old and new methods—a review. Renewable and Sustainable Energy Reviews 12, 116−140.

Ghosh, P., Mandal, S., Chattopadhyay, B.D., Pal, S., 2005. Use of microorganism to improve the strength of cement mortar. Cement and Concrete Research 35, 1980−1983.

Ghosh, S., Biswas, M., Chattopadhyay, B.D., Mandal, S., 2009. Microbial activity on the microstructure of bacteria modified mortar. Cement and Concrete Composites 31, 93−98.

Godinho, A.L., Bhosle, S., 2009. Sand aggregation by exopolysaccharide-producing *Microbacterium arborescens* AGSB. Current Microbiology 58, 616−621.

Hamdan, N., Kavazanjian, E., Rittman, B.E., Karatas, I., 2011. Carbonate mineral precipitation for soil improvement through microbial denitrification. In: Han, J., Alzamora, D.A. (Eds.), Geo-frontiers 2011: Advances in Geotechnical Engineering. American Society of Civil Engineers, Dallas.

Harkes, M.P., van Paassen, L.A., Booster, J.L., Whiffin, V.S., van Loosdrecht, M.C.M., 2010. Fixation and distribution of bacterial activity in sand to induce carbonate precipitation for ground reinforcement. Ecological Engineering 36, 112−117.

He, J., Chu, J., Ivanov, V., 2013. Mitigation of liquefaction of saturated sand using biogas. Géotechnique 63, 267−275.

Huda, M.S., Drzal, L.T., Mohanty, A.K., Misra, M., 2006. Chopped glass and recycled newspaper as reinforcement fibers in injection molded poly (lactic acid)(PLA) composites: a comparative study. Composites Science and Technology 66, 1813−1824.

Ivanov, V., Chu, J., 2008. Applications of microorganisms to geotechnical engineering for bioclogging and biocementation of soil in situ. Reviews in Environmental Science and Biotechnology 7, 139−153.

Ivanov, V., 2010. Environmental Microbiology for Engineers. CRC Press, Taylor & Francis Group, Boca Raton, 402 pp.

Ivanov, V., Stabnikov, V., Hung, Y.T., 2012. Screening and selection of microorganisms for the environmental biotechnology process. In: Hung, Y.-T., Wang, L.K., Shammas, N.K. (Eds.), Handbook of Environment and Waste Management. Air and Water Pollution Control. World Scientific Publishing Co., Inc., pp. 1137−1149.

Ivanov, V., Chu, J., Stabnikov, V., 2014a. Iron- and calcium-based biogrouts for porous soils. Proceedings of the ICE- Construction Materials 167, 36−41.

Ivanov, V., Chu, J., Stabnikov, V., Li, B., 2014b. Strengthening of soft marine clay using biocementation. Marine Georesources and Geotechnology 33, 320−324.

Jimenez-Lopez, C., Jroundi, F., Pascolini, C., Rodriguez-Navarro, C., Piñar-Larrubia, G., Rodriguez-Gallego, M., González-Muñoz, M.T., 2008. Consolidation of quarry calcarenite by calcium carbonate precipitation induced by bacteria activated among the microbiota inhabiting the stone. International Biodeterioration and Biodegradation 62, 352−363.

John, M.J., Thomas, S., 2008. Biofibres and biocomposites. Carbohydrate Polymer 71, 343−364.

Jonkers, H.M., 2007. Self healing concrete: a biological approach. In: van der Zwaag, S. (Ed.), Self Healing Materials. An Alternative Approach to 20 Centuries of Materials Science. Springer, pp. 195−204.

Jonkers, H.M., Thijssen, A., Muyzer, G., Copuroglu, O., Schlangen, E., 2010. Application of bacteria as self-healing agent for the development of sustainable concrete. Ecological Engineering 36, 230−235.

Kenyon, W.J., Esch, S.W., Buller, C.S., 2005. The curdlan-type exopolysaccharide produced by *Cellulomonas flavigena* KU forms part of an extracellular glycocalyx involved in cellulose degradation. Antonie Van Leeuwenhoek 87, 143−148.

Khanna, S., Srivastava, A.K., 2005. Recent advances in microbial polyhydroxyalkanoates. Process Biochemistry 40, 607−619.

Kim, G., Lee, S., Kim, Y., 2006. Subsurface biobarrier formation by microorganism injection for contaminant plume control. Journal of Bioscience and Bioengineering 101 (2), 142−148.

Ko, H.S., Kwon, J.H., Park, S.S., 2014. Flooring Material Using Poly Lactic Acid Resin and Construction Methods of the Same. US Patent 20140370225.

Koo, H., Xiao, J., Klein, M.I., Jeon, J.G., 2010. Exopolysaccharides produced by S*treptococcus mutans* glucosyltransferases modulate the establishment of microcolonies within multi-species biofilms. Journal of Bacteriology 192, 3024−3032.

Lee, Y.K., Kwon, K.K., Cho, K.H., Kim, H.W., Park, J.H., Lee, H.K., 2003. Culture and identification of bacteria from marine biofilms. The Journal of Microbiology 41, 183−188.

Lenz, R.W., Marchessault, R.H., 2005. Bacterial polyesters: biosynthesis, biodegradable plastics and biotechnology. Biomacromolecules 6, 1−8.

Leon-Martinez, F.M., de Cano-Barrita, P.F.J., Lagunez-Rivera, L., Medina-Torres, L., 2014. Study of nopal mucilage and marine brown algae extract as viscosity-enhancing admixtures for cement based materials. Construction and Building Materials 53, 190−202.

Li, P., Qu, W., 2012. Microbial carbonate mineralization as an improvement method for durability of concrete structures. Advanced Materials Research 365, 280−286.

Lowell, W.L., Rohwedder, W.K., 1974. Poly-beta-hydroxyalkanoate from activated sludge. Environmental Science and Technology 8, 576−579.

Maizatulnisa, O., Tan, K.H., Yusof, H.M., Halisanni, K., Ruzaidi, G., Nazarudin, Z.M., Paridah, T., Azlina, H.N., 2013. Effects of multi-walled carbon nanotubes (MWCNTS) on the mechanical and thermal properties of plasticized polylactic acid nanocomposites. Advanced Material Research 812, 181−186.

Mitchell, A.C., Ferris, F.G., 2005. The coprecipitation of Sr into calcite precipitates induced by bacterial ureolysis in artificial groundwater: temperature and kinetic dependence. Geochimica et Cosmochimica Acta 69, 4199−4210.

Mitchell, J.K., Santamarina, J.C., 2005. Biological considerations in geotechnical engineering. Journal of Geotechnical and Geoenvironmental Engineering ASCE 131, 1222−1233.

Montoya, B.M., DeJong, J.T., Boulanger, R.W., Wilson, D.W., Gerhard, R., Ganchenko, A., Chou, J.C., 2012. Liquefaction mitigation using microbial induced calcite precipitation. GeoCongress 1918−1927.

Mun, K.J., 2007. Development and tests of lightweight aggregate using sewage sludge for nonstructural concrete. Construction and Building Materials 21, 1583−1588.

Neef, A., Zaglauer, A., Meier, H., Amann, R., Lemmer, H., Schleifer, K.H., 1996. Population analysis in a denitrifying sand filter: conventional and *in situ* identification of *Paracoccus* spp. in methanol-fed biofilms. Applied and Environmental Microbiology 62, 4329−4339.

van Paassen, L., Ghose, R., van der Linden, T., van der Star, W., van Loosdrecht, M., 2010. Quantifying biomediated ground improvement by ureolysis: large-scale biogrout experiment. Journal of Geotechnical and Geoenvironmental Engineering 136, 1721−1728.

Pacheco-Torgal, F., Jalali, S., 2011. Nanotechnology: advantages and drawbacks in the field of construction and building materials. Construction and Building Materials 25, 582−590.

Pacheco-Torgal, F., Labrincha, J.A., 2013a. Biotech cementitious materials: some aspects of an innovative approach for concrete with enhanced durability. Construction and Building Materials 40, 1136−1141.

Pacheco-Torgal, F., Labrincha, J.A., 2013b. Biotechnologies and bioinspired materials for the construction industry: an overview. International Journal of Sustainable Engineering 7, 235−244.

Pacheco-Torgal, F., Jalali, S., 2013. Eco-efficient Construction and Building Materials. Springer, London, 247 pp.

Pei, R., Liu, J., Wang, S., Yang, M., 2013. Use of bacterial cell walls to improve the mechanical performance of concrete. Cement and Concrete Composites 39, 122−130.

Plank, J., 2003. Applications of biopolymers in construction engineering. In: Steinbüchel, A. (Ed.), Biopolymers, General Aspects and Special Applications, vol. 10. Wiley-VCH Verlag GmbH, Weinheim.

Plank, J., 2004. Application of biopolymers and other biotechnological products in building material. Applied Microbiology and Biotechnology 66, 1−9.

Portilho, M., Matioli, G., Zanin, G.M., de Moraes, F.F., Scamparini, A.R., 2006. Production of insoluble exopolysaccharide *Agrobacterium sp*. (ATCC 31749 and IFO 13140). Applied Biochemistry and Biotechnology 129−132, 864−869.

Ramachandran, S.K., Ramakrishnan, V., Bang, S.S., 2001. Remediation of concrete using microorganisms. ACI Materials Journal 98, 3−9.

Ramesh, B.N.G., Anitha, N., Rani, H.K.R., 2010. Recent trends in biodegradable products from biopolymers. Advanced Biotechnology 9, 30−34.

Raut, S.H., Sarode, D.D., Lele, S.S., 2014. Biocalcification using *B. pasteurii* for strengthening brick masonry civil engineering structures. World Journal of Microbiology and Biotechnology 30, 191−200.

Ray, S.S., 2012. Polylactide-based bionanocomposites: a promising class of hybrid materials. Accounts of Chemical Research 45, 1710−1720.

Rebata-Landa, V., Santamarina, J.C., 2012. Mechanical effects of biogenic nitrogen gas bubbles in soils. Journal of Geotechnical and Geoenvironmental Engineering 138, 128−137.

Rezic, T., Santek, B., Novak, S., Maric, V., 2006. Comparison between the heterotrophic cultivation of *Paracoccus denitrificans* in continuous stirred tank reactor and horizontal rotating tubular bioreactor. Process Biochemistry 41, 2024−2028.

Rodriguez-Navarro, C., Rodriguez-Gallego, M., Ben Chekroun, K., Gonzalez-Muñoz, M.T., 2003. Conservation of ornamental stone by *Myxococcus xanthus*-induced carbonate biomineralization. Applied and Environmental Microbiology 69, 2182−2193.

Roeselers, G., Van Loosdrecht, M.C.M., 2010. Microbial phytase-induced calcium-phosphate precipitation − a potential soil stabilization method. Folia Microbiologica 55, 621−624.

Ross, N., Villemur, R., Deschenes, L., Samson, R., 2001. Clogging of limestone fracture by stimulating groundwater microbes. Water Research 35, 2029−2037.

Ross, N., Bickerton, G., 2002. Application of biobarriers for groundwater containment at fractured bedrock sites. Remediation Journal 12, 5−21.

van der Ruyt, M., van der Zon, W., 2009. Biological in situ reinforcement of sand in near-shore areas. Geotechnical Engineering 162, 81−83.

Saba, N., Paridah, M.T., Jawaid, M., 2015. Mechanical properties of kenaf fibre reinforced polymer composite: a review. Construction and Building Materials 76, 87−96.

Sarda, D., Choonia, H.S., Sarode, D.D., Lele, S.S., 2009. Biocalcification by *Bacillus pasteurii* urease: a novel application. Journal of Industrial Microbiology and Biotechnology 36, 1111−1115.

Sathya, A., Bhuvaneshwari, P., Niranjan, G., Vishveswaran, M., 2013. Influence of bioadmixture on mechanical properties of cement and concrete. Asian Journal of Applied Sciences 7, 205−214.

Seifert, D., Engesgaard, P., 2007. Use of tracer tests to investigate changes in flow and transport properties due to bioclogging of porous media. Journal of Contaminant Hydrology 93, 58−71.

Seifert, D., Engesgaard, P., 2012. Sand box experiments with bioclogging of porous media: hydraulic conductivity reductions. Journal of Contaminant Hydrology 136−137, 1−9.

Seki, K., Miyazaki, T., Nakano, M., 1998. Effects of microorganisms on hydraulic conductivity decrease in infiltration. European Journal of Soil Science 49, 231−236.

Siddique, R., Chahal, N.K., 2011. Effect of ureolytic bacteria on concrete properties. Construction and Building Materials 25, 3791−3801.

Sin, L.T., Rahmat, A.R., Rahman, W.A., 2012. Polylactic Acid: PLA Biopolymer Technology and Applications. Elsevier, 329 pp.

Stabnikov, V., Chu, J., Naeimi, M., Ivanov, V., 2011. Formation of water-impermeable crust on sand surface using biocement. Cement and Concrete Research 41, 1143−1149.

Stabnikov, V., Chu, J., Myo, A.N., Ivanov, V., 2013a. Immobilization of sand dust and associated pollutants using bioaggregation. Water, Air, and Soil Pollution 224, 1631−1700.

Stabnikov, V., Chu, J., Ivanov, V., Li, Y., 2013b. Halotolerant, alkaliphilic urease-producing bacteria from different climate zones and their application for biocementation of sand. World Journal of Microbiology and Biotechnology 29, 1453−1460.

Stewart, T.L., Fogler, H.S., 2001. Biomass plug development and propagation in porous media. Biotechnology and Bioengineering 72, 353−363.

Subramaniam, K., Gandhimathi, R., Kasinathan, M., 2014. Bioclogging in porous media: influence in reduction of hydraulic conductivity and organic contaminants during synthetic leachate permeation. Journal of Environmental Health Science and Engineering 12, 126.

Sudesh, K., Abe, H., Doi, Y., 2000. Synthesis, structure and properties of polyhydroxyalkanoates: biological polyesters. Progress in Polymer Science 25, 1503−1555.

Suchomel, F., Marsche, M., 2013. TENCEL®—a high-performance sustainable cellulose fiber for the construction industry/composites. Journal of Chemical Engineering 7, 626−632.

Sudesh, K., Abe, H., 2010. Practical Guide to Microbial Polyhydroxyalkanoates. Smithers Rapra Technology, 160 pp.

Tokiwa, Y., Tsuchiya, A., 2003. Biodegradable Resin Compositions. US Patent 666977.

Tsang, P.H., Li, G., Brun, Y.V., Freund, L.B., Tang, J.X., 2006. Adhesion of single bacterial cells in the micronewton range. Proceeding of the National Academy of Sciences USA 103, 11435−11436.

Vandevivere, P., Baveye, P., 1992a. Relationship between transport of bacteria and their clogging efficiency in sand columns. Applied and Environmental Microbiology 58, 2523−2530.

Vandevivere, P., Baveye, P., 1992b. Effect of bacterial extracellular polymers on the saturated hydraulic conductivity of sand columns. Applied and Environmental Microbiology 58, 1690−1698.

Vandevivere, P., Baveye, P., 1992c. Saturated hydraulic conductivity reduction caused by aerobic bacteria in sand columns. Soil Science Society of America 56, 1−13.

Van Tittelboom, K., De Belie, N., De Muynck, W., Verstraete, W., 2010. Use of bacteria to repair cracks in concrete. Cement and Concrete Research 40, 157−166.

Vempada, S.R., Reddy, S.S.P., Rao, M.V.S., Sasikala, C., 2011. Strength enhancement of cement mortar using microorganisms − an experimental study. International Journal of Earth Sciences and Engineering 4, 933−936.

Volova, T.G., 2004. Polyhydroxyalkanoates − Plastic Materials of the 21st Century. Nova Publishers, 282 pp.

Wang K., Ivanov V., Cao J., 2012. Effect of Biopolymers on Cementation Process, unpublished data.

Warren, L.A., Maurice, P.A., Parmar, N., Ferris, F.G., 2001. Microbially mediated calcium carbonate precipitation: implications for interpreting calcite precipitation and for solid-phase capture of inorganic contaminants. Geomicrobiology Journal 18, 93−115.

Webster, A., May, E., 2006. Bioremediation of weathered-building stone surfaces. Trends in Biotechnology 24, 255−260.

Weil, M.H., DeJong, J.T., Martinez, B.C., Mortensen, B.M., Waller, J.T., 2012. Seismic and resistivity measurements for real-time monitoring of microbially induced calcite precipitation in sand. ASTM Geotechnical Testing Journal 35, 330−341.

Whiffin, V.S., van Paassen, L.A., Harkes, M.P., 2007. Microbial carbonate precipitation as a soil improvement technique. Geomicrobiology Journal 24, 417−423.

Wiktor, V., Jonkers, H., 2011. Quantification of crack-healing in novel bacteria-based self-healing concrete. Cement and Concrete Composition 33, 763−770.

Willke, T., Vorlop, K.D., 2004. Industrial bioconversion of renewable resources as an alternative to conventional chemistry. Applied Microbiology and Biotechnology 66, 131−142.

Wright, D.T., Oren, A., 2005. Nonphotosynthetic bacteria and the formation of carbonates and evaporites through time. Geomicrobiology Journal 22, 27−53.

Wu, J., Gui, S., Stahl, P., Zhang, R., 1997. Experimental study on the reduction of soil hydraulic conductivity by enhanced biomass growth. Soil Science 162, 741−748.

Xia, H., Hu, T., 1991. Effects of saturation and back pressure on sand liquefaction. Journal of Geotechnical Engineering 117, 1347−1362.

Yang, I.C., Li, Y., Park, J.K., Yen, T.F., 1993. Subsurface application of slime-forming bacteria in soil matrices. In: Proceedings of the 2nd International Symposium *In Situ* and On Site Bioreclamation, San Diego, CA, Lewis Publishers, Boca Raton, FL.

Yang, J., Savidis, S., Roemer, M., 2004. Evaluating liquefaction strength of partially saturated sand. Journal of Geotechnical and Geoenvironmental Engineering 130, 975−979.

Yegian, M., Eseller-Bayat, E., Alshawabkeh, A., Ali, S., 2007. Induced-partial saturation for liquefaction mitigation: experimental investigation. Journal of Geotechnical and Geoenvironmental Engineering 133, 372−380.

Yuan, F., Xiao, H., Wu, J., Ying, W.F., Yu, Y.P., Chi, H.X., 2013. Effect of carboxylmethyl cellulose sulfate (CMC-S) on the hydration process of cement paste. Advanced Materials Research 838−841, 123−126.

Zeiml, M., Leithner, D., Lackner, R., Mang, H.A., 2006. How do polypropylene fibers improve the spalling behavior of in-situ concrete? Cement and Concrete Research 36, 929−942.

Biotechnological production of biopolymers and admixtures for eco-efficient construction materials

3

V. Stabnikov[1,2], *V. Ivanov*[1]
[1]Nanyang Technological University, Singapore; [2]National University of Food Technologies, Kiev, Ukraine

3.1 Biotechnology for the production of construction materials

Any biotechnology for the production of construction materials includes three major stages:

1. upstream processes such as preparation of medium, equipment, and microbial inoculum (seeds);
2. core processes such as cultivation of microorganisms;
3. downstream processes such as concentration of biomass or microbial product, its drying, packing, washing of equipment, and treatment or disposal of production wastes.

The example can be the biotechnology for the production of calcium- and urea-based biocement (Figure 3.1).

The medium for microbial cultivation is a solution of chemical reagents. Different kinds of wastes, such as mining and agricultural residuals, organic fraction of municipal solid wastes, sewage sludge, and reject water of municipal wastewater treatment plants altogether with agricultural fertilizers can be used as media to reduce the cost of large-scale production because of low requirements for the purity of the product.

The microorganisms that are used to start up the bioprocess are called inoculum by microbiologists or "seeds" by civil and environmental engineers. The inoculum could be a suspended, frozen, dried, or cooled microbial biomass. Cultivation after inoculation is performed in both batch and continuous modes of operation.

Inoculum for production of construction materials or biotreatment of soil/particles is selected using the following methods:

1. Obtaining and testing of the microbial strain from the national collection of microorganisms, for example, American Type Culture Collection (ATCC, USA), or German Collection of Microorganisms and Cell Cultures (DSMZ, Germany).
2. Isolation, identification, biosafety, and application testing of wild strains from natural sites with environmental conditions close to the conditions that are needed for biotreatment, for example, with high salinity, high or low temperature, aerobic or anaerobic conditions, and

Biopolymers and Biotech Admixtures for Eco-Efficient Construction Materials. http://dx.doi.org/10.1016/B978-0-08-100214-8.00003-8
Copyright © 2016 Elsevier Ltd. All rights reserved.

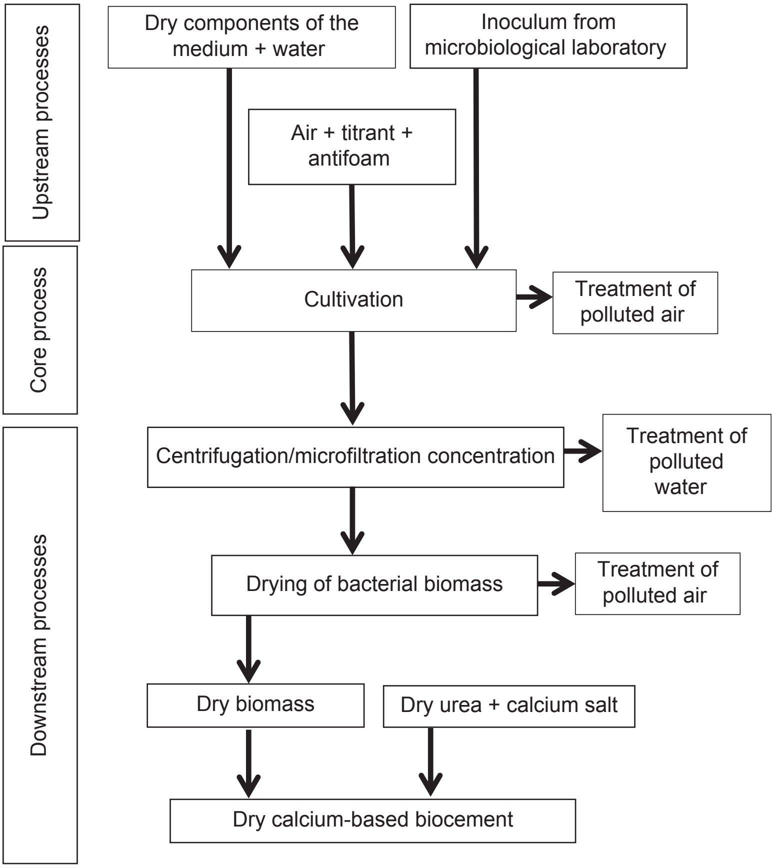

Figure 3.1 Biotechnology for the production of calcium- and urea-based biocement.

alkaline or acid pH. However, many bacteria are pathogenic (causing diseases) for humans, animals, and plants. Therefore, biosafety of biotechnological process is always an important issue, and only nonpathogenic isolated strains of bacteria can be used for civil engineering applications. Preliminary evaluation of the biosafety of an isolated strain can be done using identification data and scientific information about the biosafety of the identified species. However, a conclusion on the biosafety of the isolated strain can be done only after direct biomedical tests.

3. Autoselection in continuous culture (Cheng and Cord-Ruwisch, 2013), screening of mutants (Li et al., 2011), and construction of recombinant microbial strains from wild strains for biotreatment. However, there are many restrictions on the applications of recombinant microbial strains, so they can be used mainly for industrial production of such construction materials as polysaccharides or bioplastics.
4. Selection and testing of suspended-enrichment cultures using such selective conditions (selection pressure) as source of energy, carbon, nitrogen, and phosphorus, temperature, pH, salinity (osmotic pressure), concentration of heavy metals, concentration of dissolved oxygen, and spectrum and intensity of light (for photosynthetic microorganisms). Some

autoselected features of the enrichment culture can be genetically unstable and could disappear after several generations when the selection pressure will be absent (Ivanov et al., 2012).

5. Selection and testing of aggregated enrichment cultures, such as flocs, biofilms, and granules using such selective pressure as the settling rate of microbial aggregates and the adhesion of cells to solid surfaces. An example is the formation of bacterial cell aggregates that cannot penetrate inside sand layer, but settle onto the surface of sand, and form a calcite crust (Stabnikov et al., 2011; Chu et al., 2012).
6. In some cases, when soil is rich with indigenous microorganisms that are able to perform needed biogeochemical reactions, for example, bacteria with urease activity, soil biotreatment can be performed by indigenous microorganisms without preparation and supply of microbial inoculum (Burbank et al., 2011). To enhance the needed biogeochemical function of indigenous microorganisms, the related reagent can be introduced into soil. For example, to enhance the urease activity of indigenous microorganisms before the biotreatment, urea can be added to soil (Burbank et al., 2011). However, if microorganisms used in a geotechnical bioprocess are indigenous, it does not mean that they are safe for humans, animals, and plants, because the nonselective conditions of the soil bioprocesses, especially application of a nutrient-rich medium, can enhance the proliferation of pathogens or opportunistic pathogens in soil.

Most microorganisms applicable for Construction Microbial Biotechnology among the kingdoms of *Archaea*, *Bacteria*, and *Fungi*, *Plants*, and *Animals* are representatives of *Bacteria* for the following reasons:

1. small cell size (0.5—10 μm), enabling deep penetration into porous soil or fissured rock;
2. wide physiological diversity, for example, there are microorganisms with optimum pH in the range from 2 to 10 and optimum temperature in the range from −10 to +110 °C;
3. wide spectrum of biogeochemical reactions of oxidation—reduction with such electron donors as organic compounds and reduced inorganic compounds and such electron acceptors as oxygen, nitrate, ferric ions, and sulfate;
4. highest growth and metabolic rates among all other organisms. Generation time (time between cell divisions for binary fissured bacterial cells) can be as low as 20 min, whereas for macroorganisms it can be several years.

There are three evolutionary lines of chemotrophic (feeding by energy of chemical compounds): Gram-positive *Bacteria* (prokaryotes of terrestrial evolutionary origin with thick and rigid cell wall), Gram-negative *Bacteria* (prokaryotes of aquatic evolutionary origin with thin and elastic cell wall), and *Archaea* (prokaryotes of environments with extreme temperature, pH, or strong anaerobic conditions).

These three evolutionary lines contain four parallel physiological groups differentiated by the type of energy-yielding oxidation—reduction reactions: (1) fermenting, (2) anoxic-respiring, (3) microaerophilic and facultative anaerobic; (4) aerobic-respiring prokaryotes. In total, 12 groups of chemotrophic prokaryotes exist differentiated by the type of energy-yielding oxidation—reduction reactions (Table 3.1).

Depending on the real conditions and requirements of the construction biotechnology process, all these physiological groups can be involved in biotechnologies of construction materials or construction process biotechnologies. However, in the majority of the cases anaerobic, anoxic, facultative anaerobic/aerobic, and aerobic Gram-positive bacteria are most suitable for applications related to soil improvement

Table 3.1 Physiological groups of chemotrophic prokaryotes

Evolutionary lines of prokaryotes	Physiological groups of chemotrophic prokaryotes			
	Fermenting prokaryotes	**Anaerobically-respiring prokaryotes**	**Microaerophilic and facultative anaerobic prokaryotes**	**Aerobically respiring prokaryotes**
Gram-negative *Bacteria* (prokaryotes of aquatic evolutionary origin)	1	2	3	4
Gram-positive *Bacteria* (prokaryotes of terrestrial evolutionary origin)	5	6	7	8
Archaea (prokaryotes of extreme environments origin)	9	10	11	12

Note: Conventional number of physiological group is shown in the table cell.

because of their sustainability at high osmotic pressure of the environment and the tolerance of the cells for drying. Facultative anaerobic or aerobic Gram-negative bacteria are most suitable for industrial biosynthesis of construction biomaterials under constant and not high osmotic pressure. Applications of phototrophic (utilizing light energy) prokaryotes in civil engineering are rare. For example, the groups of Gram-negative phototrophic cyanobacteria and phototrophic microscopic algae can be used for the formation of soil crust to diminish water and wind erosion of sandy soil as well as to reduce seepage from shallow-drainage open channels and ponds. In the last case, biocementation of the bottom and slopes can be combined with the biocoating by the biofilm of cyanobacteria or algae (Figure 3.2).

Core process in the production of construction material using cultivation of microorganisms in batch, semicontinuous (sequencing batch), complete mixing continuous, or plug flow continuous mode in the bioreactor, in which the components are mixed using stirring, upflow of liquid or gas through the bioreactor, or by the horizontal rotation of the bioreactor.

Every biotechnology includes such a downstream step as the treatment of polluted air and water after biosynthesis of microbial biomass or related product.

Biotechnologies of ground improvement or surface treatment include the same upstream, core, and downstream steps, but some of these processes perform:

1. non-aseptically, i.e., without any sterilization and other measures preventing infection of material or environment;
2. using cheap media or even waste material;
3. using enrichment microbial culture or indigenous microorganisms;
4. without automatic control and comprehensive monitoring;
5. sometimes, the process operates without treatment of the secondary wastes.

In the case of on-site or off-site soil treatment, the upstream step can include the following operations: (1) crushing, grinding, sieving, homogenization of treated

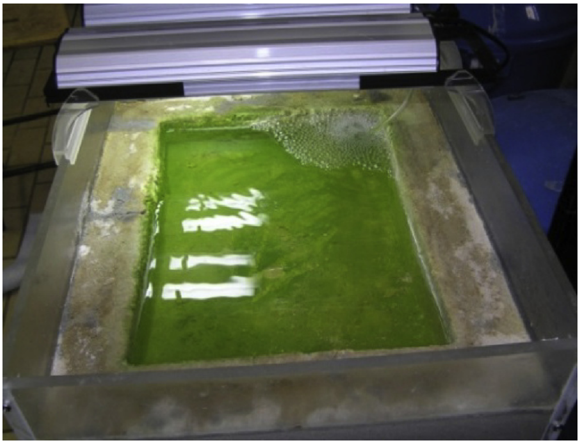

Figure 3.2 Experimental model pond made using biocementation, bioclogging, and biocoating with algae biofilm.

soil, solid particles, or soft clay; (2) chemical pretreatment of soil or particles with alkali, acids, salt solution, or surfactants; and (3) excavation, transportation, storage, and supply of soil or particles in the bioreactor in the case of the off-site biotreatment.

The medium components for ground bioimprovement (biogrout or biocement) or surface coating (biocoating composition) can be mixed together or used separately in the form of solution, suspension, or slurry by the mixing of chemical reagents and agricultural fertilizers, different kinds of wastes, or residuals. These wastes can include mining and agricultural residuals, organic fraction of municipal solid wastes, sewage sludge and reject water of municipal wastewater treatment plants. They can be used as a medium to reduce the cost of large-scale biogeotechnical work.

3.2 Biotechnological production of bioplastics for construction

The use of biodegradable bioplastics in construction industry can reduce:

1. the cost of excavation of temporary constructions because many biodegradable constructions can be left in the soil;
2. the disposal cost of the construction wastes;
3. the consumption of nonrenewable sources, thus increasing environmental and economic sustainability.

Meanwhile, the cost of bioplastics produced aseptically in fermenters is usually several times higher than the cost of petrochemical-based plastics, so the reduction of the bioplastic production costs using cheap raw materials and technological innovations is still essential for the bioplastic industry and applications. Most available types of bioplastics for construction industry are polyhydroxyalkanoates (PHAs), which are polyesters that are accumulated up to 80% of dry bacterial biomass as a storage compound. Accumulated PHAs can be extracted from bacterial biomass, and can be used in practice as bioplastic (Lowell and Rohwedder, 1974; Braunegg et al., 1998; Sudesh et al., 2000; Volova, 2004; DeMarco, 2005; Khanna and Srivastava, 2005; Lenz and Marchessault, 2005; Castilho et al., 2009; Sudesh and Abe, 2010).

The following options for raw materials, biotechnology of production, and applications of bioplastic can help to diminish the cost of the bioplastic PHAs.

1. Use of cheap raw materials (Serafim et al., 2008) such as organic fraction of municipal solid wastes, liquid wastes of municipal wastewater treatment plants, food processing waste, or agricultural wastes such as unbaled straw; corn cobs, stalks, and leaves (corn stover); silage effluent; horticulture residuals; farm yard manure; coconut fronds; husks and shells; coffee hulls and husks; cotton (stalks); nut shells; rice hull, husk, straw, and stalks; and sugarcane bagasse. Globally, 140×10^9 metric tons of biomass are generated annually from agriculture, which is equivalent to approximately 50 billion tons of oil. Therefore, biomass wastes have attractive potentials for large-scale industries and community-level enterprises (United Nations Environment Program (UNEP), 2009).
2. Batch or continuous nonaseptic cultivation for biosynthesis of bioplastic by mixed bacterial culture (Yu et al., 1999; Lu, 2007).

3. Production of crude bioplastic for the construction industry and agriculture avoiding extraction of bioplastic using chemical treatment, filtration, centrifugation, or flotation.

For the biosynthesis of PHAs under nonaseptic conditions, organic wastes can be converted to organic acids through acidogenic fermentation of organics, and then organic acids can be converted to PHAs (Yu, 2006). Most-typical material balance of acidogenic fermentation is as follows (Madigan et al., 2012):

$$\begin{aligned} C_6H_{12}O_6 + 0.82\,H_2O \rightarrow\ & 1.13\,CH_3COOH + 0.35\,C_2H_5COOH + \\ & 0.26\,C_3H_7COOH + 1.67\,CO_2 + 2.47\,H_2 \end{aligned} \tag{3.1}$$

in which $C_6H_{12}O_6$ is a monomer of cellulose, CH_3COOH, C_2H_5COOH, and C_3H_7COOH are acetic, propionic, and butyric acids, respectively.

The pH of this process must be controlled by titrant or addition of protein-containing waste because the pH drops below 5.5 during acidogenic fermentation of carbohydrate-rich wastes (Barlaz et al., 2010); meanwhile, the optimal pH for acidogens is above 6.0 (Moosbrugger et al., 1993).

The batch biosynthesis of bioplastic is simpler but less productive than the continuous process, in which productivity can be about 1 kg of PHAs/day·m^3 of the bioreactor (Ben Rebah et al., 2009). Production of PHAs can be done as semi-continuous cultivation of a mixed culture using a feast—famine cycle comprising a feast phase and a famine phase in one bioreactor. This cycling process promotes not only accumulation of PHAs in biomass but also selection of PHA-producing microorganisms (Beun et al., 2006; van Loosdrecht et al., 1997, 2008).

All known methods of PHA extraction suffer from high cost and/or environmental pollution. Therefore, crude bioplastic produced without extraction of PHAs from microbial biomass could be used for construction applications. The major advantage of PHAs for construction applications is biodegradability of bioplastic to carbon dioxide and water for about 1.5 months in anaerobic sewage, 1.5 years in soil, and 6.5 years in seawater (Mergaert et al., 1992; Reddy et al., 2003; Castilho et al., 2009). Dead bacterial biomass with PHAs contains also polysaccharides of cell wall, proteins, polynucleotides, and phospholipids, which content is about 15, 50, 25, and 10%, respectively, of dry biomass without PHAs, and biodegradation rate is higher than that of PHAs. Therefore, from the point of view of biodegradability there is no need to extract PHAs from biomass but to use dry biomass with PHAs as a crude nanocomposite material for construction purposes. Such nanocomposites should be more flexible and more quickly biodegradable than extracted PHAs. Sustainability of this biodegradable construction material is due to: (1) production of bioplastic from renewable sources or even from organic wastes, and (2) fast biodegradability of this material under the conditions of landfill or composting, so the negative effects of construction waste on the environment will be minimized.

One area of application of such nanocomposite bioplastic from bacterial biomass containing PHAs is the production and use of biodegradable construction materials, which do not require removal and incineration after temporary application. Biodegradable bioplastic foam could be used for insulation walls and partitions, construction of nonstructural (internal) elements such as separating walls and partitions, and for the temporary construction that can be landfilled for fast degradation. Other examples of potential application of crude nanocomposite from bacterial biomass and PHAs are construction silts and dust fences that can be landfilled for fast biodegradation or composted as biomass. Biodegradable plastics could be also useful for vertical drains, geotextile, geomembranes, and soil stabilization mats. These materials are used temporarily for soft-soil stabilization, filtration, and drainage (Ogbobe et al., 1998), so biodegradability of the material can eliminate the cost of extraction and disposal of the temporary objects.

Biodegradable bioplastic polylactic acid/poly-L-lactic (PLA or PLLA) is produced by chemical polymerization of lactic acid that is synthesized by anaerobic lactic acid bacteria from any source of saccharides, for example, from starch of corn or potato, or lactose of whey, or sucrose of the sugar beet or cane. This combined bio- and chemical technology produces a pure bioplastic, which is a relatively expensive material that can be applied in the construction industry only in special cases, for example, reinforcing fibers, nanocomposites, or biodegradable-resin compositions (Tokiwa and Tsuchiya, 2003; Huda et al., 2006; John and Thomas, 2008; Bajpai et al., 2013; Faludi et al., 2013; Saba et al., 2015). The price for PLA in 2009 was about 1.9 Euro/kg, whereas the prices for PHAs were 2.4—4.0 Euro/kg, and for polypropylene and polyvinylchloride they were 1.0—1.1 Euro/kg (Sin et al., 2012). Therefore, PLA can be used for the production of more expensive or more environmentally friendly materials than petrochemical plastics or crude PHAs.

The worldwide biotechnological production of L-lactic acid was about 275,000 tons in 2006 with an average annual growth of 10% (de Jong et al., 2012). The primary came from large-scale production of lactic acid, new effective biotechnologies of lactic acid fermentation, and use of inexpensive fermentative substrates, such as dairy products, food and agroindustrial wastes, glycerol, and algal biomass (Abdel-Rahman et al., 2013; Hofvendahl and Hahn-Hägerdal, 2000). Worldwide annual production of PLA in 2010 was about 110,000 tons. PLA is produced mainly from corn-based sugar raw material by Nature Works LCC (former Cargill Dow LLC) with the current production of 140,000 tons of Ingeo biopolymer with plants in USA and Thailand, Zhejiang Hisun Biomaterials Co. in China, and PURAC Biochem with plants in The Netherlands, USA, Spain, Brasil, and Thailand.

3.3 Biotechnological production of polysaccharide admixtures

Microbial extracellular polysaccharides are used in cement-based materials for dispersing, thickening, water retention, set retardation, air entrainment, and film formation. The market of microbial admixtures is estimated at the level of about US $2 billion (Plank, 2004). The major producers are Gram-negative bacteria from the genera *Xanthomonas* and *Alcaligenes*, but the spectrum of industrially available producers is continually increasing (Table 3.2).

Table 3.2 **Production of the major biotechnological admixtures used in building materials**

Admixture	Chemical type	Biotechnological process
Sodium gluconate	Organic salt	Biooxidation of glucose
Xanthan gum	Polysaccharide	Biosynthesis by bacteria *Xanthomonas campestris*
Welan gum	Polysaccharide	Biosynthesis by bacteria *Alcaligenes* sp.
Scleroglucan	Polysaccharide	Biosynthesis by fungi from the genera *Sclerotium*, *Corticium*, *Sclerotinia*, and *Stromatinia*
Succinoglycan	Polysaccharide	Biosynthesis by bacteria *Alcaligenes* sp.
Curdlan gum	Polysaccharide	Biosynthesis by bacteria from the genera *Agrobacterium* or *Alcaligenes*
Polyaspartic acid	Polyanionic polyaminoacid	Chemical synthesis
Sodium alginate	Anionic polysaccharide	Extraction from brown seaweeds
Carrageenan	Linear sulfated polysaccharide	Extraction from plants or red seaweeds
Dextran	Polysaccharide	Microbial synthesis
Pullulan	Polysaccharide	Biosynthesis by fungi *Auerobasidium pullulans*
Sewage sludge	Mixture of biopolymers	Waste biomass of municipal wastewater treatment plants
Sewage sludge ash	Incineration ash of sewage sludge	Waste of incineration plants
Bacterial cell walls	Structural polysaccharides and proteins	Aerobic cultivation of bacteria *Bacillus subtilis*; could be produced from sewage sludge

Based on Plank (2003, 2004), Mun (2007), Fytili and Zabaniotou (2008), Pacheco-Torgal and Jalali (2011), and Pei et al. (2013).

Promising exopolysaccharide ethapolan can be produced from ethanol, vegetable oil, and other organic substances using bacteria from the genus *Acinetobacter* (Pirog et al., 2003).

All microbial polysaccharides are produced by conventional biotechnology including the following steps: (1) preparation of microbial inoculum; (2) aseptic cultivation in fermenters, (3) separation of bacterial biomass if possible from viscous medium after cultivation; (4) concentration of polysaccharides, usually by precipitation after addition of ethanol; (5) separation and drying of the precipitated polysaccharide.

All these steps are relatively expensive, so the cost of product could be at the levels ranging from US $2000 to US $20,000 per metric ton.

The ways to produce cheap admixtures could be either nonaseptic cultivation on cheap organic materials or extraction of biopolymers from dry sewage sludge or dewatered dry sewage sludge of municipal wastewater treatment plants. This waste material is used in the cement industry (Mun, 2007; Fytili and Zabaniotou, 2008). It is mainly biomass of anaerobic bacteria and archaea growing in an anaerobic digester of activated sludge. This material contains various biopolymers such as linear and branched polysaccharides, globular proteins and rRNA, and linear chains of DNA and mRNA. Our experiments with the addition of pure linear (xanthan, DNA), branched (amylopectin), or globular (albumin) biopolymers to Portland cement showed that even an addition of 0.1% of these hydrophilic biopolymers changed the strength of concrete. It was higher with an addition of biopolymers than in control after three days but was lower than in control after seven days, probably because a thin layer of the hydrophilic biopolymer on the cement grain hindered its hydration (Wang et al., 2013, unpublished data). Therefore, it could be possible to expect thickening, water retention, set retardation, and air-entrainment effects using admixtures of bioplolymers extracted from sewage sludge.

3.4 Biotechnological production of biocements and biogrouts

Different types of biocements for the strengthening of soil and biogrouts for the sealing of soil can be produced using biotechnologies (Ivanov and Chu, 2008; Ivanov, 2010).

3.4.1 Production of calcium- and urea-dependent biocement

The strain used for this kind of biocement must have strong urease activity to perform the following reaction, which is used most actively in geotechnical engineering applications (DeJong et al., 2013):

$$(NH_2)_2CO + 2\,H_2O + CaCl_2 \rightarrow CaCO_3\downarrow + 2\,NH_4Cl \tag{3.2}$$

In the majority of the cases, the Gram-positive bacterial species *Sporosarcina pasteurii* (former *Bacillus pasteurii*), especially the strain *S. pasteurii* ATCC 11859 (DSM 33), is used as a bioagent of biocement because of its high urease activity and ability to grow at pH above 8.5 and at high concentration of calcium, at least at 0.75 M Ca^{2+}. Other physiologically similar species used for biocementation are the representatives of the genus *Bacillus: B. cereus* (Castanier et al., 2000); *B. megaterium* (Bang et al., 2001; Dhami et al., 2014), *B. sphaericus* (Hammes et al., 2003; De Muynck et al., 2008; Wang et al., 2012), *Bacillus subtilis* (Reddy et al., 2010), *B. alkalinitrilicus* (Wiktor and Jonkers, 2011), *B. licheniformis* (Vahabi et al., 2014), *B. lentus* (Sarda et al., 2009), and unidentified species (Hammes et al., 2003; Stabnikov et al., 2011, 2013b).

It is important to use as the biocementation agent the extreme halophiles with urease activity. This can decrease the duration of continuous biocementation or number of the batch treatments to form biocement. It is well known that some halotolerant species of genus *Staphylococcus* exhibit high urease activity (Christians et al., 1991; Jin et al., 2004). A halotolerant urease-producing strain of Gram-positive bacteria of *Staphylococcus succinus* was isolated from water of the Dead Sea with salinity 34% (Stabnikov et al., 2013b). However, the strains of *S. succinis* are often hemolytic and toxigenic (Zell et al., 2008) and have been associated with some infectious diseases (Novakova et al., 2006; Taponen et al., 2008). Therefore, the isolated strain was not used for biocementation studies and applications.

Using numerous samples from water and sediments from salt lakes in North and South America we produced an enrichment culture and then isolated and identified the bacterial strain *Jeotgalicoccus halotolerans* VS35 that grew and produced urease in the medium with 3 M NaCl (Stabnikov et al., 2015). Therefore, these halotolerant bacteria, isolated for the first time in 2003 (Yoon et al., 2003) from the traditional Korean fermented seafood, are most probably safe and could be used for one-time treatment of porous soil or fissured rock soil for bioclogging or biocementation. Known urease-active species *Haloarcula aidinensis*, *H. hispanica*, *H. japonica*, and *H. marismortui* show maximum urease activity at 18 to 23% (1.4 to 4.0 M) NaCl (Mizuki et al., 2004), so there could be possible urease activity at 4 M concentration of Ca^{2+}. One-step biocementation treatment with the solution of 4 M Ca^{2+} can produce microbially induced calcite precipitation (MICCP) with about 5% (w/w) of precipitated Ca in soil, which will be sufficient value for the majority of biocementation applications in geotechnical engineering.

The dry biogrout can contain: (1) salt of calcium (calcium chloride, calcium acetate); (2) urea in molar ratio with Ca^{2+} in the range 1:1.25−1:1.5; (3) urease-producing bacteria (UPB) or crude urease. To increase the diameter of an area of bacterial cells, distribution from the point of injection the bacterial suspension must be injected separately from calcium salt and urea because calcium ions increase an aggregation of bacterial cells from 1 to 3 μm size to large aggregates of 10 to 100 μm size, which distribution in porous soil or fissured rock is limited by the size of the pores, channels, and fissures.

3.4.2 Biocement based on activity of anoxic heterotrophic bacteria

Precipitation of calcium carbonate can be due to increase of pH and production of carbonate by heterotrophic bacteria during aerobic oxidation of organics (Wright and Oren, 2005), for example, in such biogeochemical reactions as:

$$(CH_3COO)_2Ca + 4\,O_2 \rightarrow CaCO_3\downarrow + 3\,CO_2\uparrow + 3\,H_2O \qquad (3.3)$$

Calcium carbonate precipitation due to oxidation of organics was used for biocementation of porous stones (Rodriguez-Navarro et al., 2003; Jimenez-Lopez et al., 2008). However, underground space is usually anaerobic. In this case, fermentation cannot be used for production of CO_2 and precipitation of $CaCO_3$ because of the production of organic acids, but anoxic oxidation of organics by NO_3^-, Fe^{3+}, or SO_4^{2-} can be used. All these reactions are accompanied by an increase of pH, which is necessary for the precipitation of calcium carbonate, for example:

$$(CH_3COO)_2Ca + 8/5\,NO_3^- \rightarrow CaCO_3\downarrow + 4/5\,N_2\uparrow + 3\,CO_2\uparrow + 3\,H_2O + 8/5\,OH^- \tag{3.4}$$

By one dataset, it can initiate precipitation of $CaCO_3$ (Hamdan et al., 2011) but by our data denitrification cannot be performed at high concentration of Ca^{2+}, which is necessary for biogrouting/biocementation. This inhibition of the growth of denitrifying bacteria could be due to precipitation of phosphate and sulfate from the medium by calcium ions.

The disadvantage of biocements based on aerobic or anoxic heterotrophic bacteria is that rich and expensive media must be added to the porous soil of fissured rock to initiate growth and production of CO_2 by these bacteria. Additionally, there may be a long adaptation period, from hours to days, of injected bacteria to start growth.

3.4.3 Production of calcium bicarbonate for bioclogging/biocementation

Precipitation of calcium carbonate crystals from solutions of calcium bicarbonate is going on in nature during the drying of calcium bicarbonate in air (Figure 3.3):

$$Ca(HCO_3)_2 \rightarrow CaCO_3\downarrow + CO_2\uparrow + H_2O \tag{3.5}$$

Precipitation of calcium carbonate crystals from a solution of calcium bicarbonate probably can be facilitated by an addition of urea and UPB or crude urease. This process releases a low quantity of ammonia:

$$Ca(HCO_3)_2 + CO(NH_2)_2 + H_2O \rightarrow CaCO_3\downarrow + CO_2 + (NH_4)_2CO_3 \tag{3.6}$$

Probably, the acceptable method to produce a solution of calcium bicarbonate will be the treatment of lime stone suspension solution with carbon dioxide:

$$CaCO_3 + H_2O + CO_2 \leftrightarrow Ca(HCO_3)_2 \tag{3.7}$$

Calcium bicarbonate solution produced under high pressure can spontaneously form calcium carbonate under atmospheric pressure. The problem of bicarbonate biocement produced by the treatment of $CaCO_3$ or $Ca(OH)_2$ is its low concentration and instability, so the solution must be produced and stored at elevated partial pressure of CO_2. So, liquid biogrout based on calcium bicarbonate must contain solution of calcium bicarbonate produced from suspension of $Ca(OH)_2$ or $CaCO_3$ under high pressure of CO_2. Due to its low concentration, this biogrout can be used mainly to seal the fissions with the thickness of 10–200 μm in the rock.

Figure 3.3 Precipitation of $CaCO_3$ from solution of $Ca(HCO_3)_2$ that seeps through the concrete cracks and dries on the concrete surface.

3.4.4 Iron-based bioclogging and biocementation

Iron-based biocementation could be suitable for geotechnical applications if to combine three bioprocesses shown as follows:

1. acidogenic fermentation of cellulose-containing agricultural or food-processing residuals producing mainly acetic acid;
2. bioreduction of cheap-commodity iron ore, using products of acidogenic fermentation or many organic electron donors (Ivanov et al., 2009; Guo et al., 2010); see equation for the reduction of ferric ions by iron-reducing bacteria using acetate:

$$4\,Fe_2O_3 + 17\,CH_3COOH \rightarrow 8\,Fe(CH_3COO)_2 + 2\,CO_2 + 10\,H_2O \tag{3.8}$$

3. precipitation of ferrous hydroxide (Stabnikov and Ivanov, 2006):

$$Fe^{2+} + (NH_2)_2CO + 3\,H_2O + UPB \rightarrow Fe(OH)_2\downarrow + 2\,NH_4^+ + CO_2 \tag{3.9}$$

or

Figure 3.4 Sand after bioclogging with iron-based biogrout.

4. oxidation and bioprecipitation of ferrous chelates (Stabnikov and Ivanov, 2006):

$$\begin{aligned}&\mathrm{Fe^{2+} + 1.5\,(NH_2)_2CO + 0.25\,O_2 + 5.5\,H_2O + UPB \rightarrow}\\&\quad \mathrm{Fe(OH)_3\downarrow + 1.5\,(NH_4)_2CO_3 + 2\,H^+}\end{aligned} \tag{3.10}$$

The dry iron-based biogrout must contain: (1) ferrous acetate salt or chelate as a reagent or as a crude product of anaerobic fermentation and bioreduction of ferric; (2) urea in molar ratio with Fe^{2+} 1:1 or 1:1.5 in the case of aerobic oxidation of ferrous hydroxide to ferric hydroxide; (3) acidotolerant UPB or crude urease. Sand after grouting with this biogrout became almost impermeable (Figure 3.4).

3.4.5 Eco-efficient and composite biocement

By analogy with eco-efficient concrete (Pacheco-Torgal et al., 2012), eco-efficient biocement can be produced using mining tailings/residuals of limestone, dolomite, iron ore, and organic agricultural, food-processing, or municipal wastes using acidogenic fermentation and bioreduction of iron with the production of dissolved salts of calcium, magnesium, and iron.

The problem with the brittleness of biocement could be solved using a biomimetic approach (Sarikaya, 1994; Mayer and Sarikaya, 2002) through the combination of mineral and organic nano- and microparticles. By analogy with nanomaterials in cement (Pacheco-Torgal and Jalali, 2011), applications of composite micro- and nanomaterials can also be useful to increase strength and ductility of biocement. Theoretically, ductile biocement could be made as a bioinspired material (Pacheco-Torgal and Labrincha, 2013), with the 3D-composite structure of hierarchically arranged nano- and micrometric units (Imai and Oaki, 2010), or just simply with the layers or inclusions, in which inorganic crystals of calcium carbonate (calcite, aragonite, and vaterate), calcium phosphate (hydroxyapatite), and oxides of Si and Fe create the hardness, and the organic components such as proteins and polysaccharides ensure flexibility of the biocemented structure. This property is well known from the structure of the natural biominerals such as bones, shells, and corals, as well as artificial engineering composite materials (Yao et al., 2011; Mayer and Sarikaya, 2002). However, the cost of micro- and nanocomposites could be too high to be suitable for construction practice.

Production of biocements, biogrouts, bioplastics, and polysaccharide admixtures can be more sustainable if it can be performed in the biorefinery, which is a facility for industrial production of different chemical products, first of all, a fuel, based on the biotransformation of millions of tons of renewable biomass sources (Kamm et al., 2005). This raw material could be the biomass of plants like starch of corn, sorghum, and other crops, oils of terrestrial plants and aquatic algae, cellulose and hemicellulose of trees and grasses. The common products of any fermentation from biorefinery or pyrolytic transformation of wood to fuel—ethanol, acetic acid, and hydrogen—are the most useful substances for the production of biocements, biogrouts, bioplastics, and polysaccharide admixtures. Acetic acid is neutralized by $Ca(OH)_2$ with the formation of calcium acetate as a major component of biocement. Sodium acetate and hydrogen are the best sources of carbon and energy for the production of PHAs. Ethanol is one of the best sources of carbon and energy for the production of polysaccharide admixtures. Another green solution for the bioplastic production is the utilization of hydrogen produced by photoelectric hydrolysis of water (Yu, 2014).

Biocement is not a competitive material for conventional cement because it is used only in cases in which cement is not suitable or less practical because of the high viscosity of its mixtures. Moreover, calcium bicarbonate biocement can be produced in the cement plants using the released CO_2 and CaO that could be the wastes of the cement plants:

$$\mathrm{CaO} + \mathrm{H_2O} + 2\,\mathrm{CO_2} \rightarrow \mathrm{Ca(HCO_3)_2} \tag{3.11}$$

Production and application of this type of biocement could significantly reduce anthropogenic CO_2 emissions from the cement plants, which are now about 7% of global CO_2 emissions (Rehan and Nehdi, 2005).

3.5 Conclusions

Microbial cements, polysaccharides, and construction bioplastics can be made using biotechnologies. Microbial cement could be produced with a lower cost than conventional cement. Biodegradability of bioplastic constructions after their demolition reduces the cost of construction waste disposal. Microbial polysaccharides are used to modify cement properties and soil bioclogging. The biotechnologically produced materials and construction biotechnologies have a lot of advantages in comparison to conventional construction materials and processes, so the practical implementations of construction biotechnologies could give significant economic and environmental benefits.

References

Abdel-Rahman, M.A., Tashiro, Y., Kenji Sonomoto, K., 2013. Recent advances in lactic acid production by microbial fermentation processes. Biotechnology Advances 31, 877–902.

Bajpai, P.K., Meena, D., Vatsa, S., Singh, I., 2013. Tensile behavior of nettle fiber composites exposed to various environments. Journal of Natural Fibers 10, 244–256.

Bang, S.S., Galinat, J.K., Ramakrishnan, V., 2001. Calcite precipitation induced by polyurethane-immobilized *Bacillus pasteurii*. Enzyme and Microbial Technology 28, 404–409.

Barlaz, M.A., Staley, B.F., De Los Reyes III., F.L., 2010. Anaerobic biodegradation of solid waste. In: Mitchell, R., Gu, J.D. (Eds.), Environmental Microbiology, second ed. John Wiley & Sons, Inc., Hoboken, NJ, USA, pp. 281–299.

Ben Rebah, F., Prevost, D., Tyagi, R.D., Belbahri, L., 2009. Poly-beta-hydroxybutyrate production by fast-growing rhizobia cultivated in sludge and in industrial wastewater. Applied Biochemistry and Biotechnology 158, 155–163.

Beun, J.J., Dircks, K., van Loosdrecht, M.C.M., et al., 2006. Poly-β-hydroxybutyrate metabolism in dynamically fed mixed microbial cultures. Water Research 36, 1167–1180.

Braunegg, G., Lefebvre, G., Genser, K.F., 1998. Polyhydroxyalkanoates, biopolyesters from renewable resources: physiological and engineering aspects. Journal of Biotechnology 65, 127–161.

Burbank, M.B., Weaver, T.J., Green, T.L., Williams, B.C., Crawford, R.L., 2011. Precipitation of calcite by indigenous microorganisms to strengthen liquefiable soils. Geomicrobiology Journal 28, 301–312.

Castanier, S., Le Métayer-Levrel, G., Orial, G., Loubière, J.F., Perthuisot, J.P., 2000. Bacterial carbonatogenesis and applications to preservation and restoration of historic property. In: Ciferri, O., Tiano, P., Mastromei, G. (Eds.), Of Microbes and Art. The Role of Microbial Communities in the Degradation and Protection of Cultural Heritage. Kluwer Academic/Plenum Publisher, New York, pp. 203–218.

Castilho, L.R., Mitchell, D.A., Freire, D.M.G., 2009. Production of polyhydroxyalkanoates (PHAs) from waste materials and by-products by submerged and solid-state fermentation. Bioresource Technology 100, 5996–6009.

Cheng, L., Cord-Ruwisch, R., 2013. Selective enrichment and production of highly urease active bacteria by non-sterile (open) chemostat culture. Journal of Industrial Microbiology and Biotechnology 40, 1095–1104.

Christians, S., Jose, J., Schäfer, U., Kaltwasser, H., 1991. Purification and subunit determination of the nickel-dependent *Staphylococcus xylosus* urease. FEMS Microbiology Letters 80, 271–275.

Chu, J., Stabnikov, V., Ivanov, V., 2012. Microbially induced calcium carbonate precipitation on surface or in the bulk of soil. Geomicrobiology Journal 29, 1–6.

De Muynck, W., Cox, K., Verstraete, W., De Belie, N., 2008. Bacterial carbonate precipitation as an alternative surface treatment for concrete. Construction and Building Materials 22, 875–885.

DeJong, J.T., Soga, K., Kavazanjian, E., et al., 2013. Biogeochemical processes and geotechnical applications: progress, opportunities and challenges. Geotechnique 63, 287–301.

DeMarco, S., 2005. Advances in polyhydroxyalkanoate production in bacteria for biodegradable plastics. Basic Biotechnology eJournal 1, 1–4.

Dhami, N.K., Reddy, M.S., Mukherjee, A., 2014. Synergistic role of bacterial urease and carbonic anhydrase in carbonate mineralization. Applied Biochemistry and Biotechnology 172, 2552–2561.

Faludi, G., Dora, G., Renner, K., Móczó, J., Pukanszky, B., 2013. Biocomposite from polylactic acid and lignocellulosic fibers: structure−property correlations. Carbohydrate Polymers 92, 1767−1775.

Fytili, D., Zabaniotou, A., 2008. Utilization of sewage sludge in EU application of old and new methods—a review. Renewable and Sustainable Energy Reviews 12, 116−140.

Li, M., Guo, H., Cheng, X., 2011. Application of response surface methodology for carbonate precipitation production induced by a mutant strain of *Sporosarcina pasteurii*. In: Geo-frontiers. ASCE, pp. 4079−4088.

Guo, C.H., Stabnikov, V., Ivanov, V., 2010. The removal of nitrogen and phosphorus from reject water of municipal wastewater treatment plant using ferric and nitrate bioreductions. Bioresource Technology 101, 3992−3999.

Hamdan, N., Kavazanjian, E., Rittman, B.E., Karatas, I., 2011. Carbonate mineral precipitation for soil improvement through microbial denitrification. In: Han, J., Alzamora, D.A. (Eds.), Geo-frontiers 2011: Advances in Geotechnical Engineering. American Society of Civil Engineers, Dallas.

Hammes, F., Boon, N., de Villiers, J., Verstraete, W., Siciliano, S.D., 2003. Strain-specific ureolytic microbial calcium carbonate precipitation. Applied and Environmental Microbiology 69, 4901−4909.

Hofvendahl, K., Hahn-Hägerdal, B., 2000. Factors affecting the fermentative lactic acid production from renewable resources. Enzyme Microbial Technology 26, 87−107.

Huda, M.S., Drzal, L.T., Mohanty, A.K., Misra, M., 2006. Chopped glass and recycled newspaper as reinforcement fibers in injection molded poly(lactic acid) (PLA) composites: a comparative study. Composites Science and Technology 66, 1813−1824.

Imai, H., Oaki, Y., 2010. Bioinspired hierarchical crystals. MRS Bulletin 35, 138−144.

Ivanov, V., Chu, J., 2008. Applications of microorganisms to geotechnical engineering for bioclogging and biocementation of soil *in situ*. Reviews in Environmental Science and Biotechnology 7, 139−153.

Ivanov, V., Kuang, S.L., Guo, C.H., Stabnikov, V., 2009. The removal of phosphorus from reject water in a municipal wastewater treatment plant using iron ore. Journal of Chemical Technology and Biotechnology 84, 78−82.

Ivanov, V., 2010. Environmental Microbiology for Engineers. CRC Press, Taylor & Francis Group, Boca Raton, 402 p.

Ivanov, V., Stabnikov, V., Hung, Y.T., 2012. Screening and selection of microorganisms for the environmental biotechnology process. In: Hung, Y.-T., Wang, L.K., Shammas, N.K. (Eds.), Handbook of Environment and Waste Management. Air and Water Pollution Control. World Scientific Publishing Co., Inc., pp. 1137−1149.

Jimenez-Lopez, C., Jroundi, F., Pascolini, C., Rodriguez-Navarro, C., Piñar-Larrubia, G., Rodriguez-Gallego, M., González-Muñoz, M.T., 2008. Consolidation of quarry calcarenite by calcium carbonate precipitation induced by bacteria activated among the microbiota inhabiting the stone. International Biodeterioration and Biodegradation 62, 352−363.

Jin, M., Rosario, W., Walter, E., Calhoun, D.H., 2004. Development of a large-scale HPLC-based purification for the urease from *Staphylococcus leei* and determination of subunit structure. Protein Expression and Purification 34, 111−117.

John, M.J., Thomas, S., 2008. Biofibres and biocomposites. Carbohydrate Polymers 71, 343−364.

de Jong, E., Higson, A., Walsh, P., Wellisch, M., 2012. Bio-Based Chemicals: Value Added Products from Biorefineries. IEA Bioenergy Task 42 Biorefinery. http://www.ieabioenergy.com/wp-content/uploads/2013/10/Task-42-Biobased-Chemicals-value-added-products-from-biorefineries.pdf.

Kamm, B., Kamm, M., Gruber, P.R., Kromus, S., 2005. Biorefinery systems – an overview. In: Kamm, B., Gruber, P.R., Kamm, M. (Eds.), Biorefineries – Industrial Processes and Products: Status Quo and Future Directions. Wiley-VCH Verlag GmbH, Weinheim, Germany. http://dx.doi.org/10.1002/9783527619849 (Chapter 1).

Khanna, S., Srivastava, A.K., 2005. Recent advances in microbial polyhydroxyalkanoates. Process Biochemistry 40, 607–619.

Lenz, R.W., Marchessault, R.H., 2005. Bacterial polyesters: biosynthesis, biodegradable plastics and biotechnology. Biomacromolecules 6, 1–8.

van Loosdrecht, M.C.M., Pot, M.A., Heijnen, J.J., 1997. Importance of bacterial storage polymers in bioprocesses. Water Science and Technology 33, 41–47.

van Loosdrecht, M.C.M., Kleerebezem, R., Muyzer, G., Jian, Y., Johnson, K., 2008. Process for Selecting Polyhydroxyalkanoate (PHA) Producing Micro-organisms. WO/2009/153303 June 18, 2008. International Application No.: PCT/EP2009/057571.

Lowell, W.L., Rohwedder, W.K., 1974. Poly-beta-hydroxyalkanoate from activated sludge. Environmental Science and Technology 8, 576–579.

Lu, Y., 2007. Advance on the production of polyhydroxyalkanoates by mixed cultures. Frontiers of Biology in China 2, 1673–3509.

Madigan, M.T., Martinko, J.M., Stahl, D., Clark, D.P., 2012. Brock Biology of Microorganisms, thirteenth ed. Pearson.

Mayer, G., Sarikaya, M., 2002. Rigid biological composite materials: structural examples for biomimetic design. Experimental Mechanics 42, 395–403.

Mergaert, J., Anderson, C., Wouters, A., Swings, J., Kerster, K., 1992. Biodegradation of polyhydroxyalkanoates. FEMS Microbiology Reviews 103, 317–322.

Mizuki, T., Kamekura, M., DasSarma, S., Fukushima, T., Usami, R., Yoshida, Y., Horikoshi, K., 2004. Ureases of extreme halophiles of the genus *Haloarcula* with a unique structure of gene cluster. Bioscience, Biotechnology, and Biochemistry 68, 397–406.

Moosbrugger, R.E., Wentezel, M.C., Ekama, G.A., Marais, G.V., 1993. Weak acid/bases and pH control in anaerobic systems: a review. Water South Africa 19, 1–10.

Mun, K.J., 2007. Development and tests of lightweight aggregate using sewage sludge for nonstructural concrete. Construction and Building Materials 21, 1583–1588.

Novakova, D., Sedlacek, I., Pantucek, R., Stetina, V., Svec, P., Petras, P., 2006. *Staphylococcus equorum* and *Staphylococcus succinus* isolated from human clinical specimens. Journal of Medical Microbiology 55, 523–528.

Ogbobe, O., Essien, K.S., Adebayo, A., 1998. A study of biodegradable geotextiles used for erosion control. Geosynthetics International 5, 545–553.

Pacheco-Torgal, F., Jalali, S., 2011. Nanotechnology: advantages and drawbacks in the field of construction and building materials. Construction and Building Materials 25, 582–590.

Pacheco-Torgal, F., Jalali, S., Labrincha, J., John, V.M., 2012. Eco-efficient concrete using industrial wastes: a review. Materials Science Forum 730-732, 581–586.

Pacheco-Torgal, F., Labrincha, J.A., 2013. Biotechnologies and bioinspired materials for the construction industry: an overview. International Journal of Sustainable Engineering 7, 235–244.

Pei, R., Liu, J., Wang, S., Yang, M., 2013. Use of bacterial cell walls to improve the mechanical performance of concrete. Cement and Concrete Composites 39, 122–130.

Pirog, T.P., Kovalenko, M.A., Kuz'minskaya, Y.V., 2003. Intensification of exopolysaccharide synthesis by *Acinetobacter* sp. on an ethanol–glucose mixture: aspects related to biochemistry and bioenergetics. Microbiology 72, 305–312.

Plank, J., 2003. Applications of biopolymers in construction engineering. In: Steinbüchel, A. (Ed.), Biopolymers, General Aspects and Special Applications, vol. 10. Wiley-VCH Verlag GmbH, Weinheim.

Plank, J., 2004. Application of biopolymers and other biotechnological products in building material. Applied Microbiology and Biotechnology 66, 1−9.

Reddy, C.S., Ghai, R., Rashmi, C., Kalia, V.C., 2003. Polyhydroxyalkanoates: an overview. Bioresource Technology 87, 137−146.

Reddy, S., Rao, M., Aparna, P., Sasikala, C., 2010. Performance of standard grade bacterial (*Bacillus subtilis*) concrete. Asian Journal of Civil Engineering (Build Housing) 11, 43−55.

Rehan, R., Nehdi, M., 2005. Carbon dioxide emissions and climate change: policy implications for the cement industry. Environmental Science and Policy 8, 105−114.

Rodriguez-Navarro, C., Rodriguez-Gallego, M., Ben Chekroun, K., Gonzalez-Muñoz, M.T., 2003. Conservation of ornamental stone by *Myxococcus xanthus*-induced carbonate biomineralization. Applied and Environmental Microbiology 69, 2182−2193.

Saba, N., Paridah, M.T., Jawaid, M., 2015. Mechanical properties of kenaf fibre reinforced polymer composite: a review. Construction and Building Materials 76, 87−96.

Sarda, D., Choonia, H.S., Sarode, D.D., Lele, S.S., 2009. Biocalcification by *Bacillus pasteurii* urease: a novel application. Journal of Industrial Microbiology and Biotechnology 36, 1111−1115.

Sarikaya, M., 1994. An introduction to biomimetics: a structural viewpoint. Microscopy Research and Technique 37, 360−375.

Serafim, L.S., Lemos, P.C., Albuquerque, M.G.E., Reis, M.A.M., 2008. Strategies for PHA production by mixed cultures and renewable waste materials. Applied Microbiology and Biotechnology 81, 615−628.

Sin, L.T., Rahmat, A.R., Rahman, W.A., 2012. Polylactic Acid: PLA Biopolymer Technology and Applications. Elsevier, 329 p.

Stabnikov, V.P., Ivanov, V.N., 2006. The effect of various iron hydroxide concentrations on the anaerobic fermentation of sulfate-containing model wastewater. Applied Biochemistry and Microbiology 42, 284−288.

Stabnikov, V., Chu, J., Naeimi, M., Ivanov, V., 2011. Formation of water-impermeable crust on sand surface using biocement. Cement and Concrete Research 41, 1143−1149.

Stabnikov, V., Chu, J., Ivanov, V., Li, Y., 2013b. Halotolerant, alkaliphilic urease-producing bacteria from different climate zones and their application for biocementation of sand. World Journal of Microbiology and Biotechnology 29, 1453−1460.

Sudesh, K., Abe, H., Doi, Y., 2000. Synthesis, structure and properties of polyhydroxyalkanoates: biological polyesters. Progress in Polymer Science 25, 1503−1555.

Sudesh, K., Abe, H., 2010. Practical Guide to Microbial Polyhydroxyalkanoates. Smithers Rapra Technology, 160 p.

Taponen, S., Björkroth, J., Pyörälä, S., 2008. Coagulase-negative staphylococci isolated from bovine extramammary sites and intramammary infections in a single dairy herd. Journal of Dairy Research 75, 422−429.

Tokiwa, Y., Tsuchiya, A. 2003. Biodegradable Resin Compositions. US Patent 666977.

UNEP, 2009. Converting Waste Agricultural Biomass into a Resource. Compendium of technologies. United Nations Environment Programme, 441 p.

Vahabi, A., Ramezanianpour, A.A., Sharafi, H., Shahbani, H.Z., Vali, H., Noghabi1, K.A., 2014. Calcium carbonate precipitation by strain *Bacillus licheniformis* AK01, newly isolated from loamy soil: a promising alternative for sealing cement-based materials. Journal of Basic Microbiology 53, 1−7.

Volova, T.G., 2004. Polyhydroxyalkanoates − Plastic Materials of the 21st Century. Nova Publishers, 282 p.

Wang, K., Ivanov, V., Cao, J., 2013. Effect of Biopolymers on Cementation Process, unpublished data.

Wang, J.Y., De Belie, N., Verstraete, W., 2012. Diatomaceous earth as a protective vehicle for bacteria applied for self-healing concrete. Journal of Industrial Microbiology and Biotechnology 39, 567−577.

Wiktor, V., Jonkers, H., 2011. Quantification of crack-healing in novel bacteria-based self-healing concrete. Cement and Concrete Composition 33, 763−770.

Wright, D.T., Oren, A., 2005. Nonphotosynthetic bacteria and the formation of carbonates and evaporites through time. Geomicrobiology Journal 22, 27−53.

Yao, L., Yang, J., Sun, J., Cai, L., He, L., Huang, H., Song, R., Hao, Y., 2011. Hard and transparent hybrid polyurethane coatings using in situ incorporation of calcium carbonate nanoparticles. Materials Chemistry and Physics 129, 523−528.

Yu, P.H., Chua, H., Huang, A., Ho, K.P., 1999. Conversion of food industrial wastes into bioplastics with municipal activated sludge. Macromolecular Symposia 148, 415−424.

Yu, J., November 28, 2006. Production of Biodegradable Thermoplastic Materials from Organic Wastes. US Patent 7141400.

Yu, J., 2014. Bio-based products from solar energy and carbon dioxide. Trends in Biotechnology 32, 5−10.

Yoon, J.H., Lee, K.C., Weiss, N., Kang, K.H., Park, Y.H., 2003. *Jeotgalicoccus halotolerans gen. nov., sp. nov*. and *Jeotgalicoccus psychrophilus sp. nov*., isolated from the traditional Korean fermented seafood jeotgal. International Journal of Systematic and Evolutionary Microbiology 53, 595−602.

Zell, C., Resch, M., Rosenstein, R., Albrecht, T., Hertel, C., Götz, F., 2008. Characterization of toxin production of coagulase-negative staphylococci isolated from food and starter cultures. International Journal of Food Microbiology 127, 246−251.

Life cycle assessment of biopolymers

4

A.D. La Rosa
University of Catania, Catania, Italy

4.1 Introduction

Biopolymers are innovative polymer materials within the well-known class of plastics materials. In the late 1980s and early 1990s, innovative biopolymers were introduced to the market for the first time mainly based on starch and polyhydroxyalkanoates (PHAs) manufactured by fermentation. These biologically degradable first-generation biopolymers did not successfully become established in the market, in particular because of their yet untried material properties, unfavourable political and economical circumstances, as well as a lack of political will among decision makers in industry and politics. In recent years, improved second-generation biopolymers, currently on the market, are largely comparable with conventional bulk plastics in terms of processing and use properties and increasingly competitive in certain applications, e.g. as packaging materials. Currently, these materials suffer from minor economic disadvantages, due mainly to their still low production volume. This will be compensated once disposal costs are taken into consideration and/or production volumes have increased further. Meanwhile, the manufacture of some of these second-generation biopolymers has reached industrial scale as shown in Figure 4.1. Some of the first plastics ever produced, regenerated cellulose and cellulose derivates, are among the biopolymers already being manufactured on a large industrial scale together with polycaprolactone and polyvinyl alcohol. These second-generation biopolymers were developed almost exclusively as degradable and compostable materials for the packaging, agriculture or gardening sector. Now there are polymer materials for engineering applications based on these second-generation biopolymers, gaining in interest as they enter other fields, such as the automotive and textile industries. The trend among the third-generation biopolymer materials is away from degradability and towards resistance. Furthermore, research on the use of renewable resources for the manufacturing of materials is increasing in view of limited petrochemical raw materials supply. The development of these biopolymer materials will require availability of the raw material as well as additional technological improvements (heat resistance, UV stabilization, etc.)

Biopolymers and Biotech Admixtures for Eco-Efficient Construction Materials. http://dx.doi.org/10.1016/B978-0-08-100214-8.00004-X
Copyright © 2016 Elsevier Ltd. All rights reserved.

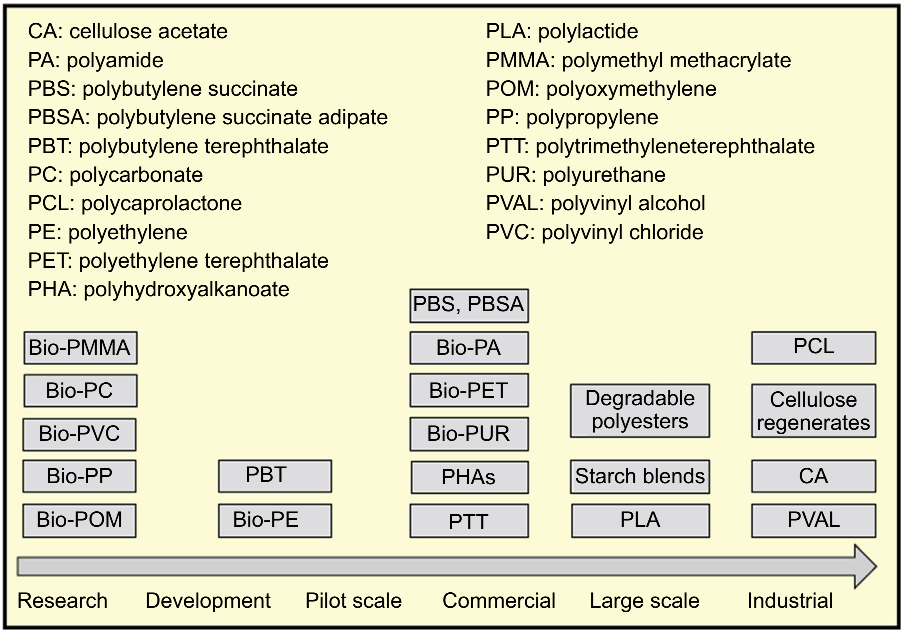

Figure 4.1 State of development of thermoplastic biopolymers.
Endres and Siebert-Raths (2012).

4.2 Biopolymers

4.2.1 Types of biopolymers

There is a lot of confusion about the terms ‘biopolymer’, ‘bioplastic’, ‘biodegradable plastic’,‘plastics from renewable resources’, etc. because biodegradable plastics can be based on petrochemical as well as on renewable resources. Degradability in biopolymeric materials is ultimately influenced only by the chemical and physical microstructure of the polymer and neither by the origin of the raw materials used nor by the process used for manufacturing these polymers (Niaounakis, 2013).

The best current general definition for the concept of biopolymers describes a polymer material that fulfils at least one of the following properties:

- Consists (partly) of bio-based (renewable) raw materials;
- Is in some way biodegradable.

Three basic groups of biopolymers exist:

1. Degradable petro-based biopolymers
2. Degradable (mainly) bio-based biopolymers
3. Nondegradable bio-based biopolymers

Possible industrial products from biorefinery process of grains and legumes are shown in Figure 4.2. Application potentials are beyond those listed in the diagram.

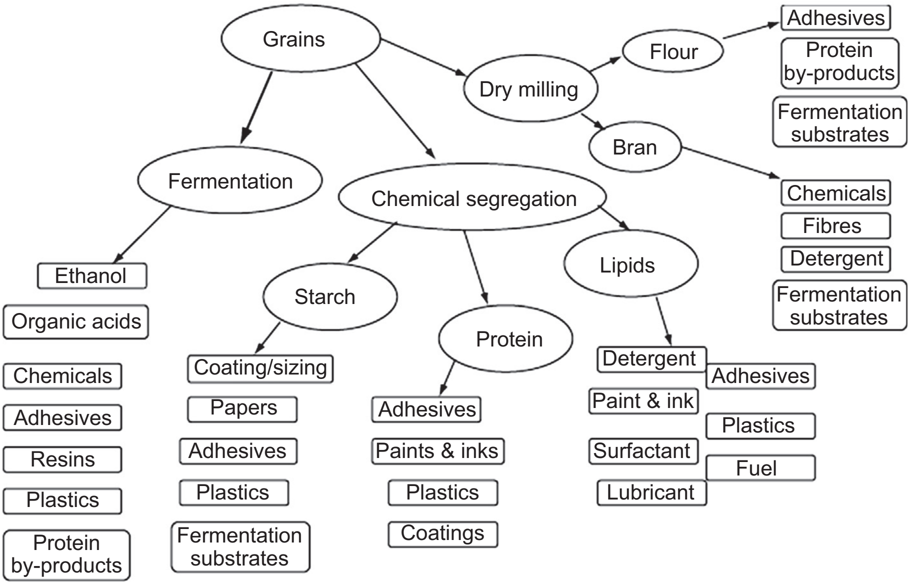

Figure 4.2 Possible industrial products from biorefinery processing of grains and legumes. Sun (2013).

4.2.2 Application of biopolymers

Recently, bio-based composites from natural fibres and bio-resins are getting increased attention. Bio-resins depending on their chemical structure can be thermoplastic or thermoset, biodegradable or not. A list of bio-derived commercially available polymers is reported in Table 4.1 and collected from technical data sheets available for each compound on each company's website. Thermoset bio-derived resins commercially available on the market are mainly epoxy resins, unsaturated polyester resins or polyurethane. These resins have a bio content ranging between 20 and 50% and are not biodegradable.

Among the thermoplastics, we can find non-biodegradable bio-resins like: biopolyolefin, bio-nylons, cellulose- and lignin-based polymers, bio-degradable bio-resins like poly(lactic acid) PLA, poly(butylene succinate) and PHAs. PLA is a commercially interesting polymer as it shares some similarities with hydrocarbon polymers such as polyethylene terephthalate (PET). It has many unique characteristics, including good transparency, glossy appearance, high rigidity and ability to tolerate various types of processing conditions. PLA is a thermoplastic polymer which has the potential to replace traditional polymers such as PET, polystyrene and polycarbonate for packaging of electronic and automotive applications (Majid et al., 2010). Although PLA has mechanical properties similar to traditional polymers, the thermal properties are not attractive due to low T_g of 60 °C. This problem can be overcome by changing the stereochemistry of the polymer and blending with other polymers and processing aids to improve the mechanical properties, e.g. varying the L and D isomer ratio which strongly influences the

Table 4.1 Commercial bio-derived resins available on the market

Tradename	Producer	Type	Biocontent %	Recycled content %
BiOH	Cargill	PU	5–20	–
Envirez	Ashland	UPR	8–22	0–44
Epobiox	Amroy Europe Oy	Epoxy	60–90	–
Palapreg eco	DSM	UPR	55	–
EcoFlex–Ecovio	Basf	Biodegradable copolyester	–	–
Eco Tek	AOC	UPR	0–30	0–45
Envirolite 31325-00	Reichold	UPR	25	–
SuperSap	Entropy	Epoxy	25–55	–
BioRez	TransFuranChemical	Furanic	–	–
Exaphen (Novocard/ Polycard)	Cimtec lab	Biobased novolac resin/polyols	–	–
Arboform	Tecnaro/Albis	Thermoplastic	100	–
Cellidor	Albis	Thermoplastic cellulose ester	45	–

crystallinity of the final polymer. However, much more work is required to improve the properties of PLA to suit various applications. Currently, Nature Works LLC, USA, is the major supplier of PLA sold under the brand name Ingeo™, with a production capacity of 100,000 ton/year (Babu et al., 2013).

A new class of totally biodegradable 'green' composites obtained by combining natural fibres with biodegradable resins are being developed (Netravali and Chabba, 2003). Furthermore, several applications are being carried out using recycled petro-based thermoplastics like polyethylene (PE) and polypropylene (PP) reinforced with natural fibres.

A Strengths, Weaknesses, Opportunities and Threats (SWOT) analysis from La Rosa and Cicala (in press), shown in Figure 4.3 and in Table 4.2, summarizes benefits and drawbacks of the use of green composites produced with natural fibres and bio-derived matrices to replace traditional composites. The benefits appear superior to the disadvantages and the market opportunities are increasing for many industrial sectors.

4.2.3 End of life of biopolymers

During the last decade, industrial production has been driven towards more sustainable policies. For 2020, the EU has committed to cutting its emissions to 20% below 1990 levels; for 2050, EU leaders have endorsed the objective of reducing Europe's greenhouse gas emissions by 80–95% compared to 1990 levels. In the field of environmental protection and resource recovery for plastics, the best practice is considered polymer recycling and reusing with properties comparable to virgin materials (Molgaard, 1995).

Some considerations on polymer products must be assumed:

- thermoplastic polymers offer the opportunity for recycling at the end of life, but they require a greater energy input in the fabrication of structures due to the melting point normally being ~200 °C above the use temperature;
- thermoset polymers are difficult to recycle and may be a potential landfill problem but large structures can be fabricated with minimal energy requirements and lower carbon emissions.

The recycling practice makes polymers 'green'; nevertheless, they are not fully eco-compatible because they are not biodegradable. Research developments during the last few years have been focused on the production of 100% eco sustainable and 'green' composites, by replacing non-biodegradable polymer matrices with biodegradable ones. PLA, a thermoplastic polymer coming from renewable sources, has been used extensively because it shows good mechanical properties, is biocompatible and easy to produce (Bax and Mussig, 2008). PLA encompasses comparable properties as well as other thermoplastics like petroleum-based PE and PP. A crucial difference is that PLA is biodegradable. The great advantage of biodegradable polymers in construction sector is that they can be left in soil after construction works increasing soil fertility, composted with other organic wastes for production of biofertilizer or digested with other organic wastes for biogas production at the end of life. Conversely, traditional thermoplastics can last for a very long time without decomposing (about

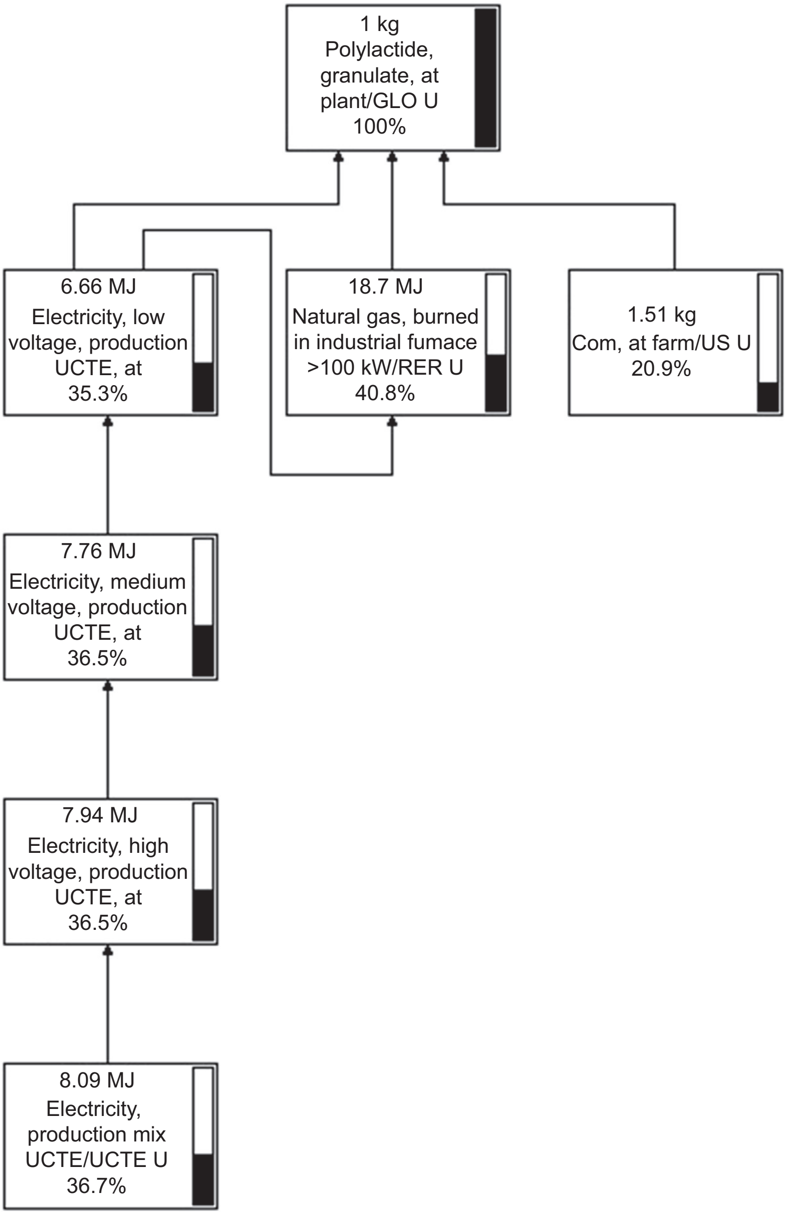

Figure 4.3 Diagram of the production step of 1 kg of PLA. Impacts in terms of percentage are referred to global warming potential.

100 years), so they are incinerated thereby polluting the atmosphere or must be extracted from soil and disposed after construction ends. On the other hand, biodegradable polymers are not yet suitable for sectors like automotive in which traditional thermoplastics are preferred because of their weatherability.

Table 4.2 Strengths, weaknesses, opportunities and threats analysis of the market of green composites compared to traditional composites

Strengths	Weaknesses
1. Reduction of the environmental impacts **2.** Cost reduction **3.** Weight reduction in composites **4.** Rural development **5.** Strong market potential **6.** Biodegradability **7.** Recyclability	**1.** Reduction of mechanical performance **2.** Reduction of thermal resistance **3.** Biomass cropping
Opportunities	**Threats**
1. New and emerging markets **2.** Emerging processing technologies **3.** Emerging emphasis on environmental issues **4.** Growing demand for green materials	**1.** Lack of production/distribution chains **2.** Infancy of the value chain **3.** Land use

La Rosa et al. (2014a).

Recycling technologies developed for thermoset composite materials comprise fundamentally three categories of processes: mechanical comminution techniques to reduce the size of the scrap to produce filler materials; chemical degradation to break the polymeric matrices into simple chemical constituents; thermal degradation to break the scrap down into materials and energy (Pimenta and Pinho, 2011). Recently, a promising solution for chemical recycling of carbon fibre (CF)/epoxy resin composites was suggested by Li et al. (2012). The composites were firstly pretreated in acetic acid. The damaged composites were then oxidized in a mixed solution of hydrogen peroxide (H_2O_2) and acetone. Clean CFs were obtained with more than 95% of their original strength, whereas above 90% of the epoxy resin was decomposed forming mainly bisphenol A and its derivatives, such as phenol derivatives. The decomposition by-products have a commercial value but they need to be further reacted and be transformed into usable products. Recently, new formulations of epoxy resin hardeners, called Recyclamines®, have been developed by Connora Technologies to obtain recyclable thermosets, which can be transformed into the readily usable thermoplastics. Key factor for recyclability was the production of hardeners modified with acid-cleavable groups.

4.3 Life cycle assessment (LCA) method and models

4.3.1 Description of LCA method

The life cycle assessment (LCA) methodology is considered the most widespread technique for evaluating the environmental impacts associated with material products

(Bovea and Vidal, 2004). LCA is a cradle-to-grave assessment of a product or service that analyses the impact of any product over a lifetime from the extraction of raw materials to the waste disposal of their various components. LCA is focused on studying the whole product system, as it is not only studying one single process but also the complete chain of production and lifetime.

An LCA includes the following main important steps: materials extraction, manufacturing and waste production, packaging, transportation, product use and product disposal. To calculate the amount of emissions and waste created during the life cycle of a product, much fundamental information is needed on manufacturing processes, materials and energy use. A life cycle inventory (LCI) is therefore compiled to record the emissions and resources consumed that can be attributed to a specific product. Databases have been developed that enable the user to input new information or data specific to their products and processes. Ecoinvent v3 (http://www.ecoinvent.org/database/) is probably the most comprehensive international LCI database. The Ecoinvent database is included in most LCA software models. Some softwares suitable for LCA of plastics are listed (O'Neill, 2003):

1. SimaPro, Pre Product Ecology Consultants, Amersfoort, Netherlands, www.pre.nl/simapro/
2. Boustead, Boustead Consulting Ltd, West Grinstead, United Kingdom, www.boustead-consulting.co.uk
3. Gabi, Polymer Institute University of Stuttgart http://www.pe-product.de/GABI/htdoc/home_englisch.htm
4. Umberto, Institute for Environmental Informatics, Hamburg, www.umberto.de/english/

LCA is governed by specific standards from the International Organization for Standards (ISO). The LCA study consists of defining the scope and goal, inventory analysis, assessing the impact and interpreting the data. ISO 14040 (2006) and ISO 14044 (2006) Environmental Management LCA provides the principles, framework, requirements and guidelines to conduct an LCA study. The impact stage involves using the inventory analysis results to come to relevant midpoint and endpoint indicators. Midpoint indicators might include acidification, radiation, climate, fossil fuel, ecotoxicity, etc. Endpoint indicators can include respiratory diseases, seawater level, resource depletion, etc.

4.3.2 Environmental impact assessment methods

A wide range of Life Cycle Impact Assessment (LCIA) methodologies has been developed, based on midpoint and/or endpoint indicators (ILCD Handbook, 2010):

- *CML 2002* (Guinée et al., 2002)
- *Eco-Indicator 99* (Goedkoop and Spriensma, 2000)
- *EDIP (1997–2003)* (Wenzel et al., 1997; Hauschild and Wenzel, 1998; Potting and Hauschild, 2005)
- *EPS2000* (Steen, 1999a,b)

- *Impact 2002+* (Crettaz et al., 2002; Jolliet et al., 2003; Payet, 2004; Pennington et al., 2005, 2006; Rochat et al., 2006; Rosenbaum, 2006; Rosenbaum et al., 2007)
- *LIME* (Itsubo et al., 2004; Hayashi et al., 2000, 2004, 2006)
- *LUCAS* (Toffoletto et al., 2007)
- *ReCiPe* (De Schryver et al., 2009; Huijbregts et al., 2005a,b; van Zelm et al., 2007a,b,c; Wegener Sleeswijk et al., 2008)
- *Swiss Ecoscarcity or Ecological scarcity* (Brand et al., 1998; Müller-Wenk, 1994; Ahbe et al., 1990; Frischknecht, 2006a,b)
- *TRACI* (Bare, 2002; Bare et al., 2003; Hertwich et al., 1997, 1998, 1999, 2001; Norris, 2002)
- *MEEuP methodology* (Kemna et al., 2005).

4.3.3 Environmental impact classification factors

The environmental issues analysed in an LCIA are called environmental impact classification factors as outlined in ISO/TR 14047 (2003). A brief description is provided:

1. Acidification Potential (AP) is a consequence of acids being emitted to the atmosphere and subsequently deposited in surface soils and waters. AP classification factors are mainly based on the contributions of SO_2, NO_x, HCl, NH_3 and HF and expressed as SO_2 equivalent.
2. Aquatic Toxicity Potential is calculated based on the maximum tolerable concentrations of different toxic substances in water by aquatic organisms.
3. Human Toxicity Potential is calculated in kg and takes into account the releases of materials toxic to humans in air (A), water (W) and soil (S) based on the human toxicological factors.
4. Eutrophication Potential (EP). Eutrophication is referred to the pollution state of aquatic ecosystems in which the over-fertilization of water and soil has turned into an increased growth of biomass. EP is calculated in kg based on a weighted sum of the emission of nitrogen and phosphorus derivatives such as N_2, NO_x, NH_4^+, PO_4^{3-}, P and chemical oxygen demand. The classification factors for EP are expressed as phosphate equivalents.
5. Global Warming Potential (GWP) is calculated for each different greenhouse gas (GHG) which are: CO_2, N_2O, CH_4 and volatile organic compounds (VOCs). GWP is expressed as CO_2 equivalent.
6. Nonrenewable/Abiotic Resource Depletion Potential is calculated for fossil fuels, metals and minerals by dividing the quantity of resource used by the estimated total world reserves of that resource.
7. Ozone Depletion Potential represents the potential of depletion of the ozone layer due to the emissions of chlorofluorocarbon compounds and other halogenated hydrocarbons.
8. Photochemical Oxidants Creation Potential. Photochemical smog is caused by the degradation of VOCs and nitrogen and is expressed in kg of ethylene.

Other factors such as land use and loss of biodiversity are considered in natural fibre production.

The output of the LCIA consists of a list of such category indicators; it does not provide an evaluation of actual environmental impact. All emissions are sorted into classes according to the effect they have on the environment. For example, chemicals that contribute to the greenhouse effect or to ozone layer depletion are divided between those two classes, whereas emissions such as nitrogen oxides may simultaneously belong to several classes, such as aquatic toxicity, acid rain and eutrophication. This is called Classification. The following step is called Characterization which means to assign and convert LCI results into numerical indicator results.

An example of output is shown in Table 4.3 (La Rosa et al., 2014a) that shows a comparative LCA between a traditional petroleum-based epoxy resin and a bio-derived epoxy resin.

Table 4.3 **Potential environmental impacts associated to 1 tonne of petroleum-based epoxy resin and 1 tonne of plant-derived SuperSap Entropy resin**

Impact Category	Units	Petroleum based-epoxy resin[a]	SuperSap entropy[b]
Abiotic depletion	kg Sb eq	59.4	0.01
Acidification potential	kg SO_2 eq	40.3	25.44
Eutrophication potential	kg PO_4 eq	6.6	6.9
Global warming potential	kg CO_2 eq	6663	4079
Ozone layer depletion potential	kg CFC-11 eq	1.26E-6	0.00
Human toxicity potential	kg 1.4-DB eq	490.44	545.17
Freshwater aquatic ecotoxicity potential	kg 1.4-DB eq	246.5	66.39
Terrestrial ecotoxicity potential	kg 1.4-DB eq	29.1	228.63
Cumulative energy demand	MJ eq	2.16	1.90

[a] Environmental impact results obtained using data from Ecoinvent v2 database.

[b] Environmental impact results purchased by Entropy resin.

In this study, the Simapro software and the CML 2002 impact assessment model were used, but other softwares (e.g. GaBi) and other impact assessment methods (e.g. Recipe; Impact 2002+) are suitable for biopolymers.

4.4 LCA of biopolymers

4.4.1 Data for the LCA of biopolymers

It is difficult to perform a comprehensive LCA for biopolymers. The main limit of the LCA methodology is data uncertainty. Existing databases for polymers and biopolymers are still uncertain and need to be continually updated and corrected. Data uncertainty also derives from the fact that studies are carried out on regional sites and the results are to some extent subject to country-specific circumstances (e.g. GHG emissions from national power production). On the other hand, the uncertainties related to conclusions can be reduced if several independent analyses for different countries arrive at similar conclusions. Despite growing interest in biopolymers and their generally simply presumed ‘eco-image’, there are still few concrete as well as testable and above all comprehensible values for assessing the life cycles of these polymer materials. The manufacturing paths, sometimes even the raw materials used, as well as the formulations of biopolymer materials are very different. Their published data are also often based only on semi-industrial or even laboratory-scale manufacturing conditions. The data provided by the few industrial manufacturers of biopolymers are too incomplete to do LCAs of industrially manufactured biopolymers.

A positive exception is represented by PLA, thanks to the effort made by Nature Works in providing the inventory data. Data for PLA are available in the Ecoinvent v3 database and an output for the manufacture phase is reported in Figure 4.4. The diagram was obtained using the Simapro 8.1. The percentage numbers reported at the bottom of each box, on the left side, are referred to the percentage of GWP. A consistent impact is associated with the corn-cropping step. Consequent impacts on land occupation, eutrophication and other categories will be discussed later in this chapter.

4.4.2 Comparison of LCA of biopolymers and conventional polymers

When different impact categories are compared for biopolymers and conventional plastics in an LCA, the biopolymers exhibit slight environmental advantages in most categories as reported by Endres and Siebert-Raths (2012) (Figures 4.4 and 4.5). Only with regard to land use, which is not relevant for conventional petro-based polymers, biopolymers clearly show higher ecological impact (Figure 4.6).

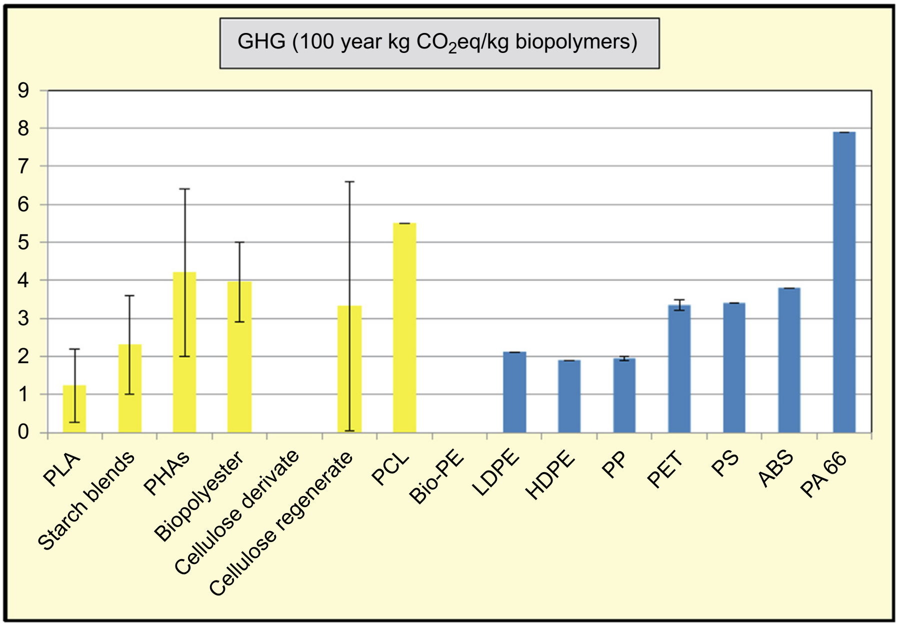

Figure 4.4 Greenhouse gas (GHG) emissions for biopolymers compared with conventional plastics. PLA, polylactide; PHAs, polyhydroxyalkanoates; PCL, polycaprolactone; PE, polyethylene; LDPE, low-density polyethylene; HDPE, high-density polyethylene; PP, polypropylene; PET, polyethylene terephthalate; PS, polystyrene; ABS, Acrylonitrile butadiene styrene; PA 66, Polyamide 6,6.
Endres and Siebert-Raths (2012).

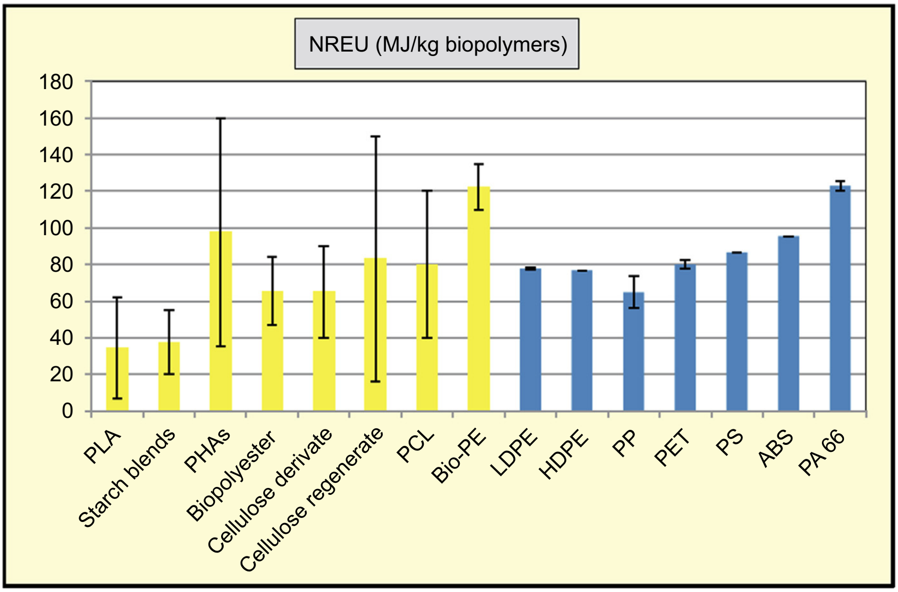

Figure 4.5 Energy input (nonrenewable energy use = NREU) for manufacturing biopolymers compared with conventional plastics. PLA, polylactide; PHAs, polyhydroxyalkanoates; PCL, polycaprolactone; PE, polyethylene; LDPE, low-density polyethylene; HDPE, high-density polyethylene; PP, polypropylene; PET, polyethylene terephthalate; PS, polystyrene; ABS, Acrylonitrile butadiene styrene; PA 66, Polyamide 6,6.
Endres and Siebert-Raths (2012).

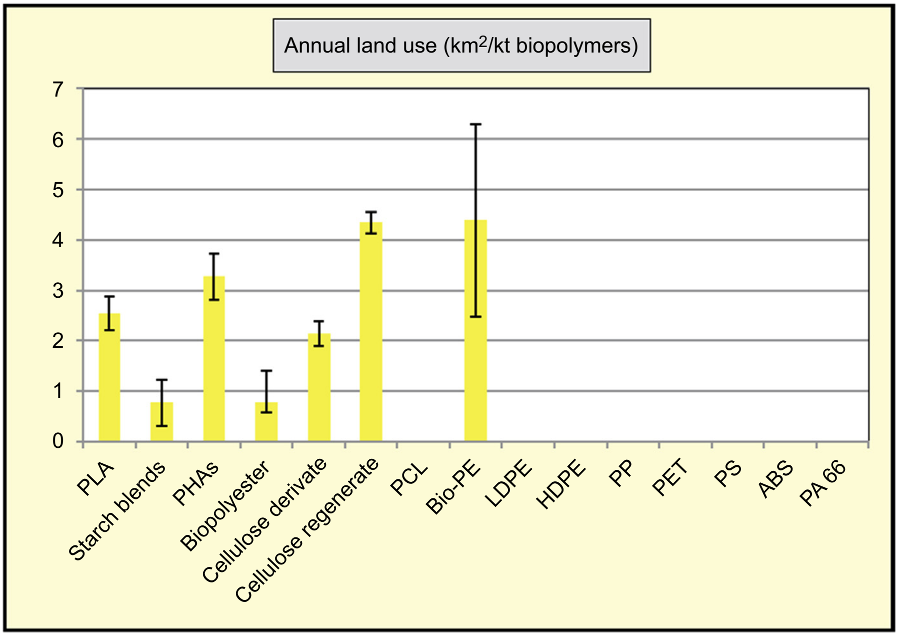

Figure 4.6 Land use for biopolymers compared with conventional plastics. See Figure 4.4 for definitions.
Endres and Siebert-Raths (2012).

Endres and Siebert-Raths (2012) stated that the biopolymers tend to emit somewhat fewer greenhouse-relevant gases and have lower energy inputs (see Figure 4.7). These advantages are due to their environmentally positive supply of renewable resources as polymer raw materials. However, when the processing energy for polymerization/polymer manufacture is involved, biopolymers usually exhibit no significant advantages over conventional plastics. For example, the fermentative manufacture of polyhydroxyalkanoate or polylactide corresponds almost exactly to that of PET. Both types require similar processing energy for so-called downstream processing to isolate and purify the polymer raw material or, in the case of PLA, for lactic acid. Hottle et al. (2013) found slightly different results when comparing the production phase of PLA with other petroleum-based polymers using the TRACI method (Figure 4.8). They state that there are environmental trade-offs between biopolymer and traditional polymer production. There are environmental impact categories, notably eutrophication, ozone depletion and noncarcinogenic human health, in which the biopolymers exhibit higher environmental impacts when compared to the petroleum-based plastics.

Similar results were found from the author of this chapter when comparing the cradle-to-manufacture phase of PLA and PP using the inventory data from the Ecoinvent v3. Table 4.4 reports the quantitative results assessed with the CML 2000 method and the Cumulative Energy Demand method. PLA shows more significant impacts for several impact categories than PP.

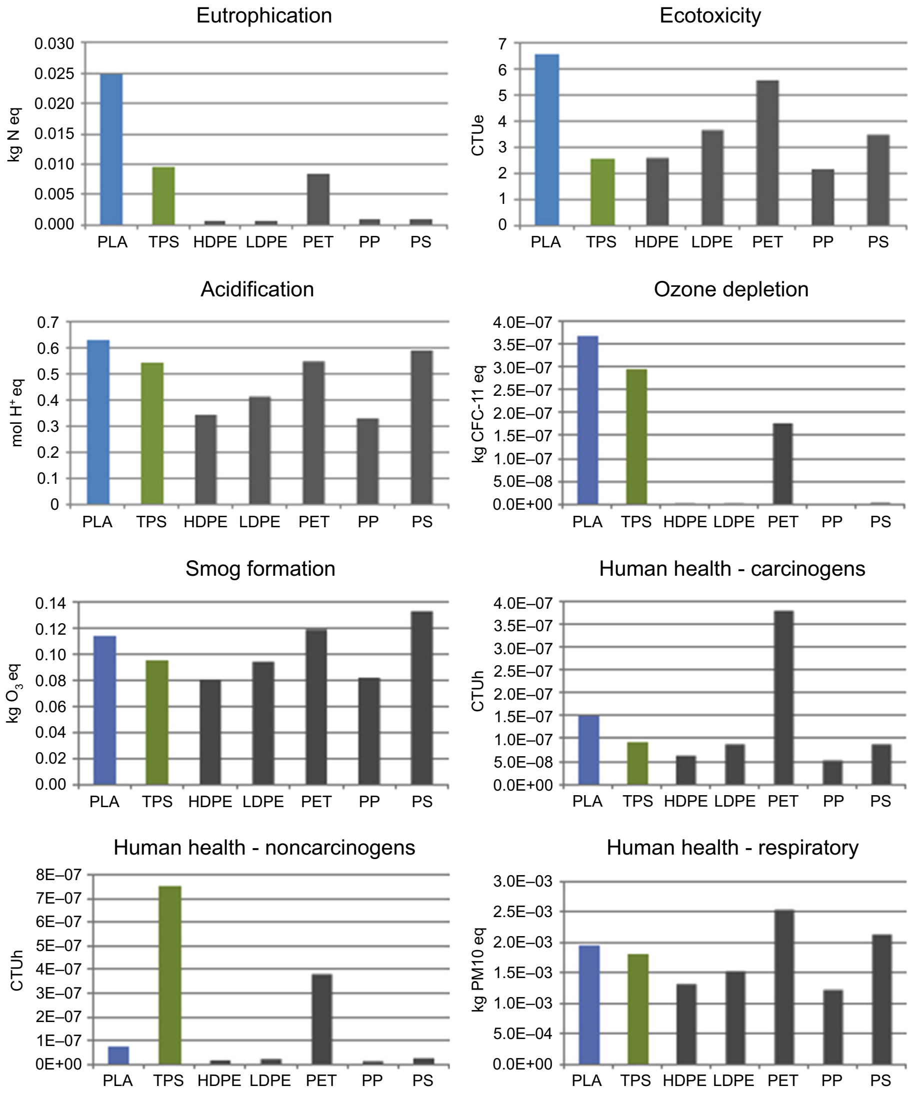

Figure 4.7 Life cycle environmental impacts of PLA and TPS compared to petroleum-based polymers per kg of granule (starch). PLA, polylactic acid; TPS, thermoplastic starch; HDPE, high-density polyethylene; LDPE, low-density polyethylene; PET, polyethylene terephthalate; PP, polypropylene; PS, polystyrene; CTUeq, Comparative Toxic Unit eco system; CTUh, Comparative Toxic Unit human health. Endres and Siebert-Raths (2012).
Data taken from Ecoinvent v2.2 and TRACI v2.00.

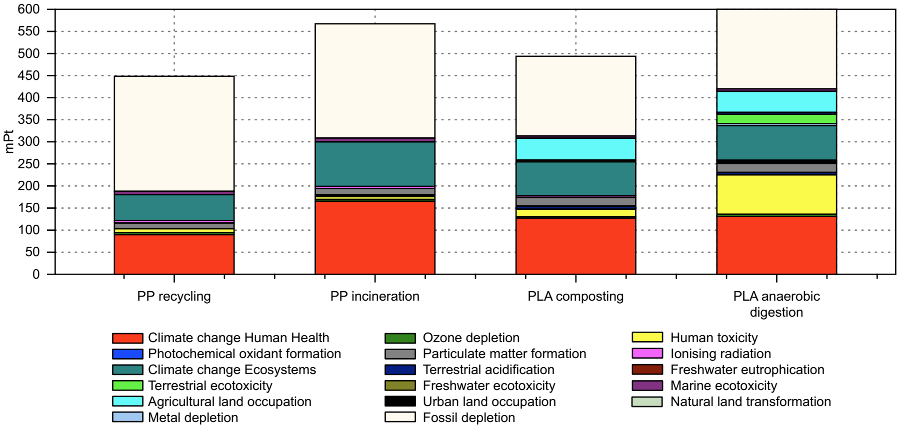

Figure 4.8 Comparison of four types of end of life of thermoplastic polymers: recycling, incineration, composting and anaerobic digestion.
Hottle et al. (2013).

For reliable statements based on LCA results, however, not only the phase of material manufacture should be considered, but also the use phase and the disposal to obtain a cradle-to-grave analysis. The end of life of biopolymers is expected to imply less burden compared to traditional polymers.

4.4.3 End of life of biopolymers

As already mentioned in Section 4.2.3, the great advantage of biodegradable polymers is that they can be composted or digested for biogas production on disposal, whereas traditional thermoplastics can last for a very long time without decomposing. On the other hand, traditional thermoplastic can undergo thermal recycling without losing the mechanical properties after several thermal cycles, whereas biodegradable polymers are yet not suitable for thermal recycles. In Figure 4.8, four different waste scenarios were evaluated and compared for thermoplastic polymers: recycling of PP, incineration of PP, composting of PLA and anaerobic digestion of PLA. As expected, incineration is the most impactive waste scenario. Recycling is only suitable for PP and not for PLA (because of its thermal degradability). According to Figure 4.8, not only does recycling seem to be the best option for petroleum-based thermoplastics, but it also creates fewer impacts than composting or digesting of PLA.

The advantage of PLA lies in the fact that the practice of recycling thermoplastics is not always easy because it involves changes in the society that are usually slow. The substitution of traditional packaging, that is up to now largely released in the environment, with biodegradable packaging (e.g. PLA), generates a reduction of impacts during the end of life.

For thermoset biopolymers, recycling is not yet suitable. Recently, new formulations of epoxy resin hardeners called Recyclamines® have been developed by

Table 4.4 **Comparative cradle-to-manufacture impacts associated with the production of 1 kg of PLA and 1 kg of PP**

Impact Category	Unit	PLA	PP
Abiotic depletion	kg Sb eq	0.03	0.04
Acidification	kg SO_2 eq	0.02	0.01
Eutrophication	kg PO_4 eq	0.01	0.00
Global warming (GWP100)	kg CO_2 eq	4.51	3.37
Ozone layer depletion (ODP)	kg CFC-11 eq	0.00	0.00
Human toxicity	kg 1.4-DB eq	2.06	0.76
Fresh water aquatic ecotoxicity	kg 1.4-DB eq	1.48	0.53
Marine aquatic ecotoxicity	kg 1.4-DB eq	2796	1071
Terrestrial ecotoxicity	kg 1.4-DB eq	0.03	0.01
Photochemical oxidation	kg C_2H_4 eq	0.001	0.001
Cumulative energy demand	MJ	109	105
Nonrenewable, fossil	MJ	63.62	91.91
Nonrenewable, nuclear	MJ	16.68	11.13
Renewable, biomass	MJ	25.91	1.13
Renewable, wind, solar, geothermal	MJ	0.30	0.13
Renewable, water	MJ	2.02	1.10

Connora Technologies, Inc., California, USA, to obtain recyclable thermosets, which can be dissolved in acetic acid and transformed into readily usable thermoplastics. A composite panel reinforced with CFs was analysed. A cradle-to-manufacture LCA was carried out of the recycling process at laboratory scale. Goal and scope of the study was the evaluation of the impacts related to the production and recycling of the recyclable thermoset-CF panel that was chosen as the functional unit. For the production phase, CF and Recyclamine are not available

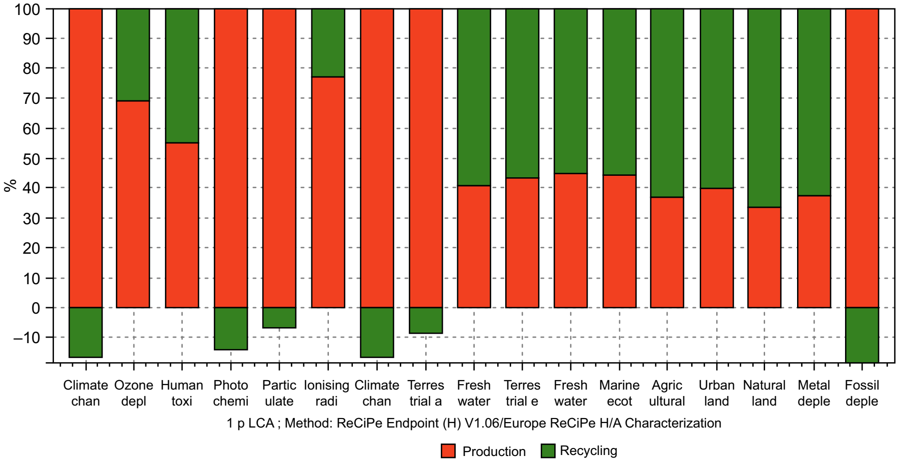

Figure 4.9 Recipe Endpoint output of the production phase (red) and recycling process (green) of a novel recyclable thermoset/carbon fibre composite.

in the Ecoinvent database; therefore, similar compounds were selected: CF was replaced by polyacrylonitrile (PAN) fibres and Recyclamine was replaced by diethanolamine. Primary data were collected at laboratory scale. Figure 4.9 shows an impact evaluation of the production phase (red) and recycling process (green) through the Recipe Endpoint. Avoided impacts, reported as negative values, were found for the abiotic depletion, acidification, GWP and cumulative energy demand of the recycling process due to the recovery of CFs and consequently to the avoided consumption of raw materials (PAN).

Consumption of electricity and acetic acid contribute to GWP, whereas a considerable amount of avoided CO_2 emission is associated with the avoided consumption of virgin PAN because of the recovery of CFs.

4.4.4 LCA case studies: biopolymers in the building sector

Several LCAs have been carried out to entire buildings (Sartori and Hestness, 2007). Most references show that a big contribution on the environmental impacts of buildings comes from their use phase, primarily due to water and energy use. Orientation, insulation, building operation, lighting, etc. are very important issues. Rossi et al. (2012) report that the phase with the highest environmental impact is the operation phase, representing approximately 62−98% of the life cycle total impacts, whereas the construction phase accounts for a total of 1−20% and the dismantling phase represents less than about 0.2−5%. Concerning the choice of materials for building applications, an optimum material solution should have the essential structural properties of concrete but with lower thermal conductivity. The reduced thermal conductivity is required to provide better thermal insulation and reduce energy consumption for cooling and heating in the use phase. Structural insulated panels are an example of energy-efficient building technology that is increasingly used for walls, partitions and flooring (Mullens and Arif, 2006). In a recent study, an eco-sandwich containing cork, plant-derived epoxy resin and flax fibre was proposed as a structural insulated solution for buildings (La Rosa et al., 2014b). Thermal conductivity was evaluated for cork (0.045−0.057 W/m K) and for the eco-sandwich (0.074−0.081 W/m K). The interesting result was that the thermal conductivity value obtained for the eco-sandwich was lower than for cement (0.9−1.5 W/m K). In the same paper, a comparative LCA method was applied to the manufacturing phase of four composite systems for building walls. The functional unit of the LCA study was defined as the material assembly used for the production of 1 m^2 of building walls with thermal transmittance $U \leq 0.46$ W/m^2 K (according to the Italian law).

The conclusion of the study was that materials with low thermal conductivity (e.g. the eco-sandwich) enable the application of relatively thin building envelopes, but the environmental impacts evaluated for the manufacture phase depend more on the type of materials used than on their weight. The system containing the eco-sandwich was the lightest but the environmental impact due to the epoxy resin was very high. Nevertheless, light walls and roofs have the advantage that they are easy to erect. Furthermore, when considering the building construction phase, lightweight systems could perform with lower impacts due to the minor energy needs both for material transportation and installation.

4.5 Future research trends and conclusion

The current bio-based industry focus is mainly on making bio-versions of existing petroleum-based monomers and polymers. Performance of these products is well known, and it is relatively easy to replace the existing product with similar performance of bio-versions. Renewable feedstocks used for manufacturing bio-based monomers and polymers often compete with requirements for food-based products. The expansion of first-generation bio-based fuel production will place unsustainable demands on biomass resources and is as much a threat to the sustainability of biochemical and biopolymer production as it is to food production (Michael et al., 2011). The European Commission has altered its targets downwards for first-generation biofuels since October 2012, indicating its preference for nonfood sources of sugar for biofuel production (EurActiv.com, 2012). Several initiatives are underway to use cellulose-based feedstocks for the production of usable sugars for biofuels, biochemicals and biopolymers (Jong et al., 2010). LCA methodology applied in the development of biopolymers is a relative new field, but it has already been widely used in many industrial sectors as a very useful tool to drive the choice of materials and processes towards a more sustainable production system. Several LCA applications to both traditional and biopolymers are making a great contribution in understanding advantages and disadvantages in the use of both bio- and fossil-based materials.

References

Ahbe, S., Braunschweig, A., Müller-Wenk, R., 1990. Methodology for Ecobalances Based on Ecological Optimization. BUWAL (SAFEL) Environment Series No. 133, Bern.

Babu, R.P., O'Connor, K., Ramakrishna, S., 2013. Current progress on bio-based polymers and their future trends. Progress in Biomaterials 2, 8. http://dx.doi.org/10.1186/2194-0517-2-8.

Bare, J.C., 2002. Developing a Consistent Decision-making Framework by Using the U.S. EPA's TRACI. Systems Analysis Branch, Sustainable Technology Division, National Risk Management; Research Laboratory, US Environmental Protection Agency, Cincinnati, OH.

Bare, J.C., Norris, G.A., Pennington, D.W., McKone, T., 2003. TRACI, the tool for the reduction and assessment of chemical and other environmental impacts. Journal of Industrial Ecology 6 (3−4). http://mitpress.mit.edu/journals/pdf/jiec_6_3_49_0.pdf.

Bax, B., Mussig, J., 2008. Impact and tensile properties of PLA/Cordenka and PLA/flax composites. Composite Science and Technology 68, 1601−1607.

Brand, G., Braunschweig, A., Scheidegger, A., Schwank, O., 1998. Weighting in Ecobalances with the Ecoscarcity Method − Ecofactors 1997. BUWAL (SAFEL) Environment Series No. 297, Bern.

Bovea, M.D., Vidal, R., 2004. Increasing product value by integrating environmental impacts, costs and customer valuation. Journal of Resources Conservation and Recycling 41, 133−145.

Crettaz, P., Rhomberg, L., Brand, K., Pennington, D.W., Jolliet, O., 2002. Assessing human health response in life cycle assessment using ED10s and DALYs: carcinogenic effects. International Journal of Risk Analysis 22 (5), 929−994.

De Schryver, A.M., Brakkee, K.W., Goedkoop, M.J., Huijbregts, M.A.J., 2009. Characterization factors for global warming in life cycle assessment based on damages to humans and ecosystems. Environmental Science and Technology 43 (6), 1689−1695.

Endres, H.J., Siebert-Raths, A., 2012. Engineering Biopolymers. Hanser Publishers, 20−22.

EurActiv.com., 2012. EU Calls Time on First-generation Biofuels. http://www.euractiv.com/climate-environment/eu-signals-generation-biofuels-news-515496.

Frischknecht, R., Steiner, R., Jungbluth, N., 2006a. Methode der ökologischen Knappheit − Ökofaktoren 2006. ö.b.u. und Bundesamt für Umwelt, Bern.

Frischknecht, R., Steiner, R., Braunschweig, A., Egli, N., Hildesheimer, G., 2006b. Swiss ecological scarcity method: the new version 2006. In: Proceedings of the 7th International Conference on EcoBalance, Tsukuba, Japan, November 2006.

Goedkoop, M., Spriensma, R., 2000. Eco-indicator 99, a damage oriented method for life cycle impact assessment. In: Methodology Report (Update April 2000).

Guinée, J.B., Gorrée, M., Heijungs, R., Huppes, G., Kleijn, R., de Koning, A., van Oers, L., Wegener Sleeswijk, A., Suh, S., Udo de Haes, H.A., de Bruijn, J.A., van Duin, R., Huijbregts, M.A.J., 2002. Handbook on life cycle assessment: operational guide to the ISO standards. In: Series: Eco-efficiency in industry and science. Kluwer Academic Publishers, Dordrecht (Hardbound, ISBN:1-4020-0228-9; Paperback, ISBN:1-4020-0557-1.

Hauschild, M.Z., Wenzel, H., 1998. Environmental Assessment of Products. In: Scientific Background, vol. 2. Chapman & Hall, United Kingdom, ISBN 0412 80810 2. Kluwer Academic Publishers, Hingham, MA, USA, 565 pp.

Hayashi, K., Itsubo, N., Inaba, A., 2000. Development of damage function for stratospheric ozone layer depletion − a tool towards the improvement of the quality of life cycle impact assessment. International Journal of Life Cycle Assessment 5 (5), 265−272.

Hayashi, K., Nakagawa, A., Itsubo, N., Inaba, A., 2006. Expanded damage function of stratospheric ozone depletion to cover major endpoints regarding life cycle impact assessment. International Journal of Life Cycle Assessment 11 (3), 150−161.

Hayashi, K., Okazaki, M., Itsubo, N., Inaba, A., 2004. Development of damage function of acidification for terrestrial ecosystems based on the effect of aluminum toxicity on net primary production. International Journal of Life Cycle Assessment 9 (1), 13−22.

Hertwich, E., McKone, T., Pease, W., 1999. Parameter uncertainty and variability in evaluative fate and exposure models. Risk Analysis 19, 1193−1204.

Hertwich, E.G., Pease, W.S., Koshland, C.P., 1997. Evaluating the environmental impact of products and production processes: a comparison of six methods. The Science of the Total Environment 196, 13−29.

Hertwich, E.G., Pease, W.S., McKone, T.E., 1998. Evaluating toxic impact assessment methods: what works best? Environmental Science and Technology 32, A138−A144.

Hertwich, E.G., Mateles, S.F., Pease, W.S., McKone, T.E., 2001. Human toxicity potentials for life cycle assessment and toxics release inventory risk screening. Environmental Toxicology and Chemistry 20 (4), 928−939.

Hottle, T.A., Bilec, M.M., Landis, A.E., 2013. Sustainability assessments of bio-based polymers. Polymer Degradation and Stability 98, 1898−1907.

Huijbregts, M.A.J., Rombouts, L.J.A., Ragas, A.M.J., Van de Meent, D., 2005b. Human-toxicological effect and damage factors of carcinogenic and non-carcinogenic chemicals for life cycle impact assessment. Integrated Environmental Assessment and Management 1 (3), 181−244.

Huijbregts, M.A.J., Struijs, J., Goedkoop, M., Heijungs, R., Hendriks, A.J., Van de Meent, D., 2005a. Human population intake fractions and environmental fate factors of toxic pollutants in life cycle impact assessment. Chemosphere 61 (10), 1495−1504. ILCD Handbook: Analysing of existing Environmental Impact Assessment methodologies for use in Life Cycle Assessment, European Union, 2010.

International Organization for Standardization ISO 14040, 2006. Environmental Management − Life Cycle Assessment − Principles and Framework. ISO 14000 International Standards Compendium, Switzerland.

International Organization for Standardization ISO 14044, 2006. Environmental Management − Life Cycle Assessment − Requirements and Guidelines. ISO 14000 International Standards Compendium, Switzerland.

ISO/TR 14047, 2003. Technical Report: Environmental Management − Life Cycle Assessment − Examples of Application of ISO 14042.

Itsubo, N., Sakagami, M., Washida, T., Kokubu, K., Inaba, A., 2004. Weighting across safeguard subjects for LCIA through the application of conjoint analysis. International Journal of Life Cycle Assessment 9 (3), 196−2005.

Jolliet, O., Margni, M., Charles, R., Humbert, S., Payet, J., Rebitzer, G., Rosenbaum, R., 2003. IMPACT 2002+: a new life cycle impact assessment methodology. International Journal of Life Cycle Assessment 8 (6), 324−330.

Jong, E.D., Higson, A., Walsh, P., Maria, W., 2010. Bio-based chemicals: value added products from biorefineries. In: IEA Bioenergy Task 42 Biorefinery, pp. 1−34. http://www.iea-bioenergy.task42-biorefineries.com/publications/reports/.

Kemna, R., van Elburg, M., Li, W., Van Holstein, R., 2005. MEEuP − The Methodology Report. EC, Brussels (Final version, Delft 28-11-2005).

La Rosa, A.D., Summerscales, J., Recca, G., Latteri, A., Cozzo, G., Cicala, G., 2014a. Bio-based versus traditional polymer composites. A life cycle assessment perspective. Journal of Cleaner Production 74, 135−144.

La Rosa, A.D., Gagliano, A., Summerscales, J., Latteri, A., Cozzo, G., Cicala, G., 2014b. Environmental impacts and thermal insulation performance of innovative composite solutions for building applications. Construction and Building Materials 55, 406−414.

La Rosa A.D., Cicala G., LCA of fibre-reinforced composites. In: Handbook of Life Cycle Assessment (LCA) of Textiles and Clothing. Woodhead Publishing Limited, in press.

Li, J., Xu, P.L., Zhu, Y.K., Ding, J.P., Xue, L.X., Wang, Y.Z., 2012. A promising strategy for chemical recycling of carbon fiber/thermoset composites: self-accelerating decomposition in a mild oxidative system. Green Chemistry 14, 3260−3263.

Majid, J., Elmira, A.T., Muhammad, I., Muriel, J., St'ephane, D., 2010. Poly-lactic acid: production, applications, nanocomposites, and release studies. Comprehensive Reviews in Food Science and Food Safety 9 (5), 552−571.

Michael, C., Dirk, C., Harald, K., Jan, R., Joachim, V., 2011. Policy Paper on Bio-based Economy in the EU: Level Playing Field for Bio-based Chemistry and Materials. www.bio-based.eu/policy/en.

Molgaard, C., 1995. Environmental impacts by disposal of plastic from municipal solid waste. Resources, Conservation and Recycling 15, 51−63.

Mullens, M.A., Arif, M., 2006. Structural insulated panels: impact on the residential construction process. Journal of Construction Engineering Management 132 (7), 786−794.

Müller-Wenk, R., 1994. The ecoscarcity method as a valuation instrument within the SETAC-framework. In: Udo de Haes, H.A., Jensen, A.A., Klöpffer, W., Lindfors, L.-G. (Eds.), Integrating Impact Assessment into LCA. SETAC-Europe, Brussels, pp. 115−120.

Netravali, A.N., Chabba, S., 2003. Composites get greener. Materials Today 6, 22−29.

Niaounakis, M., 2013. Biopolymers: Reuse, Recycling, and Disposal. http://dx.doi.org/10.1016/B978-1-4557-3145-9.00001-4.

Norris, G., 2002. Impact characterization in the tool for the reduction and assessment of chemical and other environmental impacts: methods for acidification, eutrophication, and ozone formation. Journal of Industrial Ecology 6 (3/4), 83−105.

O'Neill, T.J., 2003. Life cycle assessment and environmental impact of polymeric products. Rapra Review Report. ISSN: 0889-3144 13 (12), 156.

Payet, J., 2004. Assessing Toxic Impacts on Aquatic Ecosystems in LCA. Thesis 3112, Ecole Polytechnique Fédérale de Lausanne (EPFL, CH-1015 Lausanne).

Pennington, D.W., Margni, M., Amman, C., Jolliet, O., 2005. Multimedia fate and human intake modeling: spatial versus non-spatial insights for chemical emissions in Western Europe. Environmental Science and Technology 39 (4), 1119−1128.

Pennington, D.W., Margni, M., Payet, J., Jolliet, O., 2006. Risk and regulatory hazard-based toxicological effect indicators in life-cycle assessment (LCA). Human and Ecological Risk Assessment 12 (3), 450−475.

Pimenta, S., Pinho, S.T., 2011. Recycling carbon fibre reinforced polymers for structural applications: technology review and market outlook. Waste Management 31, 378−392.

Potting, J., Hauschild, M., 2005. Spatial Differentiation in Life Cycle Impact Assessment − The EDIP2003 Methodology. Environmental News no. 80. The Danish Ministry of the Environment, Environmental Protection Agency, Copenhagen.

Rochat, D., Margni, M., Jolliet, O., 2006. Continent-specific intake fractions and characterization factors for toxic emissions: does it make a difference? International Journal of Life Cycle Assessment 11, 55−63. Special issue 1.

Rosenbaum, R., 2006. Multimedia and Food Chain Modelling of Toxics for Comparative Risk and Life Cycle Impact Assessment. Thesis 3539, (Chapter 5) on uncertainties, Ecole Polytechnique Fédérale de Lausanne (EPFL, CH-1015 Lausanne).

Rosenbaum, R., Margni, M., Jolliet, O., 2007. A flexible matrix algebra framework for the multimedia multipathway modeling of emission to impacts. Environment International 33 (5), 624–634.

Rossi, B., Marique, A.F., Glaumann, M., Reiter, S., 2012. Life-cycle assessment of residential buildings in three different European locations, basic tool. Building and Environment 51, 395–401.

Sartori, I., Hestness, A.G., 2007. Energy use in the life cycle of conventional and low energy buildings: a review article. Energy and Building 39, 249–257.

Steen, B., 1999a. A Systematic Approach to Environmental Priority Strategies in Product Development (EPS). Version 2000-general System Characteristics. CPM report 1999:4. Chalmers University of Technology, Gothenburg, Sweden.

Steen, B., 1999b. A Systematic Approach to Environmental Priority Strategies in Product Development (EPS). Version 2000-Models and Data of the Default Method. CPM report 1999:5. Chalmers University of Technology, Gothenburg, Sweden.

Sun, X.S., 2013. Overview of plant polymers: resources, demands, and sustainability. In: Handbook of Biopolymers and Biodegradable Plastics. http://dx.doi.org/10.1016/B978-1-4557-2834-3.00001-X.

Toffoletto, L., Bulle, C., Godin, J., Reid, C., Deschênes, L., 2007. LUCAS – a new LCIA method used for a Canadian-specific context. International Journal of Life Cycle Assessment 12 (2), 93–102.

Wegener Sleeswijk, A., Van Oers, L., Guinée, J.B., Struijs, J., Huijbregts, M.A.J., 2008. Normalisation in product life cycle assessment: an LCA of the global and European economic systems in the year 2000. Science of the Total Environment 390 (1), 227–240.

Wenzel, H., Hauschild, M.Z., Alting, L., 1997. Environmental Assessment of Products. In: Methodology, Tools and Case Studies in Product Development, vol. 1. Chapman & Hall, United Kingdom, ISBN 0 412 80800 5. Kluwer Academic Publishers, Hingham, MA. USA, 544 pp.

van Zelm, R., Huijbregts, M.A.J., Harbers, J.V., Wintersen, A., Struijs, J., Posthuma, L., Van de Meent, D., 2007a. Uncertainty in msPAF-based ecotoxicological freshwater effect factors for chemicals with a non-specific mode of action in life cycle impact assessment. Integrated Environmental Assessment and Management 3 (2), 203–210.

van Zelm, R., Huijbregts, M.A.J., Van Jaarsveld, H.A., Reinds, G.J., De Zwart, D., Struijs, J., Van de Meent, D., 2007b. Time horizon dependent characterisation factors for acidification in life-cycle impact assessment based on the disappeared fraction of plant species in European forests. Environmental Science and Technology 41, 922–927.

van Zelm R., Reinds, G.J., Van Jaarsveld H.A., Huijbregts, M.A.J., 2007c. Environmental impacts of acidifying substances in life-cycle impact assessment. LCA Expertise Centre, RIVM, Bilthoven, The Netherlands.

Biotech admixtures for enhancing portland cement hydration

5

A. Vazquez[1,2], *T.M. Pique*[1,2]
[1]Instituto de Tecnología en Polímeros y Nanotecnología UBA/CONICET (ITPN), Buenos Aires, Argentina; [2]Facultad de Ingeniería, Universidad de Buenos Aires, Buenos Aires, Argentina

5.1 Introduction

Cement is the most common binder used worldwide with an annual consumption of 4180 million tons per year in 2014 (U.S. Geological Survey, 2015). Its low cost, easy application, and high compressive strength are the main reasons for its universal acceptance.

Mortar is a composite material that has a binder phase and sand. Hydrated cement, a product of the chemical reaction of cement and water, is the binder that coats the sand forming a rock-like solid. During the hydration reaction, the hydrated cement hardens and gains strength.

For decades, researchers have been working at improving hydrated cement's microstructure to improve its workability, strength, and especially its durability for making the material more environmentally friendly. This has been achieved by the incorporation of polymers into the mixture. Nowadays, several polymers used as admixtures are available for the construction material industry. It would be safe to say that every cement paste, mortar, or concrete that is now on the market has at least one admixture to enhance some specific property.

Admixtures are polymers added to the cement paste, mortar, or concrete mixture to optimize some specific property. They can accelerate or decelerate the cement paste hydration, make it more fluid with a low water-to-cement (w/c) ratio, and make it more viscous or more cohesive depending on the polymer added and its interaction with the cement paste. They can be bio-admixtures or synthetic admixtures. In many applications, bio-admixtures compete in the market with the synthetic ones, but in some applications, such as water-retention agents and viscosity-modifying agents, they are indispensable.

Bio-admixtures are molecules that include natural or modified biopolymers and biotechnological and biodegradable products. The most used are methyl hydroxypropyl cellulose, starch, guar gum, and many other polysaccharides in between.

It is expected that, due to technological advances, the bio-admixtures market will increase, especially for the microbial biopolymers, not only for their remarkable performance but also for the growing trend to use naturally based or biodegradable products in the construction materials industry (Plank, 2004).

Biopolymers and Biotech Admixtures for Eco-Efficient Construction Materials. http://dx.doi.org/10.1016/B978-0-08-100214-8.00005-1
Copyright © 2016 Elsevier Ltd. All rights reserved.

5.2 Portland cement hydration

The admixtures mentioned in this chapter act during one specific period of the cement hydration known as the dormant period. This happens before the hardening of the cement paste, when the cement paste has plastic behavior. The hardening of the cement paste is also known as setting. Before setting, the cement paste has no strength.

This period is the second of five periods that characterize the portland cement hydration process. These can be easily identified by studying the evolution of heat during hydration (Figure 5.1; Odler, 1998).

During the first minutes, when cement comes into contact with the mixing water, the alkaline sulfates and gypsum dissolve generating K^+, Na^+, Ca^{2+}, and SO_4^{2-} ions, creating a sulfate-rich environment. The tricalcium silicate (C3S) dissolves, but the silicon concentration remains low. Small sheets of calcium silicate hydrate (CSH) precipitate over the nonhydrated cement grains. Tricalcium aluminate (C3A) also dissolves and reacts with water forming a gel rich in aluminates. This gel would react with the sulfates in solution forming ettringite, which also precipitates over the anhydrous cement surface. During this stage, a large exothermic peak can be observed in the calorimetric curve.

During the first hours of hydration, the mix overcomes the so-called dormant period. This a key period of the cement paste because it delimits the period of time in which the paste can be manipulated without further altering its chemical structure. There are many theories about what happens during this period (Odler, 1998; Taylor et al., 1984; Brown et al., 1985; Jennings, 1986; Tadros et al., 1976; Young et al., 1977; Wu and Young, 1984). The rate of the reaction slows down. A layer of hydration products covers the anhydrous cement particles, separating the solution, or the concentration of ions near the surface reaches the theoretical solubility of nonhydrated products. The dormant period ends and the acceleration period begins when the nucleation of CSH begins.

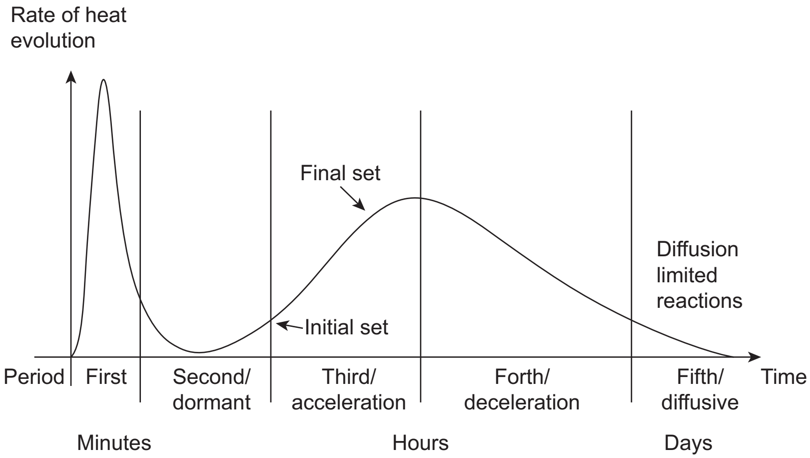

Figure 5.1 Schematic graph of cement heat evolution.

During the third period, or the acceleration period, the hydration reaction rate accelerates. The rate is controlled by the nucleation rate and the growth of the hydration products. Gypsum dissolves completely forming ettringite (AFt) and being absorbed in the CSH. More CSH is formed and $Ca(OH)_2$ precipitates.

Eventually, the amount of nonhydrated products diminishes, and the reaction begins to be controlled by chemical reactions and diffusion. This fourth period is called the deceleration period. The hydration of C3S and dicalcium silicate (C2S) continue and the amount of CSH keeps growing. When the solution does not have enough sulfates, AFt becomes monosulfate.

Finally, the process becomes completely diffusive, and then the hydration rate is very slow. The process will continue as long as water is available for the hydration products to react.

5.3 Biotech admixtures

5.3.1 Water-retention agents

5.3.1.1 Water-retention working mechanism

The working mechanism of the water-retention agents has been investigated. Desbrières (1993a,b) proposed three different working mechanisms for water retention in the case in which cement loses water to a substrate. It was first proposed that water retention was a result of increased viscosity. This would happen when the polymer is mixed with the cement paste. Increasing the viscosity of the cement paste could decelerate the filtration rate. It was also proposed that the polymer can be adsorbed on the particles of hydrated cement and then the permeability of the cement paste would be reduced. The last mechanism proposed was that water retention is a result of polymer film formation that would fill the cement pores. Then, the cement pores would be plugged, and no water loss could occur.

Patural et al. (2010a) studied the effects of the different cellulose ethers (CE) and starch ether (SE) used as admixtures in mortars. They determined the surface diffusion coefficient and the effect of the admixtures on the relative amount of water transiently present at the solid and growing interface. Their results showed that the larger the fraction, the better the water-retention capacity of the hydrated cement on mortar samples at the proximity of a solid support. They obtained that CEs had a higher water retention (98.9%) than the nonadmixed mortar (64.5%). They also studied the effect of hydroxyethyl/hydroxypropyl cellulose content and the molecular weight, but these facts had a slight effect on the water retention. Two different SEs were compared. SE with higher molecular weight produced higher water retention (92.6%) than the low-molecular-weight (66.2%) starch ether.

In different research, Patural et al. (2010b) studied the CE effect on the self-diffusion coefficient of water in solution and on the water mobility between fresh cement pastes. They used nuclear magnetic resonance to measure the CE mobility and the effect of CE and physicochemical parameters like molecular weight, substitution degrees, etc. on water retention of CE-modified cement paste and mortars. This led to the conclusion that the water loss is driven by capillary suction more than by the diffusion mechanisms at the mortar/unsaturated substrate interface. It is well known that the capillary suction depends on the substrate pore size and interface tension, as well as fluid viscosity. They suggested that the rheological properties of the aqueous CE solutions may be the key properties for water retention.

Afridi et al. (1995) established that an admixture with high molecular weight contributes to the increase of the water-retention capacity of mortars. However, Pourchez et al. (2006a) established that the molecular weight is not the only parameter affecting the water retention mechanism and suggested that other parameters, such as the porous network, should be examined.

Regarding this information, Bülichen and Plank (2011, 2012) studied the water-retention mechanism cement for hydroxyethyl cellulose (HEC), carboxymethyl hydroxyethyl cellulose (CMHEC), and hydroxyethylmethyl cellulose (MHEC). For the three CEs, they established that the working mechanism relies on two separate effects. For small dosages, there is the water-sorption capacity of the polymer in the case of the MHEC or of the additives to the polymer for the cases of HEC and CMHEC that present no water adsorption whatsoever. Then, for higher dosages, after an "overlapping concentration," there would be formation of hydrocolloid-associated polymer networks that would physically plug the cement pores, notoriously decreasing the permeability. Then, the main mechanism of water retention presents after this "overlapping concentration," whereas below it, water retention happens due to sorption of water on the cement matrix. This is shown as an example in Figure 5.2 for different concentrations of MHEC. The example shows different temperatures as the research was focused on fluid-loss additives for oil-well cement.

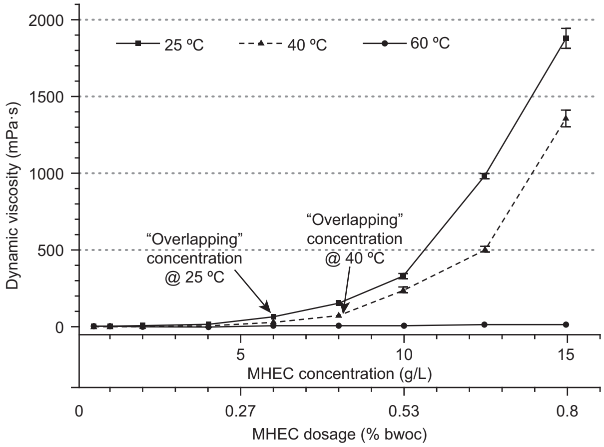

Figure 5.2 Dynamic viscosity of cement pore solutions containing methyl hydroxyethyl cellulose (MHEC) as a function of polymer concentration/dosage and temperature (Bülichen et al., 2012).

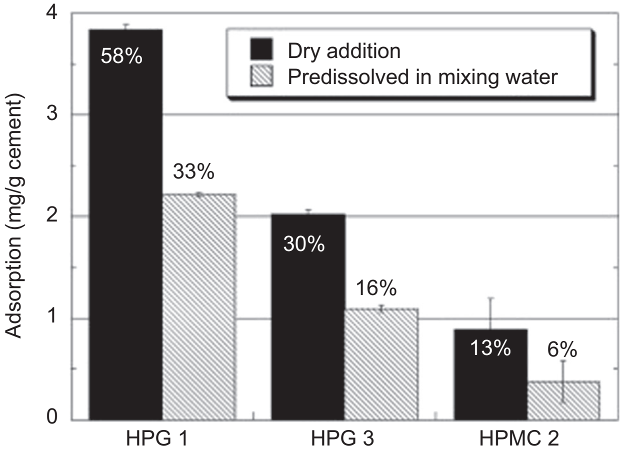

Figure 5.3 Impact of predissolution on the amount of admixture adsorbed on cement (Poinot et al., 2015).

Poinot et al. (2015) studied the polysaccharide addition to fresh mortar in two procedures: as a powder and as a solution in the mixing water. The authors used three types of polymers with different chemical structures in such a way that they exhibited strong (hydroxypropyl guar (HPG1)), medium (HPG3), and slight (hydroxypropyl methyl cellulose (HPMC2)) predissolution effects regarding cement hydration kinetics. The adsorption degree increased with the pre-dissolution property (Figure 5.3).

The authors considered that this phenomenon can be a consequence of polymer dissolution kinetics and adsorption ability of the polymer competing with the hydration kinetics. The state of the polymer, predissolved or in powder-form, determined the amount of polymer present in pore solution, which shifted the boundary between dilute and semidilute solution states and influenced the mortar properties. Figure 5.4 shows the scheme of the representation of polysaccharide-cement interaction regarding the method of addition.

5.3.1.2 Microcrystalline cellulose and cellulose derivatives

Biopolymers have been used as water-retention agents for cement mortars since the 1970s, when CE was first used in the dry-mix mortar industry (Plank, 2005). CEs are derivatives of polysaccharides, polymers that can modify cement mortar and concrete and act as water reducers, set retarders, anti-washout, and water-retention agents (Ramachandran, 1995). These polysaccharide derivatives are polymers capable of improving the water retention and workability of fresh mortar and concrete and enhance its adhesive strength to different substrates (Bertrand et al., 2004).

Cellulose is the most abundant polysaccharide in nature and is extensively used in the construction industry thanks to its nontoxic character and interesting

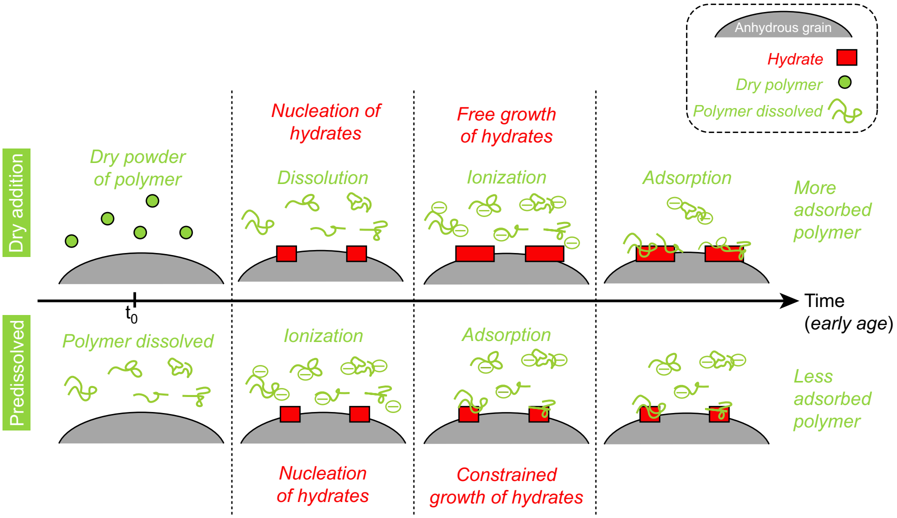

Figure 5.4 Schematic representation of the polysaccharide—cement interaction regarding the method of addition (reference Figure 11 Poinot et al., 2015).

water-retention ability in cement mortars. Neat cement pastes often suffer from hydric stress, such as evaporation, filtration under pressure, and water loss to the substrate. To compensate this, water-retention agents are added so that the calculated amount of water remains in the cement paste, and the w/c ratio does not change. Then water is retained in the fresh material, which favors cement hydration and increases the mechanical strength of the hardened material.

Adding microcrystalline cellulose (MCC), Gómez Hoyos et al. (2013) showed that the hydration degree affected the ability of interaction between the MCC, hydration products, cement particles, and water and promoted the formation of a waterproof barrier on the anhydrous particles of cement. Those interactions delayed the hydration reaction and decreased the maximum adiabatic temperature. Hydration kinetics and their relation to the microstructure and mechanical properties of cement-based materials were studied. The effect of MCC on the mechanical properties of cement mortars with 0 and 3 wt% of MCC was evaluated by flexural and compression tests. Results showed that the addition of MCC decreases the workability due to its hydrophilic character and water-retention capability.

CE also prevents the drain of water due to the highly porous unsaturated substrate (Patural et al., 2010a,b). The most used CEs in the construction industry are methyl cellulose (MC), HPMC, MHEC and CMHEC (Plank, 2004; Patural et al., 2010a,b; Desbrières, 1993a,b; Bülichen and Plank, 2012).

Cellulose is insoluble in water. It has a linear homopolymer form and consists of anhydroglucose units with β-1.4 linkages with strong intra- and intermolecular interactions via hydrogen bonds. By the substitution of anhydroglycose units, cellulose can become a water-soluble polymer. For MC, HPMC, MHEC and CMHEC,

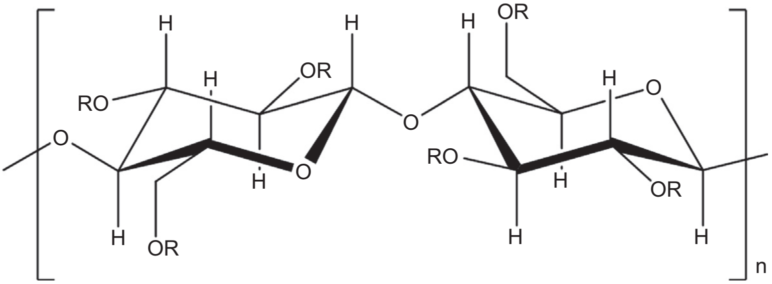

Figure 5.5 Structure of water-soluble cellulose derivatives ($R = H$ for cellulose and $R = H$, ($-CH_3$), ($-CH_2-CH_2OH$), ($-CH_2-CHOHCH_3$), or ($-CH_2-COOH$) for methyl cellulose, hydroxyethylmethyl cellulose, hydroxypropylmethyl cellulose, or carboxymethyl hydroxyethyl cellulose, respectively).

these groups are substituted by methyl, hydroxypropyl, hydroxyethyl, and carboxymethyl groups (Figure 5.5).

The difference between MCC and cellulose is that the cellulose is a polymer with repetitive unit (*n*); however, the MCC is a higher hierarchical structure with a fiber structure (Figure 5.6). MCC is not soluble in water, and it is used as a suspension of MCC in water, and the derivative cellulose can be soluble in water. MCC can act as heterogeneous nuclear agent of the cement hydration products, but not the polymer because it is liquid.

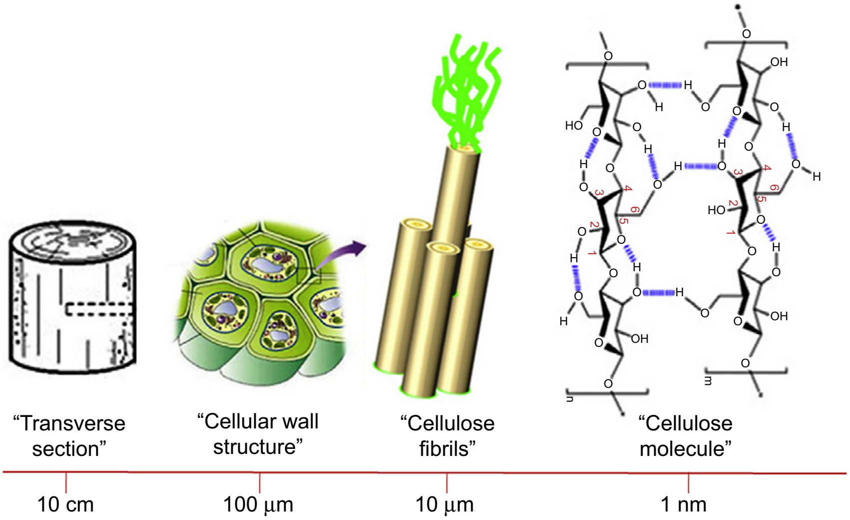

Figure 5.6 Hierarchical structure of MCC and cellulose polymer.

5.3.1.3 Water-retention agents and the hydration delay

Hydration delay is an undesired and uncontrolled secondary effect induced by some water-retention agents such as some biopolymers. Pourchez et al. (2006a,b,c) highlighted various delays on cement hydration induced by CEs (from 10 min up to several hours). Pourchez et al. (2006a, 2010) characterized HPMC, MHEC and HEC in terms of water retention. They dealt with the influence of their molecular parameters on cement hydration. They concluded that the degree of substitution is the most relevant factor in cement hydration kinetics, contrary to the molecular weight that has almost no influence on the retardation effect. This means that the concentration of the hydroxyethyl group determines the delay of cement hydration.

Weyer et al. (2005) studied the hydration kinetics by synchrotron x-ray diffraction (XRD). They saw that the lower the DS (DS = average number of substituted OH-groups per anhydroglucose unit), the stronger the delay of the hydration on the silicon phases. In addition, portlandite ($Ca(OH)_2$ or CH) precipitation is strongly DS dependant, so much that with high DS values, its formation can be inhibited.

5.3.2 Viscosity modifiers

New types of cement-based mortars and concretes require new admixtures. In the last decade, self-compacting concretes and cement grouts have been used for an increasing number of structural purposes. Self-compacting grouts and concretes are materials able to flow and consolidate under their own weight and fill formwork while maintaining homogeneity and without the need of any compaction. Łaźniewska-Piekarczyk (2013) showed that these type of cement mortars have very good deformability and high resistance to segregation. Self-compacting is usually the result of the combined use of super plasticizers and viscosity modifying admixtures that contribute to securing the high performance of highly fluid, yet cohesive, cement pastes. Thanks to these properties, the mixes are pumpable and have the ability to penetrate voids and cracks. As grouts they are used for ground treatment, repair of concrete, reduction of rock or soil permeability, embedding of anchors and posttensioning, rock and oil-well grouting, and sealing radioactive waste repositories (Sonebi et al., 2013; Şahmaran et al., 2008). As concretes, they are mostly used in highly reinforced structures (Lachemi et al., 2004).

Viscosity modifying admixtures (VMA) are water-soluble polymers that improve cement-based system cohesion, stability, and ability to retain constituents in suspension (Sonebi et al., 2013; Lachemi et al., 2004; Isik and Ozkul, 2014).

5.3.2.1 Working mechanism of the viscosity modifiers

Viscosity modifiers increase the yield stress and plastic viscosity of cement-based materials, thus thickening the mixture to provide cohesion and prevent segregation. Thereafter, they are generally used with superplasticizers to ensure the low yield stress necessary for proper flowability. Then, their mode of action depends not only on the type of additive and its concentration but also on its interaction with the superplasticizer (Şahmaran et al., 2008). Either way, it is generally accepted that the mechanism behind the viscosity buildup is related to adsorption, association, and intertwining of the long-chain structures of the VMAs (Łaźniewska-Piekarczyk, 2013; Sonebi et al., 2013; Şahmaran et al., 2008; Lachemi et al., 2004; Isik and Ozkul, 2014; Sonebi, 2006; Saric-Coric et al., 2003; Pei et al., 2015).

The adsorption is of the polymer with the mixing water. The mixing water would bind via VMA and adhere to the periphery of water molecules, thus imbibing and fixing part of the mixing water and increasing the viscosity of the cement-based material. Due to the attractive forces between adjacent polymer chains they will intertwine and entangle limiting the motion of the water molecules and causing the formation of a gel-like structure with high viscosity. At low rates of shear and above a critical polymer concentration, the long intertwined and entangled chains will increase the viscosity. With high shear rates, as these polymers are usually shear-thinning, the intertwined chains would break and align along the direction of the flow, decreasing the viscosity (Sonebi et al., 2013; Şahmaran et al., 2008; Lachemi et al., 2004; Sonebi, 2006; Saric-Coric et al., 2003).

The VMAs with anionic charges, such as welan, diutan, and xanthan gum also bind the positively charged cement particles. This will develop attraction between VMAs and cement particles, increasing the viscosity even more (Sonebi, 2006; Pei et al., 2015).

The organic VMAs show almost no influence on early cement hydration, which is one of their most important aspects: they do not change any properties of the cement-based mixture, except its viscosity (Łaźniewska-Piekarczyk, 2013; Leemann and Winnefeld, 2007).

5.3.2.2 Cement-based material rheology

Cement-based materials are thixotropic, non-Newtonian viscous, yield-stress fluids. Although their rheology is quite complicated, it changes as the hydration process starts, and the apparent viscosity of the material continually evolves over short time scales. At the very beginning, flocculation and deflocculation processes dominate, which lead to rapid thixotropic (reversible) effects (Figure 5.7). For self-compacted concrete and grouts, it is sufficient to approach the material by controlling its yield stress (Hot et al., 2014; Roussel, 2006), because for this application it is the most relevant parameter to describe the ability of a material to fill, under its own weight, a formwork or mold. It is accepted that the yield stress finds its origin in the colloidal interaction network between cement particles, which is amplified by the presence of the rigid aggregates, if these are present in the mix, and can be modified by admixtures like plasticizers (Hot et al., 2014).

To guarantee the self-compacting property of cement-based materials, the yield stress should be the lowest. For this reason, high-range water reducers are used giving the mix very high flowability. However, when cement-based material is very fluid, there is a high risk of segregation and bleeding. This has to be controlled. According to Łaźniewska-Piekarczyk (2013), segregation and bleeding stability can be obtained

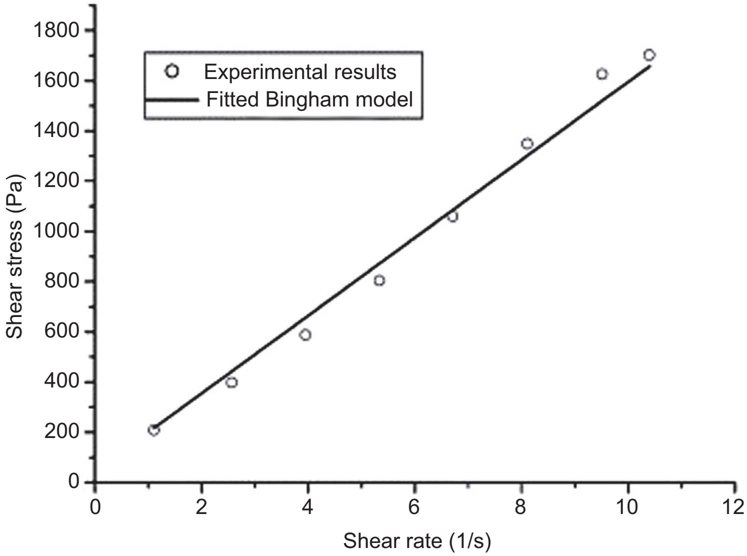

Figure 5.7 Shear stress as a function of shear rate at steady state for the concrete studied in this paper (Roussel, 2006).

in three different ways. First, formulating a mixture with a very high amount of fine material (<0.15 mm), usually in the range of 550–650 kg/m^3. Second, adding to the mixture a viscosity-modifier agent reduces the amount of fine material to 350–450 kg/m^3, and finally, it can be obtained by using a high amount of fine material (450–550 kg/m^3) and a lower dose of a viscosity-modifier admixture.

5.3.2.3 Most common viscosity modifiers

Viscosity modifying admixtures (VMA) commonly used in cement-based materials are high-molecular-weight, water-soluble organic polymers. Among these, the most commonly used are biopolymers such as polysaccharides of microbial sources: diutan gum, welan gum, and xanthan gum, or starch sources, cellulose derivatives such as hydropropyl methylcellulose and chitosan (Plank, 2004; Łaźniewska-Piekarczyk, 2013; Isik and Ozkul, 2014; Saric-Coric et al., 2003; Pei et al., 2015).

Diutan gum, welan gum, and xanthan gum are high-molecular-weight, microbial polysaccharides produced by aerobic fermentation (Plank, 2004; Isik and Ozkul, 2014; Sonebi et al., 2013; Pei et al., 2015).

Welan gum is a long-chain microbial biopolymer produced from glucose by bacteria from the *Alcaligenes* genus in aerobic fermentation. It has sugar backbones substituted with sugar side chains. It is efficient in maintaining high viscosity in alkaline solution with a high concentration of calcium ions even at high temperatures, which makes it useful for oil-well grouts. It has the ability of controlling segregation on highly fluid mixtures in very low dosages (0.01–0.1% by weight of cement) without affecting the final fluidity of the mixture (Plank, 2004).

The chain structure of diutan gum is different from welan gum. Diutan gum has two rhamnose side chains compared to welan gum that had only one rhamnose and one mannose. The molecular length of diutan gum is up to three times more than that of welan gum, and its molecular mass is higher.

Xanthan gum is also a bacterial polysaccharide obtained by aerobic fermentation. The molecular mass of xanthan molecules is very high. Similar to welan gum, xanthan is not significantly influenced by changes in the pH or temperature or by the addition of salts (Isik and Ozkul, 2014).

Starch-based VMAs consist of polysaccharides, such as amylase and amylopectin. Amylase consists of linear glucopyranose chains with very little branching and has a high molecular mass. These VMAs prevent bleeding and segregation of self-compacting concrete without affecting its ability to flow. (Isik and Ozkul, 2014).

Cellulose-based VMAs, such as hydropropyl methylcellulose (HPMC), were described in the previous section. When using these polymers as VMAs, special attention has to be given to the mixing energy. It was found that high mixing energy can destroy the bonds between the polymer chains, and a further alignment of them in the direction of flow can result in a reduction in the viscosity (Saric-Coric et al., 2003; Pei et al., 2015).

Chitosan is a biopolymer extracted from the exoskeleton of crustaceans such as crabs and shrimp (Sonebi, 2006; Pei et al., 2015). Its use as VMAs is limited because of their its high price.

5.3.3 Water reducers

Concrete's properties are usually characterized by its flowability and mechanical strength. Although flowability is mostly controlled by the dispersion of cement particles, mechanical strength is governed by the w/c ratio. Water reducers or plasticizers are used for two purposes: they can increase the dispersion of cement grains with a constant w/c ratio, resulting in better flowability of the cement-based material, or they can increase the flowability of cement-based materials with a low w/c ratio, thus improving the durability of the material and its mechanical strength (Ramachandran, 1995). Lately, normal- to high-quality concretes cannot be formulated without using a water-reducer admixture. They are actually known as the fifth component of concrete together with cement, fine and gross aggregates, and water (Ouyang et al., 2006).

The improvement in the rheological performance of cement-based materials with water reducers is generally attributed to the dispersion of agglomerated cement and hydrated cement particles. These agglomerates are formed during the mixing of cement with water, because of van der Waals attraction. The admixtures impart a stronger repulsive force at the surface–liquid interface overcoming the van der Waals forces, giving the water the ability to react with cement particles (Cheung et al., 2011).

These admixtures are not applied to modify the cement hydration; nevertheless, depending on their chemical composition or the interaction of the polymer with the cement phases, an alteration in the cement hydration kinetics might be observed. Water reducers frequently have some components that act like a set-retarding agent; then an adjustment of the hydration kinetics has to be done to satisfy industrial standards and field requirements. Cheung et al. (2011) numerated the factors that can influence the retardation as follows: cement chemical, mineralogical, and physical composition; the admixture chemistry; the behavior of the admixture with respect to sulfate availability during the cement hydration; the time when the admixture is added to the mixture; and the admixture dose.

In this section, different biopolymer-based water-reducer agents will be discussed and their influence in the hydration mechanism of cement will be explained.

5.3.3.1 Lignosulfonates

Lignosulfonate-based admixtures are the largest admixtures used, by volume, in the construction industry, typically used in dosages of 0.1−0.3% by weight of cement in concrete. They have been used as a water reducer in concrete for more than 70 years (Aitcin, 2000). They are low-cost plasticizers that can reduce up to 15% of the water content of a cement mixture. Although it is not in the range of the so-called super plasticizers or high range plasticizers, which can reduce approximately 40% of the water content, it is widely used, especially for ready-mix concrete. This area represents the largest application for lignosulfonates (Plank, 2004). These admixtures influence both the dispersion of the cement in the presence of water, and the hydration rate of single cement phases, becoming the most used water-reducing/retarding admixtures in the concrete industry (Danner et al., 2015).

The source of the admixture is lignin, a biopolymer contained at 20−30 wt% in wood (Plank, 2004). About 50% of the annually produced lignosulfonates are used as plasticizers in concrete. Pure lignin is a water-insoluble anionic surfactant obtained during wood pulping. Its surface activity may promote surface adsorption, foaming, and further particle dispersion (Ouyang et al., 2006). Sulfomethylation with sodium sulfite and formaldehyde is the most common process to obtain an optimized water-soluble lignosulfonate. It yields Na-lignosulfonates (NL) or Ca-lignosulfonates (CL) with a degree of sulfonation between 0.5 and 0.6. Lignosulfonates in solution have a wide range of molecular weights, and increasing its molecular weight usually increases the water-reducing capacity (Ouyang et al., 2006).

Unprocessed lignosulfonate may contain significant amounts of by-products such as sugars. Sugars are well known for their ability to retard the cement hydration. The role of sugar in the retarding effect of lignosulfonate is not yet fully explained. However, it is known that they are not the only factor responsible for the retarding action of lignosulfonate (Ramachandran, 1978).

Because of this, lignosulfonates have been also used as cement retarders for many years. It has been shown that they mostly affect the hydration kinetics of C3S, which extends the dormant period of cement hydration. When in contact with water, C3S forms CSH phases, which possess a negative surface charge. Ca^{2+} ions, which are abundantly present in the cement pore solution, immediately adsorb and form an ion layer on the surface of this CSH gel. However, when the mixture contains anionic lignosulfonates, these will adsorb onto this Ca^{2+} ion layer through their sulfonate and hydroxyl groups, thus coating the CSH phases with a less water-permeable layer. As a result, further hydration is slowed down by this waterproofing effect (Wang et al., 2012).

Danner et al. (2015) studied the influence of CL on the phase changes during the early hydration of cement by means of isothermal calorimetry, in situ XRD, and thermal analysis. In the presence of CL the overall hydration of cements was retarded, especially the silicate reaction. Portlandite's formation was also delayed and reduced in amount during the first 12 h. Ca-lignosulfonate (CL) was found to influence the solubility of the sulfate phase; in the case of gypsum, the initial dissolution was accelerated and the initial ettringite formation as well, whereas the dissolution of anhydrite seemed to be reduced. The second ettringite formation was retarded. The amount of bound water (H) was increased most likely due to accelerated ettringite formation (Danner et al., 2015).

CL retards the hydration of the aluminate phases (C3A and tetracalcium aluminoferrite (C4AF) between 5 and 60 min) and the silicate phases (C3S and C2S up to 30 days) (Lorprayoon and Rossingtoon, 1981). The retardation of C3S hydration by Ca- and Na-lignosulfonates is documented in several papers (Danner et al., 2015).

Wang et al. (2012) studied why using CL can lead to quick setting of cement mixtures containing anhydrite. The hydration characteristics of the C3A–anhydrite system in saturated CH solution with and without CL were studied. It was found that CL promotes the formation of ettringite, which induces a significant decrease in SO_4^{2-} concentration at the initial time of hydration. It was concluded that the quick set in the presence of CL is mainly caused by the accelerated reaction between the C3A and the anhydrite at the initial time of hydration (Wang et al., 2012).

Mollah et al. (2000) studied the influence of NL in the early stages of cement hydration by means of Fourier transform infrared spectroscopic technique. The results of these studies indicate that the NL prolongs the induction period and inhibits the hydration reaction, stabilizing and extending both the preinduction stage and the dormant stage to longer times, as well as the $Ca(OH)_2$ well into the fourth period (Mollah et al., 2000).

5.3.3.2 Starch and cellulose

Polysaccharides have been used to synthesize environment-friendly and renewable organic resource water-reducer agents (Zhang et al., 2007; Peschard et al., 2004). For this reason, starch and cellulose anionic derivatives have been investigated (Zhang et al., 2007; Peschard et al., 2004; Vieira et al., 2005).

These polymers can be equally classified as water reducers and set-retarding agents. They can be either native biopolymers (e.g., starch) or substituted polymers (e.g., CEs or starch sulfonate (SS)). Many authors have suggested that a blend of polysaccharides such as cellulose and starch could be a good water retention agent, but it has to be considered that these admixtures are also set-retarding agents, thus modifying cement hydration. Many investigations on water-reducing agents based on starch or cellulose (such as SS) have been carried out in the recent decades.

Zhang et al. (2007) studied the dispersing mechanism of SS and concluded that this water reducer is even better than the traditional naphthalene-sulfonated formaldehyde condensates (FDN). This would be because of its better dispersing capacity and stability. The dispersion capacity of SS is obtained from steric hindrance effects. The dispersions stabilized by steric hindrance, in this case by SS, have a good fluidity at low adsorption amounts (5 mg/g) and a high stability.

Polysaccharide derivatives show the disadvantage that their high molecular weight has as consequence a high viscosity, as explained previously; thus they are not appropriate to act as dispersing agents. Hence, Peschard et al. (2004) studied low-molecular-weight polysaccharides based on starch and cellulose, which act like water reducers, and their influence on cement hydration. They found out that even with low molecular weights, a small amount of polysaccharide (0.5% by weight of cement) induces a strong modification of cement hydration. The retarding effect depends on polysaccharide molecular structure; nevertheless, it was established that, generally, the action of polysaccharides on C3A hydration seems more restricted to the growth of hydrates than to nucleation. Consequently, the origin of retardation could be linked to an adsorption of admixtures on the first hydrates forming a less permeable coating on the cement particles. They established, like other authors, that the extent of retardation is higher for cement with low C3A content.

Vieira et al. (2005) studied also low-molecular-weight starch and cellulose anionic derivatives with the objective of obtaining new biodegradable dispersing agents. They also modified them chemically to obtain soluble in cold-water solutions with low viscosity. As a result, they showed that partially hydrolyzed and sulfoethylated amylomaize starch (containing 70% of amylose) provided the most efficient dispersing agent with dispersing ability comparable to polycarboxylate ethers and FDNs.

5.3.3.3 Casein

Casein is a biopolymer that is obtained by acid precipitation from milk. Its function as a cement admixture is traced back to ancient Rome. It is an outstanding water reducer with a plasticizing effect at low dosages and has good compatibility with other polymers such as retarders. Casein is a must in the formulation of self-leveling underlayers, a specific type of dry-mix cement mortar for flooring, because it provides a unique self-healing effect to the surface of the grout so that unevenness of the surface is corrected by itself. Casein has a group of different phosphoproteins, which account for approximately 80% of the total protein content of milk. The three major protein fractions are α-, β-, and κ-casein. The occurrence of these proteins differ depending on the cattle species, the food, and whether they were cattle lactates (Plank and Bian, 2010; Bian and Plank, 2013). Poor information about its working mechanism, and none of its interaction in cement hydration, suggests that

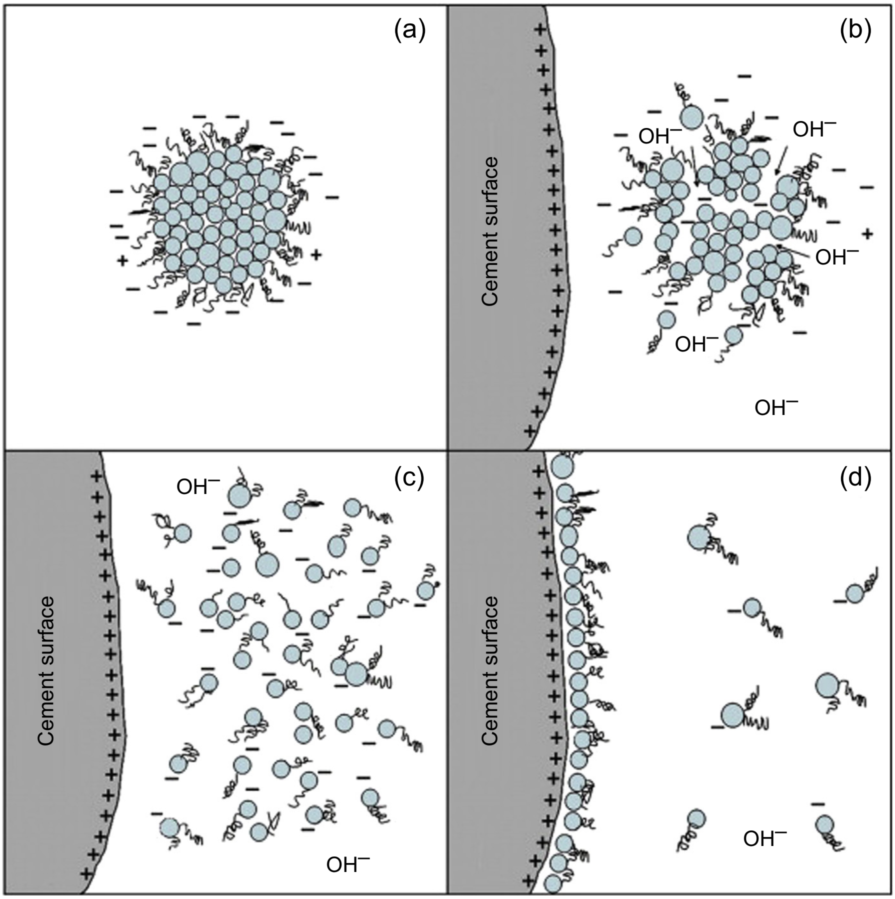

Figure 5.8 Proposed model for the interaction between casein biopolymer and cement. (a) Casein micelle exhibiting a negative surface charge from phosphate groups; (b) in the alkaline environment of cement pore solution, the micelle starts to disintegrate; (c) micelle dissociates into numerous submicelles; (d) some negatively charged submicelles adsorb onto positively charged cement surface, resulting in an adsorption equilibrium (Plank and Bian, 2010).

this biopolymer acts like a plasticizer without altering the hydration reaction. Plank and Bian (2010) suggested a model that is illustrated in Figure 5.8.

Winter et al. (2008) studied the influence of α-, β-, and κ-casein and characterized the single proteins with respect to their adsorption behavior on cement. They found that α-casein is the fraction responsible for the plasticizing effect of casein. It adsorbs on cement in high amounts, whereas β-casein shows medium and κ-casein the lowest adsorption. They established that casein micelles dissociate into submicelles of 10–20 nm in diameter. The size of the submicelles decreases with increased content of κ-casein. The smaller submicelles are supposed to show higher adsorption on the binder and consequently produce a better plasticizing effect (Plank and Bian, 2010).

5.4 Summary and future trends

The review was done in base of published papers on the subject. The effect of different biopolymers on water release, hydration delay, viscosity modification, and water reducers were discussed.

The mechanisms of hydration in the presence of each biopolymer proposed different authors were reviewed.

Each biopolymer influences usually in more than one property of the cement based materials; consequently, the optimal formulation can be a combination of different additives.

The future works in nanotechnology can contribute to improve cement based materials' properties and present different behaviors than the actual biopolymers. As examples, biopolymers can be modified with nanoparticles to produce different effects. Nanocellulose, nanochitosan, nanostarch, and their derivative products are new bio-materials for addition as cement admixtures.

References

Afridi, M.U.K., Ohama, Y., Zafar Iqbal, M., Demura, K., 1995. Water retention and adhesion of powdered and aqueous polymer-modified mortars. Cement and Concrete Composites 17 (2), 113−118.

Aitcin, P.C., 2000. Cements of yesterday and today, concrete of tomorrow. Cement and Concrete Research 30, 1349−1359.

Bertrand, L., Maximilien, S., Guyonnet, R., 2004. Wedge splitting test: a test to measure the polysaccharide influence on adhesion of mortar on its substrate. In: 11th International Congress on Polymers in Concrete. 2004. Berlin, Germany.

Bian, H., Plank, J., 2013. Effect of heat treatment on the dispersion performance of casein superplasticizer used in dry-mix mortar. Cement and Concrete Research 51, 1−5.

Brown, P., Pommersheim, J., Frohnsdorff, G., 1985. A kinetic model for the hydration of tricalcium silicate. Cement and Concrete Research 15 (1), 35−41.

Bülichen, D., Plank, J., 2012. Mechanistic study on carboxymethyl hydroxyethyl cellulose as fluid loss control additive in oil well cement. Journal of Applied Polymer Science 124, 2340−2347.

Bülichen, D., Kainz, J., Plank, J., 2012. Working mechanism of methyl hydroxyethyl cellulose (MHEC) as water retention agent. Cement and Concrete Research 42, 953−959.

Bülichen, D., Plank, J., 2011. Formation of colloidal polymer associates from hydroxyethyl cellulose (HEC) and their role to achieve fluid loss control in oil well cement. In: SPE International Symposium on Oilfield Chemistry. Texas, USA.

Cheung, J., Jeknavoriana, A., Roberts, L., Silva, D., 2011. Impact of admixtures on the hydration kinetics of Portland cement. Cement and Concrete Research 41, 1289−1309.

Danner, T., Justnes, H., Geiker, M.R., 2015. Phase changes during the early hydration of Portland cement with Ca-lignosulfonates. Cement and Concrete Research 69, 50−60.

Desbrières, J., 1993a. Cement cake properties in static filtration: influence of polymeric additives on cement filter cake permeability. Cement and Concrete Research 23, 347−358.

Desbrières, J., 1993b. Cement cake properties in static filtration. On the role of fluid loss control additives on the cake porosity. Cement and Concrete Research 1993 (23), 1431−1442.

Hoyos, C.G., Cristia, E., Vázquez, A., 2013. Effect of cellulose microcrystalline particles on properties of cement based composites. Materials & Design 51, 810−818.

Hot, J., Bey, H.B., Brumaud, C., 2014. Adsorbing polymers and viscosity of cement pastes. Cement and Concrete Research 63, 12–19.

Isik, I.E., Ozkul, M.H., 2014. Utilization of polysaccharides as viscosity modifying agent in self-compacting concrete. Construction and Building Materials 72, 239–247.

Jennings, H.M., 1986. Aqueous solubility relationships for two types of calcium silicate hydrate. Journal of the American Ceramic Society 69, 614–618.

Lachemi, M., Hossain, K.M.A., Lambros, V., Nkinamubanzib, P.-C., Bouzouba, N., 2004. Performance of new viscosity modifying admixtures in enhancing the rheological properties of cement paste. Cement and Concrete Research 34 (2), 185–193.

Łaźniewska-Piekarczyk, B., 2013. Effect of viscosity type modifying admixture on porosity, compressive strength and water penetration of high performance self-compacting concrete. Construction and Building Materials 48, 1035–1044.

Leemann, A., Winnefeld, F., 2007. The effect of viscosity modifying agents on mortar and concrete. Cement and Concrete Composites 29 (5), 341–349.

Lorprayoon, V., Rossingtom, D.R., 1981. Early hydration of cement constituents with organic admixtures. Cement and Concrete Research 11 (2), 267–277.

Mollah, M.Y.A., Yub, W., Schennach, R., Cocke, D.L., 2000. A Fourier transform infrared spectroscopic investigation of the early hydration of Portland cement and the influence of sodium lignosulfonate. Cement and Concrete Research 30 (2), 267–273.

Odler, I., 1998. Hydration, setting and hardening of Portland cement. In: Hewlett, P.C. (Ed.), Lea's Chemistry of Cement and Concrete. Arnold, London, 241–289.

Ouyang, X., Qiu, X., Chen, P., 2006. Physicochemical characterization of calcium lignosulfonate—a potentially useful water reducer. Colloids and Surfaces A: Physicochemical and Engineering Aspects 282–283, 489–497.

Plank, J., 2004. Applications of biopolymers and other biotechnological products in building materials. Applied Microbiol Biotechnology 66, 1–9.

Poinot, T., Bartholin, M.-C., Govin, A., 2015. Influence of the polysaccharide addition method on the properties of fresh mortars. Cement and Concrete Research 70, 50–59.

Patural, L., Marchal, P., Govin, A., Groisseau, P., Rout, B., Deves, O., 2010a. Cellulose ethers influence on water retention and consistency in cement-based mortars. Cement and Concrete Research 41 (1), 46–55.

Patural, L., Porion, P., Van Damme, H., Govin, A., Grosseau, P., Ruot, B., Devres, O., 2010b. A pulsed field gradient and NMR imaging investigations of the water retention mechanism by cellulose ethers in mortars. Cement and Concrete Research 40 (9), 1378–1385.

Pei, R., Liu, J., Wang, S., 2015. Use of bacterial cell walls as a viscosity-modifying admixture of concrete. Cement and Concrete Composites 55, 186–195.

Peschard, A., Govin, A., Grosseau, P., Guilhot, B., Guyonnet, R., 2004. Effect of polysaccharides on the hydration of cement paste at early ages. Cement and Concrete Research 34, 2153–2158.

Plank, J., 2005. Applications of biopolymers in construction engineering. Biopolymers Online 10.

Plank, J., Bian, H., 2010. Method to assess the quality of casein used as superplasticizer in self-levelling compounds. Cement and Concrete Research 40, 710–715.

Pourchez, J., Peschard, A., Grosseau, P., Guyonnet, R., Guilhot, B., 2006a. HPMC and HEMC influence on cement hydration. Cement and Concrete Research, Elsevier 36 (2), 288–294.

Pourchez, J., Govin, A., Grosseau, P., Guyonnet, R., Guilhot, B., Ruot, B., 2006b. Alkaline stability of cellulose ethers and impact of their degradation products on cement hydration. Cement and Concrete Research 36, 1252–1256.

Pourchez, J., Grosseau, P., Guyonnet, R., Ruot, B., 2006c. HEC influence on cement hydration measured by conductometry. Cement and Concrete Research 36 (9), 1777–1780.

Pourchez, J., Ruot, B., Debayle, J., Pourchez, E., Grosseau, P., 2010. Some aspects of cellulose ethers influence on water transport and porous structure of cement-based materials. Cement and Concrete Research 40 (2), 242−252.

Ramachandran, V.S., 1995. Concrete Admixtures Handbook, second ed. Noyes and Publications.

Ramachandran, V.S., 1978. Effect of sugar free lignosulfonates on cement hydration. Zement Kalk und Gips 31 (6), 144−146.

Roussel, N., 2006. A thixotropy model for fresh fluid concretes: theory, validation and applications. Cement and Concrete Research 36, 1797−1806.

Şahmaran, M., Ozkam, N., Keskin, S.B., Uzal, B., Yaman, I.O., Erdem, T.K., 2008. Evaluation of natural zeolite as a viscosity-modifying agent for cement-based grouts. Cement and Concrete Research 38 (7), 930−937.

Saric-Coric, M., Khayat, K.H., Tagnit-Hamou, A., 2003. Performance characteristics of cement grouts made with various combinations of high-range water reducer and cellulose-based viscosity modifier. Cement and Concrete Research 33 (12), 1999−2008.

Sonebi, M., Lachemi, M., Hossain, K.M.A., 2013. Optimisation of rheological parameters and mechanical properties of superplasticised cement grouts containing metakaolin and viscosity modifying admixture. Construction and Building Materials 38, 126−138.

Sonebi, M., 2006. Rheological properties of grouts with viscosity modifying agents as diutan gum and welan gum incorporating pulverised fly ash. Cement and Concrete Research 36 (9), 1609−1618.

Tadros, M., Skalny, J., Kalyoncu, R., 1976. Early hydration of tricalcium silicate. Journal of the American Ceramic Society 59, 344−347.

Taylor, H.F.W., Barret, P., Brown, P.W., Double, D.D., Frohnsdorff, G., Johansen, V.D., Ménétrier-Sorrentino, D., Odler, I., Parrott, L.J., Pommersheim, J.M., Regourd, M., Young, J.F., 1984. The hydration of tricalcium silicate. Materials and Structures 17 (6), 457−468.

U.S. Geological Survey, 2015. Mineral commodity summaries 2015. In: U.S. Geological Survey, U.S.D.O.T. Interior. U.S. Geological Survey, Reston, Virginia, p. 196.

Vieira, M.C., Klemm, D., Einfeldt, L., Albrechtet, G., 2005. Dispersing agents for cement based on modified polysaccharides. Cement and Concrete Research 35, 883−890.

Wang, X., Pang, Y., Lou, H., Deng, Y., Qju, X., 2012. Effect of calcium lignosulfonate on the hydration of the tricalcium aluminate−anhydrite system. Cement and Concrete Research 42 (11), 1549−1554.

Weyer, H.J., Müller, L., Müller, I., Schmitt, B., Bosbach, D., Putnis, A., 2005. Time-resolved monitoring of cement hydration: influence of cellulose ethers on hydration kinetics. Nuclear Instruments and Methods in Physics Research B 238, 102−106.

Winter, Ch., Plank, J., Sieber, R., 2008. The efficiencies of α-, β- and κ-casein fractions for plasticizing cement-based self leveling grouts. In: Calcium Aluminate Cements: Proceedings of the Centenary Conference. Avignon, France.

Wu, Z.-Q., Young, J., 1984. Formation of calcium hydroxide from aqueous suspensions of tricalcium silicate. Journal of the American Ceramic Society 67, 48−51.

Young, J., Tong, H., Berger, R., 1977. Compositions of solutions in contact with hydrating tricalcium silicate pastes. Journal of the American Ceramic Society 60, 193−198.

Zhang, D.-F., Ju, B.-Z., Zhang, S.-F., He, L., Yang, J.-Z., 2007. The study on the dispersing mechanism of starch sulfonate as a water-reducing agent for cement. Carbohydrate Polymers 70, 363−368.

Black liquor waste as a cement admixture or cement and concrete admixtures

6

H.H.M. Darweesh
National Research Center, Cairo, Egypt

6.1 Introduction

Progress in cement and concrete technology has been mostly achieved by the use of admixtures. Admixtures should be distinguished from additives or additions in that these materials are usually solids and added to the cement during its manufacture (Ramachandran, 1995; Vaysburd et al., 2000; Darweesh and Abo El-Suoud, 2014; Darweesh, 2014a,b). In the last two decades, interest in admixtures has increased along with developments in concretes, particularly to enhance their durability (Regourd and Mortureux, 1982; Vaysburd, 2001a,b; Oland and Baker, 2001; Pailere, 1995; Karim et al., 2012).

Admixtures may be regarded as active, interactive and passive materials. Active admixtures can react with the solubilized component of cement such as lime to produce a derivative that imparts the admixture effect and are not changed by these interactions, e.g. plasticizers and superplasticizers (Ohama, 1995; Ramachandran et al., 1998; Hewlett, 1998).

Passive admixtures do not change their form in passing into solution or remaining in suspension. Their contribution is mainly physical by molecular entanglement and solvent association in the case of viscosity modifiers, or simply light absorption and reflection in the case of pigments (Sonaka et al., 1997; Uchikawa et al., 1992).

The use of chemical admixtures to enhance the properties of fresh or even hardened concrete is a very common and well-accepted practice. In particular, superplasticizers are used to increase the workability of concrete at a given water/cement (w/c) ratio or to produce concrete at high w/c ratio and high compressive strength (Hewlett, 1998).

6.2 Air-entraining admixtures

Figure 6.1 shows some air-entraining admixtures. These admixtures include a group of surfactants which act at the air—water interface in the cement pastes, thereby stabilizing air entrapped during the mixing process in the form of tiny bubbles. They are characterized by a hydrocarbon chain or a backbone terminating in a hydrophilic polar group, typically a carboxylic or sulphuric acid group. The sequence is initiated by

Biopolymers and Biotech Admixtures for Eco-Efficient Construction Materials. http://dx.doi.org/10.1016/B978-0-08-100214-8.00006-3
Copyright © 2016 Elsevier Ltd. All rights reserved.

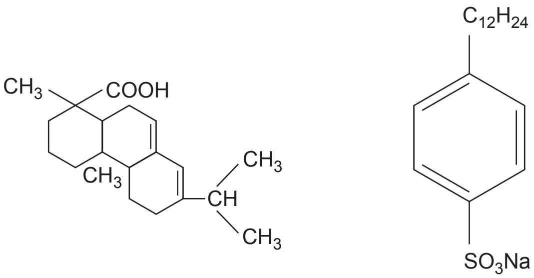

a-Abietic acid b-Sodium dodecylbenzene sulphonate

$CH_3—(CH_2)_7—CH{=}CH—(CH_2)_8—SO_4Na$

c-Sodium oleyl sulphate

$CH_3—(CH_2)_7—CH{=}CH—(CH_2)_7—COONa$

d-Sodium oleate

Figure 6.1 Some examples of air-entraining admixtures.

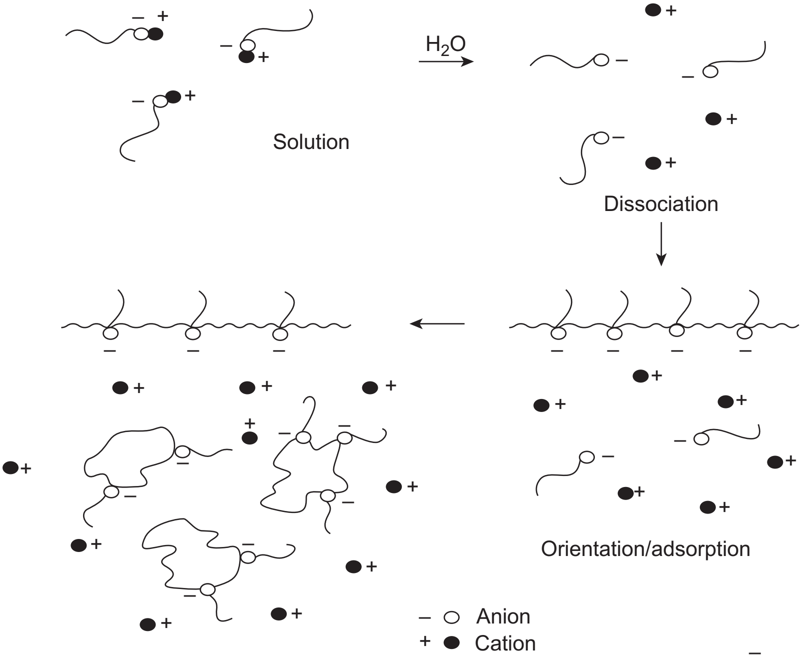

Figure 6.2 Surface activity and surfactant behaviour.
Darweesh et al. (2013).

dissolution and followed by orientation and adsorption (Figure 6.2). The ionized polar group becomes oriented into the aqueous phase, whereas the hydrocarbon chain orients into the air within the bubble (Figure 6.3). The surface tension of water is reduced, facilitating the formation of bubbles when the concrete or mortar is agitated. The

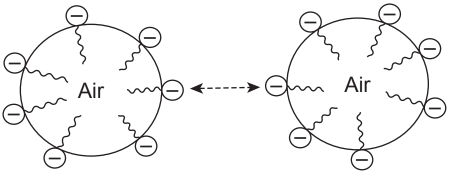

Figure 6.3 The orientation of surfactant on the surfaces of air bubbles. Darweesh et al. (2013).

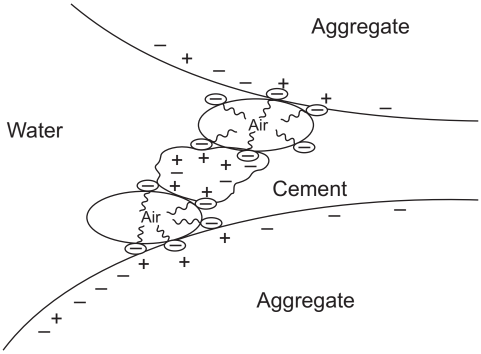

Figure 6.4 Air voids remain stable inside a concrete structure. Darweesh et al. (2013).

charged sheath of surfactants surrounding each air bubble leads to mutual repulsion. This prevents the coalescence into larger bubbles.

The surface charge causes the stabilized bubbles to adhere to the oppositely charged zones on cement and aggregate particles. The overall net effect is an aggregate—air—cement—air—aggregate type of bridge (Figure 6.4).

Such a system would permit relatively free motion in shear with the stabilized air bubbles acting like compressible bearings. Both cohesion and workability of the mix improve. When concrete admixtures are used to obtain water reduction, all types give rise to improvement of the mechanical strength, lower permeability and better freeze—thaw durability. The mechanism of action can be summarized as follows:

1. When the temperature drops below 0 °C, the liquid water converts to ice. Therefore, its volume increases by about 9%.
2. If this phenomenon occurs inside concrete, it will cause stress accompanied by internal cracks. In severe conditions, it will cause crumblings.
3. To avoid these problems, the so-called air-entraining admixtures must be added to concrete mixture with the mixing water.
4. The concrete can maintain a certain rate of air bubbles becoming entrapped inside the concrete body.
5. These air bubbles act as expansion tanks, which compensate the rate of expansion when it occurs.

On this basis, this type of admixture could only be used in very cold locations such as European, American, Russian and Scandinavian countries.

6.3 Plasticizers

The admixtures of this group are also known as 'water-reducing admixtures' because their main function is to reduce the w/c ratio, and they can be expressed as resistance to flow. Therefore, the workability of cement paste and/or concrete is greater than that of the resulting mortar which in turn is greater than for the resulting concrete (Oland and Baker, 2001; Pailere, 1995; Uchikawa et al., 1992; Kamoun et al., 2003). These are hydraulic surfactants dispersing the cement particles and then less water is required to produce a suitable paste of a particular workability. This effect is caused by adsorption on the cement surfaces of the high-molecular-weight anions, leading to a mutual repulsion of individual particles and a reduction in the interparticle friction (Cope and Ranney, 2001). Both plasticizing and air-entraining admixtures behave in a similar way. However, due to the various chemical functional groups on the backbone of molecules occurring in this group, instead of end-on adsorption occurring, the backbone is preferentially adsorbed, causing the negative end-group thrust into the solution. Figure 6.5 illustrates some examples of plasticizing admixtures. Darweesh (2014a,b) prepared Ca-lignosulphonate from lignin from black liquor waste resulting from the paper industry and used it as a plasticizer, in which, on its addition, the w/c ratio increased (Figure 6.6), whereas the setting time (initial and final) decreased (Figure 6.7). Moreover, the combined water content, bulk density and apparent porosity as well as compressive strength are improved and enhanced. The plasticizing action of this group can be utilized in three ways:

- The amount of mixing water required to produce a suitable cement paste or concrete can be reduced to produce a denser and stronger composition.
- The workability of cement paste or concrete could be improved and enhanced to provide easier placing and compaction.
- Both cement and water can be reduced in proportion to give an economic corresponding mix of unchanged workability and strength.

On this basis, this group can be divided to three subgroups as explained in the sections below.

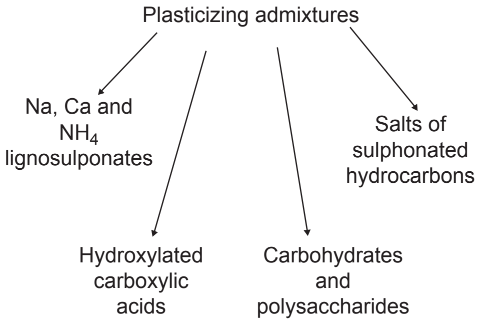

Figure 6.5 Some examples of plasticizing admixtures.

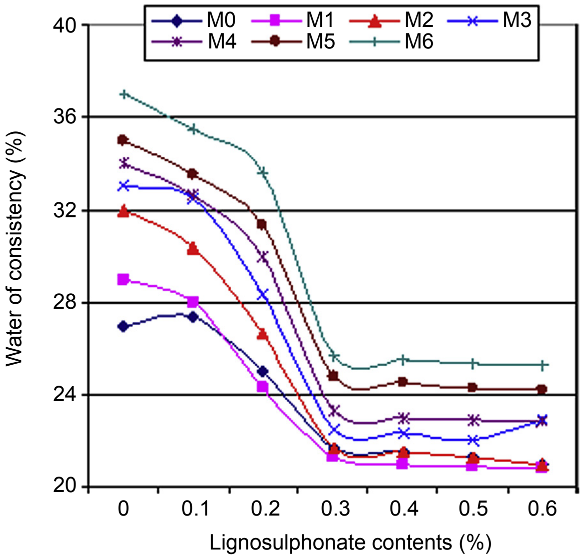

Figure 6.6 Water of consistency of cement pastes premixed with variable ratios of Ca-lignosulphonate.
Darweesh (2014a).

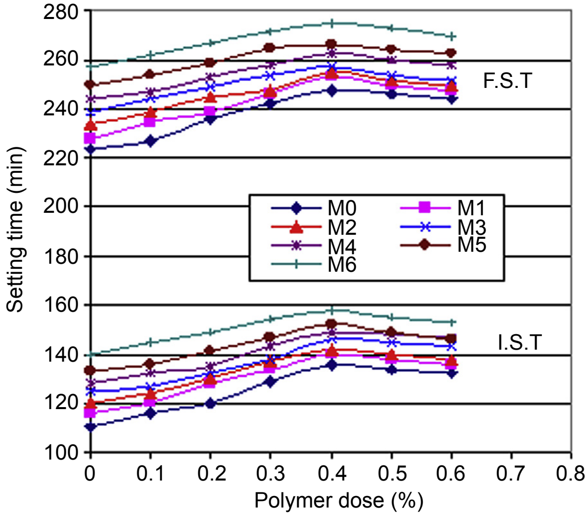

Figure 6.7 Initial and final setting times of cement pastes premixed with variable ratios of Ca-lignosulphonate.
Darweesh (2014a).

6.3.1 Normal water-reducing admixtures

Normal water-reducing admixtures have no significant effect on the subsequent hydration of the cement if added to mortar or concrete mixes at the normal dosage. However, the improved dispersion of cement grains cause a shortening of the stiffening time and the early strength can be enhanced at a constant w/c ratio. Some of these admixtures can be used in combination with certain types of cements at high dosage levels, especially with those of low tricalcium aluminate (C_3A) content, i.e. sulphate-resisting cement. This may cause retardation which can be offset by incorporating small amounts of an accelerator into the formation as $CaCl_2$, Ca-formate or triethanolamine.

The essential materials used to produce normal water-reducing admixtures are the salts of lignosulphonatic and hydrocarboxylic acids. Less commonly modified carbohydrates (sometimes known as hydroxylated polymers) have formed the basis of a series of proprietary admixtures.

Lignosulphonates are high-molecular-weight materials and can be obtained as a by-product from the acid sulphate wood-pulping process. Their crude form contains many impurities as pentose and hexose sugars. The latter are powerful retarders and are removed by fermentation followed by distillation of the resulting alcohol or incorporated into a normal water-reducing admixture. Ca- and Na-salts are most commonly used in admixture production. The former is cheaper but less effective as a water-reducing agent and the latter is more soluble and less liable to precipitation when stored at low temperatures. The hydrocarboxylic acids are normally employed as the more soluble Na-salts in proprietary admixtures (Kamoun et al., 2003).

6.3.2 Accelerating water-reducing admixtures

This type of admixtures combines water-reducing capability of the acceleration of cement hydration. The simpler formulation consists of a mixture of Ca-lignosulphonate and $CaCl_2$, or when a chloride-free admixture is represented by a blend with Ca-formate or $NaNO_2$. The Ca-lignosulphonate could be prepared from lignin of black liquor waste resulting from paper (Darweesh, 2014a,b) and used as a plasticizer, in which on its addition the w/c ratio increased whereas the setting time (initial and final) decreased as previously mentioned.

6.3.3 Retarding water-reducing admixtures

This is the most important class of concrete admixtures which includes most of the proprietary retarders of hydrocarboxylic acids. The main function is to delay the setting time of concrete which adversely affects the subsequent strength development, while permitting subsequent reduction in the w/c ratio (Uchikawa et al., 1992; Kamoun et al., 2003).

In Ca-lignosulphonate the high sugar content of the crude sulphite has been retained as much as 50–60 wt% of the lignosulphonate solids. The reducing sugars are powerful retarders, but a higher dosage level (300–1000 mL/100 kg cement) is normally required compared to the hydroxycarboxylic acid type (200–500 mL/100 kg cement). There is also a greater tendency to entrain air, which is usually offset by incorporating an air detainer. To prevent the variation in sugar content inherent in the raw material, purified lignosulphonate—hydroxycarboxylic blends are also employed to produce efficient admixtures of this class (Rixon and Waddicor, 1981). The general effect of all water-reducing admixtures on the properties of mature concrete is beneficial; however, if used to improve workability, the accelerating type can lead to a slight increase in drying shrinkage and creep. The plasticizing effectiveness also depends on the composition of the used OPC cement. This is mainly attributed to the fact that the composition of Ordinary Portland Cement (OPC) can vary from one plant to another.

It is good to remember that because high costs are unwelcome and also, for the cost effectiveness of alternative chemicals to continue, there is a tendency to use waste materials or by-products to produce these admixtures, e.g. the lignosulphonate can be produced from pulp black liquor (PBL) waste (Darweesh, 2014a,b). The mechanism of action is very complex due to the large variety of these admixtures, but the dispersion action for cement and its adsorption on cement particles, as well as the changes in surface charges, are the most vital effects to improve the specific characteristics of cement.

6.4 Superplasticizers

These admixtures are also known as ‘high-range water-reducing admixtures’, and can be used at considerably higher dosages than normal plasticizers without any adverse effects such as gross reduction of set. Superplasticizers consist of high-molecular-weight water-soluble polymers. The majority are synthetic chemicals. Solubility is ensured by the presence of adequate hydroxyl, sulphonate or carboxylic groups attached to the main organic repeating unit which is normally anionic (Negim et al., 2010; Darweesh, 2014a,b; Darweesh et al., 2013; Tagnit and Aitcin, 1993). Recently, the superplasticizers have been classified into four categories (Figure 6.8) as follows:

6.4.1 *Sulphonated melamine formaldehyde condensates*

Sulphonated melamine formaldehyde condensates are synthetic polymers that have the structural formula with each repeating unit containing one sulphonate group.

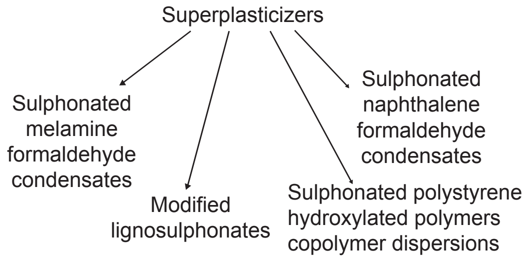

Figure 6.8 Classification of superplasticizers.

The condensation number (*n*) is usually in the range 50—60 giving a molecular weight between 12,000 and 15,000.

6.4.2 Sulphonated naphthalene formaldehyde condensates

Each repeating unit is solubilized by a single sulphonate group, which gives a very soluble salt. The condensation number (*n*) is typically 5—10 giving a molecular weight of 1000—2000.

6.4.3 Modified lignosulphonate

The activity of lignosulphonate can be considerably improved by treatment of the crude by-product to remove all carbohydrate impurities followed by selection of the higher molecular weight fraction. Lignosulphonates can approach the synthetic condensates in terms of performance, though they have a greater tendency to entrain air (Sonaka et al., 1997).

6.4.4 Sulphonated polystyrene, hydroxylated polymers, copolymer dispersions

Sulphonated polystyrene, hydroxylated polymers or copolymer dispersions can be used alone or in combination with other superplasticizers. All superplasticizers with extended workability fall into this miscellaneous category. All superplasticizers are strongly adsorbed onto cement surfaces and often build up multiple chemisorbed layers on the individual grains. The sulphonated naphthalenes do not have the backbone chemical substitution that the sulphonated melamine derivatives possess. The negative charge build-up resulting in dispersion is similar, whereas the manner of adsorption is not. A multi-adsorption layer has been suggested, but evidence for this is lacking.

The formation of hydration products on the surface of cement grains tends to negate improved workability. However, the rate of hydration may be well increased due to the finally dispersed state, causing early hydration products to result in the slump-loss phenomenon which can be very pronounced in superplasticizer concrete. The workability is greatly improved and enhanced by delaying the addition of superplasticizer rather than adding it with the mixing water. This allows time for the normal hydration between gypsum ($CaSO_4 \cdot 2H_2O$) and Portland cement clinker to take place without any competition from the superplasticizer. The delay of only a few minutes is adequate to form the ettringite phase, $C_3A \cdot 3CaSO_4 \cdot 32H_2O$. The stabilization is a dormant period during which slow changes could occur.

The effect of two different types of superplasticizers naphthalene sulphonate formaldehyde (NSF) and benzene sulphonate formaldehyde (BSF) on the physicomechanical properties of OPC pastes was studied (Abo El-Enein et al., 1997). They concluded that the dispersibility of cement particles was improved and so was the consistency of the fresh cement pastes leading to a reduction in the strength development at early stages of hydration. At later stages, however, both NSF and BSF improve the plastic and hardening characteristics of cement pastes. Accordingly, the compressive strength tends to be higher than that of the pure OPC pastes.

Torresan et al. (1997) studied the physical and mechanical properties of cement pastes and concrete of two types of cement blended with β-naphthalene sulphonate (NS) and melamine sulphonate (MS) condensate polymers. The results showed a better fluidity effect and mini-slump retention for cement pastes. For concrete, both dosage and cement type could greatly influence the performance of NS superplasticizer of high-molecular-weight. In addition, significant improvements were achieved in concrete made with high cement content, whereas with low cement content no differences in performance using NS superplasticizers of different molecular weights were noted.

Mutual particle repulsion leads to a high degree of dispersion, but the polymers employed do not entirely exclude water from the cement surface, and hydration does not proceed in a normal way (Figure 6.9(a)). The dispersion of cement agglomerates will lead to a more finely divided and uniformity dispersed material. The results from the build-up of negative charges are depicted in Figure 6.9(b).

Both plasticizing and superplasticizing admixtures cause agglomerates of cement grains to disperse. However, addition of lignosulphonate reaches its maximum effectiveness at lower wt% compared with superplasticizers. The mode of action has the ability to eliminate or at least reduce the attractive forces between particles. This is due to the high adsorption character of the cement grains. The acceptable consequences caused by the adsorption character are as follows:

1. Formation of repulsive electrostatic forces, which move the particles away from each other, i.e. dissociation of admixture particles.
2. The formation of thin layers or films.

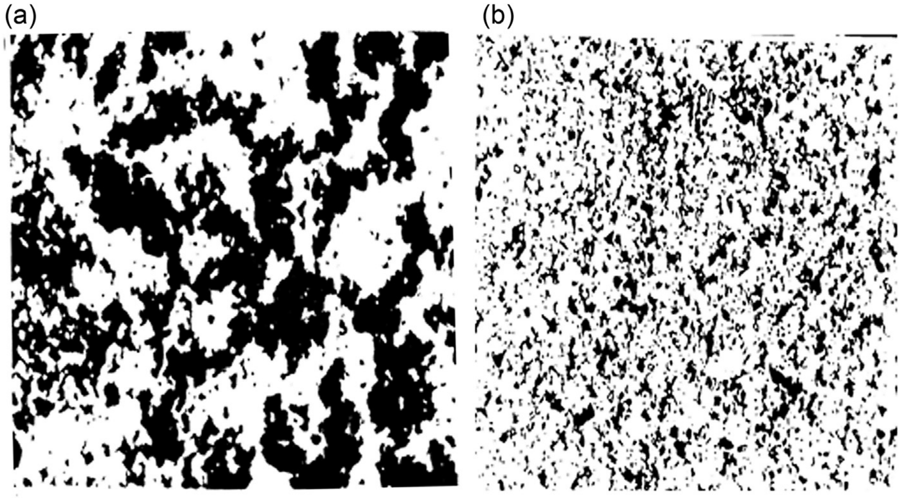

Figure 6.9 Dispersibility effect of admixtures (a) in the absence of admixture and (b) in the presence of admixture.
Darweesh et al. (2013).

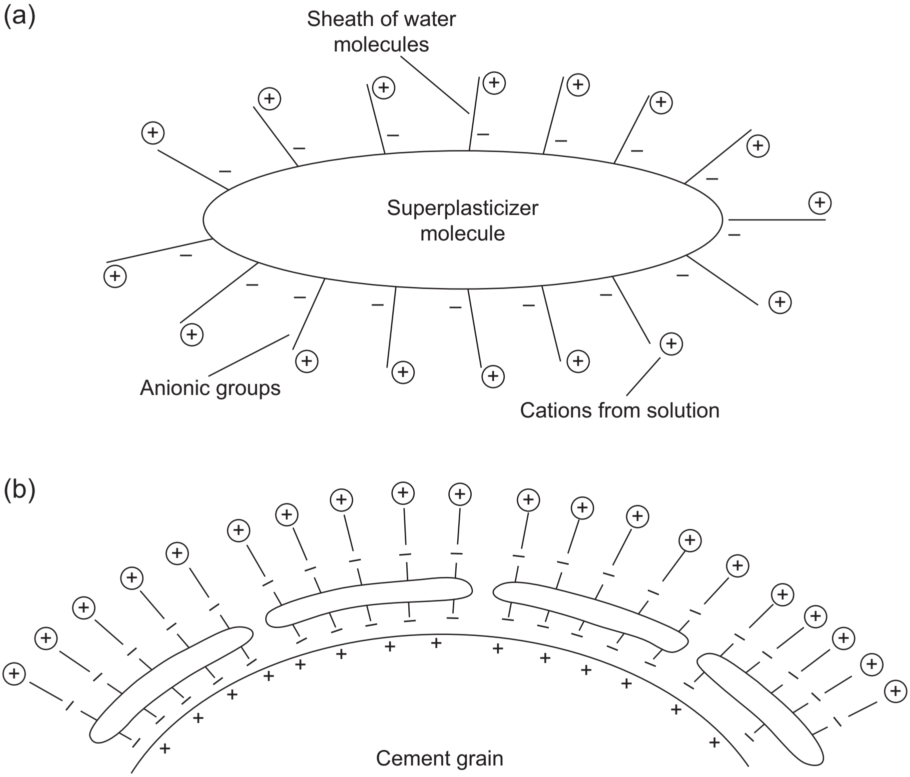

Figure 6.10 (a) Dissociation of an admixture molecule and (b) representation and mode of adsorption of admixture on a cement grain.
Darweesh et al. (2013).

3. Change in the morphology and crystalline sizes of the hydration products, i.e. dissociation and orientation of admixture particles, i.e. adsorption of admixture particles on the surfaces of cement grains (Figure 6.2).
4. Change in the hydration kinetics of cement constituents, i.e. rearrangement of charges or equilibrium (Figure 6.10).

6.5 Retarders

These admixtures, when added, would delay the setting time of the cement, i.e. the setting times lengthen. Retarders reduce the solubility of the hydrating components in cement and so are solubility reducers. Gypsum retards the dissolution of the aluminate phase (C_3A). This retards the set of the cement. Calcium sulphate in the form of plaster of Paris ($CaSO_4 \cdot {}^1\!/_2H_2O$) can also be used as a retarder (El-Mekkawi et al., 2011). Figure 6.11 shows some examples of retarding admixtures. NH_4Cl, $FeCl_2$, $FeCl_3$, Ca-borate, tartarate and oxychlorides, alkali bicarbonates (e.g. $NaHCO_3$), tannic acid, sulphuric acid in NaOH solution, various forms of starch, salts of

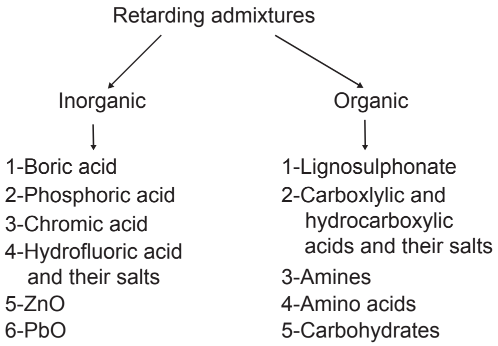

Figure 6.11 Some examples of retarding admixtures.

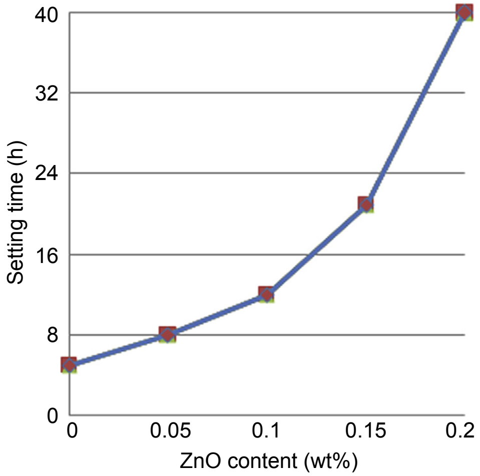

Figure 6.12 Influence of ZnO addition on initial setting time of cement pastes.

carboxymethyl cellulose or oxidized cellulose, calcium or sodium salts of lignin sulphuric acid (Hewlett et al., 1988; Aldred, 1988). Figure 6.12 indicates the influence of ZnO on the initial setting time of cement pastes. The mechanism of action could be interpreted based on two theories. The first theory suggests that the retarding admixtures are first dissociated in the solution (Figure 6.2), and then often adsorbed on the outer surfaces of cement phases (Figure 6.10). The second theory suggests that the retarding admixtures may react with the cement grains, and the resulting reaction product covers the cement grains with an impermeable (waterproof) layer. As soon as this action is removed by the diffusion of water, the hydration proceeds in the normal way.

6.6 Accelerators

These admixtures comprise a wide range of chemicals which influence the rate of cement hydration and setting times. In most cases, the rate of early strength development increases. Figure 6.13 demonstrates some examples of accelerators.

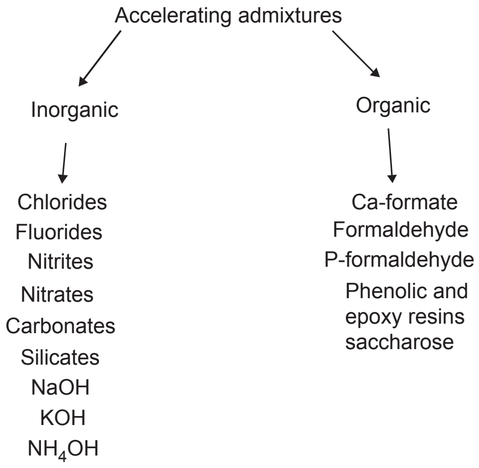

Figure 6.13 Some examples of accelerating admixtures.

6.6.1 Rapid-set accelerators

Rapid-set accelerators are referred to as ‘flash or false-set admixtures.’ These are mainly highly alkaline solution chemicals. Typical examples are alkali metal hydroxides, carbonates, aluminates and silicates. These accelerate the hydration of C_3A, resulting in a considerable evolution of heat. The precipitation of insoluble Ca salts is partially derived from the admixture itself. The increase of temperature can also stimulate the hydration of tricalcium silicate (C_3S) phase, which contributes to high early strength, but this is not sustained to give high long-term strength. A few salts derived from strong acids and weak bases accelerate the hydration of the alite phases, C_3S, and lead to a flash setting at high dosages. Little increase in strength occurs after setting (Vaysburd, 2001a,b).

6.6.2 Setting and hardening accelerators

Setting and hardening accelerators consist of chemicals principally affecting the rate of hydration of the alite phase (C_3S) resulting in an increase of heat evolution and calcium silicate hydrate (CSH) gel at early stages. The anions which cause significant acceleration are halide, nitrate, nitrite, formate, thiosulphate and thiocyanate, although their activity appears to depend on the identity of the associated counterion. The di- and trivalent cations such as Ca^{2+}, Mg^{2+} Ba^{2+}, Fe^{3+} and Al^{3+} appear to be more effective than monovalent ions such as Na^{+}, K^{+} and NH_4^{+} (Wilding et al., 1984; Hewlett, 1998).

6.6.3 Calcium chloride accelerators

The accelerator should be soluble and ionize in the mixing water. To accelerate the dissolution of lime, the acid ions should possess sufficient mobility to penetrate into the silicate particles. Consequently, their size is of major importance. On this basis,

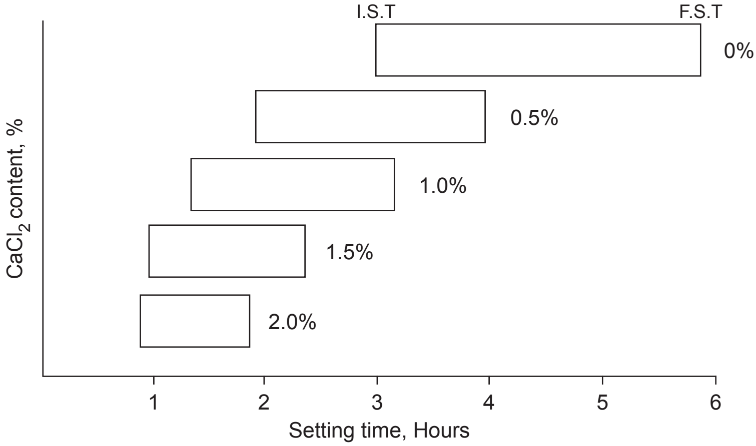

Figure 6.14 The effect of $CaCl_2$ on initial and final setting times of cement pastes.

$CaCl_2$ is suitable because it is a soluble and highly ionized salt of a strong acid and with a very small anion size (0.27 nm compared to 0.34 nm for nitrite and 0.45 nm for formate). Figure 6.14 shows the effect of $CaCl_2$ solution on the initial and final setting times of cement pastes.

Amines or base accelerators also function by upsetting the dissolution of silica and alumina. Triethanolamine is an accelerator for the initial hydration of OPC by disturbing the reaction between C_3A and gypsum ($CaSO_4 \cdot 2H_2O$). This accelerates the hydration of C_3A by both increasing the formation of the hexagonal aluminate hydrate and promoting the conversion to the cubic aluminate hydrate. It also accelerates the formation of ettringite. However, triethanolamine may also act as a retarder in the hydration of C_3S.

At high w/c ratios, the $CaCl_2$ ions react to form hydrochloroaluminate and stabilize the formation of ettringite. The aluminate ions produced from tetracalcium aluminoferrite C_4AF are also consumed together with C_3A. The $CaCl_2$ causes small fibrous crystals to appear during hydration, inactive of rapid crystallization, which in turn may be caused by the highly ionic character of water phase when $CaCl_2$ is present.

6.6.4 Non-chloride accelerators

Although they are not as effective as $CaCl_2$, non-chloride accelerators have been proposed and have become commercially available for use as accelerators, such as Ca-formate, de-acidized Ca-formate, Na-aluminate and triethanolamine. Ca-salts appear to have a superior activity compared with most other metal salts, but they commonly suffer from low solubility in water. Ca-formate acts as $CaCl_2$ in a similar manner, but high dosages are required (Dransfield and Egan, 1988).

Recently, $Ca(NO_2)_2$ has been manufactured commercially and became available as a proprietary accelerator. It has a reasonably high solubility (50 g/100 g), and the dosage rate is 0.03–2.3%. In contrast to most other chemicals, the toxicity of inorganic nitrites can be used as cement accelerators. The $Ca(NO_2)_2$ has also been promoted as an inhibitor for reinforced concretes.

6.7 Black liquor waste

6.7.1 Introduction

The use of reducing water-soluble polymer admixtures with dispersing, plasticizing and air-entraining effects, in considerably low polymer/cement ratios, is very important because these admixtures improve the workability and modify other properties of cement pastes or concrete (Singhal et al., 2008). Furthermore, they enhance the performance of concrete structures (Hewlett, 1998; Sonaka et al., 1997; Uchikawa et al., 1992; Darweesh, 2014a,b; Darweesh et al., 2013; Darweesh, 2006; Ayoub et al., 2005a,b; Ayoub et al., 2007).

The paper industry may involve three major processes: (1) chemical Kraft/sulphate digestion or mechanical and chemo-mechanical pulping; (2) fibre and chemical recycling; (3) paper-making—related processes. This industry often produces a huge amount of waste material (Figure 6.15). The by-products and residues from mechanical and chemo-mechanical pulping include wood, straw and reed residues, fibre rejects and excess sludge from external biological wastewater treatment (Sonaka et al., 1997; Ramachandran et al., 1998; Darweesh, 2006). Black and white liquors, waste products which come from the paper industry, have attracted attention due to their unique advantages such as high solubility and low viscosity. Black liquor is an important liquid fuel in the pulp and paper industry (Darweesh, 2006). It consists of the substances remaining from the digestion process by which the cellulose

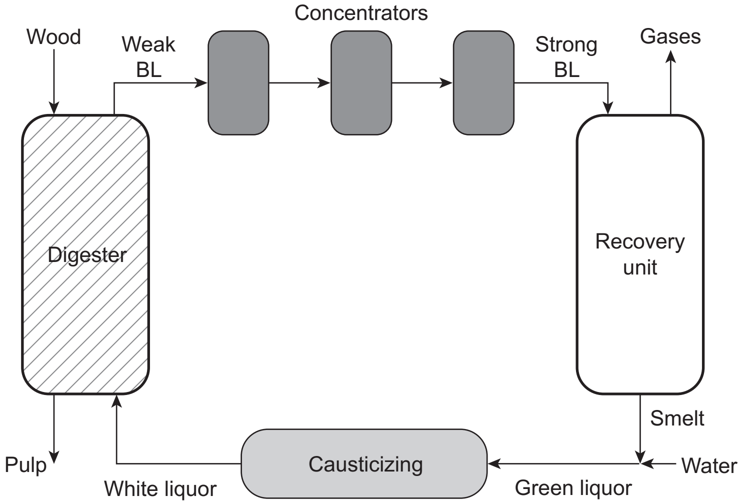

Figure 6.15 A schematic description of the pulping process.

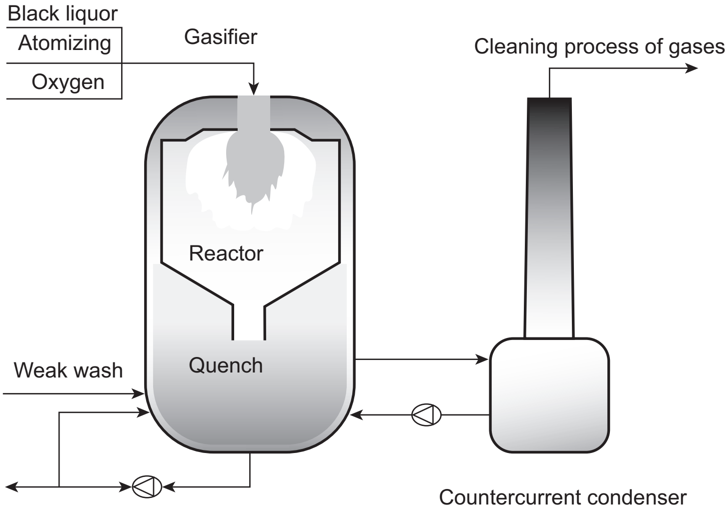

Figure 6.16 A schematic drawing of a black liquor gasification plant.

fibres have been cooked out of the wood (Figure 6.16). One of the main ingredients in black liquor is lignin, which is the material in trees that binds wood fibres together and makes them rigid, and which must be removed from wood fibres to create paper (Ayoub, 2005a,b; Ayoub et al., 2007; Bernath et al., 1998; Kim et al., 2002). Uchikawa et al. (1997) and Darweesh (2005) reported that some organic admixtures induce physical effects, which modify the bonds between particles and can act on the chemical processes of hydration, particularly on nucleation and crystal growth (Jumadurdiyev et al., 2005; Yildirim and Altun, 2012; Darweesh and Youssef, 2014).

The wide achievements of cement admixtures turned our attention to look for new suitable admixtures for cement which is the main objective of the study (El-Didamony et al., 1978; Jumadurdiyev et al., 2005; Yildirim and Altun, 2012; Abo-El-Enein et al., 1997).

On this basis, Darweesh et al. (2013) studied the possibility of using the PBL waste resulting from the paper-making industry as an admixture for cement hydration. The PBL from the paper industry was provided by Paper Factory, Alexandria, Egypt. It was tested as a cement admixture for two different types of cement: Ordinary Portland Cement (OPC) and Limestone Portland cement (LPC) with Blaine surface areas of 3300 and 3100 cm^2/g, respectively. These materials were delivered from Helwan and Tourah Cement Companies, Egypt, respectively. Table 6.1 shows the elemental analysis of black liquor, whereas the chemical compositions of the OPC and PLC cements are listed in Table 6.2.

The PBL was dissolved in the mixing water with dosage of 0%, 1%, 2% and 3% and then added to OPC and LPC cements. The pastes were poured into 1-inch cubic stainless steel moulds ($2.5 \times 2.5 \times 2.5\ cm^3$), vibrated manually for 2 min and on a mechanical vibrator for another 2 min. The surfaces of the pastes were smoothed with a spatula and then kept inside a controlled moisture chamber for 24 h, in which they were kept at 23 ± 1 °C and 100% relative humidity. Then they were demoulded and soon cured under water till the time of testing for bulk density, apparent porosity and compressive strength (1, 3, 7, 28 and 90 days). The samples were denoted as P_0, P_1, P_2 and P_3 for OPC and L_0, L_1, L_2 and L_3 for LPC.

The amount of water required to get the desirable consistency (mixing water) and the setting times (initial and final) of the prepared cement pastes were directly determined by Vicat Apparatus American Society for Testing and Materials (ASTM Standards, C187-86, 1993; ASTM Standards, C191-92, 1993; Edmonds and Majumdar, 1989). The water of consistency can be measured according to the following relation:

$$\text{W.C.\%} = \text{W/C} \times 100 \tag{3.1}$$

in which W is the quantity of water taken to produce a suitable paste and C is the used amount of cement (often 300 g).

The bulk density (BD) and apparent porosity (AP) of the hardened-cement pastes (Hewlett, 1998) were calculated according to the following equations:

$$\text{BD (g/cm}^3) = W_1/(W_1 - W_2) \times 1 \tag{3.2}$$

$$\text{AP\%} = (W_1 - W_3)/(W_1 - W_2) \times 100 \tag{3.3}$$

in which, W_1, W_2 and W_3 are the saturated, suspended and dry weights, respectively.

The compressive strength (ASTM Standards, C170-90, 1993) was measured by using a hydraulic testing machine (Type LPM 600 M1 SEIDNER, Germany), having a full capacity of 600 KN. The loading was applied perpendicular to the direction of the upper surface of the cubes. The compressive strength was determined according to the following relation:

$$\text{Cs} = \text{L (KN)/Sa (cm}^2\text{) KN/m}^2 \times 102\ \text{(Kg/cm}^2\text{)/10.2 (MPa)} \tag{3.4}$$

in which Cs: compressive strength (MPa), L: load (KN), Sa: surface area (cm^2).

The chemically combined water content (Wn) at each hydration stage was also determined on the basis of ignition loss at 1000 °C (Kondo et al., 1975; Sonaka et al., 1997) according to the following relation:

$$\text{Wn\%} = W_1 - W_2/W_2 \times 100 \tag{3.5}$$

in which W_1 and W_2 are the weights of sample before and after, respectively.

The phase composition of selected samples was investigated using infrared spectroscopy (IR) and scanning electron microscopy (SEM). The IR spectra were obtained on a Pye-Unicum SP-1100 apparatus, working in the range of 4000 to 400 cm^{-1}. The SEM images of fractured surfaces, coated with a thin layer of gold, were obtained by a JEOL-JXA-840 microscope at accelerating voltage of 30 KV.

6.7.2 Effect of PBL waste on water of consistency and setting times

The water of consistency and setting times (initial and final) of OPC and LPC cements premixed with PBL waste are plotted in Figure 6.17. Generally, the water of consistency gradually increased with PBL concentration in both types of cements: from 28% (PBL free) to 31.67% (3% PBL) with OPC and from 28.5% to 32.45% with LPC. the results are obvious that, for similar PBL concentrations, LPC-based pastes require more water than OPC counterparts. Therefore, the water of consistency was increased by 1.68% to 13.12% with OPC and by 4.11% to 13.85% with LPC in comparison with those of their blanks.

On the other hand, the PBL waste decreased the setting times (initial and final) with either OPC or LPC. With 3% PBL the initial and final setting times decreased from 140 to 119 min and from 255 to 231 min, respectively, with OPC. With LPC pastes, those changes were from 148 to 128 min and from 266 to 148 min. It is evident that setting is faster with OPC than with LPC. Hence, it could be concluded that the PBL waste can act as an accelerator for cement pastes (Cohen and Bentur, 1988; Hewlett, 1998; Darweesh, 2006).

6.7.3 Effect of PBL waste on bulk density and apparent porosity

The bulk density and apparent porosity of the OPC and LPC cement pastes premixed with 0%, 1%, 2% and 3% of PBL waste are illustrated in Figures 6.18 and 6.19,

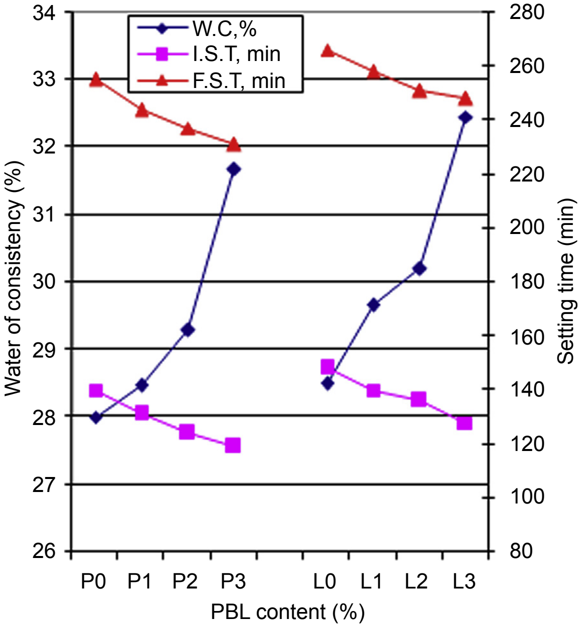

Figure 6.17 Water of consistency and setting times of the OPC and PLC cement pastes premixed with 0%, 1%, 2% and 3% PBL waste.
Darweesh et al. (2013).

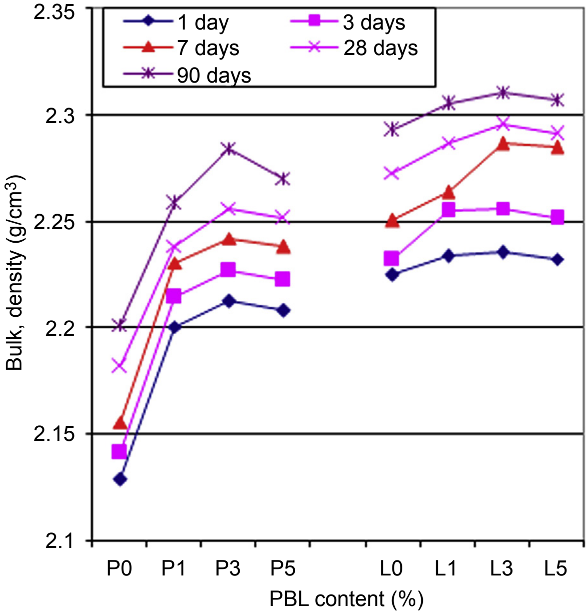

Figure 6.18 Bulk density of the OPC and PLC cement pastes premixed with 0%, 1%, 2% and 3% PBL waste cured up to 90 days.
Darweesh et al. (2013).

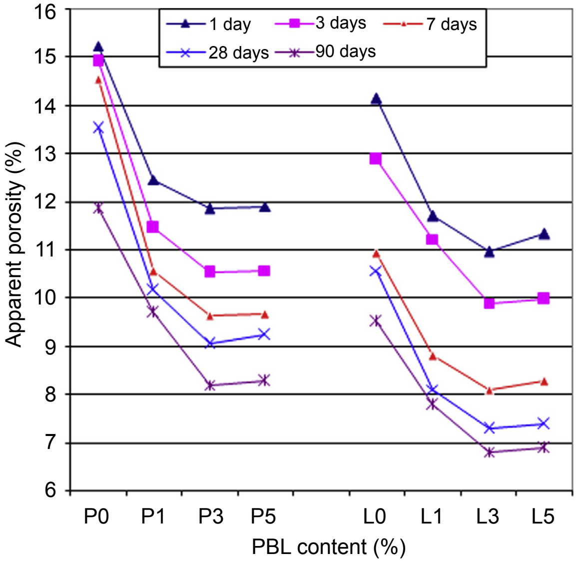

Figure 6.19 Apparent porosity of the OPC and PLC cement pastes premixed with 0%, 1%, 2% and 3% PBL waste cured up to 90 days.
Darweesh et al. (2013).

respectively. It is clear that the bulk density gradually increased with curing time, whereas the apparent porosity decreased. This is mainly attributed to the gradual and continuous deposition of the formed hydration products in the pore structure of the hardened cement pastes (Uchikawa et al., 1992). Moreover, the bulk density was further increased with PBL concentration up to 2%, whereas the apparent porosity decreased. This tendency may be attributed to the activation and improvement in the hydration process of cement phases caused by the presence of $Na(OH)_2$ in the waste liquor. Subsequently, the amount of hydration products increased in comparison to blank pastes (Luxan et al., 1989; Hewlett, 1998; Karim et al., 2012). With further increase of PBL concentration to 3%, the bulk density slightly decreased and the apparent porosity increased. Therefore, the higher PBL concentration is not desirable and hence it must be avoided (Sonaka et al., 1997; Aldred, 1988; Pailere, 1995; Ayoub et al., 2007).

6.7.4 Effect of PBL waste on combined water content

The combined water contents of the OPC and LPC cement pastes premixed with 0%, 1%, 2% and 3% of PBL waste are shown in Figure 6.20. Generally, the combined water content of all cement pastes increased with curing time up to 90 days. This was essentially attributed to the gradual and continuous formation of hydration products,

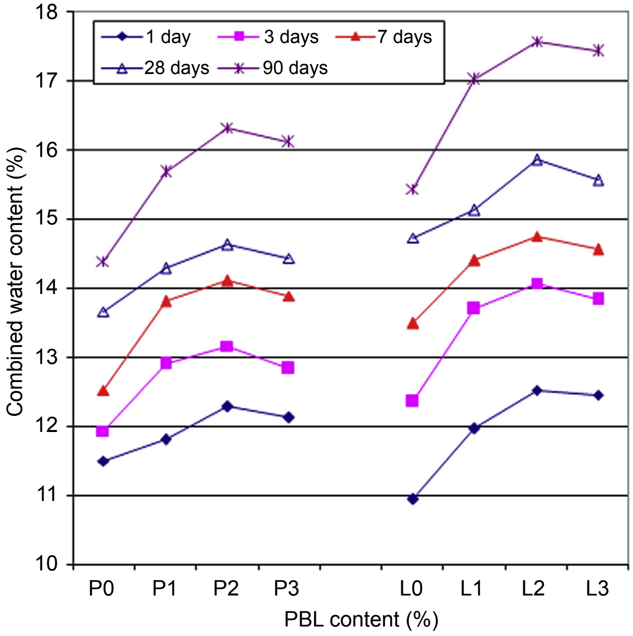

Figure 6.20 Combined water content of the OPC and PLC cement pastes premixed with 0%, 1%, 2% and 3% PBL waste cured up to 90 days.
Darweesh et al. (2013).

particularly from C_3S and β-C_2S phases (Ramachandran, 1995; Ramachandran et al., 1998; Karim et al., 2012). The combined water contents increased gradually by incorporation of PBL up to 2% with both OPC and LPC and then decreased with higher contents (Ramachandran, 1995; Ramachandran et al., 1998; Yildirim and Altun, 2012). Values tend to be slightly higher with LPC, probably because the active groups in PBL waste (−OH) are more effective with LPC than with OPC (Hewlett, 1998). The adverse effect observed with 3% PBL in both pastes again suggests that higher PBL concentrations must be avoided. This is mainly attributed to the fact that with the higher concentration of PBL (3%), the cement grains are surrounded by thin films or coats which hinder or prevent or at least reduce the hydration process of cement phases. The trends upon curing are similar with both types of cements, but the effects are more pronounced with LPC (Vaysburd, 2001a,b; Kim et al., 2002).

6.7.5 Effect of PBL waste on the compressive strength

The compressive strength of OPC and LPC cement pastes premixed with 0%, 1%, 2% and 3% of PBL waste liquor is shown in Figure 6.21. The compressive strength of the hardened cement pastes was generally increased with curing time up to 90 days, as expected from the continuous hydration process. The apparent porosity decreased gradually and the compactness of samples improved, hence the bulk density increased. This was positively reflected on the compressive strength (Ramachandran et al., 1998; Aldred, 1988; Yildirim and Altun, 2012; Abo-El-Enein et al., 1997; Darweesh, 2012).

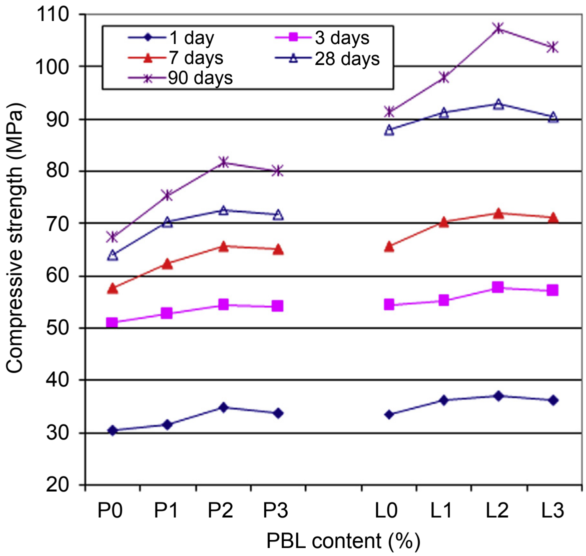

Figure 6.21 Compressive strength of the OPC and PLC cement pastes premixed with 0%, 1%, 2% and 3% PBL waste cured up to 90 days.
Darweesh et al. (2013).

The effect of PBL addition was beneficial in both cement pastes, again for concentrations up to 2%. It might be explained by activation of the $-OH^-$ groups present in the PBL, particularly at later stages (Thalcec and Zellic, 1987; Pailere, 1995; Ayoub et al., 2005a,b; Darweesh and El-Alfi, 2005).

The addition of PBL to the pastes led to the formation of electrostatic repulsive forces between cement particles which become negatively charged by the adsorption of the waste. This will reduce the attraction between the cement particles, preventing their flocculation or agglomeration and then creating a well-dispersed system (Ayoub et al., 2005a,b; Darweesh and El-Alfi, 2005; Karim et al., 2012). Consequently, the compactness will enhance and direct benefits are expected on the mechanical resistance (Mehta, 1983; Uchikawa et al., 1997). Again, the use of 3% PBL will induce adverse effects and so 2% is the optimal concentration. PBL seems more effective with LPC pastes than with OPC counterparts, as the possible result of a stronger activation effect on the hydration reactions of the first system.

The major phases of OPC are C_3S, β-C_2S, C_3A and C_4AF which can be hydrated when being in contact with water (Ramachandran, 1995; Ramachandran et al., 1998; Darweesh and El-Alfi, 2005; Rixom and Mailvaganam, 1999; Kersener et al., 2011; Darweesh, 2005; El-Didamony et al., 2008; Ettu et al., 2013; Darweesh, 2007; El-Alfi et al., 2005; Darweesh, 2013). The formation of these new phases, particularly C_3S, is responsible for strength development throughout the whole reaction stages during the various curing stages of hydration (Chindaprasirt and Rukzon, 2008; Amin et al., 2011a,b, 2012). It was evident to Darweesh and many co-researchers (Amin et al., 2011a,b, 2012, 2013) and others (Ramachandran, 1995; Oland and Baker, 2001; Ramachandran et al., 1988; Knapen and Gemert, 2009) that all cement and/or concrete admixtures including the black liquor waste had no chemical effect or reaction with the constituents or ingredients of the cement, but only have vital and physical actions on the shape, size, morphology and crystallinity of the formed hydration products. Figure 6.2(a) demonstrates the dissociation and orientation of the admixture particles as soon as it is added to the mixing water, whereas Figure 6.3 shows the adsorption of the admixture particles on the cement grains and their rearrangement to achieve equilibrium.

6.7.6 The Fourier transform infrared spectra

The IR spectra of OPC and LPC cement pastes premixed with 2% of PBL waste are shown in Figures 6.22 and 6.23, respectively. The sharp absorption band at 3644 to 3641 cm^{-1} is related to the free OH^- groups coordinated to Ca^{2+} (i.e. free lime). The intensity of the broad absorption band at 3445 to 3420 cm^{-1}, which was ascribed to the OH^- group associated to H^+ bond that related to the symmetrical stretching frequency of water, increased in the presence of PBL. The two bands at 2959 and 2856 cm^{-1} are due to $-CH_2$ and $-CH_3$ from the residual organic mixture. The two absorption bands at 1647 to 1642 cm^{-1} and 1428 to 1425 cm^{-1} are related to the main silicate band involving Si$-$O stretching vibration bands of CSH, whereas the band at 1120 to 1114 cm^{-1} may be due to calcium aluminate hydrate (CAH).

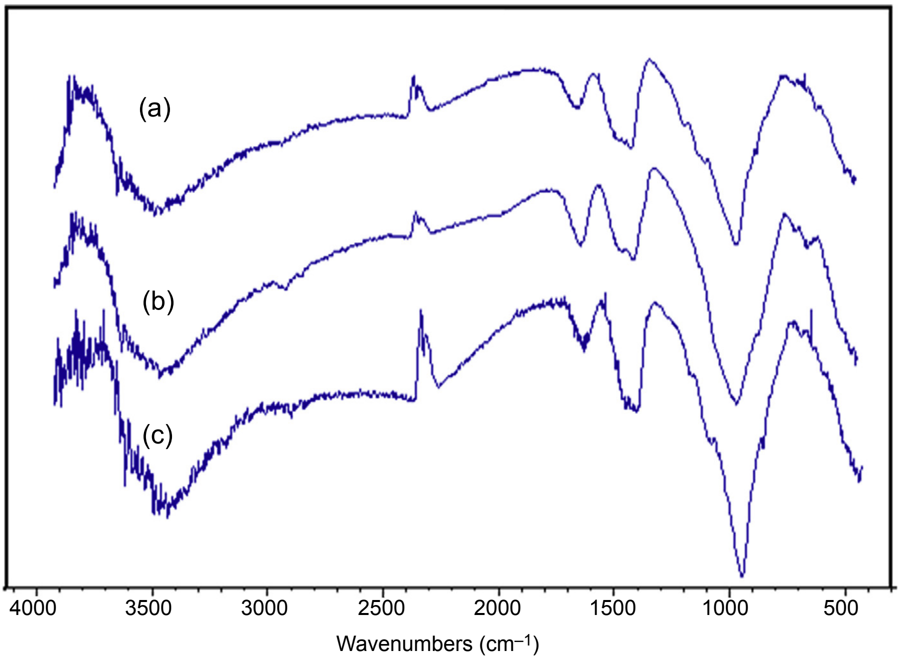

Figure 6.22 The IR spectra of the OPC pastes (a) cured up to 90 days, (b) premixed with 2% PBL waste and (c) 3% PBL waste.
Darweesh et al. (2013).

The intensity of the two absorption bands at 989 to 983 cm^{-1} and 875 cm^{-1} characterizing CO_3^{-2} and SO_4^{-2} is irregular due to the rate of carbonation or sulphonation of CSH and/or CAH, respectively, in which the vibrations of CO_3^{-2} are smaller than those of SO_4^{-2}. In addition, it is clear that the intensity of the absorption bands of Si–O, CAH, CO_3^{-2} and SO_4^{-2} are slightly higher with PBL waste/cement pastes. The intensities of the characteristic peaks were slightly improved with LPC in which a marginal effect with OPC pastes was detected.

6.7.7 SEM microscopy

The SEM images of the OPC (a–d) and LPC (e–h) cement pastes premixed with 0%, 1%, 2% and 3% of PBL waste are shown in Figure 6.24. Generally, the needle-like crystals of ettringite phase ($C_3A \cdot 3CaSO_4 \cdot 32H_2O$) that formed due to the hydration reaction of C_3A with gypsum ($CaSO_4 \cdot 2H_2O$) in presence of water are clearly demonstrated for OPC and LPC blank pastes (Figure 6.12(a) and (e)). This phase decreased or disappeared in the presence of PBL waste (Figure 6.24(b–d) and (f–h)). This was ascribed to the conversion of ettringite to monosulphate ($C_3A \cdot CaSO_4 \cdot 12H_2O$). These observations indicated a better hydration of cement phases in its presence. The PBL waste also affected the morphology of the $Ca(OH)_2$ crystals, resulted from the hydration of C_3S and/or β-C_2S phases of the cement in which the $Ca(OH)_2$ crystals represent the

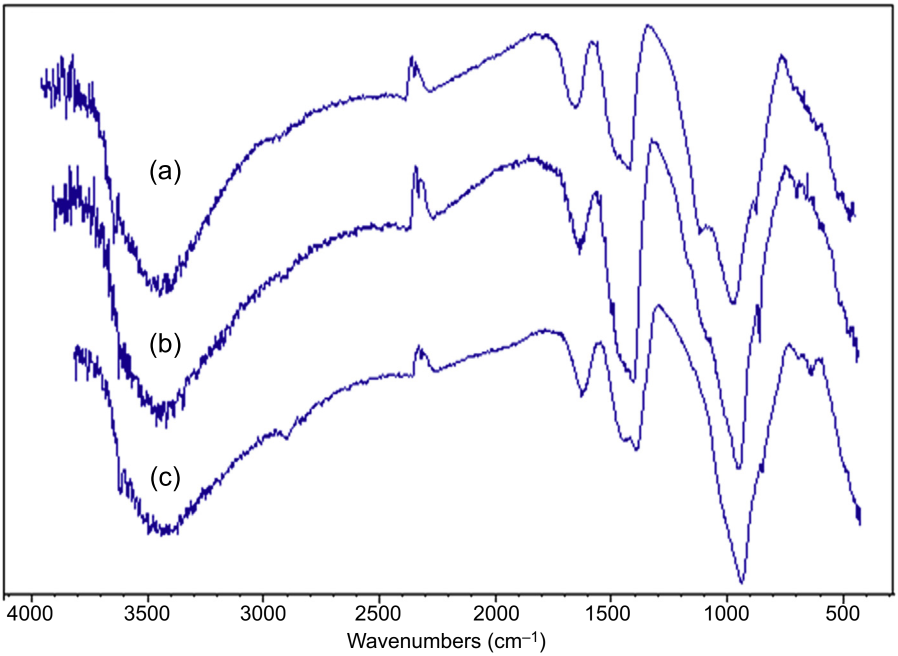

Figure 6.23 The IR spectra of LPC pastes (a) cured up to 90 days, (b) premixed with 2% PBL waste and (c) 3% PBL waste.
Darweesh et al. (2013).

weak phase in the binder matrix, the strengthening by PBL waste improves the overall strength of the binder matrix (Ayoub et al., 2005a,b; Darweesh, 2007). This in turn was reflected positively on the specific characteristics of the cement, particularly the mechanical strength. On the other hand, the phases that formed with LPC pastes were the same as with OPC pastes but with well-developed crystals, particularly with PBL waste. It could be concluded that the formed phases in the case of OPC premixed by PBL waste were the same as with LPC but with different morphologies and crystallinities due the dispersion effect of PBL in both types of cement, in which the crystals are larger and more compacted with LPC. Therefore, the PBL waste has more effect on LPC cement pastes than on OPC pastes.

6.8 Water-resisting admixtures

Water-resisting admixtures are also known as ‘integral permeability reducers’, ‘water-proofers’ or ‘damp proofers’ which reduce the hydraulic permeability of concrete and even mortars. They often confer water repellency to the exposed surfaces (Hewlett et al., 1988; Aldred, 1988). Tables 6.1 and 6.2 demonstrate the different examples of these classes and the typical properties of one type, respectively (Hewlett et al., 1988; Pailere, 1995; Ramachandran et al., 1998; Darweesh, 2006; Ayoub et al., 2007).

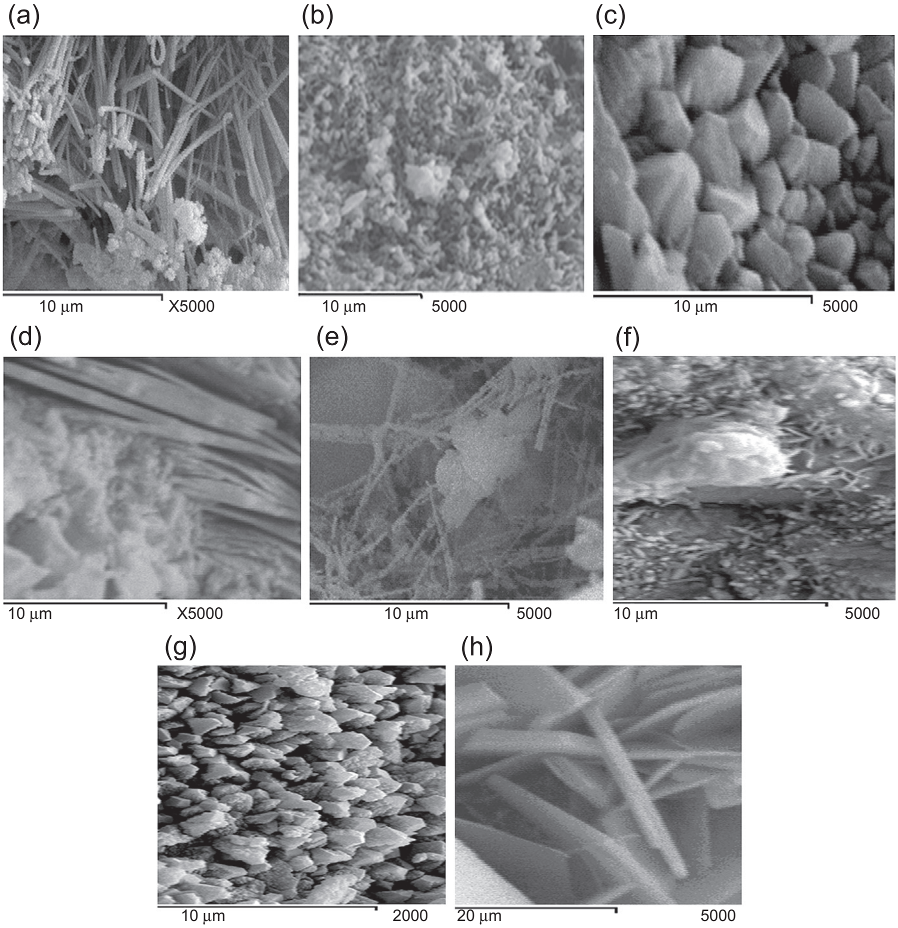

Figure 6.24 The SEM images of the OPC (a–d) and LPC (e–h) cement pastes premixed with 0%, 1%, 2% and 3% PBL waste hydrated up to 90 days.
Darweesh et al. (2013).

6.8.1 Permeability reducers

Permeability reducers are very fine and inert powders. These are added in sufficient amounts to the fresh cement and/or concrete to reduce the residual pore volume. They are often used in combination with a plasticizer or superplasticizer to maintain workability or even allow a reduction of the w/c ratio. The reactive powders such as silica fume or fly ash are preferred because they can react and combine with the resulting $Ca(OH)_2$ resulting from the hydration of C_3S and β-C_2S to form CSH gel.

The particular materials such as ground sand, whiting, bentonite, pulverized fuel ash (Pfa), silica fume (SF), granulated blast furnace slag (GbfS), pumice, diatomaceous earth, limestone, colloidal silica and fluorosilicates can be used successfully

Table 6.1 Waterproofing admixtures

Group	Property			Examples
1	Permeability reducers	a	Very fine particulate materials	Ground sand, whiting, bentonite, pulverized fuel ash, silica fume, granulated blast furnace slag, pumice, diatomaceous earth, limestone
		b	Workability and air-entraining	Lignosulphonates, wood resins, surfactants (anionic) and sulphonated naphthalenes
		c	accelerators	$CaCl_2$, Ca-formate and $NaNO_2$
2	Water repellents or hydrophobers	i	Soaps	Ca-, Na- and Al-stearate or oleate
		ii	Butyl stearate	Butyl stearate
		iii	Selected petroleum products	Mineral oils, waxes and asphalts
3	Miscellaneous	Petroleum jelly, naphthalene, wax, certain celluloses, Na-silicates and Al-powder		

Darweesh (2014a).

in this group because most of them have some degree of pozzolanic reactivity. These materials are of real benefit when the concrete mix is low in cement content or with low fineness. However, in cement-rich mixes the effect could be the reverse, because the addition of fine particles could increase the water requirement leading to a less dense and lower-strength concrete. It could be argued that as long as heat evolution is not a problem, shrinkage cracking can be avoided. The addition of extra cement to lean mixes is the best means of waterproofing (Aldred, 1988) (Tables 6.3 and 6.4).

6.8.2 Water repellents or hydrophobers

Hydrophobing agents are a group of oily or waxy compounds which are introduced into concrete as suspension, in which they precipitate often as insoluble calcium salts. They can form a water-repellent coating on the concrete surface and on the inner walls of capillary pores.

Table 6.2 **Typical properties of styrene-butadiene rubber (SBR) latex designed for use with Ordinary Portland Cement (OPC)**

Total solids	44–47 wt%
pH value	10.5
Surface tension	0.03–0.05 N/m^2
Viscosity at 20 °C (Brook field 1. VT, Spindle 2, 60 rpm)	0.004–0.01 N/s/m^2
Specific gravity	0.01
Freeze–thaw stability	Can withstand several freeze–thaw cycles, but inside storage above 0 °C recommended
Particle size	0.2 μm
Stabilization	Non-ionic
Butadiene content	33–40 wt% of SBR polymer
Antioxidant	Yes
Bacteriocide	Present
Antifoam	Usually present
Minimum film-form temperature	1–4 °C
Shelf-life (interior storage above 0 °C)	Above two years but agitate before use after prolonged storage, as creaming can occur

Darweesh (2014a).

Table 6.3 **The elemental analysis of a dry solid black liquor sample**

Element	C	Na$^+$	S^{2-}	H$^+$	K$^+$	Cl$^-$	N$^+$	O (by diff.)	Total
w/w, %	36.40	18.60	4.80	3.50	2.02	0.24	0.14	34.30	100.00

6.8.2.1 Soaps

Soaps used to be metal salts, but more recently have become sulphonium salts of fatty acids. Soluble soaps can react with Ca^{2-} ions in the aqueous-phase solution of concrete. Therefore, they precipitated out as insoluble salts, which impart a hydrophobic coating to capillary surfaces as well as blocking some pores in the fresh concrete.

Table 6.4 The chemical composition of the OPC and LPC cements, wt%

Oxides materials	L.O.I.	SiO_2	Al_2O_3	Fe_2O_3	CaO	MgO	Na_2O	K_2O	SO_3	B. S. A cm^2/g
OPC	2.64	20.12	5.25	3.38	63.13	1.53	0.55	0.3	2.54	3300
LPC	6.44	16.10	4.03	3.80	60.10	1.24	0.65	0.26	1.44	3100

6.8.2.2 Butyl stearate

The hydrophobic action of butyl stearate is much similar to that of the soups. However, it slowly hydrolyzes in the alkaline phase slowly producing calcium stearate which in turn creates much less air-entrainment, and strength reduction is not as serious.

6.8.2.3 Petroleum products

This group contains mineral oils, waxes, cutback and asphaltic emulsions. Therefore, hydrophobing and some pore-blocking properties can result.

6.8.2.4 Miscellaneous admixtures

This group comprises petroleum jelly, naphthalene, wax, certain celluloses, diluted coal tars, sodium silicate and aluminium powder. They act as waterproofing admixtures.

6.9 Conclusion

As it is well known that the progress in cement and concrete technology has been mostly achieved by the use of admixtures, particular interest in admixtures has increased during the last 30 years at least particularly to improve and enhance durability. On this basis, the possibility of utilizing PBL waste resulting from the paper-making industry has been investigated as a cement admixture. Accordingly, PBL waste activates the cement phases and improves the rate of hydration. The incorporation of PBL waste with OPC or LPC pastes enhances the water of consistency for LPC more than for OPC cement pastes but decreases the setting times (initial and final). As a result, PBL can be used as an accelerator. The combined water content, bulk density and apparent porosity at all curing ages of hydration are improved and accordingly the compressive strength is increased, particularly at later stages of hydration (28 and 90 days). No new phases have been detected by IR, but only increased intensities for the formed phases are observed by the addition of PBL waste than those for the blanks. The optimum PBL concentration is 2% because higher concentrations have an adverse effect on all cement characteristics. SEM images show that the incorporation of PBL waste with cement did not affect the OPC or LPC hydrates, but only affected the physical state, shape or morphology and crystallinity of the formed hydrates. Also, the presence of PBL waste influences the morphology of the $Ca(OH)_2$ crystals and has preferential efficiency with LPC pastes.

6.10 Future trends

In the future, the search for research points in graduate work will look for new and more effective admixtures for cement or concrete. Now, I am, with the help of my co-authors, interested in studying the possibility of using white liquor waste (PWL), also resulting from the paper industry, as a cement admixture.

Cement notation

C: CaO	S: SiO_2	A: Al_2O_3
F: Fe_2O_3	H: H_2O	CH: $Ca(OH)_2$
C_3S: $3CaO \cdot SiO_2$:	Tricalcium silicate	
C_2S: $2CaO \cdot SiO_2$:	Dicalcium silicate	
C_3A: $3CaO \cdot Al_2O_3$:	Tricalcium aluminate	
C_4AF: $4CaO \cdot Al_2O_3 \cdot Fe_2O_3$:	Tetracalcium aluminate ferrite	
CSH:	Calcium silicate hydrate	
CAH:	Calcium aluminate hydrate	
$C_3A \cdot 3CS \cdot H_{32}$:	Ettringite (tricalcium aluminate trisulphate hydrate)	
$C_3A \cdot CaSO_4 \cdot 12H_2O$:	Tricalcium aluminate monosulphate hydrate	

Acknowledgements

The current work has been supported by **National Research Centre, Egypt** through the internal research project with number 10060402. I also wish to thank my co-authors for helping me in preparing the figures of this work.

References

ASTM Standards, C187-86, 1993. Standard Test Method for Normal Water of Consistency of Hydraulic Cement, pp. 148−150.

ASTM Standards, C191-92, 1993. Standard Test Method for Setting Time of Hydraulic Cement, pp. 866−868.

ASTM Standards, C170-90, 1993. Standard Test Method for Compressive Strength of Dimension Stone, pp. 828−830.

Aldred, J.M.H.P.I., 1988. Hydrophobic blocking ingredient improves concrete durability. Concrete Institute 10 (11), 52−57.

Abo-El-Enein, S.A., El-Ashry, S.H., El-Sukkary, M.M.A., Hussain, M.H.M., Gad, E.A.M., 1997. Effect of some admixtures based on naphthalene or benzene on the mechanical properties and physicochemical properties of Portland cement pastes. Silicates Industrials 62 (3−4), 75−81.

Ayoub, M.M.H., Nasr, H.E., Darweesh, H.H.M., 2005a. Synthesis, characterization and cement application of vinyl acetate water soluble graft polymers. Polymer-Plastics Technology and Engineering 44 (2), 305−319.

Ayoub, M.M.H., Nasr, H.E., Darweesh, H.H.M., 2005b. Characterization and utilization of polystyrene and polyacrylamide-graft-methoxypolyethylene as cement admixtures. Polymer-Plastics Technology and Engineering 45 (2), 1307−1315.

Ayoub, M.M.H., Darweesh, H.H.M., Negim, S.M., 2007. Utilization of hydrophilic copolymers as superplastisizers for cement pastes. Cemento Hormigon 919, 4–15.

Amin, A., Darweesh, H.H., Morsi, S.M., Ayoub, M.M.H., 2011a. Employing of some maleic anhydride based hyper-branched polyesteramides as new polymeric admixtures for cement. Applied Polymer Science 121, 309–320.

Amin, A., Darweesh, H.H., Morsi, S.M., Ayoub, M.M.H., 2011b. Effect of phthalic anhydride based hyper-branched polyesteramide on cement characteristics. Applied Polymer Science 120, 3054–3064.

Amin, A., Morsi, S., Ayoub, M., Darweesh, H.H.M., 2012. Modification of cement with succinic anhydride-based hyperbranched polyesteramide. Applied Polymer Science 124 (2), 1483–1489.

Amin, A., Abdel-Megied, A.E., Darweesh, H.H., Ayoub, M.M., Selim, M.S., 2013. New polymeric admixture for cement based on hyperbranched poly amide-ester with pentaerithritol core. ISRN Materials Science. Hindawi ISRN Materials Science 2013, 1–7.

Bernath, P., Sinquefield, S.A., Baxter, L.L., Sclippa, G., Rohlfing, C.M., Barfield, M., 1998. In situ analysis of ash deposits from black liquor combustion. Vibrational Spectroscopy 16, 95–103.

Cohen, M.D., Bentur, A., 1988. ACI Materials Journal 83, 147–157.

Chindaprasirt, P., Rukzon, S., 2008. Strength, porosity and corrosion resistance of ternary blend Portland cement, rice husk ash and fly ash mortar. Construction and Building Materials 22 (8), 1601–1606.

Cope, B.L., Ranney, G.E., 2001. Reducing drying shrinkage of bridge-deck concrete. Concrete Internerships 23 (8), 76–82.

Darweesh, H.H.M., El-Alfi, E.A., 2005. Effect of some water-soluble polymer admixtures on the hydration characteristics of Portland cement pastes. Silicates Industrials 71 (1–2), 27–32.

Darweesh, H.H.M., 2005. Effect of combination of some pozzolanic wastes on the properties of Portland cement pastes. iiC l'industria italiana del Cemento 808 (4), 298–310.

Darweesh, H.H., 2006. Alkali-activation of slag-rich cement pastes with sodium hydroxide. iiC l'industria italiana del Cemento 826 (12), 992–1007.

Darweesh, H.H.M., 2007. Characteristics of metakaoline blended cement pastes. Silicates Industrials (Certificate in Science and Technology), Belgium 72 (1–2), 24–32.

Darweesh, H.H.M., 2012. Setting, hardening and st. properties of cement pastes with zeolite alone or in combination with slag. InterCeram International (International Ceramic review), Germany 1, 52–57.

Darweesh, H.H., Abdel-Kader, A.H., El-Meligy, M.G., 2013. Utilization of pulp black liquor waste as a cement admixture. International Journal of Basic and Applied Sciences 3 (2), 230–238.

Darweesh, 2013. Hydration, strength development and sulphate attack of some cement composites. World Applied sciences Journal 23 (2), 137–144.

Darweesh, H.M.M., 2014a. Utilization of Ca-lignosulphonate prepared from black liquor waste as a cement superplasticizer. Journal of Chemistry and Materials Research (JCMR) 1 (2), 28–34.

Darweesh, H.H.M., April 2014b. Utilization of perlite rock in blended cement-Part I: physicomechanical properties. Direct Research Journal of Chemistry and Material Science (DRCMS). ISSN: 2354-4163 2 (1), 1–12.

Darweesh, H.H.M., Abo El-Suoud, M.R., 2014. Setting, hardening and mechanical properties of some cement/agro/waste composites - Part I. American Journal of Mining and Metallurgy 2 (2), 32–40.

Darweesh, H.H.M., Youssef, H.F., 2014. Preparation of 11Å Al-substituted tobermorite from Egyptian trackyte rock and its effect on the specific properties of Portland cement. InterCeram International (International Ceramic review) 63 (7–8), 358–362.

Dransfield, J.M., Egan, P., 1988. Accelerators. Harlow: Longman Science and Technology 102−129.

El-Didamony, H., Haggag, M.Y., Abo-El-Enein, S.A., 1978. Cement and Concrete Research 8, 351−358.

Edmonds, R.N., Majumdar, A.J., 1989. Cement and Concrete Research 19, 779−782.

El-Alfi, E.A., Radwan, A.M., Darweesh, H.H.M., 2005. Low energy Portland cement clinker-Part 1. iiCL'industriaitaliana del Cemento, Italy 809 (5), 376−385.

El-Didamony, H., Darweesh, H.M.M., Mostafa, R.A., 2008. Characteristics of pozzolanic cement pastes Part I: physico-mechanical properties. Silicates Industrials (Certificate in Science and Technology), Belgium 73 (11−12), 193−200.

El-Mekkawi, S.A., Ismail, I.M., El-Attar, M.M., Fahmy, A.A., Mohammed, S.S., 2011. Utilization of black liquor as concrete admixture and set retarder aid. Advanced Research Journal 2 (2), 163−169.

Ettu, L.O., Ajoku, C.A., Nwachukwu, K.C., Awodiji, C.T.G., Eziefula, U.G., 2013. Strength variation of OPC-rice husk ash composites with percentage rice husk ash. International Journal of Applied Science and Engineering Research 2 (4), 420−424.

Hewlett, P.C., Edmeades, R.M., Holdswoth, R.L., 1988. Integral water proofers for concrete. Harlow: Longman Science and Technology 5, 63−78.

Hewlett, P.C., 1998. Lee's Chemistry of Cement and Concrete, fourth ed. John Wiley & Sons Inc, New York, Toronto.

Jumadurdiyev, A., Ozkul, M.M., Saglam, A.R., Parlak, N., 2005. The utilization of beet molasses as a retarding and water-reducing admixture for concrete. Cement and Concrete Research 35 (5), 874−882.

Kondo, R., Abo-El-Enein, S.A., Diamon, M., 1975. Bulletin of the Chemical Society of Japan 222−226.

Kim, H.J., Glu, G.Q., Jili, T., Hisadakata, M., 2002. Binding and desulphurization characteristics of pulp black liquor in biocoalbriquettes. Environmental Science and Technology 36, 1607−1612.

Kamoun, A., Jelidi, A., Chaabouni, M., 2003. Evaluation of the performance of sulphonated esparto grass lignin as a plasticizer-water reducer for cement. Cement and Concrete Research 33 (7), 995−1003.

Knapen, E., Van Gemert, D., 2009. Influence of the surfactants on hydration kinetics. Cement and Concrete Research 39, 6−13.

Kersener, Z., Darweesh, H.H.M., Routi, L., 2011. Alkali-activated slag-rich cement pastes with sodium silicate and water glass. Cemento Hormigon, Spain 4 (945), 18−26.

Karim, M.R., Zain, M.F.M., Jamil, M., Lai, F.C., Islam, M.N., 2012. Strength of mortar and concrete as influenced by rice husk ash: a review. World Applied Science Journal 19 (10), 1501−1513.

Luxan, M.P., Sanchez, M.I., Frias, M., 1989. Cement and Concrete Research 19, 69−80.

Mehta, P.K., 1983. Cement and Concrete Research 13, 401−406.

Negim, M.E., Mahyuddin, R., Khattib, J., Saad, B., Salah, M.I., 2010. Synthesis and characterization of hydraulic copolymers as superplasticizers for cement. World Applied Science Journal 10, 685−694.

Ohama, Y., 1995. Handbook of Polymer-Modified Concrete and Mortars, Properties and Process Technology. Noyes Publications, New Jersey.

Oland, C.B., Baker, J.W., 2001. Concrete structures for waste storage and disposal. Concrete Internships 23 (9), 41−46.

Pailere, A.M., 1995. Application of Admixtures in Concrete. E & PN Spon, London, pp. 131.

Rixon, N.R., Waddicor J., 1981. Detroit: Amer. Concr. Inst., SP-68, 359−379.

Regourd, M., Mortureux, B., 1982. In: Proc. 4th Intern. Conf. Cem. Microscopy, Las Vegas, pp. 249.

Ramachandran, V.S., 1995. Concrete admixtures. In: Handbook: Properties, Science and Technology, second ed. Noyes Publ., Park Ridge, NJ, pp. 1153.

Ramachandran, V.S., Malhotra, V.M., Jolicoeur, C., Sderates, N., 1998. Superplasticizers: Properties, Science and Application in Concrete (Canada).

Rixom, R., Mailvaganam, N., 1999. Chemical Admixtures for Concrete, third ed. E & FN Spon.

Sonaka, M., Kitagawa, K., Satoh, H., Izomi, T., Mizunuma, T., 1997. In: Proc. 5th NANMET-aci Intern. Conf. “Superplasticizers and Other Admixtures”, Roma, Italy, SP-173, 30, pp. 599−614.

Singhal, A., Tewari, V.K., Prakash, S., 2008. Utilization of treated spent liquor sludge with fly ash in cement and concrete. Building and Environment 43 (6), 991−998.

Thalcec, E., Zellic, J., 1987. Zement-Kalk-Gips 40, 574−579.

Tagnit, H.A., Aitcin, P.C., 1993. Cement and superplasticizer compatibility. World Cement 12, 38−42.

Torresan, I., Magaroto, R., Khurana, R., 1997. Proc. 5th CAMET-ACI-Intern. Conf., Italy. SP-173, 38, 599−583.

Uchikawa, H., Hanehara, S., Shirasaka, T., Sawaki, D., 1992. Effect of admixture on hydration of cement, adsorptive behaviour of admixture and fluidity and setting of fresh cement paste. Cement and Concrete Research 22 (6), 1115−1129.

Uchikawa, H., Hanchara, S., Sawaki, D., 1997. The role of steric repulsive force in the dispersion of cement particles in fresh paste prepared with organic admixture. Cement and Concrete Research 27 (1), 37−50.

Vaysburd, A.M., Emmons, P.H., McDonald, J.E., Poston, R.W., Kesner, K.E., 2000. Selecting durable repair materials: performance criteria. Laboratory results. Concrete Internships 22 (3), 38−46.

Vaysburd, R.V., 2001a. Shotcrete redefined. Concrete Internships 23 (9), 36−40.

Vaysburd, B.L., 2001b. Reducing drying shrinkage of bridge-deck concrete. Concrete Internships 23 (8), 76−82.

Wilding, C.R., Walter, A., Double, D.D., 1984. Cement and Concrete Research 14, 185−194.

Yildirim, H., Altun, B., 2012. Usage of molasses in concrete as a water reducing and retarding admixture. Indian Journal of Engineering and Material Sciences 19, 421−426.

High-performance superplasticizer based on chitosan

7

S.H. Lv
College of Resource and Environment, Shaanxi University of Science & Technology, Xi'an, China

7.1 Introduction

A water-reducing agent is an important and indispensable ingredient of modern concrete. It helps to produce fresh concrete that has a high fluidity and low water-to-cement (w/c) ratio; in addition, it can notably increase the mechanical strength of hardened concrete at a lower cost (Plank et al., 2008; Petit et al., 2010). The high fluidity can meet the requirements of long-distance transport of modern concrete and is beneficial to forming a compact structure (Hanehara and Yamada, 2008). The low w/c ratio can promote an ideal hydration reaction and form a compact/regular microstructure, resulting in improved mechanical properties of concrete (Felekoğlu and Sarıkahya, 2008). Therefore, water-reducing agents are now broadly applied in concrete (Winnefeld et al., 2007; Lewis et al., 2000).

Water-reducing agents are generally divided into two categories: common and high-range water-reducing agents, with the latter usually called *superplasticizers* (Xu et al., 2011; Lu et al., 2010). The major difference between the two is that common water-reducing agents have a low water-reducing rate (less than 15%), whereas superplasticizers have a high water-reducing rate (greater than 15%). A common water reducer is lignosulfonate (LS), which has a water-reducing rate of 8−12%; it comes from wastewater in sulfite pulping and consists of phenylpropane repeat units with sulfonic, phenolic hydroxyl, and alcoholic hydroxyl groups (Ji et al., 2012; Lou et al., 2013). The superplasticizers mainly include sulfonated naphthalene formaldehyde condensates (SNF; Ruckstuhl et al., 2002), sulfanilic acid−phenol−formaldehyde condensates (SPF; Ouyang et al., 2009), and polycarboxylate superplasticizers (PCs; Zhang et al., 2015; Plank et al., 2008). A schematic diagram of the chemical structures of LS, SNF, SPF, and PCs is shown in Figure 7.1.

The water-reducing rate of SNF and SF is usually in the range of 15−25%, and that of PCs is in the range of 25−40%. PCs also have many other advantages, such as low dosage, high fluidity of cement paste and concrete in the initial phase, and greater retarded effects for cement hydration processes (Lei and Plank, 2012; Ma et al., 2007). Thus, the advent of PCs is considered to be a revolutionary discovery and the beginning of a new era of superplasticizers (Lei and Plank, 2012; Lv et al., 2012a).

Biopolymers and Biotech Admixtures for Eco-Efficient Construction Materials. http://dx.doi.org/10.1016/B978-0-08-100214-8.00007-5
Copyright © 2016 Elsevier Ltd. All rights reserved.

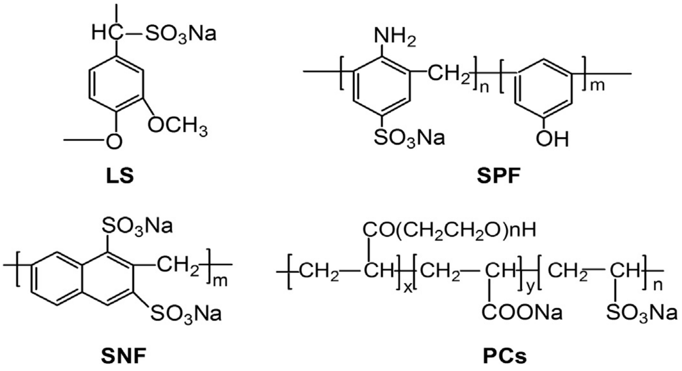

Figure 7.1 Schematic diagram of the chemical structures of LS, SNF, SPF, and PCs.

PCs have extensive application and have been rapidly developed in recent years (Yoshioka et al., 1997). However, the raw materials for PCs mainly originate from petroleum chemicals, which are faced with resource shortages, price escalations, and serious pollution issues. In summary, the progress of concrete technology has facilitated the generation of water-reducing agents and the development of superplasticizers. At the same time, superplasticizers greatly promote the properties of concrete.

Currently, the development of high-performance concrete characterized by high strength, long service life, "greenization," and low cost has become an inevitable trend (Beushausen and Dittmer, 2015; Proske et al., 2014). However, there are many difficulties and obstacles in its development—one of which is lack of the superplasticizer matched with the high-performance concrete. Therefore, a corresponding high-performance superplasticizer should first be developed (Plank et al., 2008). The high-performance concrete should first have a high water-reducing rate (greater than 25%), which can decrease the w/c ratio from its original value of 0.6 to the minimum possible value of 0.25 (Fernández et al., 2013). Only a high water-reducing rate can promote a perfect cement hydration reaction and products. The high-performance concrete also should be able to regulate and control the shape and agglomeration pattern of cement hydration products, thereby improving the strength, reducing the cracking of concrete, and achieving a longer service life. Finally, there should be little pollution from raw materials, the preparation process, and the application process.

Therefore, the development of new and high-performance superplasticizers is crucially important for the concrete industry worldwide. The current high-performance PC superplasticizers are prepared by free-radical copolymerization of vinyl monomers, such as polyethylene glycol monoether (meth)acrylate, (meth)acrylic acid, and sodium allysulfonate (Plank et al., 2008). The raw materials mainly originate from coal and petroleum, which are nonrenewable resources that are faced with shortages and produce more pollution in the process of exploiting and transforming into monomers, resulting in limits to their applications and sustainable development. Faced with the same problem, the solution for researchers in other spheres is to use natural, renewable, and abundant biopolymer resources to replace these nonrenewable resources. Some natural biopolymers, such as polysaccharides (Isik et al., 2014), starch

(Wang et al., 2010), cyclodextrin (Lv et al., 2012b), casein (Bian and Plank, 2013), and cellulose ethers (Patural et al., 2011) have been used to prepare admixtures for concrete by various methods. Inspired by the ideal and these examples, the chitosan superplasticizer has also been prepared and researched (Lv et al., 2014). This chapter mainly introduces the ideas and methods for the preparation of high-performance superplasticizers by chitosan.

7.2 Structure and properties of chitosan

7.2.1 Structure of chitosan

Chitosan is a derivative of the natural biopolymer chitin produced by stripping acetyl down, inheriting its properties of eco-friendliness, renewability, and degradation. The chemical structure of chitosan is shown in Figure 7.2. Chitosan has a high molecular weight of 100×10^4—200×10^4, and its structure is composed of units of *N*-acetyl-2-amino-2-deoxy-D-glucopyranose and 2-amino-2-deoxy-D-glucopyranose linked by (1→4)-glycosidic bonds. Each chitosan molecule mainly consists of long chains of D-glucosamine units joined together by β-1,4-glycosidic linkages. Each unit has two hydroxyl groups and one amino group (Vilela et al., 2015). The molecular structure of chitosan is very similar to that of starch and cellulose, but its properties are significantly different from starch and cellulose because of the amino group in its C_2 position.

7.2.2 Properties of chitosan

The important properties of chitosan are that it has a certain cationic at certain conditions and its solubility is closely associated with its molecular weight and deacetylation degree, as well as the pH value of aqueous. Chitosan is insoluble in water and most common organic solvents. However, it can be easily dissolved in acidic aqueous solutions

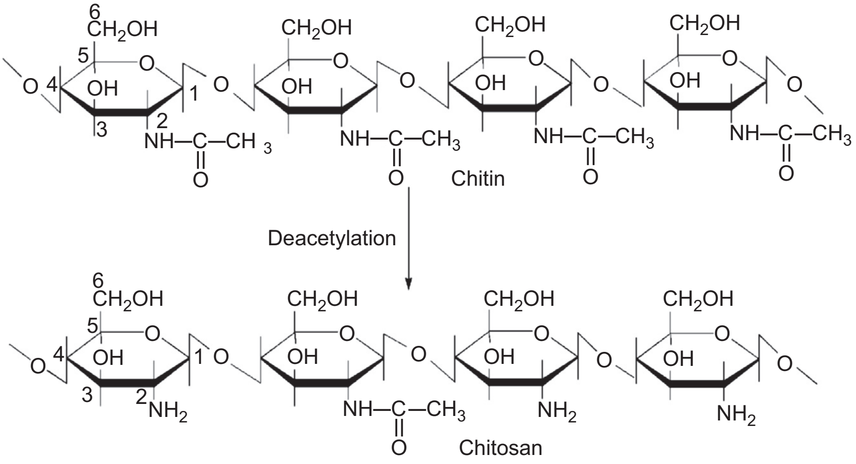

Figure 7.2 Schematic diagram of chitosan's chemical structure.

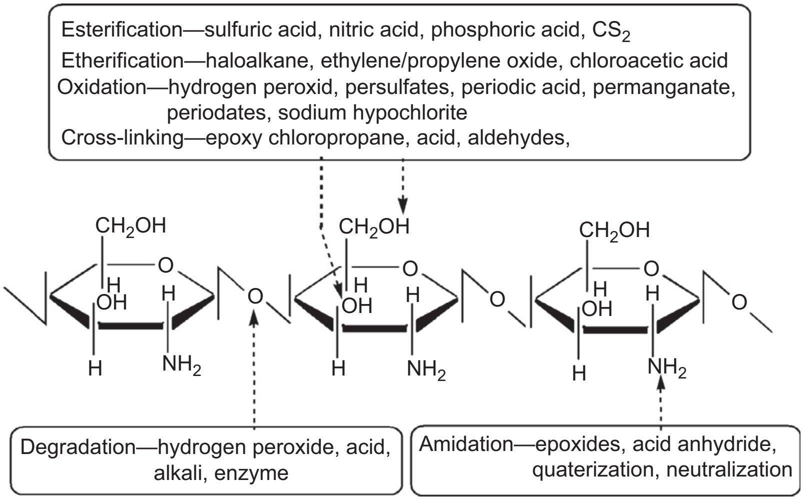

Figure 7.3 Schematic diagram of modifying chitosan.

below pH 6.3. The aqueous solution of chitosan usually has great viscosity, even in very small concentrations. A deacetylation degree of 55–70% is defined as a low deacetylated degree of chitosan, which is almost completely insoluble in water. A deacetylation degree of 70–85% is the middle deacetylation degree of chitosan, which may be partly dissolved in water. Finally, 85–95% is a high deacetylation degree of chitosan, which has good solubility in water, and 95–100% is called the ultrahigh deacetylation degree of chitosan, which is difficult to achieve. Meanwhile, reducing the molecular weight of chitosan by degradation is beneficial to increasing its solubility in water.

Modification of the structure of chitosan can greatly broaden its application areas and effects (Konwar et al., 2015; van den Brork et al.,2015). The chitosan may be modified based on hydroxyl groups and amine groups, which mainly include esterification, etherification, oxidation, cross-linking, amidation, and degradation reactions. In addition, the existence of an amino group on chitosan makes it very easy to prepare cationic materials for flocculants and bactericides. A schematic diagram of possible chemical modifications of chitosan is shown in Figure 7.3. How to build a special molecular structure for superplasticizers by modifying molecular structure and regulating molecular weight is illustrated in this chapter.

7.3 High-performance superplasticizer based on chitosan

7.3.1 Preparation of the chitosan superplasticizer

The preparation of a high-performance superplasticizer using chitosan modifies its molecular structure by a chemical reaction based on hydroxyl and amino groups. The chitosan superplasticizer is modified as suitable long molecular chains, with short

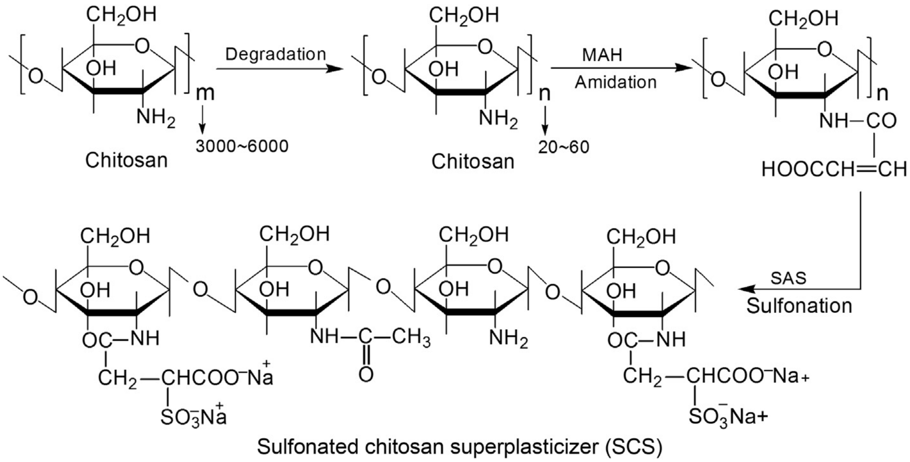

Figure 7.4 Schematic diagram of the preparation process for chitosan superplasticizer.

branched chains grafted with carboxyl and sulfonated groups. The sulfonated groups have a significant impact on the performance of the chitosan superplasticizer. The solubility of chitosan and viscosity of its solution should be first considered, which mainly depend on its molecular weight and deacetylation degree as well as increasing of the group number. Chitosan with a number-average molar mass (M_n) of 10,000–20,000 and deacetylation degree of 75–90% may be chosen as a raw material for a superplasticizer.

The preparation method for the high-performance chitosan superplasticizer is shown in Figure 7.4. It may be prepared from chitosan, maleic anhydride (MAH), and sodium metabisulfite (SM) through amidation and sulfonation reactions in turn. Chitosan and MAH first underwent amidation to introduce double bonds to the chitosan molecule. Then, the product was sulfonated with SM to prepare the sulfonated chitosan superplasticizer (SCS). The final product has carboxyl, hydroxyl, and sulfonate groups as well as a ring-shaped structure.

The SM content in the chitosan superplasticizer has a major influence on its application properties. Table 7.1 shows the application performances of chitosan superplasticizer with different SM contents, with equimolar chitosan and MAH. The results indicated that the water-reducing ratio, air content, slump retention, and compressive strength of concrete increase with increasing SM content, from 5% to 10% by weight of MAH. When the SM content is 8%, the slump, water-reducing ratio, and compressive strength at 3, 7, and 28 days reached the maximum.

7.3.2 Structure of the chitosan superplasticizer

The molecular weight of the chitosan superplasticizer was characterized by gel permeation chromatography. The molar masses, polydispersity index (PDI = M_w/M_n), and functional groups are presented in Table 7.2. The results indicated that mass average molecular weight (M_w) and number-average weight (M_n) as well as the polydispersity

Table 7.1 **Effect of chitosan superplasticizers with different SM contents on concrete performance**

SM (%)	Slump of concrete[a] (cm)				WR (%)	Air content (%)	Compressive strength (MPa)	
	0 h	1 h	2 h	3 h			3 days	28 days
0	16.3	14.1	13.5	9.1	14.1	2.1	24.3	42.3
5	17.8	19.4	17.5	14.3	18.4	3.3	30.5	62.4
8	23.5	22.8	22.1	20.7	27.6	4.2	34.5	68.5
10	22.4	21.8	206	18.4	24.6	3.5	33.1	57.8
12	20.5	20.4	19.5	18.3	24.6	5.3	31.2	63.5

SM, sodium metabisulfite; WR, water-reducing ratio.

[a] The concrete was prepared by mixing cement, sand, stone, and water in a weight ratio of 3.5:7.1:10.5:1.7. The chitosan superplasticizer solid dosage was 0.35% by weight of cement.

Table 7.2 **The physical properties of SCS and PCs**

SPs	M_w	M_n	PDI	Functional groups
SCS	18,245	14,547	1.25	$-COOH$, $-CH_2SO_3^-$, $-OH$, $-NH_2$, $-NHSO_3^-$
PCs	74,813	59,351	1.26	$-COO^-$, $-SO_3^-$, $-(OCH_2CH_2)_n-OH$

index (PDI) of chitosan superplasticizer were smaller than those of PCs. This indicates that the molecular chain length of chitosan superplasticizer was shorter and the molecular weight distribution was narrower compared to PCs.

The chemical structure of the chitosan superplasticizer was determined using a Fourier transform infrared (FTIR) spectroscopy. FTIR spectra are shown in Figure 7.5,

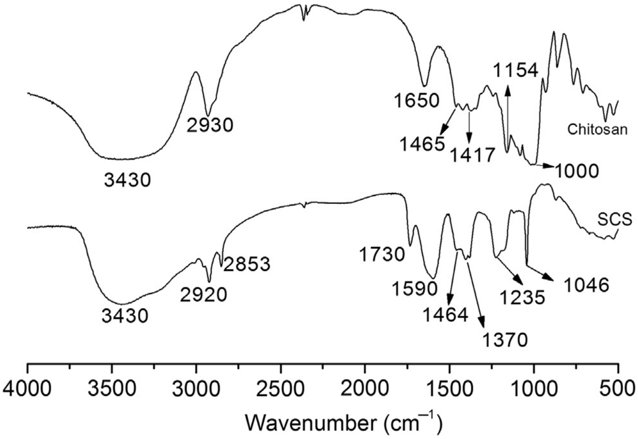

Figure 7.5 FTIR spectra of chitosan and SCS.

which confirmed that the characteristic functional groups in SCS were virtually identical to those in chitosan, MAH, and SM. The spectra included peaks at 3430 cm^{-1} (adsorption peaks of $-OH$ and $-NH_2$), 1730 cm^{-1} (adsorption peak of $-C{=}O$ in cabroxyl), 1650 cm^{-1}, 1465 cm^{-1}, 1590 cm^{-1}, 1464 cm^{-1}, and 1417 cm^{-1} (characteristic peaks of chitosan ring-shaped structure), 1370 cm^{-1}, 1235 cm^{-1} ($-NHCO-$), and 1046 cm^{-1} ($-CH_2-SO_3^-$). Thus, FTIR spectra prove that the functional groups of SCS were from chitosan, MAH, and SM, which suggest that SCS was built by chitosan, MAH, and SM.

7.4 Dispersion capacity characterization of the chitosan superplasticizer

The dispersion capacity of SCS on cement is characterized by the water-reducing ratio, concrete slump, slump loss or slump retention time, cement hydration heat, and setting time of cement paste.

7.4.1 *Water-reducing capacity*

The water-reducing ratio is an important index to evaluate the dispersion capacity of the superplasticizer. The water-reducing ratio is based on the minimum amount of water at the same concrete slump. Concrete with a slump of 22 ± 0.5 cm was prepared by mixed cement, sand, stone, and water according to the composition shown in Table 7.2. Subsequently, concrete containing SCS dosages of 0.1−0.5% by weight of cement (bwoc) were prepared. At each dosage, the w/c ratio was determined, while a constant concrete slump of 22 ± 0.5 cm was maintained. Figure 7.6 shows the relationship between the w/c ratio and the dosage of superplasticizers (SPs) at the constant

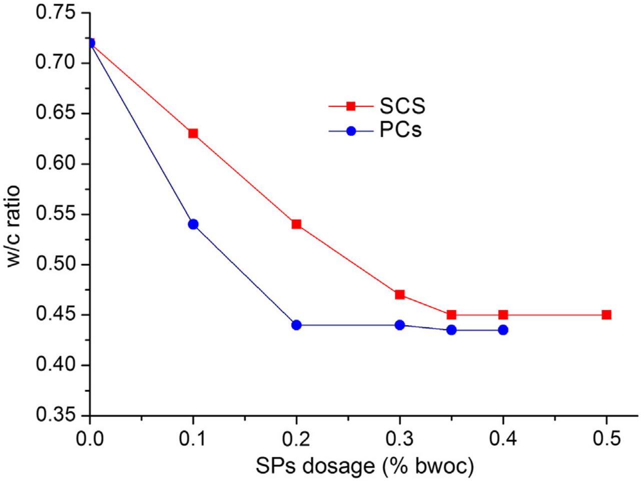

Figure 7.6 Effect of SP dosages on w/c ratio at a constant slump.

slump, indicating that the water-reducing capacity of SCS is close to that of PCs. The maximum water-reducing ratios were 28% and 27% at a dosage of 0.2% PCs and 0.35% SCS, respectively. The results also suggested that SCS has a stronger dispersion force for cement and the dispersion capacity is close to PCs.

7.4.2 Concrete slump

The slump of the concrete mixed with SCS and PCs at different dosages is shown in Figure 7.7. The results show that the slump markedly increased with the increase of SCS (PCs) dosage from 0.1% bwoc to 0.35% bwoc. At an SCS dosage of 0.35% bwoc, the slump reached a maximum. When the SCS dosage exceeded 0.35%, a serious bleeding and separation phenomenon emerged. Therefore, the optimum dosage of SCS for concrete is 0.35% bwoc. The results also indicated that the optimum dosage of PCs is 0.2% bwoc. The results of concrete slump suggested that the dispersion force of SCS in concrete is comparable to that of PCs. The reason may be that SCS is made of short-branched macromolecules, which is similar to comb-type PCs, resulting in easily occurring steric hindrance and producing a strong dispersion force. Meanwhile, there are many functional groups, such as $-COO^-$, $-CH_2SO_3^-$, $-OH$, $-NH_2$, and $-NHSO_3^-$, in the structure of SCS compared with PCs ($-COO^-$, $-(OCH_2CH_2)_n-OH$), but the length of branched chains of SCS is shorter than that of PCs, leading to the strength of the dispersion force of SCS being slightly poorer than that of PCs.

7.4.3 Concrete slump retention time

The concrete slump over time is shown in Figure 7.8. The results showed that the clump of concrete doped with SCS remained almost unchanged from onset to 120 min, then began to decrease. For PCs, the concrete slump remained unchanged until 90 min,

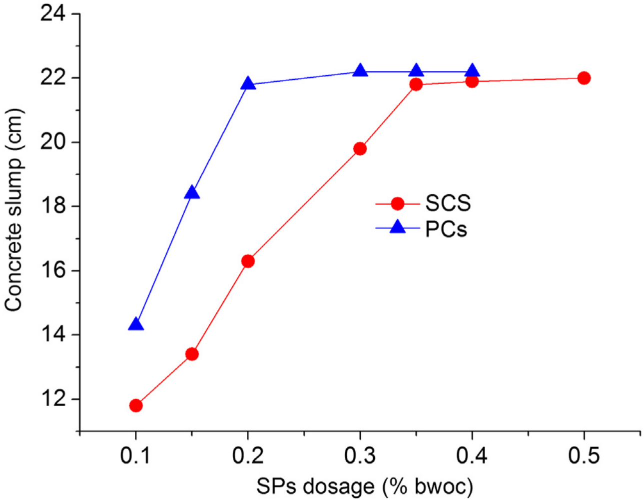

Figure 7.7 Effect of SP dosages on concrete slump.

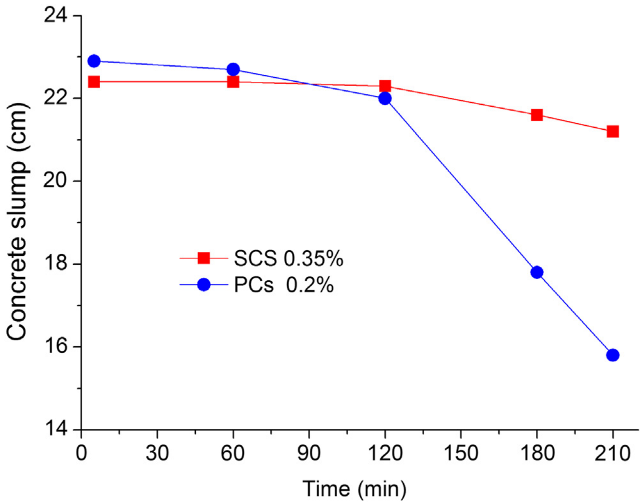

Figure 7.8 Effect of hydration time on concrete slump.

then the slump exhibited a distinct decrease over time. These results suggest that SCS shows less slump loss or longer dispersion force retention than PCs, which is likely to be because SCS has multiple functional groups ($—COO^-$, $—CH_2SO_3^-$, $—OH$, $—NH_2$, $—NHSO_3^-$), meaning that SCS exhibits strong polarity. This leads to the formation of a firm adsorption layer consisting of chitosan polymeric overlay, and it produces a stronger steric hindrance effect and electrostatic repulsion. The results suggest that the dispersion force of SCS on cement mainly originates from the synergy of steric hindrance and electrostatic repulsion.

7.4.4 Cement hydration heat

Cement paste was prepared at a w/c ratio of 0.29 containing the superplasticizer dosages (SCS 0.35% bwoc, PCs 0.2% bwoc). Figure 7.9 depicts the hydration heat—time curves, showing the effect of SCS and PCs on the cement hydration process. The results indicated that SCS can obviously delay the occurrence of hydration heat and make the rate of the production of hydration heat gentler than that of PCs. This implies that SCS can effectively inhibit the cement hydration reaction. This behavior supports the stability of the slump over the time observed for cement paste containing SCS. A noticeably delayed cement hydration reaction is characteristic of SCS.

7.4.5 Setting time of cement paste

The previous results show that SCS has a strong retarding effect on cement hydration. To explore the retarding effect on the hardening process of cement paste, the setting time of cement paste was investigated. Table 7.3 shows the initial and final setting times of cement pastes with SCS and PCs at optimum dosage. The initial and final setting times

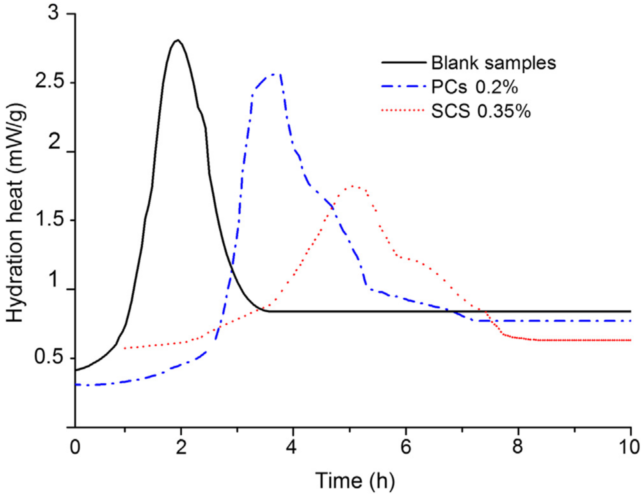

Figure 7.9 Cement hydration heat–time curves.

Table 7.3 **The setting time of cement pastes with the SCS and PCs**

SPs	Dosage (% bwoc)	Fluidity (mm)	Initial setting (min)	Final setting (min)
SCS	0.4	260	470	560
PCs	0.2	250	380	470

of cement paste with SCS (470 and 560 min) were longer than those with PCs (380 and 470 min). The results show that SCS could extend the setting time compared with PCs and that SCS could form stronger adhesion on the cement surface than PCs.

7.5 Adsorption properties of SCS on the cement surface

The previous results indicate that SCS has a strong dispersion capacity on cement particles. The strong adsorption capacity may be investigated by the adsorption behavior of SCS on the cement surface and the zeta-potential of cement particles, which will help to reveal the working mechanism.

7.5.1 Adsorption behavior of SCS on the cement surface

Adsorption behaviors mainly include the saturated adsorbed amount, adsorption isotherm, and adsorption stability. The adsorption amount of SCS and PCs was tested

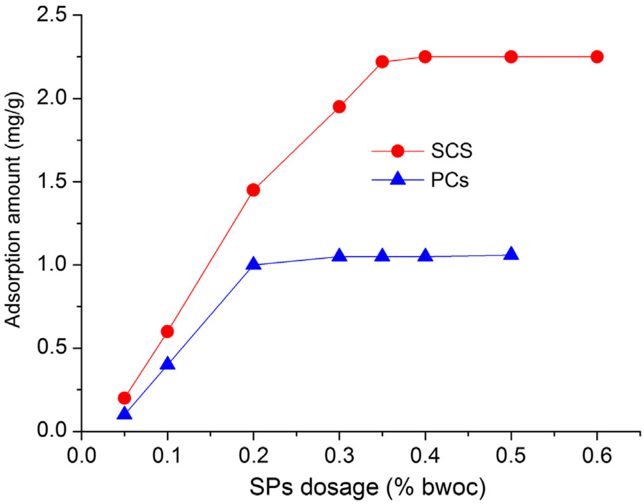

Figure 7.10 Adsorption isotherms of SCS and PCs.

at a w/c ratio of 0.5 with different dosages, and the results are shown in Figure 7.10. The results indicated that the adsorption isotherms of the three superplasticizer conform to the Langmuir adsorption model, which means that the adsorption behavior of SCS on cement can be described using the Langmuir isotherm equation. At low dosages, the adsorption amount on the cement surface increased quickly, then gradually slowed and approached the saturated adsorption. The adsorption is a monolayer adsorption and the saturated adsorption amounts of SCS and PCs are 2.1 mg/g and 1.15 mg/g of the cement surface, respectively. The results indicate that complete coverage of the cement surface requires dosages of SCS and PCs of 0.35% bwoc and 0.2% bwoc, respectively. The results correspond very well with those for the dispersion capacity displayed in Figure 7.10. The adsorption ratio and adsorption stability of SCS on the cement surface are greater than that of PCs (Table 7.4). This is because of the existence of stronger interactions between SCS and the cement surface due to multiple functional groups such as $-OSO_3^-$, $-NH_2$, $-NHSO_3^-$, $-COO^-$, and $-OH$ in the SCS molecules compared to PCs. The results demonstrated that the adsorption stability of SCS on cement particles can be attributed to electrostatic repulsion.

Table 7.4 **The adsorption amount of SCS on cement particles**

SPs	Dosage (% bwoc)	Adsorption amount (mg/g)				Adsorption ratio (%)			
		1 h	2 h	3 h	4 h	1 h	2 h	3 h	4 h
SCS	0.35	2.17	2.06	2.01	1.89	53.2	52.4	51.3	47.6
PCs	0.2	1.17	0.94	0.64	0.48	57.4	45.3	34.2	22.3

7.5.2 Zeta-potential of cement particles

The zeta-potentials of cement particles in aqueous solution with different dosages of superplasticizers are shown in Figure 7.11. The results indicate that SCS can make cement particles with similar negative zeta-potential as PCs. The minimum zeta-potential appeared at an SCS dosage of 0.35%, and the dosage is consistent with the optimal dosage of fluidity and adsorption. The results suggest that the dispersion capacity of SCS for cement particles mainly come from steric hindrance, as the dispersion capacity of PCs.

The effects of time on the zeta-potential of cement particles with superplasticizers (SCS 0.35% bwoc and PCs 0.2% bwoc) is shown in Figure 7.12. The results indicate that the cement particles adsorbed with SCS can maintain a stable zeta-potential within 200 min compared with that using PCs. The results indicate that the SCS has a stronger interaction with the cement particle surface than that of PCs. Generally, the dispersion action of PCs is mainly via steric hindrance because of its comb-type macromolecules (Frank et al., 2007), and the electrostatic repulsion plays a relatively minor role in the dispersion action due to its longer molecule chains and low charge density. Therefore, the dispersion force of SCS may come from both strong electrostatic repulsion and steric hindrance. The reason is that the SCS molecule has many functional groups with high charge density and ring-shaped longer chains with many short branches. This supports the occurrence of a powerful dispersion force of SCS on cement. The trends in the zeta-potential are consistent with the adsorption stability and the slump retention of cement paste.

7.6 The application results of SCS in concrete

The application results of SCS in concrete include water-reducing ratio, slump, and compressive strength, as shown in Table 7.5. The results indicate that the fresh

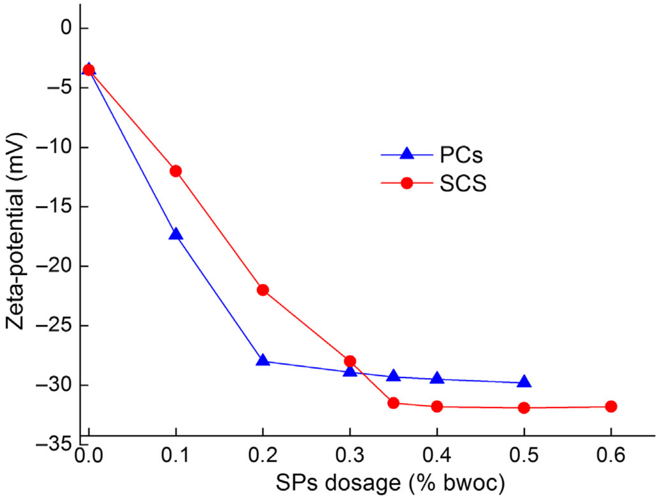

Figure 7.11 Effect of SP dosage on the zeta-potential of cement particles.

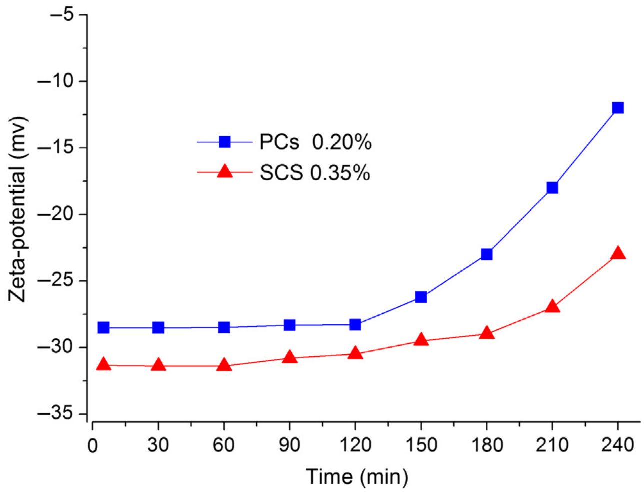

Figure 7.12 Effect of time on the zeta-potential of cement particles.

Table 7.5 **The application properties of SCS**

SPs	Dosage (%)	WR[a] (%)	Concrete slump[b] (cm)			Compressive strength (MPa)		Flexural strength (MPa)	
			0 h	1 h	3 h	3 days	28 days	3 days	28 days
SCS	0.35	28.5	22.3	21.5	18.3	38.3	67.5	5.1	10.6
PCs	0.2	29.4	22.1	20.2	13.2	36.1	64.3	4.2	8.7

[a] Water-reducing ratio.

[b] The concrete was made of cement, sand, cobble, and water according to mass ratio of 3.5:7.1:10.5:1.7.

concrete slump containing SCS was similar to PCs, but the concrete slump retention doped with SCS within 3 h was distinctly better than for PCs. For SCS, the slump differences of two different types of cements are not significant. Therefore, SCS has good dispersibility and adaptability with cements. The compressive strength of concrete doped with SCS is greater than that of PCs, while the flexural strength of concrete with SCS has a greater increase than that with PCs. The results suggest that SCS can improve the microstructure of concrete. SCS can be used as a superplasticizer and has especially durable slump retention.

Modified chitosan can be used together with existing PCs. It can ensure that the cement paste satisfies the performance requirements of viscosity, bleeding ratio, fluidity, slump, and retarding time. In particular, it can help to improve the strength of concrete and have greater potential for extending its service life.

7.7 Microstructure characterization of hardened cement paste

7.7.1 Pore structure analysis

The effect of SCS on the microstructure of hardened cement paste was investigated via pore structure measurement and scanning electron microscopy (SEM) images. The cement paste samples were prepared at a w/c ratio of 0.29 using 0.35% bwoc of SCS and 0.2% bwoc of PCs, and cured to 3 d and 28 d under standard curing conditions. The pore structure was then determined using a mercury porosimeter. Table 7.6 shows the pore structure, indicating that SCS can markedly reduce the number of large pores (>100 nm) compared with PCs. Also, SCS can lead to a greater number of smaller pores compared to PCs. This supports the finding of the greater strength of cement paste and concrete mixed with SCS than that mixed with PCs. A smaller pore diameter is associated with greater mechanical strength of cement composites.

7.7.2 SEM image analysis

Figure 7.13 shows the SEM images of hardened cement paste doped with different SPs (SNF, PCs, and SCS) at 28 d. For the blank sample, the SEM image indicates that the hardened cement paste mainly has a loose porous structure and exhibits few small rod-like crystals (Figure 7.13(a)), With SNF at 0.9% bwoc, there are many rod-like crystals blocked in the matrix of the cement paste, and it shows a loose porous structure (Figure 7.13(b)). With PCs at 0.2% bwoc, the image shows that the structure is dense and has some rod-like crystals blocked in compact hardened cement paste (Figure 7.13(c)). With SCS at 0.35% bwoc, the image indicates that the hardened

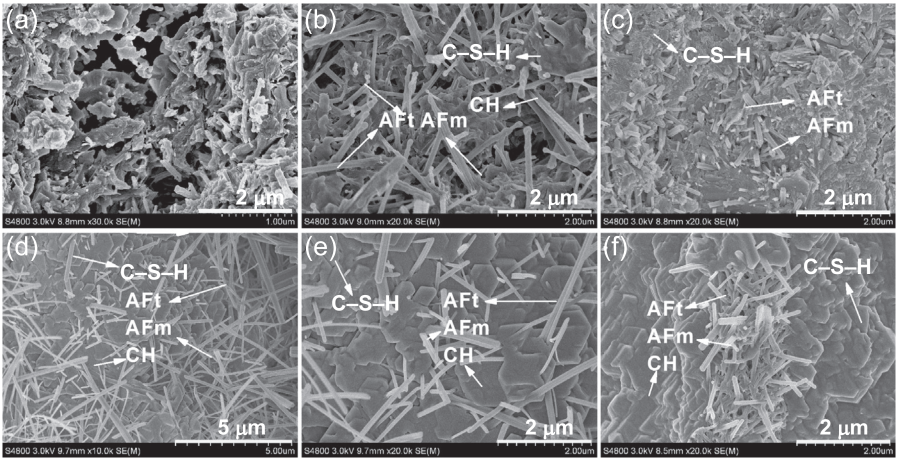

Figure 7.13 SEM images of hardened cement paste with different SPs cured for 28 d: (a) blank sample; (b) SNF 0.9% bwoc; (c) PCs 0.2% bwoc; (d−f) SCS 0.35% bwoc (Portland cement 42.5R). The w/c ratio of (a) is 0.6, whereas it is 0.29 in (b-f).

Table 7.6 **Pore structure of hardened cement paste mixed with SCS and PCs**

Pore diameter (nm)	Porosity (%)			
	Mixed with SCS		Mixed with PCs	
	3 days	28 days	3 days	28 days
<100	74.4	86.8	62.2	76.4
100–200	15.6	9.6	23.5	14.5
>200	8.2	1.6	15.7	7.8

cement paste exhibited a more compact structure and there are many rod-like crystals, which were blocked and interpenetrated in the compact matrix (Figure 7.13(d–f)). The compact matrix of cement paste was constructed with rod-like crystals (Figure 7.13(f)). This suggests that SCS can control the cement hydration reaction and promote the formation of more rod-like hydration crystals and compact structure blocked rod-like crystals. The SEM image analysis corresponds very well with the pore structure summarized in Table 7.6 and mechanical strength in Table 7.5.

7.8 Working mechanism of SCS

A possible working mechanism for SCS on cement hydration reaction and its products can be proposed, as shown in Figure 7.14. When SCS was added to the cement paste, it could strongly adhere to the cement surface because of the interactions of the multiple functional groups of SCS ($-COO^-$, $-CH_2SO_3^-$, $-OH$, $-NH_2$, and $-NHSO_3^-$) and cement surface active groups (Al_2O_3, CaO, MgO, Fe_2O_3). Moreover, SCS consists

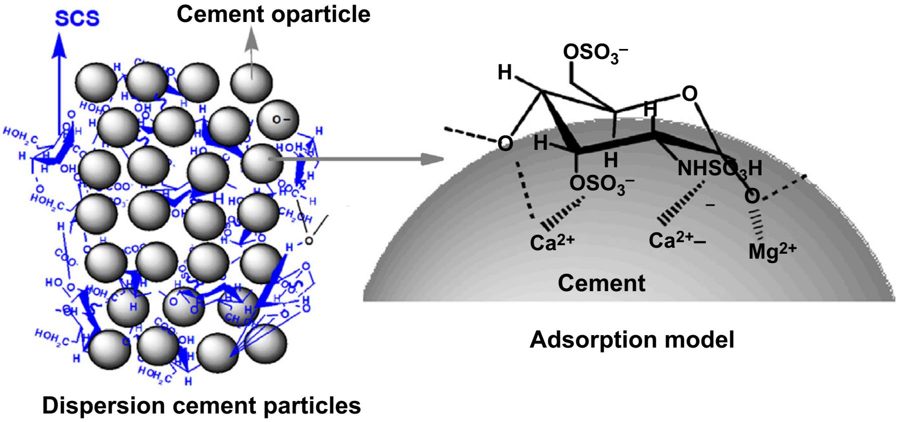

Figure 7.14 The working mechanism of SCS on the cement surface.

of ring structure units and more short branched groups to PCs. This facilitates their easy adhesion to the cement surface and further formation of a thicker and denser adsorbed double electric layer with both steric hindrance and electrostatic repulsion. In addition, the ring-shaped chain units with a larger volume and carboxyl and sulfonated groups has helped to form a stable adsorbed layer and enhance steric hindrance and electrostatic repulsion.

Cement in a hydrous state mainly consists of tricalcium silicate C_3S (Ca_3SiO_5), dicalcium silicate C_2S (Ca_2SiO_4), tricalcium aluminate C_3A ($Ca_3Al_2O_6$), tetracalcium aluminoferrite C_4AF ($Ca_4Al_nFe_{2-n}O_7$), as well as a small amount of clinker sulfate (Na_2SO_4, K_2SO_4) and gypsum ($CaSO_4\cdot 2H_2O$). In the hydration process, C_3A, C_4AF, C_3S, and C_2S will carry out a complex hydration reaction to form ettringite ($Ca_6Al_2(SO_4)_3(OH)_{12}\cdot 26H_2O$, AFt), ($Ca_4Al_2(OH)_{12}\cdot SO_4\cdot 6H_2O$, AFm), calcium hydroxide ($Ca(OH)_2$, CH), and calcium silicate hydrate ($3CaO\cdot 2SiO_2\cdot 4H_2O$, $C-S-H$) gel (Yuan et al., 2009). CH, AFt, and AFm may form rod-like, needle-like shapes with disorder or amorphous solid. The corresponding chemical reactions are represented by Eqns (7.1)–(7.4). The growth and agglomeration of these cement hydration products altogether not only form their own special structure but also fastened (fixed or binded) a sand/stone/steel bar in the structure. These shapes, as well as the numbers of such crystals in the cement paste, have an important impact on the mechanical strength of concrete (Yuan and Ji, 2009).

$$\underset{\mathbf{C_3A}}{Ca_3Al_2O_6} \rightarrow 3CaSO_4\cdot 2H_2O + 26H_2O \rightarrow \underset{\mathbf{AFt}\quad \text{rod-like}}{Ca_6Al_2(SO_4)_3(OH)_{12}\cdot 26H_2O} \tag{7.1}$$

$$\begin{aligned} &\underset{\mathbf{C_3A}}{2Ca_3Al_2O_6} + \underset{\mathbf{AFt}}{Ca_6Al_2(SO_4)_3(OH)_{12}}\cdot 26H_2O + 4H_2O \\ &\rightarrow \underset{\mathbf{AFm}\quad \text{rod-like}}{3Ca_4Al_2(OH)_{12}\cdot SO_4\cdot 6H_2O} \end{aligned} \tag{7.2}$$

$$\underset{\mathbf{C_3S}}{2Ca_3SiO_5} + 6H_2O \rightarrow \underset{\mathbf{C-S-H}\quad \text{gel}}{3CaO\cdot 2SiO_2\cdot 4H_2O} \rightarrow \underset{\mathbf{CH}\quad \text{rod- and needle-like}}{3Ca(OH)_2} \tag{7.3}$$

$$\underset{\mathbf{C_2S}}{2Ca_2SiO_4} + 4H_2O \rightarrow \underset{\mathbf{C-S-H}\quad \text{gel}}{3CaO\cdot 2SiO_2\cdot 4H_2O} \rightarrow \underset{\mathbf{CH}\quad \text{rod- and needle-like}}{Ca(OH)_2} \tag{7.4}$$

Decreasing the w/c ratio and retarded cement hydration reaction by using superplasticizers in the preparation of concrete is an appealing approach of reinforcing and toughening concrete because it can change the microstructure of cement paste. Therefore, this method has been applied widely (Anagnostopoulos, 2014). Superplasticizers can retard the hydration reaction that occurs rapidly, thus allowing more time for cement hydration products to self-assemble into compact and regular structures (Barrak et al., 2009), resulting in clear improvements in compressive strength (Prince et al., 2003). The w/c ratio has been used in evaluating the efficiency of superplasticizers (Hu et al., 2014). Of course, the high-performance superplasticizers should have stronger capacity to reduce the w/c ratio and regulate the microstructure by controlling the cement hydration reaction and product shape. This is why high-performance concrete must match with high-performance superplasticizers.

The experimental results indicated that SCS can regulate to form a compact structure blocked with many rod-like crystals, distinctly improving the tensile/flexural/compressive strength. The reason may be that the SCS molecules first stuck on the cement particle's surface by these functional groups, mainly including $-COO^-$, $-CH_2SO_3^-$, $-OH$, $-NH_2$, and $-NHSO_3^-$, as well as a ring structure to temporarily retard the hydration reaction; then, partly functional groups react preferentially with C_3S, C_2S, and C_3A and form the growth points of the hydration products. Within the retarding effect, the hydration reaction takes place slowly at the growth points, thus allowing more time and opportunity to assemble the hydration products into rod-like crystals. The rod-like crystals usually grow out from a compact matrix of cement composites and form a cross-linking and interpenetration structure, which has greatly contributed to improving the strength of cement composites.

7.9 Conclusion and future research trends

7.9.1 Conclusion

1. A high-performance superplasticizer may be prepared using the biopolymer chitosan as a raw material by chemical modification. The chitosan superplasticizer has a stronger and more stable dispersion force and high water-reducing ratio. Chitosan superplasticizer exceeds PCs with regard to retarding effect.
2. The chitosan superplasticizer can control the cement hydration reaction, as well as promote the formation of more rod-like hydration crystals and a more compact structure. The rod-like crystals usually block in a compact matrix and form a cross-linking and interpenetration structure, which has greatly contributed to improving the strength of cement composites.
3. The working mechanisms of chitosan superplasticizer suggest that the strong dispersion force and regulation capacity originates from the synergy of retardation effects and its special structure with multifunctional groups and ring-shaped units.

7.9.2 Future research trends

High-performance concrete is being paid more and more attention. However, this concrete needs many materials and has many influencing factors, with a high-performance superplasticizer being a key material. Therefore, there is an urgent need to develop a high-performance superplasticizer.

1. A high-performance superplasticizer will become the development trend of superplasticizer. Using natural biopolymer chitosan to develop a high-performance superplasticizer has certain advantages in structure, resource, and cleaner production.
2. A high-performance superplasticizer should have not only a high water-reducing ratio but also the capacity to regulate the cement hydration reaction and products. In addition, it should

help to form an ideal microstructure for reinforcing and toughening cement-based materials. Therefore, more attention should be focussed on researching the relationship between structure and properties.

3. Although natural biopolymers, including chitosan, have clear chemical structures and various modified methods, preparation of modified chitosan with the designed ideals is very difficult. Therefore, investigation into an effectively modified method is still especially important.

References

Anagnostopoulos, C.A., 2014. Effect of different superplasticizers on the physical and mechanical properties of cement grouts. Construction and Building Materials 50, 162–168. http://dx.doi.org/10.1016/j.conbuildmat.2013.09.050.

Bian, H., Plank, J., 2013. Effect of heat treatment on the dispersion performance of casein superplasticizer used in dry-mix mortar. Cement and Concrete Research 51, 1–5. http://dx.doi.org/10.1016/j.cemconres.2013.04.004.

Beushausen, H., Dittmer, T., 2015. The influence of aggregate type on the strength and elastic modulus of high strength concrete. Construction and Building Materials 74 (15), 132–139. http://dx.doi.org/10.1016/j.conbuildmat.2014.08.055.

van den Broek, L.A.M., Knoop, R.J.I., Kappen, F.H.J., Boeri, C.G., 2015. Chitosan films and blends for packaging material. Carbohydrate Polymers 116, 237–242.

Barrak, M.El, Mouret, M., Bascoul, A., 2009. Self-compacting concrete paste constituents: hierarchical classification of their influence on flow properties of the paste. Cement and Concrete Composites 31, 12–21. http://dx.doi.org/10.1016/j.cemconcomp.2008.10.002.

Felekoğlu, B., Sarıkahya, H., 2008. Effect of chemical structure of polycarboxylate-based superplasticizers on workability retention of self-compacting concrete. Construction and Building Materials 22, 1972–1980. http://dx.doi.org/10.1016/j.conbuildmat.2007.07.005.

Fernández, A.J.M., Duran, A., Navarro-Blasco, I., Lanas, J., Sirera, R., Alvarez, J.I., 2013. Influence of nanosilica and a polycarboxylate ether superplasticizer on the performance of lime mortars. Cement and Concrete Research 43, 12–24. http://dx.doi.org/10.1016/j.cemconres.2012.10.007.

Frank, W., Stefan, B., Joachim, P., Thomas, G., 2007. Effects of the molecular architecture of comb-shaped superplasticizers on their performance in cementitious systems. Cement and Concrete Composites 29, 251–262. http://dx.doi.org/10.1016/j.cemconcomp.2006.12.006.

Hu, J., Ge, Z., Wang, K., 2014. Influence of cement fineness and water-to-cement ratio on mortar early-age heat of hydration and set times. Construction and Building Materials 2014 (50), 657–663. http://dx.doi.org/10.1016/j.conbuildmat.2013.10.011.

Hanehara, S., Yamada, K., 2008. Rheology and early age properties of cement systems. Cement and Concrete Research 21, 175–195. http://dx.doi.org/10.1016/j.cemconres.2007.09.006.

Isik, I., Ozkul, E., Hulusi, M., 2014. Utilization of polysaccharides as viscosity modifying agent in self-compacting concrete. Construction and Building Materials 72, 239–247. http://dx.doi.org/10.1016/j.conbuildmat.2014.09.017.

Ji, D., Luo, Z.Y., He, M., Shi, Y.J., Gu, X.L., 2012. Effect of both grafting and blending modifications on the performance of lignosulphonate-modified sulphanilic acid–phenol–formaldehyde condensates. Cement and Concrete Research 42, 1199–1206. http://dx.doi.org/10.1016/j.cemconres.2012.05.010.

Konwar, A., Gogoi, N., Majumdar, G., Chowdhury, D., 2015. Green chitosan–carbon dots nanocomposite hydrogel film with superior properties. Carbohydrate Polymers 115, 238–245.

Lewis, J.A., Matsuyama, H., Kirby, G., Morissette, S., Young, J.F., 2000. Polyelectrolyte effects on the rheological properties of concentrated cement suspensions. Journal of the American Ceramic Society 83 (8), 1905−1913.

Lei, L., Plank, J., 2012. Synthesis, working mechanism and effectiveness of a novel cycloaliphatic superplasticizer for concrete. Cement and Concrete Research 42, 118−123. http://dx.doi.org/10.1016/j.cemconres.2011.09.003.

Lou, H.M., Lai, H.R., Wang, M.X., Pang, Y.X., Yang, D.J., Qiu, X.Q., Wang, B., Zhang, H.B., 2013. Preparation of lignin-based superplasticizer by graft sulfonation and investigation of the dispersive performance and mechanism in a cementations system. Industrial Engineering Chemistry Research 52, 16101−16109. http://dx.doi.org/10.1021/ie402169g.

Lu, S.H., Liu, G., Ma, Y.F., Li, F., 2010. Study on synthesis and application of a new vinyl graft copolymer superplasticizer. Journal of the Applied Polymer Science 117, 273−280.

Lv, S.H., Liu, J.J., Zhou, Q.F., Huang, L., Sun, T., 2014. Synthesis of modified chitosan by amidation and sulfonation and its application performance and working mechanism. Industrial and Engineering Chemistry Research 53 (10), 3908−3916. http://dx.doi.org/10.1021/ie403786q.

Lv, S.H., Duan, J.P., Gao, R.J., Cao, Q., Li, D., 2012a. Effects of poly(ethylene glycol) branched chain linkage mode on polycarboxylate superplasticizer performance. Polymer for Advanced Technologies 23, 1596−1603. http://dx.doi.org/10.1002/pat.3034.

Lv, S.H., Gao, R.J., Duan, J.P., Li, D., Cao, Q., 2012b. The effects of β-cyclodextrin side chains on the dispersing and retarding properties of polycarboxylate superplasticizers. Journal of Applied Polymer Science 125, 396−404. http://dx.doi.org/10.1002/app.35606.

Ma, G.G., Wang, X.G., Liang, W.Q., Li, X.G., He, Z., 2007. Study on early-age cracking of cement-based materials with superplasticizers. Construction and Building Materials 21, 2017−2022. http://dx.doi.org/10.1016/j.conbuildmat.2006.04.012.

Ouyang, X., Jiang, X., Qiu, X., Yang, D., Pang, Y., 2009. Effect of molecular weight of sulfanilic acid-phenol-formaldehyde condensate on the properties of cementitious system. Cement and Concrete Research 39 (4), 283−288. http://dx.doi.org/10.1016/j.cemconres.2009.01.002.

Patural, L., Marchal, P., Govin, A., Grosseau, P., Ruot, B., Deves, O., 2011. Cellulose ethers influence on water retention and consistency in cement-based mortars. Cement and Concrete Research 41, 46−55. http://dx.doi.org/10.1016/j.cemconres.2010.09.004.

Petit, J.Y., Wirquin, E., Kamal, H., 2010. Effect of temperature on the rheology of flowable mortars. Cement and Concrete Composites 32 (1), 43−53. http://dx.doi.org/10.1016/j.cemconcomp.2009.10.003.

Plank, J., Pöllmann, K., Zouaoui, N., 2008. Synthesis and performance of methacrylic ester based polycarboxylate superplasticizers possessing hydroxy terminated poly(ethylene glycol) side chains. Cement and Concrete Research 38 (10), 1210−1216. http://dx.doi.org/10.1016/j.cemconres.2008.01.007.

Prince, W., Espagne, M., Aïtcin, P.C., 2003. Ettringite formation: a crucial step in cement superplasticizer. Cement and Concrete Research 33, 635−641. http://dx.doi.org/10.1016/S0008-8846(02)01042-6.

Proske, T., Hainer, S., Rezvani, M., Graubner, C.-A., 2014. Eco-friendly concretes with reduced water and cement content - mix design principles and application in practice. Construction and Building Materials 67, 413−421. http://dx.doi.org/10.1016/j.conbuildmat.2013.12.066.

Ruckstuhl, S., Suter, M.J.-F., Kohler, H.-P.E., Giger, W., 2002. Leaching and primary biodegradation of sulfonated naphthalenes and their formaldehyde condensates from concrete superplasticizers in groundwater affected by tunnel construction. Environmental Science and Technology 36 (15), 3284−3289. http://dx.doi.org/10.1021/es010297g.

Vilela, J.A.P., Perrechil, F.de A., Picone, C.S.F., Sato, A.C.K., Cunha, R.L.da, 2015. Preparation, characterization and in vitro digestibility of gellan and chitosan—gellan microgels. Carbohydrate Polymers 117, 54—62.

Wang, T., Yan, Y., Hu, Z., Zhao, P., 2010. Synthesis and dispersion of the modified starch used as concrete water-reducing agent. Journal of the Chinese Ceramic Society 38 (7), 1191—1196.

Winnefeld, F., Becker, S., Pakusch, J., Gotz, T., 2007. Effects of the molecular architecture of comb-shaped superplasticizers on their performance in cementitious systems. Cement and Concrete Composites 29 (4), 251—262. http://dx.doi.org/10.1016/j.cemconcomp.2006.12.006.

Xu, S.L., Zhang, B.W., Chen, Z.R., Yu, J.H., Evans, D.G., Zhang, F., 2011. A general and scalable formulation of pure CaAl-layered double hydroxide via an organic/water solution route. Industrial Engineering Chemistry Research 50, 6567—6572. http://dx.doi.org/10.1021/ie102135k.

Yoshioka, K., Sakai, E., Daimon, M., Kitahara, A., 1997. Role of steric hindrance in the performance of superplasticizers for concrete. Journal of the American Ceramic Society 80, 2667—2671.

Yuan, Y.H., Ji, Y., 2009. Modeling corroded section configuration of steel bar in concrete structure. Construction and Building Materials 23, 2461—2466. http://dx.doi.org/10.1016/j.conbuildmat.2008.09.026.

Zhang, Y., Kong, X., Lu, Z., Lu, Z., Hou, S., 2015. Effects of the charge characteristics of polycarboxylate superplasticizers on the adsorption and the retardation in cement pastes. Cement and Concrete Research 67, 184—196. http://dx.doi.org/10.1016/j.cemconres.2014.10.004.

Microorganism-based bioplasticizer for cementitious materials

8

F. Martirena[1], *Y. Rodriguez-Rodriguez*[2], *A. Callico*[3], *Y. Diaz*[1], *G. Bracho*[3], *A. Hereira*[4], *J.O. Guerra de Leon*[4], *L. Sorelli*[5], *Y. Alvarado-Capó*[6]
[1]Universidad Central de las Villas, Carretera de Camajuani, Santa Clara, CP, Cuba; [2]Centro de Bioactivos Químicos (CBQ), Universidad Central "Marta Abreu" de Las Villas, Santa Clara, Cuba; [3]Institute "Carlos J. Finlay", Habana, Cuba; [4]Faculty of Chemistry and Pharmacy, Universidad Central "Marta Abreu" de Las Villas, Santa Clara, Cuba; [5]Université Laval, Département de Génie Civil, Québec, QC, Canada; [6]Instituto de Biotecnología de las Plantas, Universidad Central "Marta Abreu" de Las Villas, Santa Clara, Cuba

8.1 Introduction

Superplasticizers (SPs) can strongly influence concrete rheology: the admixture of an SP can improve flowability of concrete. Alternatively, at the same flowability requirement, the water/cement (w/c) ratio can be reduced to improve the strength and durability of concrete (Kwan and Fung, 2012). SPs currently used have different origins and properties. Most of them come in a synthesized form derived from the oil industry. The first generation of SPs was lignosulfonate-based air-entraining water-reducing agents. It was followed by the second generation of SPs, which consisted of β-naphthalene sulfonate-based products. The latest generation of SPs consists of polycarboxylate-based products, which are the main SPs in use today, with very complex molecules that yield spectacular properties. Most of these products come in a synthesized form (Kovler and Roussel, 2011).

If sustainability is sought, the industry must shift from the use of nonrenewable, oil-dependent products that ultimately lead to depletion of natural resources to the development of new renewable biomaterials, which are totally biodegradable, and can be replenished through natural processes. Applications of this approach have been experienced in several areas of industry and engineering (Pacheco-Torgal and Labrincha, 2014).

Biological additives for concrete have been developed, such as wastes of antibiotic manufacturing, lignosulfates from wastes of the paper industry, and yeast fermentation waste (YFW). For instance, YFW has been proved to be a polyfunctional hydrophilizing admixture that fluidizes concrete mixtures, mainly due to the action of melanoidine-humin complexes contained in YFW on the surface of cement particles, leading to a decrease in the flocculation of cement particles (Bolobova and Kondrashchenko, 2000).

Biopolymers and Biotech Admixtures for Eco-Efficient Construction Materials. http://dx.doi.org/10.1016/B978-0-08-100214-8.00008-7
Copyright © 2016 Elsevier Ltd. All rights reserved.

8.2 Efficient microorganisms and their use in construction

The technology "Efficient Microorganism" (EM) was created by the Japanese Teuro Higa, University of the Ryukyus, Okinawa, Japan. EM consists of mixed cultures of naturally occurring microorganisms that can be applied as inoculants to increase the microbial diversity of soils and plants. EM contains selected species of microorganisms including predominant populations of lactic acid bacteria, yeasts, and smaller numbers of phototrophic bacteria, actinomycetes, and other types of organisms. All of these are mutually compatible with one another and can coexist in liquid culture. The product has applications in agriculture and environmental control of biowastes (Higa and Wididana, 1991).

Concrete with EM was first developed in Japan with the aim of healing concrete cracks through biological activity. The product EM-1® with applications in agriculture and environmental fields was used as cement admixture (Sato et al., 2000). There are other reports of the use of bacteria to improve certain properties of concrete, among them healing concrete through microorganisms (Ramachandran et al., 2001; Wu et al., 2012); use of microorganisms to improve mortar strength (Ghosh et al., 2003); and bioconcrete with enriched bacteria culture (Ghosh et al., 2006; Achal et al., 2009). Although they reckoned that the workability of concrete was improved through the admixture of microorganisms, their effect as a plasticizer is not conclusively assessed. The use of bioproducts as an admixture for developing new concrete types is still at early stage (Ismail and Mohd Saman, 2014).

8.3 EM characterization

The authors undertook a research work to assess the plasticizing properties of an EM-like bioplasticizer, referred to as MEF (Martirena et al., 2014). The product is produced at Institute "Carlos J. Finlay" in Havana using an ad hoc technology based on previously described procedures (Sato et al., 2000; Ramachandran et al., 2001).

MEF consists of fermentation products from sequential cultures of naturally growing microorganisms. The initial inoculums comprise a combination of different species of lactic bacteria, phototrophic bacteria, and yeast. These microorganisms were cultivated in two fermentation steps in controlled conditions, starting from a solid-state process followed by large-scale liquid fermentation. Solid and liquid culturing media contain molasses as the main source of carbon and also include substrates derived from waste milk products. The manufacturing process showed to be consistent and is complete in around 15 days. Quality Control tests carried out in one-year-old material show no major variation of main properties; the product expiry date is therefore considered as one year for this investigation.

The microbial consortium in MEF consists mainly of four groups of microorganisms, with at least three species from each of four classes of organisms depending on batch. These classes of organisms are grown in a synergistic culture: yeasts, lactic acid, spore-forming bacilli, and other related undeclared organisms. Some of the species included are *Lactobacillus collinoides*, *Lactobacillus paracasei* sub *paracasei*, *Lactobacillus acidophilus*, and *Lactobacillus buchneri* (beneficial organisms widely found in fermented foods). This product also included other beneficial members of *Bacillus* spp. (*B. circulans*, *B. licheniformis*, *B. pumilus*, *B subtilis*), *Paenibacillus* spp. (*P. polymyxa*), and *Brevibacillus* spp. derived from soil samples. Yeast includes, for example, microorganisms belonging to *Candida* and *Saccharomyces*. Specific examples of this yeast are *Saccharomyces cereviciae* and other undeclared species.

The product MEF was characterized in a similar way to a commercial SP. The amount of total solids was determined according to the Cuban standard NC-271-1: 2003. Density of the final product was determined according to the Cuban standard NC-271-2:2003. pH was determined following the procedure stated in the Cuban standard NC-271-4:2003. Table 8.1 shows values of the chemical–physical characteristics determined for this bioproduct. One commercial SP, Mapefluid N-200, naphthalene based, was used as reference for comparison.

MEF has a low pH value resulting from anaerobic fermentation (Mayer et al., 2010). MEF is also more acidic than commercial superplasticizers studied in different studies (Burgos-Montes et al., 2012), something that could impact on the alkalinity of the pore solutions; this should be further studied (Yoshiokaa et al., 2002), although preliminary evaluation indicated no change in pH on cement pastes. The density of the product MEF is lower than the commercial SP N-200. It is consistent with the lower amount of total solids found in the sample of MEF tested compared to the commercial SPs. It could indicate that the product has a higher degree of dilution.

MEF electrical conductivity value is high, thus indicating that there are many dissolved electrolytes. These electrolytes can be salts, acids, or other substances dissolved in the bioproduct. The metals in MEF were Na, K, Co, Fe, Mn, Zn, Ca, Mg, Cu, and Ni, as presented in Table 8.2 (Martirena et al., 2014). The high concentration of metals such as K, Mg, Na, Fe, and Ca should be regarded in the discussion of results, especially as far as the influence of the product on hydration is concerned.

High-performance liquid chromatography was used for lactic acid and acetic acid determination. Concentrations of 90 and 60 mg/mL, respectively, were reported. Reducing sugars in MEF were also determined according to the Cuban Standard NC-712: 2009; Final molasses—determination of total reducing molasses by the Lane–Eynon method at constant volume. The concentration of reducing sugars was 0.49%, relatively low for cement chemical admixtures.

Table 8.1 **Chemical and physical properties of the bioproduct MEF and N-200**

Bioproduct	Density (picnometer) (g/mL)	% Total solids (TS)	pH	Electrical conductivity EC (mS/cm)
MEF	1.01	2.32	3.4	7.71
N-200	1.20	40.00	6.48	–

Table 8.2 Elemental composition of MEF

Elem.	Na^+ (mg/L)	K^+ (mg/L)	Fe_{total} (mg/L)	Mn^{2+} (mg/L)	Mg^{2+} (mg/L)	Cu^{2+} (mg/L)	Ni^{2+} (mg/L)	Co^{2+} (mg/L)	Zn^{2+} (mg/L)	Ca^{2+} (mg/L)	N_{total} (mg/L)	P_{total} (mg/L)
MEF	56.40	2890.13	45.44	6.97	107.11	1.13	0.79	0.54	1.80	45.12	57.40	6.09

8.4 EM as plasticizer in cement

Rheology is the logical tool to characterize and describe the flow behavior, thickening, workability loss, stability, and even compactability of a fresh cement-based particle suspension such as cement paste, mortar, and concrete (Senff et al., 2009). The rheology of cement paste normally dictates the rheology of mortar and concrete; thus, evaluating the rheological properties of cement paste could illustrate the performance of a given plasticizer (Claszewski and Szwabowski, 2004; Nunes et al., 2011).

The effect of an SP is the dispersion of fine solid-cement particles in the cement paste. When no SP is added, the solid particles would tend to form particle agglomerates, which retain water inside. With the admixture of an SP, the solid particles disperse and agglomeration would be reduced, thus allowing the solid particles to be more closely packed and the amount of excess water in concrete reduced (Wallevik and Wallevik, 2011). The effect of plasticizers can be assessed through rheological changes in cement pastes, mortars, and concrete.

The impact of MEF on cement will be assessed by evaluating the rheology of cement pastes. Pastes were prepared using a cement produced in Cienfuegos, Cuba, classified as a type I cement (Cuban norm NC-54 205:80 classifies it as P-35). Physical and mechanical properties are described in Tables 8.3–8.5.

Table 8.3 **Physical–mechanical properties of the cement used**

Properties	Value
Bulk weight	1103 kg/m^3
Density	3.15
Normal consistency	26%
Initial setting time	135″
Final setting time	3′45″
7 days Compressive strength	24.3 MPa
28 days Compressive strength	39.6 MPa
7 days Bending strength	4.3 MPa
28 days Bending strength	6.9 MPa

Table 8.4 **Chemical composition of the cement**

Oxide	CaO	SiO_2	Al_2O_3	Fe_2O_3	Na_2O	K_2O	MgO
(%)	62.64	21.20	5.79	2.70	0.00	0.61	1.22

Table 8.5 **Mineralogical phases in unhydrated cement**

Phases	C3S	C2S	C3A	C4AF	Free CaO
(%)	41.5	29.5	10.8	8.2	1.5

Abbreviations: C3S, tricalcium silicate; C2S, dicalcium silicate; C3A, tricalcium aluminate; C4AF, tetracalcium aluminoferrite.

MEF and commercial SP N-200 were used as chemical admixtures to pastes having the w/c ratio kept at 0.45. MEF was added in the proportions 4, 6, and 8% of the weight of cement. The high dosage of EM-like admixtures is commonly found in the literature, in which concentration as admixture in concrete normally ranges between 6% and 15% of the weight of cement used in the mix, probably due to the dilution effect (Ghosh et al., 2003). Water content in all MEF pastes was corrected to compensate the extra amount of liquid caused by the high dosage of the admixture. The commercial SP was tested at maximum and minimum dosages 0.5% and 1.5%, respectively, of the weight of cement, as recommended by the manufacturer.

The testing program in pastes consisted of:

- Minicone test: it has been accepted as a real but simple rheological tool that allows its user to access an intrinsic property of the tested material instead of measuring a test geometry and material density-dependent slump value (Roussel et al., 2005). Testing was done according to the Cuban Standard NC 235:2012.
- Consistency test: Pastes made with cement and plasticizers were prepared, and normal consistency was determined aided by the Vicat needle test (Cuban standard NC 524—2007). Further, setting time was determined in all pastes to assess the influence of MEF on the speed of the hydration of the cement.
- Flow test: The Marsh cone test was used to assess the flowability of cement pastes. The test method is described at Cuban standard NC-461: 2006 (similar to EN 445: 1995). It measures the time in which a certain volume of paste that fills the cone flows through a 10-mm nozzle. The test can also measure the loss of workability and the influence of temperature. The flow time can be directly linked to the material behavior, and rheological parameters such as yield stress and plastic viscosity for Bingham fluids can be predicted (Nunes et al., 2011; Roussel et al., 2005).
- Heat of hydration of cement pastes modified with chemical admixtures. With the aim of assessing the influence of the plasticizers and their dosage in the hydration of cement, isothermal calorimetry was conducted on samples to measure the heat flow and cumulated heat released during hydration of paste samples as a means of assessing the progress of cement hydration. Experiments were conducted at 30 °C to resemble Cuban environmental conditions (Martirena et al., 2014).

Figure 8.1 presents a comparison of the plasticity index of all series tested according to the testing protocol with the minicone. Although a plasticizing effect of the product MEF is clearly observed, it is significantly lower than the commercial SP used as reference, despite the higher dosage of admixture used in the series made with MEF. This could be explained through the dilution effect on the MEF product, compared to the commercial SP. Results presented in Table 8.1 prove that the ratio between total solids in MEF and N-200 ranges around 15 times, thus indicating a higher dilution rate.

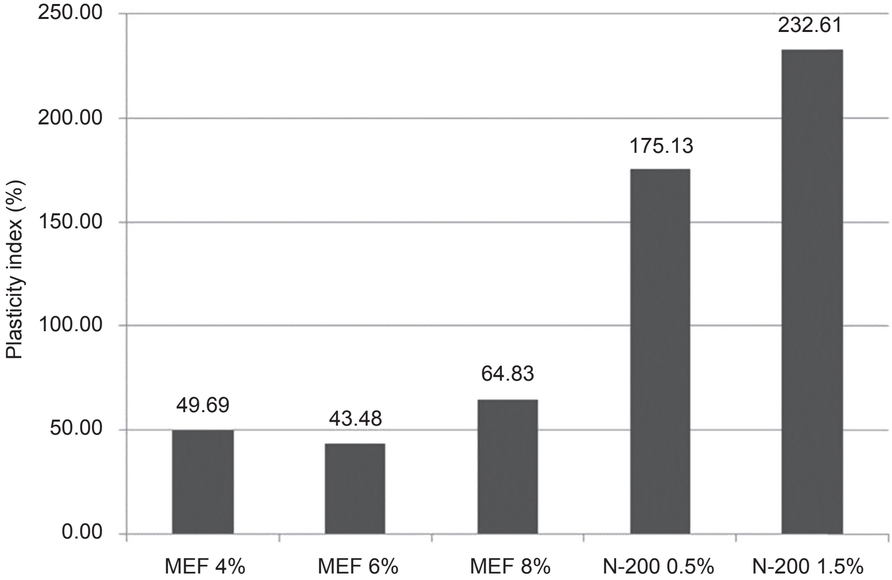

Figure 8.1 Plasticity index for all pastes tested with the minicone.

MEF is a natural product, and, accordingly, it contains a great variety of different compounds, many of which have not yet been identified. To get more clarity on its active compounds, MEF was fractioned using Soxhlet equipment, based on the polarity of the solvent, with the aim of determining which fraction has more influence on the plasticity index. The solvents used were chloroform, ethyl acetate, n-butanol, ethanol, and water. The fractions obtained were identified as follows: F2 is a mixture of extracted compounds into ethyl acetate; it represents 21.68% of the total compounds. F3 is a mixture of extracted compounds into n-butanol; it represents 16.32% of the total compounds. F4 is a mixture of extracted compounds into ethanol; it represents 4.54% of the total compounds; and F5 is a mixture of extracted compounds into water, that is, 46.74% of the total compounds with a polarity similar to that of water.

Figure 8.2 presents the plasticity index of minicone tests in which MEF has been separated into several polar fractions. The polar fraction identified as F5 corresponds to the mixture having the most polar compounds in the MEF product. It has similar solubility to that of water. For every concentration, a significant increase in plasticity is observed for the F5 polar fraction, even at smaller dosages. It could indicate that the plasticizing effect is strongly linked with the polarity of the compounds, most likely lactic acid.

Lactic and acetic acid are formed as metabolites obtained through the fermentation with different microorganisms during the manufacture of the product MEF. Through the interaction with cement particles during cement hydration, lactic acid and acetic acid could be adsorbed on the surface of the cement grains; lactate and acetate ions

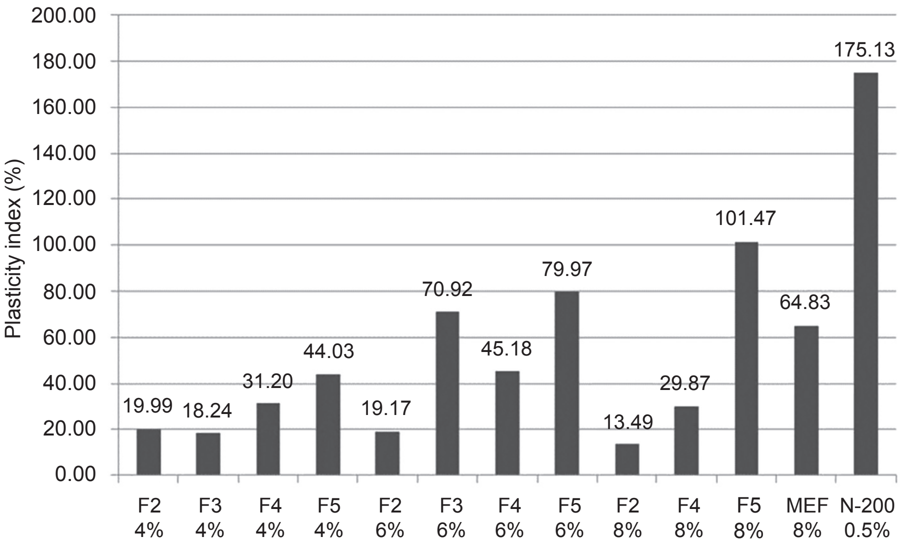

Figure 8.2 Plasticity index for polar fractions of MEF.

are formed (Singh et al., 1986). The negatively charged lactate and acetate ions repel each other and push cement grains apart. Figure 8.3 presents a scheme that illustrates the mechanisms for the electrostatic repulsion. This could likely explain the plasticizing properties observed in MEF. It is known that acetic acid is a good dispersant and decreases drastically the viscosity of the suspension for very low contents in aluminous cement paste (El Hafiane et al., 2012; El Hafiane et al., 2005).

Figure 8.4 presents the results of the Marsh cone test performed in cement pastes made with various dosages of MEF, a series with no plasticizer and a series with the commercial SP as a reference for comparison. Time T_v in cement pastes made

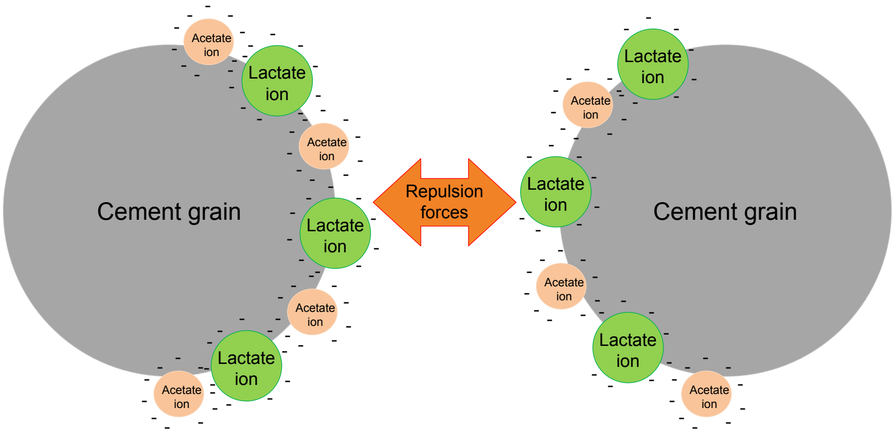

Figure 8.3 Repulsion forces between lactate ion and cement grains.

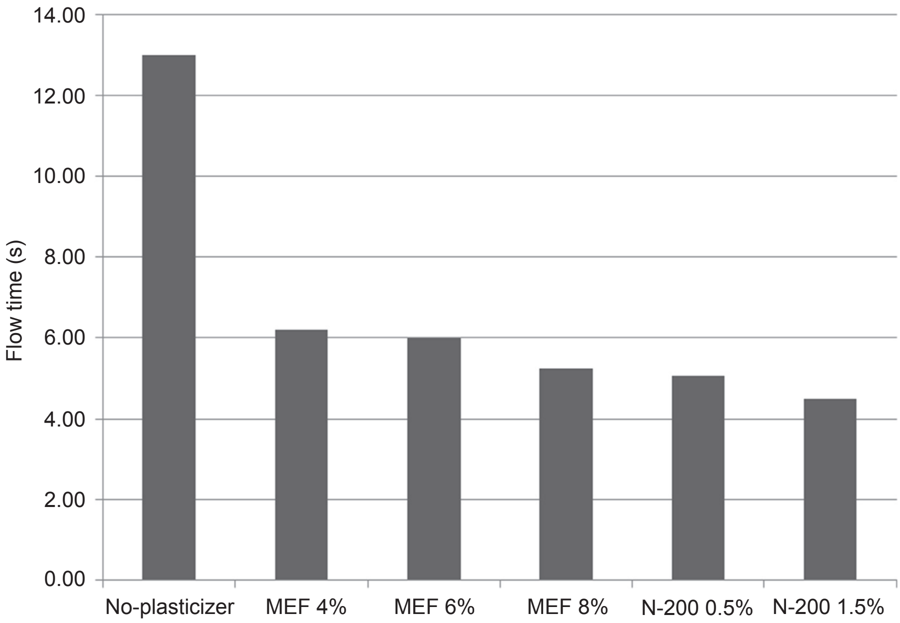

Figure 8.4 Flow time of cement pastes tested with the Marsh cone.

with MEF drops significantly compared with pastes made without SPs. The flow time is proportional to the viscosity and yield stress, thus indicating that a modification of the viscosity and the yield stress of the system occurs when MEF is used; the optimized dosage for the product evaluated appears to be 8% of the weight of cement.

The influence of MEF on the hydration of cement was assessed by measuring the heat of hydration of pastes made with MEF at different concentrations (4%, 6%, and 8% of the weight of cement). This was compared with those of the corresponding control cement pastes (OPC with no SPs) and paste containing 0.5% commercial SP N-200, as presented in Figure 8.5.

It is generally accepted that the initial setting typically occurs at the beginning of the accelerating period, in which tricalcium silicate (C3S) begins to hydrate rapidly (Xu et al., 2010). By the end of this period, once maximum rate has been reached, final set has taken place and early hardening has started. Comparing the time ranging from the end of the dormant period and the beginning of the acceleration period for the control Portland cement pastes to those with the admixtures, it seems that all the admixtures retarded the cement hydration. An increase on the heat evolution occurs as a shoulder after the first 12 h. Associated with this intensification on the cement hydration, an increase on the cumulative heat could be observed after the first 24 h for all systems when compared to control paste. This effect could be related to an increase of the heat released during hydration of the C3A phase, usually associated with an increase on ettringite formation and a delay on its conversion to monosulphate (Rixom and Mailvaganam, 1999).

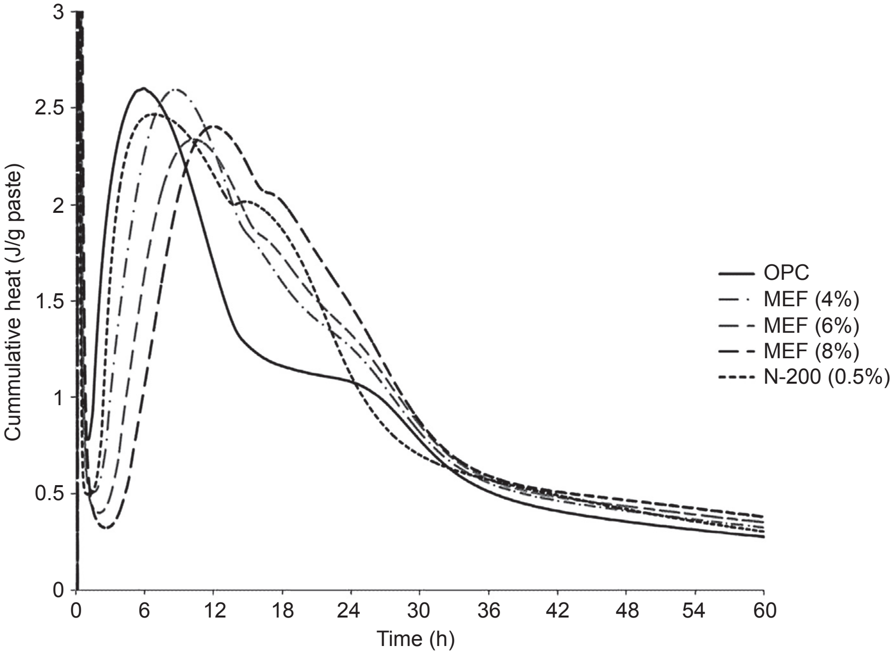

Figure 8.5 Rate of heat evolution as a means of measuring the influence of MEF on cement hydration.

The increase in the size of this shoulder was roughly proportional to the admixture concentration in pastes containing MEF. The same trend was observed for the retardation time. As MEF is the result of microbiological fermentation under anaerobic conditions, it contains a high volume of carboxylic acids such as lactic and acetic acid. Retardation effects have also been recognized for admixtures based on hydroxyl carboxylic acids at high concentrations (Taylor, 1990). However, because of its complex nature, further research is needed to unveil the nature of the MEF over cement hydration.

8.5 EM as plasticizer in concrete

The authors decided to prove the effectiveness of MEF by using it as admixture to produce self-compacting concrete (SCC) (Martirena et al., 2014). SCC is a high-performance concrete developed in Japan in the late 1980s. Its main feature is that it spreads under its own weight, and therefore can be placed without vibration. The high degree of flowability at relatively low w/c ratio can only be accomplished using high-range water-reducing admixtures (HRWR) or SPs, combined with stabilizing agents to ensure homogeneity of the mixture. A successful SCC must comply with workability requirements, including deformability, passing ability, and resistance to segregation. Deformability is the ability of SCC to flow into and completely fill all

Table 8.6 **Proportions of the SCCs made with the bioplasticizer and the reference**

Mixture	Cement (kg)	Water (L)	Zeolite (kg)	Sand (kg)	Gravel (kg)	N-200 (L)	Bioplasticizer (L)
Reference	450	459	364	594.6	528	6.7	0
Bioplasticizer	450	426	364	594.6	528	0	40

Fernando Martirena et al. (2014).

spaces within the formwork under its own weight (Hwang et al., 2006; Walraven, 2003).

Concrete mixture was proportioned on the principle of SCC (Aggarwal et al., 2008). Fine and coarse aggregates used were sourced from quarries in the south-central part of Cuba. Both aggregates fulfill all requirements from Cuban Standard NC 251. Bioplasticizer was added in up to 7% of the weight of cement and water was corrected to avoid differences in the w/c ratio, as explained previously. The bioplasticizer and the reference mixture were cast with water-to-fines ratio of 0.56, which was obtained for the flow condition.Table 8.6 presents the composition of each mix.

The testing procedure proposed by the Self-Compacting Concrete European Project Group (2005) (Walraven, 2003) was assumed to assess the properties of fresh SCC made with the bioplasticizer and the reference. The tests performed are the slump flow, the Japanese ring, the V flow, and the L-box.

Table 8.7 summarizes the main results of the entire experimental program carried out with fresh SCC made with bioplasticizer and the reference. The Slump Flow (SF) falls in the group SF1, slump flow between 550 and 650 mm, according to the classification given in the European Guidelines for SCC. This means SCC is suitable for unreinforced or slightly reinforced-concrete structures that are cast from the top, for instance, housing slabs; also it can be used for a pumped injection system, for instance, in tunnel linings.

Viscosity is characterized by the T_{500} during the slump flow test or by the V-funnel flow time. T_{500} in both cases (SCC made with bioplasticizer and reference SP) was under 2 s. T_V was for SCC made with bioplasticizer and the reference less than 8 s. Both results show, according to European Guidelines for SCC, a concrete with good filling capacity, even with congested reinforcement.

Passing ability is measured through the difference between the heights H_1 and H_2 when SCC passes through the L-box and the difference in height at the Japanese ring. For both mixtures, the height difference was below 10 mm, which classifies as SCC with good passing ability. Visual assessment was only done to verify segregation on SCC made with bioplasticizer. Figure 8.6 presents a detail of the material, which appears to be very homogenous, with no segregation or bleeding.

Table 8.8 presents the results of mechanical properties of SCC made with bioplasticizer and the reference. The relatively high presence of fines through the SCM used (zeolite) increases water demand in both concretes to 1.0. However, the water-to-fines ratio is kept around 0.55. After 28 d, compressive strength is around

Table 8.7 **Summary of experimental results for SCC made with bioplasticizer and reference**

	Slump flow		J-ring			V-funnel	L-box			
	SF (cm)	**T_{500} (s)**	**SF (cm)**	**H_1 (cm)**	**H_2 (cm)**	**T_v (s)**	**H_1 (cm)**	**H_2 (cm)**	**T_{40} (s)**	**T_{60} (s)**
N-200	62	1.0	60	15	12	3	7.5	5	0.75	1.5
Bioplasticizer	60	1.5	59	20	15	5	8.9	7.5	1.00	2.0

Abbreviations: SF, Slump Flow; T_{500}, Time = 500 s; H_1, Height 1; H_2, Height 2; T_v, Time variable; T_{40}, Time = 40 s; T_{60}, Time = 60 s.
Fernando Martirena et al. (2014).

Figure 8.6 Details of the edge of slump flow, SCC made with bioplasticizer. Fernando Martirena et al. (2014).

20 MPa, which for the foreseen applications (floors, slabs) is reasonable. After one year, concrete strength tends to increase on SCC made with bioplasticizer, thus indicating some marginal contribution of MEF to late strength gain.

8.6 Assessment of the impact of EM on the microstructure of concrete

An explanation of the strength gain described in the previous section was found while evaluating the mechanical properties of hardened concrete made with MEF aided by statistical nano-indentation techniques (Venkovic and Sorelli, 2014). The properties of calcium silicate hydrates (C—S—H) governs the viscoelastic behavior and the long-term durability of concrete. The relevance of studying the microstructure of such systems is twofold: (i) concrete admixtures, such as EM-based bioplasticizers, may affect the morphology of C—S—H hydrates and their variability (Bolobova and Kondrashchenko, 2000); and (ii) a difference in the structure of C—S—H and its spatial distribution can have important repercussions on the macroscale properties, such as strength, long-term creep, and drying shrinkage (Jennings, 2000; Vandamme and Ulm, 2009).

The advantages of applying a nano-indentation technique to characterize the aforementioned concretes were essentially the following: (i) nano-indentation technique provides a quantitative and statistical assessment of the mechanical properties of the hydrates, in particular the C—S—H phases, whereas macroscopic approaches are limited to the investigation of the overall composite behavior. (ii) The tiny volume of material probed by nano-indentation shortens the characteristic time of the viscous behavior (creep or relaxation) by several orders of magnitudes with respect to a macroscopic test. The later allows characterizing the long-term viscoelastic behavior of

Table 8.8 Mechanical properties of SCC made with bioplasticizer and reference SP

	Cem (kg/m^3)	Water L	Zeol (kg/m^3)	Agg. (kg/m^3)	Plast L	W/F	W/C	Slump (cm)	CS$_{28d}$ (MPa)	CS$_{365d}$ (MPa)
SCC with EM	450	426	364	1122	40	0.52	1.0	60	20.53	27.49
SCC reference	450	459	364	1122	6.7	0.56	1.0	62	18.58	25.13

Fernando Martirena et al. (2014).

C—S—H in few 100 s only (Vandamme and Ulm, 2009, 2013). More important, the long-term creep of C—S—H measured by nano-indentation was found to be representative (i.e., linearly correlated) with the long-term creep observed after years on macroscale compressive creep tests (Vandamme and Ulm, 2009).

Following the latest methodology of nano-indentation techniques for heterogeneous material (Ulm et al., 2007; Vandamme et al., 2010), a statistical analysis has been applied to consider the randomness nature of the microstructure of a cement paste (Venkovic and Sorelli, 2014). The statistical analysis of a large grid of nano-indentation tests has allowed identifying the statistical distributions of the following properties: the packing density, the elastic stiffness, the strength properties associated with the measured hardness (i.e., cohesion and friction for pressure sensitive materials like concrete), and the long-term rate of relaxation. Additionally, a cluster technique has been applied to the statistical results for identifying the volume fractions and properties of the (mechanically) representative phases composing the microstructure. Although the so-identified phases are not pure phases, but rather an intermix of hydrated products and clinker phases, it is possible to identify phases in which C—S—H are predominant (Chen et al., 2010).

As for the distribution of the packing density, the sample produced with MEF shows a maximal value of the packing density of about 72%, whereas 12% of tests on N-200 have showed packing densities larger than 72% spanning up to 79%. For a given water-to-binder ratio, the addition of MEF to concrete seems to inhibit the precipitation of C—S—H with high packing density. Figure 8.7 shows the statistical relationship between packing density and hardness for the C—S—H of the two samples: for a given packing density, the C—S—H of MEF always exhibits a greater hardness than that of N-200. Considering the side windows of Figure 8.7, one notes also that MEF is endowed with a lower packing-density distribution and greater hardness distribution than the N-200.

It was also possible to estimate that the cohesion and friction of the C—S—H matrix in the sample with MEF are 30% and 90% larger than the ones obtained for the sample with N-200, respectively. Those results support the idea that the addition of MEF to concrete improves the strength properties of C—S—H. This is consistent with the observation of Bolobova and Kondrashchenko (Bolobova and Kondrashchenko, 2000) for which the addition of bioplasticizer of the same nature as EM increases the rate of formation of fine crystalline structure and new fully crystallized structures of hydrated-silicate phases. As for the long-term relaxation rate, the mechanical work of relaxation is larger in the sample produced with MEF. Hence, the results support the idea that the addition of MEF to concrete decreases the rate of long-term relaxation of C—S—H.

In conclusion, the addition of EM-based bioplasticizer to concrete was found to (i) improve the strength of C—S—H by enhancing the cohesion and friction of solid nanograins; (ii) decrease the absolute rate of long-term relaxation; and (iii) inhibit the precipitation of C—S—H of higher density (Venkovic and Sorelli, 2014). This is actually confirmed by the measurements of compressive strength that were performed at the macroscale of the two samples under study (see Table 8.8). Hence, for a water-to-binder ratio of 0.60, the compressive strength of concrete is improved by 10.5% and 9.6% at 28 and 365 days, respectively.

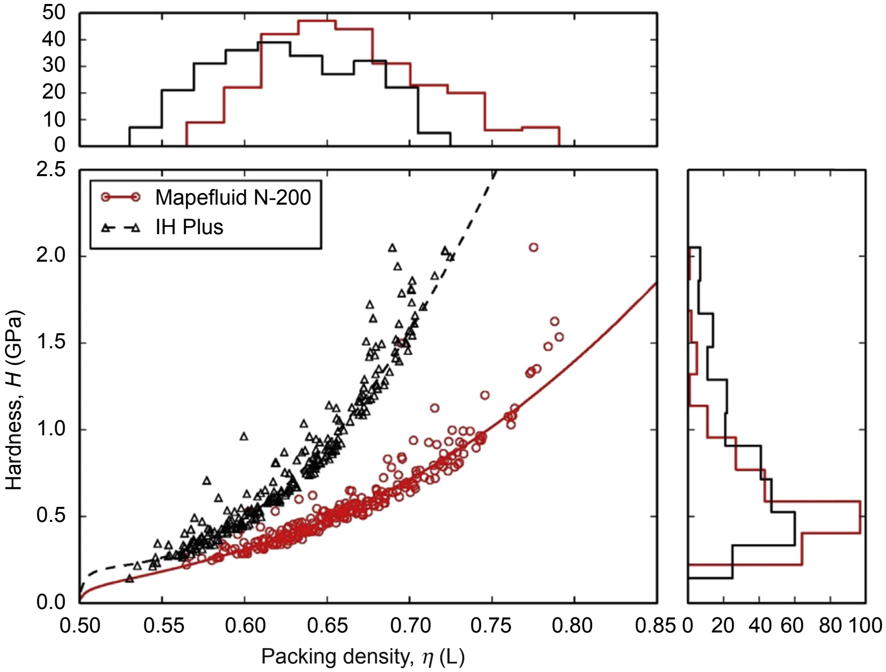

Figure 8.7 Statistical relationship between hardness and packing density for N-200 and MEF with a view of the frequency distributions in the side windows.
Venkovic and Sorelli (2014) and Fernando Martirena et al. (2014).

8.7 EM as viscosity modifier in concrete

The relationship between the shear stress τ that is applied on a fluid element and its resulting shear rate $\dot{\gamma}$ is named apparent viscosity η. Many fluids show plastic behavior (also called Bingham), in which flow only initiates when the forces created through flocculation of cement particles are broken by shear, thus the flocculated network is disrupted and the suspension begins to flow. The stress at which such a breakdown occurs is called the yield stress (τ_0) (Struble and Ji, 2001; Mahmoodzadeh and Chidiac, 2013).

Viscosity of a cement suspension is affected by the increase of the volume fraction of solids (φ). Flocculation produces plastic behavior with the yield stress reflecting the forces holding particles together. Often this breakdown is not complete at the yield stress so the suspension is still somewhat flocculated even though it flows and this remaining flocculation is progressively disrupted as the strain rate is increased further (Struble and Ji, 2001; Wallevik, 2009).

The adsorption of polymers on commercial SPs on the surface of cement grains modifies static charge, thus inducing repelling forces (Collepardi, 2005a). The macroscopic impact is the reduction of the yield stress τ_0 and the start of the flow. If a second

SP having similar ionic effect but a higher degree of dilution, for instance, MEF, is supplied to the system, a competence for absorption would take place. The commercial SP would adsorb first, because of the higher ion concentration, and the second SP would be adsorbed later, as the first one is depleted.

As the suspension flows, the second SP acts on remaining flocculation on the system, producing pseudoplastic (shear thinning) behavior often accompanied by *thixotropy*, a progressive and reversible decrease in viscosity on application of a constant stress level. The second admixture modifies viscosity of the suspension and acts like improved Viscosity Modifying Admixtures (VMA), also referred to as Stabilizers or Viscosity Enhancing Admixtures (VEA) (Collepardi, 2005b).

The authors decided to test a cocktail of N-200 and MEF as rheology modifier of concrete. N-200 would act as superplasticizer and MEF would act as VMA. N-200 has many sulfonate groups in its complex chemical structure, and they are distributed in the linear chain and side chains. Moreover, they form several charge sites to be absorbed on the cement particles with a strong ionic effect. They can be responsible for the starting of the cement paste flow.

The presence of carboxylic acids in MEF is well established. Dilution of MEF counteracts its ionic effect, and therefore sulfonate groups from N-200 tend to adsorb more on cement grains than do carboxylate groups, thus a competition for adsorption takes place between carboxylate and sulfonate groups. The carboxylate groups will continue to adsorb as the sulfonates are depleted, thus influencing the viscosity of the mix.

To assess the impact of a cocktail of N-200 and MEF, 15 × 30 cm cylinders of a 25 MPa concrete were cast with different proportions of both admixtures and rheology and mechanical properties were assessed. Same aggregates used in Section 8.5 were used to make this concrete. Two reference concretes were cast, one with 8% MEF and another with 0.95% N-200. Table 8.9 presents mix proportion for the concrete, as well as rheology and strength results.

Rheology of concrete was assessed aided by the vibrating table following the DIN EN 12350-5:2009. The use of MEF and N-200 cocktails do not compromise flow, although the total dosage of both is decreased in reference to the reference. The best results in terms of w/c ratio are obtained for a combination of 0.3% of N-200 (30% of initial dosage) and 3% of MEF (40% of initial dosage). Further to improving rheology, the resulting concrete decreased segregation and retained more water than the normal concrete made with one single admixture.

Compressive strength was measured at 7 and 28 days. Results of both 7 and 28 days strength do correlate well with the w/c ratio. Again, best results are obtained for a combination of 0.3% of N-200 (30% of initial dosage) and 3% of MEF (40% of initial dosage). Water absorption was measured at 28 days following the Cuban standard NC 345:2005, to assess impact on pore structure of concrete. No negative impact of the cocktail on porosity is reported.

These are still preliminary but encouraging results. The authors continue to assess the properties of concrete made with combination of superplastcizer and a VMA. The underlying mechanisms for the benefits observed should be further clarified.

Table 8.9 Concrete made with cocktails of N-200 and MEF

Mix	Cement (kg/m^3)	Sand (kg/m^3)	Gravel (kg/m^3)	Water (L/m^3)	N-200 (L/m^3)	MEF (L/m^3)	W/c	Spread (cm)	7 days	28 days	Wt Abs. (%)
									Strength (MPa)		
ME—1	440	735	974	190	–	35 (8%)	0.46	39.0	18.3	26.04	0.59
ME—2	440	735	974	205	3.6 (0.95%)	–	0.43	36.5	27.7	34.28	1.6
ME—3	440	735	974	200	2.2 (0.58%)	2.2 (1%)	0.46	38.8	19.36	28.65	1.6
ME—4	440	735	974	200	2.2 (0.58%)	1.54	0.45	39.5	21.56	30.02	2.43
ME—5	440	735	974	195	2.95 (0.67%)	8.8	0.45	35.2	22.1	32.3	1.63
ME—6	440	735	974	190	1.32 (0.3%)	13.2	0.44	38.2	21.9	33.5	1.72

8.8 Conclusions

The emergence of new biopolymers such as the one referred to as MEF in this chapter could contribute to changing the paradigms of the use of admixtures in concrete. The EM-based admixture has been proved to have potential for a broad use in construction. This research has proved its moderate plasticizing effect and its impact as a VMA combined with powerful superplasticizers in concrete. The wide spectrum of compounds present in MEF favors its broad impact on concrete, so it could replace several individual admixtures that are used to modify concrete properties, with an impact on both cost and environmental profile of concrete.

There are, however, challenges to face. The conventional admixture industry does not have either equipment or experience for the industrial production of biological products. A choice would be to establish cooperation with the pharmaceutical industry, which has the equipment, experience, and research capacity to embrace development and massive production of such products. Some steps have been given in Cuba, where the vaccine production center "Institute Carlos J. Finlay" has set up a production capacity of up to 2 million liters a year of MEF. The Cuban Ministry of Construction has labeled the product as suitable for its use as VMA in concrete production.

Another challenge would be to modify the fermentation process or the final bioproduct to obtain a solid product, for current technology is based on fermentation of a liquid solution. This could expand production further, and could foster global export of the product. In terms of global trade, biohazard issues should be also considered. This work has proved that a bacteria-free MEF product could have a similar effect as the original one (Martirena et al., 2014). However, cost-effective ways of removing bacteria are yet to be explored.

References

Achal, V., Mukherjee, A., Basu, P.C., Reddy, M.S., 2009. Lactose mother liquor as an alternative nutrient source for microbial concrete production by sporosarcinapasteurii. Journal of Industrial Microbiology and Biotechnology 36, 433–438.

Aggarwal, P., et al., January–June 2008. Self-compacting concrete – procedure for mix design. Leonardo Electronic Journal of Practices and Technologies (12), 15–24.

Bolobova, A.V., Kondrashchenko, V.I., 2000. Use of yeast fermentation waste as a biomodifier of concrete (review). Applied Biochemistry and Microbiology 36 (3), 205–214.

Burgos-Montes, O., Palacios, M., Rivilla, P., Puertas, F., 2012. Compatibility between superplasticizer admixtures and cements with mineral additions. Construction and Building Materials 31, 300–309.

Chen, J.J., Sorelli, L., Vandamme, M., Ulm, F.J., Chanvillard, G., 2010. A coupled nanoindentation/SEM-EDS study on low water/cement ratio portland cement paste: evidence for C–S–H/Ca (OH) 2 nanocomposites. Journal of the American Ceramic Society 93 (5), 1484–1493.

Claszewski, G., Szwabowski, J., 2004. Influence of superplasticizers on rheological behavior of fresh cement mortars. Cement and Concrete Research 34, 235–248.

Collepardi, M., 2005a. Chemical admixtures today. Proceedings of Second International Symposium on Concrete Technology for Sustainable, Development with Emphasis on Infrastructure (Hyderabad, India).

Collepardi, M., 2005b. Guidelines for Viscosity Modifying Admixtures for Concrete. September 2006. European Federation of National Associations Representing Producers and Applicators of Specialist Building Products for Concrete, EFNARC, and European Federation of Concrete Admixture Associations. www.efnarc.org.

El Hafiane, Y., Smith, A., Bonnet, J.P., Tanouti, B., 2005. Effect of a carboxylic acid on the rheological behavior of an aluminous cement paste and consequences on the properties of the hardened material. Journal of the European Ceramic Society 25, 1143–1147.

El Hafiane, Y., Smith, A., Chartier, T., Abouliatim, Y., Nibou, L., Bonnet, J.P., 2012. Role of dispersant and humidity on the setting of millimetric films of aluminous cement prepared by tape casting. Journal of the European Ceramic Society 32, 2103–2111.

Fernando, Martirena, Yaset, Rodriguez-Rodriguez, Camilo, Gonzalez, Raul, Gonzalez, Alvarado-Capo, Y., 2014. “Bioplasticizer for Concrete”, *Proceedings of the International RILEM Conference on Application of Superabsorbent Polymers and Other New Admixtures in Concrete Construction*. RILEM Publications Sarl.

Ghosh, P., Mandal, S., Chattopadhyay, B.D., Pal, S., 2003. Use of microorganism to improve the strength of cement mortar. Cement and Concrete Research 35, 1980–1983.

Ghosh, P., Mandal, S., Pal, S., Bandyopadhyaya, G., Chattopadhyay, B.D., 2006. Development of bioconcrete material using an enrichment culture of novel thermophilic anaerobic bacteria. Indian Journal of Experimental Biology 44, 336–339.

Higa, T., Wididana, G.N., 1991. The Concept and Theories of Effective Microorganism. University of Ryukyus, 118–124.

Hwang, S.-D., Khayat, K.H., Bonneau, O., March–April 2006. Performance-based specifications of self-consolidating concrete used in structural applications. ACI Materials Journal 121–129.

Ismail, N., Mohd Saman, H., 2014. Microstructure examination and strength characteristics of effective microbed cement. In: International Conference on Biological, Civil and Environmental Engineering (BCEE-2014 (Dubai, UAE).

Jennings, H.M., 2000. A model for the microstructure of calcium silicate hydrate in cement paste. Cement Concrete Research 30 (1), 101–116.

Kovler, K., Roussel, N., 2011. Properties of fresh and hardened concrete. Cement and Concrete Research 41, 775–792.

Kwan, A.K.H., Fung, W.W.S., 2012. Roles of water film thickness and SP dosage in rheology and cohesiveness of mortar. Cement and Concrete Composites 34, 121–130.

Mahmoodzadeh, F., Chidiac, S.E., 2013. Rheological models for predicting plastic viscosity and yield stress of fresh concrete. Cement and Concrete Research 49, 1–9.

Martirena, F., Rodriguez-Rodriguez, Y., Callico, A., Gonzalez, R., Diaz, Y., Bracho, G., Alujas, A., Guerra de Leon, J.O., Alvarado-Capó, Y., 2014. Microorganism-based bioplasticizer for cementitious materials. Construction and Building Materials 60C 91–97.

Martirena, F., Rodriguez-Rodriguez, Y., Gonzalez, C., Gonzalez, R., Alvarado-Capó, Y., 2014. Bioplasticizer for concrete. In: Mechtcherine, V., Schroefl, C. (Eds.), Application of Superabsorbent Polymers and Other New Admixtures in Concrete Construction. RILEM Publication S.A.R.L., Proceedings PRO 95, ISBN 978-2-35158-147-6.

Mayer, J., Scheid, S., Widmer, F., Fließbach, A., Oberholzer, H.-R., 2010. How effective are “Effective microorganisms® (EM)”? Results from a field study in temperate climate. Applied Soil Ecology 46, 230–239.

Nunes, S., et al., 2011. Rheological characterization of SCC mortars and pastes with changes induced by cement delivery. Cement and Concrete Composites 33, 103–115.

Pacheco-Torgal, F., Labrincha, J., 2014. Biotechnologies and bioinspired materials for the construction industry: an overview. International Journal of Sustainable Engineering 7 (3), 235–244.

Ramachandran, S.K., Ramakrishnan, V., Bang, S.S., 2001. Remediation of concrete using microorganism. American Concrete Institute Materials Journal 98, 3–9.

Rixom, R., Mailvaganam, N., 1999. Chemical Admixtures for Concrete. E & FN Spon, London, UK.

Roussel, N., et al., 2005. From mini-cone test to Abrams cone test: measurement of cement-based materials yield stress using slump tests. Cement and Concrete Research 35, 817–822.

Sato, N., Higa, T., et al., 2000. Some Properties of Concrete Mixed with Effective Microorganism and the On-site Investigation of the Completed Structures. Hachinohe Institute of Technology, Japan.

Senff, L., et al., 2009. Mortar composition defined according to rheometer and flow table tests using factorial designed experiments. Construction and Building Materials 23, 3107–3111.

Singh, P., et al., 1986. Effect of lactic acid on the hydration of Portland cement. Cement and Concrete Research 16 (4), 545–553.

Struble, L.J., Ji, X., 2001. 9-Rheology. In: Ramachandran, V.S., Beaudoin, J.J. (Eds.), Handbook of Analytical Techniques in Concrete Science and Technology. William Andrew Publishing, Norwich, NY, pp. 333–367.

Taylor, H.F.W. (Ed.), 1990. Cement Chemistry. Academic Press, London, UK, p. 491.

Ulm, F.-J., Vandamme, M., Bobko, C., Alberto Ortega, J., Tai, K., Ortiz, C., 2007. Statistical indentation techniques for hydrated nanocomposites: concrete, bone, and shale. Journal of American Ceramic Society 90 (9), 2677–2692.

Vandamme, M., Ulm, F.J., 2009. Nanogranular origin of concrete creep. Proceedings of the National Academy of Science of the United States of America 106 (26), 10552–10557.

Vandamme, M., Ulm, F.-J., 2013. Nanoindentation investigation of creep properties of calcium silicate hydrates. Cement and Concrete Research 52 (0), 38–52.

Vandamme, M., Ulm, F.-J., Fonollosa, P., 2010. Nanogranular packing of CSH at substochiometric conditions. Cement and Concrete Research 40 (1), 14–26.

Venkovic, N., Sorelli, L., Martirena, F., 2014. Nanoindentation study of calcium silicate hydrates in concrete produced with effective microorganism-based bioplasticizer. Cement and Concrete Composites 49 (2014), 127–139.

Wallevik, J.E., 2009. Rheological properties of cement paste: thixotropic behavior and structural breakdown. Cement and Concrete Research 39, 14–29.

Wallevik, O.H., Wallevik, J.E., 2011. Rheology as a tool in concrete science: the use of rheographs and workability boxes. Cement and Concrete Research 41, 1279–1288.

Walraven, J., 2003. Structural applications of self-compacting concrete. In: Wallevik, O., Nielsson, I. (Eds.), Proceedings of 3rd RILEM International Symposium on Self Compacting Concrete, Reykjavik, Iceland. RILEM Publications PRO 33, Bagneux, France, pp. 15–22.

Wu, M., et al., 2012. A review: self-healing in cementitious materials and engineered cementitious composite as a self-healing material. Construction and Building Materials 28, 571–583.

Xu, Q., et al., 2010. Isothermal calorimetry tests and modeling of cement hydration parameters. Thermochimica Acta 499, 91–99.

Yoshiokaa, K., Tazawab, E.-I., Kawaib, K., Enohatac, T., 2002. Adsorption characteristics of superplasticizers on cement component minerals. Cement and Concrete Research 32, 1507–1513.

Fly ash-based geopolymer with kappa-carrageenan biopolymer

9

Z. Li, L. Zhang
University of Arizona, Tucson, AZ, USA

9.1 Introduction

The utilization of biopolymers in construction materials has been in rapid development since the last century (Plank, 2004). The first biopolymer massively used in construction materials was lignosulfonate for concrete plasticization in the 1920s (Ramachandran, 1995). Since then, biopolymers have become much more popular as admixtures for enhanced engineering construction materials, and these biopolymers have included starch (Pilla and Datta, 2011), xanthan gum (Sakata et al., 1996), cellulose ethers (Knaus and Bauer-Heim, 2003), and polyaspartic acid (Vijn et al., 2004). Typically, biopolymers can provide desired properties, functioning as plasticizers, viscosifiers, water-retention agents, shrinkage-reduction agents, and retarders. In the early 2000s, more than one billion dollars in sales at the manufacturer's level were estimated for biopolymer additives in the global market of building materials (Plank, 2003).

Biopolymers are high-molecular-weight organic materials that are either produced by microorganisms, plants, or animals or synthesized chemically from biological starting materials such as amino acids, sugars, and oils (USCOTA, 1993; Plank, 2004; Kumar et al., 2007; Griggs, 2010). They have a number of advantages over the commonly used petroleum-based polymers. For example, biopolymers are renewable because they are derived from sustainable and reproducible natural resources. They are also environmentally friendly because of their biodegradability and low toxicity (Rhim and Ng, 2007). Owing to their unique properties and the growing awareness of environmental sustainability, biopolymers have been increasingly used in diverse areas (Menefee and Hautala, 1978; Jha et al., 1988; Deans and Dixon, 1992; Deans, 1994; Chandra and Rustgi, 1998; Orts et al., 2000; Kosbar et al., 2000; Vekshin, 2002; Steinbuchel, 2003; Kumar et al., 2007; Rhim and Ng, 2007; John et al., 2008), especially for the enhancement of construction materials (Kim et al., 2005; Bezerra et al., 2011; Li et al., 2013). Of all construction materials, concrete represents the main one using biopolymer additives. Concrete is by far the most extensively used material in the construction industry to maintain the ongoing development of the world. Each year, more than 10 billion tons of concrete is manufactured worldwide (Meyer, 2009). It is of great significance to enhance its performance regarding strength, ductility, durability, etc. Therefore, much research has been conducted on utilizing biopolymers to enhance the performance of concrete. For example,

Biopolymers and Biotech Admixtures for Eco-Efficient Construction Materials. http://dx.doi.org/10.1016/B978-0-08-100214-8.00009-9
Copyright © 2016 Elsevier Ltd. All rights reserved.

Bezerra et al. (2011) investigated the mechanical and durability performance of concrete containing both synthetic latex and chitosan biopolymer. The results indicated that the combination of the two polymer additives was able to improve the mechanical properties, with an increase up to 21% for the tensile and compressive strength. Scanning electron microscope (SEM) studies further showed that the chitosan had electrostatically immobilized the calcium in concrete leading to lower mobility of water and an increase of tensile strength. On the other hand, the presence of latex was found to connect the pores of concrete in the form of networks, although to a lesser degree, also contributing to the enhancement of mechanical and other properties. Kim et al. (2005) studied biopolymer-modified concrete systems for disposal of cathode ray tube glass. The use of biopolymers (xanthan gum, guar gum, and chitosan) in concrete produced a stable interpenetrating cross-linking composite, which showed a 30% increase in compressive strength and a substantial decrease in lead leachability.

However, the production of ordinary Portland cement (OPC) that binds concrete together not only consumes significant amounts of raw materials and energy, but also emits enormous amounts of carbon dioxide (CO_2). To produce 1 ton of OPC, about 1.5 tons of raw materials are needed, and 0.81 ton of CO_2 is released to the atmosphere (Hendriks et al., 2000). Worldwide, the OPC industry alone is responsible for about 7% of all human-generated CO_2 (Malhotra, 2000; McCaffrey, 2002). Growing environmental concerns and the need for sustainable construction materials have driven civil engineers and materials scientists to search for viable alternatives to OPC (Bakharev, 2005a; Ahmari and Zhang, 2013b). During the past decades, geopolymer has emerged as such a promising material and has attracted increasing research interest (Davidovitz, 2005, 2008; Duxson et al., 2007; Dimas et al., 2009; Provis and Van Deventer, 2009; Van Deventer et al., 2012; Provis, 2014). Geopolymer is a synthetic material produced through the alkaline activation of aluminosilicates at ambient or slightly elevated temperatures, having an amorphous to semicrystalline polymeric structure with Si^{4+} and Al^{3+} cations tetrahedrally coordinated and linked by oxygen bridges (Davidovitz, 2005, 2008; Duxson et al., 2007; Dimas et al., 2009; Provis and Van Deventer, 2009; Van Deventer et al., 2012; Provis, 2014):

$$M_n[-(SiO_2)_z-AlO_2-]_n \tag{9.1}$$

where M is an alkali cation (Na^+ or K^+), n the degree of polymerization, and z the Si/Al molar ratio, which can be 1, 2, 3, or >>3. Geopolymer can be synthesized from a wide range of low-cost aluminosilicate materials or even industrial wastes, such as metakaolin, volcanic ash, fly ash, furnace slag, red mud, and mine tailings (Wang et al., 2005; Chindaprasirt et al., 2007; Granizo et al., 2007; Pacheco-Torgal et al., 2007, 2009; Hu et al., 2008; Rangan, 2008; Rattanasak and Chindaprasirt, 2009; Guo et al., 2010; Li et al., 2010; Sarker, 2010; Temuujin et al., 2010; Zhang et al., 2011; Ahmari and Zhang, 2012, 2013a,b). The two commonly used alkali activators are sodium and potassium hydroxides (Krivenko et al., 2006; Davidovits, 2008), and sodium silicate is used together with the hydroxides. In general, activation with sodium silicate in the process can increase the compressive strength, because it not only regulates the Si/Al and Si/Na ratios in the raw material mix, but also catalyzes polycondensation by providing extra SiO_4^- monomers to initiate polymerization between SiO_4^- and AlO_4^- units (Kaps and Buchwald, 2002; Granizo et al., 2007).

Geopolymer not only provides performance comparable to OPC in many applications, but also shows additional advantages, such as rapid development of mechanical strength, excellent adherence to aggregates, superior resistance to chemical attack, ability to immobilize contaminants, and significantly reduced energy usage and greenhouse gas emissions (Hardjito et al., 2004; Bakharev, 2005b; Sofi et al., 2007; Duxson et al., 2005, 2007; Provis and Van Deventer, 2009; Van Deventer et al., 2012; Provis, 2014). However, as OPC, geopolymer exhibits brittle behavior with low tensile strength, ductility, and fracture toughness, which imposes constraints in structural design and adversely affects its wide application in practice (Zhao et al., 2007; Zhang et al., 2010a,b; Pernica et al., 2010). To overcome the aforementioned disadvantages, extensive research has been conducted on utilization of engineered fibers to reinforce geopolymer, including steel, PVA, carbon, and basalt (Balaguru and Shah, 1992; Dias and Thaumaturgo, 2005; Zhang et al., 2006, 2008; Sun and Wu, 2008; Lin et al., 2008, 2009; Li and Xu, 2009; Bernal et al., 2010; Metaxa et al., 2010; He et al., 2010). However, these studied fibers are all produced by a high-energy-consuming process, and there is concern about how to deal with these materials at the end of their life cycle (Merta et al., 2010; Pacheco-Torgal and Jalali, 2011). The other problem is that these fibers usually have a cross-sectional dimension at the micro/macroscale and thus can only increase the tensile strength, ductility, and toughness by bridging micro/macrocracks, transferring loads, and delaying the development of micro/macrocracks (Balaguru and Shah, 1992; Dias and Thaumaturgo, 2005); but cracks initiate at the nanoscale in which micro/macrofibers do not function effectively (Metaxa et al., 2010). The cracks (even at micro/nanoscale) and possible ingress of corrosive ions can lead to degradation of geopolymer and its reinforcing fibers. To resolve this issue, fine-tuning of geopolymer matrix at the nanoscale is required so that the formation and propagation of micro/nanocracks can be hindered at the very beginning (i.e., at the nanoscale). As such, reinforcement of geopolymers using nanofibers, such as carbon nanotubes (CNTs) and carbon nanofibers (CNFs), has been investigated. For example, MacKenzie and Bolton (2009) investigated the effect of incorporating single-wall CNTs on the electrical and mechanical properties of geopolymers. Although nanofibers possess excellent physical and mechanical properties, such as exceptional high strength, stiffness, and aspect ratio, they have a major drawback for matrix reinforcement: poor dispersion, usually due to van der Waals attractions and other surface forces, resulting in a particular difficulty to produce uniformly dispersed fibers within the matrix (Xie et al., 2005; Moniruzzaman and Winey, 2006; Ashton, 2010; Yazdanbakhsh et al., 2010). To truly achieve nanoscale fiber reinforcement in a composite, it is critical to achieve uniform dispersion (i.e., no aggregation) of nanofibers within the matrix (Xie et al., 2005; Groert, 2007; Ashton, 2010). Therefore, research is required to develop methods for reinforcing geopolymers at the nanoscale.

Utilization of biopolymer to enhance geopolymer can be a very promising way, but has seldom been previously reported. Recently, our research group has successfully used a chitosan derivative, N-carboxymethyl chitosan, to enhance fly ash-based geopolymer (Li et al., 2013). However, although commercially available, the N-carboxymethyl chitosan has relatively high cost and is not so environmentally "green" because its synthesis through carboxymethylation of chitosan involves consumption of large amounts of chemicals and energy. In this chapter, we study the feasibility of using kappa-carrageenan (KC) to enhance fly ash-based geopolymer. KC is a natural high-molecular-weight polysaccharide produced from the seaweed plant. More importantly, the presence of ester sulfate groups in KC makes it soluble in water at appropriate temperature, which is of great importance to produce homogeneous solutions for geopolymer production. The study is based on the hypothesis that the cross-linked gel networks of KC function with the amorphous interconnected geopolymer structure to form the hybrid high-performance cementitious material (Figure 9.1), in which KC macromolecules exist as random coils in the biopolymer solution but agglomerates to form a three-dimensional interpenetrating network with geopolymer during geopolymerization and curing. Unconfined compression and splitting tensile tests were conducted to investigate the improvement of the mechanical properties of fly ash-based geopolymer paste specimens after different amounts of KC were added. To better understand the enhancement mechanism, SEM and Fourier transform infrared spectroscopy (FTIR) were used to investigate the microstructural and chemical evolution of geopolymer paste specimens containing different amount of KC.

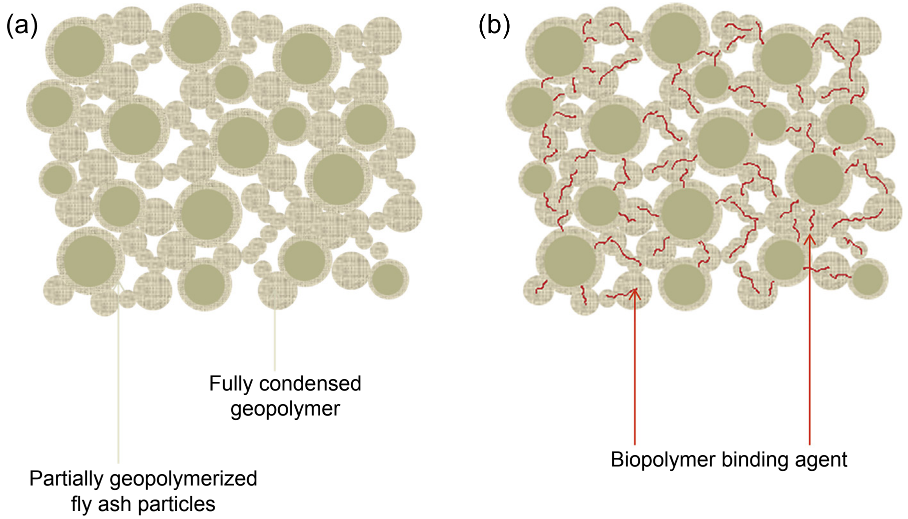

Figure 9.1 Proposed mechanism for enhancement of geopolymer paste through incorporation of biopolymer macromolecules: (a) plain fly ash-based geopolymer, and (b) biopolymer-enhanced fly ash-based geopolymer.

9.2 Experimental study

9.2.1 Materials

Class F fly ash and sodium hydroxide solutions were used as the starting materials to prepare the geopolymer paste specimens. The paste specimens were used so that the enhancement effect of the KC biopolymer could be better studied with no need to consider the effect of the presence of aggregates. The fly ash was provided by Salt River Materials Group (SRMG) in Phoenix, Arizona, which contains about 57% (weight percentage) SiO_2, 29% Al_2O_3, and 6.1% CaO and has 71% particles passing #325 (44 μm) sieve. The specific gravity of fly ash is 1.97. The sodium hydroxide flakes (98%) were purchased from Alfa Aesar in Ward Hill, Massachusetts. The KC was acquired from Gum Technology in Tucson, Arizona. The KC is off-white to light brown powder with moisture less than 14%. The gel strength of the KC is found at minimum 500 g/cm^2 measured by Brookfield Texture Analyzer. The KC has min. 90% of particles passing through a U.S. Std 80-mesh sieve. The pH value for 1.5% KC solution is between 7.0 and 11.0. The basic structure of KC is a high-molecular-weight linear polysaccharide with a repeating disaccharide sequence and contains a large number of ester sulfate and hydroxyl functional groups.

To incorporate KC macromolecules into a geopolymer matrix at the molecular scale, it was essential to maintain the solubility of KC in an alkaline solution so that no phase separation occurred when combined with geopolymer reaction mixtures. So KC was first dissolved in water and then sodium hydroxide flakes were added to this solution to prepare a uniform biopolymer alkaline solution for geopolymer synthesis. Due to the high viscosity of KC macromolecules in the alkaline solution, only low contents of KC, 0.025%, 0.05%, 0.075%, 0.1%, 0.125%, and 0.15% of fly ash by weight, were used.

9.2.2 Specimen preparation

First, KC at a specified weight percentage was dissolved in deionized water under vigorous stirring at ambient conditions. Then sodium hydroxide (NaOH) flakes were added to this solution to produce a 10 M NaOH solution containing KC. The stirring was continued for 1 h until a homogeneous solution was formed. The resulted solution was subsequently mixed with fly ash under stirring at ambient conditions for 20 min. The obtained geopolymer paste containing KC was then placed in cylindrical Plexiglas molds with the size of 25 mm inner diameter and 50 mm length. The mold was shaken by a vibrator during casting to release the trapped air bubbles. Subsequently, the specimens were aged at room temperature for one day before they were demolded and placed in an oven at 60 °C for curing up to 6 days before they were tested.

9.2.3 Unconfined compression tests

Unconfined compression tests were performed at room temperature on the 7-day cured cylindrical specimens using an ELE Tri Flex 2 loading machine at a constant loading rate of 0.2 mm/min, following ASTM C39/C39M-12a. The tests were carried out to measure the unconfined compressive strength (UCS) of geopolymer paste specimens containing different contents of KC. For each condition, at least four specimens were tested, and the average and standard deviation of the measured UCS values were analyzed. Before conducting the tests, the end surfaces of the specimens were polished to make sure they were flat and parallel.

9.2.4 Splitting tensile tests

The splitting tensile tests were performed at room temperature on the 7-day cured cylindrical specimens using an ELE Tri Flex 2 loading machine at a constant loading rate of 0.2 mm/min, following ASTM C496/C496M-11. The tests were conducted to measure the tensile strength (T) of geopolymer paste specimens containing different contents of KC. The same specimen size as in the unconfined compression tests was used. Based on the tests, the splitting tensile strength was calculated as follows:

$$T = \frac{2P}{\pi DL} \tag{9.2}$$

in which T is the splitting tensile strength (MPa); P is the maximum load on the specimen (N); D is the diameter of the specimen (mm); and L is the length of the specimen (mm). For each condition, at least four specimens were tested, and the average and standard deviation of the measured values were analyzed.

Additionally, by studying the force–displacement curves obtained from the splitting tensile tests, the effect of inclusion of KC on the toughness of geopolymer paste specimens was also evaluated. In this chapter, the toughness is simply defined as the prepeak toughness or the area under the force–displacement curve before the peak (Figure 9.2).

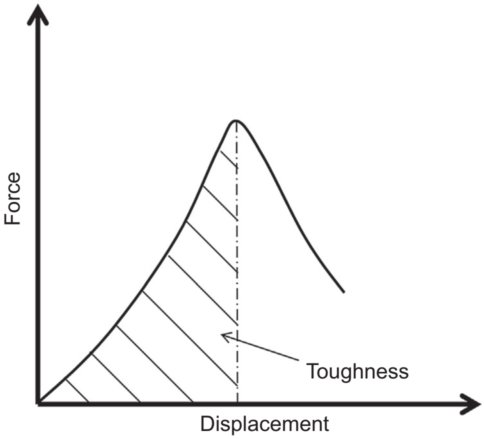

Figure 9.2 Definition of toughness used in this chapter.

9.2.5 Scanning electron microscopy characterization

To elucidate the effect of KC on the microstructure and mechanical performance of the biopolymer—geopolymer composite, SEM imaging was carried out under SE conventional mode using the FEI INSPEC-S50/Thermo-Fisher Noran 6 microscope. The freshly failed surfaces from the splitting tensile tests, without polishing to keep the fractured surface "un-contaminated," were used for the SEM imaging.

9.2.6 Fourier transform infrared spectroscopy characterization

To determine the presence of KC in the hybrid geopolymer and further analyze the interactions between KC and geopolymer, FTIR analysis was performed using a Thermo Nicolet 370 FTIR/EZ Omnic with a smart performance ATR ZnSe crystal and covering wavelengths from 600 to 4000 cm^{-1}.

9.3 Results

9.3.1 Unconfined compressive strength

Figure 9.3 shows the effect of inclusion of KC on the UCS of geopolymer paste specimens. The addition of KC led to an increase of UCS at all KC contents, and the

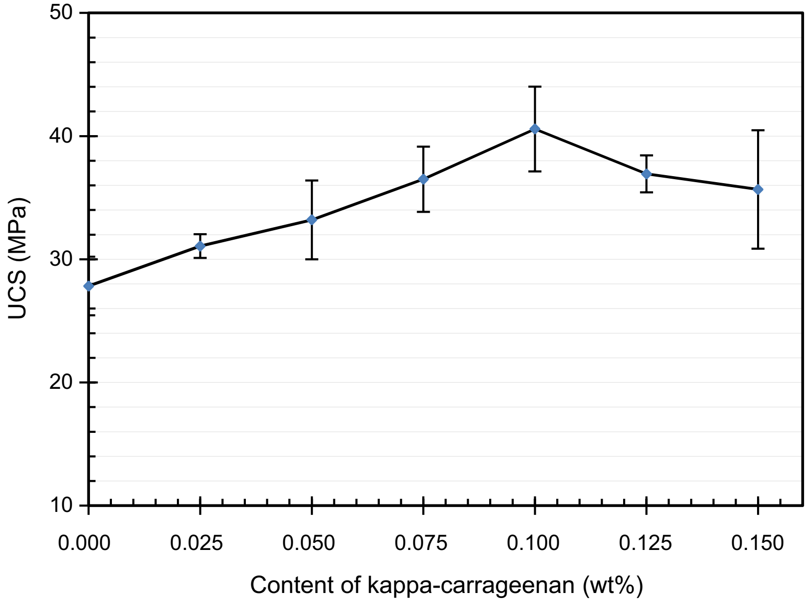

Figure 9.3 Effect of kappa-carrageenan content on the unconfined compressive strength (UCS) of fly ash-based geopolymer.

maximum increase was obtained at 0.1 wt% KC. The UCS increased remarkably from 27.8 MPa with no KC to 40.6 MPa (45.8%) at 0.1 wt% KC. Further increase of the KC content beyond 0.1 wt% slightly reduced the UCS of the biopolymer—geopolymer composite, but the UCS was still greater than that of the plain geopolymer paste. The general trend is in agreement with our previous research on the utilization of N-carboxymethyl chitosan to enhance fly ash-based geopolymer (Li et al., 2013). However, our results were contrary to the results of many previous studies on the utilization of fibers to reinforce geopolymer, which showed a decrease of compressive strength with inclusion of fibers (Al-Oraimi and Seibi, 1995; Kriker et al., 2005; De Gutiérrez et al., 2005; Li et al., 2006).

9.3.2 Splitting tensile strength

The variation of the splitting tensile strength (*T*) with the content of KC in geopolymer paste specimens is shown in Figure 9.4. The *T* increased remarkably with the addition of KC up to 0.1 wt% content. The *T* of geopolymer paste containing 0.1 wt% of KC was found as high as 4.68 MPa, which was approximately 22.4% greater than that of the plain geopolymer paste. However, the *T* was observed to decrease with KC content beyond 0.1 wt%, although the *T* was still greater than that of the plain geopolymer paste. This is in agreement with the results in the previous studies using fibers or organic resins to reinforce geopolymer, in which the *T* increased with the inclusion of fibers or resins up to a certain content and then decreased beyond the optimum content (Su and Wu, 2008; Zhang et al., 2010a). This was presumably due to the formation of additional

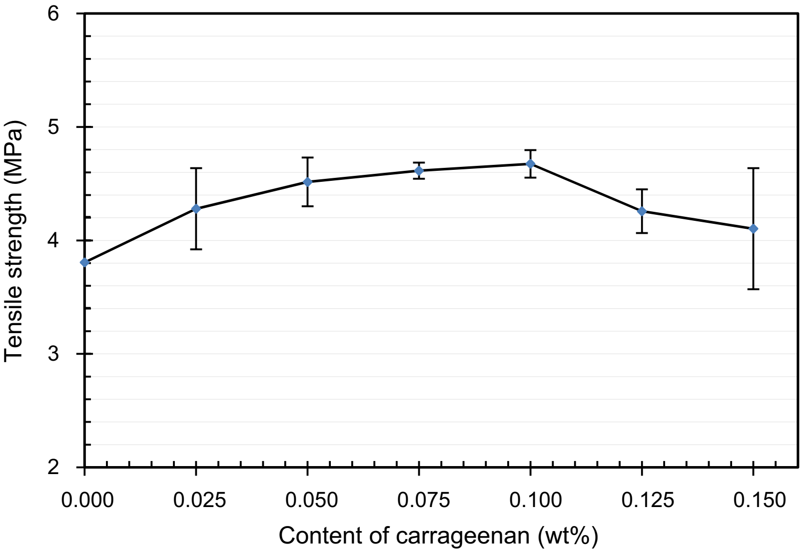

Figure 9.4 Effect of kappa-carrageenan content on the tensile strength (*T*) of fly ash-based geopolymer.

voids as a result of the poorer workability of geopolymer paste containing excessive amounts of fibers or resins (Su and Wu, 2008; Zhang et al., 2010a).

9.3.3 Prepeak toughness based on splitting tensile tests

Figure 9.5 shows the typical splitting tensile test load and displacement curves of geopolymer paste specimens containing different contents of KC. The plain geopolymer paste specimen failed suddenly at the peak load, and the incorporation of KC was not found to significantly change the postpeak ductility. However, the addition of KC led to an increase of the displacement at the peak load, and the maximum increase of about 27.1% happened at 0.1 wt% KC. The peak load also increased with the addition of KC until 0.1 wt% content. Beyond 0.1 wt% KC, the peak load and the displacement at the peak load both decreased but were still greater than those of the plain geopolymer paste.

The prepeak toughness (*H*) as defined in Figure 2 versus the content of KC in the geopolymer paste specimens is summarized in Figure 9.6. The *H* increased with the addition of KC up to 0.1 wt%, and the maximum increase of approximately 45.6% happened at 0.1 wt% KC. Further increase of KC content beyond 0.1 wt% resulted in a slight decrease in *H*, but the *H* was still much higher than that of the plain geopolymer paste specimen. This substantial increase of *H* combined with the increase of *U*, *T*, and the displacement at the peak load because of addition of KC makes it very promising to produce a green high-performance hybrid biopolymer—geopolymer cementitious material.

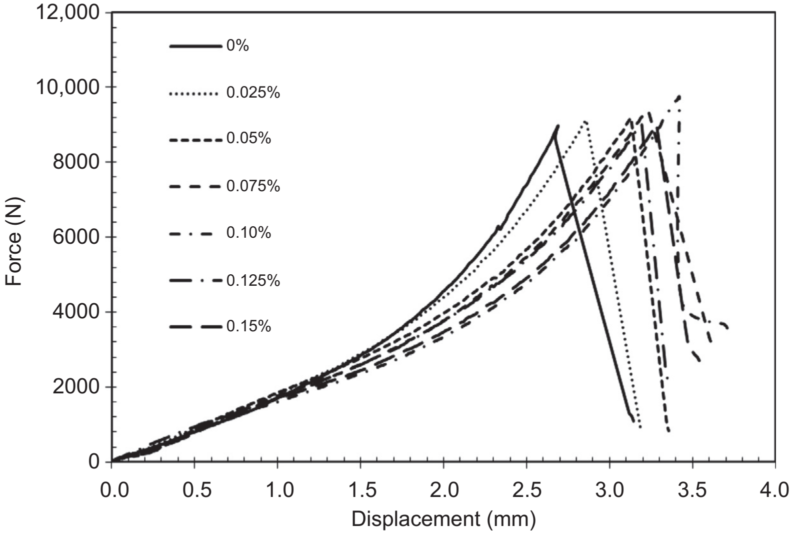

Figure 9.5 Splitting tensile test load and displacement curves of fly ash-based geopolymer containing different contents of kappa-carrageenan.

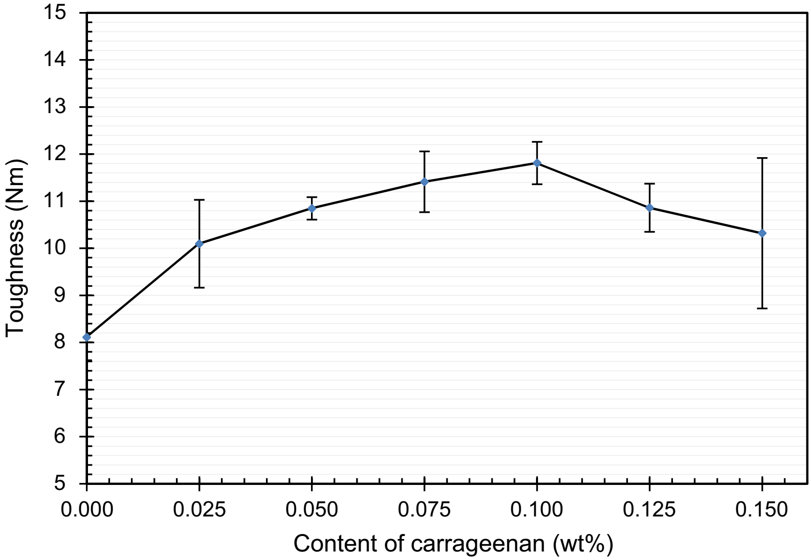

Figure 9.6 Effect of kappa-carrageenan content on the prepeak toughness (*H*) of fly ash-based geopolymer.

9.3.4 SEM images

Figure 9.7 shows representative SEM micrographs of KC-enhanced geopolymer paste specimens tested after 7 days' curing. When no KC was added, it could be clearly seen that the fly ash particles were geopolymerized to form a cross-linked three-dimensional network (Figure 9.7(a) and (b)). With the inclusion of 0.05 wt% KC, the KC biopolymer gel encapsulated and bridged the geopolymerized fly ash particles to produce a more condensed geopolymer structure (Figure 9.7(c) and (d)), which was responsible for the enhancement of mechanical properties of the biopolymer–geopolymer composite. In addition, the KC macromolecules could penetrate into the voids or interstitial pores in the geopolymer paste through diffusion and thus contribute to the improvement of mechanical performance. Further increase of the KC content up to 0.1 wt% led to a higher degree of encapsulation and bridging of fly ash particles in the biopolymer–geopolymer composite and further improvement of the mechanical properties (Figure 9.7(e) and (f)). However, when the KC content was beyond 0.1 wt%, the large amount of biopolymer macromolecules heavily coated the unreacted and partially hydrolyzed fly ash particles and hindered their geopolymerization with other hydrolyzed fly ash particles (Figure 9.7(g) and (h)).

9.3.5 FTIR spectra

The FTIR spectra for geopolymer paste specimens containing different contents of KC are shown in Figure 9.8 and Table 9.1. The geopolymer containing no KC

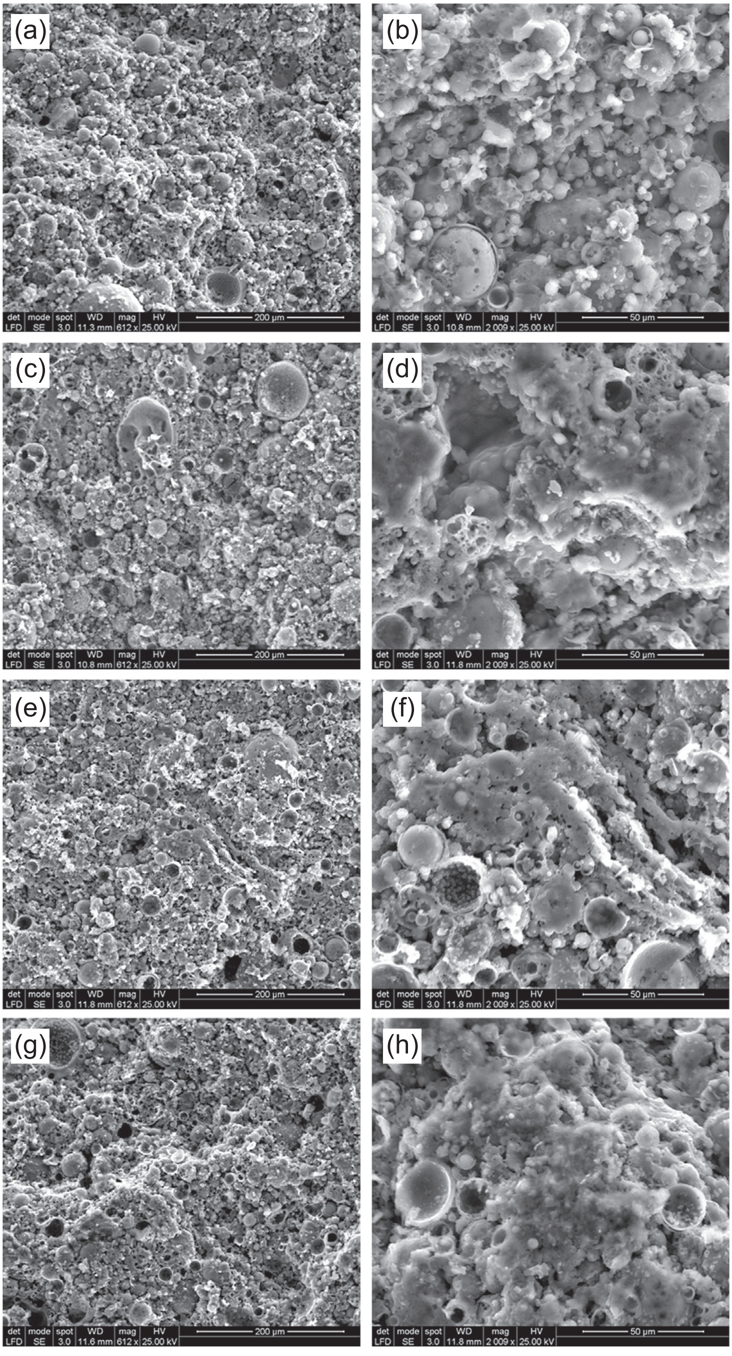

Figure 9.7 SEM images of geopolymer paste specimens containing different contents of kappa-carrageenan: (a,b) 0 wt%; (c,d) 0.05 wt%; (e,f) 0.1 wt%; and (g,h) 0.15 wt%.

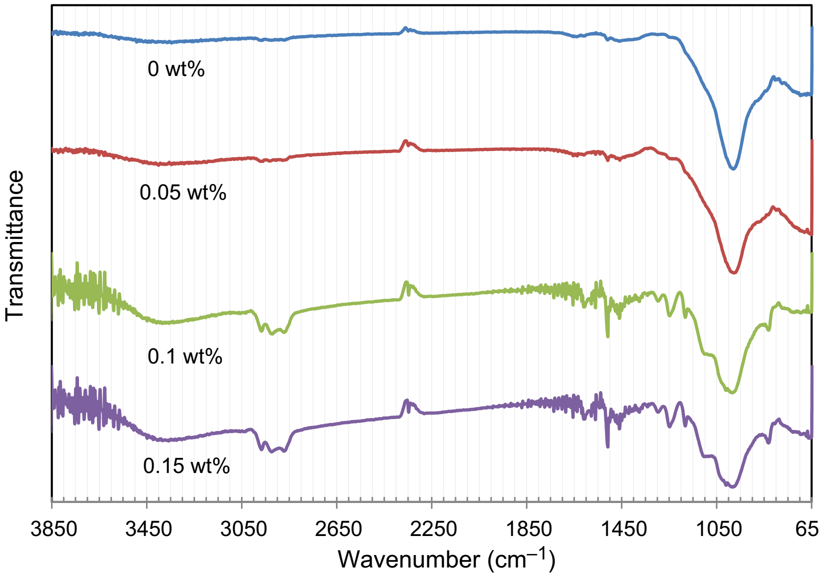

Figure 9.8 FTIR spectra of geopolymer paste specimens containing different contents of kappa-carrageenan.

Table 9.1 **FTIR characteristic bands identified in the KC-enhanced fly ash-based geopolymer shown in Figure 9.8**

Wavenumber (cm^{-1})	Characteristic bands	References
650–750	Symmetric stretching vibrations of Si–O–Si and Si–O–Al	Panias et al. (2007)
830	Si–O stretching vibrations of SiO_4	Buchwald et al. (2007)
970	Stretching vibration mode of Si–O (ν_3)	Buchwald et al. (2007)
1110	Si–O stretching vibrations of SiO_4	Buchwald et al. (2007)
1250, 1373	S=O stretching in the ester sulfate	Sankalia et al. (2006)
1425	C–H deformation	Sankalia et al. (2006)
1460–1520	O–C–O stretching vibrations resulting from carbonation of the contained Na	Swanepoel and Strydom (2002) and Phair et al. (2004)
1600–1650	Bending mode (ν_2) of H–O–H	Buchwald et al. (2007)
2350	C–O vibrations in CO_2 constrained in the amorphous phase of geopolymer	Treadwell et al. (1996)
2850, 2970	C–H stretching vibrations	Sankalia et al. (2006)
3200–3600	O–H stretching in polyhydroxyl groups	Sankalia et al. (2006)

showed the weak bands between 650 and 750 cm^{-1} due to the symmetric stretching vibrations of Si—O—Si and Si—O—Al bonds (Panias et al., 2007). The strong absorbance band at 970 cm^{-1} could be attributed to the stretching vibration mode of Si—O bond (Buchwald et al., 2007). The peaks in the region of 1460—1520 cm^{-1} due to O—C—O stretching vibrations resulted from the carbonation of contained Na during geopolymerization (Swanepoel and Strydom, 2002; Phair et al., 2004). The peaks at 1650 and 2350 cm^{-1} were also observed due to the bending mode of H—O—H bond and the vibrations of C—O bond from carbon dioxide constrained in the amorphous phase of geopolymer, respectively (Treadwell et al., 1996; Buchwald et al., 2007).

With the addition of KC up to 0.05 wt%, the FTIR spectra were not found to change significantly, presumably due to the relatively low KC content and the insufficient sensitivity of the IR technique. Further increase of the KC content beyond 0.05 wt% led to remarkable changes of the FTIR spectra. The appearance of peaks at 830 and 1110 cm^{-1} could be attributed to the Si—O stretching vibrations of SiO_4 units (Buchwald et al., 2007), which suggested the promotion of geopolymerization in the presence of KC. The peaks at 1250 and 1373 cm^{-1} correspond to the S=O stretching in the ester sulfate, indicating the presence of KC macromolecules in the hybrid geopolymer (Sankalia et al., 2006). The peaks between 2850 and 2970 cm^{-1} could be due to the C—H stretching vibrations, which further suggested the presence of KC (Sankalia et al., 2006). The very broad band spreading in the region of 3200—3600 cm^{-1} could be assigned to the polyhydroxyl (—OH) groups (Sankalia et al., 2006), which may have resulted from the water trapped in the specimens or the hydrogen bonds present in the KC-enhanced geopolymer. Moreover, the bands between 1460 and 1520 cm^{-1} were found sharper, suggesting that KC modified the geopolymerization by promoting the movement of a large amount of Na to surface and then enhancing its carbonation (Swanepoel and Strydom, 2002; Phair et al., 2004).

9.4 Discussion

The enhancement of fly ash-based geopolymer due to the inclusion of KC could be attributed to the modification of geopolymerization process and the promotion of mineralization (Shchipunov and Karpenko, 2004; Shchipunov et al., 2005). It is worth noting that the addition of biopolymer has been previously reported to manipulate the sol—gel process and influence the microscopic morphology of the final hybrid material (Shchipunov 2003; Shchipunov et al., 2005; Ruiz-Hitzky et al., 2008). Furthermore, the production of biopolymer-enhanced geopolymer resembles the formation of some high-performance natural organic—inorganic composites (e.g., diatoms through polymerization and precipitation of silicic acid) (Manfred, 2002; Zhang et al., 2004). Therefore, it is reasonable to assume that geopolymer can exhibit remarkably improved mechanical properties with the involvement of appropriate amount of polysaccharides and the formation of cross-linking networks through the sol—gel process. The main effect of incorporation of KC into geopolymer could be attributed to the presence of large amounts of hydrogen bonds in the

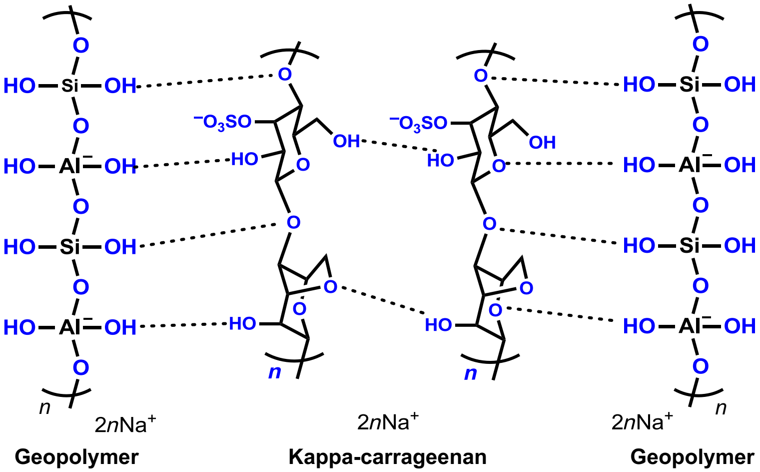

Figure 9.9 Hydrogen bonds (represented by the dashed lines) formed between kappa-carrageenan and fly ash-based geopolymer as well as within kappa-carrageenan macromolecules.

biopolymer macromolecules (Figure 9.9). The hydroxyl and ester sulfate groups in the KC macromolecules could also be associated with the geopolymer gels through interactions such as van der Waals forces and coordination bonds. Furthermore, the silanol monomers and oligomers produced from hydrolysis of fly ash during geopolymerization were likely to condense with the hydroxyl groups in the KC macromolecules to form covalent bonds (Shchipunov et al., 2005). Hence, the formation of KC-enhanced geopolymer composites could be depicted by three stages: (1) hydrolysis of fly ash to produce silanol monomers and oligomers; (2) formation of hydrogen bonds between the geopolymer and KC macromolecules, linkage of hydroxyl groups between geopolymers through hydrogen bonds, and reaction of hydroxyl groups between geopolymer and KC macromolecules; and (3) condensation of silanols to produce the final three-dimensional cross-linked KC-enhanced geopolymer composite. This could be used to explain the substantial increase of UCS, *T*, and *H* because of inclusion of KC. Further increase of the KC content beyond 0.1 wt%, however, led to the decrease of the mechanical properties, possibly due to two reasons. First, the addition of KC beyond 0.1 wt% significantly increased the viscosity of the biopolymer alkaline solution and adversely affected the workability of the biopolymer—geopolymer paste, leading to a less condensed structure with higher porosity in the final paste specimens. Second, excessive amount of KC macromolecules might heavily encapsulate the unreacted and partially hydrolyzed fly ash particles during geopolymerization and hinder their further dissolution and condensation and subsequent formation of three-dimensional cross-linking geopolymer networks. Similar trend was also reported for fiber-reinforced cement paste specimens (Mansur and Aziz, 1982) and N-carboxymethyl chitosan-enhanced fly ash-based geopolymer paste specimens (Li et al., 2013).

9.5 Conclusions and suggestions for future work

The feasibility of using low-cost naturally occurring kappa-carrageenan (KC) biopolymer to enhance fly ash-based geopolymer was studied. Based on the experimental results, the following conclusions can be drawn.

1. The unconfined compressive strength (UCS) of geopolymer paste increased with the addition of KC up to 0.1 wt% and the maximum increase was about 45.8% at 0.1 wt% KC. Further increase of KC content beyond 0.1 wt% resulted in a slight decrease in UCS, but the UCS was still much higher than that of the plain geopolymer paste.
2. The splitting tensile strength (*T*) of geopolymer paste increased with the addition of KC until 0.1 wt% and then decreased. At 0.1 wt% KC, the *T* increased by approximately 22.4% compared to that of the plain geopolymer paste.
3. The prepeak toughness (*H*) of geopolymer paste increased with the addition of KC up to 0.1 wt% and then slightly decreased. At 0.1 wt% KC, the *H* increased by approximately 45.6%.
4. The added KC coated and bridged the (geopolymerized) fly ash particles and led to formation of a more condensed geopolymer structure, thus improving the mechanical behavior of the biopolymer—geopolymer composite. However, when too much KC was involved, the significantly increased viscosity of the biopolymer alkaline solution adversely affected the workability of the biopolymer—geopolymer paste and led to a less condensed structure with higher porosity in the final paste specimens. In addition, excessive amount of KC led to heavy coating and encapsulation of unreacted and partially hydrolyzed fly ash particles, hindering their geopolymerization and deteriorating the mechanical behavior of the biopolymer—geopolymer composite. This was why the maximum enhancement of mechanical properties was obtained at 0.1 wt% KC.

The current research provides very promising results regarding utilization of biopolymer to enhance geopolymer. However, because the study is in laboratory scale and focuses only on the short-term properties of geopolymer paste enhanced by KC, further research needs to be conducted to promote the application of biopolymer-enhanced geopolymer products in practice, including:

1. Study the enhancement of different geopolymer products such as paste, mortar, and concrete using different types of biopolymers, aiming to find the most effective biopolymer for the enhancement of a specific geopolymer product.
2. Study not only the short-term but also the long-term properties of biopolymer-enhanced geopolymer products, especially the durability of the biopolymer-enhanced geopolymer products at field conditions.
3. Conduct full-scale study to investigate the different practical aspects related to field applications such as the commercial production method and the costs.

References

Ahmari, S., Zhang, L., 2012. Production of eco-friendly bricks from copper mine tailings through geopolymerization. Construction and Building Materials 29, 323—331.

Ahmari, S., Zhang, L., 2013a. Durability and leaching behavior of mine tailings-based geopolymer bricks. Construction and Building Materials 44, 743—750.

Ahmari, S., Zhang, L., 2013b. Utilization of cement kiln dust (CKD) to enhance mine tailings-based geopolymer bricks. Construction and Building Materials 40, 1002−1011.

Al-Oraimi, S.K., Seibi, A.C., 1995. Mechanical characterization and impact behavior of concrete reinforced with natural fibers. Composite Structures 32, 165−171.

Ashton, H.C., 2010. The incorporation of nanomaterials into polymer media. In: Gupta, R.K., Kennel, E., Kim, K.-J. (Eds.), Polymer Nanocomposites Handbook. CRC Press, Boca Raton, FL, pp. 21−44.

Bakharev, T., 2005a. Geopolymeric materials prepared using class F fly ash and elevated temperature curing. Cement and Concrete Research 35, 1224−1232.

Bakharev, T., 2005b. Resistance of geopolymer materials to acid attack. Cement and Concrete Research 35, 658−670.

Balaguru, P.N., Shah, S.P., 1992. Fiber-Reinforced Cement Composites. McGraw-Hill, New York.

Bernal, S., Gutierrez, R.D., Delvasto, S., Rodriguez, E., 2010. Performance of an alkali-activated slag concrete reinforced with steel fibers. Construction and Building Materials 24, 208−214.

Bezerra, U.T., Ferreira, R.M., Castro-Gomes, J.P., 2011. The effect of latex and chitosan biopolymer on concrete properties and performance. Key Engineering Materials 466, 37−46.

Buchwald, A., Hilbig, H., Kaps, C., 2007. Alkali-activated metakaolin-slag blends—performance and structure in dependence of their composition. Journal of Materials Science 42, 3024−3032.

Chindaprasirt, P., Chareerat, T., Sirivivatnanon, V., 2007. Workability and strength of coarse high calcium fly ash geopolymer. Cement and Concrete Composites 29, 224−229.

Chandra, R., Rustgi, R., 1998. Biodegradable polymers. Progress in Polymer Science 23, 1273−1335.

Davidovitz, J., 2005. Geopolymer, Green Chemistry and Sustainable Development Solutions: Proceedings of the World Congress Geopolymer 2005. Saint-Quentin, France.

Davidovitz, J., 2008. Geopolymer: Chemistry & Applications, second ed. Institut Géopolymère, France.

De Gutiérrez, R.M., Díaz, L.N., Delvasto, S., 2005. Effect of pozzolans on the performance of fiber-reinforced mortars. Cement and Concrete Composites 27, 593−598.

Deans J.R., 1994. Removing polyvalent metals from aqueous waste streams with chitosan and halogenating agents. US Patent 5336415.

Deans, J.R., Dixon, B.G., 1992. Uptake of Pb^{2+} and Cu^{2+} by novel biopolymers. Water Research 26, 469−472.

Dias, D.P., Thaumaturgo, C., 2005. Fracture toughness of geopolymeric concretes reinforced with basalt fibers. Cement and Concrete Composites 27, 49−54.

Dimas, D.D., Giannopoulou, I.P., Panias, D., 2009. Utilization of alumina red mud for synthesis of inorganic polymeric materials. Mineral Processing and Extractive Metallurgy Review. An International Journal 30, 211−239.

Duxson, P., Fernández-Jiménez, A., Provis, J.L., Lukey, G.C., Palomo, A., van Deventer, J.S.J., 2007. Geopolymer technology: the current state of the art. Journal of Materials Science 42, 2917−2933.

Duxson, P., Provis, J.L., Lukey, G.C., Mallicoat, S.W., Kriven, W.M., van Deventer, J.S.J., 2005. Understanding the relationship between geopolymer composition, microstructure and mechanical properties. Colloids and Surfaces A 269, 47−58.

Groert, N., 2007. Carbon nanotubes becoming clean. Materials Today 10, 28−35.

Granizo, M.L., Blanco-Varela, M.T., Martmez-Rarmrez, S., 2007. Alkali activation of metakaolins: parameters affecting mechanical, structural and microstructural properties. Journal of Materials Science 42, 2934−2943.

Griggs, C., 2010. Modified biopolymers as an alternative to petroleum-based polymers for soil modification. Environment, Energy Security, and Sustainability Symposium and Exhibition, E^2S^2.

Guo, X., Shi, H., Dick, W.A., 2010. Compressive strength and microstructural characteristics of class C fly ash geopolymer. Cement and Concrete Composites 32, 142−147.

Hardjito, D., Wallah, S.E., Sumajouw, D.M.J., Rangan, B.V., 2004. On the development of fly ash-based geopolymer Concrete. ACI Materials Journal 467−472.

He, P., Jia, D., Lin, T., Wang, M., Zhou, Y., 2010. Effects of high-temperature heat treatment on the mechanical properties of unidirectional carbon fiber reinforced geopolymer composites. Ceramic International 36, 1447−1453.

Hendriks, C.A., Worrell, E., de Jager, D., Blok, K., Riemer, P., 2000. IEA Greenhouse Gas R&D Programme. http://www.ieaghg.org.

Hu, S., Wang, H., Zhang, G., Ding, Q., 2008. Bonding and abrasion resistance of geopolymeric repair material made with steel slag. Cement and Concrete Composites 30, 239−244.

Jha, I.N., Iyengar, L., Prabhakara Rao, A.V.S., 1988. Removal of cadmium using chitosan. Journal of Environmental Engineering 114, 962−975.

John, M.J., Anandjiwala, R.D., Wambua, P., Chapple, S., Klems, T., Doecker, M., Goulain, M., Erasmus, L., 2008. Bio-based Structural Composite Materials for Aerospace Applications, 2nd South African International Aerospace Symposium (Cape Town, South Africa).

Kaps, C., Buchwald, A., October 2002. Property controlling influences on the generation of geopolymeric binders based on clay. In: Proc Int Conf Geopolymer 2002, Melbourne, Australia.

Kim, D., Petrisor, I.H., Yen, T.F., 2005. Evaluation of biopolymer-modified concrete systems for disposal of cathode ray tube glass. Journal of Air Waste Management Association 55, 961−969.

Knaus, S., Bauer-Heim, B., 2003. Synthesis and properties of anionic cellulose ethers: influence of functional groups and molecular weight on flowability of concrete. Carbohydrate Polymers 53, 383−394.

Kosbar, L.L., Gelorme, J.D., Japp, R.M., Fotorny, W.T., 2000. Introducing biobased materials into the electronics Industry. Journal of Industrial Ecology 4, 93−105.

Kriker, A., Debicki, G., Bali, A., Khenfer, M.M., Chabannet, M., 2005. Mechanical properties of date palm fibers and concrete reinforced with date palm fibers in hot-dry climate. Cement and Concrete Composites 27, 554−564.

Krivenko, P.V., Shi, C., Roy, D., 2006. Alkali-activated Cements and Concretes, first ed. Taylor & Francis, New York, NY.

Kumar, A., Srivastava, A., Galaev, I.Y., Mattiasson, B., 2007. Smart polymers: physical forms and bioengineering applications. Progress in Polymer Science 32, 1205−1237.

Li, C., Sun, H., Li, L., 2010. A review: the comparison between alkali-activated slag (Si+Ca) and metakaolin (Si+Al) cements. Cement and Concrete Research 40 (9), 1341−1349.

Li, W., Xu, J., 2009. Mechanical properties of basalt fiber reinforced geopolymeric concrete under impact loading. Material Science and Engineering: A 505, 178−186.

Li, Z., Chen, R., Zhang, L., 2013. Utilization of chitosan biopolymer to enhance fly ash-based geopolymer. Journal of Materials Science 48, 7986−7993.

Li, Z., Wang, L., Wang, X., 2006. Properties of hemp fiber reinforced concrete composites. Composites A 37, 497−505.

Lin, T., Jia, D., He, P., Wang, M., Liang, D., 2008. Effects of fiber length on mechanical properties and fracture behavior of short carbon fiber reinforced geopolymer matrix composites. Materials Science and Engineering: A 497, 181−185.

Lin, T., Jia, D., Wang, M., He, P., Liang, D., 2009. Effects of fibre content on mechanical properties and fracture behaviour of short carbon fibre reinforced geopolymer matrix composites. Bulletin of Materials Science 32, 77−81.

MacKenzie, K.J.D., Bolton, M.J., 2009. Electrical and mechanical properties of aluminosilicate inorganic polymer composites with carbon nanotubes. Journal of materials Science 44, 2851−2857.

Malhotra, V.M., 2000. In: Gjorv, O.E., Sakai, K. (Eds.), Concrete Technology for a Sustainable Development in the 21st Century. E&FN Spon, London.

Manfred, S.A., 2002. Phase separation model for the nanopatterning of diatom biosilica. Science 295, 2430−2433.

Mansur, M.A., Aziz, M.A., 1982. A study of jute fibre reinforced cement composites. International Journal of Cement Composites and Lightweight Concrete 4, 75−82.

McCaffrey, R., 2002. Global Cement Lime Magazine (Environmental Special Issue) 15.

Menefee, E., Hautala, E., 1978. Soil stabilization by cellulose xanthate. Nature 275, 530−532.

Merta, I., Tschegg, E.K., Kolbitsch, A., 2010. Fracture mechanical properties of concrete reinforced with straw fibers. In: Proceedings of the Cost Strategic Workshop: Principles and Development of Bio-inspired, Vienna, Austria, pp. 145−146.

Metaxa, Z.S., Konsta-Gdoutos, M.S., Shah, S.P., 2010. Carbon nanofiber−reinforced cement-based materials. Transportation Research Record - Journal of Transportation Research Board 2142, 114−118.

Meyer, C., 2009. The greening of the concrete industry. Cement and Concrete Composites 31, 601−605.

Moniruzzaman, M., Winey, K.I., 2006. Polymer nanocomposites containing carbon nanotubes. Macromolecules 39, 5194−5205.

Orts, W.J., Glenn, G.M., Sojka, R.E., 2000. Biopolymer additives to reduce erosion-induced soil losses during irrigation. Industrial Crops and Products 11, 19−29.

Pacheco-Torgal, F., Castro-Gomes, J., Jalali, S., 2007. Investigations about the effect of aggregates on strength and microstructure of geopolymeric mine waste mud binders. Cement and Concrete Research 37, 933−941.

Pacheco-Torgal, F., Castro-Gomes, J., Jalali, S., 2009. Tungsten mine waste geopolymeric binder: preliminary hydration products investigations. Construction and Building Materials 23, 200−209.

Pacheco-Torgal, F., Jalali, S., 2011. Cementitious building materials reinforced with vegetable fibers: a review. Construction and Building Materials 25, 575−581.

Panias, D., Giannopoulou, I.P., Perraki, T., 2007. Effect of synthesis parameters on the mechanical properties of fly ash-based geopolymers. Colloid and Surfaces: A 301, 246−254.

Pernica, D., Reis, P.N.B., Ferreira, J.A.M., Louda, P., 2010. Effect of test conditions on the bending strength of a geopolymer-reinforced composite. Journal of Materials Science 45, 744−749.

Phair, J.W., van Deventer, J.S.J., Smith, J.D., 2004. Effect of Al source and alkali activation on Pb and Cu immobilisation on fly-ash based “geopolymers”. Applied Geochemistry 19, 423−434.

Pilla, S., Datta, C., 2011. Starch as a biopolymer in construction and civil engineering. In: Handbook of Bioplastics and Biocomposites Engineering Applications, vol. 11. Wiley, pp. 317−346.

Plank, J., 2003. Applications of biopolymers in construction engineering. In: Steinbüchel, A. (Ed.), Biopolymers, vol. 10. Wiley-VCH, Weinheim, pp. 29−95.

Plank, J., 2004. Applications of biopolymers and other biotechnological products in building materials. Applied Microbiology and Biotechnology 66, 1–9.

Provis, J., 2014. Geopolymers and other alkali activated materials: why, how, and what? Journal of Materials Structures 47, 11–25.

Provis, J., Van Deventer, J.S.J., 2009. Geopolymers: Structure, Processing, Properties and Industrial Applications. Woodhead Publishing, Cambridge, UK.

Ramachandran, V.M., 1995. Concrete admixtures handbook. Properties, Science and Technology, second ed. Elsevier.

Rangan, B.V., 2008. Fly-Ash Based Geopolymer Concrete. Research Report GC 4, Engineering Faculty. Curtin University of Technology, Perth, Australia.

Rattanasak, U., Chindaprasirt, P., 2009. Influence of NaOH solution on the synthesis of fly ash geopolymer. Minerals Engineering 22, 1073–1078.

Rhim, J.W., Ng, P.K.W., 2007. Natural biopolymer-based nanocomposite films for packaging applications. Critical Reviews in Food Science and Nutrition 47, 411–433.

Ruiz-Hitzky, E., Darder, M., Aranda, P., 2008. An introduction to bio-nanohybrid materials. In: Bio-inorganic Hybrid Nanomaterials: Strategies, Syntheses, Characterization and Applications. Wiley, pp. 1–40.

Sakata, N., Maruyama, K., Minami, M., 1996. Basic properties and effects of welan gum on self-consolidating concrete. In: Production Methods and Workability of Concrete. E & FN Spon.

Sankalia, M.G., Mashru, R.C., Sankalia, J.M., Sutariya, V.B., 2006. Stability improvement of alpha-amylase trapped in kappa-carrageenan beads: physicochemical characterization and optimization using composite index. International Journal of Pharmaceutics 312, 1–14.

Sarker, P.K., 2010. Bond strength of reinforcing steel embedded in fly ash-based geopolymer concrete. Materials and Structures 44 (5), 1021–1030.

Shchipunov, Y.A., 2003. Sol–gel-derived biomaterials of silica and carrageenans. Journal of Colloid and Interface Science 268, 68–76.

Shchipunov, Y.A., Karpenko, T.Y., 2004. Hybrid polysaccharide-silica nanocomposites prepared by the sol-gel technique. Langmuir 20, 3882–3887.

Shchipunov, Y.A., Karpenko, T.Y., Krekoten, A.V., 2005. Hybrid organic-inorganic nanocomposites fabricated with a novel biocompatible precursor using sol-gel processing. Composite Interfaces 11, 587–607.

Sofi, M., van Deventer, J.S.J., Mendis, P.A., Lukey, G.C., 2007. Engineering properties of inorganic polymer concrete (IPCs). Cement and Concrete Research 37, 251–257.

Steinbuchel, A., 2003. Biopolymers: General Aspects and Special Applications. Wiley.

Sun, P., Wu, H.C., 2008. Transition from brittle to ductile behavior of fly ash using PVA fibers. Cement and Concrete Composites 30, 29–36.

Swanepoel, J.C., Strydom, C.A., 2002. Utilisation of fly ash in a geopolymeric material. Applied Geochemistry 17, 1143–1148.

Temuujin, J., Van Riessen, A., MacKenzie, K.J.D., 2010. Preparation and characterisation of fly ash based geopolymer mortars. Construction and Building Materials 24 (10), 1906–1910.

Treadwell, D.R., Dabbs, D.M., Aksay, I.A., 1996. Mullite ($3Al_2O_3$–$2SiO_2$) synthesis with aluminosiloxanes. Chemistry of Materials 8, 2056–2060.

USCOTA, 1993. Biopolymers: Making Materials Nature's Way – Background Paper. OTA-bp-e-102. US Government Printing Office, Washington, DC.

Van Deventer, J.S.J., Provis, J., Duxson, P., 2012. Technical and commercial progress in the adoption of geopolymer cement. Minerals Engineering 29, 89–104.

Vekshin, N.L., 2002. Photonics of Biopolymers. Springer.

Vijn J.P., Spindler C.E., Keilhofer G., Plank J., 2004. Cementing subterranean zones using cement compositions containing biodegradable dispersants. US Patent 0099416 A1.

Wang, H., Li, H., Yan, F., 2005. Synthesis and mechanical properties of metakaolinite-based geopolymer. Colloids and Surfaces A: Physicochemical and Engineering Aspects 268, 1−6.

Xie, X.L., Mai, Y.W., Zhou, X.P., 2005. Dispersion and alignment of carbon nanotubes in polymer matrix: a review. Material Science and Engineering 49, 89−112.

Yazdanbakhsh, A., Grasley, Z., Tyson, B., Al-Rub, R.K.A., 2010. Distribution of carbon nanofibers and nanotubes in cementitious composites. Transportation Research Record: Journal of the Transportation Research Board 2142, 89−95.

Zhang, L., Ahmari, S., Zhang, J., 2011. Synthesis and characterization of fly ash modified mine tailings-based geopolymers. Construction and Building Materials 25 (9), 3773−3781.

Zhang, S., Gong, K., Lu, J., 2004. Novel modification method for inorganic geopolymer by using water soluble organic polymers. Materials Letters 58, 1292−1296.

Zhang, Y., Li, S., Xu, D., Wang, B., Xu, G., Yang, D., Wang, N., Liu, H., Wang, Y., 2010a. A novel method for preparation of organic resins reinforced geopolymer composites. Journal of Materials Science 45, 1189−1192.

Zhang, Y., Sun, W., Li, Z., 2006. Impact behavior and microstructural characteristics of PVA fiber reinforced fly ash-geopolymer boards prepared by extrusion technique. Journal of Materials Science 41, 2787−2794.

Zhang, Y., Sun, W., Li, Z., Zhou, X., Chau, C., 2008. Impact properties of geopolymer based extrudates incorporated with fly ash and PVA short fiber. Construction and Building Materials 22, 370−383.

Zhang, Y.J., Wang, Y.C., Xu, D.L., Li, S., 2010b. Mechanical performance and hydration mechanism of geopolymer composite reinforced by resin. Material Science and Engineering: A 527, 6574−6580.

Zhao, Q., Nair, B., Tahimian, T., Balaguru, P., 2007. Novel geopolymer based composites with enhanced ductility. Journal of Materials Science 2, 3131−3137.

Biopolymers with superplasticizer properties for concrete

10

U.T. Bezerra
Federal Institute of Paraíba, João Pessoa-PB, Brazil

> *God should not let poets and scientists die*
>
> ***Tupan Tebano Bezerra***

10.1 Introduction

"One naturally wonders who or what people first discovered that lime, when burnt and slaked with water, together with sand as an additive, can be used as a mortar? The answer has to be: we will never know - it just happened." This inquiry, spoken by Hamelau (1997), may very well be paraphrased as the problem of this book and be rewritten as: "one naturally wonders who or what people first discovered that concrete, together with *biopolymer*, can be used as a *greenconcrete*? The answer has to be: we will never know - it just happened."

As seen in Part II of this book, the following sequence allows reaching the concept of concrete:

1. Portland cement paste: well-proportioned mixture between Portland cement and water in which some additives can be included;
2. Portland cement mortar: well-proportioned mixture between the aforementioned paste and sand; and
3. Portland cement concrete: currently, concrete is a well-proportioned mixture between the aforementioned paste and gravel.

Why was the term *currently* previously mentioned? This is because until the beginning of the last century, around the year 1906, a discussion was incited about the difference between the expressions *betón* (in French) and *concrete* (in English). From one point of view, the French believed that betón was a mixture of mortar and gravel and, from another perspective, the English people held the position that stated that concrete was a mixture of cement, sand, gravel, and water, not existing a consensus on a unique concept between both sides. After some dissensions, the French and the English concluded that both expressions represented the same concept and the mixture order, which seemed to be the difference between both concepts, did not imply the need for different nomenclatures. In fact, even today there is no consensus on the mixture order of concrete components so that there are divergences about the quantity of materials to be added in concrete preparation as well as the adequate moment to add them to such mixture.

Biopolymers and Biotech Admixtures for Eco-Efficient Construction Materials. http://dx.doi.org/10.1016/B978-0-08-100214-8.00010-5
Copyright © 2016 Elsevier Ltd. All rights reserved.

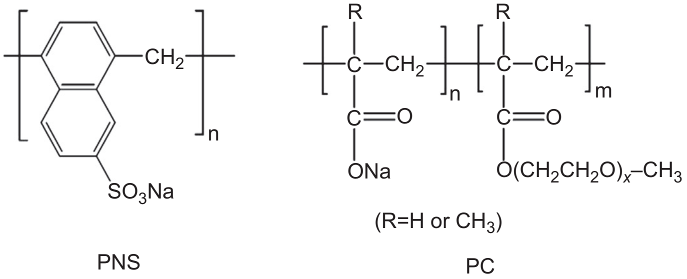

Figure 10.1 Chemical structure of commonly used petrochemical-based superplasticizers (PNS, polynaphthalene sulfonate; PC, polycarboxylate) (Petit et al., 2014).

Thus, it can be contemporarily said that, with permission from the French and the English, concrete is a mixture of Portland cement, sand, gravel, water, additions, and additives.

In this work, additions and additives have the following definitions:

1. Addition: fine-grained inorganic material added to cement with the aim of improving some specific cementing properties. Includes two types: inert or nearly inert additions, and pozzolanic or latent hydraulic additions. Quantities are usually ranging from 5.0% to 50.0% per unit mass of powder (EN 206-1, 2000); and
2. Additives: material added to the concrete mixture in small quantities at time of mixing to modify the properties of fresh and/or hardened (not usually) concrete. Quantities usually range from 0.2% to 4.0% per unit mass of powder. Admixtures are commercialized commonly in liquid form (EN 206-1, 2000).

In civil construction, the use of polymers dates back to the beginning of the twentieth century, with intensification starting from the decade of 1950 (Vertematti, 2004).

In relation to the structure of this material, according to what was presented in the previous chapters, a monomer is the basic repetition unit of a polymer that, in its turn, is an artificial material obtained from typical processes, for example, of the oil industry. Following this premise, a biopolymer is produced by agents and/or natural processes (animals, bacteria, fungi, humans, etc.) that generate macromolecules that increase in size and, then, are called biopolymers (i.e., naturally originated polymers).

Roughly, the subjacent idea of current superplasticizers is separating of anhydrous Portland cement particles from each other during the time in which concrete is cast into forms of the structural elements. It is important that superplasticizers act only in this interval of time and, afterward, these materials must be capable of being inert with respect to the cementitious products. Obviously, if the presence of superplasticizers is still capable of adding some increment of any property, after the material hardens, the superplasticizer is considered even better.

In general, the chemical structure of the current superplasticizers is presented in Figure 10.1.

In this structure, the basic characteristics of organic materials can be observed, with the presence of benzene rings and pendant functional groups. Three physicochemical

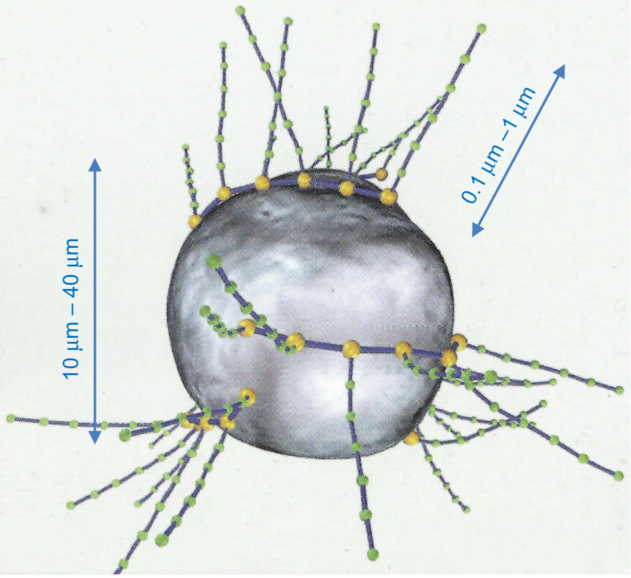

Figure 10.2 Stereo effect.
Adapted from MC-Bauchemie Catalogue (2011) and Oliveira et al. (2015).

effects have been adopted in the conception of superplasticizers for concrete and further cementitious materials:

1. The first one is the *electrostatic effect*: the idea is providing Portland cement particles with negative electrostatic charges, so that some cement particles repulse the other ones and then retard the beginning of hydration time. This is not exactly an easy task because the entire system is immersed in a super electrolyte, which is water, capable of making incommensurable ion exchanges between concrete phases, superplasticizers, and many materials that are added into the mixture, without defined limits;
2. The second one is the *stereo effect*: this effect is characterized by the adoption of long polymeric chains to the Portland cement particles (Figure 10.2) as to slightly separate them from each other, which makes the mixing water not reach these particles and also allows a reduction of the system viscosity.

   Also in Figure 10.2 can be noted a spatial repulsion of polymeric chains in a lower order of magnitude regarding Portland cement particles. In other words, particles tend to remain spaced around two polymeric chains, before the concrete pouring in forms and, consequently, before the hydration process starts with more intensity; and
3. The third is the stereo effect in the superplasticizer itself. This effect was proposed by Xiangming et al. (2014) and brings a new concept in conceiving superplasticizers. These authors developed a polyethylene-based superplasticizer that is stereo-wrapped by the *macro-monomer methoxy polyethylene glycol methacrylate* (PNP) polymer (Figure 10.3).

In this case, the goal is to shield cement particles with a stereo-structured polymer and, having even smaller dimensions than the pure stereo effect (30 nm), the density of polymers (PNP) around the particles is so large that they do not come into contact with water.

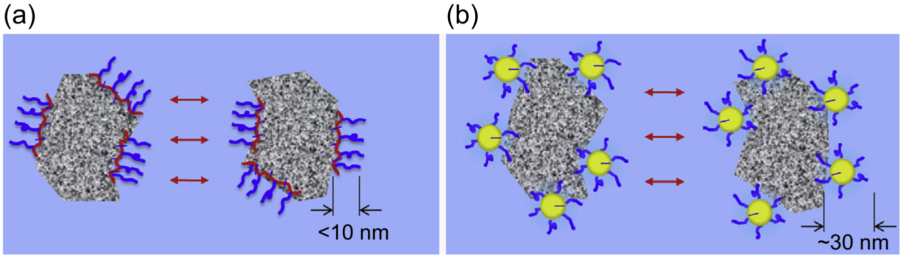

Figure 10.3 The proposed dispersing mechanisms of PCE superplasticizer (a) and PNPs (b). Adapted from Xiangming et al. (2014).

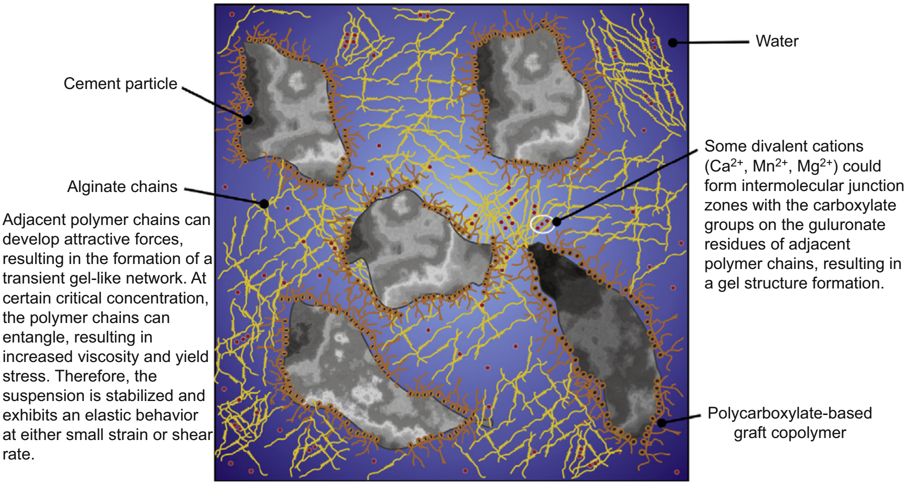

Adjacent polymer chains can develop attractive forces, resulting in the formation of a transient gel-like network. At certain critical concentration, the polymer chains can entangle, resulting in increased viscosity and yield stress. Therefore, the suspension is stabilized and exhibits an elastic behavior at either small strain or shear rate.

Some divalent cations (Ca^{2+}, Mn^{2+}, Mg^{2+}) could form intermolecular junction zones with the carboxylate groups on the guluronate residues of adjacent polymer chains, resulting in a gel structure formation.

Figure 10.4 Schematic representation of the network formation between the marine brown algae extract (ALG) polymer chains in cement pastes.
Adapted from León-Martínez et al. (2014).

Another interesting research conducted by León-Martínez et al. (2014) presents a possible structure of the effect of a viscosity-enhancing admixture obtained of nopal mucilage and marine brown algae extract (Figure 10.4).

The proposed structure shows a complex steric effect provided by the presence of the alginate chains that deviate cement particles. The result of this effect is shown in Table 10.1 below in terms of fresh properties.

In general, the presence of nopal mucilage and marine brown algae extract increased the viscosity of the concrete. Some concentrations were able to improve performance in some tests, but not all. For example, the concrete prepared with 0.25% of nopal mucilage, although it had a good spread, had excessive bleeding and segregation. Figure 10.5 shows the visual appearance of some of the specific spreading tests at room temperature. Note that the concrete with 0.25% of marine brown algae extract

Table 10.1 **Fresh properties of SCC mixtures containing different types of VEAs**

Test	Measurement	RSCC welan gum-0.065%	SCC1 MUC-0.250%	SCC2 MUC-0.374%	SCC3 ALG-0.250%	SCC4 ALG-0.250%	SCC5 ALG-0.500%
Slump flow	Flow spread (mm)	753	800	701	736	705	430
	$T_{50\ cm}$ time (s)	1.3	1.2	1.2	1.5	0.3	c
	VSI (0−3)	0	3	1	2	0	0
	Yield-stress (Pa)[a]	191.65 (179.45)	169.56 (167.45)	223.62	201.10 (374.30)	211.64	561.17 (1403.01)
J-ring with inverted slump cone	J-ring flow spread (mm)	723	730	645	625	640	395
	Height difference (mm)	0.48	1.30	0.50	1.50	0.83	1.40
V-funnel	T-0 (s)	4.32	3.43	5.10	6.74	3.42	5.52
	T-5 (s)	4.52	29.00	5.11	6.81	3.48	5.68
	Average flow-through speed, V_m(m/s)[b]	0.475	0.598	0.402	0.304	0.600	0.372
	Flow-through index, $S_f(-)$[b]	0.046	7.454	0.002	0.01	0.017	0.029

Continued

Table 10.1 **Continued**

Test	Measurement	RSCC welan gum-0.065%	SCC1 MUC-0.250%	SCC2 MUC-0.374%	SCC3 ALG-0.250%	SCC4 ALG-0.250%	SCC5 ALG-0.500%
L-box	Blocking ratio $h_2/h_1(-)$	0.94	0.51	0.67	0.46	0.93	0.51
Segregation column	Percentage of static segregation (%)	0.28	7.70	0.48	4.54	3.28	2.36
Other properties	Air content (v%)	0.80	0.60	1.25	2.57	6.00	6.20
	Unit weight (kg/m^3)	2280	2280	2310	2290	2210	2180
	Temperature (°C)	17	21	18	21	20	19
Observations		A highly stable mixture was observed	Excessive bleeding was observed together with visible segregation	A slight aggregate pile in the center of the concrete mass was observed	A stable and homogeneous mixture with a slight halo of bleeding was observed	A stable and homogeneous mixture was observed	A stable and homogeneous mixture was observed

$T_{50\ cm}$: elapsed time to 50 cm spreading in seconds;
a: data calculated using the Murata equation with 3D yield criteria;
b: these were calculated using the equations reported in ACI 238.1R-08, 2008;
c: there was not any flow due to very high yield-stress of the mixture.
Source: León-Martínez et al. (2014).

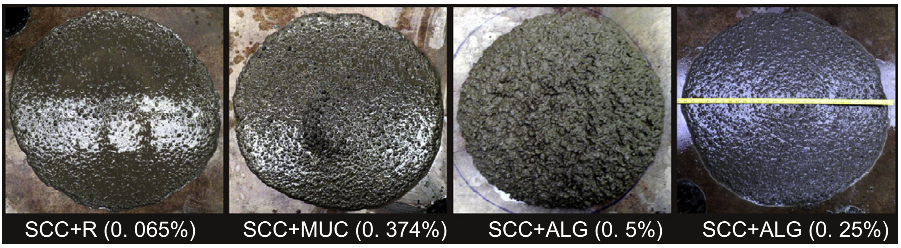

Figure 10.5 Visual appearance of SCC mixtures containing nopal mucilage (MUC), marine brown algae extract (ALG), and a commercial VEA (R) during the flow spread test at room temperature.
Adapted from León-Martínez et al. (2014).

seems to be the best tested mixture, as well as presenting a good spread, low segregation, and bleeding, also had a high air content (>6%), which is a good evidence of concrete suitable to resist freeze—thaw cycles.

When studying the rheology of concrete, it is still not possible to use a single test that is able to predict behavior from its mixing to the curing. A promising attempt has been the adoption of the concept of robustness (Nunes et al., 2006), involving mini slump-flow tests, mini V-funnel, and air content.

Seeking to increase the robustness of a self-compacting concrete, Van Der Vurst and De Schutter (2014) used small amounts of additions, including diutan gum and welan gum; Table 10.2 shows the results obtained.

Table 10.2 **Effect of fine additions in robustness of fresh self-compacting concrete**

Mortar mix	Robustness
Eqm1 (reference mix)	2.85
Eqm2 (more robust mix)	15.64
Ref + 0.02% welan gum	3.61
Ref + 0.01% diutan gum	17.18
Ref + 1% silica fume	1.57
Ref + 1% ground granulated blast furnace slag	4.31
Ref + 1% fly ash	1.25
Ref + 1% zeolite	1.10
Ref + 0.02% purified attapulgite clay	1.32
Ref + 1% kaolinite clay	2.36
Ref + 1% metakaolin clay	1.62

Adapted from Van Der Vurst and De Schutter (2014).

In Table 10.2, the enormous effect provided by diutan gum in robustness (502.81%), relative to a reference concrete without additives, can be seen. This value shows the importance of microbial-based biopolymers for the increase of self-compacting concrete robustness.

Another aspect of superplasticizers refers to the fact that such materials are not limited to the function of significant reduction of water—cement ratio with maintaining the workability. Peng and Jacobsen (2013) report the importance of compatibility verification of the cement—superplasticizer system. In most situations the compatibility is synergistic, but there are some important cases of overdose or chemical differences, in which the superplasticizer is capable of, inclusively, generating bleeding and segregation. Thus, either zeta-potential or hydrostatic tests (sedimentation verification) are recommended as to avoid such problems. Simple rheological tests are also useful for compatibility verification of the system, but, in this case, the cause of the problem will not be known.

In another direction, nonopposite and parallel, a family of superplasticizers and additives has been recently developed, known as Superabsorbent Polymers (SAP). These materials began to be studied during the decade of 1980 toward disposable nappy applications (Friedrich, 2012 *apud* Mechtcherine and Reinhardt, 2012 p. 13). In 2007, International union of laboratories and experts in construction materials, system and structures RILEM established the Technical Committee 225-SAP (Mechtcherine and Reinhardt, 2012), in charge of categorizing different studies performed so far. The results have not been as promising as predicted, because, although the material can control concrete cure (which is its main function), other properties are impaired (such as compressive and tensile strength, and shrinkage). In other words, like Toledo Filho et al. (Mechtcherine and Reinhardt, 2012) said: "the implementation of a new technique such as the use of SAP on concrete must require preliminary and extensive research in order to use the material with safety and effectiveness."

In principle, it can be supposed that currently there is a slow replacement period of oil-based superplasticizers, but it is not exactly what history reports. Torgal and Jalali (2010) discuss the employment of natural organic materials (biopolymers) in mortars at least 500 years ago. Sá (2005) and Cechova et al. (2010) indicate that olive oil and linseed oil were used in mortars at least five centuries ago. In fact, concretes used in Brazil, for example, at the time of discovery of the Brazilian territories, were prepared with lime, sand, limestone rocks, and whale oil. These organic materials, precursors of current biopolymers, were added to concrete mixtures at low concentrations, providing workability (fresh state), durability (waterproofing), but not high mechanical resistance (Santiago, 2001, 2007). The presence of such materials was so efficient that many constructions are still fully operating in this century, such as several buildings in the world.

Therefore, it can be said that biopolymers, as superplasticizers developed by nature, were replaced by human-produced superplasticizers and, currently, they are undergoing a transformation. This transformation refers to the gradual substitution of synthetic superplasticizers by biopolymers.

In this context, additives have been employed in concrete since the last century, and superplasticizers obtained from biopolymers have been employed more recently, without defined systematization, by both the construction industry and manufacturers.

10.2 Biopolymers with superplasticizer properties

Biopolymers are natural materials, structurally classified as polysaccharides, polyesters, polyamides, and hydrocarbons. Some examples of natural polymers commonly found in everyday life are rubber, starch, cotton, leather, wool, silk, etc. They can be found in three basic forms (Costa et al., 2014):

1. Powder form: biopolymers that can be either added to cement or diluted in water for concrete preparation. Examples: chitin, chitosan, starch, etc.;
2. Liquid form: biopolymers that are usually diluted in water for concrete preparation. Examples: many latex materials (rubber, avelós, *Araucária*, diutan, welan, xanthan, gelan, gutta-percha, guar, etc.); and
3. Fiber form: biopolymers that have suffered the biopolymerization process and that will increase the tensile strength of the concrete (these types of biopolymers are not treated here, due to the fact that they do not present a superplasticizing effect). Examples: natural fibers (curauá, coconut, sisal, Spanish broom, hemp, juta, kenaf, pineapple, etc.).

Biopolymers offer some advantages in relation to synthetic polymers, such as lower cost in some cases, easy extraction, biocompatibility, and biodegradability (Nóbrega, 2009). Biodegradability is a dubious property; a concrete that degrades over time is not accepted.

The most abundant biopolymer is *cellulose*, a polysaccharide produced by plant photosynthesis. Cellulose is found abundantly in several bamboo species (Sobrinho et al., 2012). The second is *chitin*, a polysaccharide found in marine animals, insects, and fungi (Antonino, 2007). Chitin was isolated for the first time in mushrooms, in 1811, by the French professor Henri Braconnot when he was studying fungi, calling it *fungina*. In 1823, Odier isolated the same substance through insect carapaces, which gave the name of chitin. Posteriorly, Odier observed the presence of chitin in crab carapaces (Chiandotti, 2005; Antonino, 2007). Today, the commercially produced chitin is obtained from both crab carapaces and shell shrimps.

The derived product of chitin that has given rise to scientific and commercial interests is the *chitosan* (Dutta et al., 2004; Rinaudo, 2006). This polymer was first described around 1859 by Professor C. Rouget. The name *chitosan* only came to be proposed in 1894 by Hoppe-Seyler, due to the fact that this substance has nitrogen at an equal level as it is found in original chitin (Antonino, 2007). Chitosan is nothing more than a product from deacetylation of chitin (Bezerra, 2006); moreover, chitosan is a stable material in alkaline environments and of low acidity (Craveiro et al., 1999).

These three biopolymers (cellulose, chitin, and chitosan) have similar chemical structures (Figure 10.6 and Chapter 7), differing only in their pendant functional groups. It is worth noting that cellulose is the only one that does not present nitrogen in its pendant functional groups.

Some of these biopolymers can be employed in concrete, as additions. For instance, chitosan is capable of increasing the compressive strength of concretes by up to 30% (Bezerra, 2006). However, rheological properties become impaired, once chitosan is slightly soluble in water. From this finding, Nóbrega (2009) carried out research by using diluted chitosan from 0.25 to 2.00 M of glacial acetic acid (99%). Thus, chitosan

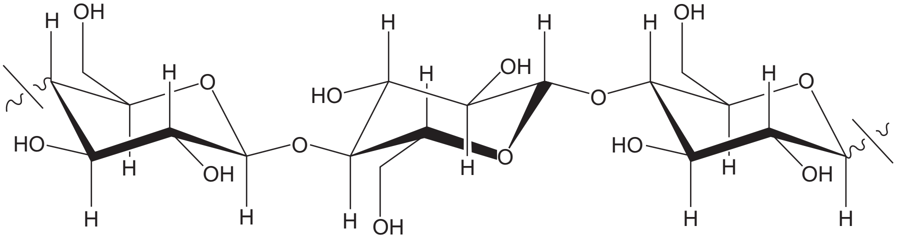

Figure 10.6 Cellulose chemical structure.

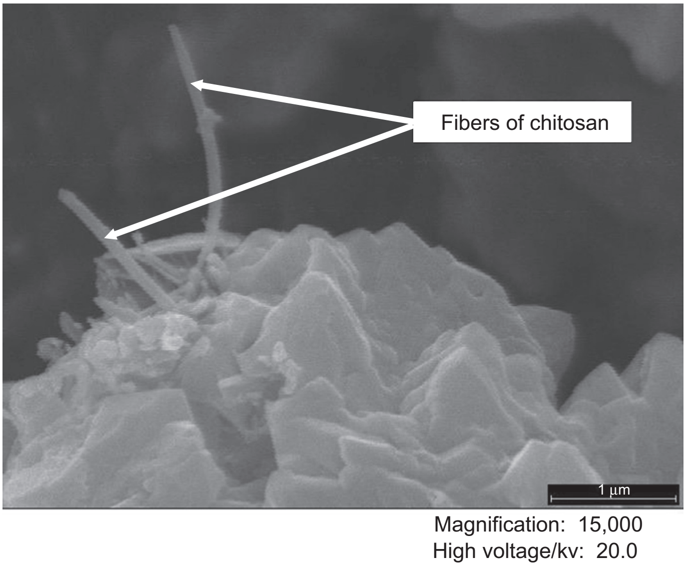

Figure 10.7 Scanning electronic microscopy of concrete with chitosan (Bezerra et al., 2011).

suffers an acetylation process and returns to chitin form, which is a polymer that is more soluble than chitosan. Then, when introduced into the strongly alkaline environment provided by Portland cement, the chitin becomes deacetylated again, being converted into chitosan. At this stage, the formation of chitosan occurs inside the microstructure of the cement paste, which favors the formation of polymeric networks. Furthermore, due to the fact that chitin is initially diluted in water, the rheological properties are not affected as they are in the case of direct employment of chitosan. These polymeric networks, in their turn, provide higher gain of mechanic properties, once they involve Portland cement hydrates more efficiently (Figure 10.7).

The study conducted by Bezerra et al. (2011) shows a correspondence between the pore distribution in the microstructure and the absorption of water through capillarity in concrete prepared with chitosan and latex.

Figures 10.8 and 10.9 show results of pore size distribution obtained by mercury intrusion to chitosan and latex addition. There, one can see a larger number of smaller

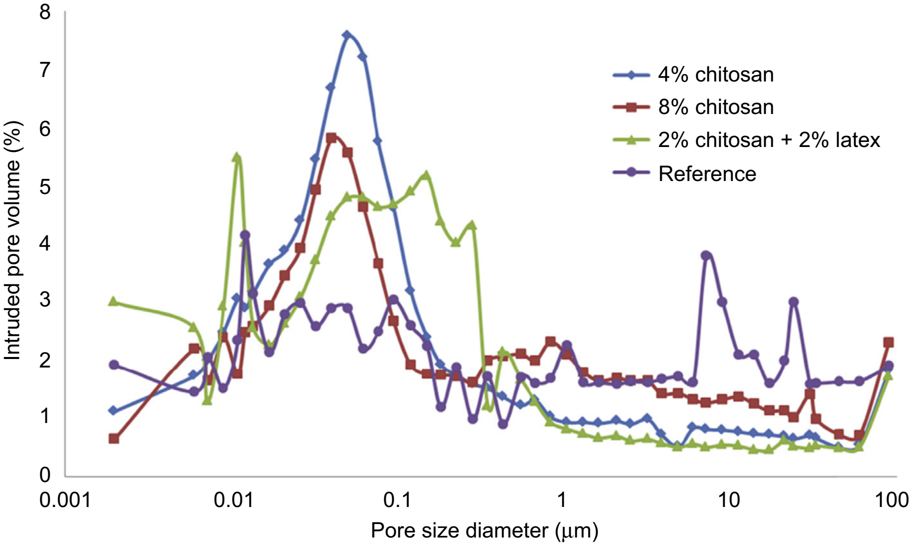

Figure 10.8 Intruded pore distribution for concrete—chitosan—latex system.

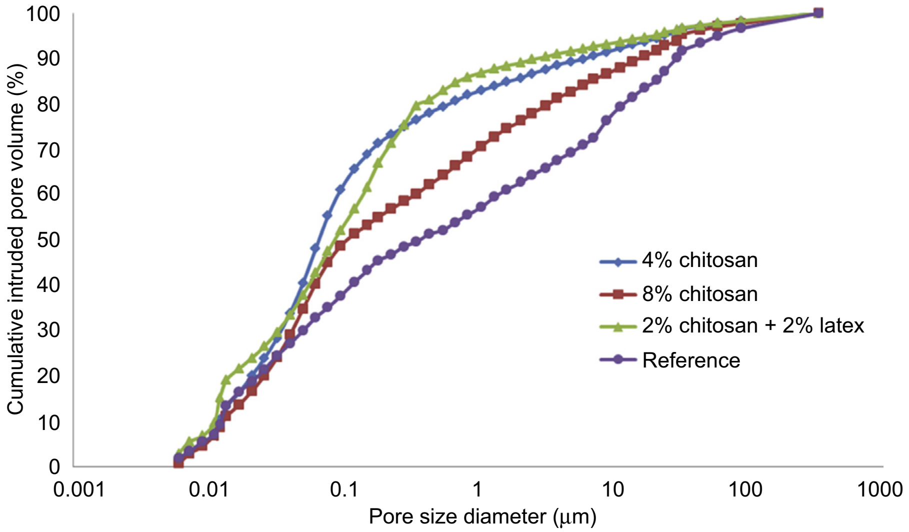

Figure 10.9 Cumulative intruded pore distribution for concrete—chitosan—latex system.

pores (0.01 μm < ϕ < 0.3 μm) for concrete with the biopolymers, in contrast to the reference concrete, which has larger pores and larger size (ϕ > 8 μm). Similarly, the cumulative distribution shows a predominance of larger diameter pores for reference, instead of concrete with 2% chitosan and 2% latex.

Figure 10.10 shows the effect of latex as a concrete permeability reducer, aiding chitosan in the formation of a biopolymeric network (see Figure 10.7). These

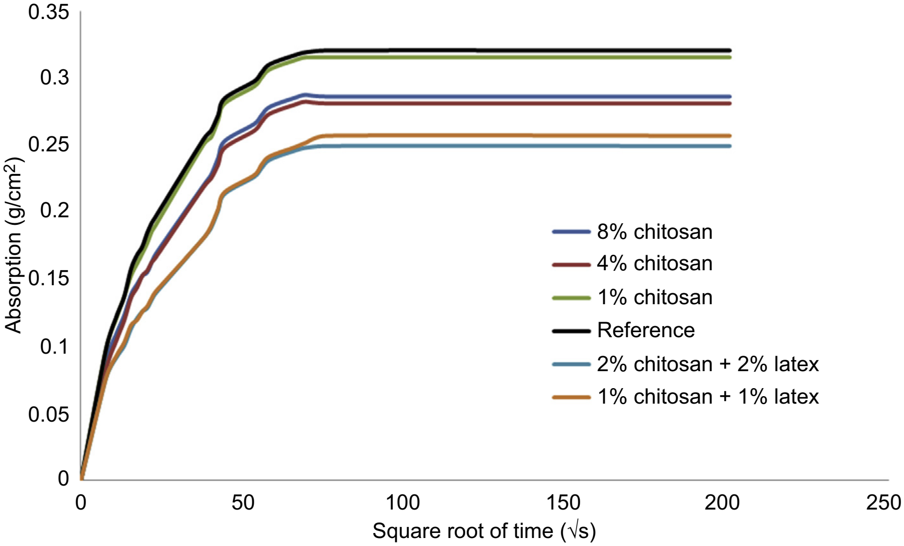

Figure 10.10 Evolution of capillary water absorption.

biopolymers act both to reduce the porosity (Figures 10.8 and 10.9) and the permeability (Figure 10.10).

Since the 1960s (ICPIC, 1991), polymers have been added to concrete mixtures. In the paper entitled "polymer-based admixtures," Ohama (1998) deeply discussed this issue and studied the effect caused by polymers in the microstructure of concrete. The polymers act involving Portland cement hydrates, offering them improved mechanical properties. This is not because added polymers directly contribute with these properties, as purely mechanical composite components, but they actually reduce permeability, diminish the quantity of large pores as well as refine them, hinder the propagation of cracks, etc. In other words, polymers can better organize the microstructure of concrete.

Likewise, biopolymers present similar performance, seeking for the best possible organization for microstructure of concrete.

Many biopolymers have been incorporated to concrete; some were carried by pure curiosity, such as the use of biopolymers for increasing concrete viscosity to avoid segregation in self-compacting concrete (Khayat, 1998; Panesar et al., 2014). Khayat indicates the use of natural glues (i.e., welan gum based on sugar backbones) to avoid separation of concrete constituent phases, which afford integrity to concrete. The same biopolymer was used by Zhao et al. (2012) with the intention of assessing the hydration retardation of the tricalcium aluminate (C3A)—calcium sulphate. These authors employed zeta potential analysis and confirmed that welan gum absorbs C3A, hindering its immediate reaction with water and allowing longer concrete workability (see Figure 10.11). Following the same line of thought, other authors, like Sonebi (2006), incorporated other polysaccharides to concrete, such as gelam gum, diutan gum, xanthan gum, gutta-percha, or guar gum, but results were not that promising

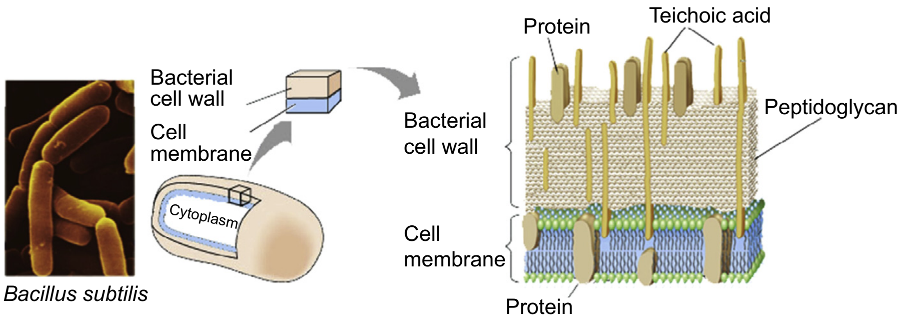

Figure 10.11 The cell wall of the Gram-positive bacterium *Bacillus subtilis*. The cell wall contains peptidoglycan as the major component.
Adapted from Pei et al. (2015).

as were the tests with welan gum. However, Kwasny et al. (2009), studying several kinds of welan and diutan gums like superplasticizers, achieved that diutan gum improved both fresh and hardened states of concretes. These authors concluded that the chemical compatibility of superplasticizers and Portland cement is fundamental for gain in properties.

On the other hand, Bian and Plank (2013) used the biopolymer *casein*, obtained from bovine, as a superplasticizer. They found that the increase in temperature (up to 110 °C), in its industrial production, reduced the performance of such material and, consequently, diminished the workability of the system. This fact is not strange, because biopolymers tend to maintain their properties at temperatures near room temperature than at temperatures for which these materials were bioconceived.

In a similar direction, Pei et al. (2015) employed peptidoglycan obtained from the bacterium *Bacillus subtilis*. The cell walls have very similar chemical structure (Figure 10.9) to biopolymers commonly used in concrete; these walls have to reach 50% peptidoglycan (Pei et al., 2015).

With the use of peptidoglycan, Pei et al. (2015) had increases in apparent viscosity of the several compositions employed (Figure 10.12).

However, although this is not desired viscosity when working with concrete, increasing the dosage of the superplasticizer (Figure 10.12) was able to rapidly reduce this value. Moreover, the presence of peptidoglycan reduces segregation and bleeding of the material.

Research studies from Álvarez et al. (2012) on chitosan derivatives verified the ionic character effect on workability parameters and setting time of concrete. The studied derivatives were the nonionic *hydroxypropyl-chitosan* and *hydroxyethyl-chitosan*, and ionic *carboxymethyl-chitosan* (Figure 10.13).

As can be seen in Figure 10.13, the result shows that nonionic materials did not significantly modify the workability or the setting time, unlike the chitosan, which considerably altered both properties, reaching a zero setting time for an added concentration of 0.5% in relation to cement mass.

Similar studies were performed by Martinelli et al. (2013) with synthetic polyurethane and the same outcomes were obtained. In other words, only the nonionic

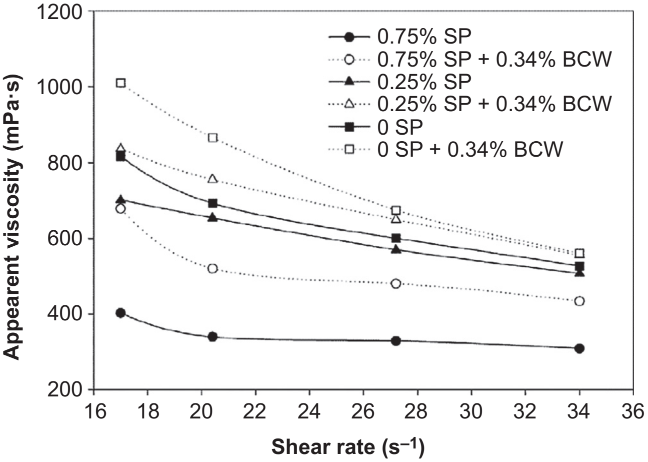

Figure 10.12 Effect of SPs of various dosages together with 0.34% Bacterial Cell Walls (BCW) amended in cement paste of water–cement ratio 0.4.
From Pei et al. (2015).

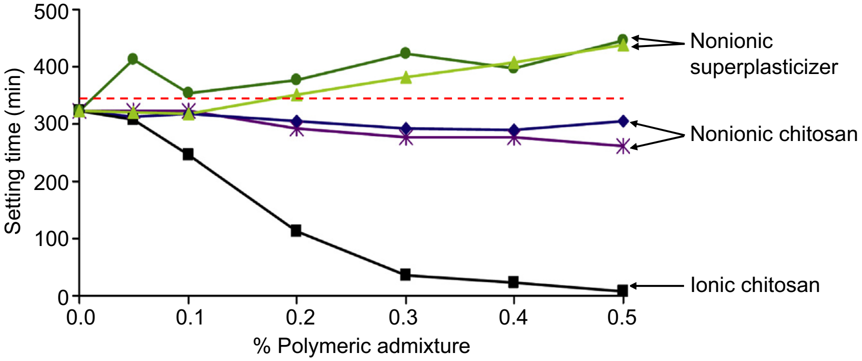

Figure 10.13 Workability evolution of different admixture vs. increasing amounts of admixtures (setting time).
Adapted from Álvarez et al. (2012).

polyurethane did not modify the rheological properties of the studied systems, as opposed to cationic and anionic polyurethanes, which significantly interfered with these properties.

Apparently, the presence of cationic charges presents a strong chemical interaction to the cement particles, leading to an early hydration (Álvarez et al., 2012).

The fact that a polymer is of natural origin does not modify the procedure of its preparation or alter the order of its mixture. Concretes have been prepared through different forms (and receiving distinct nomenclatures) in many countries. The construction industry has not yet achieved unification of procedures for concrete preparation, probably because it is not of main importance.

General rules of material mixtures are followed in the same manner, for example, biopolymer in liquid state must be mixed into kneading water; biopolymer in powder form must be mixed with Portland cement.

An interesting case that can occur is the employment of two liquid biopolymers (for example, polyurethane and vegetable-sourced latex). In this case, a previous simple test has to be done with reduced quantities of the material (it would be the same, if polymers were of synthetic origin):

1. To mix both biopolymers with each other e, afterward, with water;
2. To mix a biopolymer with water and with another biopolymer a posteriori; and
3. Vice-versa.

Then, if any sort previous agglutination of the mixtures occurs, opt for one that presents the lower viscous aspect.

Why does such a simple test need to be performed? In face of biopolymerization reaction, the strong polar character of water makes this substance to behave as a poison. In other words, water inhibits the biopolymerization process. Here, it is interesting that such process is retarded because, if it occurs early, biopolymers will not totally perform their function, which can be the involvement of Portland cement hydrates, hindering the hydration reaction. It is not the current practice; usually only one biopolymer (in liquid state) is added. If the previous test does not result in fluid aspect, it is recommended to request assistance from a specialized laboratory in concrete technology.

For biopolymers in powder form, chitosan, for example, neither bleeding nor segregation must occur, but the viscosity should increase. Thus, it is common to employ a superplasticizer for workability correction. However, if the biopolymer is in liquid state, this need no longer exists.

Further pumping operations, spreading, and cure of concrete follow the same traditional procedures for conventional concretes that are prepared with Portland cement.

The inclusion of biopolymers with superplasticizing properties do not always increase the compressive strength of a concrete. Other properties are also important, such as durability, low permeability, and high modulus of elasticity, but the compressive strength is always referenced to studies on concrete. Specifications for concrete construction rarely approach the need for concrete to last 100 years or permit the layer of chloride ions to penetrate 5 mm, at most, but the concrete must have a minimum compressive strength.

Bezerra (2006) employed chitosan in cement pastes obtaining excellent results: 30% increase in compressive strength, gain of impermeability, filling of porosity, reduction of filtrate losses, etc. (Figure 10.14).

However, when the same biopolymer was employed in concrete, results were not promising (Bezerra et al., 2011). Chitosan did not provide benefits in the presence of concrete system, which is more complex than the Portland cement paste (Figure 10.15).

Then, the authors decided to evaluate the concrete from the introduction of another biopolymer: a latex. Thus, results became relevant and increments in properties were achieved (Figure 10.16).

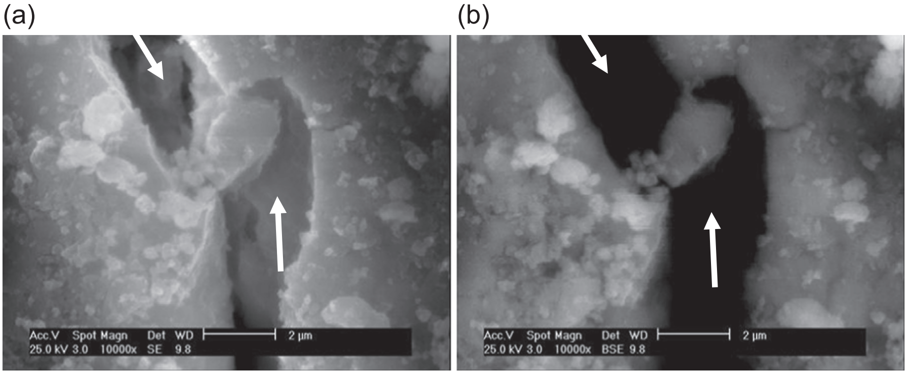

Figure 10.14 Chitosan in paste: (a) secondary electron, (b) backscattering electron. Source: Bezerra (2006).

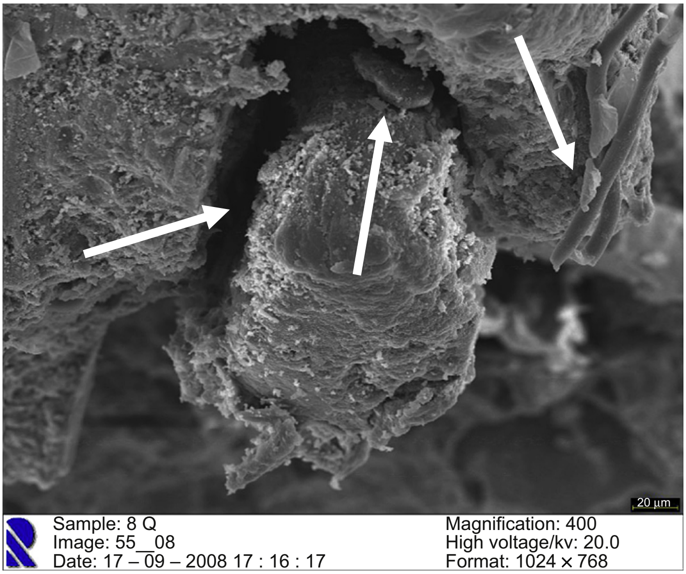

Figure 10.15 Chitosan in concrete: low adhesion, macrostructure, and microstructure with several pores.

Another study including a biopolymer based on castor oil was carried out by Bezerra et al. (2005). The biopolymer was obtained from castor oil hydrogenation, resulting in natural polyurethane. The goal of this study was to increase the tensile strength of the material, but it eventually increased the compressive strength. The same principle of involvement of Portland cement hydrates was repeated (Figure 10.17).

In Figure 10.17, the presence of connecting bridges between Portland cement hydrates can be clearly seen. The bridges, formed by polyurethane, confirm the gain in the obtained mechanical properties.

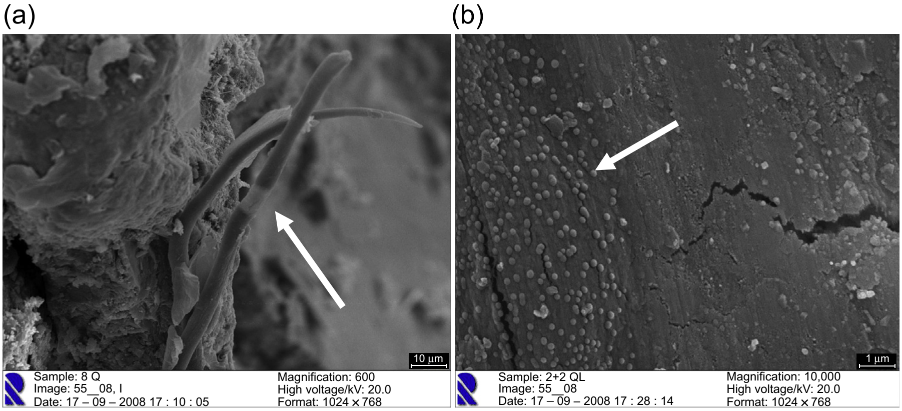

Figure 10.16 Concrete: presence of chitosan (a) and latex (b).
Source: Bezerra et al. (2011).

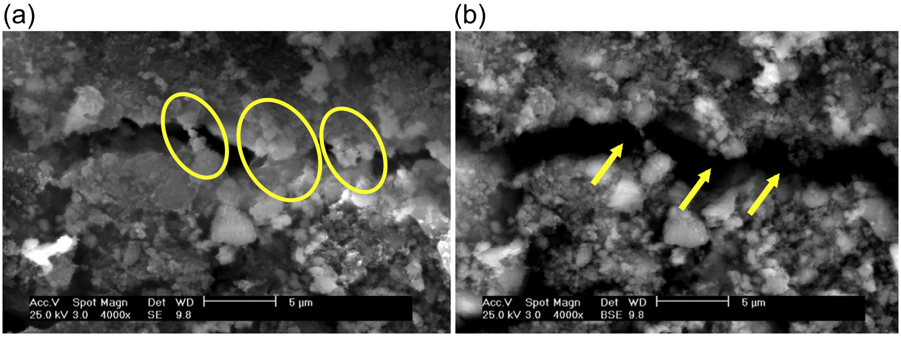

Figure 10.17 Presence of natural polyurethane: (a) secondary electron image (bond bridge), (b) back-scattered electron.
Source: Bezerra et al. (2005).

Regarding the tensile strength, it is possible to say that this property is a mechanical property related to the compressive strength of concrete, setting the ratio of 1/10 between them. For conventional concretes ($\sigma_c < 50$ MPa), it is quite reasonable to accept such a ratio, but for other types of concrete the ratio moves away from 1/10. The inclusion of pozzolanic materials, additions, and additives causes the compressive strength to rise significantly and the tensile–compressive ratio is reduced to 1/12. In other words, the gain in tensile strength does not occur in the same proportion as it occurs in compressive strength. On the other hand, the addition of polymers or biopolymers, either as superplasticizers or as fibers, increments tensile strength and, commonly, reduces compressive strength, which makes the ratio increase up to 1/7 (Mehta and Monteiro, 2006; Bezerra, 2006).

Regarding biopolymers, Bezerra (2006) presents correlations (exponential pattern a σ_c^b) that area similar to the ones shown in common literature, from a total of 1440 of concrete specimens with chitosan, as shown in Figure 10.18.

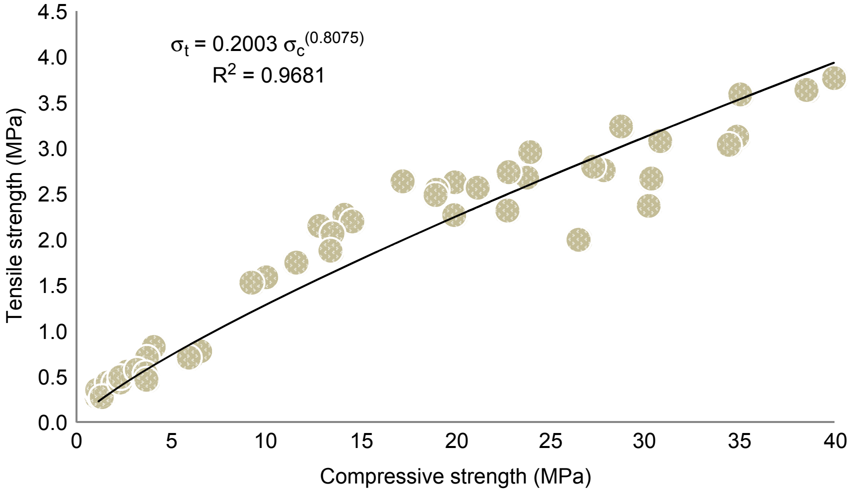

Figure 10.18 Correlation between tensile strength and compressive strength for chitosan system.

However, by adding concrete with biopolymer (natural latex), Bezerra et al. (2008) obtained results that demonstrated the gain in tensile strength of concrete rather than compressive strength at 7 and 28 days of curing (Figure 10.19 and 10.20).

From Figures 10.19 and 10.20, it can be noted that compressive strength, for both dates, suffered a more intense decrease than did the tensile strength. It means that if the goal is the gain in compressive strength, latex is not a reasonable alternative, once it only contributes to the increment in tensile strength. It is also worth noting that the ratio between strengths varied from 1/10 to 1/6, which are similar values to the ones found in other scientific research studies.

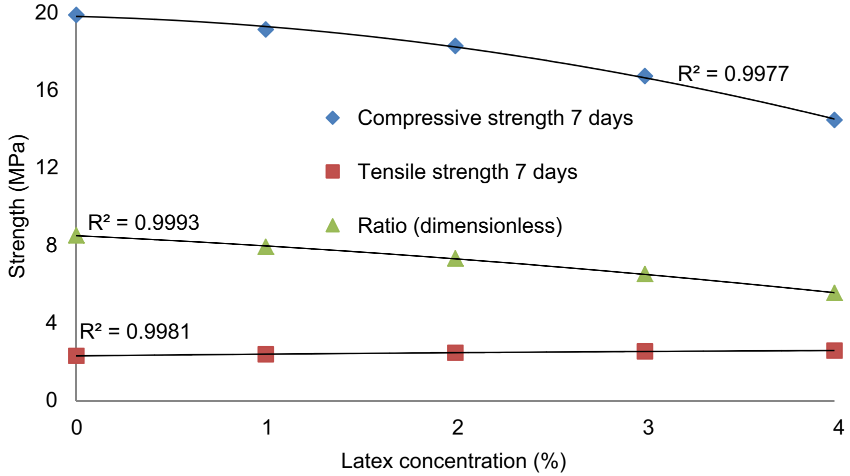

Figure 10.19 Mechanical properties of latex–concrete system for 7 days.
Adapted from Bezerra et al. (2008).

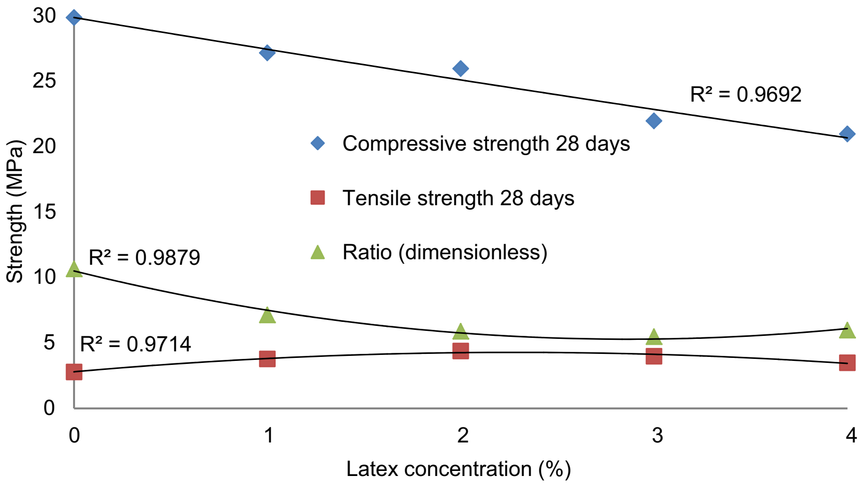

Figure 10.20 Mechanical properties of latex–concrete system for 28 days.
Adapted from Bezerra et al. (2008).

By studying the interaction between chitosan (biopolymer) and latex applied to concrete, Bezerra et al. (2011) concluded that additives do not reach the best outcomes when applied alone or without verification of their synergy. According to the authors, the combination of additives with each other, even with distinct effects, can produce concrete with relevant properties. Figure 10.21 presents the obtained effect in this study, in which can be identified as an optimum region for results around 1.2% of latex and 2.8% of chitosan.

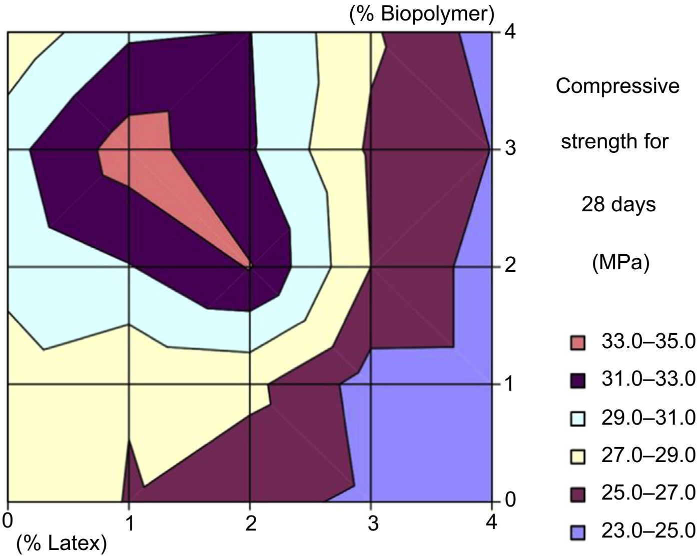

Figure 10.21 Latex–biopolymer (chitosan) system.
Source: Bezerra et al. (2011).

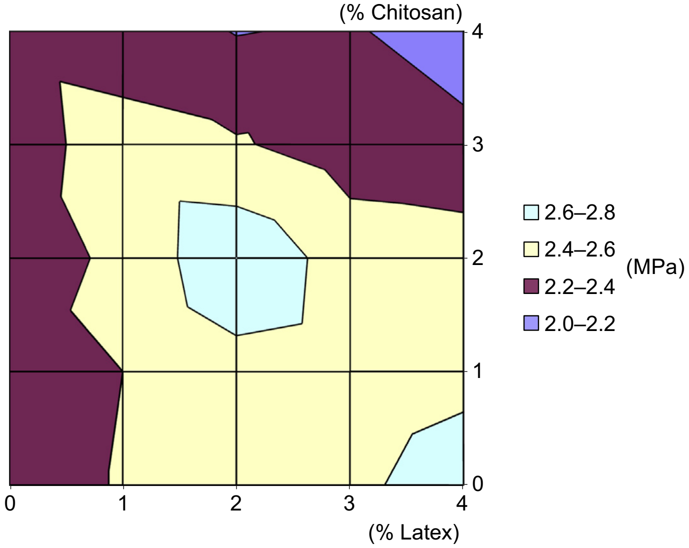

Figure 10.22 Tensile strength for concrete—latex—chitosan system.
Source: Bezerra et al. (2011).

The behavior described previously is common when it comes to latex in concrete, but a different result was obtained by Muhammad et al. (2012). These authors used six types of latex, and, for four latexes, the compressive strength was reduced about 12.4%; however, for the other two, the strength was increased by 2% and 4%. Although this increase is not significant, it demonstrates that the use of latex can increase tensile strength without loss of compressive strength. The authors attributed the results to high levels of volatile fatty acids and zinc. Thus, the final presence of organic materials in the concrete is reduced, which explains the maintenance and even increase in compressive strength obtained.

The presence of biopolymers, as well as polymers, modifies some mechanical properties of concrete, particularly in making the final product more elastoplastic, tough, and resilient. Concrete with higher toughness and, mainly, higher resilience, is required for situations in which structures are designed to support relevant thermal variations or dynamic loads followed by fatigue. The presence of biopolymers in latex form, for example, is capable of reducing up to 30% the modulus of elasticity. It means that deformation in concrete will be much higher before reaching a critical state of the concrete, either a conventional yield stress or a breaking stress (Martinelli et al., 2005).

For concretes with latex and chitosan, the tensile strength was higher than referential concretes (Figure 10.22) (Bezerra et al., 2011).

Moreover, the resilience and tenacity of the material increased by 56% and 77%, respectively, in relation to the referential concrete (Bezerra et al., 2011).

The presence of biopolymers under these conditions can significantly increment the performance of the material, even though no gain in compressive strength is presented.

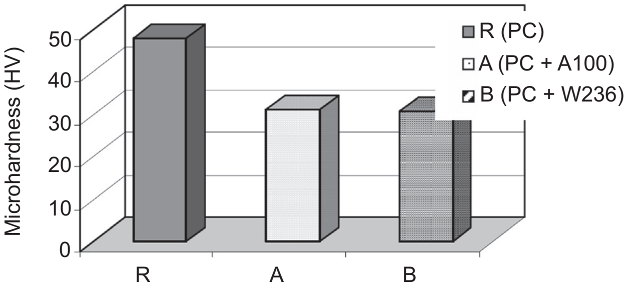

Figure 10.23 Microhardness: (R) reference; (A) polyurethane A100; (B) polyurethane W236, average of 30 different points.
Adapted from Martinelli et al. (2005).

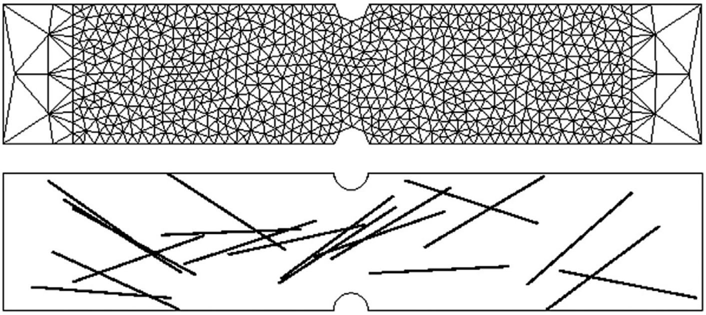

Figure 10.24 Discretization and stochastic disposal of some fibers.
Adapted from Radtke et al. (2008).

In the same way, the addition of polyurethane could reduce the microhardness of cement pastes at 35% in comparison with referential cement concrete (Figure 10.23).

In the year 2008, Universities of Delft—Netherlands and Gent—Belgium, with the support of RILEM, promoted a symposium regarding concrete modeling (Schlangen and Schutter, 2008). In this event, some papers studied concrete modeling in many situations and different perspectives, some of them on high-strength concretes with incorporation of synthetic superplasticizers. But no scientific paper considered biopolymers, a fact that demonstrates the lack of knowledge on this subject.

One prominent work that can make feasible the process of biopolymer modeling in concrete is the paper of Radtke et al. (2008). It presents a way for incorporating metallic fibers in concrete (Figure 10.24).

The authors can simulate a fiber as a pair of opposite forces actuating inside the structure in a certain direction. The distance between the point of application of a force to the point in which the other force acts is equivalent to the fiber length. These forces can be either of attraction or of repulsion. Then, many fibers (force pairs) are randomly distributed into the structure (nonasymmetric solid) of the material. The authors considered only 20 fibers. Another limiting aspect of the model refers to the fact that only one fiber, though, has forces localized at the fiber ends, which is unrealistic, because along fiber length shear forces emerge between the fiber surface and the cement hydrates. The principle adopted by this model can be employed in simulation of concretes with biopolymers. However, it must be considered that forces act along its length. Thus, biopolymeric networks would be represented more realistically, and it would be possible to note the effect provided to microstructure of concrete by these materials.

10.3 Use of biopolymers in concrete: case studies

Two applications for biopolymers in concrete were chosen. The first one refers to a biopolymer obtained from the *Araucária* tree; and the second one refers to a biopolymer obtained from rubber trees.

10.3.1 Concrete blocks with Araucária resin

Only in southern Brazil and in a small Argentinian region, a tree species grows known as Araucária (*Araucária angustifolia*, pinales order, pinopsida class). From this tree a thermoplastic biopolymer of complex chemical composition has been extracted, which resembles a modified pitch.

This biopolymer is already commercialized by an enterprise in many ways, and it does not have a patent, due to industrial secrecy. Its applications vary from simple mortars for bricklaying to superplasticizers for concretes, waterproofing materials, and thermal and acoustic protection, including significant resistance to direct exposure to fire.

The biopolymer obtained by Araucária can be applied as a waterproofing substance for concrete slabs or as a refractory material for concrete blocks (heat insulation up to 300 °C between faces of blocks), etc. The product is insoluble in water, but soluble in ethanol and aromatic hydrocarbons, has a softening point between 110 °C and 120 °C, bulk density of 1.06 to 1.09 g/cm^3, and an acid index of 200–300 mg KOH/g (www.carbonos.com.br).

The product was approved by the Toxic Substance Control Act of the United States (CAS: 65997-04-8 and US, EINECS: 266-040-8) and it is according ISO 11014 (2009) and NBR 14725 (2010).

Although this book does not aim to broadcast products from specific companies, two interesting video suggestions of application of this biopolymer, which can be accessed through internet connection:

1. For waterproofing: https://www.youtube.com/watch?v=rKWOsIzX5lwandfeature=youtu.be
2. For fire protection: https://www.youtube.com/watch?v=49YygTvb4ugandfeature=youtu.be

10.3.2 Shotcrete with latex of the rubber tree

From the rubber tree (*Hevea brasiliensis*), high-quality latex (60% purity, Panrat et al., 2012) is obtained for rubber production. Historically established, this industrial branch also produces latex for waterproofing use and as a superplasticizer of concretes (Hughes, 1992).

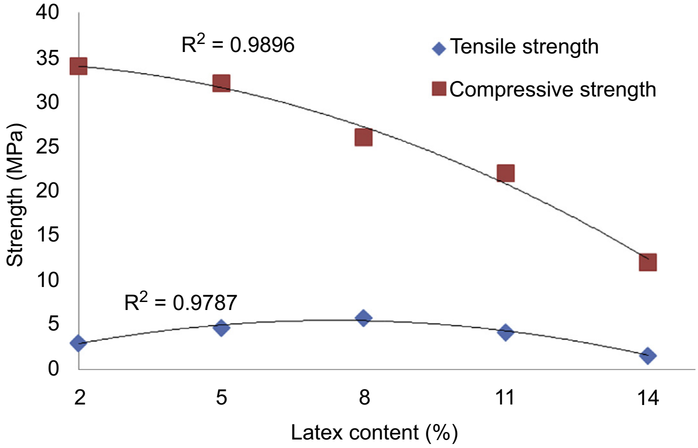

Figure 10.25 Concrete with latex of *Hevea brasiliensis*: compressive and tensile strength results.
Adapted from Oliveira et al. (2008).

This biopolymer, of diverse usage, has been traditionally employed in waterproofing of shotcretes on slopes that offer downside risk (Hughes, 1992).

The use of *Hevea brasiliensis* latex is not restricted to shotcretes, but to common concretes when it is necessary to increase tensile strength and decrease modulus of elasticity (Oliveira et al., 2008). The following Figure 10.25 shows the variation of the compressive strength and tensile strength of a concrete with latex from *Hevea brasiliensis* (Oliveira et al., 2008).

As will be seen, latex acts by reducing the compressive strength, and the tensile strength increases up to a point. In the case of compression, this is expected, because the increase in latex (low compressive strength material) implies the reduction of the cementitious phases (material with high compressive strength). However, in the case of a tensile phase such as latex, it can fill the pores and involve the cement hydrates, the tensile behavior receiving a significant contribution.

10.4 Final considerations

The chapter deals with biopolymers with superplasticizer properties for concrete. One conclusion is that there is a natural tendency to use biopolymers in groups and not only alone, because several properties of the concrete can be simultaneously optimized. Moreover, these materials should be used in greater quantities in the near future, because the sources of the traditional polymers will not last, unlike the sources of biopolymers that are virtually inexhaustible.

What is the availability of petroleum in the Earth? According to Berge (2009), oil will last for 41 more years. Therefore, humankind can keep employing superplasticizers from petroleum for four decades, or maybe for a slightly longer time due to new research studies. However, it is a short interval of time! What is the availability of biopolymers in the Earth? This answer is unknown because they are partially recycling materials. And why are these materials partially recycling? It is because the planet is not in its full form for assuring such renovation, and this full capacity depends on the species *Homo sapiens*, which is the only species, unfortunately, able to maintain (or not) a sustainable planet.

References

ACI Committee 238, 2008. Report on measurements of workability and rheology of fresh concrete (ACI 238.1R-08.). Farmington Hills, Michigan: ACI.

Álvarez, J.I., Lasheras-Zubiate, M., Navarro-Blasco, I., Fernández, J.M., 2012. Effect of the addition of chitosan ethers on the fresh state properties of cement mortars. Cement and Concrete Composites 34, 964−973.

Antonino, N.A., 2007. Otimização do processo de obtenção de quitina e quitosana de exoesqueletos de camarões oriundo da indústria pesqueira paraibana. Dissertação de Mestrado. UFPB/CCEN.

Berge, B., 2009. The Ecology of Building Materials, second ed. Architectural Press. Elsevier Science.

Bezerra, U.T., Martinelli, A.E., Melo, D.M.A., Henrique, D.M., Rodrigues, E.M., Lima, F.M., 2005. Composites of Portland cement and natural polymers. Materials Science Forum 498−499, 407−412.

Bezerra, U.T., 2006. Compósitos Portland-biopolímero para cimentação de poços de petróleo (Doctorate thesis). UFRN, Brazil.

Bezerra, U.T., Ferreira, R.M., Fonseca, C.S.M., 2008. Avaliação do desempenho de betões com incorporação de biopolímero e látex. BE2008-Encontro Nacional de Betão Estrutural. Guimarães. Portugal.

Bezerra, U.T., Ferreira, R.M., Castro-Gomes, J.P., 2011. The effect of latex and chitosan biopolymer on concrete properties and performance. Key Engineering Materials 466, 37−46.

Bian, H., Plank, J., 2013. Effect of heat treatment on the dispersion performance of casein superplasticizer used in dry-mix mortar. Cement and Concrete Research 51, 1−5.

Cechova, E., Papayianni, I., Stefanidou, M., 2010. Properties of lime-based restoration mortars modified by the addition of linseed oil. In: Valek, J., Groot, C., Hughes, J. (Eds.), Proceedings of the 2nd Conferende and of the Final Workshop of RILEM TC 203-RHM. RILEM Publications, Prague, Cezch Republic, pp. 937−944.

Chiandotti, R.S., 2005. Síntese e propriedades de derivados de quitosana: lauroil quitosana (Master dissertation). UFPR, Brazil.

Costa, C.R., Ratti, A., Curto, B., 2014. Product development using vegetable fibers. International Journal of Design and Nature and Ecodynamics 9 (3), 237−244.

Craveiro, A.A., Craveiro, A.C., Queiroz, D.C., 1999. Quitosana: a fibra do futuro. PADETEC, Fortaleza.

Dutta, P.K., Dutta, J., Tripathi, V.S., 2004. Chitin and chitosan: chemistry, properties, and applications. Journal of Scientific and Industrial Research 63, 20−31.

EN 206-1, 2000. Concrete − Part I: Specification, Performance, Production, and Conformity.

Hamelau, K., 1997. The History of Cement. Autumn Seminar. Krupp Polysius, Leipzig.

Hughes, K., 1992. Foundations and Masonry, second ed. Taunton Press, USA.

Innovation Center Iceland, 2009. ICI Rheocenter catalogue.

International Congress on Polymers in Concrete – ICPIC, September 24–27, 1991. North American Workshop. Prime Co-sponsor and Organizer American Concrete Institute, San Francisco, California, United States of America.

International Organization for Standardization, 2009. ISO 11014: Safety Data Sheet for Chemical Products – Content and Order of Sections. Geneva.

Khayat, K.H., 1998. Viscosity-enhancing admixtures for cement-based materials: an overview. Cement and Concrete Composites 20, 171–188.

Kwasny, J., Sonebi, M., Taylor, S.E., Bai, Y., Basheer, P.A.M., Owens, K., Cleland, D.J., 2009. The influence of different viscosity-modifying admixtures on the fresh properties of superplasticized cement-based grouts. In: Rheology of Cement Suspensions Such as Fresh Concrete. 3rd International RILEM Symposium. Proceedings PRO 58.

León-Martínez, F.M., Cano-Barrita, P.F.J., Lagunez-Rivera, L., Medina-Torres, L., 2014. Study of nopal mucilage and marine brown algae extract as viscosity-enhancing admixtures for cement based materials. Construction and Building Materials 53, 190–202.

Martinelli, A.E., Melo, D.M.A., Lima, F.M., Bezerra, U.T., Marinho, É.P., Henrique, D.M., 2005. Addition of polyurethane to Portland cement. Materials Science Forum 498–499, 401–406.

Martinelli, A.E., Nóbrega, A.C.V., Melo, D.M.A., Melo, M.A.F., Freitas, J.C.O., Oliveira, O.S., 2013. Effect of mud acid on Portland-aqueous polyurethane composites to oil well cementing. Materials Science Forum 730-732, 307–312.

Mechtcherine, V., Reinhardt, H.W., 2012. Application of Superabsorbent Polymers (SAP) in Concrete Construction: State of the Art Report Prepared by Technical Committee 225-SAP.

Mehta, P.K., Monteiro, P.J.M., 2006. Concrete: Microstructure, Properties, and Materials, third ed. McGraw-Hill Companies, New York.

Muhammad, B., Ismail, M., Bhutta, M.A.R., Abdul-Majid, Z., 2012. Influence of non-hydrocarbon substances on the compressive strength of natural rubber latex-modified concrete. Construction and Building Materials 27 (1), 241–246.

Muraplast, 2011. Superplastificantes de alto desempenho. MC-Bauchemie catalogue.

Nóbrega, A.K.C., 2009. Formulação de pastas cimentícias com adição de suspenção de quitosana para cimentação de poços de petróleo. Doctorate Thesis. UFRN, Brazil.

Nunes, S., Figueiras, H., Oliveira, P.M., Coutinho, J.S., Figueiras, J., 2006. A methodology to assess robustness of SCC mixtures. Cement and Concrete Research 36 (12), 2115–2122.

Ohama, Y., 1998. Polymer-based admixtures. Cement and Concrete Composites 20 (2–3), 189–212.

Oliveira, G.M., Bezerra, U.T., Barbosa, N.P., Alves, S.M.S., 2008. Resistencia a la tracción del hormigón utilizando látex. In: III Congreso Internacional “Ing. Jose Fermín Colina”. Argentina, pp. 577–583.

Oliveira, D.N.S., Bezerra, U.T., Beltrão, L.S.D., Chaves, A.C., Mendonça, A.M.G.D., Neves, G.A., 2015. Oil well cement developed from common cement: physical, chemical, and mineral characterization. Materials Science Forum 805, 558–563.

Panesar, P.S., Kaur, V., Bera, M.B., Kumar, H., Kennedy, J.F., 2014. Welan gum: microbial production, characterization, and applications. International Journal of Biological Macromolecules 65, 454–461.

Panrat, K., Boonme, P., Taweepreda, W., Pichayakorn, W., 2012. Formulations of natural rubber latex as film former for pharmaceutical coating. Procedia Chemistry 4, 322–327.

Pei, R., Liu, J., Wang, S., 2015. Use of bacterial cell walls as a viscosity-modifying admixture of concrete. Cement & Concrete Composites 55, 186–195.

Peng, Y., Jacobsen, S., 2013. Influence of water/cement ratio, admixtures, and filler on sedimentation and bleeding of cement paste. Cement and Concrete Research 54, 133–142.

Petit, J.-Y., Crépy, L., Wirquin, E., Martin, P., Joly, N., 2014. Synthesis and evaluation of starch-based polymers as potential dispersants in cement pastes and self leveling compounds. Cement and Concrete Composites 45, 29–38.

Radtke, F.K.F., Simone, A., Stroeven, M., Sluys, L.J., 2008. Multiscale framework to model fibre reinforced cementitious composite and study its microstructure. In: Schlangen, E., Schutter, G.D. (Eds.), Concrete Modelling: CONMOD'08. International Rilem Symposium. Proccedings PRO 58.

Rinaudo, M., 2006. Chitin and chitosan: properties and applications. Progress in Polymer Science 31, 603–632.

Sá, A.F.G., 2005. Rebocos em paredes de pedra e cal. Dissertação de Mestrado, Universidade Técnica de Lisboa, IST.

Santiago, C.C., 2001. Estudo dos materiais de construção de Vitrúvio até ao século XVIII: uma visão crítica interpretativa à luz da ciência contemporânea. Universidade de Évora (Portugal). Doctorate Thesis.

Santiago, C.C., 2007. Argamassas tradicionais de cal. EDUFBA, Salvador.

Schlangen, E., Schutter, G.D., 2008. In: Concrete Modelling: CONMOD'08. International Rilem Symposium. Proccedings PRO 58.

Sobrinho Jr., A., Torres, S.M., Barbosa, N.P., Ortiz, S.R., Ghavami, K., 2012. Impregnation of *Bambusa vulgaris* with polymeric resins. Key Engineering Materials 517, 27–33.

Sonebi, M., 2006. Rheological properties of grouts with viscosity modifying agents as diutan gum and welan gum incorporating pulverised fly ash. Cement and Concrete Research 36, 1609–1618.

Torgal, F.P., Jalali, S., 2010. A sustentabilidade dos materiais de construção, second ed. TecMinho, Guimarães,.

Van Der Vurst, F., De Schutter, G., 2014. Improving the robustness of fresh self-compacting concrete using small quantities of fine additions. In: 3rd International Symposium on Design, Performance and Use of Self-consolidating Concrete, pp. 195–204.

Vertematti, J.C., 2004. Manual brasileiro de geossintéticos, first ed. Edgard Blücher, São Paulo www.carbonos.com.br.

Xiangming, K., Zhihua, S., Zichen, L., 2014. Synthesis of novel polymer nano-particles and their interaction with cement. Construction and Building Materials 68, 434–443.

Zhao, Q., Ma, L., Yao, C., Zhou, M., 2012. Impact of welam gum on tricalcium aluminate-gypsum hydration. Materials Characterization 64, 88–95.

Biopolymers with viscosity-enhancing properties for concrete

11

P.F. de J. Cano-Barrita, F.M. León-Martínez
Instituto Politécnico Nacional/CIIDIR Unidad Oaxaca, Oaxaca, México

11.1 Introduction

The annual global production of Portland cement reached 2.8×10^9 tonnes in 2011, and is expected to increase to 4×10^9 tonnes per year by 2050 owing to the major growth forecast in China and India as well as in the Middle East and Northern Africa (Schneider et al., 2011). On the other hand, the use of chemical admixtures has increased the quality and the range of applications of hydraulic concrete. In some countries, 70% to 80% of all concrete produced contains one or more admixtures (Mehta and Monteiro, 2006).

Modern concrete technology produces specialized types of concrete, including lightweight, high-strength, high-performance, self-consolidating, underwater, shotcrete, and pumped concrete. Some of these types of concrete may require the use of special chemical admixtures such as viscosity-enhancing admixtures (VEAs) to obtain the desired fresh-state properties. The most commonly used VEAs are based primarily on high-molecular-weight polymers that are soluble in water and can support the alkaline environment of the cement paste. Other VEAs are based on mineral admixtures such as microsilica. Polymers used as VEAs can be synthetically obtained (e.g., poly acrylates, polyethylene oxides, and polyvinyl alcohol) or by a biotechnological process (e.g., microbial exopolysaccharides), extracted directly from natural sources (e.g., plant and microbial gums, mucilages, cell wall polysaccharides) or chemically modified from natural sources (e.g., ethers and esters from cellulose and starch).

The main function of VEAs in concrete is to make the mixture stable and cohesive during flow and under static forces, by modifying the rheological properties of the cement paste. This chapter will provide an overview of the basic concepts of rheology and the properties of the biopolymers commonly used as VEAs to produce stable and homogeneous cement-based materials, as well as those from renewable sources with potential for future use.

Biopolymers and Biotech Admixtures for Eco-Efficient Construction Materials. http://dx.doi.org/10.1016/B978-0-08-100214-8.00011-7
Copyright © 2016 Elsevier Ltd. All rights reserved.

11.2 Basic concepts of rheology and viscosity-enhancing admixtures

11.2.1 Rheology

Rheology is "the science of the deformation and flow of matter" (Hackley and Ferraris, 2001). In concrete technology, the rheological behavior of concrete is important because concrete must flow during placing and compacting operations, without causing any segregation. Self-consolidating concrete (SCC) is a special type of concrete that does not require mechanical vibration to consolidate, thus making rheology even more important because of its high fluidity and high resistance to segregation required to flow and fill in the forms under the action of gravity (Okamura, 1997).

It is generally accepted that concrete behaves as a viscoplastic fluid described by the Bingham equation (Eqn (11.1)). In Figure 11.1 the plot of shear rate $\dot{\gamma}$ versus shear stress σ shows that the intercept of the stress–strain rate curve with the y-axis is the yield stress σ_B. The slope of this curve is the plastic viscosity η_{pl}, defined as the "excess of the shear stress over the yield stress divided by the shear rate, and equal to the differential viscosity" (Hackley and Ferraris, 2001).

$$\sigma = \sigma_B + \eta_{pl}\dot{\gamma} \tag{11.1}$$

The Bingham yield stress σ_B is a critical shear stress value below which an ideal plastic or viscoplastic material behaves like a solid (i.e., will not flow). When the fluid behaves as a purely viscous material, the resistance to flow is called dynamic viscosity η and represents the internal molecular friction.

Other researchers have suggested that the Herschel–Bulkley equation (Eqn (11.2)) better represents fresh concrete flow (de Larrard et al., 1998), avoiding the problem of negative yield stress obtained when the Bingham model is used to fit the experimental

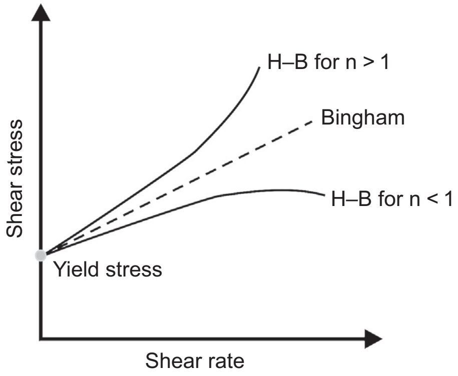

Figure 11.1 Stress–strain rate diagrams for the Bingham and Herschel–Bulkley types of concrete.
Wallevik and Wallevik (2011).

data. However, as seen from Eqn (11.2), it has three parameters that make the model impractical from the perspective of specifying the rheological properties of concrete and then controlling them in the field. In this equation, there is a power-law relationship between the shear stress and shear rate above the yield stress σ_y. When $n = 1$, Eqn (11.2) reduces to Eqn (11.1).

$$\sigma = \sigma_y + k\dot{\gamma}^n \tag{11.2}$$

In addition to the yield stress and plastic viscosity, there is another important rheological property called thixotropy that makes concrete exhibit different rheological behavior between resting and flowing states. Thixotropy refers to "a reversible time-dependent decrease in viscosity at a particular shear rate" (Hackley and Ferraris, 2001). This phenomenon occurs due to the structural buildup when concrete is at rest, and structural breakdown when concrete is sheared. This property has an influence on both the pressure concrete exerts on the formwork, and its segregation resistance. In fact, in SCC, the pressure exerted on the formwork is inversely proportional to the breakdown area of concrete, and it never reaches the full hydrostatic pressure (Assaad and Khayat, 2006).

To determine the workability of concrete, the slump test has traditionally been used in both the laboratory and the field owing to its simplicity. However, the slump is only a one-parameter test that is usually correlated to the yield stress of concrete (Roussel, 2006), which is only one of the parameters characterizing a Bingham or a Herschel–Bulkley type of fluid. Other tests such as the modified slump test (Ferraris and de Larrard, 1998) allows, in addition to estimating the yield stress, obtaining the plastic viscosity of concrete.

Devices that are more sophisticated are now used to characterize the rheology of concrete with a more scientific approach. Coaxial cylinders (Couette geometry) and parallel plate types of rheometers have been developed to measure the yield stress and the plastic viscosity of concrete mixtures. Parallel-plate rheometers, such as the BTRHEOM, and coaxial cylinder rheometers such as the BML and the CEMAGREF-IMG are some of the devices that provide information to calculate the rheological characteristics of concrete in fundamental units (Banfill et al., 2001; de Larrard et al., 1996). Other rheometers such as the IBB and the ICAR do not allow for direct calculation of rheological parameters in fundamental units (Banfill et al., 2001), which makes it difficult to compare results obtained with different rheometers. The Danish Technological Institute developed an apparatus called the 4-C rheometer. In fact, it is not a mechanical rheometer like those previously described. Instead, it is a robotic system that automatically performs the slump flow test. The flow curve is then fitted to a database of simulated-flow curves using the spread versus time information, using digital image analysis (Thrane et al., 2010).

Rheometers such as those described provide information that is used to characterize the effects of different mineral and chemical admixtures on the plastic behavior of concrete. Figure 11.2 shows the effect of distinct additions to the rheology of a reference concrete. The easiest and most economical solution would appear to be just adding water to the mixture, which reduces both the plastic viscosity and the yield stress,

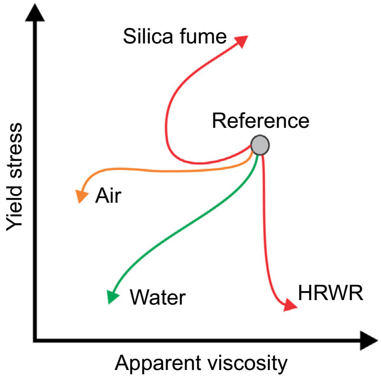

Figure 11.2 Effect of adding different constituents to a reference mixture.
Adapted from Wallevik and Wallevik (2011).

whereas if a high-range water reducer (HRWR) is used, the yield stress is significantly reduced while having only a minimum effect on the viscosity. Of course, just adding water would cause segregation in the mixture because of inadequate viscosity of the cement paste. In addition to those effects, the inclusion of air decreases the apparent viscosity and maintains an almost unchanged yield stress. Specific concentrations of silica fume may even reduce the plastic viscosity, contrary to the usual behavior observed in high-performance concrete containing silica fume that produces a highly viscous and cohesive concrete. If concrete requires a higher viscosity as in the case of SCC, one solution is to increase the amount of fine powders. Another approach is to use VEAs without the need for changing the mixture proportions, and one more alternative is to use a combination of the two previous approaches.

11.2.2 Viscosity-enhancing admixtures

An admixture is defined as "a material other than water, aggregates, cementitious materials, and fiber reinforcement, used as an ingredient of a cementitious mixture to modify its freshly mixed, setting, or hardened properties and that is added to the batch before or during its mixing" (ACI Committee 212, 2010). Among several types of admixtures available for the concrete industry, VEAs are used to enhance the rheology of cement-based materials, mainly their viscosity and cohesion.

Most VEAs are water-soluble polymers of high-molecular-weight polysaccharides possessing high affinity for water that increase the viscosity and cohesion of fresh cement-based materials. This enhancement is essential to avoid segregation of the constituent materials, thus improving the homogeneity of concrete, mortar, or grouts. The main challenge for a VEA is thus to increase the stability of cement-based materials during transport, placement, and consolidation without having adverse effects on their mechanical and durability properties at early and later ages. Of course, VEAs must be compatible with HRWR admixtures often needed to counteract the increase in yield stress caused by the addition of VEAs.

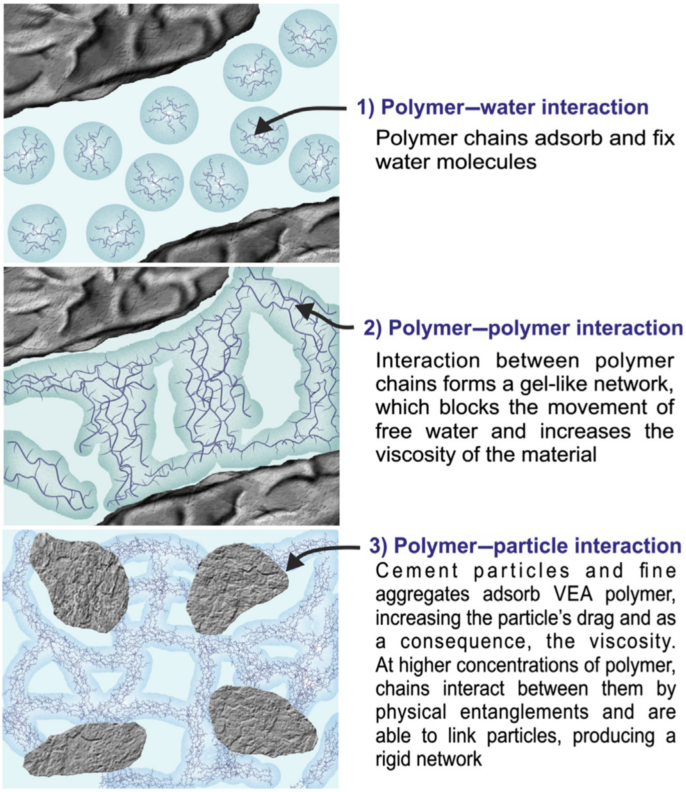

Figure 11.3 Schematic representation of the modes of action of polymer-based VEAs in cement systems.

There are three modes of action of VEAs (Figure 11.3) depending on the type and concentration of the polymer (Khayat and Mikanovic, 2012):

1. **Polymer–Water interaction**. The chains of the polymer molecules adsorb and fix free-water molecules into the periphery by electrostatic forces, mainly hydrogen bonds, resulting in swelling of the polymer chains. This enhances the viscosity of the mixing water, which in turn increases the viscosity of the cement paste. This mechanism of action is dependent upon the molecular weight, number of dipoles in the molecule, and concentration of the polymer in the solution.
2. **Polymer–Polymer interaction**. When adjacent polymer chains are closer to each other, attractive forces between them develop. This results in a weak gel-like network, which blocks the motion of free water and increases the viscosity of the whole system. At higher concentration levels of the polymer, entanglements result in an increased yield stress and viscosity of the system.
3. **Polymer–Particle interaction**. Adsorption of polymer onto the particle surface leads to an increase in the particle size, resulting in an increase in the drag. At higher concentration levels of the polymer, particle–particle bridging produces a relatively rigid network.

VEAs can work by a combination of these modes of action at the same time, depending mainly on the biopolymer type and concentration. In addition, these biopolymers may alter or change their molecular conformation because of the highly alkaline conditions in the cement paste or by chemical reaction with hydration products or the ionic species present in the pore solution. The molecular conformation of the polymer is influenced by changes in ionic strength, solvent type, pH, and temperature. Important changes in the viscosity of solutions prepared with chitosan, xanthan, carrageenan, and welan gums are observed when NaCl is added; this effect is attributed to conformational changes of the polymer chains in the solution (Wyatt et al., 2011).

VEAs based on polysaccharides exhibit shear-thinning behavior, which means that the viscosity decreases in response to increasing shear rate. This is attributed to their long-chain structures. As shear rates increase, the intertwined chains break down and align along the flow direction, and an overall shape rearrangement can be induced over the polymer chains by shearing, decreasing the viscosity. VEAs with anionic charges such as welan and diutan gum also bind the positively charged cement particles, enhancing their attractions and thereby increasing the viscosity of the material. Welan gum and diutan gum exhibit a more pronounced shear-thinning behavior than cellulose ethers and effectively prevent sagging and bleeding at low concentrations (Margheritis et al., 2009).

Figure 11.4 shows a qualitative representation of how the rheology of cement-based materials is influenced by the use of the most common VEAs that will be described later in this chapter. In Figure 11.4(a) and (b), a significant difference occurs in slump flow and thixotropy in concrete containing either welan or diutan gum compared to the behavior observed when concrete contains either cellulose or starch derivatives. The latter two have a less pronounced effect when the concentration is increased. Increasing thixotropy of concrete reduces the formwork pressure (Assaad and Khayat, 2006). Figure 11.4(c) and (d) shows that increasing the concentration of VEAs increases the plastic viscosity and, as a result, the segregation coefficient decreases. Some VEAs, especially cellulose and starch derivatives, increase the yield stress of concrete, in addition to increasing the viscosity of the cement paste.

As observed, the main purpose of using VEAs is to modify the rheology of cement-based materials in a fresh state. However, in a hardened state, VEAs may enhance the durability properties of concrete. For instance, VEAs increase the viscosity of the pore solution and may decrease the chloride diffusion rates (Bentz et al., 2009). The combination of the type of HRWR and VEA is an important consideration because they affect workability, compressive strength, and air content in high-performance SCC (Łaźniewska-Piekarczyk, 2013). These effects do not show a unique trend and are entirely dependent on the combination of admixtures, even if they have similar chemical compositions.

In addition to measurements undertaken using rheometers or viscometers, several empirical tests have been used to characterize the performance of VEAs in cement-based materials; these include mini slump, Marsh cone flow time, bleeding, segregation resistance, water-retaining capacity, and washout resistance tests (ACI Committee 238, 2008).

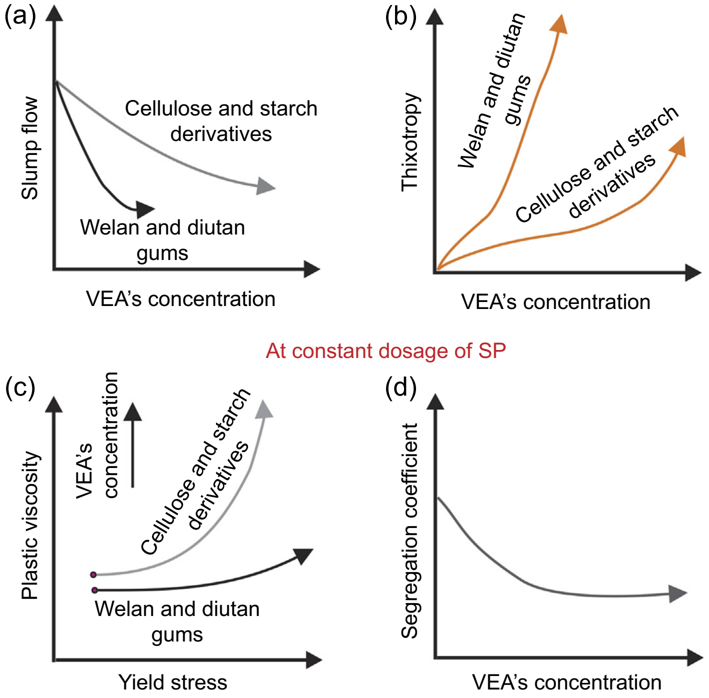

Figure 11.4 Effect of adding VEAs based on microbial exopolysaccharides (diutan and welan gums), cellulose derivatives, and starch to a reference concrete mixture. (a) Slump flow, (b) Thixotropic behaviour, (c) Plastic viscosity, and (d) Segregation coefficient. Graphs obtained and adapted from Khayat and Mikanovic (2012).

11.2.3 Applications of VEAs

VEAs may be used for a wide range of applications in concrete technology, including self-consolidating, pumped, underwater, sprayed, and lightweight concrete, as well as grouts.

11.2.3.1 Self-consolidating concrete

Self-consolidating concrete (SCC) was developed by Okamura (Okamura, 1997) and is essentially a highly fluid concrete that does not segregate when flowing through the reinforcing steel and can be compacted without any vibration (Okamura and Ouchi, 2003). The modern design of SCC always considers the use of HRWR to decrease the yield stress, whereas the viscosity of the paste is increased by using a high amount of fine powder (Okamura and Ouchi, 2003), a VEA, or a combination of both. Therefore, VEAs are incorporated into SCC to improve its resistance to bleeding, segregation, and surface settlement (Khayat, 1998). In any case, the volume of coarse aggregate is usually less than 50% of the total solids volume to reduce the aggregate interlock (Okamura and Ouchi, 2003). The robustness of SCC to variations in moisture content of the sand is increased when using microbial anionic polysaccharides compared to cellulose-based VEAs (Naji et al., 2011).

SCC may be modeled by the Bingham model, although some researchers consider that SCC is better represented by the Herschel–Buckley model, which avoids the negative yield stress obtained when the Bingham model is used (de Larrard et al., 1998). This type of concrete requires a reduced yield stress and an adequate viscosity of the cement paste to make it resistant to static and dynamic segregation. An increased thixotropy is also required to reduce the pressure exerted on the forms, especially before the initial setting time. Several empirical tests, some of them already standardized, are employed to characterize this type of concrete, including the slump flow, V-funnel, J-ring, L-box, U-box, and others available (ACI Committee 238, 2008).

11.2.3.2 *Pumped concrete*

Pumped concrete is used for the construction of high-rise buildings or structures in which the transport of fresh concrete by other means is difficult or costly. The main advantages of pumping concrete are the speed of casting, casting in places with difficult access, and constant rate of concrete supply. The concrete is pumped through a pipe using a pump that applies pressure to the concrete such that it flows along the pipeline. During the flow of conventional concrete, a lubrication layer of a few millimeters (about 2 mm) is formed at the interface between the concrete and the pipe (Choi et al., 2013), which is composed mainly of mortar because the coarse aggregates migrate toward the center of the pipe. Therefore, the rheological properties of this layer are more important to the flow during pumping than the properties of the bulk concrete (Choi et al., 2013). However, when pumping highly fluid concrete such as SCC, the pumping pressure required is dictated by the concrete viscosity (Feys, 2012). In this type of concrete, VEAs are considered to be pumping aids to reduce segregation and bleeding that cause aggregate blockage in the pipe, usually at a bend. Additionally, high pumping pressures may produce separation of the lubrication layer from the mix and cause blockage of aggregates. Therefore, these admixtures decrease the pumping pressure owing to the better lubricating properties and reduced segregation of concrete.

11.2.3.3 *Underwater concrete*

VEAs developed for underwater concrete placement or repairs are better known as antiwashout admixtures. Underwater concrete is normally placed by pumping or by tremie in still or flowing water, and it is required to resist the loss of cement paste, which can be reduced as much as 50% if an antiwashout admixture is used in the mixture (ACI Committee 212, 2010).

11.2.3.4 *Other uses*

Other uses of viscosity-enhancing admixtures include sprayed concrete, in which rebound and sagging must be minimized by increasing the cohesion of the concrete. Lightweight concrete also benefits from the use of VEAs that reduce both the flotation of low-density aggregates and the absorption of water when pumping concrete containing unsaturated lightweight aggregate. They may be used to minimize bleeding in cement grouts for post-tensioning ducts.

11.3 Biopolymers currently used as viscosity-enhancing admixtures

11.3.1 Introduction

Polysaccharides are the most common biopolymers used as VEAs. They can be extracted directly from biological sources (e.g., steams, leaves, fruits, seeds of plants, or cell walls of microorganisms) or generated as a by-product during the metabolic processes of microorganisms (e.g., welan gum is obtained from aerobic fermentation of *Sphingomonas* sp.). Some of them are obtained from these sources by chemical modification (e.g., cellulose and starch derivatives). Biopolysaccharides used nowadays as VEAs for cement-based materials include cellulose ether derivatives, welan gum, and diutan gum, although some research has involved the use of guar gum, xanthan gum, and starch ether (Plank, 2004). The robustness of SCC to variations in moisture content in the sand is better when using microbial anionic polysaccharides than when using cellulose-based VEAs (Naji et al., 2011).

Regarding their chemical structure, polysaccharides can be homopolysaccharides, which are constituted by a single monosaccharide, or heteropolysaccharides, which consist of more than one monosaccharide. In addition, polysaccharides can be linear or branched polymers, because glycosidic linkages can be made to any of the hydroxyl groups of a monosaccharide. Hydrogen bonds are formed between polymer chains owing to the presence of hydroxyl groups in the monosaccharide structure. Differences in the monosaccharide composition, linkage types and patterns, chain shapes, and molecular weight, dictate their physical properties, including solubility, flow behavior, gelling potential, and/or surface and interfacial properties (Gomes et al., 2012; Rudin and Choi, 2013).

The main disadvantage of currently used VEAs is their high cost of production that restricts the widespread use of special types of concretes such as SCC. Therefore, as will be noted later, obtaining and characterizing new VEAs based on biopolymers is an open area for research and development. In addition, VEAs should increase the viscosity and cohesion of the cement-based materials without affecting the mechanical and durability properties at early and later ages.

11.3.2 Cellulose derivatives

Cellulose (Figure 11.5) is the basic structural material of the cell walls of plants and some seaweed (Mark, 1999). It is a macromolecule with a nonbranched chain of variable length of 1→4 linked β-D-anhydroglucopyranose units (Wüstenberg, 2014). Cellulose consists of amorphous and mostly crystalline domains of parallel-oriented polymer molecules, which are insoluble in water. Intermolecular H—H bridging bonds

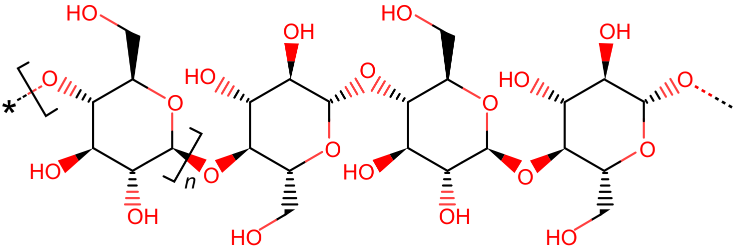

Figure 11.5 A cellulose unit, aggregate of linear polymers of D-glucopyranose residues in chain shape, which are linked in the β-(1→4) configuration.

at the hydroxyl groups of the anhydroglucose units bond them to each other. These bonds also exist within one molecule as intramolecular H—H bridging bonds.

The chain length of the polymer molecule depends on the source raw material (Müller, 2006). Natural sources of cellulose are wood, bamboo, cotton, hemp, straw, jute, flax, reed, and sisal. Cellulose is separated from plant cell walls and is never in a pure form in nature. It is always associated with lignin and hemicellulose and is separated from them by pulping. Naturally occurring cellulose has a degree of polymerization (DP) over 1×10^4, which corresponds to a molecular weight of about 2×10^6 g mol^{-1}. Depending on the method of isolation and source, cellulose has a DP range of 1×10^3 to 1.5×10^4 (Wüstenberg, 2014).

Common forms of cellulose in VEAs are the ether derivatives, which are obtained by chemical modification of natural forms of cellulose. Alkylation is determined by the hydroxyl groups of the C6, C2, and C3 in the anhydroglucose monomer of cellulose (Wüstenberg, 2014). The annual consumption of cellulose ethers for dry-mix mortars is 1×10^5 tonnes (Plank, 2004). They are used as thickeners, binders, film formers, and water-retention agents in construction materials. They increase the viscosity of the fluid phase to provide higher consistency to the cement paste, which is dependent on molecular weight and dosage. For a specific dosage, higher DP produces higher viscosity in the cement paste (Müller, 2006). The viscosity of methyl-cellulose and hydroxyl-ethyl-cellulose solutions are lower under alkaline conditions compared to solutions in deionized water (Sakata et al., 1996).

Cellulose ethers are characterized by three parameters (Patural et al., 2011): (1) the average molecular mass; (2) the number of substituted hydroxyl groups per anhydroglucose unit, expressed as degree of substitution (DS); and (3) the molar ratio of alkoxy groups in the side chains to cellulose, expressed as the average molar substitution (MS). The most important properties of the cellulose ethers are their solubility combined with chemical stability and nontoxicity. Water solubility and/or organosolubility can be controlled within wide limits via the constitution and the combination of ether groups at the cellulose chain, as well as via the DS, and to some extent via the pattern of substitution (Klemm et al., 1998). For methylation, typical DS ranges from 1.4 to 2.0 and for propoxylation from 0.1 to 0.7. Aqueous dissolutions at 2% show a Brookfield viscosity over 1.5 to 6.0×10^4 mPa s^{-1} (Plank, 2004). Cellulose-based VEAs when added at 0.02% to 0.05% of water show compatibility with polynaphthalene sulfonate and polycarboxylate ether-based HRWR (Naji et al., 2011).

11.3.2.1 Hydroxy-ethyl-cellulose

Hydroxy-ethyl-cellulose (HEC) is the most common cellulosic agent used as a VEA in cement-based materials. It is a white, free-flowing granular powder prepared from the alkali cellulose and ethylene oxide (or ethylene chlorohydrin) by etherification, and belongs to nonionic soluble cellulose ethers. Various molecular weights of this polymer are used, depending upon the density of the cement slurry. Its molecular structure is given in Figure 11.6. Although no sodium hydroxide is directly consumed during the preparation of HEC from ethylene oxide, sodium hydroxide is necessary to swell the cellulose and to catalyze the reaction. Ethylene chlorohydrin is also suitable to catalyze the reaction (Ott et al., 1954).

HEC is soluble in cold and hot water at an MS above 1.0, and also becomes soluble at higher MS in mixtures of water with some polar organic liquids such as lower alcohols. Its biodegradability decreases with increasing DS, whereas the length of the side chains is of marginal relevance to enzymatic attack (Klemm et al., 1998). Its apparent viscosity of aqueous solutions depends on the DP, the polymer concentration, and the shear rate. In solution, it is compatible with starch and starch derivatives, gelatin, natural gums, and sodium carboxymethyl cellulose, but it is only partly compatible with methyl cellulose and polyvinyl alcohol (Ott et al., 1954).

The active sites are the ethylene oxide links and carboxyl groups (Nelson et al., 1990). For constant molecular weight of HEC, its water retention in cement-based mortars improves when the MS decreases (Patural et al., 2011). Moreover, when the molecular weight increases the water retention increases, with a plateau at approximately 6×10^5 g mol^{-1} in which the retention capacity is constant (~98%). The working mechanism of HEC as a cement fluid-loss additive relies on a dual effect (Bülichen and Plank, 2012). At HEC concentrations <15 g L^{-1} (0.66% cement weight basis), the fluid-loss control is mainly achieved through the water-binding

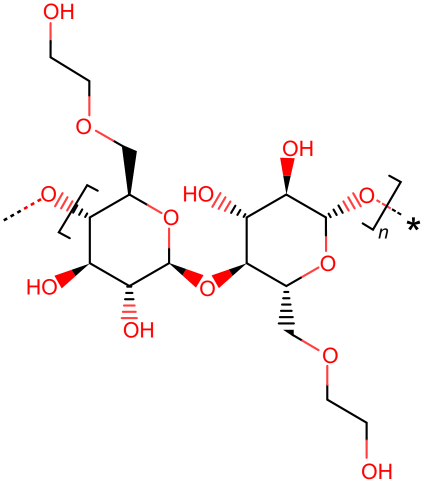

Figure 11.6 Hydroxy-ethyl-cellulose (HEC), DS = 1.0.

capacity of hydrocolloidal HEC. For concentration >15 g L^{-1}, the formation of highly associated polymer networks is the responsible mechanism.

HEC significantly retards cement hydration (Knapen and Van Gemert, 2009), probably as a result of the adsorption of the polymer onto the surface of cement particles. Binary mixtures of HEC-oxalic acid added to Portland cement mortar increase the heat of hydration, strength, fracture toughness, and corrosion resistance compared to the control. The water absorption of mortar is reduced by sealing of the pores with calcium oxalate products (Singh et al., 2003).

11.3.2.2 Methyl-hydroxy-ethyl-cellulose

Methyl-hydroxy-ethyl-cellulose (MHEC) is a hygroscopic white granule or powder. In cold water, MHEC swells into a colloidal dispersion, and its solubility is not influenced by its pH value. It is highly soluble in water and has a high gel temperature (60–90 °C). Figure 11.7 shows its molecular structure. MHEC solutions at concentrations of 0.01% to 0.1% exhibit Newtonian rheological behavior (Pierre et al., 2015). However, at concentrations above 0.2% and at high shear rates, a shear-thinning behavior is observed. The viscosity of solutions at 2% concentration under high shear rates ranges from 50 to 2×10^5 mPa s.

Increasing MHEC molecular weight from 9×10^4 to 3.8×10^5 g mol^{-1}, at a constant concentration of 0.27% with respect to the total solids in mortars, decreases both the yield stress and the flow behavior index, whereas the consistency index and the water retention increase (Patural et al., 2011). The increase of MS reduces the water-retention capacity. However, this effect becomes less significant compared to the effect of the molecular weight. A stearic hindrance could explain their results. This effect is dependent on the MHEC chain length that produces a better separation of the cement particle aggregates. Consequently, a reduction of the yield stress in the

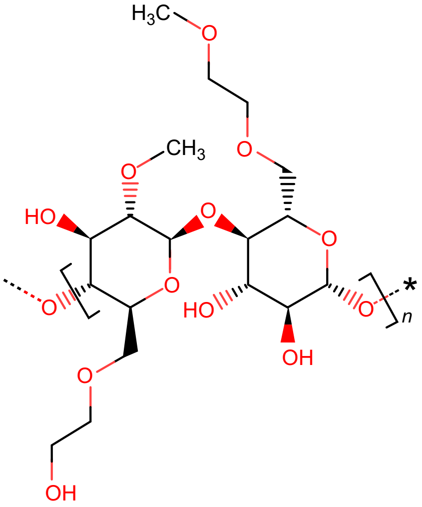

Figure 11.7 Methyl-hydroxy-ethyl-cellulose, DS = 1.5.

mortars is observed. A similar trend has been observed for MHEC in a concentration range of 0.3% to 0.2% (Cappellari et al., 2013). For MHEC of higher molecular weight the reduction of the yield stress is given at a certain critical concentration below which the yield stress increases with increasing concentration. This effect was attributed to the competition between two opposing effects of the polymers: the dispersing and lubricant effects versus the associative effect.

In general, an increase in both yield stress and consistency index is expected when the dosage of the admixture is increased. However, at lower concentrations, the increase in yield stress cannot be noted because the polymer must reach a critical concentration in the solution to show physical entanglements between the polymer chains, which produce the increase in the yield stress.

The increase in viscosity is related to the water adsorption on the polymer chain by van der Waals forces and hydrogen bonds, which increase the viscosity of mortars. At low dosages, MHEC achieves water retention by intramolecular sorption of water and concomitant swelling. At higher dosages, MHEC molecules agglomerate into large hydrocolloidal microgel particles ($d > 1$ μm), which effectively plug the pores in the mortar matrix (Bülichen et al., 2012). They stabilize air voids in the cement paste. Studies related to the effect of MHEC on the hydration of pure tricalcium silicate (C3S) using NMR relaxation times and calorimetric analysis (Alesiani et al., 2004) indicate that MHEC at 0.27% with respect to C3S weight acts as regulator of water release during the whole hydration process. For C3S/water/MHEC paste, the acceleration period ends when only 20% of water remains unreacted, whereas for C3S/water paste the unreacted water is nearly 60%. MHEC retards the hydration rate of C3S and dicalcium silicate (C2S) in pure phases but does not affect the hydration thermodynamics (Ridi et al., 2005). It also has a significant influence on the water availability and changes the morphology of calcium silicate hydrate (CSH) products at later ages. In addition, there is a significant inhibition of the crystallization of the stable cubic phases and a stabilization of the amorphous gel of C3AH6 and C3(AF)H6 during hydration of the pure C3A and tetracalcium aluminoferrite (C4AF) phases (Ridi et al., 2005).

11.3.2.3 Methyl-hydroxy-propyl-cellulose

Methyl-hydroxy-propyl-cellulose (MHPC) is a yellowish, odorless, and nontoxic powder. It is partially etherified with methyl groups, with a small number of substituted hydroxyl-propyl groups. The viscosity of aqueous solutions remains constant within a pH range of 3.0–11.0. MHPC has the same characteristics as pure methyl-cellulose (MC) (Wüstenberg, 2014). The molecule of MHPC has a cellulose backbone made of β-D-glucose units with a (1→4) linkage. The three free-hydroxyl groups are partially etherified with methyl groups. The hydroxyl-propyl and methyl groups can be attached to both the naturally occurring hydroxyl groups of the cellulose and to newly formed hydroxyl-propyl groups through an ether bridge. The MHPC molecule is illustrated in Figure 11.8. The gravimetric content of methyl groups is 19–30% and the content of hydroxyl-propyl groups is 3–12% (on dry basis). The molecular weight is between 1.3×10^4 and 2×10^5 g mol^{-1}, which correlates with a DP of 70 to 1100

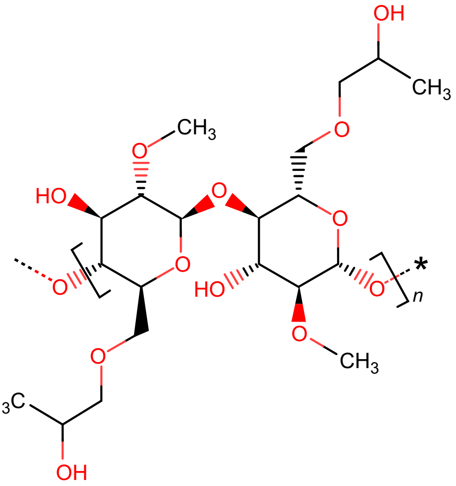

Figure 11.8 Methyl-hydroxy-propyl-cellulose, DS = 2.0.

glucose monomers. MHPC with a DS of 1.5 to 2.0 is very soluble in cold water (0–30 °C) and polar organic solvents. The viscosity of the aqueous solution increases in the presence of sugars. MHPC in pure water gels at 58 °C and calcium sulfate at 10% decreases the gelation temperature to 4 °C.

Increasing the polymer molecular weight (Patural et al., 2011) from 2.25×10^5 g mol^{-1} to 9.1×10^5 g mol^{-1} leads to an increase in both water retention and consistency coefficient in mortars. The water retention of MHPC was studied by Bülichen and Plank (2013) in cement pastes and in a gypsum plaster utilizing the filter paper test. The water-retention capacity decreased significantly in the calcium sulfate system. Thus, higher dosages of MHPC were required in the gypsum plaster to attain water-retention values comparable to those in cement. It was determined that sulfate anions hinder the formation of colloidal associates, which presents the key process to achieve water retention. This observation explains the higher dosages required in $CaSO_4$ systems.

The flexural strength of cement pastes decreases with increasing MHPC/cement ratio, which is a result of the retarding action of the polymer on cement hydration. A chemical interaction via cross-linking between MHPC-oxygen and the metal ions/free valences on the cement surface forms an organo-mineral phase responsible for this effect (Coarna et al., 2004).

11.3.3 Microbial exopolysaccharides

Producing microorganisms under controlled conditions makes the production of polysaccharides most homogeneous, offering a wide range of polymers with unique structural properties. However, microbial production and recovery of polysaccharides are highly expensive (Kaur et al., 2014). Some examples of these polysaccharides are xanthan from *Xanthomonas campestris*, sphingans from *Sphingomonas* sp., alginates from *Pseudomonas* sp., *Azotobacter vinelandii*, and *Azotobacter chrococcum*, cellulose from *Acetobacter xylinium*, hyaluronic acid from *Streptococcus equii*, succinoglycan from *Rhizobium*, and pullulan secreted by *Aureobasidium pullulans* (Bülichen et al., 2012; Kaur et al., 2014). Sphingans (e.g., gellan, welan, diutan, rhamasan) are structurally similar polysaccharides with a backbone structure except for the location of side chains. This group has a common linear tetrasaccharide backbone structure [$\rightarrow$3)-β-Glcp-(1$\rightarrow$4)-β-D-GlcpAc-(1$\rightarrow$4)-β-D-Glcp-(1$\rightarrow$4)-α-L-Rha-(1$\rightarrow$ or -β-L-Manp(1$\rightarrow$], in which Glcp is glucose, GlcpAc is glucuronic acid, Rha is rhamnose, and Manp is mannose to which different side groups are attached.

The most commonly used polymers in cement-based materials from microbial production are welan, diutan, and xanthan gums.

11.3.3.1 Welan gum

Welan gum is an anionic polysaccharide produced by bacteria *Sphingomonas* sp., also known as *Alcaligenes* sp., a Gram-negative microorganism, under aerobic submerged fermentation at an optimal temperature between 28 and 35 °C and a pH between 6.5 and 7.5 (Kaur et al., 2014). Its molecular structure is shown in Figure 11.9. It is composed of a long chain with a molecular weight of approximately 6.6×10^5 g mol^{-1} and an intrinsic viscosity of approximately 4479 mL g^{-1} (Xu et al., 2013). Its sugar backbone consists of D-glucose, which is substituted on C3 of every glucose unit with side chains containing either L-rhamnose or L-mannose linked (1$\rightarrow$4) (Kaur et al., 2014; Pei et al., 2015). It has polyelectrolyte properties owing to the presence of D-glucoronic acid in its chemical structure.

It is among the most commonly used VEAs in cement-based materials and produces a substantial increase in water-retention capacity and thus increases the viscosity of the cement paste. In aqueous solutions, welan gum increases viscosity with increasing concentration and exhibits shear-thinning behavior. The side chain can fold back on the main chain to form hydrogen bonds with the carboxylate groups, and a double helix is produced, avoiding cross-linking gelation. Temperature has a negligible effect on the viscosity of welan gum solutions (Sakata et al., 1996; Xu et al., 2013), remaining unchanged in the range of 5 to 75 °C. The pH of the solutions in the range of 2 to 12 has little effect on the viscosity (Isik and Ozkul, 2014) and the presence of calcium ions slightly increases the viscosity (Sakata et al., 1996).

In cement pastes, the long-chain molecules of welan gum adhere to the periphery of water molecules, thus adsorbing and fixing part of the mixing water, increasing both the yield stress and the plastic viscosity as well as controlling bleeding. Dosages of welan gum at 0.01% to 0.1% by weight of cement have been shown to stabilize concrete without affecting its fluidity, which is attributed to its shear-thinning behavior. For a given dosage of naphthalene-based HRWR, increasing the welan gum concentration in cement pastes with a w/c ratio of 0.40 reduced the mini-slump and the fluidity over time, and increased the flow time in the Marsh cone. In addition, it increased the resistance to forced bleeding and slightly increased the setting times (Khayat and Saric-Coric, 2000). Other studies indicate that increasing welan gum content in grouts causes a proportional increase in the apparent viscosity, yield stress, and thixotropy

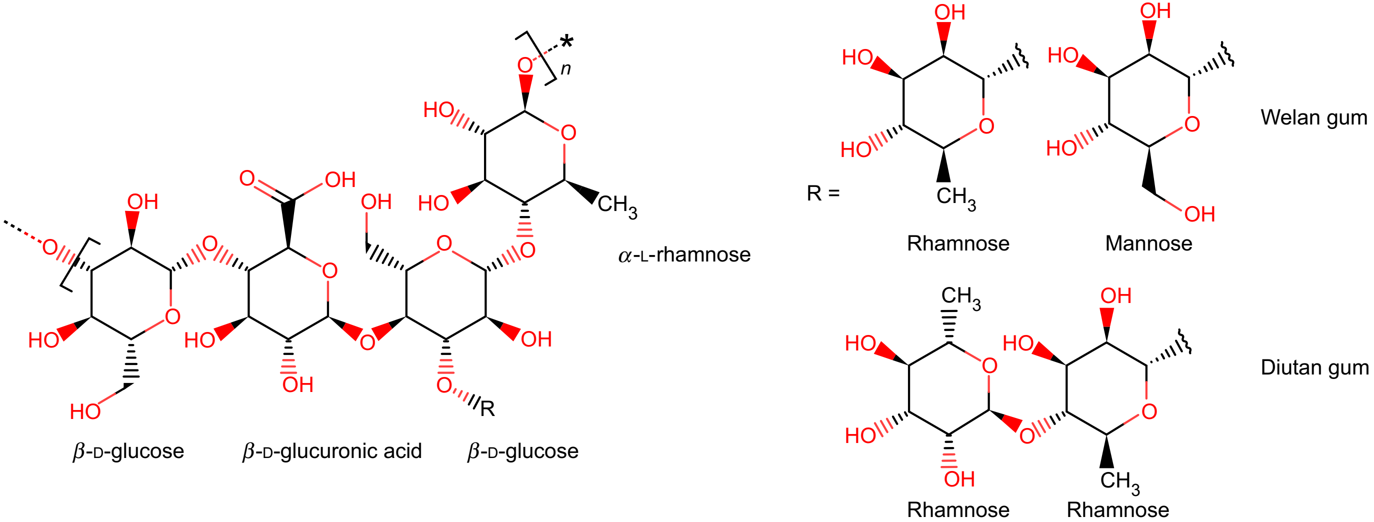

Figure 11.9 Basic tetrasaccharide backbone structure in the sphingan family showing side chains and their linkage position in welan and diutan gums.

(Khayat and Yahia, 1997). In underwater concrete, the addition of welan gum as 0.15% of cement mass reduced the mass loss from 9% in the reference mix to 0.5% in the mix containing welan gum (Khayat, 1995). The superplasticizer dosage to maintain the same level of fluidity increased more than 100% in low- and medium-strength concrete mixtures containing welan gum. This gum has shown compatibility with melamine-based, naphthalene-based, and polycarboxylate-based HRWR (Khayat and Assaad, 2008).

Several VEAs, including welan gum, were tested to investigate their effect on cement hydration (Ciobanu et al., 2013). The degree of hydration, assessed by the amount of $Ca(OH)_2$ determined by thermal analysis, indicates a higher amount of calcium hydroxide promoted by a better dispersion of particles that result in a higher interaction between water and cement. This behavior is contrary to that observed, for instance, with cellulose ethers, which slow down the hydration process. The addition of welan gum changes the morphology of ettringite and retards hydration in a tricalcium aluminate (C3A)−gypsum system, which was attributed to the adsorption of welan gum on ettringite, producing its variation in size and morphology (Ma et al., 2012).

11.3.3.2 Diutan gum

Diutan gum is a natural high-molecular-weight gum produced by carefully controlled aerobic fermentation. The repeating unit is composed of a six-sugar unit. The backbone is made up of D-glucose, D-glucuronic acid, D-glucose, and L-rhamnose, and the side chain of two L-rhamnose (Figure 11.9). When added to cement grouts, diutan gum exhibits a shear-thinning behavior compared to a control grout without VEA (Sonebi, 2006). At low shear rates, the grout showed a high apparent viscosity that resulted from entanglement and intertwining of the polymer, whereas at high shear rates the viscosity decreases because of the alignment of the polymer along the direction of the flow, thus enhancing fluidity. Compared to welan gum, it was observed that diutan gum is more shear thinning and exhibited higher viscosity at low shear rates at the same dosages of VEA and superplasticizer. This difference is attributed to the higher-molecular-weight and longer chain of the diutan gum. It is also known that the viscosity of diutan gum is higher under alkaline environment and in the presence of calcium ions, such as that found in fresh cement paste.

At early ages, the diutan gum showed a set retarding behavior and reduced strength of the cement pastes, compared to the control. With respect to the effects of diutan gum on cement hydration, samples of cement paste studied by thermal analysis have shown that the addition of diutan gum causes a higher content of calcium hydroxide compared to control cement paste (Ciobanu et al., 2013). This indicates a higher degree of hydration promoted by the adsorption of water molecules on the surface of cement particles. However, the compressive strength was lower in cement pastes containing diutan gum compared to the control.

11.3.3.3 Xanthan gum

Xanthan gum is a natural, fully biodegradable within two days (Katzbauer, 1998), high-molecular-weight (approximately 2×10^6 g mol^{-1}) bacterial polysaccharide obtained by aerobic fermentation of *Xanthomonas campestris*. Its backbone structure is the same as that of cellulose (Figure 11.10). It is a linear polymer with the D-glucopyranosyl unit of its main chain backbone as a trisaccharide unit containing, from the reducing end outward, an α-D-mannopyranosyl 6-acetate unit, a β-D-glucuronopyranosyl unit, and a β-D-mannopyranosyl unit at the nonreducing end. Some of the nonreducing end units are terminated with a 4,6-*O*-pyruvyl cyclic acetal group (BeMiller, 2008; Plank, 2005). It is an anionic and nongelling polysaccharide, the viscosity of which is unaffected by pH or most salts. It behaves as if it were a neutral gum. Xanthan gum forms solutions exhibiting highly shear-thinning behavior, which is due to the stiffness of its molecules and/or the intermolecular associations of two or more molecules.

Xanthan molecules have the shape of a five-fold helix, rather than the two-fold helical shape of cellulose. They often are in the form of double helixes and bundles of double helixes. Xanthan undergoes a conformational transition as the properties of the solvent are altered. An ordered helical conformation is stabilized by high ionic strength and/or low temperature. Average molecular weight values for xanthan gum range from 3×10^5 to 7.5×10^6 g mol^{-1} or greater, an indication of the ability of xanthan molecules to aggregate. Xanthan molecules behave as rather rigid, linear molecules, and the stiffness of these molecules gives them unique properties. The actual properties of xanthan gum preparations can vary with the strain of the organism used and the conditions of fermentation, so not all xanthan products are identical (BeMiller, 2008). Xanthan gum has been used in the food, textile, and paper industries as well as in ceramics processing and oil drilling (Isik and Ozkul, 2014).

The rheological behavior of xanthan gum in aqueous solutions at room temperature indicates a shear-thinning behavior related to the orientation of molecules along the flow (Xu et al., 2013). At low shear rates, the stretching polysaccharide molecules intertwine to form aggregates that cause high viscosity. As the shear rate is increased, the aggregates are destroyed, the molecules orient along the flow direction, and the apparent viscosity decreases. It does not show any incompatibility with polycarboxylate-based HRWR. When used in SCC concrete, xanthan gum has performed satisfactorily compared to other VEAs such as welan gum and starch ether (Isik and Ozkul, 2014). The flow and segregation resistance of SCC containing xanthan gum was similar to those obtained with welan gum and starch ether. However, its performance regarding bleeding has been shown to be superior compared to welan gum, being able to reduce bleeding to zero. From the perspective of macroscopic effects on hydration, the use of xanthan gum did not adversely affect the compressive strength of SCC compared to the other VEAs used (Isik and Ozkul, 2014).

11.3.4 Starch

Starch is found in almost all plants and consists of a mixture of two polysaccharides: amylose, a linear α-(1→4)-glucan, DP between 1×10^2 and 4×10^5, and amylopectin, a branched α-(1→4)-glucan with α-(1→6)-glucan branches every 19–25 units, DP between 1×10^4 and 4×10^7. Amylose has a molecular mass of approximately 1×10^5 to 1×10^6 g mol^{-1} and amylopectin has a molecular mass of approximately 1×10^7 to 1×10^8 g mol^{-1}. Its molecular structure is given in Figure 11.11. It can

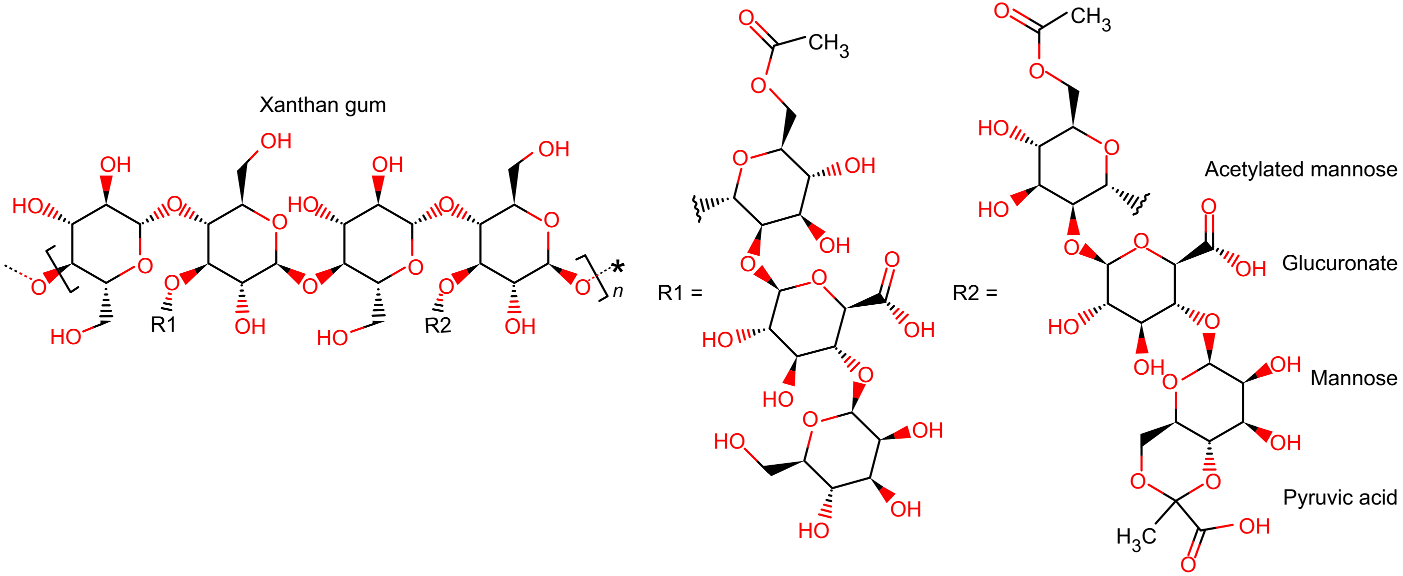

Figure 11.10 Basic structure of xanthan gum.

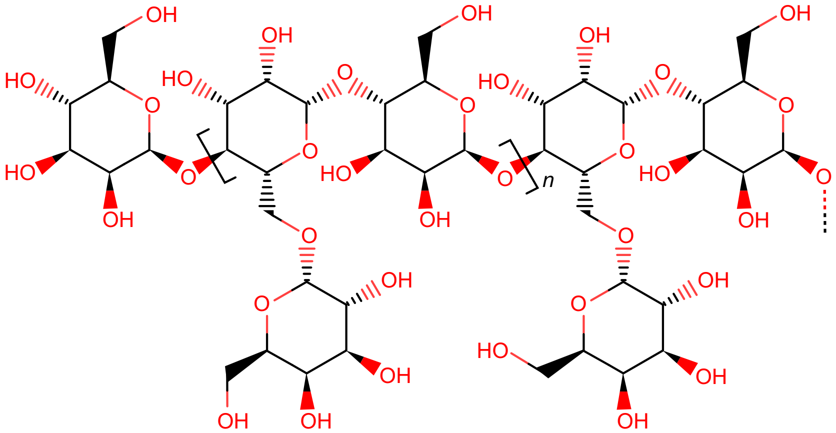

Figure 11.11 Amylose unit, aggregate of linear polymers of D-glucopyranose residues in chain form, which are linked in the α-(1→4) configuration.

be commercially produced using various sources such as potato, tapioca, corn, and wheat. In most cases, starch-based polymers used in the industry are usually modified products derived from native starch via chemical, physical, and/or enzymatic modifications. In general, the starch-based polymers for commercial use include unmodified starch, oxidized starch, hydroxyethylated starch, acetylated starch, and cationic starch. Starch is insoluble in water at ambient temperature. However, in hot water it gelatinizes to form an opalescent dispersion (Gross and Scholz, 2001).

Rols et al. (1999) used starch and a waste from the starch industry as VEAs. They obtained good results using only the raw starch. It increased the viscosity and improved the resistance to the segregation of self-leveling concrete when used at 0.05% with respect to cement weight. Leemann and Winnefeld (2007) used both mineral and high molecular polymer VEAs, including a natural polysaccharide and a starch derivative in a range of concentrations of 0.2% to 0.8% with respect to cement weight. They found that all VEAs used decreased the mortar flow and increased the flow time. They observed that the yield stress and the plastic viscosity of mortars increased when the VEAs, compatible with polycarboxylate-based HRWR, were added.

11.4 Biopolymers with potential for future use as viscosity-enhancing admixtures

11.4.1 Introduction

An increase in the use of VEAs for the production of special types of concrete can be generated if the cost of these admixtures is reduced in the near future. Therefore, researchers have had an interest in obtaining renewable and environmentally friendly VEAs with appropriate rheological and physical properties to be used in concrete technology. In developing countries, the production of highly industrialized VEAs is difficult. Therefore, their use depends on the cost of importation and transport, which increase the production cost of special types of concrete. The study of local biological sources of polymers with potential for use as VEAs, such as plants, algae, animals, or microorganisms, is very important to provide these countries with low-cost and environmentally friendly chemical admixtures. Some of these biopolymers are cactus mucilage, alginates, guar gum, peptidoglycan, and chitosan, among many other available but yet unexplored for use in cement-based materials.

11.4.2 Mucilages and gums

There is no chemical category for mucilages, which are sometimes called gums. Mucilage is a term used to refer to substances that produce slimy or tacky aqueous dispersions, which are properties manifested by various types of water-soluble plant, animal, or microbial polysaccharides. Both terms are sometimes indistinctly used (BeMiller, 2008). However, considering some aspects that are relevant in plants, a gum is considered to be an exudation from fruit, trunk, or branches of trees spontaneously or after mechanical injury of the plant by incision of the bark or removal of a branch, or after invasion by bacteria or fungi (Jones and Smith, 1949). These gums result from normal plant metabolism and appear to be produced by some protective mechanism to heal an injured area. Remarkable features of plant gums are that they form gels, have uniformity in their chemical structure, are hydrophilic, and possess high solubility in water. When these gums are not dissolved in water and form a colloidal dispersion, they are called mucilages. Plant mucilages differ from pectin in that they do not form gels. Mucilages are generally heteropolysaccharides, with varying uronic acid content. They are produced in the cells of some plants or in the outer layers of cells in seed coats or root cap (Trachtenberg and Mayer, 1980). Mucilage sometimes is used as a food reserve, and, in dry climates, it may act as a water reservoir.

11.4.2.1 Cactus mucilage

The mucilage produced by the cladodes of cactus is a complex heteropolysaccharide, which is formed by a neutral mixture of approximately 55 high-molecular-weight sugar residues composed basically of arabinose, galactose, rhamnose, xylose, and galacturonic acid (Figure 11.12). Mucilage has the ability to interact with metals, cations, and biological substances. Mucilage swells in water but is insoluble, which provides it with great potential to precipitate ions, bacteria, and particles from aqueous solutions (Trachtenberg and Mayer, 1980). Mucilage of *Opuntia* genus has been of interest to research because it has a traditional use in Latin America, especially in Mexico. It has been used in the restoration of historical buildings as an admixture that prevents moisture transport to the interior of lime mortars (Cárdenas et al., 1998). The plasticity and resistance of Portland cement are also increased when it is mixed with cactus mucilage, owing to the complex formation with $Ca(OH)_2$ (Chandra et al., 1998). It has been shown to increase the setting times as well as decrease the hydration rate of cement-based materials in the hardened state (Ramírez-Arellanes et al., 2012). The indirect measure of cement hydration by compressive strength on concrete has

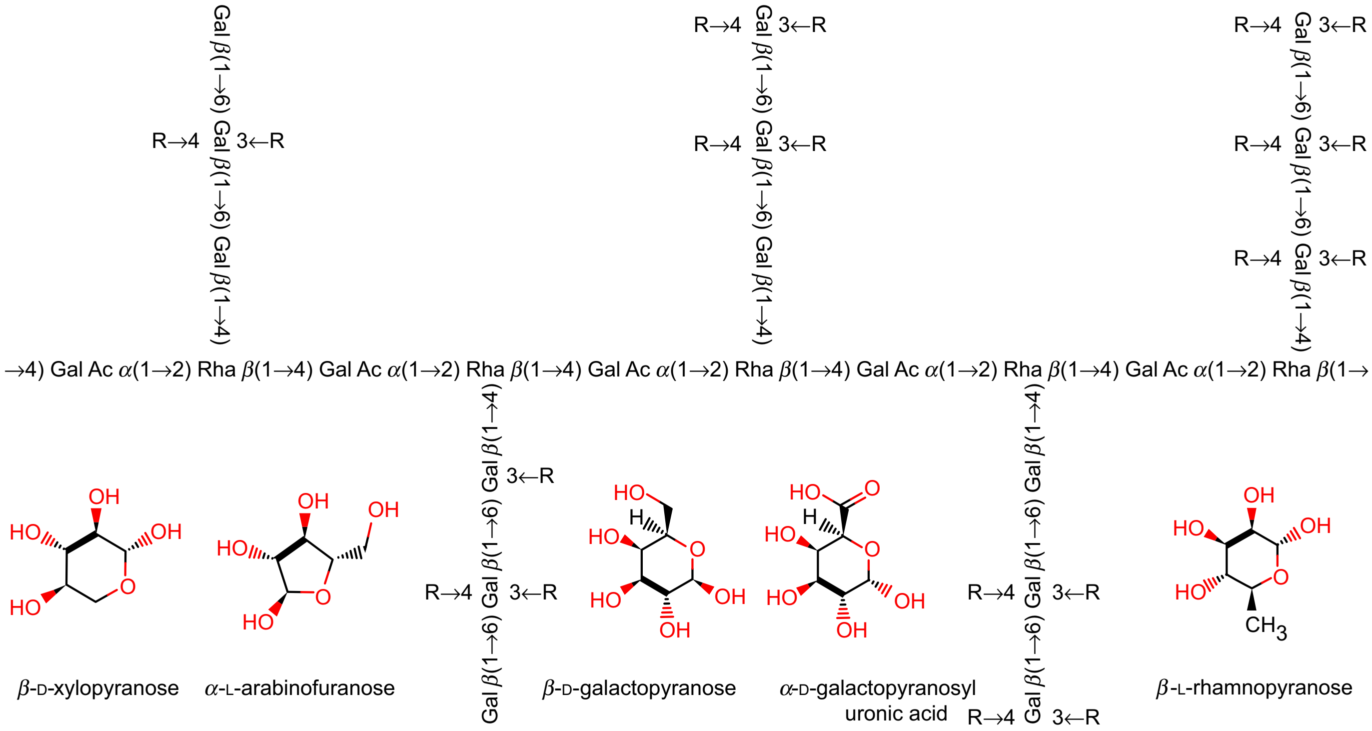

Figure 11.12 Molecular structure of *Opunti ficus indica* mucilage.

not provided a conclusive indication of improved hydration when cactus mucilage is added. León-Martínez et al. (2014) studied the use of cladodes' mucilage of *Opuntia ficus-indica* as VEA in SCC. In aqueous solutions, it exhibits a shear-thinning behavior, which is a function of the mucilage concentration in the solution. Mucilage increases the viscosity of cement pastes, mortars, and SCC as well as increases the Herschel—Bulkley yield stress. The shear-thinning behavior of cement pastes and mortars is affected with inclusion of mucilage, being more significant when the concentration increases from 0.25% to 0.435%, obtaining a rapid decrease in viscosity with increasing shear rate. The authors suggested an adsorption-of-water mechanism of action for this biopolymer in the range of concentrations used.

11.4.2.2 Alginates

Alginate is a linear polysaccharide made up of a binary copolymer composed of α-L-guluronic (G) and β-D-mannuronic (M) residues of widely varying composition and sequence (Figure 11.13). These residues are (1→4) linked. The stiffness of the chain blocks increases in the order MG < MM < GG (BeMiller, 2008; Gomes et al., 2012). They are structural components of marine brown algae (*Phaeophyceae*), composing up to 40% of the dry matter and as capsular polysaccharides in soil bacteria. Alginate is used in the industry as a water retainer, gelling agent, viscosifying agent, and stabilizer. Alginates are polydisperse, and the solutions prepared with sodium alginates

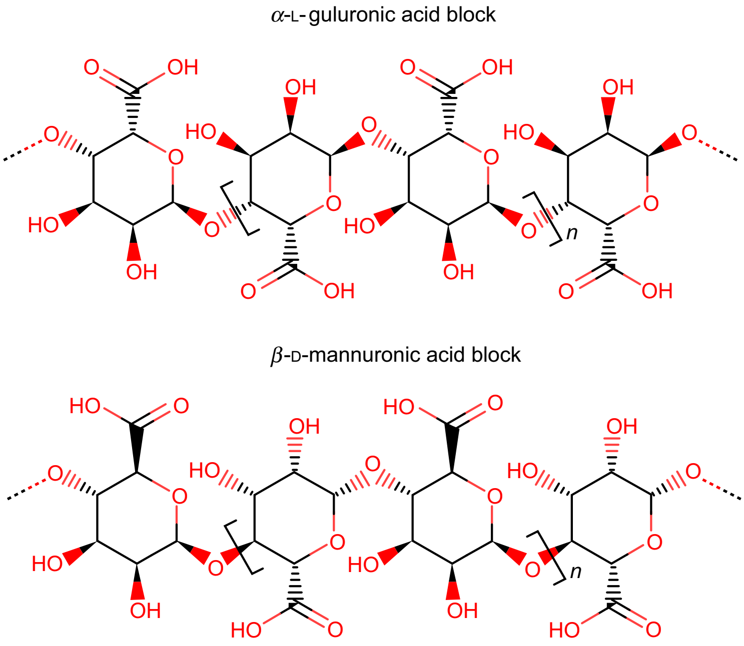
α-L-guluronic acid block

β-D-mannuronic acid block

Figure 11.13 β-(1→4)-D-mannuronic acid and α-(1→4)-L-guluronic acid blocks that form the alginate chains.

are highly viscous. León-Martínez et al. (2014) have studied the use of marine brown algae extract from *Macrocystis pyrifera* as VEA in cement-based materials. In aqueous solutions, the extract exhibits shear-thinning behavior and affects cohesion, viscosity, and slump of cement-based materials. The Herschel—Bulkley yield stress is highly affected by the use of this admixture, increasing with increasing extract concentration in a potential way with a power factor of ~2. This behavior was attributed to the formation of a gel network between the cations in dissolution present in the cement paste with the guluronic residues in the alginate polymer. In addition, alginate has been used as a bonding agent in the preparation of clay soil composites, in which it increases the compressive strength compared to control specimens (Galán-Marín et al., 2010). More studies on the effect of this type of polysaccharide in the hydration process are needed.

11.4.2.3 Guar gum

Guar gum is a polysaccharide belonging to the family of galactomannans, extracted from the seed endosperm of a leguminosae *Cyamopsis tetragonolobus*, which grows in semi-dry regions of tropical countries, particularly in India and Pakistan. It is a galactomannan consisting of a (1→4) linked β-D-mannopyranose backbone, with random branch points of galactopyranose via α-(1→6) linkage (Figure 11.14). It has a high-molecular-weight in the range of 1 to 2×10^6 g mol^{-1}. However, incomplete hydration of guar gum at ambient temperatures, poor solution clarity, and the desire for products with modified or special properties led to the development of a variety of commercial ether derivatives. Guar gum and its derivatives show shear-thinning behavior in solution (Maier et al., 1993), increasing with increasing concentration and molecular weight. The viscosity of aqueous solutions increases linearly with increases in guar gum concentration and do not exhibit yield stress. Aqueous solutions of guar gum develop a gel structure when they are treated with cross-linking agents (e.g., borates and transition-metal ions) under controlled pH conditions.

Its hydroxypropyl and hydroxyethyl derivatives (HPG and HEG, respectively) are commonly employed in the textile industry as printing-paste thickeners, in the paints and coatings and building industry as rheology modifiers, in the drilling industry, in paper and explosives production, and in other industry sectors (Gross and Scholz, 2001).

Hydroxypropyl guar (HPG) has been used as water-retaining agent in lime-based mortar under aggressive conditions (Izaguirre et al., 2010). Its use increased the

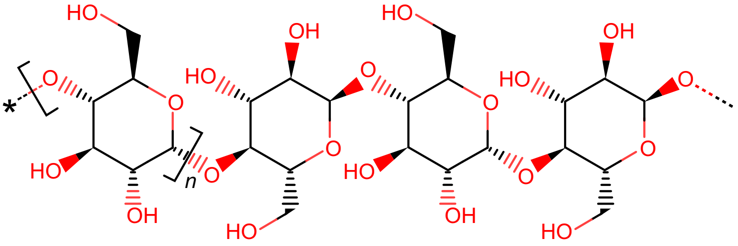

Figure 11.14 Chemical structure of guaran, the principal polysaccharide of guar gum.

compressive strength and improved the durability of mortar compared to the control. Shear-thinning behavior and reduction in shear viscosity are observed when the pH is increased from 7 to 13 and NaCl is added at 1 M to HPG solutions. An increase in the concentration of HPG increases the shear-thinning behavior, yield stress, and consistency of cement mortars (Poinot et al., 2014). HPG delays the cement hydration, which is due to its influence on the growth of hydrates. This is caused by the adsorption of the HPG via the interaction between hydroxyl groups and the highly polar hydrated phases (Poinot et al., 2013). The addition method of HPG in cement mortars affects their properties in the fresh state. A dry addition produces mortars with lower water-retention capacity and lower consistency but higher yield stress and marginal cement hydration delay (Poinot et al., 2015).

11.4.2.4 Peptidoglycan from the cell wall of bacteria

The main structural features of peptidoglycan are linear glycan strands cross-linked by short peptides. The backbone is composed of repeating units of disaccharide, N-acetylglucosamine, and N-acetylmuramic acid residues linked by $\beta(1 \rightarrow 4)$ bonds (Figure 11.15). Peptidoglycan is an important and specific component of the bacterial cell wall found on the outside of the cytoplasmic membrane of almost all bacteria. The side group contains a short peptide composed of four amino acids (Vollmer et al., 2008). Pei et al. (2015) and Vollmer et al. (2008) proposed this type of biopolymer to be used as VEA in hydraulic concrete. They observed an increase

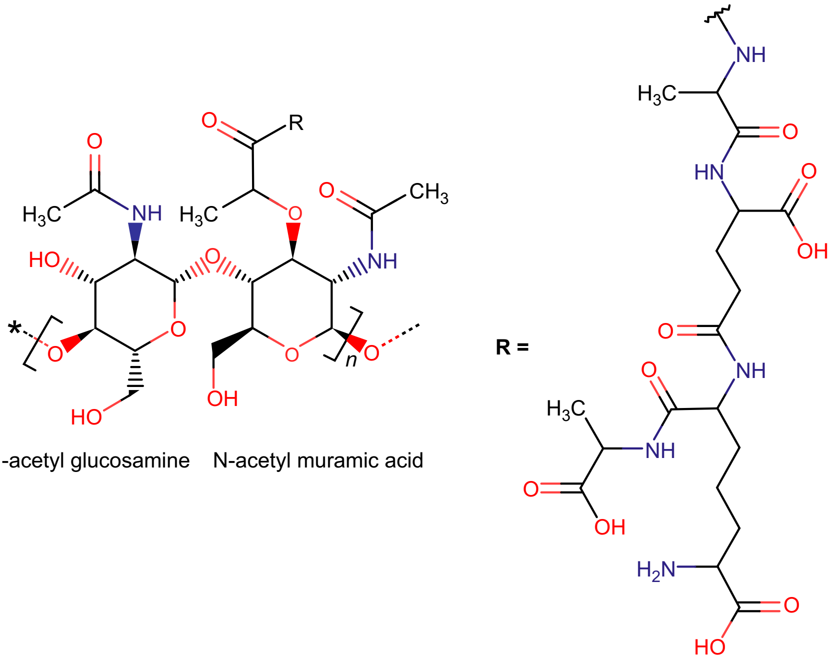

Figure 11.15 Molecular structure of peptidoglycan.

in the apparent viscosity and yield stress of cement pastes when the peptidoglycan was used at concentrations of 0.068% and 0.34% with respect to the cement weight. A shear-thinning behavior was observed, and it was compatible with naphthalene sulfonate-based HRWR. A lower viscosifying effect was found when the peptidoglycan was compared to diutan gum at 0.02%. This was attributed to the conformational shape of the molecule in space that has a cage-like structure. According to Pei et al. (2013), the peptidoglycan of *B. subtilis* does not affect $CaCO_3$ formation, which is responsible for a significant increase in the compressive strength of concrete.

11.4.2.5 Chitosan

Chitin is a skeletal polysaccharide, poly(2-acetamido-2-deoxy-D-glucopyranose), found in many organisms in nature in which it serves a critical function for their survival. For example, it is found in a wide range of insects, crustaceans, annelids, mollusks, coelentera, and most fungi. This homopolymer consists of β(1→4)-N-acetyl-D-glucosamine units. Chitosan, poly(2-amino-2-deoxy-D-glucopyranose), is obtained by base-catalyzed chemical de-acetylation of chitin (Figure 11.16). It represents a group of cationic biopolymer. The extraction and modification of this natural polymer demonstrate unique properties such as biocompatibility, antimicrobial activity, biodegradability, film- and fiber-forming ability, as well as heavy metal absorption. Chitin is insoluble in aqueous solutions and organic solvents, due to its highly crystalline nature; in

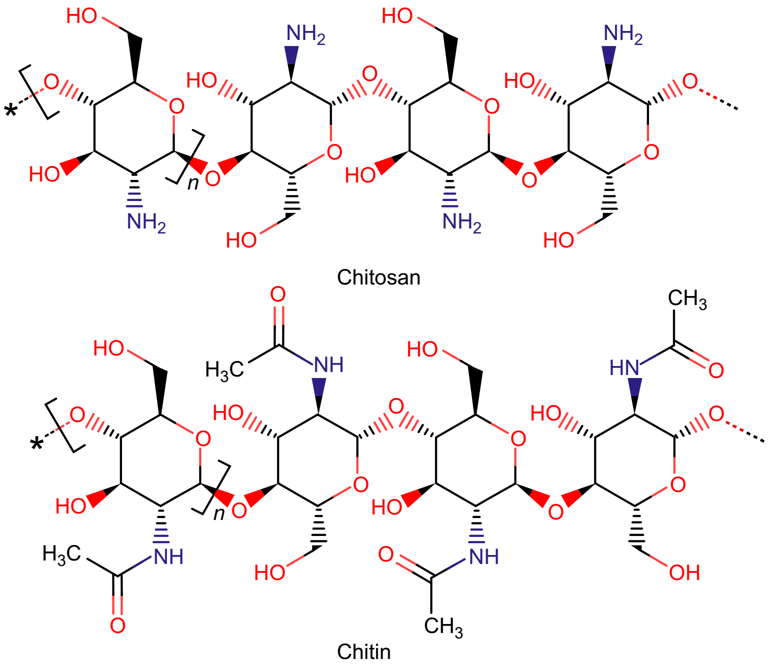
Chitosan

Chitin

Figure 11.16 Basic structure of chitosan and chitin.

contrast, chitosan is soluble in water and acidic solutions and is slightly soluble in weakly alkaline solutions (Gross and Scholz, 2001). Chitosan is a versatile biopolymer and can be used in various fields, such as agriculture, construction materials, horticulture, water treatment, biomedicine—pharmaceuticals, food, nourishments, cosmetics, and paper making. Recent studies on the use of chitosan (Lasheras-Zubiate et al., 2011) and chitosan ethers (Lasheras-Zubiate et al., 2012) indicate that their addition causes a delay in hydration of the cement in mortars. Chitosan increases the viscosity and the yield stress, retards the setting time as a result of interaction between the polymer and cement particles, and increases the number of coarse pores. Nonionic chitosan derivatives show that the dosage does not significantly affect the fresh-state properties, but the ionic derivatives show a marked effect.

11.5 Future trends

In 2003, the total amount of cellulose used by the chemical industry was approximately 5×10^6 tonnes. From this amount, 12% and 25% were used to produce ether and ester derivatives (Wüstenberg, 2014). According to Plank (Plank, 2005, 2004), about 1×10^5 tonnes of cellulose ethers and 3×10^4 tonnes of starch and derivatives were consumed as admixtures in dry-mix mortars, whereas <500 tonnes of microbial exopolysacharides (welan and xanthan) were used. This indicates that cellulose will continue to be the main biopolymer for the production of VEAs. The amount consumed by the construction industry is expected to increase, as consumers demand more-specialized cement-based materials.

Recent patents propose the generation of rheology-modifying admixtures that still use ether- and ester-cellulose derivatives as well as starch derivatives. They consider mixing them with microbial exopolysaccharides, synthetic polymers, and mineral particles to improve the rheological properties of cement-based materials. On the other hand, improvements in the biotechnological process and cost reductions are necessary to increase the competitiveness of the biopolymers obtained from microorganisms such as welan, diutan, and xanthan gums. The alteration of the biosynthetic pathway for welan gum production via genetic engineering techniques can also maximize the production of this exopolysaccharide. Recent research has shown that mixing xanthan and locust bean gums produces a strong interaction that results in a rheological enhancement of the mix (Renou et al., 2013) that may benefit the performance of cement-based materials.

On the other hand, alternative VEAs from natural sources such as cactus mucilage and alginates from brown seaweeds have shown promising results in cement-based materials. Figure 11.17 shows a comparison of the rheological behavior of cactus mucilage and VEAs such as welan gum, xanthan gum, and HEC. Despite having a reduced viscosity, the cactus mucilage has been used to produce stable SCC mixtures (León-Martínez et al., 2014). However, appropriate methods of extraction and purification must be developed to obtain VEAs with consistent properties that ensure reproducible results for the construction industry. Other VEAs such as guar gum, peptidoglycan, and chitosan are additional potential sources of biopolymers that also need further exploration.

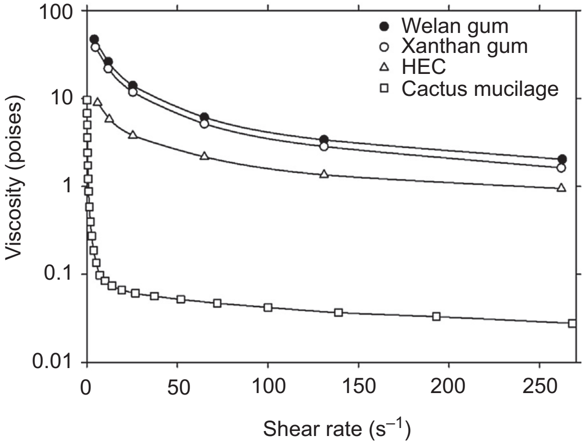

Figure 11.17 Relationship between shear rate and viscosity for pore solution-extracted cement pastes containing VEAs at a concentration around 1%.
Graph adapted from Sakata et al. (1996) and from unpublished data from the authors.

References

ACI Committee 212, 2010. Report on Chemical Admixtures for Concrete. Farmington Hills, MI.

ACI Committee 238, 2008. Report on Measurements of Workability and Rheology of Fresh Concrete. Farmington Hills, MI.

Alesiani, M., Capuani, S., Giorgi, R., Maraviglia, B., Pirazzoli, I., Ridi, F., Baglioni, P., 2004. Influence of cellulosic additives on tricalcium silicate hydration: nuclear magnetic resonance relaxation time analysis. The Journal of Physical Chemistry B 108, 4869–4874. http://dx.doi.org/10.1021/jp037876n.

Assaad, J.J., Khayat, K.H., 2006. Effect of viscosity-enhancing admixtures on formwork pressure and thixotropy of self-consolidating concrete. ACI Materials Journal 103, 280–287. http://dx.doi.org/10.14359/16612.

Banfill, P., Beaupré, D., Chapdelaine, F., de Larrard, F., Domone, P., Nachbaur, L., Sedran, T., Wallevik, O., Wallevik, J.E., 2001. Comparison of Concrete Rheometers: International Tests at LCPC (Nantes, France) in October 2000, NISTIR 6819. Gaithersburg (USA).

BeMiller, J.N., 2008. Gums and related polysaccharides. In: Fraser-Reid, B.O., Tatsuta, K., Theim, J. (Eds.), Glycoscience. Springer Berlin Heidelberg, pp. 1513–1533.

Bentz, D., Peltz, M., Snyder, K., Davis, J., 2009. VERDiCT: viscosity enhancers reducing diffusion in concrete technology. Concrete International 31, 31–36.

Bülichen, D., Kainz, J., Plank, J., 2012. Working mechanism of methyl hydroxyethyl cellulose (MHEC) as water retention agent. Cement and Concrete Research 42, 953–959. http://dx.doi.org/10.1016/j.cemconres.2012.03.016.

Bülichen, D., Plank, J., 2013. Water retention capacity and working mechanism of methyl hydroxypropyl cellulose (MHPC) in gypsum plaster—which impact has sulfate? Cement and Concrete Research 46, 66–72. http://dx.doi.org/10.1016/j.cemconres.2013.01.014.

Bülichen, D., Plank, J., 2012. Role of colloidal polymer associates for the effectiveness of hydroxyethyl cellulose as a fluid loss control additive in oil well cement. Journal of Applied Polymer Science 126, E25–E34. http://dx.doi.org/10.1002/app.36529.

Cappellari, M., Daubresse, A., Chaouche, M., 2013. Influence of organic thickening admixtures on the rheological properties of mortars: relationship with water-retention. Construction and Building Materials, 25th Anniversary Session for ACI 228 — Building on the Past for the Future of NDT of Concrete 38, 950—961. http://dx.doi.org/10.1016/j.conbuildmat.2012.09.055.

Cárdenas, A., Arguelles, V.M., Goycoolea, F.M., 1998. On the possible role of *Opuntia ficus-indica* mucilage in lime mortar performance in the protection of historical buildings. Journal of the Professional Association for Cactus Development 3, 64—71.

Chandra, S., Eklund, L., Villarreal, R.R., 1998. Use of cactus in mortars and concrete. Cement and Concrete Research 28, 41—51. http://dx.doi.org/10.1016/S0008-8846(97)00254-8.

Choi, M., Roussel, N., Kim, Y., Kim, J., 2013. Lubrication layer properties during concrete pumping. Cement and Concrete Research 45, 69—78. http://dx.doi.org/10.1016/j.cemconres.2012.11.001.

Ciobanu, C., Lazǎu, I., Pǎcurariu, C., 2013. Investigation regarding the effect of viscosity modifying admixtures upon the Portland cement hydration using thermal analysis. Journal of Thermal Analysis and Calorimetry 112, 331—338. http://dx.doi.org/10.1007/s10973-012-2655-1.

Coarna, M., Georgescu, M., Puri, A., Diaconu, D., 2004. ESCA, MIP and mechanical characterization of some Portland cement — methyl-cellulose composites. Key Engineering Materials 264-268, 2153—2156. http://dx.doi.org/10.4028/www.scientific.net/KEM.264-268.2153.

Ferraris, C.F., de Larrard, F., 1998. Modified slump test to measure rheological parameters of fresh concrete. Cement Concrete and Aggregates 20, 241—247.

Feys, D., 2012. Understanding the pumping of conventional vibrated and self-compacting concrete. In: Roussel, N. (Ed.), Understanding the Rheology of Concrete. Elsevier, pp. 331—353. http://dx.doi.org/10.1533/9780857095282.3.331.

Galán-Marín, C., Rivera-Gómez, C., Petric, J., 2010. Clay-based composite stabilized with natural polymer and fibre. Construction and Building Materials 24, 1462—1468. http://dx.doi.org/10.1016/j.conbuildmat.2010.01.008.

Gomes, M., Azevedo, H., Malafaya, P., Silva, S., Oliveira, J., Silva, G., Joao Mano, R.S., Reis, R., 2012. Natural polymers in tissue engineering applications. In: Ebnesajjad, S. (Ed.), Handbook of Biopolymers and Biodegradable Plastics- Properties, Processing and Applications. William Andrew Publishing, Boston, pp. 385—425.

Gross, R.A., Scholz, C. (Eds.), 2001. Biopolymers from Polysaccharides and Agroproteins. American Chemical Society. ACS Symposium Series No. 786.

Hackley, V.A., Ferraris, C.F., 2001. The Use of Nomenclature in Dispersion Science and Technology. Washington.

Isik, I.E., Ozkul, M.H., 2014. Utilization of polysaccharides as viscosity modifying agent in self-compacting concrete. Construction and Building Materials 72, 239—247. http://dx.doi.org/10.1016/j.conbuildmat.2014.09.017.

Izaguirre, A., Lanas, J., Álvarez, J.I., 2010. Ageing of lime mortars with admixtures: durability and strength assessment. Cement and Concrete Research 40, 1081—1095. http://dx.doi.org/10.1016/j.cemconres.2010.02.013.

Jones, J.K.N., Smith, F., 1949. Plant gums and mucilages. Advances in Carbohydrate Chemistry 4, 243—291.

Katzbauer, B., 1998. Properties and applications of xanthan gum. Polymer Degradation and Stability 59, 81—84. http://dx.doi.org/10.1016/S0141-3910(97)00180-8.

Kaur, V., Bera, M.B., Panesar, P.S., Kumar, H., Kennedy, J.F., 2014. Welan gum: microbial production, characterization, and applications. International Journal of Biological Macromolecules 65, 454—461. http://dx.doi.org/10.1016/j.ijbiomac.2014.01.061.

Khayat, K.H., 1998. Viscosity-enhancing admixtures for cement-based materials—an overview. Cement and Concrete Composites 20, 171–188. http://dx.doi.org/10.1016/S0958-9465(98)80006-1.

Khayat, K.H., 1995. Effects of anti-washout admixtures on fresh concrete properties. ACI Materials Journal 92, 164–171.

Khayat, K.H., Assaad, J.J., 2008. Use of thixotropy-enhancing agent to reduce formwork pressure exerted by self-consolidating concrete. ACI Materials Journal 105, 88–96. http://dx.doi.org/10.14359/19211.

Khayat, K.H., Mikanovic, N., 2012. Viscosity-enhancing admixtures and the rheology of concrete. In: Roussel, N. (Ed.), Understanding the Rheology of Concrete. Elsevier, pp. 209–228. http://dx.doi.org/10.1533/9780857095282.2.209.

Khayat, K.H., Saric-Coric, M., 2000. Effect of welan gum-superplasticizer combinations on properties of cement grouts. ACI Special Publication 195, 249–268. http://dx.doi.org/10.14359/9916.

Khayat, K.H., Yahia, A., 1997. Effect of welan gum-high-range water reducer combinations on rheology of cement grout. ACI Materials Journal 94, 365–372.

Klemm, D., Philipp, B., Heinze, T., Heinze, U., Wagenknecht, W., Klemm, D., 1998. Comprehensive Cellulose Chemistry. In: Functionalization of Cellulose, vol. 2. Wiley-VCH, Weinheim, New York.

Knapen, E., Van Gemert, D., 2009. Cement hydration and microstructure formation in the presence of water-soluble polymers. Cement and Concrete Research 39, 6–13. http://dx.doi.org/10.1016/j.cemconres.2008.10.003.

de Larrard, F., Ferraris, C.F., Sedran, T., 1998. Fresh concrete: a Herschel-Bulkley material. Materials and Structures 31, 494–498.

de Larrard, F., Sedram, T., Hu, C., Sitzkar, J.C., Joly, M., Derkx, F., 1996. Evolution of the workability of superplaticized concretes: assessment with BTRHEOM rheometer. In: Proceedings International RILEM Conference on Production Methods and Workability of Concrete. Paisley, pp. 377–388.

Lasheras-Zubiate, M., Navarro-Blasco, I., Fernández, J.M., Alvarez, J.I., 2011. Studies on chitosan as an admixture for cement-based materials: assessment of its viscosity enhancing effect and complexing ability for heavy metals. Journal of Applied Polymer Science. 120, 242–252. http://dx.doi.org/10.1002/app.33048.

Lasheras-Zubiate, M., Navarro-Blasco, I., Fernández, J.M., Álvarez, J.I., 2012. Effect of the addition of chitosan ethers on the fresh state properties of cement mortars. Cement and Concrete Composites 34, 964–973. http://dx.doi.org/10.1016/j.cemconcomp.2012.04.010.

Łaźniewska-Piekarczyk, B., 2013. Effect of viscosity type modifying admixture on porosity, compressive strength and water penetration of high performance self-compacting concrete. Construction and Building Materials 48, 1035–1044. http://dx.doi.org/10.1016/j.conbuildmat.2013.07.076.

Leemann, A., Winnefeld, F., 2007. The effect of viscosity modifying agents on mortar and concrete. Cement and Concrete Composites 29, 341–349. http://dx.doi.org/10.1016/j.cemconcomp.2007.01.004.

León-Martínez, F.M., Cano-Barrita, P.F.J., Lagunez-Rivera, L., Medina-Torres, L., 2014. Study of nopal mucilage and marine brown algae extract as viscosity-enhancing admixtures for cement based materials. Construction and Building Materials 53, 190–202. http://dx.doi.org/10.1016/j.conbuildmat.2013.11.068.

Ma, L., Zhao, Q., Yao, C., Zhou, M., 2012. Impact of welan gum on tricalcium aluminate–gypsum hydration. Materials Characterization 64, 88–95. http://dx.doi.org/10.1016/j.matchar.2011.12.002.

Maier, H., Anderson, M., Karl, C., Magnuson, K., Whistler, R.L., 1993. Guar, locust bean, tara, and fenugreek gums. In: Whistler, R.L., Bemiller, J.N. (Eds.), Industrial Gums. Academic Press, London, pp. 181–226.

Margheritis, G., Baldaro, E., Perrone, L., Li, B.G., 2009. Rheology Modifying Admixture.

Mark, J.E., 1999. Polymer Data Handbook. Oxford University Press.

Mehta, P.K., Monteiro, P.J.M., 2006. Concrete: Microstructure, Properties, and Materials, third ed. McGraw-Hill.

Müller, I., 2006. Influence of Cellulose Ethers on the Kinetics of Early Portland Cement Hydration. Universitätsverlag Karlsruhe, Karlsruhe.

Naji, S., Hwang, S.-D., Khayat, K.H., 2011. Robustness of self-consolidating concrete incorporating different viscosity-enhancing admixtures. ACI Materials Journal 108, 432–438. http://dx.doi.org/10.14359/51683116.

Nelson, E.B., Baret, J.-F., Michaux, M., 1990. 3 Cement additives and mechanisms of action. In: Nelson, E.B. (Ed.), Developments in Petroleum Science, Well Cementing. Elsevier, pp. 3–1.

Okamura, H., 1997. Self-compacting high-performance concrete. Concrete International 19, 50–54.

Okamura, H., Ouchi, M., 2003. Self-compacting concrete. Journal of Advanced Concrete Technology 1, 5–15. http://dx.doi.org/10.3151/jact.1.5.

Ott, E., Spurlin, H.M., Grafflin, M.W., Bikales, N.M., Segal, L., 1954. Cellulose and Cellulose Derivatives. Interscience Publishers.

Patural, L., Marchal, P., Govin, A., Grosseau, P., Ruot, B., Devès, O., 2011. Cellulose ethers influence on water retention and consistency in cement-based mortars. Cement and Concrete Research 41, 46–55. http://dx.doi.org/10.1016/j.cemconres.2010.09.004.

Pei, R., Liu, J., Wang, S., Yang, M., 2013. Use of bacterial cell walls to improve the mechanical performance of concrete. Cement and Concrete Composites 39, 122–130. http://dx.doi.org/10.1016/j.cemconcomp.2013.03.024.

Pei, R., Liu, J., Wang, S., 2015. Use of bacterial cell walls as a viscosity-modifying admixture of concrete. Cement and Concrete Composites 55, 186–195. http://dx.doi.org/10.1016/j.cemconcomp.2014.08.007.

Pierre, A., Perrot, A., Picandet, V., Guevel, Y., 2015. Cellulose ethers and cement paste permeability. Cement and Concrete Research 72, 117–127. http://dx.doi.org/10.1016/j.cemconres.2015.02.013.

Plank, J., 2005. Applications of biopolymers in construction engineering. Biopolymers Online 29–39. http://dx.doi.org/10.1002/3527600035.

Plank, J., 2004. Applications of biopolymers and other biotechnological products in building materials. Applied Microbiology and Biotechnology 66, 1–9. http://dx.doi.org/10.1007/s00253-004-1714-3.

Poinot, T., Bartholin, M.-C., Govin, A., Grosseau, P., 2015. Influence of the polysaccharide addition method on the properties of fresh mortars. Cement and Concrete Research 70, 50–59. http://dx.doi.org/10.1016/j.cemconres.2015.01.004.

Poinot, T., Govin, A., Grosseau, P., 2014. Influence of hydroxypropylguars on rheological behavior of cement-based mortars. Cement and Concrete Research 58, 161–168. http://dx.doi.org/10.1016/j.cemconres.2014.01.020.

Poinot, T., Govin, A., Grosseau, P., 2013. Impact of hydroxypropylguars on the early age hydration of Portland cement. Cement and Concrete Research 44, 69–76. http://dx.doi.org/10.1016/j.cemconres.2012.10.010.

Ramírez-Arellanes, S., Cano-Barrita, P.F.J., Julián-Caballero, F., Gómez-Yañez, C., 2012. Concrete durability properties and microstructural analysis of cement pastes with nopal cactus mucilage as a natural additive. Materiales de Construcción 62, 327–341. http://dx.doi.org/10.3989/mc.2012.00211.

Renou, F., Petibon, O., Malhiac, C., Grisel, M., 2013. Effect of xanthan structure on its interaction with locust bean gum: toward prediction of rheological properties. Food Hydrocolloids 32, 331−340. http://dx.doi.org/10.1016/j.foodhyd.2013.01.012.

Ridi, F., Fratini, E., Mannelli, F., Baglioni, P., 2005. Hydration process of cement in the presence of a cellulosic additive. A calorimetric investigation. The Journal of Physical Chemistry B 109, 14727−14734. http://dx.doi.org/10.1021/jp050237n.

Rols, S., Ambroise, J., Péra, J., 1999. Effects of different viscosity agents on the properties of self-leveling concrete. Cement and Concrete Research 29, 261−266. http://dx.doi.org/10.1016/S0008-8846(98)00095-7.

Roussel, N., 2006. Correlation between yield stress and slump: comparison between numerical simulations and concrete rheometers results. Materials and Structures 39, 501−509. http://dx.doi.org/10.1617/s11527-005-9035-2.

Rudin, A., Choi, P., 2013. Biopolymers. In: Rudin, A., Choi, P. (Eds.), The Elements of Polymer Science & Engineering. Academic Press, Boston, pp. 521−535.

Sakata, N., Maruyama, K., Minami, M., 1996. Basic properties and effects of welan gum on self-consolidating concrete. In: Bartos, P.J.M., Marrs, D.L., Cleland, D.J. (Eds.), Production Methods and Workability of Concrete. E & FN Spon, London, pp. 237−253.

Schneider, M., Romer, M., Tschudin, M., Bolio, H., 2011. Sustainable cement production—present and future. Cement and Concrete Research 41, 642−650. http://dx.doi.org/10.1016/j.cemconres.2011.03.019.

Singh, N.K., Mishra, P.C., Singh, V.K., Narang, K.K., 2003. Effects of hydroxyethyl cellulose and oxalic acid on the properties of cement. Cement and Concrete Research 33, 1319−1329. http://dx.doi.org/10.1016/S0008-8846(03)00060-7.

Sonebi, M., 2006. Rheological properties of grouts with viscosity modifying agents as diutan gum and welan gum incorporating pulverised fly ash. Cement and Concrete Research 36, 1609−1618. http://dx.doi.org/10.1016/j.cemconres.2006.05.016.

Thrane, L.N., Pade, C., Nielsen, C.V., 2010. Determination of rheology of self-consolidating concrete using the 4C-rheometer and how to make use of the results. Journal of ASTM International 7, 10.

Trachtenberg, S., Mayer, A.M., 1980. Biophysical properties of *Opuntia ficus-indica* mucilage. Phytochemistry, An International Journal of Plant Biochemistry 21, 2835−2843. http://dx.doi.org/10.1016/0031-9422(80)85052-7.

Vollmer, W., Blanot, D., De Pedro, M.A., 2008. Peptidoglycan structure and architecture. FEMS Microbiology Reviews 32, 149−167.

Wallevik, O.H., Wallevik, J.E., 2011. Rheology as a tool in concrete science: the use of rheographs and workability boxes. Cement and Concrete Research 41, 1279−1288. http://dx.doi.org/10.1016/j.cemconres.2011.01.009.

Wüstenberg, T., 2014. Cellulose and Cellulose Derivatives in the Food Industry: Fundamentals and Applications, first ed. Wiley-VCH Verlag GmbH & Co. KGaA.

Wyatt, N.B., Gunther, C.M., Liberatore, M.W., 2011. Increasing viscosity in entangled polyelectrolyte solutions by the addition of salt. Polymer (Guildf) 52, 2437−2444. http://dx.doi.org/10.1016/j.polymer.2011.03.053.

Xu, L., Xu, G., Liu, T., Chen, Y., Gong, H., 2013. The comparison of rheological properties of aqueous welan gum and xanthan gum solutions. Carbohydrate Polymers 92, 516−522. http://dx.doi.org/10.1016/j.carbpol.2012.09.082.

Biotech solutions for concrete repair with enhanced durability

12

H.M. Jonkers, R.M. Mors, M.G. Sierra-Beltran, V. Wiktor
Faculty of Civil Engineering and Geosciences, Materials and Environment Section,
Delft University of Technology, Stevinweg, Delft, The Netherlands

12.1 Introduction

Durability of materials or structures is commonly defined as the ability to withstand wear, decay, pressure, or damage over a relatively long period and is thus linked to certain functional properties and performance over time. In line with this general definition, loss or decrease of durability would mean that at a certain moment during the service lifetime of a material or construction a set criterion for a certain performance level is approached or even no longer met. The functional performance of that construction would at that moment be at risk, and repair action is required to restore required functionality and/or lifetime expectancy to an acceptable or originally intended level. Task and challenge of the modern engineer is, therefore, to design a construction in such a way that it meets, nearly exactly, its intended functional service life.

Preferably, for both economic and sustainability reasons, the amounts of materials and other resources required for construction should be minimized while expected maintenance and repair actions during the construction service lifetime should be limited or completely avoided. In practice, however, concrete construction will always need a certain amount of maintenance and repair actions. This may be due to accidental overloading, unexpected wear or weathering, microcrack formation, increased porosity, or other phenomena related to specific, changing, environmental conditions resulting in early loss of functional properties.

12.2 Biotechnological strategies for durable repair of concrete structures

In view of existing design strategies, an interesting major difference in building concept between classical humanmade construction and natural biobased construction was observed and defined by van der Zwaag (2007). Although humanmade construction is typically designed to avoid damage (or loss of durability) and is therefore being defined by these authors as "damage prevention" design, nature designs in a fundamentally different way, and that is by being able to cope with (unexpected) occurring damage by activation of an in-built self-repair or self-healing mechanism. The latter

Biopolymers and Biotech Admixtures for Eco-Efficient Construction Materials. http://dx.doi.org/10.1016/B978-0-08-100214-8.00012-9
Copyright © 2016 Elsevier Ltd. All rights reserved.

strategy was defined by van der Zwaag as “damage management” design. Following this design strategy, nature ensures building structures using minimal amounts of materials and energy during the full-intended service lifetime of a construction.

The strategy of building according to the “damage management” design is now adopted in a relatively recent but already well-established field of material science in which humanmade self-healing materials, thus mimicking nature, are being developed (White et al., 2001; van der Zwaag, 2007). In a number of studies, however, the concept of developing self-repairing materials or improving durability aspects of materials was taken a step further by not only mimicking nature but also using natural biobased processes for enhancing durability aspects of humanmade construction. Bacteria that, under specific environmental conditions, produce limestone were applied to improve the durability aspects of ornamental stone and degraded limestone (Rodriguez-Navarro et al., 2003; Dick et al., 2006), consolidate soils (Schlegel, 1993; Gollapudi et al., 1995; Stocks-Fischer et al., 1999; DeJong et al., 2006; Whiffin et al., 2007; van Paassen et al., 2010a,b), seal cracks and pores in concrete to retain water tightness (De Muynck et al., 2008a,b; Qian et al., 2009b; Li and Qu, 2012; Achal et al., 2013; Kim et al., 2013), biocontainment of toxic compounds (Okwadha and Li, 2011), regain strength (Bang et al., 2001; Ramachandran et al., 2001), and improve frost resistance in concrete (Wiktor and Jonkers, 2015). In all these studies, biotechnology in the form of bacteria that can improve one or more specific durability aspects of concrete construction has thus been applied.

12.3 Bacterial production of limestone in alkaline environments

Limestone, $CaCO_3$, can be precipitated due to metabolic activity of bacteria and other microorganisms such as unicellular micro-algae and foraminifera (protozoa, see Figure 12.1). Unlike the latter two groups of microorganisms, bacteria other than a recently found cyanobacterium (Couradeau et al., 2012) generally do not intracellularly deposit limestone. Although micro-algae such as coccolithophorids and foraminifera actively regulate limestone precipitation intracellularly through transport of calcium ions over the cellular and intracellular vacuole membranes for the purpose of structural skeleton formation (Erez, 2003), bacterial extracellular limestone precipitation rather occurs as a by-product of metabolic activity.

In that sense bacteria do not “purposely” produce limestone like coccolithophorids and foraminifera, but precipitation occurs because, due to metabolic activity, the ion concentration product of calcium and carbonate ions ($[Ca^{2+}] * [CO_3{}^{2-}]$) in the direct vicinity of cells exceeds the solubility product of calcium carbonate (Zeebe and Wolf-Gladrow, 2001; Ludwig et al., 2005). Although metabolic activity of bacteria hardly affects the concentration of calcium ions, it can strongly influence the concentration of carbonate ions by changing the carbonate equilibrium system:

$$CO_2 + OH^- \leftrightarrow HCO_3{}^- \leftrightarrow H^+ + CO_3{}^{2-} \quad (12.1)$$

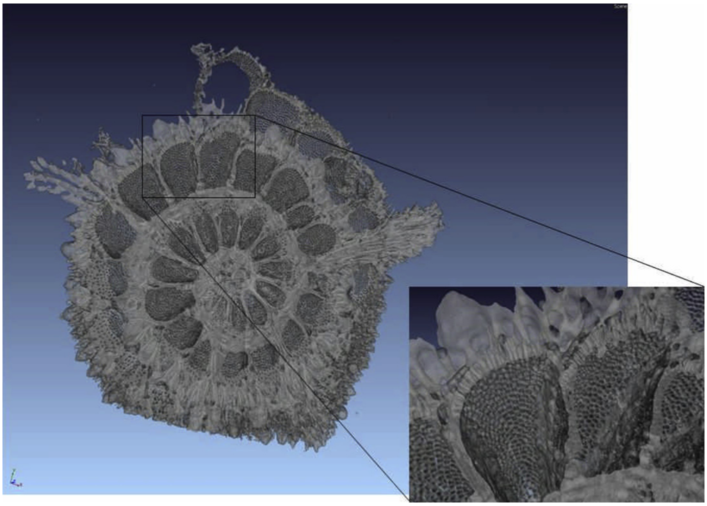

Figure 12.1 X-ray nanocomputed tomographic image of intracellular calcium carbonate skeleton of 1-mm sized unicellular foraminifera *Calcarina* sp.
Image by Arjan Thijssen, Section Materials and Environment, Delft University of Technology.

by either producing or consuming protons (H^+) or hydroxide ions (OH^-) or one or more of the carbonate equilibrium compounds. For example, during the process of photosynthesis both CO_2 and protons are consumed resulting in a shift in the carbonate equilibrium toward higher concentrations of carbonate ions that may result in precipitation of calcium carbonate in case its solubility product is exceeded. Likewise, also microbial deamination of amino acids and sulfate and nitrate reduction are examples of metabolic processes that produce alkalinity (increase of OH^- ion concentration) shifting the carbonate equilibrium toward ${CO_3}^{2-}$, increasing the potential for calcium carbonate precipitation.

In general terms, it can thus be stated that in environments where calcium ions are available, microbial metabolic processes that result in increase in alkalinity or otherwise in production of carbonate ions, increase the potential of calcium carbonate precipitation. Two specific microbial metabolic pathways, i.e., enzymatic hydrolysis of urea and heterotrophic CO_2 production under alkaline conditions, respectively, have been applied in a number of documented studies to promote calcium carbonate precipitation for the benefit of improving the durability aspects of concrete. These two biotechnological solutions will be critically reviewed in the following paragraphs.

12.3.1 Ureolytic bacterial limestone production

The possibility of using bacteria for consolidation of soils via precipitation of limestone using ureolytic bacteria was suggested by Schlegel already in the early 1990s (Schlegel, 1993). Some species of bacteria produce the enzyme urease that enables them to get access to nitrogen required for growth in the form of ammonia, a product of enzymatic hydrolysis of urea according to reaction (12.2):

$$CO(NH_2)_2 + H_2O \rightarrow CO_2 + 2NH_3 \tag{12.2}$$

The hydrolysis of one molecule of urea thus yields one molecule of CO_2 and two molecules of ammonia. Due to the alkalinity of ammonia, part of it becomes protonated in water yielding according to reaction (12.3) hydroxide and ammonium ions:

$$NH_3 + H_2O \leftrightarrow NH_4^+ + OH^- \tag{12.3}$$

This latter equilibrium reaction features a pK value of 9.2, meaning that in a water-based solvent system, at a pH of 9.2, 50% of nitrogen is in the form of ammonia (NH_3) and 50% in the form of ammonium ions (NH_4^+). The hydrolysis of urea in pH neutral to acidic waters therefore results in an increase in pH due to the production of hydroxide ions up to a pH of 9.2. The production of hydroxide ions (alkalinity) drives the carbonate equilibrium to the right in two steps according to reactions (12.4) and (12.5) in favor of formation of carbonate ions (CO_3^{2-}):

$$CO_2 + OH^- \rightarrow HCO_3^- \tag{12.4}$$

$$HCO_3^- + OH^- \rightarrow CO_3^{2-} + H_2O \tag{12.5}$$

The overall reaction of urea hydrolysis (12.6) yielding carbonate ions can be written as:

$$CO(NH_2)_2 + 2H_2O \rightarrow CO_3^{2-} + 2NH_4^+ \tag{12.6}$$

What can also be seen from the latter reaction is that hydrolysis of one molecule of urea yields besides one carbonate ion also two ammonia ions. Microbially driven calcium carbonate precipitation can thus potentially occur in calcium-containing environments in case hydrolysis of urea results in ion concentration products of calcium and carbonate ions exceeding the solubility product of calcium carbonate (Schlegel, 1993). However, it should be realized that for each molecule of calcium carbonate produced in this way two molecules of ammonium are produced as well.

The advantage of the ureolytic pathway is that microbially driven calcium carbonate precipitation potentially readily occurs in pH neutral environments, as the hydrolysis of urea produces the alkalinity that is required for production of carbonate ions, which subsequently react with calcium ions to form calcium carbonate. As suggested by Schlegel, this process was used in a number of later studies to solidify loose soils and sediments (e.g., Gollapudi et al., 1995; Stocks-Fischer et al., 1999; Whiffin et al., 2007; van Paassen et al., 2010a,b and others) and also to precipitate limestone on the surface of cracked and porous concrete specimens in laboratory studies (e.g., Bang et al., 2001; Ramachandran et al., 2001; De Muynck et al., 2008a,b and others in subsequent studies) and outdoor applications for the benefit of limestone monument restoration (Rodriguez-Navarro et al., 2003; Dick et al., 2006).

Although the hydrolysis of urea used for precipitation of limestone in the aforementioned studies is a microbially driven and thus biobased process, it is not necessarily sustainable due to the massive by-production of ammonium ions. As excess ammonium poisons groundwater, results in health problems and eutrophication of surface water (FAO, 1996), and can initiate corrosion of the steel reinforcement in concrete (Neville, 1996), it must be removed afterward to avoid such environmental and material durability problems (Ivanov and Chu, 2008; van Paassen et al., 2010b). The claim in many published studies that microbial calcium carbonate precipitation, or "biocementation," via the ureolytic pathway is environmental friendly, sustainable, or resulting in "green" products appears therefore unsubstantiated. Life-cycle assessment (LCA) studies are required to quantitatively compare sustainability performance of ureolytic versus traditional techniques used for stabilization of soils or improving durability of concrete. In such LCA studies, at least the use of required raw materials (e.g., urea, cement, energy) as well as the emission of environmental harmful compounds (e.g., ammonium or CO_2) must be included. In some LCA studies, the monetarization of environmental effects is applied, i.e., costs are assigned to quantities of emitted compounds. These costs, expressed as prevention or shadow costs, relate to the amount of money that needs to be spent to compensate environmental damage in a way to bring it to a societally acceptable sustainable level. For example, environmental costs for a kg of emitted CO_2 is set at 0.05 Euro, whereas those of ammonia per kg, assigned to the three environmental impact effect categories of human toxicity potential (HTP), eutrophication potential (EP), and acidification potential (AP), amounts to 0.009, 7.52, and 3.15 Euro, respectively (Groot and Borén, 2010; De Bruyn et al., 2010), thus more than two orders of magnitude higher in comparison to CO_2! Although the urease-driven hydrolysis of urea is a biological process, it does thus not necessarily mean that it is more sustainable than conventional concrete repair techniques.

12.3.2 Heterotrophic bacterial limestone production

To avoid excess production of ammonium and related environmental problems, alternative microbial metabolic pathways to the urea hydrolysis route have been explored for improving durability aspects of concrete. Microbially controlled precipitation of calcium carbonate in association with concrete is relatively easy because the required alkalinity for the process can be provided by the material itself. In the process of the cement hydration reaction, calcium hydroxide (Portlandite) is produced as secondary reaction product next to the formation of calcium silicate hydrate (CSH). Calcium hydroxide is chemically converted (12.7) to calcium carbonate upon reaction with CO_2:

$$Ca(OH)_2 + CO_2 \rightarrow CaCO_3 + H_2O \tag{12.7}$$

This process of carbonation results in densification of the porous matrix in concrete as long as calcium hydroxide is present in sufficient amounts. The naturally occurring carbonation process, i.e., the reaction of atmospheric CO_2 with calcium hydroxide residing in the concrete matrix can be significantly accelerated by application of CO_2-producing heterotrophic bacteria. Heterotrophic bacteria produce CO_2 by metabolic conversion of organic compounds, and several species are adapted to strongly alkaline environments. These "alkaliphilic" heterotrophic bacteria appear therefore suitable candidates for improving durability aspects of concrete as no other potentially detrimental metabolic by-products, such as ammonium as in the ureolytic pathway, are produced (Jonkers, 2007). Moreover, alkaliphilic species of the genus *Bacillus* are not only adapted to be metabolically active in highly alkaline environments, but are also able to produce spores, i.e., specific robust "dormant" cells (Figure 12.2), which survive incorporation in the concrete matrix (Jonkers et al., 2010).

In a number of studies, these alkaliphilic spore-forming bacteria were used to improve durability properties of both new and existing concrete structures and mortars (see Sections 12.4 and 12.5). Calcium carbonate production by these bacteria results from initial metabolic conversion of a concrete-compatible feed such as calcium lactate according to reaction (12.8):

$$Ca(C_3H_5O_3)_2 + 6O_2 \rightarrow CaCO_3 + 5CO_2 + 5H_2O \tag{12.8}$$

and subsequent chemical conversion (12.9) of calcium hydroxide (present in the concrete matrix) with metabolically produced CO_2:

$$5CO_2 + 5Ca(OH)_2 \rightarrow 5CaCO_3 + 5H_2O \tag{12.9}$$

In the overall reaction, one molecule of calcium lactate is thus converted into six molecules of calcium carbonate without any other metabolic by-product other than water.

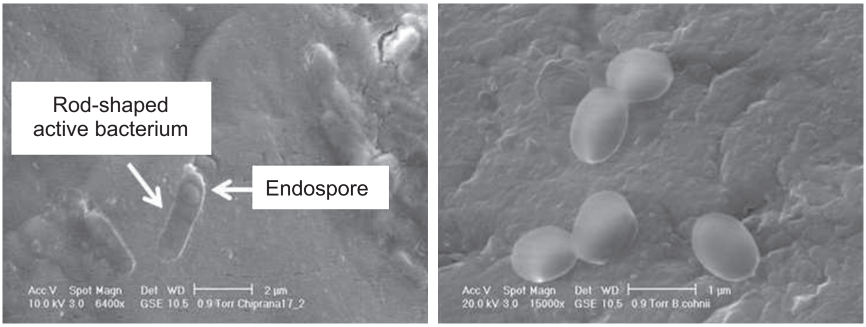

Figure 12.2 Spore-forming alkaliphilic bacteria of the genus *Bacillus*. Active rod-shaped bacteria (left image) form intracellular spores that remain as dormant cells after disintegration of the mother cell (right image).
Images by Arjan Thijssen, Section Materials and Environment, Delft University of Technology.

12.4 Liquid bacteria-based system for durable repair of porous concrete structures

In a series of studies Wiktor and coworkers developed a liquid bacteria-based system for durable and sustainable repair of leaking and porous concrete structures (Wiktor et al., 2012, 2013; Wiktor and Jonkers, 2015; Sangadji et al., 2013). Aim of these studies was to develop a system that produces calcium carbonate for plugging and waterproofing cracks and pores in concrete without concomitant production of environmentally harmful excess ammonium. Calcium carbonate is a concrete-compatible material and can therefore be considered to result in durable repair as long as the concrete remains alkaline because calcium carbonate is soluble under acidic conditions.

Bacterially controlled calcium carbonate production of the system is based on metabolic conversion of organic salts in a calcium-containing alkaline solution. Wiktor developed a two-component system which requires sequential application of both components to avoid immediate chemical precipitation of minerals such as Portlandite ($Ca(OH)_2$). The composition of the two-component liquid repair system is listed in Table 12.1 below.

When sequentially applied, the two components start to form a soft gel due to the chemical reaction of calcium and silicate ions. Slowly, in a process taking several weeks, the gel components are converted to calcium carbonate that results in a durable plugging (waterproofing) of cracks in concrete.

12.4.1 Improvement of frost damage resistance

Before application in situ on cracked and porous concrete structures, Wiktor and coworkers studied and quantified functional aspects of the liquid two-component system under combined in situ and laboratory conditions. To quantify durability improvement of concrete suffering from frost damage, the system was applied on a porous concrete slab positioned at the entrance of a parking garage. After a several

Table 12.1 Composition of the bacteria-based two-component system developed by Wiktor and coworkers

Component 1	Quantity	Component 2	Quantity (g/L)
Na-gluconate	125 g/L	Either Ca-lactate	80 g/L
Yeast extract	1 g/L	Or $Ca(NO_3)_2$	500 g/L
Bacillus spp.	1.6×10^8 spores/L	*Bacillus* spp.	1.6×10^8 spores/L
Na_2SiO_3	4.8 g/L	Yeast extract	1 g/L

After Sangadji et al. (2013).

week period to allow the bacteria to precipitate calcium carbonate in the concrete pores, triplicate 10-cm diameter cores of treated and nontreated (control) sites were drilled and subjected to freeze/thaw cycles in the laboratory to evaluate frost damage resistance. Mass loss of cores showed that significantly less scaling occurred on cores treated with the bacteria-based liquid repair system (Figure 12.3).

Although the treatment did not completely inhibit scaling of concrete cores when subjected to freeze/thaw cycles, a significant difference of an almost 50% reduction in scaling was observed. Further experiments are required to clarify whether replicate application of the repair system further reduces scaling and thus improves frost resistance of damaged concrete construction.

12.4.2 Waterproofing of cracked-concrete structures

The capacity of crack repair by waterproofing of the liquid repair system was also functionality quantified in a series of laboratory tests before in situ application of the system. Cracked mortar disks (dimensions diameter 17 cm and thickness 2 cm) were subjected to a water permeability test before and after treatment with the liquid repair system, and the effective durability of the treatment was furthermore analyzed by subjecting the treated specimens to five freeze/thaw cycles (Wiktor and Jonkers, 2014). Control specimens were treated with water only. Results of this test are shown in Figure 12.4.

Results showed that water-treated specimens are highly permeable, whereas the liquid repair system-treated specimens became waterproof (left part of image). Subjection to freeze/thaw cycles showed that permeability increased in both control and liquid repair system-treated specimens indicating that one treatment might not be sufficient for durable repair (waterproofing) of cracked-concrete construction.

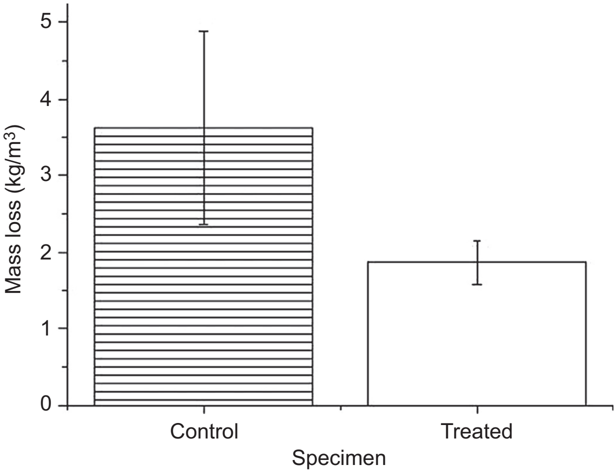

Figure 12.3 Mass loss of cores due to scaling after being subjected to seven freeze/thaw cycles. Control cores (depicted as gray bars) that were not treated with the bacteria-based liquid repair system suffered from about twice as much scaling compared to treated cores.

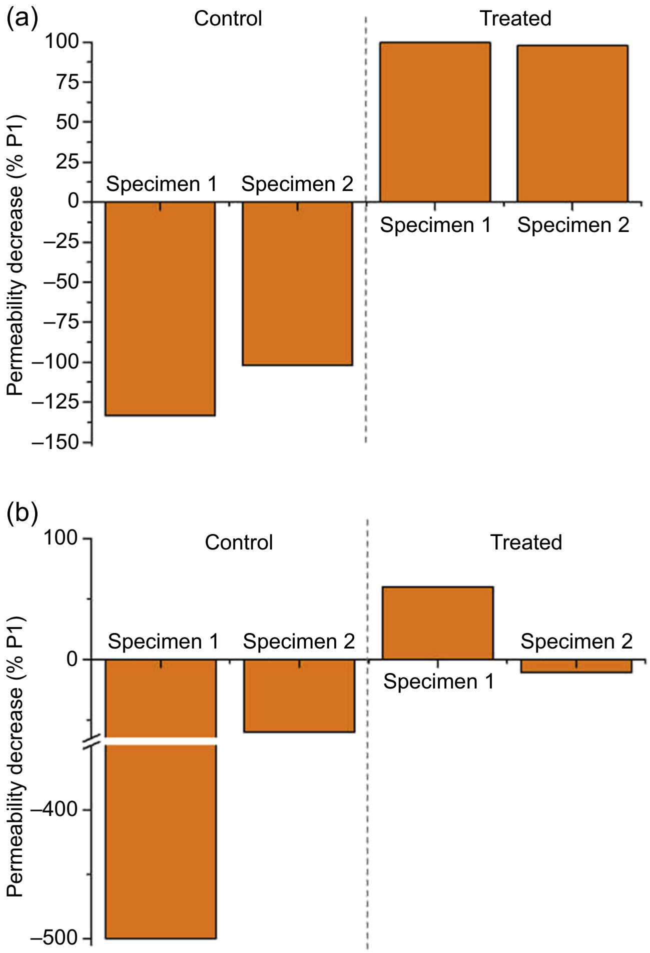

Figure 12.4 Cracked specimens, treated with either water alone (controls) or with the bacteria-based liquid repair system, subjected to water permeability tests: before and 28 days after treatment (a) as well as after subjection to five freeze/thaw cycles after treatment (b).

12.4.3 Practical applications of liquid bacteria-based repair system

The bacteria-based liquid repair system was applied on the full scale in situ with the aim of achieving durable repair of cracked and water-permeable parking decks of two parking garages located in the Netherlands. The two-component repair system (see Table 12.1 for its composition) was applied using handheld spray units that are commercially available for use of application of, e.g., liquid herbicides or pesticides. The system was applied on cracked surfaces, preferably directly sprayed in visible cracks with crack widths up to 0.8 mm. Upon sequential application of the two

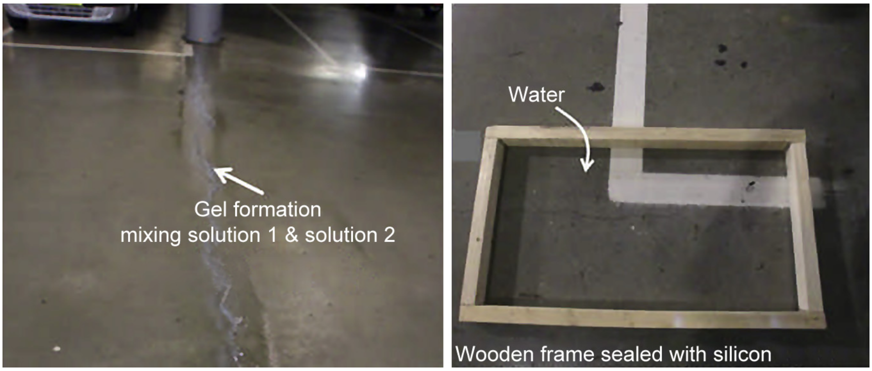

Figure 12.5 Application of the bacteria-based liquid repair system results in gel formation directly after sequential application of solutions 1 and 2 (left image). A wooden frame temporarily glued on a cracked parking deck area (right image) is used for in situ quantification of water permeability.

components, immediate gel formation could be visually detected (see Figure 12.5). Due to bacterial metabolic conversion of gluconate under alkaline conditions provided by the sodium silicate (see Figure 12.6), the gel is slowly converted into limestone (calcium carbonate) that results in a more permanent sealing of the cracked parking-deck areas.

The effectiveness of the treatment was established by applying an in situ water-permeability test. For this test, a rectangular wooden frame with dimensions of 1 × 0.5 m was placed on a cracked area and filled with 5 L tap water. Permeability

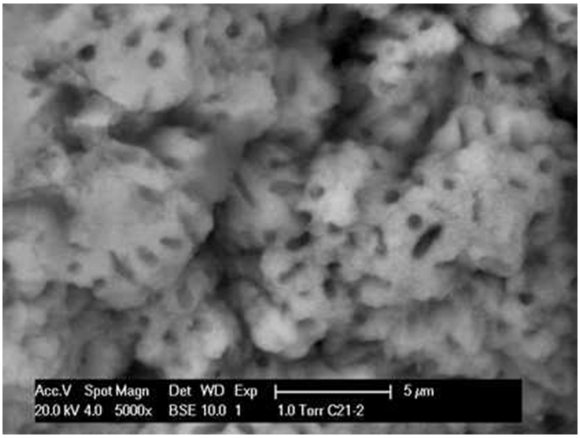

Figure 12.6 Calcium carbonate minerals produced by bacterial metabolic conversion of gluconate under alkaline conditions. Imprints of rod-shaped bacteria (see Figure 12.2 for size and shape of active vegetative bacterial cells) are clearly visible within the mineral matrix. Image by Arjan Thijssen, Section Materials and Environment, Delft University of Technology.

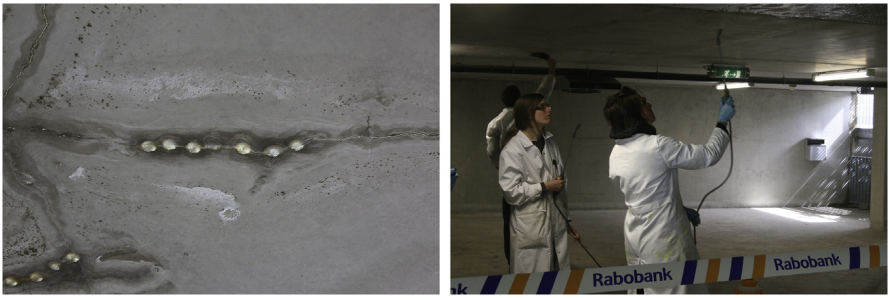

Figure 12.7 In situ application of the bacteria-based liquid repair system. Manual application using handheld spray units (right image) and counting of water drops permeating per minute through the cracked parking deck (left image).

of cracks within the wooden frame area was quantified by counting number of water drops dripping per minute from the bottom part of the cracked-concrete parking deck (ceiling of the lower parking deck level) (see Figure 12.7). As a control for the applied treatment, cracked reference areas were treated with tap water only.

Repeated permeability tests performed 8 weeks after the application of the liquid repair system showed that permeability of two of three cracked areas was reduced by more than 90%, whereas the third cracked area was completely waterproof. No significant reduction in water permeability was observed at areas that were treated with tap water only (control sites), showing that the treatment was effective (Wiktor and Jonkers, 2015).

12.5 Biobased mortar systems for structural repair of concrete defects

Concrete repair systems often face durability-related problems because compatibility with aged underlying concrete construction is generally low. This problem has a substantial impact on national economies, e.g., it is estimated that in the United States of America the cost for maintenance and repair of just concrete highway bridges already amounts to more than 4 US$ billion yearly (FHWA, 2001). Besides low in durability, traditional repair mortars also perform low in sustainability as they are commonly based on environmental unfriendly materials like acrylic resins, epoxy systems, or silicone-based polymers. In a series of recent studies, a novel type of repair mortar has been developed based on fibers for control of crack formation, and a bacteria-based "healing agent" for autonomous repair of freshly occurring cracks. The objective of these studies was to develop a more durable and simultaneously sustainable mortar for repair of damaged aged-concrete structures (Sierra-Beltran et al., 2014a,b). Synthetic fiber-based mortars had been previously developed, as fibers increase the tensile capacity and limit the width of occurring cracks in these mortars (Bentur and Mindness, 2007). Targeted application areas were specifically overlays in pavements and patch repair of damaged concrete construction (Yang et al., 2009; Qian et al., 2009a). A common durability problem associated with repair mortars is due to differential shrinkage deformation, a phenomenon that leads to tensile stress development often resulting in cracking and ultimately to debonding and detachment of the repaired patch. Fiber-based mortars can, however, carry higher tensile loads and therefore accommodate more tensile strain compared to nonfiber-based repair mortars. Although tensile strain in fiber-based repair mortars does result in crack formation, the freshly occurring crack widths remain small and the risk of debonding is much lower. Durability of repair is therefore typically considerably smaller in fiber-based repair mortars (Zhou, 2011). Self-repair of occurring microcracks, e.g., by incorporation of calcium carbonate-precipitating bacteria can contribute to further durability increase of fiber-based repair mortars (Sierra-Beltran et al., 2014a,b).

12.5.1 Properties of biobased self-healing repair mortars

To improve durability aspects of synthetic fiber-based repair mortars, Sierra-Beltran and coworkers proposed to incorporate a biotechnological agent composed of alkali-resistant bacteria and a suitable food source, inspired by bacteria-based self-healing concrete and the concrete liquid repair system previously described in Section 12.4. Upon crack formation and water ingress, incorporated bacterial spores germinate and start to convert the food source into calcium carbonate minerals that block cracks from further water and chemical ingress and, moreover, also result in improved bonding with the underlying aged-concrete substrate (Sierra-Beltran et al., 2014a). Typical mortar composition used by Sierra-Beltran and others in their studies is shown in Table 12.2.

Specimens with dimensions of 120 × 30 × 10 mm were subjected to four-point bending to induce crack formation. This procedure resulted in a typical crack pattern of multiple 0.02-mm-wide cracks, due to polyvinyl alcohol (PVA) fiber crack-width control. Subsequent submersion of specimens resulted in autonomous healing of cracks due to formation of calcium carbonate. Repeated loading of healed specimens resulted in new crack formation deflecting, however, from healed cracks, indicating that healing of cracks resulted in an improvement of mechanical properties (see Figure 12.8).

Table 12.2 **Composition of fiber-based control and bacterial repair mortars by weight (kg/m^3)**

Mortar type	CEMI 42.5N	Fly ash	Limestone powder	Healing agent	Water	SP	PVA fiber
Mix 1 control	485	582	415	–	416	5	25
Mix 2 bacterial	442	530	258	121	384	20	25

SP indicates superplasticizer, Cretoplast SL01, Cugla BV, The Netherlands; PVA fiber, polyvinyl alcohol fiber, 8 × 0.04 mm, tensile strength 1600 MPa, density 1300 kg/m^3, elastic modules 42.8 GPa, and maximum elongation of 6%.

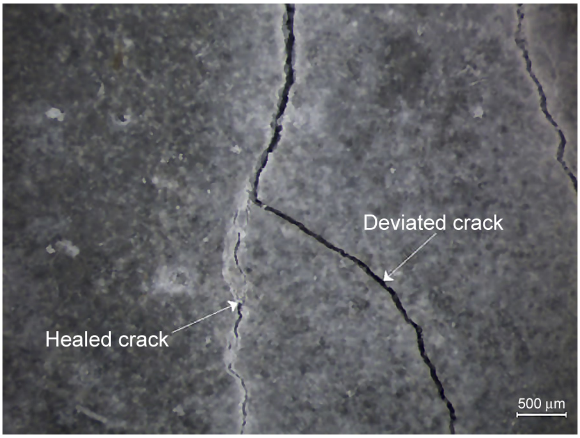

Figure 12.8 Self-healed crack due to bacterial metabolic conversion of calcium lactate into calcium carbonate. Subsequent reloading of specimen resulted in a newly formed crack deflecting from the previously healed crack, indicating that bacterially controlled crack-healing improved mechanical properties.
After Sierra-Beltran et al. (2014a).

That healing of cracks was largely controlled by bacterial activity was furthermore supported by oxygen profile measurements on water-submerged specimens. Control specimens that did not contain bacteria-based healing agent did not consume oxygen, whereas specimens with incorporated healing agent (mix 2) did consume considerable amounts of oxygen. This is proof that incorporated bacteria were metabolically active as the used bacteria consume oxygen during metabolic conversion of calcium lactate, food source of the bacteria and part of the healing agent (see Figure 12.9).

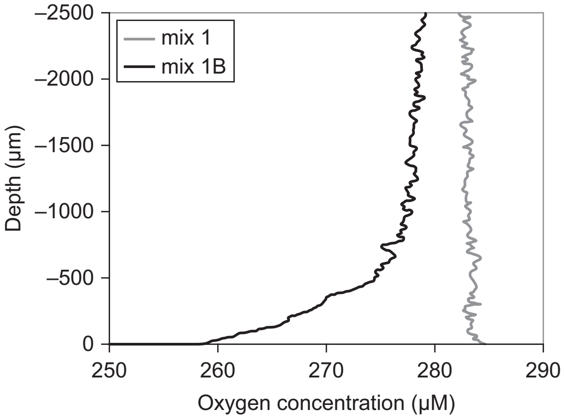

Figure 12.9 Oxygen consumption of bacteria-based healing agent-incorporated specimens (mix 1B) shown by decrease of oxygen concentration toward the specimen surface as measured by oxygen microsensor techniques, but not in control specimens that did not contain healing agent (mix 1).
After Sierra-Beltran et al. (2014a).

The bacteria-based healing agent applied in these repair mortars was composed of spores of resistant bacterial spores of the genus *Bacillus* and calcium lactate plus trace amounts of yeast extract required for spore germination upon crack formation. One part of the active healing agent ingredients was loaded into porous silicate-based aggregates and another part encapsulated in a polylactic acid-derived polymer matrix (Mors and Jonkers, 2012).

The average compressive 28 days strength of control and healing agent-containing specimens was 39.8 and 38.5 MPa, respectively. Both types of mortars showed ductile behavior under flexural loading and produced multiple cracks prior to failure. The healing agent-containing mortar applied on aged-concrete substrate showed reduced delamination and sufficient bond strength in comparison to the control mortar, showing promising functionality and capacity for durable in situ repair actions (Sierra-Beltran et al., 2014a,b).

12.5.2 Practical applications biobased repair mortars

The PVA fiber- and bacterial healing agent-based repair mortar developed by Sierra-Beltran and coworkers was applied in several outdoor trials. One of the outdoor repair applications was done on a cracked and leaking underground basement wall, part of a parking garage in the East region of the Netherlands. Spalled concrete patches showed brownish discoloration indicating initial corrosion of the embedded-steel reinforcement. One of the problematic areas had already been treated several times previously with traditional repair mortar; however, repair was not durable as newly formed cracks showed continued leakage. Previous repair patches were therefore manually removed by chisel, including traces of bitumen applied previously for waterproofing of leaking cracks (Figure 12.10(a)). The mortar was applied in place without prior application of primer (Figure 12.10(b)). Four weeks and 6 months after repair the patch was checked, and no signs of debonding or spalling were visible, indicating that the repair was successful and durable (Figure 12.10(c)).

Another application was done in October 2014 on an aged tunnel, built in the late 1930s. A large patch affected by steel rebar corrosion and spalling was treated.

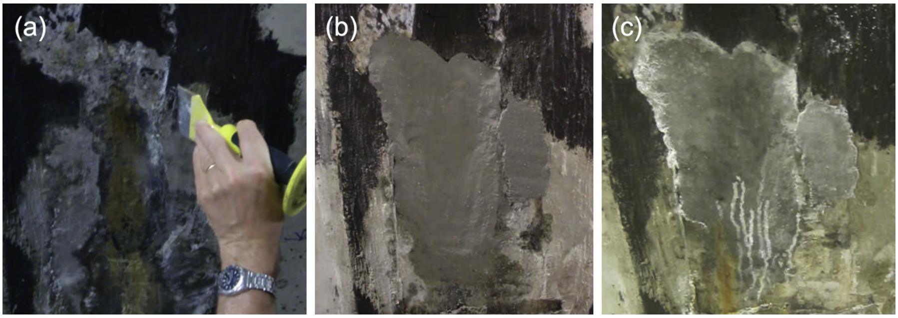

Figure 12.10 Self-healing bacteria-based repair mortar applied under moist conditions. (a) Surface preparations; (b) fresh repair patch directly after application; (c) repair patch one month after application, microcracks and limestone formation visible.
After Sierra-Beltran and Jonkers (2015).

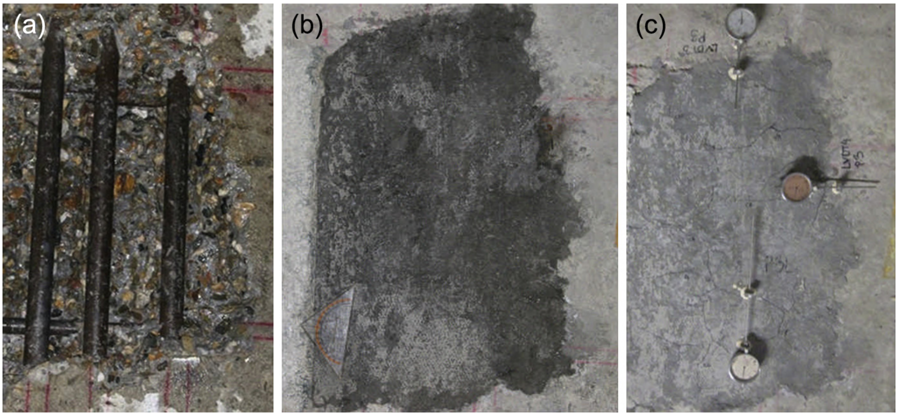

Figure 12.11 Self-healing mortar applied at an aged 80-year-old tunnel in the Netherlands. (a) Surface preparations; (b) fresh repair patch directly after application; (c) monitoring for shrinkage and possible delamination.
After Sierra-Beltran and Jonkers (2015).

Surface concrete was removed over an area of 25 × 50 × 11 cm, exposing the steel rebars. The rebars were cleaned from traces of corrosion prior to application of the bacteria-based repair mortar (Figure 12.11(a)). The PVA fiber- and bacteria-based healing agent-containing mortar was prepared on the site and immediately applied (Figure 12.11(b)). Directly after application the repaired patch was covered for seven days with wet geotextile to ensure proper curing. The durability of the repair was monitored during the following 2 months to check for possible cracking and delamination that could be expected due to restrained shrinkage of the fresh mortar applied on the aged-concrete substrate (Figure 12.11(c)). Only minor small shrinkage cracks but no delamination was observed indicating durable repair of this patch. However, ongoing monitoring is required to ensure that applied repair was indeed durable.

12.6 Conclusions and future trends

Microbially controlled precipitation of calcium carbonate for the benefit of improving the durability aspects of concrete has been developed based on primarily two different metabolic pathways. The first one makes use of urease active bacteria that during hydrolysis of urea produce both ammonium and carbonate ions. Although the latter ions promote precipitation of calcium carbonate for the benefit of improving concrete properties such as reducing permeability, waterproofing, and protection of the embedded steel reinforcement against corrosion, ammonium ions cause negative environmental effects such as health problems, eutrophication, and contamination of groundwater when not removed. The second metabolic pathway is based on heterotrophic bacteria that produce CO_2 that under alkaline conditions in the presence of calcium ions precipitates in the form of calcium carbonate. The latter metabolic pathway does not produce environmental harmful products such as ammonium. For practical full-scale outdoor concrete repair, the second heterotrophic pathway appears, therefore, more suitable for both environmental and economic reasons as no removal of excess ammonium is required.

The bacteria-based two-component liquid repair system discussed in Section 12.4, being composed of alkali-resistant bacteria of the genus *Bacillus*, diluted sodium silicate, sodium gluconate, calcium lactate or calcium nitrate, and some yeast extract, was used to successfully reduce water permeability of cracked parking decks. Applying the system can result in direct formation of a gel due to the chemical reaction of calcium and silicate ions present in solutions 1 and 2, respectively. In time, the gel is converted into limestone due to bacterial metabolic conversion of gluconate resulting in a permanent sealing of the cracks. The durability of this biobased repair technology is still under investigation as the in situ sealing effectiveness of the early 2015 treated parking decks will be monitored in subsequent years. Advantage of this novel biotechnological repair system is that no environmental unfriendly by-products such as excess ammonia are produced.

The development of bacteria-based self-healing repair mortar is still in its pioneering stage. Biotechnological applications such as bacteria that mediate the formation of calcium carbonate minerals that can improve the durability of repair mortars by reducing shrinkage, cracking, and debonding risks has so far been applied in only a few studies. However, results appear promising as laboratory results show good properties and initial outdoor field trials have so far been successful. Continued research and monitoring of applied patch repairs must be done to ensure that performance of such biotechnological mortars are indeed superior to traditional ones.

The cases discussed here, development and application of bacteria-based liquid repair systems and repair mortars for durable repair of concrete construction, do indicate that combining apparently unrelated fields of science, i.e., biotechnology and concrete technology, have potential. These may result in a series of truly new products which might, due to improved durability and sustainability properties, both save money and lower the environmental impacts of civil engineering activities.

Acknowledgments

This work has been financially supported by the Dutch Technology Foundation STW project number 11342 and Netherlands Enterprise Agency (Rijksdienst voor Ondernemend Nederland) project numbers IOP SHM01018 and IOP SHM012020.

References

Achal, V., Mukerjee, A., Reddy, M.S., 2013. Biogenic treatment improves the durability and remediates the cracks of concrete structures. Construction and Building Materials 48, 1–5.

Bang, S.S., Galinat, J.K., Ramakrishnan, V., 2001. Calcite precipitation induced by polyurethane-immobilized *Bacillus pasteurii*. Enzyme and Microbial Technology 28, 404–409.

Bentur, A., Mindness, S., 2007. Fibre Reinforced Cementitious Composites. Taylor and Francis, New York.

Couradeau, E., Benzerara, K., Gérard, E., Moreira, D., Bernard, S., Brown Jr., G.E., López-García, P., 2012. An early-branching microbialite cyanobacterium forms intracellular carbonates. Science 336, 459−462.

De Bruyn, S., Korteland, M., Markowska, A., Davidson, M., De Jong, F., Bles, M., Sevenster, M., 2010. Shadow Prices Handbook—Valuation and Weighting of Emissions and Environmental Impacts. CE Delft, Delft.

DeJong, J., Fritzges, M., Nüsslein, K., 2006. Microbially induced cementation to control sand response to undrained shear. Journal of Geotechnical and Geoenvironmental Engineering 132, 1381−1392.

De Muynck, W., Debrouwer, D., De Belie, N., Verstraete, W., 2008a. Bacterial carbonate precipitation improves the durability of cementitious materials. Cement and Concrete Research 38, 1005−1014.

De Muynck, W., Cox, K., De Belie, N., Verstraete, W., 2008b. Bacterial carbonate precipitation as an alternative surface treatment for concrete. Construction and Building Materials 22, 875−885.

Dick, J., DeWindt, W., DeGraef, B., Saveyn, H., VanderMeeren, P., DeBelie, N., Verstraete, W., 2006. Bio-deposition of a calcium carbonate layer on degraded limestone by *Bacillus* species. Biodegradation 17, 357−367.

Erez, J., 2003. The source of ions for biomineralization in foraminifera and their implications for paleoceanographic proxies. In: Dove, P.M., De Yoreo, J.J., Weiner, S. (Eds.), Reviews in Mineralogy and Geochemistry, vol. 54. Mineralogical Society of America, Washington, DC, pp. 115−149.

FAO, 1996. Control of Water Pollution from Agriculture. Irrigation and Drainage, Paper 55. Food and Agriculture Organization of the United Nations, Rome.

FHWA-RD-01-156, 2001. Corrosion Cost and Preventive Strategies in the United States. Report by CC Technologies Laboratories, Inc. to Federal Highway Administration (FHWA), Office of Infrastructure Research and Development.

Gollapudi, U.K., Knutson, C.L., Bang, S.S., Islam, M.R., 1995. A new method for controlling leaching through permeable channels. Chemosphere 30, 695−705.

Groot, W.J., Borén, T., 2010. Life cycle assessment of the manufacture of lactide and PLA biopolymers from sugarcane in Thailand. International Journal of Life Cycle Assessment 15 (9), 970−984.

Ivanov, V., Chu, J., 2008. Applications of microorganisms to geotechnical engineering for bioclogging and biocementation of soil in situ. Reviews in Environmental Science and Biotechnology 7, 139−153.

Jonkers, H.M., 2007. Self healing concrete: a biological approach. In: van der Zwaag, S. (Ed.), Self Healing Materials: An Alternative Approach to 20 Centuries of Materials Science. Springer, Dordrecht, The Netherlands, pp. 195−204.

Jonkers, H.M., Thijssen, A., Muyzer, G., Copuroglu, O., Schlangen, E., 2010. Application of bacteria as self-healing agent for the development of sustainable concrete. Ecological Engineering 36, 230−235.

Kim, H.K., Park, S.J., Han, J.I., Lee, H.K., 2013. Microbially mediated calcium carbonate precipitation on normal and lightweight concrete. Construction and Building Materials 38, 1073−1082.

Li, P., Qu, W., 2012. Microbial carbonate mineralization as an improvement method for durability of concrete structures. Advanced Materials Research 365, 280−286.

Ludwig, R., Al-Horani, F.A., deBeer, D., Jonkers, H.M., 2005. Photosynthesis-controlled calcification in a hypersaline microbial mat. Limnology and Oceanography 50 (6), 1836−1843.

Mors, R.M., Jonkers, H.M., 2012. Towards a bacteria-based agent to make concrete self-healing. imrc12-1488-7b-006 MRS Proceedings 1488. http://dx.doi.org/10.1557/opl.2012.1543.

Neville, A.M., 1996. "Properties of Concrete", Pearson Higher Education, fourth ed. Prentice Hall, New Jersey.

Okwadha, G., Li, J., 2011. Biocontainment of polychlorinated biphenyls (PCBs) on flat concrete surfaces by microbial carbonate precipitation. Journal of Environmental Management 92, 2860−2864.

van Paassen, L.A., Ghose, R., van der Linden, T.J.M., van der Star, W.R.L., van Loosdrecht, M.C.M., 2010a. Quantifying biomediated ground improvement by ureolysis: large-scale biogrout experiment. Journal of Geotechnical and Geoenvironmental Engineering 136, 1721−1728.

van Paassen, L.A., Daza, C.M., Staal, M., Sorokin, D.Y., van der Zon, W., van Loosdrecht, M.C.M., 2010b. Potential soil reinforcement by biological denitrification. Ecological Engineering 36, 168−175.

Qian, S., et al., 2009a. Self-healing behavior of strain hardening cementitious composites incorporating local waste materials. Cement & Concrete Composites 31, 613−621.

Qian, C., Wang, J., Wang, R., Cheng, L., 2009b. Corrosion protection of cement-based building materials by surface deposition of $CaCO_3$ by *Bacillus pasteurii*. Materials Science & Engineering, C 29 (4), 1273−1280.

Ramachandran, S.K., Ramakrishnan, V., Bang, S.S., 2001. Remediation of concrete using micro-organisms. ACI Materials Journal 98, 3−9.

Rodriguez-Navarro, C., Rodriguez-Gallego, M., BenChekroun, K., Gonzalez-Munoz, M.T., 2003. Conservation of ornamental stone by *Myxococcus xanthus*-induced carbonate biomineralization. Applied and Environmental Microbiology 69, 2182−2193.

Sangadji, S., Wiktor, V., Jonkers, H.M., Schlangen, E., 2013. Injecting a liquid bacteria-based repair system to make porous network concrete healed. In: Proceedings of the Fourth International Conference on Self-healing Materials ICSHM2013, Belgium—Ghent 16-20 June 2013, ISBN 9789082073713, pp. 118−122.

Sierra-Beltran, M.G., Jonkers, H.M., Schlangen, E., 2014a. Characterization of sustainable bio-based mortar for concrete repair. Construction and Building Materials 67, 344−352.

Sierra-Beltran, M.G., Jonkers, H.M., Schlangen, E., 2014b. Performance of SHCC with bacteria for concrete patch repair. In: Forde, M.C. (Ed.), Structural Fault and Repair, Proc. London, 6−8 July.

Sierra-Beltran, M.G., Jonkers, H.M., 2015. Crack self-healing technology based on bacteria. Journal of Ceramic Processing Research, Vol 16, Special. 1, pp.1s−7s.

Schlegel, H.G., 1993. General Microbiology, seventh ed. University Press, Cambridge.

Stocks-Fischer, S., Galinat, J.K., Bang, S.S., 1999. Microbiological precipitation of $CaCO_3$. Soil Biology and Biochemistry 31, 1563−1571.

Whiffin, V.S., van Paassen, L.A., Harkes, M.P., 2007. Microbial carbonate precipitation as a soil improvement technique. Geomicrobiology Journal 24 (5), 417−423.

White, S.R., Sottos, N.R., Geubelle, P.H., Moore, J.S., Kessler, M.R., Sriram, S.R., Brown, E.N., Viswanathan, S., 2001. Autonomic healing of polymer composites. Nature 409, 794−797.

Wiktor, V., Jonkers, H.M., 2014. Protection of aged concrete structures: application of bio-based impregnation system. In: AMS'14 Proceedings of the Int. Conference on Ageing of Materials & Structures Delft 26−28 May 2014, The Netherlands, pp. 295−301.

Wiktor, V., Jonkers, H.M., 2015. Field performance of bacteria-based repair system: pilot study in a parking garage. Case Studies in Construction Materials 2, 11−17.

Wiktor, V., Thijssen, A., Jonkers, H.M., 2012. Development of a liquid bio-based repair system for aged concrete structures. In: Alexander, et al. (Eds.), © 2012, Concrete Repair, Rehabilitation and Retrofitting III. Taylor & Francis Group, London, ISBN 978-0-415-89952-9, pp. 955−960.

Wiktor, V., Sangadji, S., Jonkers, H.M., Schlangen, E., 2013. Potential of bacteria-based repair solution as healing agent for porous network concrete. In: Proceedings of the Fourth International Conference on Self-healing Materials ICSHM2013, Belgium—Ghent 16−20 June 2013, ISBN 9789082073713, pp. 592−596.

Yang, Y., Lepech, M.D., Yang, E., Li, V.C., 2009. Autogenous healing of engineered cementitious composites under wet-dry cycles. Cement and Concrete Research 39, 382−390.

Zeebe, R.E., Wolf-Gladrow, D., 2001. CO_2 in Seawater: Equilibrium, Kimetics, Isotopes. Elsevier.

Zhou, J., 2011. Performance of Engineered Cementitious Composites for Concrete Repairs (PhD thesis). Delft University of Technology, Netherlands.

van der Zwaag, S., 2007. Self healing materials: an alternative approach to 20 centuries of materials science. Springer Series in Materials Science 100.

Rigid biofoam composites as eco-efficient construction materials

13

V. Chevali[1], *E. Kandare*[2]
[1]University of Southern Queensland, Toowoomba, QLD, Australia; [2]RMIT University, Melbourne, VIC, Australia

13.1 Introduction

Rigid foams are derived from a variety of metallic and nonmetallic sources, of which polymeric foams are the most common because they are relatively easy to formulate and their processing is less energy intensive. Polyurethane (PUR) foams can be flexible or rigid foams (Chevali et al., 2011; Fuqua et al., 2010a), and they often compete with expanded thermoplastics such as poly(ethylene), poly(propylene) and poly(acrylonitrile butadiene styrene). Biopolymer foams, including ethylene vinyl alcohol, poly(vinyl alcohol), poly(caprolactone), poly(lactic acid), poly(saccharide) and starch, are also gaining market share because of their low CO_2 footprint (Javadi et al., 2011).

PUR rigid foams are mostly derived from petrochemical resources and are leaving behind a substantial carbon footprint and increasing the demand for fossil fuel worldwide (Chevali et al., 2011). Today, the constituents of polymeric foams are scoped to be derived from biobased resources, the most common of which are functionalised, vegetable-oil-based reactants that are relatively benign and potentially biodegradable in comparison to their petrochemical counterparts (Petrović, 2008). These biobased microcellular foams are now rapidly replacing the traditional petrochemical or synthetic foams in many engineering applications. This chapter describes the state-of-the-art of rigid biofoams and their reinforced composites.

At the current annual growth rate of about 7%, the global foam market comprises flexible foams, rigid foams and semirigid integral skin foams, of which a 26% market share is attributed to rigid foams (Allport et al., 2003). The global foam market is expected to reach a value of about $62 million by the end of year 2018 (Anonymous, 2014). The building and construction industries are predicted to be major consumers of PUR foam in the near future with diverse applications such as sealants, thermal barriers and flooring. Whilst the growth and market share remains steady in Europe and North America, the Asia–Pacific region is projected to show high growth in the utilisation of polymeric foams (Anonymous, 2014).

Research and development is indicated as a key part in this progression, where companies, professional associations and associated stakeholders are making efforts to fuel

Biopolymers and Biotech Admixtures for Eco-Efficient Construction Materials. http://dx.doi.org/10.1016/B978-0-08-100214-8.00013-0
Copyright © 2016 Elsevier Ltd. All rights reserved.

future advancements and technology reforms (Anonymous, 2014). This transformation can be attributed to the feasibility offered by the PUR market economics, largely because of a beneficial cost-to-performance ratio.

The major source for biofoam constituents are vegetable oils whose renewable source is native to the particular geographical location, and whose selection is dependent on the relative abundance and availability. Additional reinforcement and additives in the biofoam systems are common for commercial applications where multifunctionality is a necessity. The biofoam systems can comprise biobased fillers and reinforcements that may effectively increase their resistance to moisture, fire, physical ageing or photo-oxidative degradation (Szycher, 2013).

The overall ecological impact of biofoams on the environment can be reduced by increasing the fraction of biodegradable constituents. However, replacing conventional materials with their biodegradable equivalents is a comprehensive and complex task. In addition to identifying and evaluating suitable alternatives, it takes a passionate effort to change the status quo on established materials that have been rigorously evaluated, certified and exhibit a testament to meeting performance requirements. Furthermore, there is always a great deal of resistance from the manufacturers of contemporary processing equipment and intermediate trade entities to maintain steady production schedules and achieve consistent product quality for their long-term sustainability. As such, the task is cut out for university-based researchers in collaboration with industry to work towards the transformation of the foam industry to accept biofoams as a viable alternative to synthetic or petrochemical-derived foams. Increasing availability and awareness of biodegradability incentives, and tax and environmental credits from federal governments across the world, are fostering change concerning builders and foam producers to direct emphasis and effort in developing biofoams for the construction industry.

The main applications of rigid biofoams are in abating noise and absorbing energy during a mechanical input. Rigid foams work with the basic principle of creating a network of closed cells through which density is reduced, as the bulk is replaced by air pockets. The cell density determines the degree of foam rigidity. For example, polyurethane foams with densities ranging between 8 and 320 kg/m^3 are dimensionally stable, whilst foams exhibiting densities lower than 24 kg/m^3 show negligible dimensional stability (Szycher, 2013) and hence may be regarded as flexible foams.

During processing, a volume of cells is constricted to a constant thickness. Based on the available volume and the foaming characteristics of the foam, the foam density can somewhat be predicted. Hence, the ratio of the skeleton density to the foam density (Gibson and Ashby, 2010) in the solidified part is critical in determining the properties, and thereby the possible end application.

Originally manufactured for use as core panels in sandwich composites, lightweight rigid foams can greatly reduce the overall weight whilst ensuring increased bending stiffness. Upon compression or bending, the foam structure resists deformation through a collapsing network of open cells (Chevali et al., 2011). Hence, even with a great reduction in the thickness through cell compression, a loaded foam structure retains its stiffness.

Properties of biofoams and their composites can be attributed to the constituent properties and the design philosophy, specifically materials selection. The following sections provide a critical analysis of current literature and case studies in the development and application of rigid biofoams.

13.2 Rigid foams

The development of lightweight dimensionally stable or structural materials is a topic of interest in the transportation industry, where a reduction in vehicle weight improves the fuel efficiency whilst reducing CO_2 emissions. One option available to the materials scientist to achieve this objective is the utilisation of rigid foams in developing lightweight structures. However, the majority of precursor materials for making rigid foam are derived from a finite resource—petroleum oil. In the past decade, there has been growing interest in replacing petroleum-based rigid foam precursors with those derived from natural and renewable resources (Lligadas et al., 2013; Pfister et al., 2011; Raquez et al., 2010; Seniha Güner et al., 2006).

Vegetable oil-derived polyols have so far been the preferred choice in the development of environmentally benign rigid composite polyurethane foams. However, before vegetable oils can be used in developing rigid foams, they need to be modified in order to increase their hydroxyl value (Petrović, 2008). Synthesis routes involving the hydroxylation of the carbon—carbon double bonds or alcoholysis of vegetable oils to produce mono-, di- and triglycerides are commonly used. The hydroxylation of the carbon—carbon double bonds or alcoholysis increases the hydroxyl group concentration, and hence the cross-linking density and the rigidity of the resultant foam. This section is dedicated to reviewing research efforts focused on the development of biobased rigid foams.

Rigid foam prepolymers require a highly functional polyalcohol of functionality greater than 3. A pre-polymer may be employed in the formation of a polyurethane with a polyol and an isocyanate content lower than 12 wt%. However, when the isocyanate content exceeds 25 wt%, the mixture is termed a quasi-prepolymer that features low viscosity. The quasi-prepolymer technique is a combination of the pre-polymer and one-step technique in which a polyol is mixed with diisocyanate in the first component, and water, amine and additives are mixed with a polyol in the second component. For the processing of rigid foams, the aforementioned components are often mixed in equal volumes.

Biofoams produced using pre-polymer methods are shock absorbent and moisture resistant. Biofoams formulated using a vegetable oil can constitute rigid or semi-rigid foam systems; however, use in semi-rigid and energy-absorbing applications such as packaging is a major avenue for utilisation of these systems (Szycher, 2013). The nature of castor oil foams, for example, is temperature dependent as they are rigid at temperatures lower than room conditions and pliable at higher temperatures, limiting their usage in structural applications. In addition, they exhibit shrinkage during processing that is otherwise mitigated with the dispersion of elastic particulates, such as silica.

13.2.1 Foam chemistry

PUR is the most common foam compound obtained from vegetable oil-based precursors. The PUR foam reaction proceeds by the interaction between a diol or a triol, commonly classified as a polyol, with an isocyanate in the presence of a blowing agent, a surfactant and necessary additives. The reaction ensues with the formation of carbon dioxide, which promotes the blowing action and the formation of a cellular network with polyurea/polyurethane linkages. A typical PUR reaction involving a castor oil-based fatty acid is shown in Figure 13.1.

In the PUR reaction, the degree of polymerisation of 50 is expected to produce a high conversion/yield to meet or exceed a threshold value for mechanical properties. The chemical composition and associated variables dictate the load bearing properties of the developed biofoam. High isocyanate fraction, high functionality of the isocyanate (Lim et al., 2008) and higher triol concentration are beneficial for obtaining a structurally effective foam.

Nonconventional synthesis routes are now commonplace for polyurethane production (Guan et al., 2011), including nonisocyanate routes (Türünç et al., 2008; Figovsky, 2000; Lee and Deng, 2015). These methods include the ring opening of cyclic carbonates with amines, producing urethane bonds, as shown in Figure 13.2. PUR foams produced using this method possess higher thermal stability over isocynate-derived ones. Overall, as a result of the elimination of isocynate, this route also possesses a low toxicity potential for the development of PUR (Kreye et al., 2013; Benyahya et al., 2011).

The PUR foam thus obtained is essentially a segmented polymer where the isocyanate and polyol cause the formation of rigid and soft segments, respectively. The higher fraction of isocyanate leads to greater rigidity as a result of a greater number of rigid domains formed during the foaming reaction.

13.2.2 Isocyanate

Isocyanates are used in the form of methylene diisocyanate (MDI) and polymethylene polyphenyl diisocyanate (PMDI), with rigid foam applications being the largest consumer of MDIs in the recent past (Anonymous, 2015b). Isocyanates, upon the

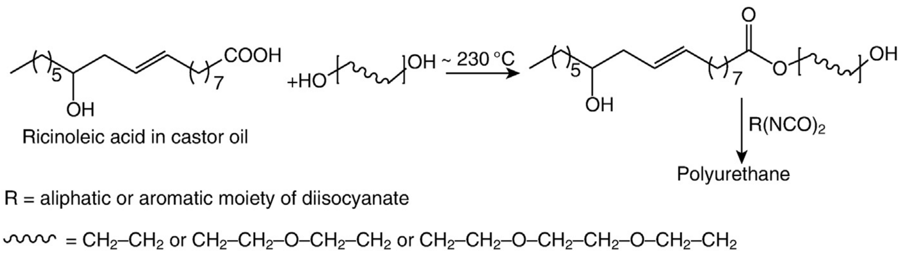

Figure 13.1 A chemical reaction schematic for the production of PUR foam from a castor oil polyol and diisocyanate reactants.
Reprinted with permission from Karak (2012).

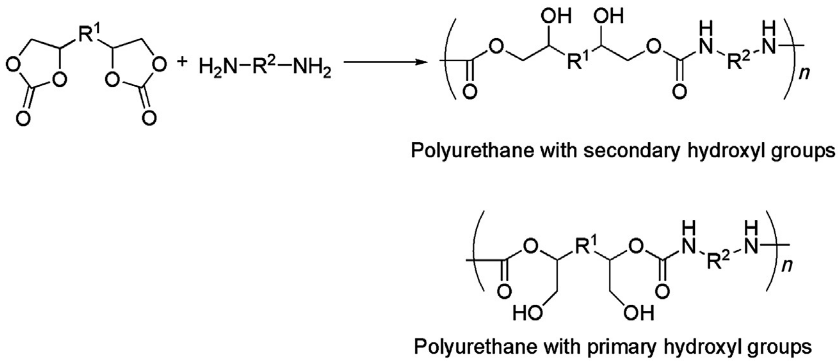

Figure 13.2 A non-isocyanate route for the synthesis of PUR foams with secondary and primary hydroxyl groups.
Reprinted with permission from Tomita et al. (2001).

action of water, release CO_2 that facilitates the formation of a microcellular foam. In addition, as a polyfunctional reactant, PMDI enables the polyol linkages through interaction with hydroxyl groups, gradually establishing a cross-linked polymer through the formation of polyurea or polyurethane linkages, which controls the rigidity and thermal resistance of rigid foams. Often, the usage of high-activity isocyanates is restricted because of their scorching potential, and instead lower assay isocyanates are used for a one-step and relatively more cost-effective rigid foam formulation.

Within the isocyanates, aromatic tri-isocyanates often result in higher-density foam, higher glass transition temperature and ultimately higher mechanical properties in comparison to aliphatic isocyanates, which produce foams with enhanced ductility. Maintaining the stoichiometric ratio of carbonate to amine group in the formulations often is suitable for engineering applications.

Isocyanates, however, bear the risk of a violent reaction with water and creation of toxic methyl amine gas, which was attributed as the root cause of the 1984 Bhopal Gas Tragedy (Varma and Guest, 1993). The impetus to produce sustainable, ecofriendly isocynates has been well explored (Kreye et al., 2013). Some of these syntheses include reductive carbonylation of nitro arenes (Le and Ganem, 2011, 2003) and oxidation of isocyanides to isocyanates using dimethyl sulfoxide in the presence of trifluroacetic anhydride (Paul, 2000; Kreye et al., 2013).

13.2.3 Polyol

The hydroxyl group-carrying compound also dictates the properties of urethane polymer, which is the polyol. The increased exploration of biobased polyols to achieve ecofriendly materials can be attributed to the limited selection of MDIs. Three predominant sources of hydroxyl bearing chemicals are polyethers, polyesters and vegetable oils with hydroxyl groups. The polyethers and polyesters are largely synthetic petrochemical-based chemicals.

13.2.3.1 Synthetic polyols

Polyethers assume high importance within these three classes of compounds. Polyethers with high functionality are derivatives of alcohol containing groups such as glycerine or sorbitol (Szycher, 2013).

The hydroxyl number of polyols required for rigid foams ranges from 350 to 600. Polyesters are obtained from dibasic acids such as adipic acid and currently restricted to use in foam laminates as polyethers become increasingly ubiquitous. Nevertheless, the polyol component determines the foam density, ductility and permeability to common gases and solvents. It is important to note that rigid foams are obtained from lower molecular weight resins with high degree of branching. A thorough analysis of the equivalent weight, functionality and rigidity of the chain units is critical in understanding the polymeric foam properties.

Polyol characteristics, such as the equivalent weight and functionality, define the characteristics of the rigid foam. Higher heat is generated as the equivalent weight of polyol decreases and hence it is important to monitor this property to preclude excessive heat up and scorching of the foam when processing. The functionality of polyols also bears an effect on heat resistance and dimensional stability inasmuch as these properties increase with the functionality, albeit with a trade-off in decreasing flexibility.

Polyethers cause the formation of foams with higher resilience and resistance to hydrolysis over polyesters, which feature a higher resistance to oil, solvent or oxidative action. With higher cross-linking in either of the synthetic polyols, the elastic modulus and glass transition temperature of the foam increase, however, with a decrease in strain to failure and overall flexibility of the foam.

The polyether polyol in the presence of isocyanate and chlorofluorocarbon can be often achieved as a low-density foam, which is used for sound abating applications. Polyether-based polyols are relatively inexpensive, possess a narrow molecular weight distribution and have low chemical resistance but high stability towards hydrolytic attack. Polyesters are often used in hydroxyl-terminated varieties and often are based on adipic acid or diethylene glycol. Polyester polyols can be formulated from halogenated dibasic acids to gain fire resistance without the need for additives.

13.2.3.2 Biobased polyols

Biofoams are obtained from polyols obtained from vegetable oils such as soybean oil (Banik and Sain, 2008; Beltrán and Boyacá, 2011; Fan et al., 2012, 2013; Ji et al., 2015a,b; Luo et al., 2011, 2012, 2013; Tan et al., 2011; Yu et al., 2012; Zhu et al., 2012), castor oil (Corcuera et al., 2010; Lin et al., 2013; Ristić et al., 2012; Wang et al., 2008; Zhang et al., 2014) and palm oils (Ang et al., 2014; Arniza et al., 2015; Chuayjuljit et al., 2010; Farhana et al., 2014; Kalita et al., 2015; Septevani et al., 2015), and rapeseed oil (Cabulis et al., 2014; Gaidukov et al., 2013; Kairyte and Vejelis, 2015; Kirpluks et al., 2013; Rojek and Prociak, 2012; Stirna et al., 2014; Zieleniewska et al., 2015). Additional sources of vegetable oils include tung oil (Mosiewicki et al., 2009; Ribeiro Da Silva et al., 2013a), tannin (Celzard et al., 2013; Čop et al., 2015; Link et al., 2011; Martinez de Yuso et al., 2014; Zhou et al., 2013), which are relatively emergent in comparison.

For biofoam polyols, triglycerides act as reactive species, which grow the hydroxyl groups through (a) hydroxylation of carbon–carbon double bond, (b) alcoholysis of triglyceride or (c) esterification of fatty acid/glycerol to form a monoglyceride. An example of a functionalised vegetable oil is the acrylated epoxidised soybean oil (Lu et al., 2005), which is derived using the reaction scheme as outlined in Figure 13.3.

In spite of major momentum in the synthesis of vegetable oil-based polyols, there has been a lack of commercialisation at an equivalent rate. However, commercially available soy polyols for PUR systems are increasing in number and are shown in Table 13.1. Biopolyols obtained from vegetable can be cost-effective in synthesis; however, the postsynthesis purification and homogenisation of the chemicals often is an added cost (Petrović, 2008).

A growing list of key chemical companies is now investing in green or biobased polyols for major engineering application areas including automotive and building and construction. The formulations vary vastly depending on the end-use application. Overall, polyols with induced higher functionality and higher hydroxyl content can be surmised to produce foams with higher compressive or tensile properties and increased elongation.

Mazzon et al. (2015) reported the synthesis of a new generation of highly reactive epoxy foams by using hybrid mixtures of epoxidised-plant-oil derivatives—namely, linseed oil (ELO) or glycerol (EG) together with a cycloaliphatic amine hardener, isophorone diamine (IPDA) and a foaming agent sodium bicarbonate ($NaHCO_3$).

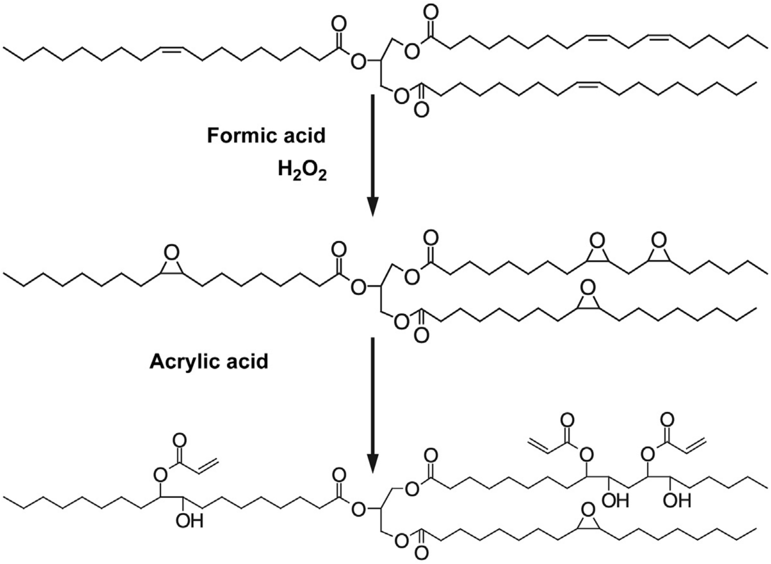

Figure 13.3 Acrylated epoxidised soybean oil synthesised from soybean oil triglyceride through formication to produce epoxidised soybean oil (ESO), which is acrylated to form acrylated epoxidised soybean oil (AESO).
Reprinted with permission from Lu et al. (2005).

Table 13.1 **A list of commercially available biobased polyols and their key properties (Nodelman et al., 2011; Muller et al., 2009; Anonymous, 2015a)**

Grade	Hydroxyl value (mg KOH/g)	Functionality (eq_{OH}/mol)	Density $(g/cm)^3$	Viscosity at 25 °C (mPa·s)
Lupranol Balance 50	50	2.7	0.99	650–800
Agrol 2.0	65–75	1.7	0.96	233
Agrol 3.6	107–117	3	0.98	720
Agrol 4.3	125–137	3.6	0.98	1320
Agrol 5.6	151–170	50	0.99	4770
X-0210	235	4.4	1.01	8900
Voranol 490	475–510	4.3	1.11	5500–6600
HB-150	140–160	2	–	140
HB-230	220–240	2	–	375
HB-230M	225–250	2	–	4000

The authors optimised the chemical formulation of this reactive mixture by integrating varied chemical additives to control the exothermicity of the curing reaction. When epoxidised glycerol and linseed oil were used as precursors in the ratio 9:1, a rigid biofoam with an apparent density of 0.17 g/cm^3 and glass transition temperature of 48 °C was produced in 3 min. In addition to increasing the 'green' credentials of rigid foams, the measured T_g values were comparable to those obtained when synthetic polyols are used. The hybrid foam containing equal weight fractions of ELO and EG retained more than 50% of its room-temperature modulus of elasticity at temperatures as high as 50 °C, demonstrating potential application of the developed material in tertiary engineering structures.

Rigid polyurethane foam exhibiting properties similar to those used in commercial thermal insulation foam and prepared from modified soybean and castor oil was reported by Veronese et al. (2011). The authors performed transesterification on formicated soy polyol and castor oil in order to increase the number of hydroxyl functional groups. The resultant foams had apparent densities of 50 kg/m^3, an average through-thickness Young's modulus greater than 3 MPa and through-thickness yield strength above 150 kPa. Whilst the measured mechanical response of the rigid foams prepared using vegetable oil was inferior to that exhibited by foams containing synthetic polyols, these research findings confirmed the potential viability of using vegetable oils as alternate and renewable polyol sources.

Zieleniewska et al. (2015) fabricated rigid polyurethane foams using rapeseed oil-based and/or petrochemical-derived polyols. Prior to the fabrication of the rigid foams, rapeseed oil was epoxidised using peracetic acid generated in situ following the reaction of H_2O_2 and glacial acetic acid at 60 °C in the presence of H_2SO_4 as a catalyst. The authors then converted the epoxidised oil into polyols using diethylene glycol. The progressive replacement of commercial polyol, Rokopol G500, within the polyols premix with its rapeseed-derived counterpart did not alter the apparent density of the fabricated hybrid foam. The hybrid foams exhibited relatively high glass transition temperatures in the range 80−90 °C. The premix containing 50% by weight of rapeseed oil-derived polyol was considered optimal when environmental friendliness and application requirements were considered. The premix with 1:1 ratio of commercial and biobased polyols represented the highest renewable constituent content with the preservation of compressive strength (>750 and 600 kPa in the parallel and perpendicular dimensions, respectively), water absorption, dimensional stability, high ageing resistance and low friability.

13.3 Foam processing

Selection of polyol based on molecular weight is dictated by the end use. Higher molecular weight polyols are chosen for semirigid or flexible foams, whereas short-chain polyols are pursued for rigid foam preparation.

For rigid foams, closed cells are designed and the foam system is formulated to limit breakage in cell walls. To preclude gas contraction-initiated shrinkage, chemical formulation becomes a key consideration, and higher cross-linking at the initial stages of the reaction is amenable to this effect. In addition, excess isocyanate is used to increase dimensional stability, albeit at the cost of ductility.

Blowing agents compatible with the hydroxyl group of a vegetable oil are used in processing, which governs the mechanical properties to an extent. The selection criteria for blowing agents include their thermodynamic properties, suitability of use in a particular processing technique, and the targeted application. The amount of water in the reaction mixture also affects the rate of stiffening of the domains, and hence the formation of rigid cells. A surfactant may also be used to assist the mixing of the various components and a resultant uniform distribution of the cells.

The temperature of the reaction mixture is another critical variable in processing design, as the modulus of the foam is a result of the temperature of the reaction, which controls the evolution and growth of bubbles, fill rate of bubble/fluid foam, phase separation and cell opening and curing (Szycher, 2013).

13.3.1 Reaction injection moulding

Reaction injection moulding (RIM) traditionally offers benefits in high flexural modulus foams, achievable light weight and low tooling costs, along with part size flexibility. In addition, a range of shapes and forms for automotive to commodity areas can be processed using this method.

The RIM method (Figure 13.4) consists of a PUR processing system of tanks with the precursor chemicals that are gravity fed using a metering device to a mixing

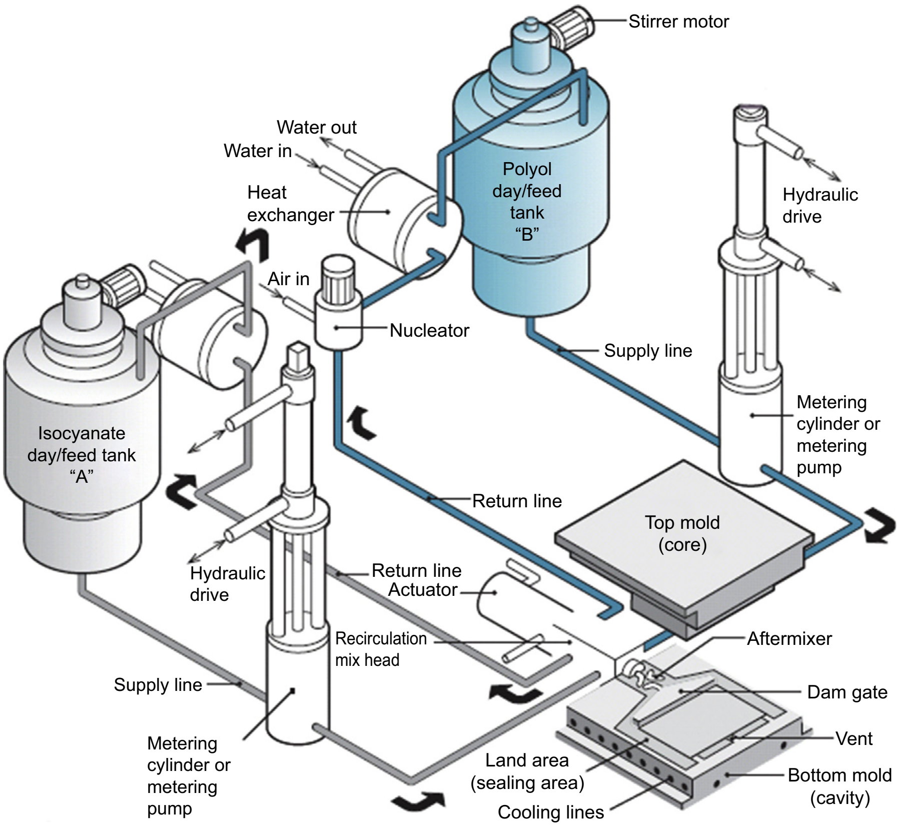

Figure 13.4 A drawing of PUR foam system production at an industrial level is shown in this schematic with the major components in the foam reaction and moulding section.
Courtesy of Shanghai New Product Technologies Ltd.

head. The materials can be filtered or gauged, and the flow can be controlled. The mixing and dispensing occurs through the mixing head, and the temperature is subsequently controlled via a heat exchanger.

A mixing head allows the chemicals to be mixed at high pressures through an impingement action, which starts the reaction. The reaction mixture is then deposited in a mould, following which a scraper removes all of the mixture to prevent contamination for the next batch. For a mixing head, the selection demands knowledge of recirculation and impingement capabilities, and the size requirement for housing in a production environment. In addition, the viscosity and temperature of the precursor chemicals should also be maintained to allow seamless production.

The reaction mixture is then poured into the mould and allowed to cure for a specific period of time before demoulding. It is critical to understand the hot tear strength of the foams to insure that the foam part is demoulded from the system without disintegration. The moulds for foam production can be chosen from steel, aluminium, zinc alloys and other constructions; regardless, these materials should be polished to a mirror finish and usually a quality check should be performed every 100,000 cycles to ensure high part quality.

The temperature control also plays a critical part in the RIM process, whereas the moulds require to be at 70 °C for certain systems. In addition, a mould parting agent may be required for easy peel-off of the foam when the reaction is complete. In terms of occupational health guidelines, it is advisable to use well-ventilated facilities to mitigate occupational health risks.

13.4 Foam morphology and characterisation

The morphology of free rise foams and fibre-filled foam systems can be closely analysed using electron microscopy imaging (Kuranska and Prociak, 2012; Luo et al., 2013). An example of the closed cellular network and lignin-filled foam (Luo et al., 2013) is shown in Figure 13.5. The open cell structures cause challenges in moisture resistance and may show dilatation upon solvent intake. To a great extent, the majority of foam properties are directly related to the foam density and these properties can be tailored through density variations (Szycher, 2013). The polyol equivalent weight, the cross-linking extent and surfactant levels have an influence of the closed cell fraction, which in turn defines the mechanical properties. A comprehensive list of constituents and their corresponding effects can be found in Michael (2012).

Density and hardness are often used for benchmarking polymeric foams. The density of a foam is the result of the foam kinetics and the water/blowing agent content; the hardness, on the other hand, is a consequence of the hard segments of the rigid foam system that arise from the MDI content. The hardness of the foam increases with a ratio of polyol to MDI ratio of 1:1 to 1:1.15, at which point the critical hardness is reached and there is no further effect on the hardness with increasing MDI content. The thermal conductivity of the voids in the cell walls is lower than ambient air; however, in use, the cell wall conductivity may approach that of the ambient air as a steady state is reached.

13.4.1 Chemical characterisation

Fourier transform infrared spectroscopy (FTIR) is an effective tool in determining the surface chemical composition of rigid foams. The absorbance of a sample to an incident infrared spectrum in the range of 900 to 3600 cm^{-1} constitutes the analysis. The major bands and their significance are shown in Table 13.2. The FTIR in the embodiment of diffuse reflectance or attenuated total reflectance FTIR can be used to determine the correlation between temperature gradients generated during the processing with gradients in chemical constitution in the foam dimensions. FTIR can also effectively highlight incomplete polymerisation when compared with a standard sample.

Scanning electron microscopy and optical microscopy can be valuable in imaging the cellular structure of foams and are useful also in understanding the failure modes in

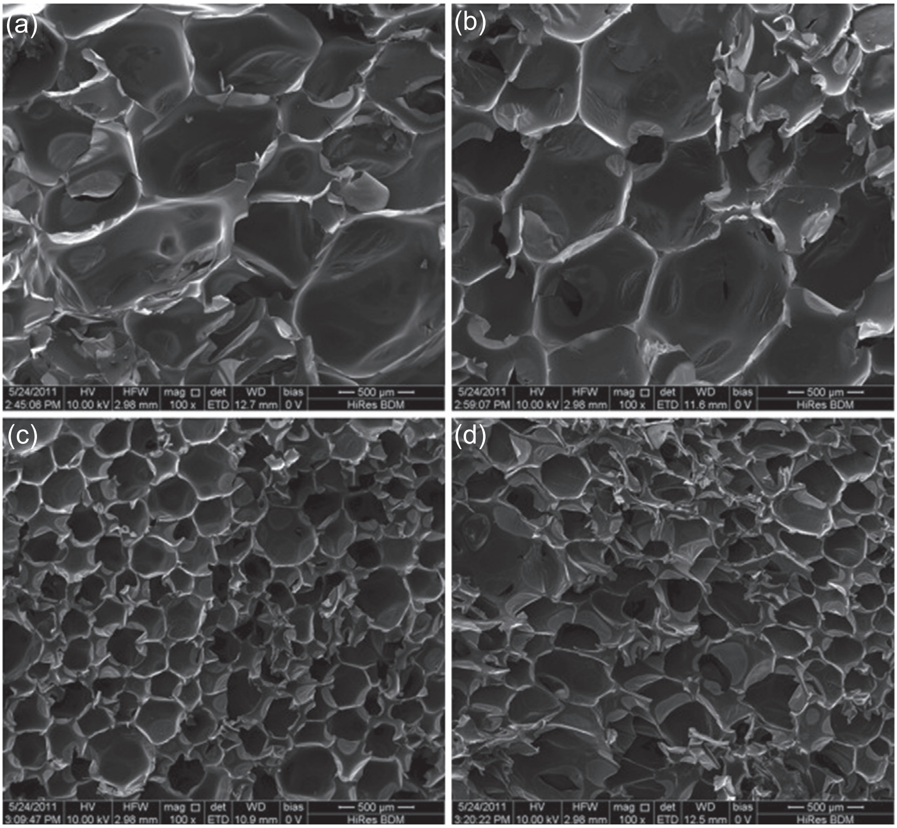

Figure 13.5 Electron microscopy images of (a) neat biofoam, (b) with 5 wt% lignin, (c) with 10 wt% lignin and (d) 15 wt% lignin.
Reprinted with permission from Luo et al. (2013).

foams or their composites. Phenomenon such as cell wall crazing can be well mapped using advanced electron microscopy techniques.

13.4.2 Mechanical characterisation

The physical properties and geometrical aspects of the cells dictate the overall mechanical properties of the foams, which may be customised to a specific relative density, cell size and edge connectivity (Hollaway, 1993). Relative density is the ratio of foam density to the solid fraction of the foam (ρ_f/ρ_s), and this ratio forms the basis of several theoretical models of foams, including the compressive strength, energy absorption, thermal conductivity and collapse strength of the foams. The Ashby—Gibson model for the elastic modulus foam is shown in Eqn (13.1) and the relationship for shear modulus is shown in Eqn (13.2) (Saint-Michel et al., 2006). In this equation, a shape factor ϕ governs the mechanical properties.

Table 13.2 **A list of chemical structure as function of FTIR absorbance (Szycher, 2013)**

	Absorbance (Cm^{-1})
Aliphatic amine	1280, 1180
Aromatic amine	1350, 1250
−NH stretching (urethane)	3349
−NH−COO− (urethane)	1680, 1650, 1640, 1610
−N=C=O (diisocyanate)	2275, 2250, 1350
C=C (aromatic)	800, 1610, 1500
−OH (hydroxyl)	3200, 3400
C−O−C (ether)	1150, 1070, 1062
−CH vibration	2900
−NH	1703−1699
−CN	1519
−CN−CO stretching	1174
−C=O	1020

$$\frac{E_{\mathrm{f}}}{E_{\mathrm{s}}} \approx \phi^2\left(\frac{\rho_{\mathrm{f}}}{\rho_{\mathrm{s}}}\right) + (1-\phi)\frac{\rho_{\mathrm{f}}}{\rho_{\mathrm{s}}} + \frac{\rho_0(1-2\nu_{\mathrm{f}})}{E_s(1-\rho_{\mathrm{f}}/\rho_{\mathrm{s}})} \tag{13.1}$$

$$\frac{G_{\mathrm{f}}}{G_{\mathrm{s}}} \approx \phi^2\left(\frac{\rho_{\mathrm{f}}}{\rho_{\mathrm{s}}}\right) + (1-\phi)\frac{\rho_{\mathrm{f}}}{\rho_{\mathrm{s}}} \tag{13.2}$$

where subscripts f and s refer to the foam and skeleton, E refers to the Young's modulus, G refers to the shear modulus and ν is the Poisson's ratio.

Under a deformational compressive load, foams exhibit several stages of progressive response, as shown in Figure 13.6. The strain proceeds as a linear elastic until the yield point, where it transitions into a plateau region and eventually reaches a stage where further deformation is possible only through cell densification and ultimately failure.

13.4.2.1 Compression

Compression in rigid foams is a result of Euler buckling in and out of plane deformation. The Poisson's ratio indicates the lateral versus longitudinal deformation characteristics of the foam.

The compressive properties are determined using ASTM C365 (Fam and Sharaf, 2010), where the compressive properties are tested in the thickness direction

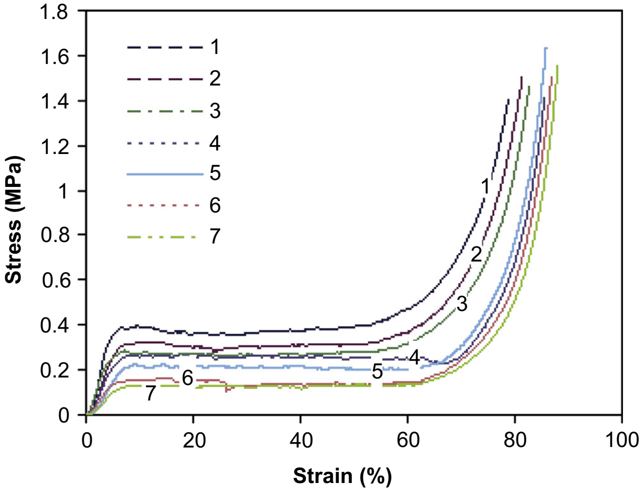

Figure 13.6 Typical stress-strain graph of foams showing the various regions of progressive deformation and failure for foams with different bulk densities.
Reprinted with permission from Martinez de Yuso et al. (2014).

(out-of-plane) and in the width direction as the in-plane direction. The compressive stress is the recorded and reported failure value under 10% strain; otherwise, the strength is reported corresponding to a load value at 10% strain.

13.4.2.2 Tension

Tension in rigid foams can lead to crack initiation and growth under a 5% strain where the foam exhibits tearing (Hollaway, 1993). In tension as well, the Poisson's ratio of the foam indicates the expansion of the foam in the in-plane and axial deformation. The specimen is often bonded to steel blocks for testing.

13.4.2.3 Bending

Bending in rigid foams follows the theory of neutral axis where the moments in the planes below the neutral axis are tensile and those above are compressive in nature. Bending in foams follows a thickness to width ratio of 1:16 or 1:32. However, a three-point bending apparatus may be insufficient for the testing of foams in flexure. A four-point bending apparatus is used for determining the flexural strength and modulus of a foam.

Failure in bending occurs through crack formation in the tensile (outer) fibre, and through cell densification and collapse in the compressive (load) fibre. For foams of high rigidity, a three-point bending method can be used if the failure strain is low (<5%). However, for low-rigidity foams that fail beyond the 5% strain, a four-point bending method is used. The stress and strain equations associated with the three- and four-point bending test methods are compared in Table 13.3. The flexural secant modulus of elasticity is the ratio of stress to corresponding strain at any given point on the stress—strain curve.

Table 13.3 **Mechanical properties in three-point and four-point bending tests (ASTM International, 2012)**

Method	Stress (MPa)	Maximum strain (mm/mm)	Secant modulus (GPa)
Three-point bending	$\frac{3PL}{2bh^2}$	$\frac{6\delta h}{L^2}$	$\frac{L^3 m}{4bh^3}$
Four-point bending	$\frac{3PL}{4bh^2}$	$\frac{4.36\delta h}{L^2}$	$\frac{0.17L^3 m}{4bh^3}$

13.4.2.4 Shear

The shear properties of rigid foams in correlation to the end application can be in-plane shear, twisting shear or interlaminar shear. In-plane shear corresponds to shear deformation constricted within the composite material, whereas twisting shear corresponds to the distortion seen in a bar or thin section of the material. The interlaminar shear, more common for composite materials, is the deformation normal to the plane of the section.

The common method of measuring the shear properties follows the ASTM C273, where a deflection is recorded against an applied load and translated into a shear stress and a shear strain (Fam and Sharaf, 2010). A complete list of testing standards can be found in ASTM D1623-09 standard (ASTM International, 2009).

13.5 Rigid foam composites

Rigid foam composites often comprise a rigid foam system, a divergent range of additives and a fibre/reinforcement whose surface is functionalised to be compatible with the polymeric foam. In the alternative embodiment, rigid foams can simply be sectioned into slabs of desired thickness and used as cores for sandwich composites applications.

For use with a low-aspect-ratio filler/additive/fibre, the intended use is a foam as a standalone entity, such as a backing for sporting floors or insulative walls. In many engineering applications, a nanoscale additive or a functional additive such as a fire retardant may be utilised (Chevali et al., 2011). Alternatively, a chopped fibre mat may be used for providing a framework for the expanding foam to provide structural rigidity, given that the cell size is lower than the inter-fibre distance and the cellular foam can penetrate around these fibres.

An average aspect ratio fibre may be added to the foam if impact properties are targeted for improvement. Longer fibres and reinforcements are often reserved for high-performance applications and as sandwich composite facesheets or veneers.

Short or particulate additives and fillers influence the foaming behaviour and increase the cell density as they create constricted spaces between the fibres. Inorganic additives, such as layered silicates, modify the reaction mixture viscosity and hence the foaming behaviour. Lignocellulosic fillers and short fibres, on the other hand, cause secondary reactions because of their nucleation-friendly size, residual moisture and chemical makeup, ultimately resulting in increased density.

Overall, the presence of these fibres and fillers is favourable in gaining higher compressive strength. In addition, the damping behaviour is improved in comparison to neat foams as evidenced by a broadening tan δ peak. The thermal stability and glass transition temperature also increase with the addition of a filler/fibre in biofoams. The inherent flammability of the foams is relieved by addition of flame retardant additives such as boric/phosphoric acid particulates.

The foam composites with long or continuous fibres provide benefits similar to the short fibres, albeit with greater gains in mechanical property improvements. The reaction mixture may require additional adjustment in case of a woven or advanced architecture because the foam structure is required to penetrate fibre tows, which may provide resistance and prevent full fibre/foam consolidation.

Numerous researchers have investigated the inclusion of particles and/or fibres in polyurethane foams in order to provide structural reinforcement (Azmi et al., 2013; Fuqua et al., 2010b; Garcia et al., 2008; Gu and Sain, 2013; Sharma and Sripathy, 2012; Xue et al., 2014; Yu et al., 2015; Zhu et al., 2012). The reinforcement fillers come in various shapes and sizes (Chuayjuljit et al., 2010; Gaidukov et al., 2013; Palanisamy, 2013; Türünç et al., 2008) ranging from nanosized inclusions such as nanoclays, carbon-based nanomaterials, nanocellulosic fibres and inorganic nanomaterials to continuous fibres including glass, carbon and natural fibres.

Natural fibres especially are pitted to be combined with renewable vegetable oil polyol because of the added potential of biodegradability (Chevali et al., 2011). Natural fibres include flax (Kuranska and Prociak, 2012; Fuqua et al., 2010b), hemp (Ristić et al., 2012; Yu et al., 2012; Aranguren et al., 2007), kenaf (Munusamy et al., 2012) and sisal (Wu et al., 2009). Particulate natural fibres also add value to foams in the composite form. Key particulate filler sources include rice husk (Ribeiro Da Silva et al., 2013a,b) and microscale cellulose and lignin (Faruk et al., 2014; Lin et al., 2013; Luo et al., 2011, 2012; Zhu et al., 2012). A list of key natural fibres and their reinforcement ability can be found in Table 13.4. The reader is referred to Sain and Faruk (2015) for a detailed list of critical aspects of using natural fibres for composite applications. This section presents research findings related to strategies adopted in order to enhance the rigidity/structural properties of foams.

Zhu et al. (2012) reported on properties of soy-based polyurethane matrix reinforced by cellulose microfibres and nanoclays. Whilst the integration of cellulose microfibres at concentrations between 0.5 and 2.0 per hundred parts (php) had no significant effect on the foam density, the inclusion of nanoclays generally increased the foam density. The incorporation of microfibres or nanoclays resulted in the reduction in cell size and the fraction of large cells within the foam. Combined, the decrease in average cell size and increase in the number of cells per unit volume resulted in increased compression strength. The profound reinforcing effect revealed following the incorporation of cellulose microfibres or nanoclays demonstrates inherent strengthening characteristics of the fillers, strong interfacial adhesion between the filler and matrix and/or uniform dispersion of filler particles.

Table 13.4 Lignocellulosic fibres and their physical/mechanical properties

Fibre	Density (g/cm^3)	Length (mm)	Diameter (μm)	Strain at break (%)	Tensile strength (MPa)	Young's modulus (GPa)	Specific strength (MPa)	Specific modulus (GPa)	Moisture content (%)	2015 Price (per kg) (USD)
Cotton	1.21	15–56	12–35	2–10	287–597	6–10	194–452	4–6.5	33–34	~$1.5–$2.2
Jute	1.23	0.8–6	5–25	1.5–3.1	187–773	20–55	140–320	14–39	12	~$0.926
Flax	1.38	10–65	5–38	1.2–3	343–1035	50–70	345–620	34–48	7	~$3.11
Sisal	1.2	0.8–8	7–47	1.9–3	507–855	9–22	55–580	6–15	11	~$0.65
Ramie	1.44	40–250	18–80	2–4	400–938	61.4–128	590	29	12–17	~$2
Hemp	1.35	5–55	10–51	1.6–4.5	580–1110	30–60	210–510	20–41	8	~$1.55
Coir	1.2	0.3–3.0	7–30	15–25	175	6	92–152	5.2	10	~$0.2–$0.4
Kenaf	1.2	1.4–11	12–36	2.7–6.9	295–930	22–60	246–993	18–50	6.2–12	~$0.378
Banana	1.35	0.9–0.4	12–30	5–6	529–914	27–32	392–677	20–24	10–11	–
Pineapple	1.5	3–8	8–41	1–3	170–1627	60–82	287–1130	42–57	10–13	~$0.40–$0.55
Abaca	1.5	4.6–5.2	10–30	2.9	430–813	31.1–33.6	–	–	14	~$0.345
Bamboo	0.6–1.1	1.5–4	88–25	1.3–8	140–441	11–36	383	18	–	~$0.5
Nettle	1.51	5.5	20–80	1.7	650	38	–	–	11–17	–
Hardwood	0.3–0.88	3.3	16	–	51–120.7	5.2–15.6	–	–	–	~$0.44–$0.55
Softwood	0.30–0.59	1	30	4.4	45.5–11.7	3.6–14.3	–	–	–	~$0.44–$0.55
E-glass	2.5	–	15–25	2.5	2000–3500	70–73	800–1400	29	–	~$2
S-glass	2.5	–	–	2.8	3–3.5	63–67	1.8	34.4	–	~$2

Reprinted from Gurunathan et al. (2015).

Similar observations were independently reported by Palanisamy (2013) when montmorillonite-based nanoclays were incorporated into castor oil-based polyurethane foam at weight fraction ranging between 0.5% and 5%. With increasing nanoclays content, the cell size decreased thereby increasing the cell number density. Palanisamy attributed the increase in cell number density to the presence of nanoclays particles, which acted as nucleation sites.

Using soy-based polyols, Gu et al. (2013) prepared rigid polyurethane foams reinforced by microfibres derived from hardwood pulp. The inclusion of 13.3-php pulp fibre increased the density of the neat polyurethane foam by 22% from 28.5 to 34.8 kg/m^3 but did not alter the mechanical properties of the neat PUR foam. The glass transition temperature of the polyurethane foam shifted from 66 to 86 °C as a result of the fibre particles participating in the formation of networking polymer chains and precluding free segmental motion. The increased T_g coupled with the retention in mechanical properties following the addition of wood fibres revealed a potential strategy to impart desirable environmental characteristics without compromising the utilization of polyurethane foam in engineering applications. It has been demonstrated that the structural integrity of bio-foams can be enhanced by integrating fillers into the foam material. The next section discusses the design methodology for foam hybrid materials particularly the sandwich composites. The mechanical response of sandwich foam composites under varied loading conditions forms the primary focus point.

13.5.1 Design of foam composites

Structural insulated panels (SIPs) are defined as the sandwich material comprising a structural facing material and a foam core (Mullens and Arif, 2006; Mousa and Uddin, 2011; Anonymous, 2011, 2015c). The requirements for design follow the Allowable Stress Design method. The design for SIPs is governed by aspects of (a) design loads, (b) serviceability, (c) load combinations and (d) stress increase (Anonymous, 2011). The minimum design loads should converge with the corresponding building code, whereas the serviceability dictates the adequate stiffness able to limit deflection and lateral drift, which in either case, should be lower than the limitation of building code and minimum design load guidelines. The design guidelines also consider the moisture to be lower than 19% by mass and within a sustained service temperature of 37 °C.

The design considerations are classified into three distinct load categories, i.e. (1) bending loads, (2) compression loads and (3) combined loads. It is critical to understand that the design considerations change depending on whether a continuous support is present at the end of the span ($C_v = 1.0$) or absent ($C_v < 1.0$) based on which the shear support is subsequently variant.

13.5.1.1 Bending members

SIPs in simple, continuous and cantilevered bending should be designed with central consideration to the span length, which the face-to-face distance supports (Anonymous, 2011). In addition, special consideration should be placed for load cases where a spline is used to provide continuity for contiguous SIPs. The flexural strength upon a transverse loading should satisfy $M \leq F_tS$ or F_cS where M is the applied moment, F_t or F_c is the allowable tensile or compressive stress and S is the flexural modulus under transverse loading.

For SIPs in shear under transverse loading, the shear strength of the SIP should satisfy $V \leq F_vC_{Fv}C_vA_v$, where C_{Fv} is the size factor for shear, C_v is the shear support correction factor, A_v is the shear area of the panel given by $6(h+c)$, F_v is the allowable shear stress. The shear design for an SIP is closely dependent on the type of support, the shear force and the panel size effect.

Deflection in SIP bending members is the resultant of the bending and shear effects and is defined through Eqn (13.3):

$$\Delta = \Delta_b + \Delta_s = \frac{1728\left(5wL^4\right)}{384E_bI} + \frac{3wL^2}{2A_vG} \tag{13.3}$$

In Eqn (13.3), the total deflection is a sum of the flexural deflection and shear deflection, on an SIP of shear modulus G, span length L, transverse tensile modulus E_b and subjected to uniform load w.

The long-term loading can be treated as a summation of creep effects according to Eqn (13.4).

$$\Delta_T = \sum K_{cr}\Delta_i \tag{13.4}$$

where K_{cr} is a constant that depends on the core material and for a urethane foam core, the value of K_{cr} ranges from 1 to 7, under standard load types defined in the ASCE 7-05 Standard. Additional creep information on creep can be found in (Garrido et al., 2012, 2014; Taylor et al., 1997). The fatigue properties of sandwich core composites are a function of the incipient damage in the form of debonding at the facesheet and core, and arising from flawed joints (Burman and Zenkert, 1997a,b; Zenkert and Burman, 2011). In general, damage starts in regions of high shear stress, primarily at the middle of the sandwich composite during the initiation phase, which accounts for about 90% of the fatigue life. The damage regions coalesce to create a large crack that is a function of support span, and high shear zone. The larger cracks eventually grow towards the facesheets causing debonding at the interface.

The total deflection of the SIP for structural and non-structural members is understood to be safe below L/120 or a standard building code/design standard that supersedes this condition. In addition, when an SIP is designed for bearing or concentrated loading, a minimum of 38 mm continuous support is advisable.

13.5.1.2 Compression members

SIP design for compression requires the panels to be of a suitable size and load bearing capacity that meet the allowable design values (Anonymous, 2011). Under axial compression, the SIP should meet the condition $P \leq P_e$. $P_e = C_eF_cA_f$ where P is the axial load, P_e is the load component at the eccentric load, F_c is the allowable compressive stress on the facesheet and A_f is the cross sectional area. C_e is defined through Eqn (13.5).

$$C_\mathrm{e} = \frac{1}{\left(1 + \frac{ey_\mathrm{c}}{r^2}\left(\frac{12L}{2r}\sqrt{\frac{3P}{A_\mathrm{f}E_\mathrm{b}}}\right) + \frac{2Pey_\mathrm{c}}{2A_\mathrm{v}GI}\right)} \tag{13.5}$$

where e is the load eccentricity, y_c is the distance from the centroid to the outer (compression) fibre and r is the radius of gyration.

SIPs under pinned column upon axial loading is designed to meet the condition $P \leq P_\mathrm{cr}$ where P_cr is defined through Eqn (13.6).

$$P_\mathrm{cr} = \frac{\pi^2 E_\mathrm{b} I}{3(12L^2)(1 + \pi^2 E_\mathrm{b} I / 12L^2 A_\mathrm{v} G)} \tag{13.6}$$

The compressive bearing strength similar to the shear bearing is a function of the appropriate design guidelines and the splines if used should be able to conduct efficient load transfer.

Tensile forces in SIPs are generally not considered as they are dissipated through a designed load path to preclude any sustained loads on the facesheets or the core.

13.5.1.3 Combined loading

For combined loading scenarios on SIPs, the strength under compression, bending and shear are understood to satisfy the considerations (Anonymous, 2011) as shown in Eqns (13.7) and (13.8).

$$\frac{P}{P_\mathrm{e}} + \frac{M_\mathrm{max}}{F_\mathrm{c}S} + \frac{V_\mathrm{ip}}{F_\mathrm{vip}} \leq 1.0 \tag{13.7}$$

$$\frac{P}{P_\mathrm{cr}} + \frac{M_\mathrm{max}}{F_\mathrm{c}S} + \frac{V_\mathrm{ip}}{F_\mathrm{vip}} \leq 1.0 \tag{13.8}$$

where $M_\mathrm{max} = 1.5wL^2 + P\Delta_\mathrm{2nd}$, V_ip is the applied shear force and Δ_2nd is the total immediate deflection considering secondary effects.

The reader is recommended to refer to SIP Engineered Design Guides available through the Structural Insulated Panel Association and through references (Anonymous, 2011) and (Anonymous, 2015c) for further information.

13.6 Environmental impact

Understanding the ecological impact and efficiency of biofoams is critical in understanding the utilisation of these materials for building or construction. Often, the usage of biobased materials is incentivised by many governments in promoting energy-efficient materials in their nations (Stevenson and Ingwersen, 2012). However, it is noteworthy that biobased materials do not always meet the eco-design criteria, and hence extensive analysis of ecological footprint is warranted for design. ISO 14040 and ISO14044 describe common life cycle analysis (LCA) frameworks, and are applicable to biofoam and their respective composites (Weitz, 2012).

In a life cycle analysis of carbon dioxide emissions, the largest impact in insulative materials such as foams with a large fraction of this impact from evaporated water and energy consumed during foam manufacturing. Nevertheless, the final disposal of the materials in incinerators also was purported to cause a global warming risk (Zabalza Bribián et al., 2011).

The ISO 14040 method of life cycle analysis is critical in understanding the ecological impact of materials. This standard method is comprised of the following steps (Margni and Curran, 2012).

Step 1: The functions are identified in terms of the final use or product system.
Step 2: The functions are determined and defined, and ranked according to their criticality including a mandatory primary function.
Step 3: A functional unit is defined using key parameters for proper functioning of the system, and a unit system is selected, most often the SI system. Alternative systems that may affect the analysis are also considered at this stage.
Step 4a: An equivalent product system that is identical to the functional unit is selected for comparison. Any omissions made are identified and justification for doing so is provided.

Describe the consequences of not considering certain functionally comparable systems for the validity of the study's results and conclusions.

Step 4b: Reference flows are determined using the base function and related standards or recommended use testing methods. The underlying information regarding the flow is carefully described in detail, with step-by-step justification of each step.

It is critical to explain the flows in a proper and unambiguous manner as comparisons are involved. The system performance, boundaries and data collection and categorisation procedures, and strategic decision making constitute the key indicators of the efficacy of the LCA performed. It is also important to note that the variations, alternative terminology or parallel systems should be carefully defined for posterity.

The ISO 14040 framework can be implemented for comparison of a biobased foam with a baseline petrochemical foam as the alternative product system. As shown in Figure 13.7, the key steps in understanding the efficiency of the biofoam system would entail analysis of various aspects, including energy, emissions, toxicity, risk associated, raw materials flow and land use, as this is a bio-derived system. For Lupranol Balance 50 (Muller et al., 2009), a study based on this framework concluded that the toxicity, emissions and energy consumption with biofoams was considerably lower than that of its petrochemical counterpart. However, the land use, and risk potential were higher with the novel biofoam system, owing to a general lack of standardised methods and guidelines for best uses.

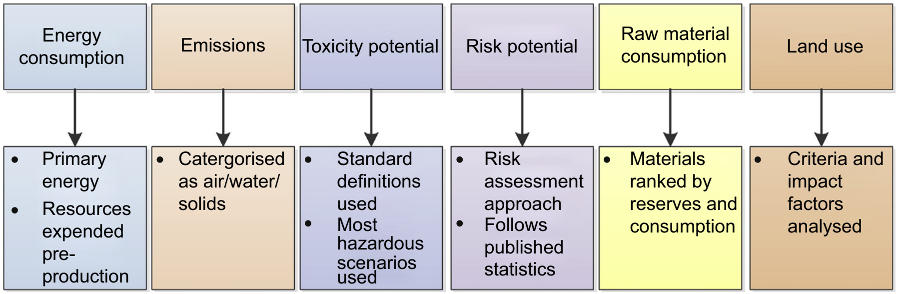

Figure 13.7 The major elements of eco-efficiency analysis and the associated descriptions of the underlying sampling mechanisms.
Adapted from Muller et al. (2009).

13.6.1 Degradation and biodegradability

Degradation in polymeric materials is undesirable in service but remains an environmental challenge at the end-of-service life. Biodegradation is the action of microorganisms that causes decomposition of polymeric chains into smaller molecules (Nakajima-Kambe et al., 1999). In PUR foams and biofoams overall, the biodegradation is a function of the chemical structure, molecular orientation, degree of crystallinity and the density of cross-linking. The decomposition routes are defined by the polyol type, and by the hydrolysis-susceptible ester bonds (Howard, 2002). Most pathways of biodegradation can be surmised as enzymatic actions on the chemical species through esterases and proteases (Gómez et al., 2014; Loredo-Treviño et al., 2012; Cregut et al., 2013).

Biofoams show a higher tendency to biodegrade in comparison to their synthetic counterparts (Gómez et al., 2014), with identical degradation pathways in composting or anaerobic digestion (Wang et al., 2008). The ester bonds are considered the primary degradation sites in biofoams, whereas the synthetic foams show resistance or incubation to degradation at equivalent decomposition conditions (Gómez et al., 2014). The urethane and urea groups are hydrolysis-susceptible sites; however, the enzymatic degradation is difficult at these sites because of shielding caused at the polymer surface that features secondary structures and hydrogen bonding within the hard segments (Santerre et al., 1994). Additionally, the increase in chain length of polyesters, and increase in the size of the hard segment show positive correlation with tendency of PUR foams to biodegrade. Microbial attack is carried out faster in the amorphous regions of the foam (Cregut et al., 2014) in comparison to the crystalline segments. Polyester PUR foams show a higher overall degradation potential in comparison to polyether-based foams, with fungi as the predominantly active microbial agent causing the material to biodegrade in soil (Barratt et al., 2003). A comprehensive list of microorganism activity for polyurethane foams and the corresponding enzymatic activity can be found in the review by Loredo-Treviño et al. (2012).

13.6.2 Recycling and recovery

Recycling and recovery of polymeric foams is critical for long-term sustainability of the industry. With diversification of foam products, novel methods for recycling and recovery of foams are constantly emerging (Zia et al., 2007). The methods of recycling can be classified into four major categories, i.e. (1) mechanical recycling, (2) chemical recycling, (3) thermochemical processing and (4) energy recovery.

Mechanical recycling of rigid foams and composites is often the preferable route for obtaining these materials for reuse. Mechanical recycling encompasses a number of size reduction processes followed by reprocessing/shaping through secondary manufacturing processes, such as compression/injection moulding after regrinding or milling (Zia et al., 2007). Chemical recycling methods involve chemical decomposition routes (Molero et al., 2006; Zia et al., 2007; Ulrich et al., 1978; Modesti and Simioni, 1996) including hydrolysis, glycolysis, alcohololysis, fractionation, hydroglycolysis and aminolysis as the basic methods. Additional information can be found through the specific reference works (Cregut et al., 2013; Modesti and Simioni, 1996; Ulrich et al., 1978; Zia et al., 2007).

Thermochemical recovery processes (Cai et al., 1998; Lattimer et al., 1998) include pyrolysis, gasification and hydrogenation, which require capital investments and energy for processing. The underlying methodology is to breakdown the foam materials into gas and oil for secondary uses. Energy recovery (Zia et al., 2007) is a group of processes that is constituted by combustion or incineration of the foams in the lack of a perceived benefit or end market.

13.7 Application case studies

In a study by Munusamy (2012) and Yu et al. (2012), soy oil-based PUR foam was used as a core in a sandwich construction with facesheets of hybridised kenaf and E-glass fibre in a vinyl ester matrix to replace traditionally used plywood sheeting on steel frame for a mass transit bus flooring system. Upon identifying a suitable biobased foam material that has an equivalent property set as a commercial product, the sandwich composite was fabricated using a vacuum infusion method. The sandwich composite was evaluated to determine key mechanical properties for a flooring application in flexure, shear and compression. The sandwich biocomposite showed greater flexural strength and flexural modulus over the traditional plywood material. Upon further analysis, the soy-based PUR foam used as a core for the sandwich composite showed favourable potential for flooring in mass transit. The flexural strength and modulus showed increases by about 200% over the existing plywood, along with higher bio-content.

In a study on fibre-reinforced soy foams, flexural properties and fastener pullout tests were investigated for a flax fibre-reinforced, soy-PUR composite (Fuqua et al., 2010b). Results indicated that these composites constituted a fraction of 0.55−0.70 of biomaterials. Higher fibre volume fraction and a higher density of the foam were suggested for achieving higher performance for plywood-like applications at low cost. The yielding behaviour of the fibre-reinforced foams was comparable to plywood at a lower potential for frequent replacement requirements.

13.8 Conclusions and future trends

The utilisation of biofoam in insulation and building materials requires a comprehensive understanding of the background and engineering principles for design purposes. Biofoams derived from functionalised vegetable oils and associated precursors are beneficial in providing potentially higher biodegradability. A major hurdle in acceptance of this technology is the lack of parametric technical data in understanding the utility of vegetable oil polyols in specific engineering applications. The commercialisation of these materials is not concomitant with the increasing volume of literature on vegetable oil-based polymers, a hindrance for industrial-scale usage of these polyol systems. In addition, non-isocyanate-based PUR systems require alternative chemicals for obtaining a foam, which may cause the shift in research and development towards precursors other than polyols for rigid foams. However, in PUR foams and composites, understanding structure—property relationships is the key in developing new chemicals from renewable vegetable oils. The production of non-isocyanate/vegetable oil-polyol based foams will increase the emphasis on a renewable, nontoxic and biodegradable foam, which in conjunction with an appropriate lignocellulosic fibre will perhaps provide a 100% green biofoam composite in the future.

References

Allport, D.C., Gilbert, D.S., Outterside, S.M., 2003. MDI, TDI and the Polyurethane Industry. MDI and TDI: Safety, Health and the Environment. A Source Book and Practical Guide, pp. 11—23.

Ang, K.P., Lee, C.S., Cheng, S.F., Chuah, C.H., 2014. Synthesis of palm oil-based polyester polyol for polyurethane adhesive production. Journal of Applied Polymer Science 131.

Anonymous, 2011. Engineered Design of SIP Panels. NTA, INC.

Anonymous, 2014. Global Polyurethane Market to Cross US$73,607 mln by 2020 (Online). Smartech Global Solutions Ltd. Available: http://www.plastemart.com/plastic-facts-information.asp?news_id=26303&news=Global-Polyurethane-market-to-cross-US73607-mln-by-2020 (accessed 10.05.15.).

Anonymous, 2015a. HONEY BEE™ Soy Polyols (Online). Available: http://honeybee.cc/products-2/ (accessed 10.03.15.).

Anonymous, 2015b. Rigid Foam Application Segment to Lead Global Methylene Diphenyl Diisocyanate Market between 2011 and 2016 (Online). Transparency Market Research. Available: http://www.transparencymarketresearch.com/pressrelease/methylene-diphenyl-diisocyanate-market.htm (accessed 15.05.15.).

Anonymous, 2015c. SIPA- Structural Insulated Panel Association (Online). Available: http://www.sips.org/ (accessed 15.04.15.).

Aranguren, M.I., Rácz, I., Marcovich, N.E., 2007. Microfoams based on castor oil polyurethanes and vegetable fibers. Journal of Applied Polymer Science 105, 2791—2800.

Arniza, M.Z., Hoong, S.S., Idris, Z., Yeong, S.K., Hassan, H.A., Din, A.K., Choo, Y.M., 2015. Synthesis of transesterified palm olein-based polyol and rigid polyurethanes from this polyol. JAOCS, Journal of the American Oil Chemists' Society 92, 243−255.

ASTM International, 2009. ASTM D1623-09 Standard Test Method for Tensile and Tensile Adhesion Properties of Rigid Cellular Plastics. ASTM Volume 08.01 Plastics (I). ASTM International, West Conshohocken, PA.

ASTM International, 2012. ASTM D7249 Standard Test Method for Facing Properties of Sandwich Constructions by Long Beam Flexure. ASTM Volume 15.03 Space Simulation; Aerospace and Aircraft; Composite Materials. ASTM International, West Conshohocken, PA.

Azmi, M.A., Abdullah, H.Z., Idris, M.I., 2013. Properties of polyurethane foam/coconut coir fiber as a core material and as a sandwich composites component. IOP Conference Series: Materials Science and Engineering 50.

Banik, I., Sain, M.M., 2008. Water blown soy polyol-based polyurethane foams of different rigidities. Journal of Reinforced Plastics and Composites 27, 357−373.

Barratt, S.R., Ennos, A.R., Greenhalgh, M., Robson, G.D., Handley, P.S., 2003. Fungi are the predominant micro-organisms responsible for degradation of soil-buried polyester polyurethane over a range of soil water holding capacities. Journal of Applied Microbiology 95, 78−85.

Beltrán, A.A., Boyacá, L.A., 2011. Production of rigid polyurethane foams from soy-based polyols. Latin American Applied Research 41, 75−80.

Benyahya, S., Desroches, M., Auvergne, R., Carlotti, S., Caillol, S., Boutevin, B., 2011. Synthesis of glycerin carbonate-based intermediates using thiol-ene chemistry and isocyanate free polyhydroxyurethanes therefrom. Polymer Chemistry 2, 2661−2667.

Burman, M., Zenkert, D., 1997a. Fatigue of foam core sandwich beams—1: undamaged specimens. International Journal of Fatigue 19, 551−561.

Burman, M., Zenkert, D., 1997b. Fatigue of foam core sandwich beams—2: effect of initial damage. International Journal of Fatigue 19, 563−578.

Cabulis, U., Sevastyanova, I., Andersons, J., Beverte, I., 2014. Rapeseed oil-based rigid polyisocyanurate foams modified with nanoparticles of various type. Polimery/Polymers 59, 207−212.

Cai, Y., Jiang, Z., Yang, D., Liu, P., 1998. Structure and thermal properties of PU/P(BMI−UBMI) IPNs. Journal of Applied Polymer Science 68, 1689−1694.

Celzard, A., Fierro, V., Pizzi, A., Zhao, W., 2013. Multifunctional porous solids derived from tannins. Journal of Physics: Conference Series 416.

Chevali, V., Fuqua, M., Ulven, C.A., 2011. Vegetable Oil Based Rigid Foam Composites. Handbook of Bioplastics and Biocomposites Engineering Applications. John Wiley & Sons, Inc.

Chuayjuljit, S., Maungchareon, A., Saravari, O., 2010. Preparation and properties of palm oil-based rigid polyurethane nanocomposite foams. Journal of Reinforced Plastics and Composites 29, 218−225.

Čop, M., Lacoste, C., Conradi, M., Laborie, M.-P., Pizzi, A., Sernek, M., 2015. The effect of the composition of spruce and pine tannin-based foams on their physical, morphological and compression properties. Industrial Crops and Products 74, 158−164.

Corcuera, M.A., Rueda, L., Fernandez D'arlas, B., Arbelaiz, A., Marieta, C., Mondragon, I., Eceiza, A., 2010. Microstructure and properties of polyurethanes derived from castor oil. Polymer Degradation and Stability 95, 2175−2184.

Cregut, M., Bedas, M., Assaf, A., Durand-Thouand, M.-J., Thouand, G., 2014. Applying Raman spectroscopy to the assessment of the biodegradation of industrial polyurethanes wastes. Environmental Science and Pollution Research 21, 9538−9544.

Cregut, M., Bedas, M., Durand, M.J., Thouand, G., 2013. New insights into polyurethane biodegradation and realistic prospects for the development of a sustainable waste recycling process. Biotechnology Advances 31, 1634–1647.

Fam, A., Sharaf, T., 2010. Flexural performance of sandwich panels comprising polyurethane core and GFRP skins and ribs of various configurations. Composite Structures 92, 2927–2935.

Fan, H., Tekeei, A., Suppes, G.J., Hsieh, F.H., 2012. Physical properties of soy-phosphate polyol-based rigid polyurethane foams. International Journal of Polymer Science 2012.

Fan, H., Tekeei, A., Suppes, G.J., Hsieh, F.H., 2013. Rigid polyurethane foams made from high viscosity soy-polyols. Journal of Applied Polymer Science 127, 1623–1629.

Farhana, S.M.A., Mohd Haziq, D., Nurfatmah Pz, N., Majid, R.A., 2014. Effects of silicone surfactant on the water absorption and surface morphology of rigid palm oil-based polyurethane foam. Applied Mechanics and Materials 554.

Faruk, O., Sain, M., Farnood, R., Pan, Y., Xiao, H., 2014. Development of lignin and nanocellulose enhanced bio PU foams for automotive parts. Journal of Polymers and the Environment 22, 279–288.

Figovsky, O.L., 2000. Hybrid Nonisocyanate Polyurethane Network Polymers and Composites Formed Therefrom. Google Patents.

Fuqua, M., Chevali, V., Gibbon, L., Ulven, C., Reck, D., Mccord, S., 2010a. Usage of corn cob as reinforcement in post-industrial recycled HDPE. In: Society of Plastics Engineers – Global Plastics Environmental Conference 2010, GPEC 2010.

Fuqua, M.A., Huo, S., Chevali, V.S., Ulven, C.A., 2010b. Development of flax fiber/soy-based polyurethane composites for mass transit flooring application. In: SAE 2010 World Congress and Exhibition, April 13, 2010. SAE International, Detroit, MI, USA, pp. 230–236.

Gaidukov, S., Cabulis, U., Gromilova, K., Tupureina, V., Grigalovica, A., 2013. Preparation and structural properties of free films from rapeseed oil-based rigid polyurethane-montmorillonite nanocomposites. International Journal of Polymer Science 2013.

Garcia, A., Alvarado, P., Sibaja, M., Jimenez, G., Vega, J., 2008. Thermal degradation of fiber-reinforced bio-based rigid polyurethane foams. Technical Papers, Regional Technical Conference – Society of Plastics Engineers 581–584.

Garrido, M., Correia, J.R., Branco, F., Sá, M., 2012. Creep behaviour of GFRP sandwich panels with PU foam cores for civil engineering structural applications. In: Proceedings of the 6th International Conference on FRP Composites in Civil Engineering, CICE 2012.

Garrido, M., Correia, J.R., Branco, F.A., Keller, T., 2014. Creep behaviour of sandwich panels with rigid polyurethane foam core and glass-fibre reinforced polymer faces: experimental tests and analytical modelling. Journal of Composite Materials 48, 2237–2249.

Gibson, L.J., Ashby, M.F., 2010. Cellular Solids: Structure and Properties. Cambridge University Press, Cambridge, USA.

Gómez, E.F., Luo, X., Li, C., Michel Jr., F.C., Li, Y., 2014. Biodegradability of crude glycerol-based polyurethane foams during composting, anaerobic digestion and soil incubation. Polymer Degradation and Stability 102, 195–203.

Gu, R., Sain, M.M., 2013. Effects of wood fiber and microclay on the performance of soy based polyurethane foams. Journal of Polymers and the Environment 21, 30–38.

Gu, R., Sain, M.M., Konar, S.K., 2013. A feasibility study of polyurethane composite foam with added hardwood pulp. Industrial Crops and Products 42, 273–279.

Guan, J., Song, Y., Lin, Y., Yin, X., Zuo, M., Zhao, Y., Tao, X., Zheng, Q., 2011. Progress in study of non-isocyanate polyurethane. Industrial & Engineering Chemistry Research 50, 6517–6527.

Gurunathan, T., Mohanty, S., Nayak, S.K., 2015. A review of the recent developments in biocomposites based on natural fibres and their application perspectives. Composites Part A: Applied Science and Manufacturing 77, 1−25.

Hollaway, L., 1993. Polymer Composites for Civil and Structural Engineering. London, Angleterre: London: Chapman and Hall, Blackie Academic & Professional.

Howard, G.T., 2002. Biodegradation of polyurethane: a review. International Biodeterioration & Biodegradation 49, 245−252.

Javadi, A., Pilla, S., Gong, S., Turng, L.-S., 2011. Biobased and biodegradable PHBV-based polymer blends and biocomposites: properties and applications. In: Handbook of Bioplastics and Biocomposites Engineering Applications. John Wiley & Sons, Inc.

Ji, D., Fang, Z., He, W., Luo, Z., Jiang, X., Wang, T., Guo, K., 2015a. Polyurethane rigid foams formed from different soy-based polyols by the ring opening of epoxidised soybean oil with methanol, phenol, and cyclohexanol. Industrial Crops and Products 74, 76−82.

Ji, D., Fang, Z., He, W., Zhang, K., Luo, Z., Wang, T., Guo, K., 2015b. Synthesis of soy-polyols using a continuous microflow system and preparation of soy-based polyurethane rigid foams. ACS Sustainable Chemistry and Engineering 3, 1197−1204.

Kairyte, A., Vejelis, S., 2015. Evaluation of forming mixture composition impact on properties of water blown rigid polyurethane (PUR) foam from rapeseed oil polyol. Industrial Crops and Products 66, 210−215.

Kalita, H., Jayasooriyamu, A., Fernando, S., Chisholm, B.J., 2015. Novel high molecular weight polymers based on palm oil. Journal of Oil Palm Research 27, 39−56.

Karak, N., 2012. 6-Vegetable oil-based polyurethanes. In: Karak, N. (Ed.), Vegetable Oil-Based Polymers. Woodhead Publishing.

Kirpluks, M., Cabulis, U., Kurańska, M., Prociak, A., 2013. Three different approaches for polyol synthesis from rapeseed oil. Key Engineering Materials 559.

Kreye, O., Mutlu, H., Meier, M.A.R., 2013. Sustainable routes to polyurethane precursors. Green Chemistry 15, 1431−1455.

Kuranska, M., Prociak, A., 2012. Porous polyurethane composites with natural fibres. Composites Science and Technology 72, 299−304.

Lattimer, R.P., Polce, M.J., Wesdemiotis, C., 1998. MALDI-MS analysis of pyrolysis products from a segmented polyurethane. Journal of Analytical and Applied Pyrolysis 48, 1−15.

Le, H.V., Ganem, B., 2003. A Practical Synthesis of Isocyanates from Isonitriles: Ethyl 2-Isocyanatoacetate. Organic Syntheses. John Wiley & Sons, Inc.

Le, H.V., Ganem, B., 2011. Trifluoroacetic anhydride-catalyzed oxidation of isonitriles by DMSO: a rapid, convenient synthesis of isocyanates. Organic Letters 13, 2584−2585.

Lee, A., Deng, Y., 2015. Green polyurethane from lignin and soybean oil through non-isocyanate reactions. European Polymer Journal 63, 67−73.

Lim, H., Kim, S.H., Kim, B.K., 2008. Effects of the functionality of polyol in rigid polyurethane foams. Journal of Applied Polymer Science 110, 49−54.

Lin, S., Huang, J., Chang, P.R., Wei, S., Xu, Y., Zhang, Q., 2013. Structure and mechanical properties of new biomass-based nanocomposite: castor oil-based polyurethane reinforced with acetylated cellulose nanocrystal. Carbohydrate Polymers 95, 91−99.

Link, M., Kolbitsch, C., Tondi, G., Ebner, M., Wieland, S., Petutschnigg, A., 2011. Formaldehyde-free tannin-based foams and their use as lightweight panels. BioResources 6, 4218−4228.

Lligadas, G., Ronda, J.C., Galià, M., Cádiz, V., 2013. Renewable polymeric materials from vegetable oils: a perspective. Materials Today 16, 337−343.

Loredo-Treviño, A., Gutiérrez-Sánchez, G., Rodríguez-Herrera, R., Aguilar, C., 2012. Microbial enzymes involved in polyurethane biodegradation: a review. Journal of Polymers and the Environment 20, 258–265.

Lu, J., Khot, S., Wool, R.P., 2005. New sheet molding compound resins from soybean oil. I. Synthesis and characterization. Polymer 46, 71–80.

Luo, X., Mohanty, A., Misra, M., 2012. Water-blown rigid biofoams from soy-based biopolyurethane and microcrystalline cellulose. JAOCS, Journal of the American Oil Chemists' Society 89, 2057–2065.

Luo, X., Mohanty, A., Misra, M., 2013. Lignin as a reactive reinforcing filler for water-blown rigid biofoam composites from soy oil-based polyurethane. Industrial Crops and Products 47, 13–19.

Luo, X., Mohanty, A., Misra, M., Kazemizadeh, M., 2011. Rigid biofoam composites from functionalized soy oil based biopolyurethane and microcystalline cellulose (MCC) for automotive applications. In: 26th Annual Technical Conference of the American Society for Composites 2011 and the 2nd Joint US-Canada Conference on Composites, pp. 43–52.

Margni, M., Curran, M.A., 2012. Life Cycle Impact Assessment. Life Cycle Assessment Handbook. John Wiley & Sons, Inc.

Martinez De Yuso, A., Lagel, M.C., Pizzi, A., Fierro, V., Celzard, A., 2014. Structure and properties of rigid foams derived from quebracho tannin. Materials & Design 63, 208–212.

Mazzon, E., Habas-Ulloa, A., Habas, J.-P., 2015. Lightweight rigid foams from highly reactive epoxy resins derived from vegetable oil for automotive applications. European Polymer Journal 68, 546–557.

Michael, S., 2012. Rigid Polyurethane Foams. Szycher's Handbook of Polyurethanes, second ed. CRC Press.

Modesti, M., Simioni, F., 1996. Chemical recycling of reinforced polyurethane from the automotive industry. Polymer Engineering & Science 36, 2173–2178.

Molero, C., De Lucas, A., Rodríguez, J.F., 2006. Recovery of polyols from flexible polyurethane foam by "split-phase" glycolysis with new catalysts. Polymer Degradation and Stability 91, 894–901.

Mosiewicki, M.A., Casado, U., Marcovich, N.E., Aranguren, M.I., 2009. Polyurethanes from tung oil: polymer characterization and composites. Polymer Engineering and Science 49, 685–692.

Mousa, M.A., Uddin, N., 2011. Global buckling of composite structural insulated wall panels. Materials & Design 32, 766–772.

Mullens, M., Arif, M., 2006. Structural insulated panels: impact on the residential construction process. Journal of Construction Engineering and Management 132, 786–794.

Muller, J., Van Biesen, W., Saling, P., 2009. Lupranol BALANCE 50 High Performance. Naturally (Online). UTECH Europe 2009 Conference, Maastricht, The Netherlands. Available: https://www.basf.com/documents/corp/en/sustainability/management-and-instruments/quantifying-sustainability/eco-efficiency-analysis/examples/lupranol-balance-50/Lupranol_BALANCE_EEA.pdf (accessed 01.05.15.).

Munusamy, S., Whitacre, R., Chevali, V., Ulven, C., Alcock, M., Yu, Z.C., Potter, S., 2012. Development of Biobased Sandwich Structures for Mass Transit Applications. International SAMPE Technical Conference.

Munusamy, S.R., 2012. Development of Biobased Sandwich Structures for Mass Transit Application.

Nakajima-Kambe, T., Shigeno-Akutsu, Y., Nomura, N., Onuma, F., Nakahara, T., 1999. Microbial degradation of polyurethane, polyester polyurethanes and polyether polyurethanes. Applied Microbiology and Biotechnology 51, 134–140.

Nodelman, N., Shackelford, N., Hall, L., Parker, W., Qian, J., 2011. Polyurethane Rigid Foams from Agrol® Polyols. Available: http://www.agrolinside.com/img/pdf/BioBased%20Technologies%20PU2011%20Paper.pdf (accessed 27.05.15.).

Palanisamy, A., 2013. Water-blown polyurethane–clay nanocomposite foams from biopolyol—effect of nanoclay on the properties. Polymer Composites 34, 1306–1312.

Paul, F., 2000. Catalytic synthesis of isocyanates or carbamates from nitroaromatics using Group VIII transition metal catalysts. Coordination Chemistry Reviews 203, 269–323.

Petrović, Z.S., 2008. Polyurethanes from vegetable oils. Polymer Reviews 48, 109–155.

Pfister, D.P., Xia, Y., Larock, R.C., 2011. Recent advances in vegetable oil-based polyurethanes. ChemSusChem 4, 703–717.

Raquez, J.M., Deléglise, M., Lacrampe, M.F., Krawczak, P., 2010. Thermosetting (bio)materials derived from renewable resources: a critical review. Progress in Polymer Science 35, 487–509.

Ribeiro Da Silva, V., Mosiewicki, M.A., Yoshida, M.I., Coelho Da Silva, M., Stefani, P.M., Marcovich, N.E., 2013a. Polyurethane foams based on modified tung oil and reinforced with rice husk ash I: synthesis and physical chemical characterization. Polymer Testing 32, 438–445.

Ribeiro Da Silva, V., Mosiewicki, M.A., Yoshida, M.I., Coelho Da Silva, M., Stefani, P.M., Marcovich, N.E., 2013b. Polyurethane foams based on modified tung oil and reinforced with rice husk ash II: mechanical characterization. Polymer Testing 32, 665–672.

Ristić, I.S., Budinski-Simendić, J., Krakovsky, I., Valentova, H., Radičević, R., Cakić, S., Nikolić, N., 2012. The properties of polyurethane hybrid materials based on castor oil. Materials Chemistry and Physics 132, 74–81.

Rojek, P., Prociak, A., 2012. Effect of different rapeseed-oil-based polyols on mechanical properties of flexible polyurethane foams. Journal of Applied Polymer Science 125, 2936–2945.

Sain, M., Faruk, O., 2015. Biofiber Reinforcement in Composite Materials. Cambridge; Amsterdam, Woodhead Publishing; Elsevier.

Saint-Michel, F., Chazeau, L., Cavaillé, J.-Y., Chabert, E., 2006. Mechanical properties of high density polyurethane foams: I. Effect of the density. Composites Science and Technology 66, 2700–2708.

Santerre, J.P., Labow, R.S., Duguay, D.G., Erfle, D., Adams, G.A., 1994. Biodegradation evaluation of polyether and polyester-urethanes with oxidative and hydrolytic enzymes. Journal of Biomedical Materials Research 28, 1187–1199.

Seniha Güner, F., Yağci, Y., Tuncer Erciyes, A., 2006. Polymers from triglyceride oils. Progress in Polymer Science 31, 633–670.

Septevani, A.A., Evans, D.A.C., Chaleat, C., Martin, D.J., Annamalai, P.K., 2015. A systematic study substituting polyether polyol with palm kernel oil based polyester polyol in rigid polyurethane foam. Industrial Crops and Products 66, 16–26.

Sharma, K.V., Sripathy, M., 2012. Comparative studies of crushing behavior of various fiber reinforced skin polyurethane foam cored composite sandwich structures. TMS Annual Meeting 387–394.

Stevenson, M.J., Ingwersen, W.W., 2012. Environmental Product Claims and Life Cycle Assessment. In: Life Cycle Assessment Handbook. John Wiley & Sons, Inc.

Stirna, U., Fridrihsone-Girone, A., Yakushin, V., Vilsone, D., 2014. Processing and properties of spray-applied, 100% solids polyurethane coatings from rapeseed oil polyols. Journal of Coatings Technology Research 11, 409–420.

Szycher, M., 2013. Szycher's Handbook of Polyurethanes (Online). CRC Press, Boca Raton, Fla.

Tan, S., Abraham, T., Ference, D., Macosko, C.W., 2011. Rigid polyurethane foams from a soybean oil-based polyol. Polymer 52, 2840–2846.

Taylor, S., Manbeck, H., Janowiak, J., Hiltunen, D., 1997. Modeling structural insulated panel (SIP) flexural creep deflection. Journal of Structural Engineering 123, 1658−1665.

Tomita, H., Sanda, F., Endo, T., 2001. Model reaction for the synthesis of polyhydroxyurethanes from cyclic carbonates with amines: substituent effect on the reactivity and selectivity of ring-opening direction in the reaction of five-membered cyclic carbonates with amine. Journal of Polymer Science Part A: Polymer Chemistry 39, 3678−3685.

Türünç, O., Kayaman-Apohan, N., Kahraman, M.V., Menceloğlu, Y., Güngör, A., 2008. Nonisocyanate based polyurethane/silica nanocomposites and their coating performance. Journal of Sol-Gel Science and Technology 47, 290−299.

Ulrich, H., Odinak, A., Tucker, B., Sayigh, A.A.R., 1978. Recycling of polyurethane and polyisocyanurate foam. Polymer Engineering & Science 18, 844−848.

Varma, D.R., Guest, I., 1993. The Bhopal accident and methyl isocyanate toxicity. Journal of Toxicology and Environmental Health 40, 513−529.

Veronese, V.B., Menger, R.K., Forte, M.M.D.C., Petzhold, C.L., 2011. Rigid polyurethane foam based on modified vegetable oil. Journal of Applied Polymer Science 120, 530−537.

Wang, H.J., Rong, M.Z., Zhang, M.Q., Hu, J., Chen, H.W., Czigány, T., 2008. Biodegradable foam plastics based on castor oil. Biomacromolecules 9, 615−623.

Weitz, K.A., 2012. Life Cycle Assessment and End of Life Materials Management. In: Life Cycle Assessment Handbook. John Wiley & Sons, Inc.

Wu, S.P., Qiu, J.F., Rong, M.Z., Zhang, M.Q., Zhang, L.Y., 2009. Plant oil-based biofoam composites with balanced performance. Polymer International 58, 403−411.

Xue, B.L., Wen, J.L., Sun, R.C., 2014. Lignin-based rigid polyurethane foam reinforced with pulp fiber: synthesis and characterization. ACS Sustainable Chemistry and Engineering 2, 1474−1480.

Yu, Y.H., Nam, S., Lee, D., Lee, D.G., 2015. Cryogenic impact resistance of chopped fiber reinforced polyurethane foam. Composite Structures 132, 12−19.

Yu, Z.C., Townsley, M., Alcock, M., Ulven, C., Potter, S., 2012. Developing natural fibre-based composite materials for Canadian industry sectors. Journal of Biobased Materials and Bioenergy 6, 515−520.

Zabalza Bribián, I., Valero Capilla, A., Aranda Usón, A., 2011. Life cycle assessment of building materials: comparative analysis of energy and environmental impacts and evaluation of the eco-efficiency improvement potential. Building and Environment 46, 1133−1140.

Zenkert, D., Burman, M., 2011. Failure mode shifts during constant amplitude fatigue loading of GFRP/foam core sandwich beams. International Journal of Fatigue 33, 217−222.

Zhang, L., Zhang, M., Hu, L., Zhou, Y., 2014. Synthesis of rigid polyurethane foams with castor oil-based flame retardant polyols. Industrial Crops and Products 52, 380−388.

Zhou, X., Pizzi, A., Sauget, A., Nicollin, A., Li, X., Celzard, A., Rode, K., Pasch, H., 2013. Lightweight tannin foam/composites sandwich panels and the coldset tannin adhesive to assemble them. Industrial Crops and Products 43, 255−260.

Zhu, M., Bandyopadhyay-Ghosh, S., Khazabi, M., Cai, H., Correa, C., Sain, M., 2012. Reinforcement of soy polyol-based rigid polyurethane foams by cellulose microfibers and nanoclays. Journal of Applied Polymer Science 124, 4702−4710.

Zia, K.M., Bhatti, H.N., Ahmad Bhatti, I., 2007. Methods for polyurethane and polyurethane composites, recycling and recovery: a review. Reactive and Functional Polymers 67, 675−692.

Zieleniewska, M., Leszczyński, M.K., Kurańska, M., Prociak, A., Szczepkowski, L., Krzyżowska, M., Ryszkowska, J., 2015. Preparation and characterisation of rigid polyurethane foams using a rapeseed oil-based polyol. Industrial Crops and Products 74, 887−897.

Biopolymers for wood preservation

14

S. Patachia, C. Croitoru
Transilvania University of Brasov, Brasov, Romania

14.1 Introduction

Wood is a structural organic tissue found in the stems and roots of trees and other woody plants, in which it serves mainly as support and nutrient transport system for the photosynthesis-bearing part of the plant. It has been used by mankind since the beginning as fuel or construction material (Schweingruber, 2007).

Due to its organic nature, consisting of cellulose fibers embedded in a lignin matrix together with some minor components such as terpenoids, resin, fatty acids, pectin, proteins, and inorganics, it is fairly susceptible to the action of external environmental and/or (micro-) biological degradative factors (Timar, 2003a).

The natural durability of wood is imparted by the wood extractives that are located mainly in the actively growing part of this plant species (the heartwood), thus making the lumber containing a larger proportion of sapwood less resistant to these degradative factors (Figure 14.1). The most resistant wood species are the Mediterranean softwoods (juniper, cypress) and exotic hardwoods such as catalpa, yew, black locust, and so forth. The majority of the commonly used wood species possess only a low to moderate resistance to decay (oak, fir, spruce, beech, pine, poplar, and so forth) (Taylor et al., 2002; Hashemi and Latibari, 2011).

Wood quality is mainly influenced by the following external factors (Figure 14.2):

- Humidity
- Oxygen presence
- Nutrients
- Microbiological organisms such as fungi, molds, insects
- Temperature
- Presence of electromagnetic radiation (mainly from the UV, IR, high-energy β or γ).

These factors act interdependently; high humidity and oxygen presence, as well as optimal temperatures, are good conditions for fungus and mold growth (Evans et al., 1992; Tao et al., 2013).

Wood is traditionally considered a renewable resource, having an overall annual biological production of 10 billion tons, to minimize the intensive and often irresponsible exploitation of this natural resource, as well as for other economic reasons, the maintaining of wood product quality as long as possible is an important aspect to consider (Schweingruber, 2007; Vinden and Butcher, 2005).

Biopolymers and Biotech Admixtures for Eco-Efficient Construction Materials. http://dx.doi.org/10.1016/B978-0-08-100214-8.00014-2
Copyright © 2016 Elsevier Ltd. All rights reserved.

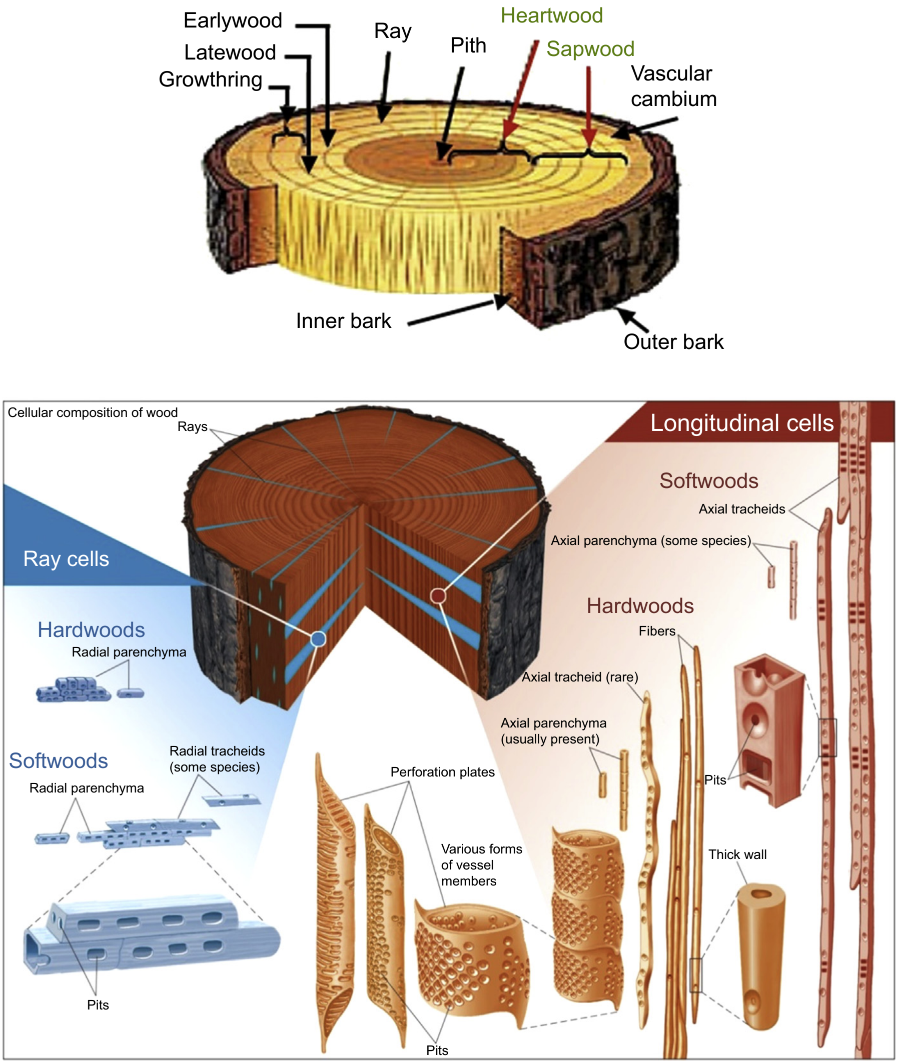

Figure 14.1 The structure of wood (Tsoumis, 2000).

14.2 Wood preservation mechanisms

The maintaining of wood quality is achieved by diminishing the effect of the previously mentioned external factors (Timar, 2003b) according to the following mechanisms:

- Introduction of hydrophobization agents into the wood's structure (water repellents);
- The "sealing" of wood's structure to prevent the access of moisture, air, and microorganisms;

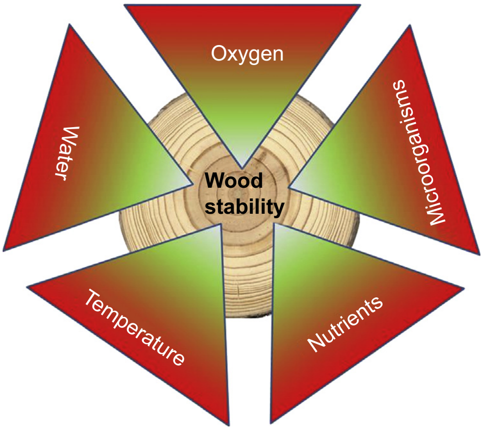

Figure 14.2 Factors affecting wood stability.

- Fixing of several substances with biocidal character into the structure of the wood;
- Reducing the availability of nutrients for microorganisms from the wood structure, impeding their nourishment, thus limiting their proliferation.

The maintaining of wood quality in time is usually achieved with the help of preservatives. These are individual chemical compounds or mixtures that make wood less susceptible to attack from a large variety of degradative factors or organisms. These organisms include insects, marine borers, and various types of fungi such as stain and decay. Some of these chemicals are effective against a wide range of organisms, whereas others are very specific and protect wood from only one type of organism. It is to be noted that no preservative will protect wood from all the degrading factors (Clausen, 2010; Freeman et al., 2003; Kjellow and Henriksen, 2009).

Regardless of their nature, wood preservatives must meet the following criteria (Freeman et al., 2003; Wilcox et al., 1991):

- They must be compatible with at least one of the wood's natural components;
- They must not leach from wood;
- They must be nontoxic for mammals;
- They must enable the wood to be recycled at the end of its life cycle;
- They must be ecologic and biodegradable;
- They must be economically efficient (i.e., readily available and cheap);
- The impregnation technology must be ecological.

14.2.1 Traditional wood preservatives

Traditionally, the majority of wood preservatives in use up to this date are small-molecular compounds obtained by chemical or thermal decay (tar of pyrolysis). Until recently, wood preservation implied the use of aromatic impregnating agents (insecticides or fungicides) such as creosote, halogenated carbamates, benzothiazoles, pentachlorophenol, (alkyl)imidazoles, bis (tributyltin) oxide, or salt-based impregnants such as borates, quinolinolates, naphthenates of copper, zinc, or chromated copper arsenate-based preservatives (CCA) in several commercial variants (Betts, 2005; Bull, 2001; Krzyzewsky, 1987).

All of these preservatives are highly toxic and biocumulative. When they are exposed to rainwater, a significant amount of these preservatives could be leached from the wood, contaminating the environment. Furthermore, the presence of these preservatives in the wood materials at the end of their life cycle limits their recycling perspectives (Adam et al., 2009; Lin et al., 2009; Temiz et al., 2006).

14.2.2 Biopolymer wood preservatives

Extending the service life of wood and wood-derived products by using "green" compounds as preservatives currently represents an attractive approach for wood protection from the perspectives of human health and environmental protection. An alternative "green" solution for wood preservation could be represented by the use of biopolymers (Pizzi, 2015).

14.2.2.1 Biopolymer definition

Biopolymers have been initially defined as compounds with high molecular mass, produced by living organisms. They can be categorized as a function of their monomer unit into several classes, such as polysaccharides and modified polysaccharides (cellulose, hemicellulose, chitin, chitosan, glucans, starch), proteins (gelatin, zein, fibroin, casein in non-cross-linked or cross-linked form), and derived polypeptides (gelatin, collagen peptides, non-cross-linked or in cross-linked form), and polyphenols or modified polyphenols (tannins, cross-linked tannins, lignin) (Niaounakis, 2013; Vroman and Tighzert, 2009).

Waxes and resins of vegetal or animal origin with molecular masses close to those of oligomers could be also included into the biopolymers category (carnauba, beeswax, or paste wax, and rosin, dammar, copal, and shellac resins). These natural substances are able to polymerize or polycondensate in situ in the structure of wood, generating tridimensional biopolymer networks (Pizzi, 2015; Singh and Singh, 2012).

Vegetable oils that contain at least one double bond in the alkyl chain (mainly oleic, linoleic, linolenic acids) could also polymerize, generating biopolymers in situ. These are able to hydrophobize wood and could be fixed into the wood structure by reactions with the wood's components (for example, with lignin: substitution at the aromatic ring or at the lateral chain). For the purpose of wood impregnation, alpha-linoleic acid oils, such as tall oil, tung oil, or linseed oil are frequently employed (Schultz and Nicholas, 2008; Singh and Singh, 2012).

Copper soaps with carboxylic acid groups of unsaturated fatty acids such as those of edible vegetable oils, which are nontoxic, such as maize oil, sunflower oil, and others, as well as with resin acids of rosin, were shown to have effectiveness and long-term durability as ground-contact wood preservatives, polymerizing into the structure of wood (Pizzi, 1993, 2015). Ammonium borate oleate preservative (fungicide, fire retardant) can be fixed into the wood structure by polymerization (Pizzi, 2015) (Figure 14.3).

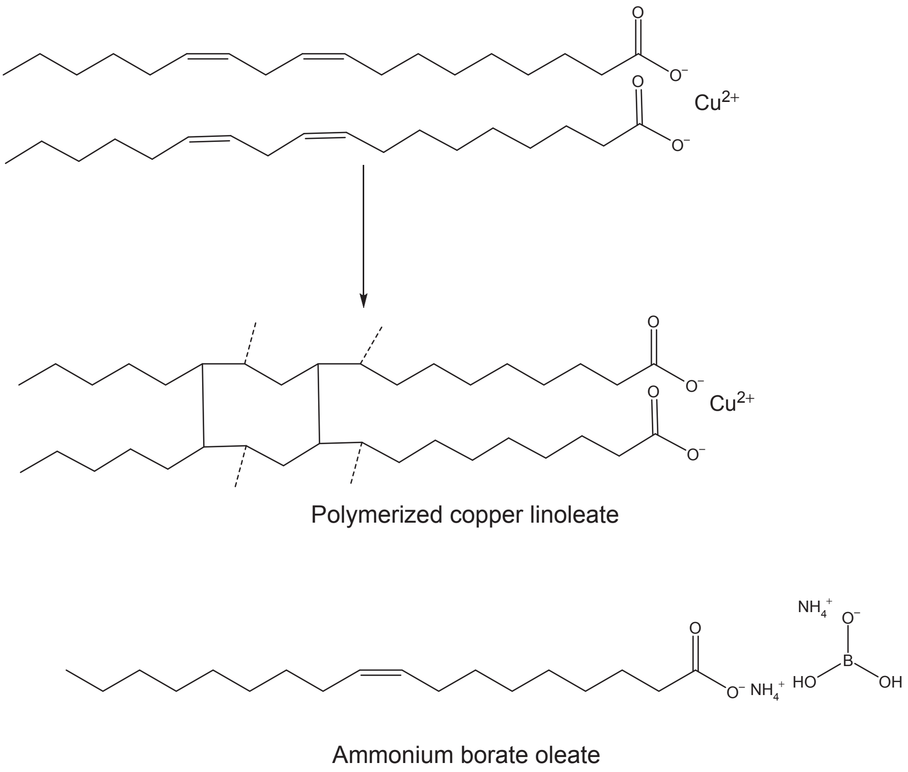

Figure 14.3 Fatty acid-derived wood preservatives (Pizzi, 2015).

Also, in the category of biopolymers could be included the macromolecular synthetic compounds obtained by polymerization or polycondensation of the monomers obtained from bio-resources. Examples of such polymers include furanic resins obtained from bioderived furfural and furfuryl alcohol, which is categorized in the European Union as an environment-friendly and nontoxic preservative (Srivastava and Pizzi, 2014).

14.2.2.2 Techniques of wood impregnation with biopolymers

The general methods for introducing biopolymers into the wood structure include the following techniques:

- Biopolymers with low molecular mass generate solutions (aqueous or organic solvent-based) with low viscosity, that are able to diffuse into the wood, impregnating it. Inside the wood, they could close the pores and/or they could form a continuous film on the wood lumen, which could act as a water repellent. They could protect the wood internal structure from biologic attack or favor the adsorption of several metallic ions that either are nutrients for the micro-organisms, diminishing their quantity, or they present antibacterial effect (Cu^{2+}, CrO_4^{2-}, Zn^{2+}, AsO_3^{2-}). These low-molecular biopolymer solutions could be introduced into wood either by immersion (superficial impregnation) or by high-pressure impregnation (Freeman et al., 2003; Singh et al., 2008);

- Biopolymers with high molecular mass form viscous solutions that could form a continuous coating at the surface of the wood or in neighboring tissues (surface impregnation), which diminishes the access of moisture, oxygen, or micro-organisms inside the wood structure. They can also minimize the leaching of biocidal compounds former introduced into the wood, protecting the environment, and prolonging the life cycle of wood (for example, the borate-based preservatives are fixed into the wood structure by proteins). These high-molecular biopolymer solutions could be applied to the wood surface by immersion, spraying, or brushing (Singh et al., 2010);
- Biopolymers that form hydrogels introduced into the wood structure through holes bored into the material could be loaded with biocidal agents (for example, rosin hydrogels). An increase in the humidity of the environment favors the swelling of the hydrogel and the diffusion of the biocidal compound into the wood. The controlled delivery of the biocidal agent leads to its efficient use (Passialis et al., 1995).
- Amphiphilic biopolymers in the form of self-assembling nanoparticles (100–150 nm in diameter) loaded with biocides can penetrate the pit pairs of solid wood, in which they are able to minimize leaching of biocide from the wood structure. They also act as emulsifiers for organic biocides in water. Such mechanism has been applied for the impregnation of southern pine sapwood with self-assembling chitosan-g-PMMA nanoparticles (∼100 nm diameter by scanning electron microscope (SEM)), containing ∼25–28 wt% (∼82–93% capture efficiency) of the fungicide tebuconazole (Ding et al., 2011);
- The monomers introduced into the wood lumen by diffusion (unsaturated vegetable oils, tannins, furfural and furfuryl alcohol, etc.) could polymerize, polycondensate, or graft on the macromolecular components of wood, generating tridimensional cross-linked structures that consolidate wood (Pizzi, 1993);
- “Self-impregnation” of wood with its natural components (cellulose, hemicellulose, and lignin) with the help of suitable solvents, such as ionic liquids, especially from the alkylimidazolium and alkylpiridinium class. The treatment of wood with the ionic liquid under controlled temperature conditions is able to promote swelling of wood components. By eliminating the ionic liquid through water addition, the natural wood components precipitate, closing the pits and chambers of the wood rays, thus acting as a natural barrier to moisture, air, and biological agents (Croitoru et al., 2015);
- Impregnation of ionic liquid-swollen wood with biopolymers. Ionic liquid acts as a carrier for the biopolymer into the structure of the wood. Biomacromolecule access into the wood’s structure is facilitated by the wood-swelling ability of certain ionic liquids. Ionic liquid is further removed, and the biopolymer precipitates into the wood structure, sealing it from the external degradative factors (Croitoru et al., 2011a, 2015).

14.2.2.3 Mechanisms of antibacterial action of biopolymers

Antibacterial activity is a very complex process that involves living organisms whose every step of life like sustenance, metabolism, respiration, and capacity of reproduction could be affected by the presence of toxic substances (Kenawy et al., 2007). Many mechanisms of interaction between different classes of substances and different types of fungi, molds, and termites have been proposed. However, some aspects are still unclear, and future studies are needed to deeply understand these processes.

One of the proposed mechanisms considers that the functional groups of biopolymers could present biocidal character through direct interaction with the cellular membrane components of the bacteria, fungi, or molds (for example, phospholipids). Such interaction could modify their permeability, disturb the osmotic equilibrium through electrolyte release from the cytoplasm and/or modify DNA conformation, or impede cellular reproduction or RNA synthesis (Ikeda et al., 1984; Wojciechowskia and Klodzinska, 2015).

Literature reports show that the dominating factors that influence the antimicrobial character of biopolymers are (a) molecular mass, (b) their concentration, (c) their ability to be fixed into the wood structure, and (d) their electrical charge (Goy et al., 2009).

It has been determined that optimal biocidal activity is achieved for a molecular weight in the range of 140 to 940 kDa. Generally, biopolymers with higher molecular masses present a decrease in the biocidal activity, due to their low diffusion coefficients through the bacterial cell wall and cytoplasm (Badawy and Rabea, 2011).

The antibacterial properties of several ionic biopolymers could be explained in terms of electrostatic interaction between the charged macromolecule and the bacterial membrane surface. For example, in the case of Gram-negative bacteria, the NH_3^+ groups (protonated NH_2 groups) compete with Ca^{2+} ions for electronegative sites on the membrane surface. Thus, the greater the number of cationized amino groups on the polymer backbone, the more pronounced is the antibacterial activity (Badawy and Rabea, 2011; Goy et al., 2009).

14.3 Examples of biopolymer wood preservatives

14.3.1 Chitin and chitosan

Chitin $(C_8H_{13}O_5N)_n$ is an important renewable resource and the second most abundant biopolymer after cellulose. It is a polymer comprising N-acetyl-D-glucosamine units β (1−4) linked and is the major structural component of the exoskeleton of invertebrates, the cuticles of insects, and the cell walls of fungi. The polymerization degree of chitin typically ranges from 2000 to 4000, with average molecular weights from 1.03×10^6 to 2.5×10^6 Da, and degree of acetylation between 85% and 95%. By deacetylation, it could be converted to chitosan (Figure 14.4) (Rinando, 2006).

The usage of this biopolymer as wood preservative is mainly focused in two directions:

- Partial deacetylation and depolymerization of chitin (with the help of chitinase enzymes), a process that converts chitin into chitosan or chitosan oligomers (Barikani et al., 2014; Muzzarelli et al., 2012). The usage of chitosan as wood preservative will be further discussed in this chapter.
- Obtaining chitin gels loaded with CCA, zinc, and copper salts, as well as organic biocides, which are either applied on wood to form a protective surface coating by solvent evaporation or are introduced into holes specially drilled into wood for the controlled release of the biocide into the wood structure. This process uses N,N-dimethylacetamide and N-methyl-2-pyrrolidone as solvents for chitin in the presence of 5% LiCl at temperatures in the range

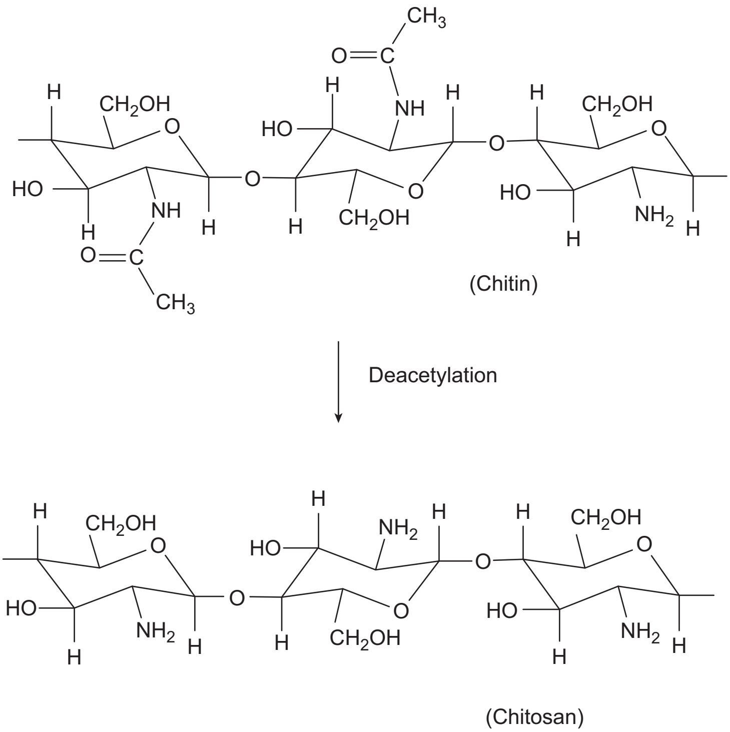

Figure 14.4 Structure of chitin and chitosan biopolymers.

of 60–105 °C. It appears that the shorter the duration of this process, the greater the molecular mass of chitin from the obtained gels. It has been determined that a higher molecular weight of chitin from the gel determines a lower diffusion coefficient of the biocide from the loaded gel, allowing for a more timed release of the biocide into the wood structure (Hirano and Horiuchi, 1989; Tamura et al., 2006).

Chitosan is a nontoxic biodegradable polymer comprising β-1,4-glucosamine produced commercially by alkaline deacetylation of chitin obtained mainly from crustacean shells. Chitosan is reported to present antifungal activity against forest-pathogenic and wood-decaying fungi, either alone or in combination with CCA or zinc and copper salts (Kumar, 2000; Leuba and Stössel, 1986).

In this respect, Kobayashi and Furukawa (1995a,b) have reported that Sugi wood (*Cryptomeria* sp.) treated with chitosan (11.6 kg/m^3) had a significantly lower average mass loss (15.9% by *Tyromyces palustris* and 4.9% for *Trametes versicolor* attack) compared to 34.8 and 19.7% for the untreated reference samples. Schmidt et al. (1995) determined that Scots pine sapwood with an impregnation solution uptake of 5.6% to 6.8% kg/m^3 was more resistant to the attack of *Coniophora putena* and *Gloeophyllum trabeum*, determined from the average mass losses of 1.6–3.2% and 3.7–6.0% compared to 18.2% and 35.6% for the untreated controls. Eikenes et al. (2005) reported that Scots pine treated with chitosan solutions at 4.8% (weight/volume) had an average mass loss during fungal attack of 1.6% for *Coniophora puteana* and 0.1% for *Poria placenta* (60% and 45% for untreated controls, respectively).

The mechanism of chitosan biocidal action could be summarized as following:

1. Chitosan interacts with the phospholipids from the cellular membrane of the bacteria and fungi, increasing its permeability and determining the electrolytes and protein release from the cellular media, leading to a pronounced cell disorganization and eventually to plasmolysis (Gorgija et al., 2014);
2. Chitosan could enter the fungi or bacterial cell and interact with the DNA, altering its conformation and inhibiting RNA synthesis (Eikenes et al., 2005);
3. Chitosan could form a membrane at the wood lumen surfaces that both acts as a barrier against air and moisture and determines a higher uptake of metals with antimicrobial activity (CCA, Zn^{2+}, Cu^{2+}). It has been determined that weathering did not easily remove the inorganic biocides from the chitosan membrane and the cell wall (Kobayashi et al., 1995);
4. Chitosan and *T. harzianum* (simultaneously inoculated) into the wood lumen produces lytic enzymes that are able to completely degrade the cellular membrane of bacteria and fungi (synergic effect). This method could be applied immediately after wood harvesting, eliminating its "pre-infection" (Chittenden and Singh, 2009).

Antimicrobial activity of chitosan appears related to its molecular weight as well as degree of deacetylation (Rabea et al., 2003). However, opinion is divided as to whether low-or high-molecular-weight chitosan and chitosan products are most effective. Some research groups suggest the higher effectiveness of high-molecular-weight chitosan on wood decay fungi (Eikenes et al., 2005), but there are also indications that certain fractions of low-molecular-weight chitosan oligomers are quite effective against *T. harzianum*, *L. procera*, and *S. sapinea* (Hirano and Horiuchi, 1989; Chittenden and Singh, 2009). Mellegård et al. (2011) reported that no trends in antibacterial action related to increasing or decreasing molecular weight.

The preparation of chitosan oligomers can be performed by chemical or enzymatic methods (Hussain et al., 2012; Jeon et al., 2000). Depolymerization is carried out by nitrous acid deamination (Tømmeraas et al., 2001), flurolysis in anhydrous hydrogen fluoride (Defaye et al., 1994), or oxidative–reductive reaction by hydrogen peroxide (Nordtveit et al., 1994). Enzymatic methods consist of hydrolysis of chitin and chitosan with hydrolytic enzymes (Jeon et al., 2000) or synthesis from smaller oligosaccharides with enzymes having transglycosylation activities (Hussain et al., 2012).

However, several researches have reported that chitosan is able to leach from the wood structure in time, thus limiting the application of this type of treatment. The chitosan content in wood after leaching was reported to be just above 25 mg/g of wood, which corresponds to a 50 kg/m^3 chitosan solution uptake with dry wood density of 500 kg/m^3 (Larnøy et al., 2005).

For these considerations, generally a chitosan formulation with high molecular weight is desirable. However, the higher the average molecular weight of the chitosan in a solution the higher is the viscosity of the solution. Furthermore, the higher the viscosity of an impregnation solution, the less is the uptake in wood during impregnation. Schmidt et al. (1995) concluded that by a vacuum treatment of pine sapwood with a 2% (weight/volume) solution chitosan produced a weight percent gain (WPG) of 2.7% but did not result in any swelling of the wood in either tangential or radial direction. This suggests that chitosan was located in the cell lumens rather than penetrating into the cell wall. The chitosan leaches from the wood structure, signifying weak physical interaction between wood polysaccharides and chitosan molecules (Kiljunen et al., 2012).

Several methods are currently used to fix chitosan and chitosan-compatible small-molecule biocides into the wood structure, among which two are the most common:

- Variants of the so-called royal process: impregnation of wood with chitosan under pressure (8—10 bar), fixation of the chemicals into wood for a period of 24 h followed by oil (tall, linseed) treatment of the chitosan-impregnated wood for several hours at 80 to 100 °C under reduced pressure (80 to 100 mbar). The unsaturated oil polymerizes and forms a hydrophobic barrier that impedes chitosan and other co-impregnated biocides (if any) leaching from the wood structure (Liibert et al., 2011);
- Fixing of chitosan on (hemi) cellulose by cross-linking it with citric acid to the (hemi) cellulose from the wood cell walls using sodium hypophosphite or *p*-toluenesulfonic acids as catalysts (Kiljunen et al., 2012).

Experimental results have confirmed that chitosan has higher antibacterial and anti-fungal activity than chitin, from which it is obtained by deacetylation. It is worth observing that the amount of polycationic chitosan available to bind to a charged bacterial surface is apparently reduced as the concentration of chitosan increases. A possible explanation is that in the presence of a larger number of charged sites, the chains tend to form clusters by molecular aggregation while they are still in solution. In such conditions, adjustments on pH could be decisive for a good solubility and to keep the chains apart from each other (Goy et al., 2009).

Similar to bacteria, the chitosan activity against fungus is assumed fungistatic rather than fungicidal. Generally, chitosan has been reported as being very effective in inhibiting bacterial spore and ascospore germination, hyphae development, germ tube elongation, and radial growth (Badawy and Rabea, 2011; Goy et al., 2009). The anti-fungal mechanism of chitosan involves cell wall morphogenesis with chitosan molecules interfering directly with fungal growth, similarly to the effects observed in bacteria cells (El Ghaouth et al., 1992; Goy et al., 2009). Microscopic observation reported that chitosan oligomers diffuse inside hyphae interfering with the enzyme activities responsible for the fungal growth (Eweis et al., 2006; Goy et al., 2009). The intensity of degradation action of chitosan on fungal cell walls is also dependent upon the concentration, degree of acetylation, and local pH (Stössel and Leuba, 1984). Inhibition rate on the order of 80% against several fungal strains have been known to occur at chitosan concentrations of 20 to 150 mg/L. Several researchers have noted that the optimum concentration of chitosan is 5% (w/vol) in aqueous solutions of pH from 2 to 5.5 as antibacterial agent. Other researchers report that a 1% solution of chitosan is able to completely inhibit the development of fungi from spores on agar plates. When using chitosan formulations at acidic pH, it is to be noted that pH values lower than 3 could lead to hemicellulose hydrolysis or lignin solubilization and leaching from wood (Eikenes et al., 2005).

Chitin and chitosan present unique features that deem them suitable for use as natural wood preservatives. However, the limited solubility of chitin in conventional wood-preservation solvents and rigorous control of pH (in the case of chitosan) due to their macromolecular nature, currently limit the use of chitin-derived biopolymers as wood preservatives (Kumar, 2000). In addition, the high viscosity of the impregnation solutions that ensures only surface penetration of the polymers into the wood structure, would require more complex vacuum-impregnation treatments.

An alternative method is to use mild organic solvents for chitin-derived biopolymers such as ionic liquids (ILs). These compounds comprise a large and highly asymmetric alkylimidazolium-, alkylpiridinium-, alkylpyrolydynium-, alkylphosphonium-, or alkylammonium-based organic cation and an anion of organic or inorganic origin (Plechkova and Seddon, 2008; Rogers and Seddon, 2003). The asymmetric bulky organic cation is able to disrupt the inter- and/or intramolecular bonds in the biopolymer's supramolecular architecture, dissolving them.

The dissolution usually occurs at temperatures between 80 and 130 °C, depending on the structure of the polymer, its molecular mass, heating conditions, the nature of the IL anion, and so forth. ILs have been successfully used as solvents for polysaccharides (celluloses, chitin, and chitosan), proteins (keratin, fibroin, zein, silk proteins, etc.), and other types of biopolymers, thus introducing the means to avoid the use of expensive toxic volatile organic solvents (Biswasa et al., 2006). In addition, recent studies have proven ILs efficient as wood preservatives (Han et al., 2009), antistatic agents for wood (Croitoru et al., 2011b; Li et al., 2004), and thermal and UV stabilizers (Patachia et al., 2012) for wood and cellulose.

Recently, our research group from Transilvania University of Brasov, Romania, has proposed an alternative impregnation method with biopolymers from the polysaccharide class, among which chitosan and chitin are included (Croitoru et al., 2011a). This impregnation process includes four steps, as follows: (1) the preparation of biopolymer solutions, in alkylimidazolium ionic liquids; (2) the impregnation of wood samples by immersing them into the obtained solutions at 40 °C; (3) the precipitation of the impregnant into the wood structure by adding water and eliminating the ionic liquid carrier; and (4) the drying of the material and conditioning it at 55% relative humidity. The ratio of the volume of the impregnation dispersion to the volume of the sample was set at 1.25, to ensure a complete covering of the sample with the dispersion (Croitoru et al., 2015).

Testing performed on the impregnated-wood specimens have revealed wood percent gains (WPGs) of 18% to 21% for the chitosan impregnation process (at 600 to 680 kg/m^3 impregnation solution uptake) and WPGs of 13% to 16.5% for chitin (at 485 kg/m^3 impregnation solution uptake). The precipitated impregnant is able to form a continuous barrier on the surface of the wood, and to penetrate into the wood structure, acting as a moisture barrier.

The chitosan- and chitin-impregnated wood presents a water uptake value of only 2% to 5%, by comparing with reference wood (120%). Studies regarding the impregnation of spruce wood using ILs as carriers have indicated that chitosan is able to increase the Brinell hardness of the wood to 88 MPa, similar to the values of more exotic wood species. SEM analysis has been performed to evidence the wood morphology changes as a result of the impregnation process that could explain the

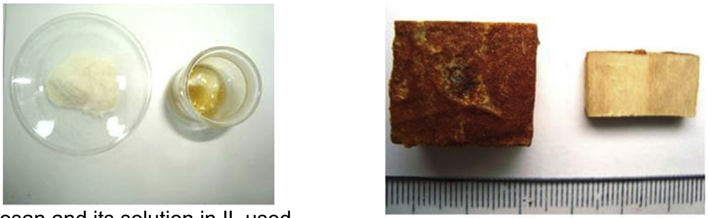

Chitosan and its solution in IL used for impregnation

Macrostructure of chitosan-impregnated wood

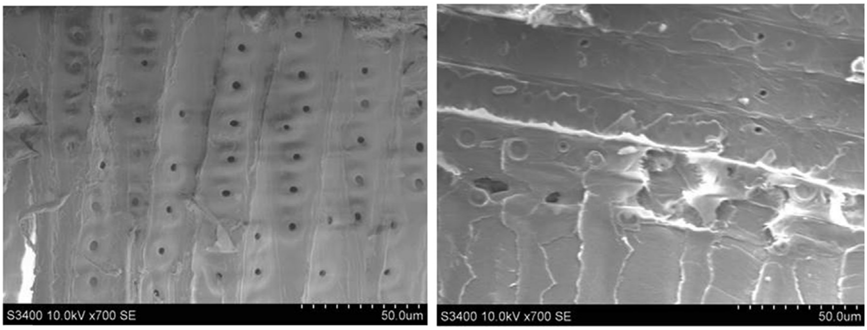

Reference wood

Chitosan-impregnated wood

Microstructure

Figure 14.5 Structure of chitosan-impregnated wood and reference samples.

properties of the impregnated wood. Figure 14.5 presents the SEM cross-section images of impregnated samples and reference wood.

For the reference wood, several structural features, such as tracheids displaced in parallel radial rows, bearing inside circular areolate pits (500×) could be observed. It could be noted that the impregnated-wood structure seems to be more consolidated due to tracheid shrinking.

This could explain the higher Brinell hardness values obtained for impregnated wood, in comparison with the reference. In addition, even if the tracheid walls are still visible in the impregnated samples, the areolate pits inside them seem to be covered by the impregnant. The covering of the areolate pits inside the tracheids could also be accounted for by the lower water-absorption values and lower volume modification of the impregnated samples (Croitoru et al., 2011a, 2015).

14.3.2 Proteins used in wood preservation

Proteins are macromolecules that could be found in all organisms. Although the majority of micro-organisms and plants can biosynthesize all 20 common amino acids, some micro-organisms, animals, and humans must obtain some of them from the diet (Voet and Voet, 2004). A large number of proteins are nontoxic compounds; the presence of nitrogen atoms in their molecule could contribute to microorganism nourishment.

To understand why proteins have been proposed for use in wood preservation, some remarks have to be made. First, the use of synthetic polymers in wood preservation is well known. Some of them exert a direct biocide action, but most of them, impregnated into the wood structure, act as barriers against the release of classical biocide systems such CCA. In this way, the biocide is kept for longer time in the wood structure, protecting it from fungal, mold, and insect attack. The biocide will be more efficiently used, in smaller amount, and the decreased release into environment will ensure its protection. Nevertheless, synthetic polymers are oil-based products, obtained by polluting technologies, and they are nonbiodegradable. In addition, technologies of wood preservation based on synthetic polymers are polluting, because volatile organic solvents need to be used. Wood protected with synthetic polymers become environmental issues at its end life cycle, due to problems related to its recycling. For these reasons, natural polymers have to replace synthetic polymers use in wood preservation.

Proteins are very available and renewable materials. They are biodegradable, nontoxic, and some of them are water soluble (globular proteins). From the chemical point of view, proteins are polyamides. They consist of one or more long chains of amino acid residues named polypeptides. Most proteins consist of linear polymers built from a series of up to 20 different L-α-amino acids (Figure 14.6). Proteinogenic amino acids possess common structural characteristics, including an amino group, a carboxyl group, and variable side chains bonded to an α-carbon.

R radicals could contain different functional groups such as $-NH_2$ amine groups (i.e., lysine, arginine, or histidine), carboxylic or amid groups (glutamic acid or glutamine), alcoholic groups (i.e., serine), or sulfur (i.e., cysteine or methionine) (Voet and Voet, 2004).

The high number of protein functional groups, containing atoms bearing unbonded electrons, determines their capacity to avidly chelate metallic ions (Cu, Zn, Mg, Fe, In, etc.) (Figure 14.7). Some of the metal ions are antimicrobials (for example, Cu^{2+}, Zn^{2+}). Due to the protein chelation equilibrium, Cu^{2+}, commonly used in wood preservation, will be slowly released from the chelate, ensuring the antimicrobial effect for a long time.

Also, the mild basic character of $-NH_2$ amine and $-NH-$ amide groups from the protein structure allows reaction with a well-known, nontoxic to mammals biocide, used in wood preservation: boric acid. Protein borates and polyborate could be easily obtained by just mixing aqueous solutions of protein with boric acid.

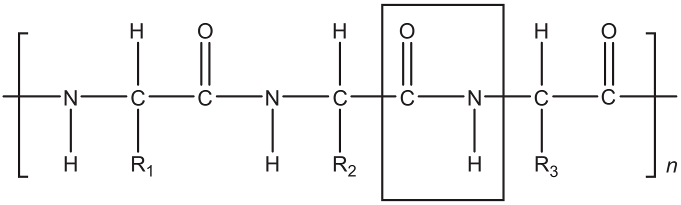

Figure 14.6 Structural moiety of proteins.

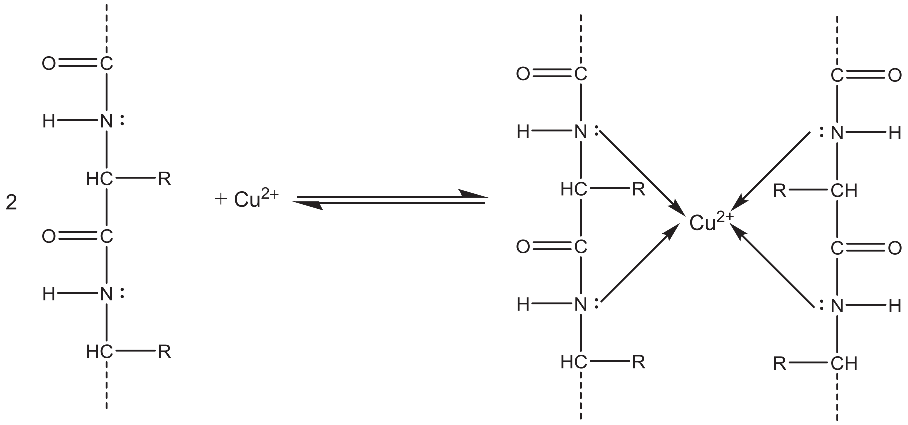

Figure 14.7 Chelating of proteins with metal cation mechanism.

The use of premanufactured-protein borate salts could be also a good method of greatly retarding the leaching of boron from treated timber (Thevenon et al., 1997; Thevenon and Pizzi, 2003).

As in case of chelation, protein borate formation is a reversible process. When equilibrium is reached, a small amount of boron coexists with other chemical species, being free to exercise its anti-fungal activity. Protein bonding drastically diminishes the boron tendency to diffuse and greatly retards its leaching from the wood (Mazela and Polus-Ratajczak, 2003).

Proteins differ from one another by their sequence of amino acids that determines folding of the protein into a specific three-dimensional structure. This complex structure is developed on four levels: *primary structure*, given by the covalent bonds of atoms in polyamide chain; *secondary structure*, given by H bonds created between N—H groups and C=O groups from the local polyamide backbone and having as an effect the obtaining of alpha helix, beta sheet, and turns; *tertiary structure*, given by interaction between different secondary structures through hydrophobic interaction, salt bridges, hydrogen bonds, disulphide bonds, having as an effect a general stabilization of the folded protein molecule; and *quaternary structure* that consists in complexes generated by interaction between several polypeptide macromolecules that function as a single protein complex.

The complex superstructure of proteins makes them very sensitive to environmental factors such as high temperatures, strong bases or acids, alcohols, ionizing radiation, and other actions. They determine protein irreversible precipitation, called denaturation.

Denaturation causes the breaking of bonds, which are responsible for supporting the secondary structure of proteins, and thus induces changes in protein conformation (such as peptide chain unfolding), and consequently changes in their physical, chemical, and biological properties. The majority of proteins start their denaturation at temperatures above 50 °C. The longer and more intensive the action of the destabilization factor on the proteins structure is, the more severe are the changes found in protein natural structure.

The denatured proteins have a much lower solubility in water, by comparing to the initial proteins. This property of proteins makes them suitable to be used in wood preservation, first, due to the limitation of water diffusion into the wood structure. The absorbed water determines the dissolution of preservatives initially impregnated into the wood and leads to their leaching. Second, the denatured proteins coagulated into the wood structure modulate the preservative release. This process is controlled both by the chemical equilibrium of protein chelation or complexation and by diffusion of the biocide species through the denser wood structure obtained by pores filling with denatured proteins.

The performance of protein complexes and the nature of coagulum depend on the ratio of biocide agent (boric acid, polyborate ions, metal ions) and proteins, as well as on the pH.

It was observed that the increased protein concentration in the solution of impregnation decreased the leaching of copper (II) sulfate. These results show that the addition of protein caused a significant improvement of the fixation of the copper-based formulation to the wood structure (Polus-Ratajczak and Mazela, 2004). In the presence of Solutein animal protein in wood impregnation solution, the level of copper retention increased at 2.75 g/kg by comparing to the wood treatment with copper alone, when the retention is approximately 1.6 g/kg (Ratajczak et al., 2008). Obanda et al. (2008) showed that protein—boron retention was 3—4 times higher on cellulose than on lignin, possibly because the aromatic acyclic lignin system is less susceptible to the action of amino acid groups. It was also found that copper concentration in the impregnating solution should not exceed 0.5%. For higher concentrations, the precipitation of $CuSO_4 \cdot 5H_2O$ salt appears in wood, and this precipitated salt is easily leached out. For pH values higher than 4.8, an increase in the chelating strength with the wood components have been observed (Ratajczak et al., 2008).

In addition, albumin at an acidic pH provides a more durable performance than at alkaline pH, due to the higher relative proportion of covalent bonds between boric acid and protein at the lower pH. In the alkaline range, ionic charge of functional groups determines the prevalence of hydrolysis process. At $pH < 7$, the protein coagulates with boric acid moieties attached to suitable alkaline sites on the protein. The boron compound does not form bridges between different sites of the protein but is only a pendant group grafted onto it. At alkaline pH, polyborate bridges between different sites of the protein are ionic and hydrolyzable (Thevenon and Pizzi, 2003; Polus-Ratajczak and Mazela, 2004).

Aqueous solution of proteins can impregnate or coat the wood by soaking, injection (vacuum and vacuum-pressure methods), spraying, or brushing techniques. Then, in situ denaturation of the proteins by heat-induced treatment leads to protein insolubilization. This process determines the wood structure consolidation, by pores filling with insoluble polymer that acts also as an efficient barrier against the water adsorption and the fungicide leaching from the wood (Mazela and Bartkowiak, 2007).

Due to the high molecular mass of the proteins, as well as to their complex structure, the water dissolution until reaching the molecular level is difficult and the viscosity of the obtained solutions is high. To decrease the solution viscosity aiming to make easier its sorption into the wood structure and to optimize the energetic efficiency of the process (reducing the heat, pressure and corrosive chemicals amount) the proteins have been enzymatically hydrolyzed. Protease produced by bacteria from genus *Bacillus* has been successfully used to obtain peptides (Ahn et al., 2010).

Among the preservatives used in association with proteins, $CuSO_4$, $CuCl_2$, $Na_2B_4O_7 \cdot 10H_2O$, and $Na_2B_8O_{13} \cdot 4H_2O$ are the most frequently used. The reference literature mentions the following wood species impregnated with proteins: Scots pine (*Pinus sylvestris* L.) sapwood; aspen poplar (*Populus tremula* L.) against a large variety of pathogenic fungi (*Coniophora puteana*, *Coriolus versicolor*, *Lentinus squarrosulus Coriolus*, *Pycnoporus sanguineus versicolor*, *Antrodia* sp., *Poria placenta*) and insects (*Heterotermes indicola*, *R. Flavipes*).

Different types of proteins have been tested in wood preservative formulation such as:

- Collagen, a fibrous triple-helix protein, insoluble in water, with an atypical amino acid composition for proteins, particularly with respect to its high hydroxyproline content. After hydrolysis it will be irreversibly transformed into gelatin, a soluble form of collagen (Thevenon et al., 1998),
- Casein, a protein family commonly found in mammalian milk (80% proteins in the cow milk), relative hydrophobic and then insoluble in water; it could be dispersed in water (Thevenon et al., 1998),
- Soy flour, obtained by soybeans finely ground. It contains approximately 50% protein and 5% fiber and does not contain gluten (Thevenon et al., 1998),
- Defatted soy flour (Honey Mill 90; (Harvest State, Mankato, Minnesota: HM), Arpro 2100 (ADM, Decatur, Illinois (IL): Arpro), and Supro 760 (ProteinTechnologies International, Palatine, IL: Supro)). Dry HM soy flour has a typical composition of 55% protein, 37% carbohydrates, and 8% other components, mainly salts. Arpro is a soy protein isolate in granular form, obtained by a salt-precipitation process and typically containing over 90% protein and 10% salts. Supro is also a soy protein isolate, obtained by spray-drying from a neutral pH solution (Yang and Myers, 2006);
- Hydrolyzed Okara (OK) that is the residue generated as a by-product during soymilk and tofu production (containing about 27% proteins, 53% fibers and carbohydrates, 12% fats and oils, and 8% ash) (Ahn et al., 2010) or OK free of moisture, containing 8−15% fats, 12−14.5% crude fiber, and 24% protein (Kim et al., 2011);
- Egg albumin (Thevenon et al., 1998); the main components of whole egg are egg-white (albumin) (58%) and yolk (31%) (Audic et al., 2003). Egg-white contains about 11% proteins with the most abundant ovalbumin, conalbumin, ovomucoid, and lysozyme. Ovalbumin, the major egg-white protein fraction constituting 54−60% of the egg white, is a phosphorylated and glycosylated globular protein (Coughlan et al., 2004) of 385 amino acids (45 kDa) the secondary structure of which consists of approximately 30% α-helixes and 30% β-sheets. Albumen has the ability to form gel networks, increase solution viscosity, and stabilize emulsions and foams. Egg albumen is also a good candidate for producing edible film for food package (Song and Zheng, 2014);
- Animal blood plasma (in the form of the spray-dried animal blood plasma; commercial products called SOLUTEIN™ and AP 820™ (APC, Poznan, Poland) containing albumin (50% of total plasma proteins with MW 66 000 Da), γ-globulin (15% of total plasma protein with MW 150 000 Da), α-globulin (approx. 15% of total plasma proteins) and β-globulin (approx. 15% of total plasma proteins; 1−10% concentration) (Polus-Ratajczak and Mazela, 2004), freeze-dried blood plasma (Mazela and Bartkowiak, 2007; Ratajczak et al., 2008);

- Zein is the prolamine fraction of corn protein (Padua et al., 2003) belonging to the prolamins proteins group. The prolamins are a group of globular proteins found in grasses, above all in cereal crops such as corn (zein), wheat (gliadin), and oats (avenin), and are characterized by a high amount of the amino acids proline and glutamine from which the name prolamine is derived. Prolamins contain only small amounts of the amino acids arginine, lysine, and histidine. Zein is a nontoxic, combustible, white to light-yellow powder with no odor or taste. Zein is produced as a by-product from corn processing (Murray et al., 1995). It consists of 17 amino acids and is completely free of the amino acids cystine, lysine, and tryptophan. Zein is soluble in diluted alcohol but insoluble in water, diluted acids, esters, anhydrous alcohols, turpentine, oils, and fats. Zein is recognized for its ability to form films and provides a relatively good barrier to oxygen and water. Zein is one of the few proteins commercially used to impart surface gloss and to act as an O_2, lipid, and/or moisture barrier. Formation of zein films from aqueous alcohol casting solutions involves development of hydrophobic, hydrogen, and limited disulfide bonds between zein chains in the film matrix during the alcohol evaporation (Song and Zheng, 2014).

Samples of wood treated with Zein + Acetem (acetylated mono- and diglyceride), with Acetem + Natamax (natamicin antimicrobial), or with glycerol-plasticized zein presented fungi-inhibiting properties, providing a barrier against moisture and oxygen that is necessary for mold growth. In addition, Acetem has acidic properties providing even more inhibiting effect (Thomas and Delves-Broughton, 2005).

Croitoru et al. (2011, 2015) have proposed a mild impregnation of spruce (*Picea abies* sp.) with 5% zein solution in 1-alkyl-3-methylimidazolium chlorides at 40 °C. The alkylimidazolium ionic liquids are able to readily dissolve zein in a higher amount than in the case of traditional volatile organic solvents, such as ethanol, acetone, or their mixtures (maximum solubility of 2%), resulting a solution with low viscosity that could be readily adsorbed (relative solution uptakes of 520 kg/m^3) and rapidly diffuse into the wood structure (Figure 14.8).

By removing the ionic liquid carrier by water addition, zein precipitates into the chamber pits of the wood tracheids and on the surface of the impregnated wood, providing a barrier to oxygen, micro-organisms, and moisture (WPG's of 15–17%). In addition, the zein coating increases the hardness of spruce wood with 10%, thus increasing its wear resistance. In addition, the impregnated wood could be protected due to zein antimicrobial effect.

Another important finding concerning the wood preservative formulations is the beneficial influence of the addition of tannin extracts to the protein–borate complexes. Tannins are a class of complex biomolecules of polyphenolic nature synthesized by a large variety of plants, in which they are used as antipredation or pesticide agents. Their molecular weight ranges from 500 (in the case of oligotannins) to 20,000. There are currently four types of tannins: gallotannins (esters of gallic acid), ellagitannins (formed by oxidative linkage of galloyl groups from 1,2,3,4,6-pentagalloyl glucose), condensed tannins (formed by C4 glycosidic linkage of catechin to gallotannin or ellagitannin units), and complex tannins, in which a catechin unit is bound glycosidically to a gallotannin or an ellagitannin unit (Figure 14.9).

The tannin–protein combination helps to fix the boric acid into the wood structure, greatly retarding its leaching. The tannin effect is strongly dependent on the type of

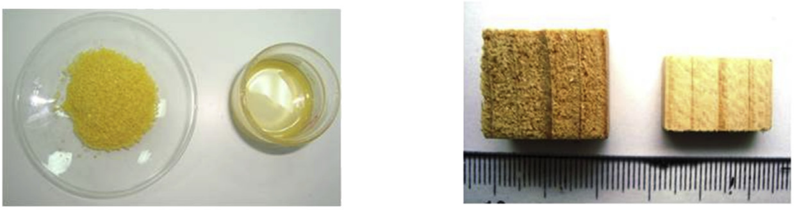

Zein and its solution in IL used for impregnation

Macrostructure of zein-impregnated wood

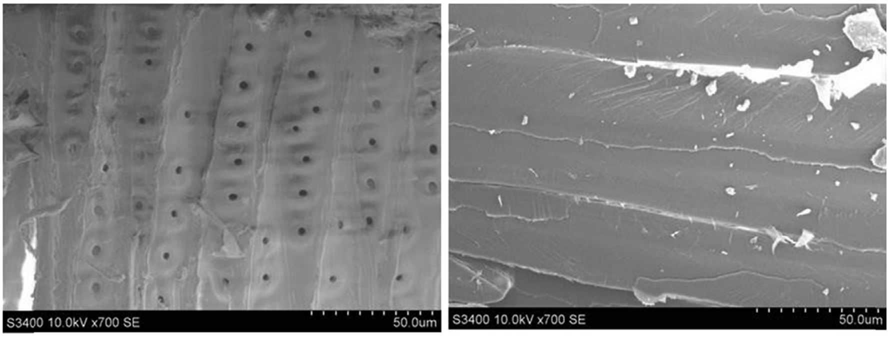

Reference wood

Zein-impregnated wood

Microstructure

Figure 14.8 Structure of zein-impregnated wood and reference samples.

protein used. Although the top-performing albumin borate does not show any marked improvement when tannin is added in relation to albumin borate alone (Thevenon et al., 1997), the collagen borate performance improves markedly when tannin is present in relation to soluble collagen borate alone (Thevenon et al., 1997). This is due to the insolubilization of collagen by reaction with tannin, identical to the process that occurs in leather tanning. If not coupled with tannin, collagen-based animal glue and collagen borates have been proved to remain soluble (Thevenon et al., 1997) leading to much worse performances. If both albumin borate and collagen borate are added together with the tannin solution in a single impregnation step into the wood, the stability at ambient temperature of the mixed solutions would be low due to the low tannin concentration (at much higher tannin concentrations this would not be possible). This allows, then, a single-step water-borne treatment with its consequent economic and technical advantages (Thevenon et al., 1998).

It was also demonstrated that tannic acid addition to the protein-based impregnation solution is very effective in copper ion retention (5.83 g/kg, by comparing to 2.75 g/kg retained when protein alone is used and 1.6 g/kg retained when copper sulfate alone is used) (Ratajczak et al., 2008).

Despite these remarkable results obtained in both biocide retention level and its slow release when proteins are used in wood preservative formulations, new studies look for alternatives to biocide (boron) complexation, addressing its bioavailability.

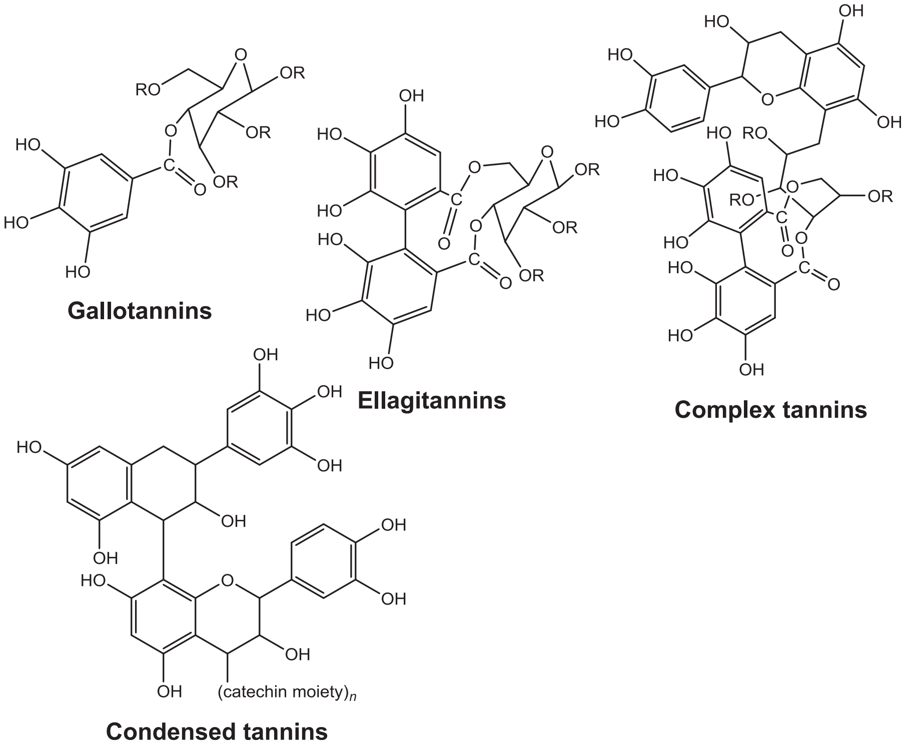

Gallotannins

Ellagitannins

Complex tannins

Condensed tannins

Figure 14.9 Structure of tannin moieties.

Starting from the idea that the biological activity of borate is primarily due to tetrahydroxyborate ions $[B(OH)_4]^-$, which are able to form complexes with polyols of wood-destroying fungi through extracellular and intracellular substrate sequestration, enzyme inhibition, and changes in membrane function, Obounou-Akong et al. (2015) proposed a new strategy in wood preservatives obtaining: loading of biocide (boron) in a smart tripeptides thermos-reversible hydrogel. They reported that small amounts of hydrogelators (2–3%) improved boron retention in wood, allowing its protection against the brown rot fungus *Poria placenta* and termites (*R. flavipes*) even after leaching, whereas blocks treated with the same concentration of borax were strongly degraded after leaching.

14.3.3 Polylactic acid

Polylactic acid (PLA) is a thermoplastic biopolymer belonging to the polyester class. It is obtained either by enzymatic conversion of starch or by catalytic ring-opening polymerization of its corresponding lactone. It has many uses in the domain of the food industry and the pharmaceutical industry, especially as packaging material (Placket and Sodengard, 2005).

It has been used in the manufacturing of biocomposites from wood, due to its oxygen- and moisture barrier-forming properties (Altun et al., 2013). Although not biocidal itself, PLA could be loaded with anti-fungal or antimicrobial agents to prolong the life cycle of impregnated-wood materials (Pizzi, 2015).

14.3.4 Biobased resins

14.3.4.1 Biobased polyurethane resins

Polyurethanes are a class of resins obtained as the product of the reaction of an isocyanate (more frequently a polymeric isocyanate) with a polyol. Due to this composition as regards green chemistry, the fundamental approach to obtain biobased polyurethanes has been to substitute the synthetic polyol with natural polyols. However, this approach still makes use of toxic isocyanates.

Only recently, successful attempts to produce polyurethanes not only from natural polyols but also without any use of isocyanates have appeared in the literature (Thebault et al., 2014a,b). In the first step, such a reaction employs the reaction between the hydroxyl groups of gallic acid moieties from hydrolyzable chestnut tannins with dimethyl carbonate, which could take place in three successive steps: a, b and c (Fig. 14.10). This process has a yield of 50% (Pizzi, 2015).

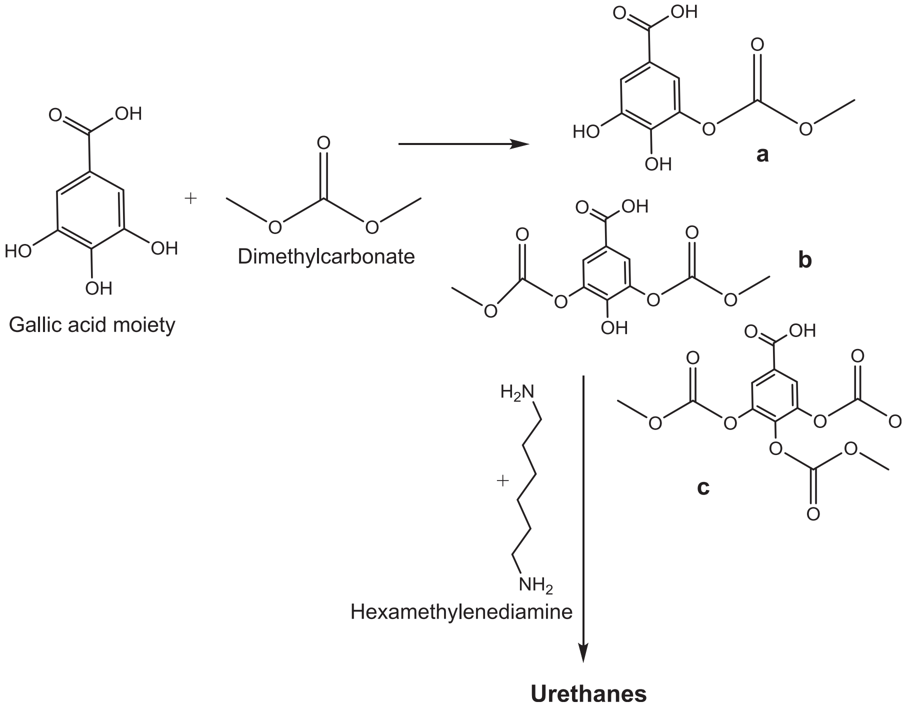

Figure 14.10 Obtaining of biobased urethanes (based on Pizzi, 2015).

Instead of hydrolyzable tannins, Thebault et al. (2014b) have used different condensed flavonoid tannins from maritime pine (*Pinus pinaster*), mimosa (*Acacia mearnsii*), radiata pine barks, and quebracho (*Schinopsis lorentzii* and balansae) wood. Braghiroli et al. (2013) have used aminized tannins as a source of amino groups, thus 80% of the final polymer resin is biosourced. The formed polyurethanes presented good rigidity, imparting high mechanical strength to wood. They also provide a moisture and oxygen barrier, thus protecting the structure of the wood from the external degrading factors (Pizzi, 2015).

14.3.4.2 Biobased epoxy resins

Although traditional synthetic epoxy resins are rarely used for wood impregnation due to their high price, nonetheless it is of interest that epoxy resins derived from wood- and bark-derived natural materials have been developed (Aouf et al., 2013) in competition with biobased epoxy resins obtained from vegetable oils (Stemmelen et al., 2011).

Catechin moieties from wood bark tannins have been reacted with epichlorohydrin to form glycidyl ethers (GEs), as precursors to epoxy resins. Epoxy resins formulated with GEs had slightly lower storage moduli but induced a decrease of the swelling percentage, suggesting GE-enhanced cross-linking in the epoxy resin networks (Pizzi, 2015).

14.3.4.3 Natural oligomeric and polymeric resins

Rosin is considered one of the oldest raw materials used in the wood industry, either as adhesive or as preservative. It is obtained by pine resin or tall oil distillation and contains oligomer (partially condensed) esters of abietic and pimaric-derived acids (Mildenberg et al., 2008).

Rosin-sizing agents designed to impregnate wood and immobilize copper in wood cells for protection against decay have been extensively investigated. Poplar (*Populus ussuriensis*) wood impregnated with combinations of 3% $CuSO_4$ solution and 1.0%, 2.0%, or 4.0% rosin-sizing agent the average weight losses of the samples degraded by fungi were less than 4%, by comparing to the weight losses of untreated control blocks (70.45% by *Trametes versicolor* and 61.84% by *Gloeophyllum trabeum*). Results showed that the amount of copper ions released from the samples treated with the copper–rosin solutions was half those from the samples treated with copper alone (Hyen et al., 2012). The mechanism employs the formation of a copper complex with the carboxyl groups from the abietic acid moiety. Waterproofing of wood lumber and veneers by the addition of rosin does increase considerably the dry mechanical resistance of the impregnated wood (Pizzi, 2015).

Guaiac resin (or guaiacum) is a natural product obtained from natural oxidation and polycondensation of plant sap belonging mainly to the Zygophyllaceae family. It is soluble in alcohols, acetone, and ether and insoluble in cold water. It is used mainly as a preservative in food and wood industry, due to its antimicrobial properties (Ash and Ash, 2004).

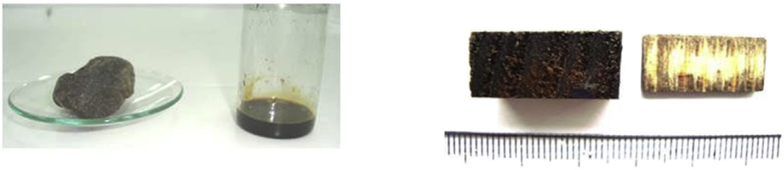

Guaiac resin and its solution in IL used for impregnation

Macrostructure of guaiac resin-impregnated wood

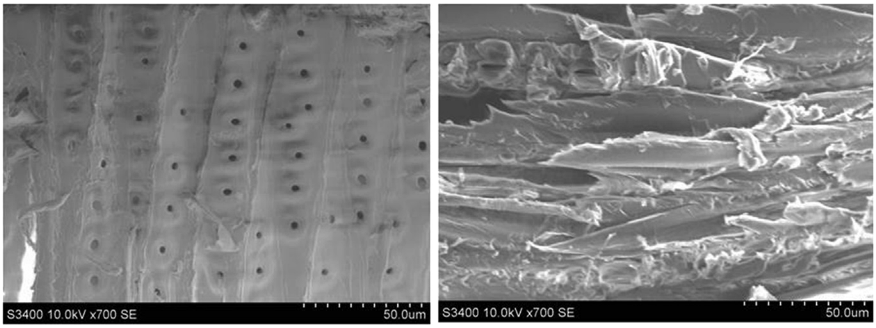

Reference wood

Guaiac resin-impregnated wood

Microstructure

Figure 14.11 Guaiac resin-impregnated wood and reference samples.

Croitoru et al. (2011, 2015) have used guaiac resin to impregnate spruce (*Abies* sp.) wood samples by using an 1-alkyl-3-methylimidazolium chloride ionic liquid as carrier for the resin (Figure 14.11).

The impregnation solution used was of 5% (weight/volume of IL), and the solution uptake of wood was 600 kg/m^3, proving good adsorption and compatibility with the tested wood. By elimination of the IL by water addition, the resin precipitates into the wood structure, closing the pits inside the tracheids, thus providing an efficient barrier to moisture and air.

14.4 Conclusions and future trends

As discussed throughout this chapter, the potential for developing innovative wood protection technologies based on the use of biopolymers as biocides or barrier-forming compounds penetrated into the structure of wood is rather enormous. The results show that a great deal of benefit occurs when designing protection systems based on natural compounds. These include cost-effectiveness due to the high availability and renewability of biopolymers and their capacity to act on multiple levels by complex mechanisms. Biopolymers enhance compatibility with the main components of wood that ensures a good penetrability of biopolymer into the wooden mass. In addition, it is possible to enhance the biopolymer biocidal activity through addition of other substances/agents, e.g., antioxidants, metal sequestering agents, or metal ions. Other benefits include prolonged maintaining of biocidal agent in the wood structure, minimizing the amount of toxic substances needed to obtain the same effect, protecting the environment and avoiding the issues linked to wood recycling.

Besides the traditional use of biopolymer in wood impregnation as aqueous dispersion or emulsion, new techniques of wood preservation have recently been designed. One such is the insertion of biopolymer hydrogels loaded with biocides into holes drilled into the wood mass that ensures controlled release of the biocide correlated with environmental factors (temperature and moisture). Another involves insertion of biopolymers by using as carrier an organic nonvolatile solvent for wood components (ionic liquids) that determines their swelling, ensuring a better penetrability and immobilization of the preservative into the wood structure.

All the reviewed studies took into consideration both the high value of the wood as construction material, furniture, packages, heritage objects, and usual goods, and environmental protection.

Even though a large number of studies have been published in the field of biopolymers used as wood preservatives, due to the great variability of their properties, depending on their provenance, contradictory results have been reported. More research and information are required to allow the technological transfer to industrial scale.

References

Adam, O., Badot, P.M., Degiorgi, F., Crini, G., 2009. Mixture toxicity assessment of wood preservative pesticides in the freshwater amphipod *Gammarus pulex* (L.). Ecotoxicology and Environmental Safety 72, 441–449.

Ahn, S., Oh, S.C., Choi, I., Han, G., Jeong, H., Kim, K., Yoon, Y., Yang, I., 2010. Environmentally friendly wood preservatives formulated with enzymatic-hydrolyzed okara, copper and/or boron salts. Journal of Hazardous Materials 178, 604–611.

Altun, Y., Dogan, M., Bayramli, E., 2013. Effect of alkaline treatment and pre-impregnation on mechanical and water absorbtion properties of pine wood flour containing poly (lactic acid) based green-composites. Journal of Polymers Environment 21, 850–856.

Aouf, C., Nouailhas, H., Fache, M., Calliol, S., Boutevin, B., Fulcrand, H., 2013. Multi-functionalisation of gallic acid. Synthesis of a novel bio-based epoxy resin. European Polymer Journal 49, 1185–1195.

Ash, M., Ash, I., 2004. Handbook of Preservatives. Synapse Information Resources Inc., New York, USA, pp. 406–407.

Audic, J.L., Chaufer, B., Daufin, G., 2003. Non-food applications of milk components and dairy co-products: a review. Lait 83, 417–438.

Badawy, M.E.I., Rabea, E.I., 2011. A biopolymer chitosan and its derivatives as promising antimicrobial agents against plant pathogens and their applications in crop protection. International Journal of Carbohydrate Chemistry 3, 100–129.

Barikani, M., Oliaei, E., Seddiqi, H., Honarkar, H., 2014. Preparation and application of chitin and its derivatives: a review. Iranian Polymer Journal 23, 307–326.

Betts, W.D., 2005. The properties and performance of coal-tar creosote as wood preservative. In: Thompson, R. (Ed.), The Chemistry of Wood Preservation. Woodhead Publishing, Elsevier, Amsterdam, pp. 117–135.

Biswasa, A., Shogrena, R.L., Stevensonb, D.G., Willetta, J.L., Bhowmikc, P.K., 2006. Ionic liquids as solvents for biopolymers: acylation of starch and zein protein. Carbohydrate Polymers 66, 546–550.

Braghiroli, F., Fierro, V., Celzard, A., Pizzi, A., Rode, K., Radke, W., Delmotte, L., Parmentier, J., 2013. Condensation reaction of flavonoid tannins with ammonia. Industrial Crops and Products 44, 330–335.

Bull, D.C., 2001. The chemistry of chromated copper arsenate II. Preservative wood-interactions. Wood Science and Technology 34, 459–466.

Chittenden, C., Singh, T., 2009. In vitro evaluation of combination of *Trichoderma harzianum* and chitosan for the control of sapstain fungi. Biological Control 50, 262–266.

Clausen, C.A., 2010. Biodeterioration of wood. In: Forest Products Laboratory. United States Department of Agriculture Forest Service, Madison, Wisconsin.

Coughlan, K., Shaw, N.B., Kerry, J.F., Kerry, J.P., 2004. Combined effects of proteins and polysaccharides on physical properties of whey protein concentrate-based edible films. Journal of Food Science 69, 271–275.

Croitoru, C., Patachia, S., Lunguleasa, A., 2011a. Solutions for Wood Impregnation, Based on Natural Polymers, Method of Preparation and Process for Application. RO126930 (A0).

Croitoru, C., Patachia, S., Lunguleasa, A., 2015. A mild method of wood impregnation with biopolymers and resins using 1-ethyl-3-methylimidazolium chloride as carrier. Chemical Engineering Research and Design 93, 257–268.

Croitoru, C., Patachia, S., Cretu, N., Boer, A., Friedrich, C., 2011b. Influence of ionic liquids on the surface properties of poplar veneers. Applied Surface Science 257, 6220–6225.

Defaye, J., Gadelle, A., Pedersen, C., 1994. A convenient access to β-(1-4)-linked 2-amino-2-deoxy-D-glucopyranosyl fluoride oligosaccharides and β-(1→4)-linked 2-amino-2-deoxy-D-glucopyranosyl oligosaccharides by fluorolysis and fluorohydrolysis of chitosan. Carbohydrate Research 261, 267–277.

Ding, X., Richter, D., Matuana, L., Heiden, P., 2011. Efficient one-pot synthesis and loading of self-assembled amphiphilic chitosan nanoparticles for low-leaching wood preservation. Carbohydrate Polymers 86, 58–64.

Eikenes, M., Alfredsen, G., Christensen, B.E., Militz, H., Solheim, H., 2005. Comparison of chitosans with different molecular weights as possible wood preservatives. Journal of Wood Science 51, 387–394.

Evans, P.D., Michell, A.J., Schmalzl, K.J., 1992. Studies of the degradation and protection of wood surfaces. Wood Science Technology 26, 151–163.

Eweis, M., Elkholy, S.S., Elsabee, M.Z., 2006. Antifungal efficacy of chitosan and its thiourea derivatives upon the growth of some sugar-beet pathogens. International Journal of Biological Macromolecules 38, 1–8.

Freeman, M.H., Shupe, T.F., Vlosky, R.P., Barnes, H.M., 2003. Past, present, and future of the wood preservation industry. Forest Products Journal 53, 8–15.

El Ghaouth, A., Arul, J., Grenier, J., Asselin, A., 1992. Antifungal activity of chitosan on two postharvest pathogens of strawberry fruits. Phytopathology 82, 398–402.

Gorgija, R., Tarmianb, A., Karimic, A.N., 2014. Effect of chitosan on the mold resistance of wood and its surface properties. International Journal of Lignocellulosic Products 1, 39–49.

Goy, R.C., de Britto, D., Assis, O.B.G., 2009. A review of the antimicrobial activity of chitosan. Polímeros 19, 241–247.

Han, S., Li, J., Zhu, S., Chen, R., Wu, Y., Zhang, X., Yu, Z., 2009. Potential applications of ionic liquids in wood related industries. Bioresources 4, 825–834.

Hashemi, S.K.H., Latibari, A.J., 2011. Evaluation and identification of walnut heartwood extractives for protection of poplar wood. BioResources 6, 59−69.

Hirano, S., Horiuchi, K., 1989. Chitin gels. International Journal of Biological Macromolecules 11, 253−254.

Hussain, I., Singh, T., Chittenden, C., 2012. Preparation of chitosan oligomers and characterization: their antifungal activities and decay resistance. Holzforschung 66, 119−125.

Hyen, T.T.H., Li, J., Li, S., 2012. Effects of water-borne rosin on the fixation and decay resistance of copper-based preservative treated wood. BioResources 7, 3573−3584.

Ikeda, T., Yamaguchi, H., Tazuke, S., 1984. New polymeric biocides: synthesis and antibacterial activities of polycations with pendant biguanide groups. Antimicrobial Agents and Chemotherapy 26, 139−144.

Jeon, Y.J., Shahidi, F., Kim, S.K., 2000. Preparation of chitin and chitosan oligomers and their applications in physiological functional foods. Food Reviews International 16, 159−176.

Kenawy, E.R., Worley, S.D., Broughton, R., 2007. The chemistry and applications of antimicrobial polymers: a state-of-the-art review. BioMacromolecules 8, 1359−1384.

Kiljunen, S., Kosk, A., Kunttu, M., Valkonen, T., 2012. Impregnation of Chemicals into Wood. EP 2485880 A1.

Kim, H.Y., Jeong, H.S., Min, B.C., Ahn, S.H., Oh, S.C., Yoon, Y.H., Choi, I.G., Yang, I., 2011. Antifungal efficacy of environmentally friendly wood preservatives formulated with enzymatic-hydrolyzed okara, copper, or boron salts. Environmental Toxicology and Chemistry 30, 1297−1305.

Kjellow, A.W., Henriksen, O., 2009. Supercritical wood impregnation. The Journal of Supercritical Fluids 50, 297−304.

Kobayashi, T., Furukawa, I., 1995a. Optimum conditions for the formation of chitosan-metal salts and their fixation in wood. Journal of Antibacterial and Antifungal Agents 23, 263−269.

Kobayashi, T., Furukawa, I., 1995b. Wood-preserving effectiveness of chitosan-metal salts against wood decaying fungi. Journal of Antibacterial and Antifungal Agents 23, 343−348.

Krzyzewsky, J., 1987. Arsenical Creosote Wood Preservatives. US 4656060 A.

Kumar, M.N.V.R., 2000. A review of chitin and chitosan applications. Reactive and Functional Polymers 46, 1−27.

Larnøy, E., Eikenes, M., Militz, H., 2005. Uptake of chitosan based impregnation solutions with varying viscosities in four different European wood species. Holz als Roh- und Werkstoff 63, 456−462.

Leuba, J.L., Stössel, P., 1986. Chitosan and other polyamines: antifungal activity and interaction with biological membranes. In: Muzzarelli, R., Jeauniaux, C., Gooday, G.W. (Eds.), Chitin in Nature and Technology. Plenum, New York, USA, pp. 215−222.

Li, X., Geng, Y., Simonsen, J., Li, K.C., 2004. Application of ionic liquids for electrostatic control in wood. Holzforschung 58, 280−285.

Liibert, L., Treu, A., Meier, P., 2011. The fixation of new alternative wood protection systems by means of oil treatment. Materials Science 17 (4), 402−406.

Lin, L.D., Chen, Y.F., Wang, S.Y., Tsai, M.J., 2009. Leachability, metal corrosion, and termite resistance of wood treated with copper-based preservative. International Biodeterioration & Biodegradation 63, 533−538.

Mazela, B., Polus-Ratajczak, I., 2003. Reduction of preservative leaching by animal proteins in wood. Holzforschung 57, 593−596.

Mazela, B., Bartkowiak, M., 2007. Animal protein impact on fungicidal properties of treatment formulations. Wood Research 52, 12−22.

Mellegård, H., From, C., Christensen, B.E., Granum, P.E., 2011. Inhibition of *Bacillus cereus* spore outgrowth and multiplication by chitosan. International Journal of Food Microbiology 149, 218–225.

Mildenberg, R., Zander, M., Colin, G., 2008. Hydrocarbon Resins. VCH Publishers Inc., New York, USA, pp. 41–50.

Murray, R.K., Granner, D.K., Mayes, R.A., Rodwell, V.W., 1995. Harper's Biochemistry, 24th ed. Appleton & Lange, Stamford, USA, pp. 65–68.

Muzzarelli, R.A.A., Boudrant, J., Meyer, D., Manno, N., DeMarchis, M., Paoletti, M.G., 2012. Current views on fungal chitin/chitosan, human chitinases, food preservation, glucans, pectins and inulin: a tribute to Henri Braconnot, precursor of the carbohydrate polymers science, on the chitin bicentennial. Carbohydrate Polymers 87, 995–1012.

Niaounakis, M., 2013. Biopolymers Reuse, Recycling, and Disposal. Elsevier, Amsterdam, The Netherlands, pp. 1–75.

Nordtveit, R.J., Varum, K.M., Smidsrod, O., 1994. Degradation of fully water-soluble, partially N-acetylated chitosans with lysozyme. Carbohydrate Polymers 23, 253–260.

Obanda, D.N., Shupe, T.F., Barnes, H.M., 2008. Reducing leaching of boron-based wood preservatives–a review of research. Bioresource Technology 99, 7312–7322.

Obounou-Akong, F., Gerardin, P., Thevenon, M.F., Gerardin-Charbonnier, C., 2015. Hydrogel-based boron salt formulations for wood preservation. Wood Science and Technology 49, 443–456.

Padua, G.W., Rakotonirainy, A.M., Wang, Y., 2003. Thermal behavior of zein-based biodegradable films. Starch/Stärke 55, 25–29.

Passialis, C., Grigoriou, A., Voulgaridis, E.V., 1995. Utilization of oleoresin and bark extractives from *Pinus halepensis* Mill in wood products. Forêt méllilermnéenne 16, 19–27.

Patachia, S., Croitoru, C., Friedrich, C., 2012. Effect of UV exposure on the surface chemistry of wood veneers treated with ionic liquids. Applied Surface Science 258, 6723–6729.

Pizzi, A., 1993. A new approach to non-toxic, wide-spectrum, ground contact wood preservatives, part 1: approach and reaction mechanisms. Holzforschung 47, 253–260.

Pizzi, A., 2015. Wood products and green chemistry. Annals of Forest Science. http://dx.doi.org/10.1007/s13595-014-0448-3.

Placket, D., Sodengard, A., 2005. Natural Fibers, Biopolymers and Biocomposites. Taylor and Francis, Boca Raton, USA, pp. 55–68.

Plechkova, N.V., Seddon, K.R., 2008. Applications of ionic liquids in the chemical industry. Chemical Society Reviews 37, 123–150.

Polus-Ratajczak, I., Mazela, B., 2004. The use of blood protein in wood preservatives. Holz als Roh- und Werkstoff 62, 181–183.

Rabea, E.I., Badawy, M., Steven, C.V., Smagghe, G., Stebuaut, W., 2003. Chitosan as antimicrobial agent: application and mode of action. Biomacromolecules 4, 1457–1465.

Ratajczak, I., Hoffmann, S.K., Goslar, J., Mazela, B., 2008. Fixation of copper (II)-protein formulation in wood: part 1. Influence of tannic acid on fixation of copper in wood. Holzforschung 62, 294–299.

Rinando, M., 2006. Chitin and chitosan: chitin and chitosan properties and applications. Progress in Polymer Science 31, 603–632.

Rogers, R.D., Seddon, K.R., 2003. Ionic liquids–solvents of the future? Science 31, 792–793.

Schmidt, O., Müller, J., Moreth, U., 1995. Potentielle Schutzwirkung von Chitosan gegen Holzpilze Fachzeitschrift. Holz-Zentralblatt 121, 2503–2513.

Schultz, T.P., Nicholas, D.D., 2008. Improving the performance of organic biocides by using economical and benign additives. In: Schultz, T.P., Militz, H., Freeman, M.H., Goodell, B., Nicholas, D.D. (Eds.), Development of Commercial Wood Preservatives; Efficacy, Environmental and Health Issues. American Chemical Society, Washington, USA, pp. 272−284.

Schweingruber, F.H., 2007. Wood Structure and Environment. Springer, Berlin, Germany, pp. 33−44.

Singh, A.P., Singh, T., Rickard, C., 2010. Visualising impregnated chitosan in *Pinus radiata* early wood cells using light and scanning electron microscopy. Micron 41, 263−267.

Singh, T., Chittenden, C., Singh, A.P., Franich, R., 2008. Chitosan as a potential wood preservative. Wood Processing Newsletter 42, 11−23.

Singh, T., Singh, A.P., 2012. A review on natural products as wood protectant. Wood Science and Technology 46, 851−870.

Song, Y., Zheng, Q., 2014. Ecomaterials based on food proteins and polysaccharides. Polymer Reviews 54, 514−571.

Srivastava, V.K., Pizzi, A., 2014. Characterization and preparation of wood/furanic foams. Journal of Renewable Materials 2, 201−206.

Stemmelen, M., Pessel, F., Lapinte, V., Calliol, S., Habas, J.P., Robin, J.J., 2011. A fully biobased epoxy resin from vegetable oils: from the synthesis of the precursors of thiol-ene reaction to the study of the final material. Journal of Polymer Science A 49, 2434−2444.

Stössel, P., Leuba, J.L., 1984. Effect of chitosan, chitin and some aminosugars on growth of various soilborne phytopathogenic fungi. Journal of Phytopathology 111, 82−90.

Tamura, H., Nagahama, H., Tokura, S., 2006. Preparation of chitin hydrogel under mild conditions. Cellulose 13, 357−364.

Tao, W., Shi, S., Kroll, C.N., 2013. Influences of wood preservation, lumber size, and weather on field leaching of red pine lumber. Journal of Hazardous Materials 260, 296−304.

Taylor, A.M., Gartner, B., Morrell, J.J., 2002. Heartwood formation and natural durability − a review. Wood and Fiber Science 34, 587−611.

Temiz, A., Yildiz, U.C., Nilsson, T., 2006. Effects of the wood preservatives on mechanical properties of yellow pine (*Pinus sylvestris* L.) wood. Building and Environment 41, 910−914.

Thebault, M., Pizzi, A., Dumarcay, S., Gerardin, P., Fredon, E., Delmotte, L., 2014a. Polyurethanes from hydrolysable tannins obtained without using isocyanates. Industrial Crops and Products 59, 329−336.

Thebault, M., Pizzi, A., Essawy, H., Baroum, A., Van Asche, G., 2014b. Isocyanate free condensed tannin-based polyurethanes. European Polymer Journal. http://dx.doi.org/10.1016/j.eurpolymj.2014.10.022.

Thevenon, F., Pizzi, A., Haluk, J.P., 1997. Non-toxic albumin and soja protein borates as ground-contact wood preservatives. European Journal of Wood and Wood Products 55, 293−296.

Thevenon, F., Pizzi, A., 2003. Polyborate ions' influence on the durability of wood treated with non-toxic protein borate preservatives. European Journal of Wood and Wood Products 61, 457−464.

Thevenon, M.F., Pizzi, A., Haluk, J.P., 1998. One-step tannin fixation of non-toxic protein borates wood preservatives. Holz als Roh- und Werkstoff 56, 90−98.

Thomas, L.V., Delves-Broughton, J., 2005. Natamycin (Technical Paper, TP 21-1e). Danisco Innovation, Beaminster, Dorset, UK.

Timar, M.C., 2003a. Wood Chemistry. Editura Universitatii Transilvania din Brasov, Brasov, Romania, pp. 50−66.

Timar, M.C., 2003b. Ameliorarea lemnului. Editura Universitatii Transilvania din Brasov, Brasov, Romania, pp. 10−22 (in Romanian).

Tømmeraas, K., Strand, S.P., Tian, W., Kenne, L., Varum, K.M., 2001. Preparation and characterisation of fluorescent chitosans using 9-anthraldehyde as fluorophore. Carbohydrate Research 336, 291−296.

Tsoumis, G.T., 2000. Wood: Cellular Composition of Wood. Types of Cells Present in Hardwoods and Softwoods. Encyclopaedia Britannica Inc. http://www.britannica.com/media/full/603935/55253.

Vinden, P., Butcher, J.A., 2005. Wood preservation: strategies for the future. In: Thompson, R. (Ed.), The Chemistry of Wood Preservation. Woodhead Publishing, Elsevier, Amsterdam, pp. 117−135.

Voet, D., Voet, J.G., 2004. Biochemistry, third ed., vol. 1. Wiley, Hoboken, NJ.

Vroman, I., Tighzert, L., 2009. Biodegradable polymers. Materials 2, 307−344.

Wilcox, W.W., Botsai, E.E., Kubler, H., 1991. Wood as a Building Material: A Guide for Designers and Builders. John Wiley & Sons, New York, pp. 125−130.

Wojciechowskia, K., Klodzinska, E., 2015. Zeta potential study of biodegradable antimicrobial polymers. Colloids and Surfaces A: Physicochemical and Engineering Aspects. http://dx.doi.org/10.1016/j.colsurfa.2015.04.033.

Yang, M.K., Myers, D.J., 2006. Soy protein combined with copper and boron compounds for providing effective wood preservation. JAOCS 83, 31−44.

Biopolymers for paints and surface coatings

15

N. Karak
Tezpur University, Napaam, Tezpur, Assam, India

15.1 Introduction

Paints and surface coatings are compounded liquids or liquefiable polymeric products, which form thin continuous solid films with definite color after application on the surfaces of desired objects. They are the mixtures of a film former, binder, or vehicle, as well as a pigment or colorant along with a large number of other additives (Eiri, 2008). Almost all manmade objects are generally painted or coated with a suitable thin film to protect from external damage and/or to enhance the aesthetic appeal of the applied object surfaces (Malshe and Sikchi, 2004). In addition, this thin film may also provide some special properties, such as inhibition of microorganism growth, radar absorption, or tolerance to different adverse chemical environments.

In the construction sector, the use of paints and coatings is inevitable as both the exterior and interior parts of constructed articles, including buildings, are painted or coated for the above mentioned purposes. Roof and masonry paints and coatings, and concrete coatings, decorative construction specialty paints and coatings are a few examples from this sector. However, almost all such paints and surface coatings have a suitable solvent or a solvent mixture for processing and application. Although this solvent is not a part of the final painted film, it assists in the homogenization or dispersion of additives and pigments into the binder, as well as promotes easy brushing, spraying, dipping, or any other method of application. Today, most of the building constructors prefer to protect and decorate surfaces using waterborne low volatile organic compound (VOC) paints; low VOC paints are easy to apply, quick to dry, and odorless, with good washability, excellent finishing, and environmentally friendly (Wilson et al., 1991).

In paints and coatings, binders and film formers are the most important components because they hold all other components together in the painted film. They not only form the continuous thin film over the applied object surface, but they tether/hold pigment and other additives uniformly by cohesive force and to the object's surface by adhesive force. Thus, the binder imparts adhesion, binds the pigments and other additives together, and strongly influences the basic characteristics of paints, such as gloss, drying time, hardness, exterior durability, flexibility, toughness, abrasion resistance, impact resistance, chemical resistance, and adhesion (Morgans, 2000). The behavior of the binders in paint is tested by looking at the transparency, block resistance, hardness development, drying time, and gloss of the paint. The pigment is another important ingredient of paint. Its functions are to provide required aesthetic appearance (e.g., color) and hiding capacity of the paint, help to protect the paint

Biopolymers and Biotech Admixtures for Eco-Efficient Construction Materials. **http://dx.doi.org/10.1016/B978-0-08-100214-8.00015-4**
Copyright © 2016 Elsevier Ltd. All rights reserved.

from ultraviolet (UV) light and corrosion, and assist in attaining elasticity, hardness, and abrasion resistance. The efficiency of a pigment depends on its particle size distribution and the level of dispersion into the binder system. A large number of other additives for wetting, dispersing, viscosity controlling, antistatic attribute, hardening, thixotropic behaviour, antifoaming, antisettling, antirusting, protective colloid, biocide, adhesion promoter, etc., are also used to perform some specific functions in paints and coatings. Mainly polymers and resinous organic materials are used as binders, although a few inorganic materials can also be used. However, polymers have many advantages over the other categories of materials, such as metals and ceramics, and hence are preferred binders for paints and coatings (Karak, 2009). The advantages include versatility in feedstock, versatility in structure and properties, ease of modification, processing and fabrication, high speed of mass production, a wide range of colorability, low overall cost, and light weight.

Due to their advantages, the use of polymers has increased greatly in almost all sectors. Furthermore, almost all synthetic (manmade) petroleum-based polymers are nonbiodegradable and remain as they are, even after their useful service, for a long time (many years). These nonbiodegradable polymers cause problems like waste disposal, risk to aquatic and terrestrial living systems, garbage, and landfills, thereby creating overall adverse environmental impacts. Moreover, all of these polymers are generally obtained from petroleum resources, and dependence on fossil fuels is leading to depletion of petroleum reserves. Thus, scientists and industrialists are searching for alternative renewable, ecofriendly, and cheap resources to reduce dependency on petroleum products, allowing oil reserves to be stored for future generations. Natural polymers, such as natural rubber (*cis*-1,4-polyisoprene), cellulose, starch, polypeptides, and chitin, as well as natural products such as glue, gum, lignin, shellac, rosin, vegetable oil, and cashew nut shell liquid, are used for many industrial purposes. These natural materials are biodegradable, ecofriendly, and renewable; thus, they are used in many sectors, especially in agriculture, packaging, and paints and coatings. A large number of publications are coming out from these fields, with biodegradable polymers obtained from naturally renewable resources are attracting great attention in recent years (Karak, 2012). Hence, this chapter provides details of biopolymers used in paints and coatings.

15.2 Concept of biopolymers in paints and coatings

Polymers, including biopolymers, are macromolecules with high molecular weights. They are formed by covalent linkages of small and simple (but a large number of) repeating units. This number is so high that the addition or subtraction of a few such units does not alter the ultimate properties of polymers. These polymers are of different types and are classified based on their origin, mode of formation, thermal response, main linkages through which they formed, physical properties, type of repeating unit, etc. Biopolymers are derived from biological origins and are sustainable (Nair and Laurencin, 2007). These polymers are formed by biochemical processes in the presence or absence of some specific enzymes or catalysts. Biopolymers are also broadly defined as the polymers obtained from renewable agriculture/forestry resources or biomass-based feedstock, which are capable of behaving like conventional manmade polymers with characteristics of biodegradability upon disposal after their services; such polymers are better termed as *bioderived* or *biobased* polymers. Biodegradation is the degradation of the materials into environmentally acceptable products such as water, carbon dioxide, and biomass by the action of naturally available microorganisms under normal environmental conditions. Thus, in a broad sense, biopolymers used in paints and coatings are naturally derived biodegradable polymers.

These biopolymers are classified into different types based on their biological origin or from where they are obtained. "Plant-produced biopolymers" are polysaccharides such as cellulose and starch. "Animal, insect, and microbial-produced biopolymers" include proteins or polypeptides, lipids, poly(lactic acid), chitin, and collagen. These biopolymers generally suffer from poor mechanical properties, including dimension stability. "Bioderived polymers," such as polymers based on vegetable oil, cashew nut shell liquid, and tannic acid, have versatility in structure and properties; in addition, their performance can be modified depending on requirements (Shogren et al., 2004). This type of biopolymer is, therefore, more useful as a binder for surface coatings and paints.

15.3 Naturally obtained biopolymers used in paints and coatings

This section briefly describes different types of naturally obtained biopolymers used in paints and coatings.

15.3.1 Cellulose

Cellulose is the most abundant natural biopolymer, with 33% of all plant matter being cellulose. It is a linear polymer with high molecular weight and the repeating unit is cellobiose. Some important sources of cellulose are cotton (94%), wood (50%), and hemp pulp (45%). However, cellulose is insoluble and infusible due to the presence of strong H-bonding, its crystalline nature, high molecular weight, and stiffness (Chandra and Rustgi, 1998), so it is difficult to use directly in paints and coatings. Thus, cellulose has to be modified by transforming the hydroxyl groups present in its structure to corresponding ether, ester, and acetal derivatives. A large number of cellulose derivatives, such as hydroxyl ethyl cellulose, hydroxyl ethyl methyl cellulose, hydroxyl methyl propyl cellulose, and carboxyl methyl cellulose, are used as film formers in waterborne coatings, protective colloid in emulsion paints, and thickening agents for paints and coatings. These derivatives are available in a variety of grades based on molecular weight, degree of substitution, and dispersion ability in water.

The importance of cellulose products in different sectors, including building additives and water-based paints, is increasing. For example, AkzoNobel Company is investing ERU 60 million to improve the production capacity of cellulose derivatives. Hydroxyl ethyl cellulose—a white, odorless, tasteless, hygroscopic, nonionic, water-soluble cellulosic polymer—is used as a film former and rheological modifier in paints. It also improves adhesion and density of cement-based mortar, wall putting, and tile adhesive. Hydroxyl ethyl cellulose possesses the properties of a thickener, pseudo-plastic fluid, protective colloid, and film former, as well as a high level of salt tolerance and water retention. Thus, hydroxyl ethyl cellulose-based paint is best suited for the construction industry. Noncellulosic polysaccharide such as hydroxyl propyl gaur, a modified gaur gum, is also used in coatings and paints and provides more shear thinning (pseudo-plastic) and antisag characteristics than cellulose derivative-based systems.

15.3.2 Starch

Starch is a polysaccharide formed by covalent linkages of a large number of glucose units and is obtained from plants. The main sources of starch are potatoes, wheat, maize (corn), and rice. It is a white, tasteless, and odorless powder that is insoluble in cold water and organic solvents, such as alcohol. Starch is a well-known hydrocolloid biopolymer. It possesses a linear crystalline amylose and a branched and amorphous amylopectin (Ratnayake et al., 2001). This is a low-cost polysaccharide, abundantly available and one of the cheapest biodegradable biopolymers. Dissolved starch in warm water is used as a thickening, stiffening, or gluing agent in paints and coatings.

Starch-based products suffer from water sensitivity, brittleness, and poor mechanical properties. To overcome these problems, starch is modified by acetylation using acetic acid and pyridine. Lorama Chemical Incorporation (Canada) produced a starch polysaccharide-based resin, LPR™, which provides significant cost savings on the total paint cost and VOC reduction to allow manufacturers to meet environmental regulations. It also provides excellent gloss, film hardness, adhesion, compatibility with a wide range of alkyds (polyesters) and other materials, improved drying time, stability, and reduced yellowing effect (Dredge and Knight, 2008).

15.3.3 Protein

Proteins are obtained both from animal and plant sources. However, most proteins are insoluble and infusible. Common fibrous proteins include silk, wool, and collagen. Thus, it is difficult to use them as such in paint and coatings, although they can be used as reinforcing agents. Collagen is enzymatically and chemically degraded to gelatin. Gelatin is a translucent, colorless, brittle (when dry), and flavorless material. Thus, it is an irreversibly hydrolyzed product of collagen. Hydrophilic and water-soluble dry gelatin with relatively high jelly strength is obtained by pulverizing using dimethyl formamide in an atmosphere where moisture is excluded. Paints containing synthetic resin solutions in dimethyl formamide with gelatin particles are pulverized into 30 μm or smaller in size. Paint layers with excellent moisture permeability can be obtained by eluting gelatin particles with hot water (Nishibori, 1992).

The combination of gelatin with other biopolymers, such as soybean protein, vegetable oil, and fatty acid or polysaccharide, results in improved coating performance. Similarly, wheat gluten contains gliadin and glutenin proteins. Properly chemically modified gluten can produce aqueous protein dispersions with excellent film-forming characteristics and strong adhesion to various surfaces, which are requirements of binders used in paints and coatings. Wheat gluten-based films exhibit very interesting mechanical properties with extensibility over 600%, tunable gas and moisture permeability, tailored durability, and water resistance. Thus, the modified protein can be used as a binder for novel, organic solvent-free paints and coatings (Johannes et al., 1996). Here, it is pertinent to mention that the use of proteins in nonfood sectors is increasing due to the enrichment of protein technology and chemistry, such as the isolation and characterization of proteins, elucidation of their structures, structure–function relationships, and modifications. The relatively low cost of proteins compared to that of synthetic polymers, particularly plant proteins, are thus attractive for use in paints and coatings.

15.3.4 Chitosan

Chitosan is deacetylated product of chitin, a nitrogen-containing polysaccharide obtained from the exoskeleton of crustacean waste (head, chaw, and shell of sea organisms such as lobsters, crabs, and shrimps). Glucosamine units are predominant in chitosan. It is only soluble in a few dilute acid solutions. The self-healing coating—a most desired surface coating—is prepared by using chitosan-based polyurethane. This type of coating could minimize upkeep and repair on a variety of products, saving consumers money and reducing waste. The chitosan is incorporated as one of the components in polyurethane, which is used in the outer coatings to protect the applied object surface. The chemical structure of the polymer is damaged on formation of scratch on the outer coating, and chitosan responds to the UV component of the used sunlight. Chemical chains are then formed with other materials present in the coating formulation, eventually filling the scratch. This process is very efficient, taking less than an hour, and eventually leads to a “scratch-free surface” (Ghosh and Urban, 2009).

15.3.5 Lignin

Lignin is a complex product of aromatic alcohols known as monolignols. It is generally obtained from wood and is a by-product of the paper and pulp industry. Lignin is an integral part of the secondary cell walls of plants and some algae. It is a tasteless, insoluble material in water and alcohol but soluble in weak alkaline solutions. The alkaline solution of lignin can be precipitated by an acid solution. Lignin is an unusual biopolymer because of its heterogeneity in structure, which is a lack of a defined primary structure. It provides the strength of wood in trees. A large number of reports, including patents, are available in the literature on the use of lignin in surface coating applications. A Chinese patent describes an environmentally friendly preparation process of a low-cost inner wall coating, which uses straw powder (containing lignin) as one of the components (Xu, 2012). Lignin is also used to prepare phenolic, polyester, polyurethane, and epoxy resins, which are subsequently used in coating industry. Lignin modified polyurethane is obtain from hydroxypropyl lignin derivatives and hexamethylene diisocyanate or toluene diisocyanate. The coating performance is dependent on the type of lignin, nature of diisocyanate, and NCO/OH ratio. In phenol-formaldehyde resin, up to 40% phenol can be replaced by lignin as a renewable, low-cost resource without influencing the ultimate properties of the resin.

15.3.6 Shellac

Shellac is a resinous product obtained from the secretion of the female “lac bug” (*Kerria lacca*) on trees, mostly in the forests of India and Thailand. The dry flake processed shellac is dissolved in ethanol to obtain liquid shellac, which is used as a brush-on colorant, food glaze, and wood finish. It functions as a tough natural primer, sanding sealant, tannin blocker, odor blocker, stain, and high-gloss varnish. Shellac may be used on an object for a its good insulation qualities, sealing out moisture. The biopolymer is thermoplastic in nature and provides good adhesion to other objects. An alcoholic (ethanol or methanol) solution of shellac yields a coating with good durability and hardness. Furthermore, this coating does not darken as it ages because shellac is an UV-resistant material. Shellac is important in the fields of surface coatings and paints due to the formation of smooth, hard, and glossy film with high adherence.

Because of its brittleness and poor chemical resistance properties, shellac has limited use in paints for building surfaces. However, maleated shellac, a product of maleic anhydride reacted shellac and acrylic resin-based coating, exhibited good adhesion finish, smoothness and lack of flaking on the surfaces, and good water and chemical resistance for applied substrates such as plaster of Paris, cement, and limed surface (Patel and Patel, 2010). Furthermore, modification of shellac with acrylic resin resulted in improved film performance with respect to adhesion, finishing (smoothness), and flexibility. The film does not show any flaking/detachment from the applied surfaces. This is because of the esterification between shellac and acrylic resin (Ansari and Goswami, 2006).

15.3.7 Rosin

Rosin is a solid resin obtained from pine trees and some other conifers. It is produced by heating fresh liquid resin to vaporize the volatile liquid terpene components. Rosin is semitransparent and varies in color from yellow to black. At room temperature it is brittle, but it melts at elevated temperatures. Thus it is brittle and friable, with a faint piney odor. The main component of rosin is abietic acid, an unsaturated monobasic acid, although other organic acids are also present. Rosin is mainly used in varnish, as well as in paint and coating industries. It is added in small quantities to traditional linseed oil/sand gap fillers that are used in building materials. Rosin-modified alkyd resins are preferred in paints and surface coating applications because of improvement of some specific properties, such as gloss and hardening of the film (Sanderson, 1934). Rosin or its derivates are also used in special paints, such as antifouling paints (Yebra et al., 2005).

15.3.8 Vegetable oil

Vegetable oils are triglyceride esters of fatty acids; generally, both saturated and unsaturated fatty acids are present in almost all such oils (Figure 15.1). They are obtained from the seeds of the plants. Depending on the amount of unsaturation present in the

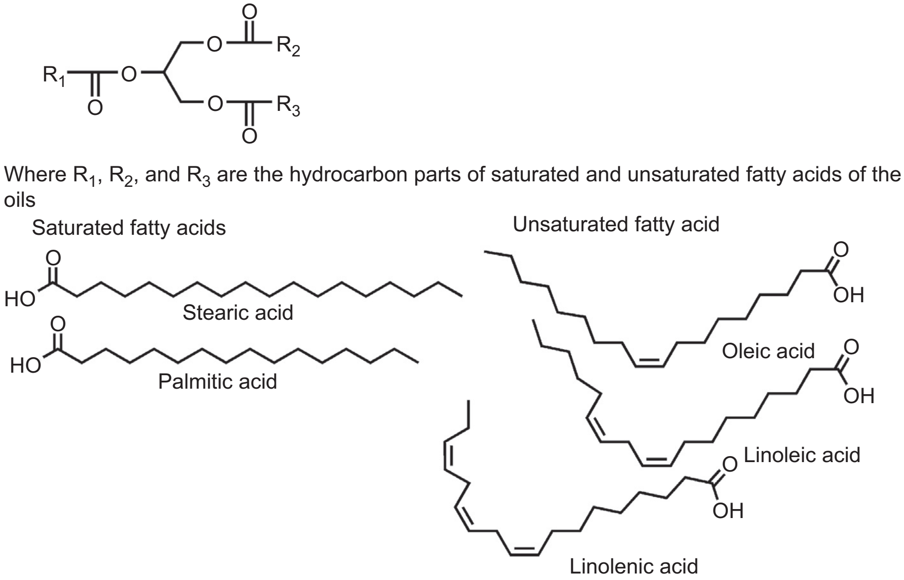

Figure 15.1 General structural representation of vegetable oil with fatty acids.

oils, they can be classified as drying, semidrying, and nondrying oils. In paints and coatings for the building sector, generally drying oil is used because of its easy film-forming property. Thus, even though drying oil is not a biopolymer, after drying (curing by free radical cross-linking reactions), it forms a continuous thin film with a three-dimensional network structure; because the precursor is obtained from bio-origin, the final thermoset can be treated as the product of biopolymers. A few such oils are used for this purpose (Erhan, 2005), including linseed, tung, perilla, oiticica, and walnut oils. Besides direct use of drying oils as binders, some vegetable oils, such as neem and karanja oils, are used as biocides; soybean, cotton seed, sunflower, safflower, and canola oils are used in ink formulation; and a large number of oleo-chemicals such as surface active agents, curing agents (fatty acid based polyamine/poly(amido amine)), industrial solvents (low volatility and may become the part of final products) are used in paints and coating industries.

Vegetable oils such as *Euphorbia lagascae* and *Vernonia galamensis* seed oils possess >60% of an epoxy fatty acid (vernolic acid) that can be used as a reactive diluents for paint and coating applications (Johannes et al., 1996). *Calendula officinalis*, or “marigold” oil, contains >63% of a C18 conjugated triene fatty acid (calendic acid), similar to tung oil, which possesses film-forming abilities. The chemical derivatives of this oil are very useful, particularly in emulsion systems as film-forming materials. Similarly, castor oil and lesquerella oil contain hydroxyl-bearing fatty acids and can be used in the preparation of different biobased resins to be used in paints and coatings. Dimer acids, the Diels−Alder product of polyunsaturated fatty acids/esters, are very useful vegetable oil-based components for coatings and paints (Cecil et al., 1988).

They are noncrystalline liquid dibasic acids with relatively high molecular weight. Dimer acids are used in the preparation of polyesters with good coating performance, particularly with isocyanate treatment.

However, almost all of the biopolymer-based paints and coatings discussed here are not able to provide adequate mechanical strength and resistance against adverse environmental impacts, particularly under harsh conditions. Hence, biobased polymers are essential as binders for such applications. Thus, the details of biobased or bioderived polymers are presented in this chapter.

15.4 Background and importance of biobased polymers

The problems associated with petroleum-based nonbiodegradable synthetic polymers are well understood. Again, directly obtained biopolymers from nature also have some inadequacies as binders for paints and coatings; thus, there is a strong demand for biodegradable biobased ecofriendly polymers, which can provide the desired performance to the paints and coatings; at the same time, they also address the problems associated with petroleum-based synthetic polymers. Therefore, the desired biopolymers should possess the following qualities: minimum or low dependence on fossil fuels to avoid the depletion of petroleum reserves, environmentally benign and biodegradable, easy and adequate availability, acceptable handling and transportation. Furthermore, the development should be sustainable; through this route, high carbon credits (minimizing the carbon footprint by reducing CO_2 generation) should be achieved. Development should also follow the concept of the triple bottom-line approach, which is associated with social, ecological, and economical balance. Additionally, such development has to follow the tenets of green chemistry as much as possible, as these are inevitable for today’s material development. Thus, the literature and experience support the fact that properly designed biobased polymers are the right choice (Karak, 2012).

Among all the bioresources, plant seed oil is the most preferred for this purpose, as it has many advantages over the others. This is due to the fact that the resource is naturally renewable (agriculture and or forestry based), easily available in large quantities, environmentally benign, biodegradable, relatively low cost, easy to modify to different desired products, easy to handle, and versatile in structure and composition; in addition, the existing knowledge of material chemistry helps to transform it to an industrially useful binder for paints and coatings. Furthermore, the development of biobased polymers from different vegetable oils for a specific purpose is sustainable development. This is because of the fact that the used vegetable oil is obtained from the seeds of a plant, which is transformed to the desired biopolymers by chemical processes and subsequently employed as a binder for paints and coatings. After their useful service, these paints and coatings are degraded to water, carbon dioxide, and biomass, which are utilized for the growth of the plant and conservation of soil, from which seeds are obtained; hence, it is a sustainable development, as the cycle can be repeated for an endless number of times. Furthermore, this route follows a few principles of green chemistry: effective utilization of the renewable resource-based raw

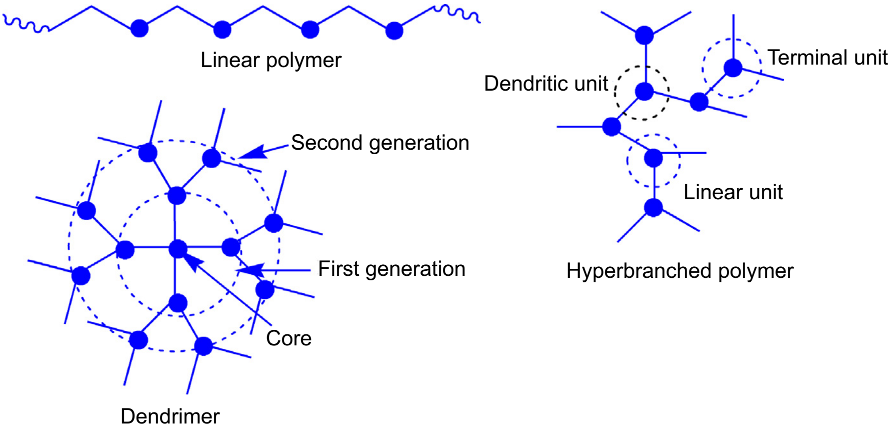

Figure 15.2 General structural presentations of dendrimer, hyperbranched, and linear polymers.

material for an industrially important products uses a catalyst with minimum energy and without creating any unwanted or toxic by-products. Thus, a large number of industrial binders or film formers, such as polyesters, poly(ester amide)s, epoxies, and polyurethanes, are reported in the literature and used by the paint and coating industries (Karak, 2012).

In addition to conventional polymers, a good number of hyperbranched polymers (a class of dendritic polymers) have also been reported. This is because of the fact that hyperbranched polymers exhibit superior properties over their liner analogs with equivalent molecular mass and can be prepared on a large scale by a single-step process (Voit and Lederer, 2009). The advantages include a highly branched structure with a large number of freely exposed terminal groups; hence, they possess low melt and solution viscosity as well as high solubility. The compatibilizing ability of hyperbranched polymer with others is much higher than its linear analog. The general structural representations of dendritic polymers along with the linear polymers are shown in Figure 15.2. In the subsequent sections, the details of such polymers related to paints and coatings are briefly discussed.

15.5 Biobased polymers used for paintings and coatings

The conventional and hyperbranched biobased polyesters, poly(ester amide)s, epoxies, and polyurethanes used for paints and coatings are presented in this section. The importance of such bioderived polymers is easily revealed from the increasing number of research papers published each year. Vegetable oil-based polymers are obtained directly from these oils or from their immediate derivatives by very simple routes (Figure 15.3).

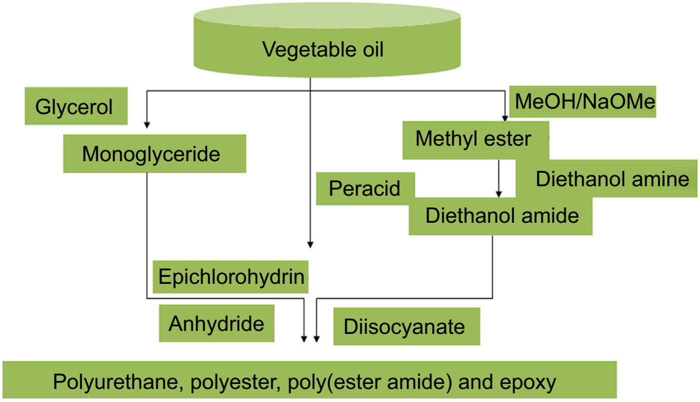

Figure 15.3 Simple routes for obtaining vegetable oil-based polymers.

15.5.1 Polyester

15.5.1.1 Basic concept and importance

Polyester, especially as modified from vegetable oil (also known as alkyd), is one of the important biobased polymers used in the paint and coating industries. Polyester is the polycondensation products of di/polybasic acid or anhydride and di/polyhydric alcohol, where at least one of the components is derived from vegetable oil. Almost all available vegetable oils are used for this purpose. This biobased polyester has high popularity in paints and coatings industries, because of the ready availability of all the reactants, easy and simple preparative methods, excellent pigment dispersion, high gloss, good adhesion, and long-term durability of the final product. Depending on the amount of oil used in the preparation of such polyesters, they are of three types: long oil polyester or alkyd (oil content >60 wt%), medium oil alkyd (oil content 40—60 wt%), and short oil polyester (oil content <40 wt%) (Biemans and Thomas, 2014).

15.5.1.2 Raw materials

The raw materials used for the preparation of polyesters include all types of vegetable oils, fatty acids, and their derivatives, such as monoglyceride and dimer acid; polyhydric alcohols such as glycols of ethylene, propylene, butylenes, and hexylene; glycerol, trimethylol propane, pentaerythritol, sorbitol, xylitol, etc.; polybasic acid/anhydride such as phthalic anhydride, isophthalic acid, maleic anhydride, adipic acid, hexahydrophthalic anhydride, pyromellitic anhydride, and terephthalic acid and monobasic acid such as fatty acid, benzoic acid, and rosin (abietic acid). (Karak, 2012). However, the use of monobasic acid is optional and only used either to control viscosity (molecular weight) or to modify the structure of prepared polyester. In almost all processes, a number of catalysts such as acid, base, or enzyme are used. These include lithium hydroxide, calcium oxide, sodium methoxide, calcium octoate, dibutyl tin, and lipozyme. A large variety of vegetable oil-based polyesters are reported in literature using different vegetable oils like linseed oil, castor oil, sunflower oil, safflower oil, rubber seed oil, karanja oil, jatropha curcas seed oil, *M. ferrea* L. seed oil, melon seed oil, or a combination of more than one oil, with variety of structures and compositions along with different di/polybasic acids and di/polyols (Karak, 2012).

15.5.1.3 Preparation

This biopolymer is prepared industrially by different methods such as “alcoholysis” or “glycerolysis,” “fatty acid,” “acidolysis,” and “fatty acid-oil” processes using either a fusion or solution technique. The monoglyceride of *M. ferrea* L. seed oil as the biobased component is reacted with phthalic anhydride as saturated and maleic anhydride as unsaturated anhydrides at 125 °C for 3−4 h to obtain the desired polyester resin, which on curing provided desired good coating performance (Dutta et al., 2004). In the case of hyperbranched polyester, a multifunctional reactant (functionality greater than two) must be used and the reaction has to be performed under precisely controlled conditions using an appropriate method, such as high dilution and slow addition technique. Karak and coworkers reported a few hyperbranched polyester resins by reacting monoglyceride of *M. ferrea* L. seed oil with conventional anhydrides in the presence of polyfunctional carboxylic or polyol compounds such as trimellitic anhydride or 2,2-bis(hydroxymethyl) propionic acid or hyperbranched polyol under controlled reaction conditions (Konwar et al., 2009; Konwar and Karak, 2011). Figure 15.4 represents

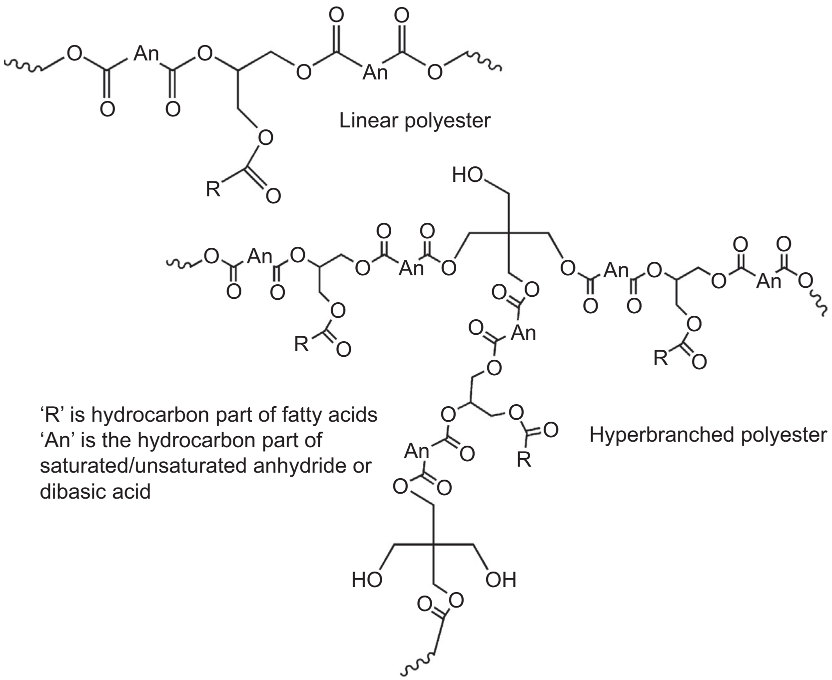

Figure 15.4 General structure of biobased linear and hyperbranched polyesters.

the general structure of vegetable oil-based linear and hyperbranched polyesters. The studies indicate that all these polyesters could be used as binders for anticorrosive and nonpolluting surface coatings, and bis(hydroxymethyl) propionic acid based hyperbranched polyester thermoset exhibited the best coating performance among the studied thermosets.

As already stated earlier, waterborne coatings and paints are preferred because of their environmentally benign nature with low or no VOC. Polyesters are the most popular in waterborne binders for paints and coatings and such systems offer low VOC, reduced odor and flammability, improved safety, and easy cleaning. The waterborne polyesters are obtained by the reaction of suitable vegetable oil directly (lesquerella oil) or monoglyceride of oil with phthalic anhydride and trimethyllol propane or pentaerythritol or bis(hydroxyl methyl) propionic acid. Water-reducible polyesters are also prepared by the reaction of monoglyceride of oil with carboxy-functionalized acrylic polymer (Wang et al., 2000). To reduce VOC in coatings and paints, polyester emulsion is blended with acrylic dispersion and the final product exhibited good performance (Indeikin et al., 2002).

15.5.1.4 Modification

To fulfill the demands of different service requirements, conventional and hyperbranched polyesters may be modified by proper functionalization, copolymerization, blending with other polymers, formation of interpenetrating network, etc., instead of designing new polyesters; the latter is expensive, time intensive, and labor consuming, and new setups may be required for their industrial productions. For example, diglycidyl ether epoxy or melamine-formaldehyde or phenol-formaldehyde resin modified polyester showed better drying ability, chemical resistance, mechanical performance, etc., than that of pristine systems. Similarly, diisocyanate such as toluene diisocyanate, isophorone diisocyanate, and isocyanate terminated pre-polymer, and modified polyesters improved film hardness, durability, drying rate, and chemical resistance over unmodified polyester.

15.5.1.5 Curing

Biobased polyesters are generally cured by a conventional peroxide curing system consisting of methyl ethyl ketone peroxide, styrene or methacrylate, and cobalt or manganese octoate for drying and semidrying vegetable oil-based polyesters, as well as epoxy resin with amine/poly(amido amine) or melamine-formaldehyde resin with *para*-toluene sulfonic acid curing system for semidrying and nondrying oil-based polyesters. Di/polyisocyanate or isocyanate terminated polyurethane prepolymer or polyurethane curing systems are used for all types of biobased polyesters. The temperature for curing is generally varied from room temperature to elevated temperatures up to 150 °C for specified period of time until the desired level of cross-linking density is obtained.

15.5.1.6 Properties

Polyesters obtained using different vegetable oils with a variety of compositions of reactants possess large varieties of structure and hence properties. The structure of this biobased polymer mainly consists of ester linkages along with unsaturation, hydroxyl, carboxylic, aromatic, and aliphatic moieties. The ester linkage is chemically weak, particularly against alkali and undergoes hydrolysis, aminolysis, and ester exchange reactions. Furthermore, this polar ester group can undergo polar−polar and H-bonding interactions with other groups and components of a similar nature, thereby increasing intra- and intermolecular attractions among the chain molecules and increasing the rigidity of the matrix. However, an ether linkage of an ester group also provides flexibility; hence, the combined effect is almost canceled out by each other. The chemical resistance of polyester is also influenced and improved by the presence of a rigid moiety in two sides of an ester linkage. The polymer is soluble in most of the commonly used industrial organic solvents, although a long oil-based polyester is easily soluble in aliphatic hydrocarbon, whereas the short oil polyester is soluble in aromatic hydrocarbon solvents (Talbert, 2008). The density of this polyester binder is generally less than 1.0 (0.81−0.96 g/cc at 25 °C), maybe due to the absence of any heavy element and crystallinity in the structure. However, the required mechanical properties are obtained by the right choice of the components with their appropriate ratios to achieve a balance between rigidity and flexibility, by choosing the correct reaction conditions to obtain the right molecular weight with good flowability and mechanical strength, and correctly choosing the amount and reactivity of cross-linker to maintain optimum cross-linking density.

Table 15.1 represents the coating performance of epoxy-cured biobased polyester thermosets with different compositions. The rheological or flow behavior of biobased polyester is similar to pseudoplastic fluid, and viscosity generally decreases with the increase of shear rate. Thus, application by brushing, spraying, etc., becomes easy at a high shear rate. The polymers are generally transparent because of their amorphous nature and possess high gloss because of the smooth surface and good dimensional stability. Low oil content polyester possesses good color stability and gloss retention, but if the unsaturation level is high in the cured films, then gloss deteriorates with passage of time (Wicks et al., 1999). They are electrically insulated and have a high dielectric constant. The thermal properties and chemical resistance of biobased polyesters are very important; these properties are governed by rigidity of the matrix, presence of intra- and intermolecular attraction forces among the chain molecules, compactness in the structure, ultimate molecular weight of the polymer, chemical linkages, other components present in the system, etc. Polyesters are thermostable up to 200 °C and hence adequate for most of their paint and coating applications (Dutta et al., 2007).

Although all such biobased polyesters possess acceptable biodegradability, the poor chemical resistance, particularly under basic conditions, is a matter of concern; hence, such polymers are restricted for many advanced applications. However, the modification of these biobased polyesters by the formation of suitable nanocomposites with appropriate functionalized/modified nanomaterials, such as organically modified nanoclay, functionalized multiwalled carbon nanotubes, and reduced graphene oxide, resulted in tremendous improvements of all desired properties for paints and coatings. Silver and organoclay nanomaterials modified highly branched polyester resin of *M. ferrea* L. seed oil-based carboxyl terminated pre-polymer and 2,2-bis(hydroxymethyl) propionic acid exhibited high antibacterial activity, good thermostability, high chemical resistance,

Table 15.1 **Coating performance of epoxy and poly(amido amine) cured *Mesua ferrea* L. seed oil-based polyester thermosets with different compositions**

Property	**Monoglyceride (MG) + Phthalic anhydride (PA) + Maleic anhydride (MA)**	**MG + PA + MA + hyperbranched polyether polyol**	**MG + PA + MA + bis(hydroxyl methyl) propionic acid**	**MG + bis(hydroxymethyl) propionic acid**	**MG + PA**	**MG + PA + MA**
Tensile strength (MPa)	6–7	5–6	3–4	20–25	4–5	5–6
Elongation at break (%)	30–35	90–100	20–30	80–90	70–75	75–80
Scratch hardness (kg)	6–7	8–9	7–8	8.5–9	5–6	6–7
Impact resistance (m)	0.5–0.6	>1	>0.8	>1	>0.7	>0.75
Bending (m)	<0.002	<0.002	<0.001	<0.001	<0.001	<0.001
Gloss (60°)	75–80	90–95	80–85	75–80	60–65	65–70
Adhesion (MPa)	80–90	100–110	120–130	250–300	100–110	115–120
Hard drying time (at 120 °C, min)	230–250	80–90	180–190	45–50	60–70	50–60

very good tensile strength, and scratch hardness; hence, they have great potential to be used as antibacterial surface coating materials (Konwar et al., 2010).

15.5.2 Poly(ester amide)

15.5.2.1 Basic concept and importance

To overcome the problem of poor alkali resistance of biobased polyester and to retain its good flexibility, some of the ester linkages are replaced by alkali resistance amide linkages in polyester; thus, poly(ester amide) is obtained. Hence, this type of biobased polymer is obtained from different vegetable oils and possesses both ester and amide linkages in its molecular chains. The amide linkages provide rigidity like polyamide and ester linkages offer flexibility like polyester. Therefore, poly(ester amide)s have advantages of both polyester and polyamide within the same polymer. Hence, biobased poly(ester amide)s exhibit better performance with respect to hardness, chemical resistance, thermal resistance, durability, and physicomechanical properties over the analogous biobased polyesters.

15.5.2.2 Raw materials

A large number of vegetable oils, such as linseed, castor, sunflower, karanja, *M. ferrea*, coconut, safflower, argemone, and soybean oils, and their fatty acids, such as stearic, palmitic, oleic, linoleic, linolenic, and ricinoleic acids, are used to obtain the biobased component, dihydroxy fatty amide for poly(ester amide)s. The other components of poly(ester amide)s are dibasic acids/anhydrides similar to polyesters, di/polyhydroxylamines such as diethanol amine, hydroxyethylamino propanol, and diisopropanol amine. The catalysts are the same as polyester.

15.5.2.3 Preparation

Bioderived poly(ester amide)s are obtained by a similar type polycondensation reaction of di/polyhydroxy fatty amide(s) with dibasic acid/anhydride in the absence or presence of other di/polyhydroxyl compound(s) as polyesters (Mahapatra and Karak, 2004). The hydroxyl fatty amides are obtained from their respective vegetable oils or methyl ester of fatty acids by a reaction with di/polyhydroxy alkylamine. Here, it is pertinent to mention that the polycondensation reaction of diethanol fatty amide of castor oil with phthalic anhydride, maleic anhydride, and isophthalic acid resulted in conventional linear poly(ester amide), but controlled polycondensation of the above reactants with diethanol amine produces hyperbranched poly(ester amide) (Pramanik et al., 2012, 2013). Metal, such as zinc, containing biobased poly(ester amide) is prepared by the polycondensation reaction of linseed oil fatty amide diols, phthalic anhydride, and zinc acetate (Zafar et al., 2007). Waterborne poly(ester amide)s are also prepared from different vegetable oils such as castor oil and niger oil (Zafar et al., 2012). The fatty amide diols of these oils are reacted with isophthalic acid followed by neutralization with varying percentages of triethylamine to yield waterborne biobased poly(ester amide)s.

15.5.2.4 Modification

Semidrying and particularly nondrying oil-based poly(ester amide)s required a long time for drying, so attempts have been made to reduce their curing time by modifying such poly(ester amide) by butylated melamine-formaldehyde resin, urethane resin, and poly(styrene-co-maleic anhydride). Thus, there are some reports on the modification of vegetable oil-based poly(ester amide)s to improve their performance. For example, room temperature-cured poly(ester amide) is modified by the incorporation of phthalic anhydride in poly(styrene-co-maleic anhydride). Similarly, toluene diisocyanate is used to modify the poly(ester amide) of linseed oil fatty amide diol and ethylene diamine tetra-acetic acid. The biobased poly(ester amide)s are also modified by incorporation of different metals such as alumina, antimony, cadmium, zinc, and boron. This type of modification improves physicomechanical, thermal, and anticorrosive properties, as well as antibacterial activity and curing time (Ahmad et al., 2001, 2005, 2006a). Thus, metal containing poly(ester amide) is resistant against rusting and corrosion, and finds application as an anticorrosive binder for paints and coatings. Physical blending of these poly(ester amide)s with numbers of thermoplastic polymers, such as poly(methyl acrylic acid) and poly(vinyl alcohol), is also reported in the literature for improvement of properties. For example, linseed and dehydrated castor oil-based poly(ester amide)s are blended with poly(methyl acrylic acid) or poly(vinyl alcohol) to obtain a resultant free-standing film with low water sensitivity, transparency, and good stiffness by exploiting the superior properties of individual components (Ashraf et al., 2007). The dimer acids are also used to obtain poly(ester amide)s.

15.5.2.5 Curing

Biobased poly(ester amide)s are cured by similar methods as described previously for biobased polyesters. However, the temperature for curing is reduced by using a proper curing system. For example, the curing time is reduced drastically from more than 150 °C for a conventional methyl ethyl ketone peroxide curing system with organo metallic compound such as cobalt or manganese naphthenate or octoate in presence of reactive diluent such as styrene or methyl methacrylate to ambient temperature for acrylated poly(ester amide) with phthalic anhydride system. Room temperature (~25 °C) cured biobased poly(ester amide) thermoset is produced by using drying such an oil-based polymer with poly(styrene-co-maleic anhydride), along with little amount of phthalic anhydride. However, most of the biobased poly(ester amide)s, such as polyesters, are being cured by epoxy resin in the presence of different types of polyamine or bio-based poly(amido amine) to form three-dimensional network structures (Figure 15.5).

15.5.2.6 Properties

Similar to polyesters, biobased poly(ester amide)s also have varieties of structures and compositions and hence properties. As stated earlier, the functional groups and chemical moieties present are same in both cases. In addition, thermostable

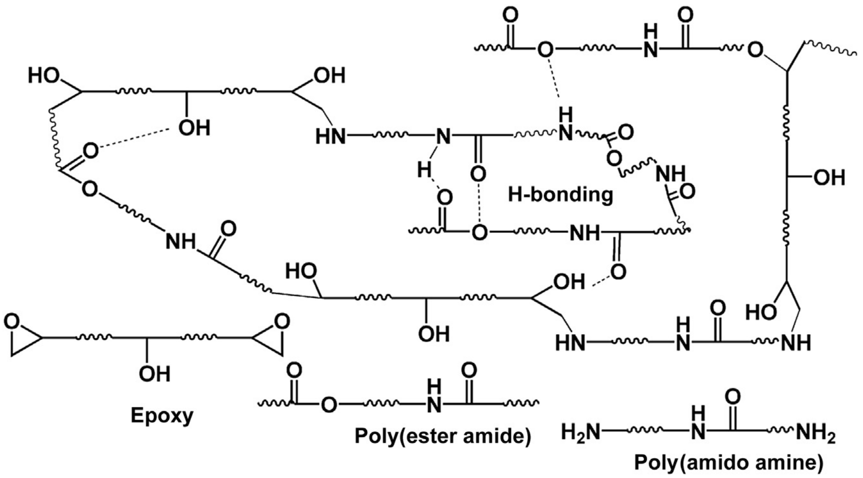

Figure 15.5 Three-dimensional network structure of polyester amide on cross-linking with epoxy resin in the presence of poly(amido amine).

and alkali resistance amide linkage is also present in poly(ester amide). The ultimate properties of such poly(ester amide)s depend on the amount of various linkages and moieties present in the molecular chains. The literature showed the combination of equimolar quantities of fatty amide diol with dibasic acid that produces an almost equal amount of ester and amide linkages containing poly(ester amide) with good drying time, hardness, and chemical resistance. However, the alkali resistance is improved by using more amide linkages, although biodegradability is found to be easier with more ester linkages. Similarly, incorporation of metal or urethane linkages enhances physicomechanical, thermal, chemical resistance, etc., properties of surface coatings and paints. The hardness and dimensional stability of poly(ester amide) increase with the increase of amide linkages, aromatic and heterocyclic moieties, cross-linking density, gloss, and adhesion properties of properly cured biobased poly(ester amide)s are found to be good.

Table 15.2 shows the coating performance of biobased poly(ester amide) thermosets with different compositions of the components. Furthermore, the presence of urethane linkages in such poly(ester amide)s enhances coating performance with respect to toughness, weather and chemical resistance, and adhesive strength. Hyperbranched aromatic polyamine cured biobased poly(ester amide) exhibited short cure time, enhanced thermostability, flame retardancy, impact and scratch resistance, and chemical resistance (Mahapatra and Karak, 2007). Thus, biobased poly(ester amide)s exhibited optimum performance with acceptable cost and hence are preferred in many paints and surface coatings. Furthermore, the literature supports the formation of a special type of antistatic and antimicrobial biobased hyperbranched poly(ester amide) nanocomposites with a judicious choice of nanomaterials, such as polyaniline nanofibers and silver nanoparticles decorated with multiwalled carbon nanotubes as a binder for paints and coatings (Pramanik et al., 2014).

Table 15.2 **Coating performance of epoxy and poly(amido amine) cured biobased poly(ester amide) thermosets with different compositions**

Property	Phthalic anhydride (PA) + Maleic anhydride (MA) + isophthalic acid (IA) + diethanol amine (DEA)	Dihydroxy fatty amides (DFA) + PA + MA + IA	DFA + PA + MA + IA + 5 wt% DEA	DFA + PA + MA + IA + 10 wt% DEA	DFA + PA + MA + IA + 15 wt% DEA
Tensile strength (MPa)	10−12	8−9	14−16	30−35	20−25
Elongation at break (%)	85−90	100−115	20−30	18−20	40−45
Scratch hardness (kg)	7−8	7−8	7.5−8	8−8.5	9−9.5
Impact resistance (m)	>0.8	>0.9	>1	>1	>1
Bending (m)	<0.002	<0.001	<0.001	<0.001	<0.001
Gloss (60°)	65−70	80−85	80−85	85−90	80−85
Adhesion (MPa)	120−130	100−110	120−130	185−190	260−270
Hard drying time (at 185 °C, h)	2−2.1	2.1−2.2	2.2−2.5	2.0−2.1	1.9−2.0

15.5.3 Epoxy

15.5.3.1 Basic concept and importance

Epoxy thermoset is treated as an engineering material because of its excellent attributes like favorable physical property, high mechanical strength, high thermal stability, high chemical resistance, excellent adhesive strength, low or no shrinkage during curing, and high dimensional stability. The organic low-molecular compounds or relatively high-molecular-weight polymers with at least two epoxy groups in each molecule are termed *epoxy resins*. The presence of a highly strained three-member oxirane ring of epoxy resin makes it very reactive; hence, a variety of curing systems are employed to obtain the desired thermosets. Thus, there is widespread interest in epoxy thermosets because of their excellent properties and high reactivity toward different chemicals coupled with outstanding formulation versatility at a reasonable cost to produce many useful properties. However, inherent brittleness, high flammability, and low toughness restrict the thermoset to use as a sole component in paints and surface coatings. Therefore, they are always used in combination with some flexible polymeric binders such as polyester, poly(ester amide), and polyurethane. In this respect, vegetable oil-based epoxy has very good compatibility with the aforementioned polymers and helps in surface wetting of other components present in the paint and coating systems.

15.5.3.2 Raw materials

Vegetable oil-based epoxies are of two types: non-glycidyl ether type and glycidyl ether type. Epoxy resin produced by direct epoxidation of unsaturation present in the unsaturated fatty acids of the vegetable oils by in situ generated peracids such as performic acid, peracetic acid (formic/acetic acid with hydrogen peroxide), and perbenzoic acid is in the first category. Polycondensation of monoglyceride of vegetable oil or fatty amide diol with epichlorohydrin in the presence or absence of conventional aromatic diol, such as bisphenol-A, bisphenol-S, tetrabromobisphenol-A, bisphenol-H, bisphenol-F, and bis(hydroxyl phenyl) methane, in alkaline aqueous solution resulted in the second category of epoxy. The catalysts used are sodium hydroxide, sodium carbonate, potassium carbonate, calcium carbonate, potassium hydroxide, and potassium bicarbonate. A large number of vegetable oils such as sunflower, karanja, *Annona squamosa*, linseed, soybean, cotton-seed, castor, and *M. ferrea* oils are used for producing these biobased epoxies (Das and Karak, 2010; Sharmin et al., 2007; Wang and Schuman, 2013).

The preparative steps for a typical biobased epoxy are shown in Scheme 15.1. Here, it is worthy to mention that *Vernonia* oil is a naturally obtained epoxidized vegetable oil produced by *Vernonia galamensis* and hence has potential to be used commercially. Oleic, linoleic, and linolenic acids and their methyl or ethyl esters are also epoxidized by urea and hydrogen peroxide in the presence of niobia supported methyl trioxo-rhenium catalyst. However, epoxidized vegetable oils, because of their low epoxy value, cannot be formed thermoset with desired properties. On the other hand, they possess very low viscosity and relatively good reactivity due to the presence of an epoxy group, so they are mainly used as reactive diluents and plasticizer for other epoxies to produce high-solid, low-VOC paints and coatings.

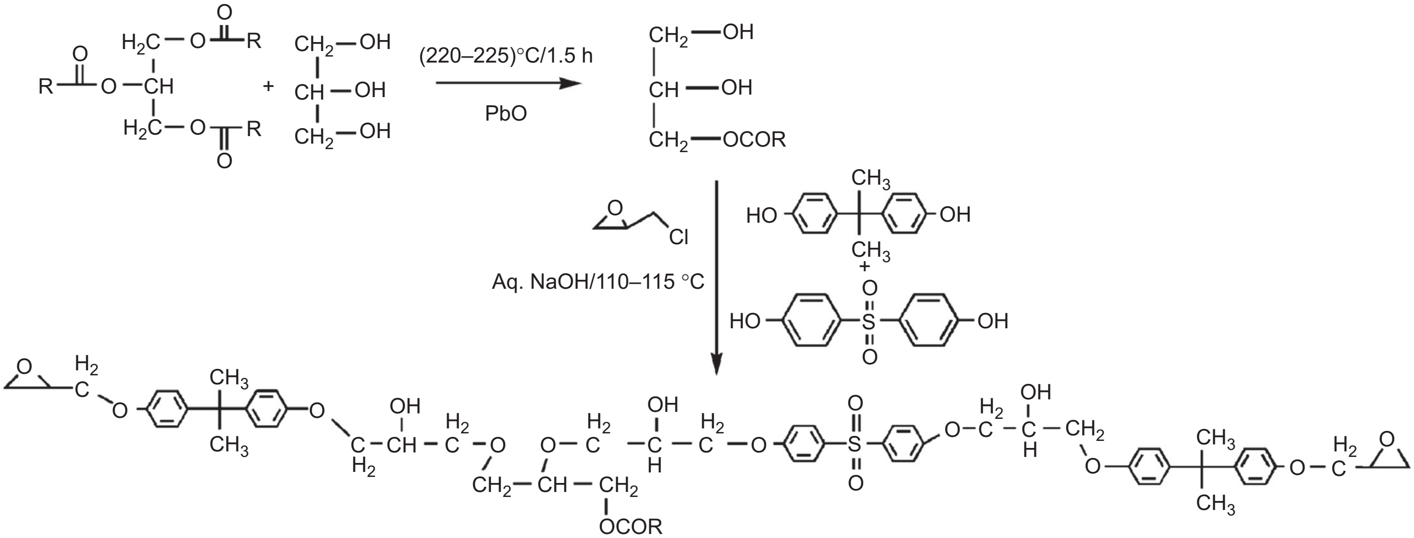

R is the hydrocarbon part of the mixture of oleic, linoleic, stearic, and palmitic acids

Scheme 15.1 Typical preparation of biobased epoxy resin.
Reproduced with permission from Das and Karak (2010); Copyright Elsevier, 2010.

15.5.3.3 Preparation

The epoxidized vegetable oils are generally produced by four different methods: epoxidation by peracid, such as peracetic acid, in the presence of a mineral acid catalyst, such as sulfuric acid, or perbenzoic acid; epoxidation by peroxide, including transition metal catalysts; epoxidation by halohydrin, such as hypohalous acid and its salts; and epoxidation by molecular oxygen. Peracid is generally preferred because of the ready availability of reactants and low-cost process, although other processes are sometimes used. For example, high oleic sunflower oil is epoxidized industrially by 16% hydrogen peroxide in the presence of tetrakis (diperoxotungsto) phosphate catalyst in dichloroethane solvent at 70 °C for 5 h (Shabeer et al., 2005). Epoxidized soybean oil is commercially obtained (trade name Drapex 6.8 of Witro Corp) with epoxy functionality 4.1−4.6 per vegetable oil molecule. Epoxidized soybean oil and epoxidized linseed oil (trade name Vikoflex 7190 of Elf Atochem Inc.), among others, are prepared by peracetic acid under ambient conditions over an extended period of time until the desired epoxidation is obtained. A variety of epoxidized oils with photocurable capability are also produced. For example, nobornyl linseed oil is epoxidized using hydrogen peroxide in the presence of ammonium tetrakis (diperoxotungsto) phosphate catalyst (Chen et al., 2002).

15.5.3.4 Modification

The essence of waterborne epoxy is well known. Thus, waterborne vegetable oil-based epoxies are produced by esterification of vegetable oil epoxy of drying oils or their fatty acids to half ester of dicarboxylic epoxy esters or maleinized epoxy esters by the reaction with polybasic acid or anhydrides, followed by neutralization with dimethyl ethanolamine. Similarly, ecofriendly biobased flame retardant epoxies are obtained from diepoxy fatty derivatives of oils containing phosphaphenanthrene, epoxidized vegetable oil, and epoxidized methyl-tris(undecenoyloxy) benzoate. Other types of modification of expoxidized oils are also reported in the literature (Saithai et al., 2013). Epoxidized soybean oil is modified acrylic acid in the presence of tertiary amine to obtain acrylated epoxidized soybean oil. Similarly, epoxidized karanja oil is modified by acrylonitrile and methyl methacrylate using benzoyl peroxide in an inert atmosphere to produce acrylated epoxies, which are further treated with diisocyanate to obtain acrylated epoxy polyurethane (Goud et al., 2007). The waterborne interpenetrating network (IPN) can also be produced from acrylated epoxy by the reaction with oleic acid using ammonium persulphate initiator followed by treatment with butylated melamine-formaldehyde resin (Zafar et al., 2009). The physical blending of vegetable oil-based epoxy, such as epoxidized allyl soyate with bisphenol-A based glycidyl ether epoxy, is prepared to improve physicomechanical properties. *Mesua ferrea* L. seed oil-based epoxies are modified with polyester and polyurethane of the same oil at different ratios; the resultant thermosets exhibit better performance than the parent epoxy-based thermoset (Das et al., 2013).

15.5.3.5 Curing

All of the previously discussed biobased epoxies are cured by using a required amount of suitable hardener system. A wide variety of hardener systems are used for this purpose. They are mainly three types: active hydrogen containing compounds or materials, ionic initiators, and reactive cross-linkers. Polyamines of both aliphatic and aromatic, hyperbranched polyamines and polyols, poly(amido amine) of dimer acids, di/polybasic acids and anhydrides, diisocyanates, polythiols, etc., or their combinations are classified as the first type; boron trifluoride monoethylamine and benzylpyrazinium hexafluoroantimonate are the second category; and melamine-formaldehyde resin, urea-formaldehyde resin, and phenol-formaldehyde resin, are the third type of agent used for curing biobased epoxies. These low viscous liquid epoxy resins are transformed to solid thermosets by chemical reactions with suitable hardeners. Biobased epoxy with low epoxy equivalent (amount of resin in gram per epoxy group or oxirane ring) is cured in less time than that of high epoxy equivalent epoxy resin. However, the overall reactivity of biobased epoxy of the same epoxy equivalent of bisphenol-A based glycidyl ether epoxy is less due to the presence of the long-chain hydrocarbon of fatty acid part of oil, which hindered the accessibility of resin to the hardener. The thermally latent initiator, N-benzylpyrazinium hexafluoroantimonate, cured biobased epoxy of diglycidyl ether epoxy of bisphenol-A and epoxidized soybean and castor oils by complex formation mechanism (Park et al., 2004; Jin and Park, 2008).

15.5.3.6 Property

The biobased epoxies in their original form are low viscous liquids with good solubility in a number of solvents; the epoxy equivalent generally varies from 120 to 750 g/epoxy depending on the molecular weight and number of epoxy groups present in each molecule. The viscosity varies with temperature and shear rate, such as Newtonian fluid, although high-molecular-weight epoxy with polar groups behaves differently. The thermosets of such epoxies exhibit relatively low mechanical strength but high flexibility and good impact resistance. The scratch hardness of such thermosets depends on the overall toughness, whereas gloss is influenced by dimensional stability and smoothness of the surface; generally, they are found to be good. Adhesive strength with different substrates is also good, although the value is relatively less than that of bisphenol-A-based glycidyl ether epoxy.

Table 15.3 represents the coating performance of biobased epoxy thermosets with different compositions. The study showed that the waterborne interpenetrating network of acrylated biobased epoxy, oleic acid, and butylated melamine-formaldehyde-based thermoset exhibited good mechanical, chemical, thermal, and antimicrobial properties (Zafar et al., 2009). The thermal stability of such biobased epoxy thermosets varies from 200 °C to 250 °C. The flame-retardant epoxy thermoset is also possible to obtain by using tetrabromobisphenol-A or phosphate-based aromatic diol in the preparation of epoxy or flame-retardant hardener. The glass transition temperature of the thermosets increases with increasing rigidity in the system by increasing cross-linking density,

Table 15.3 Coating performance of biobased epoxy thermoset with varying compositions and amounts of vegetable oil

Property	Bisphenol-A (BPA) + epichlorohydrin (ECH)	Monoglyceride (MG) + ECH	MG + ECH + BPA	5 wt% MG + ECH + BPA + Tiethanol amine (TEA)	10 wt% MG + ECH + BPA + TEA	15 wt% MG + ECH + BPA + TEA
Tensile strength (MPa)	20−22	0.5−1	4−6	30−35	20−25	10−15
Elongation at break (%)	5−8	30−40	20−30	18−20	40−45	55−60
Scratch hardness (kg)	7−8	1−2	4−5	8.5−9	8−8.5	7.5−8
Impact resistance (m)	0.6−0.8	>0.4	>0.8	>1	>1	>1
Bending (m)	<0.003	<0.001	<0.002	<0.002	<0.001	<0.001
Gloss (60°)	55−60	50−55	55−60	65−70	70−75	75−80
Adhesion (MPa)	120−130	155−165	220−230	1850−1900	1680−1700	1450−1500
Hard drying time (at 100 °C, min)	50−60	280−300	110−130	45−50	60−70	75−80

using more aromatic and heterocyclic moieties, etc. The chemical resistance of such epoxy thermosets is very good in almost all chemical environments, such as water, dilute acid, dilute alkali, and salt solution. However, in some cases, adhesion failure of the coated surface is observed due to relatively poor alkali resistance of the ester linkages that are present in the component of vegetable oil or in triglyceride itself. Epoxidized *Annona squmosa* oil is cured with a combination of amine and acid-like propane diamine with phthalic acid, *p*-phenylenediamine with adipic acid, etc. (Ahmad et al., 2006b), Here, it is pertinent to mention that a large number of reports clearly show the advantages of different biobased epoxy nanocomposites as superior binders with special attributes for paints and coatings over the pristine epoxies (Das and Karak, 2012; Das et al., 2014). Thus, properly formulated biobased epoxy along with other flexible resin-based thermosets are very good binders for paints and coatings.

15.5.4 Polyurethane

15.5.4.1 Basic concept and importance

Among all the biobased polymers, polyurethane is the most versatile because of its inherent molecular inhomogeneity; thus resin, plastic, elastomer, adhesive, etc., can be produced by judicious choice of structure and composition of the components under appropriate reaction conditions. Both biobased thermosetting and thermoplastic polyurethanes are used in paints and coating. The properties of polyurethanes can be manipulated by varying the ratio and structure of the components (Hepburn, 1992). They are prepared by the reaction of di/polyhydroxyl compounds with di/polyisocyanates under controlled reaction conditions, where at least one component is obtained from a biobased resource. These biobased polymers are formed by urethane linkage ($-$NHCOO$-$), which is a combination of amide ($-$CONH$-$) and ester ($-$COO$-$) bonds and transformed to a single chemical linkage with carbonyl part (C$=$O) common to both. In this linkage, the $-$NH group acts as proton donor and the ether ($-$O$-$) or carbonyl (C$=$O) part of ester linkage acts as proton acceptor and thus strong intra- and intermolecular H-bonding are formed through this urethane linkage among the chain molecules. Thus, this part of polyurethane provides rigidity in the structure. On the other hand, the flexibility is obtained from the flexible hydrocarbon part or ether linkage of the biobased component and macroglycol, present in the polyurethane chains. The ratio of isocyanate groups (NCO) to hydroxyl groups (OH) in the polyurethane is very critical and important. A room-temperature moisture curable binder for coatings and paints can be obtained by using polyurethane with NCO/OH greater that 1. The wide acceptability of biobased polyurethane in such industries is due to its outstanding mechanical strength, flexibility, toughness, scratch hardness, abrasion, chemical, thermal, and weather resistance. Furthermore, the processing and properties can be tuned by varying composition, structure, and reaction conditions. Thermoplastic polyurethanes are used in paints and coatings, but they can also be transferred to thermosetting depending on requirements using the appropriate amount and nature of cross-linkers.

15.5.4.2 Raw materials

The main components for the preparation of biobased polyurethanes are castor oil (main component recinoleic acid, a hydroxyl containing fatty acid), monoglyceride or dihydroxy fatty amides of different vegetable oils, and other polyols of vegetable oils (hydrolyzed epoxidized oils); macroglycol (for segmented polyurethanes) of relative high molecular weight (400—4000 g/mol) dihydroxy polyester, polyether, polycarbonate, or polyhydrocarbon; a chain extender of low-molecular-weight (<400 g/mol) di/polyols, aminoalcohols, and di/polyamines such as ethylene glycol, butane diol, cyclohexane dimethanol, trimethlol propane, or ethylene diamine, which is used sometimes in combination with vegetable oil-based polyol; and di/polyisocyanates of both aromatic and aliphatic, including cycloaliphatic such as toluene diisocyanate, methylene diphenyl diisocyanate, isophorone diisocyanate, or hexamethylene diisocyanate (Karak, 2012). Soybean oil-based polyisocyanate, obtained by the reaction of brominated triglyceride with silver-isocyanate, is also used for this purpose (Cayli and Kusefoğlu, 2008). Although diisocyanate reacts with diol or diamine at a very fast rate, sometimes to accelerate the reaction rate and particularly to reduce the reaction temperature, various catalysts are used in the polyurethane polymerization process. Mainly organometallic compounds such as dibutyltin dilaurate, dibutyl tin oxide, bismuth/zinc and carboxylates are preferred, although basic tertiary amines such as triethyl amine, triethylene diamine, and dimethylcyclohexyl amine can also be used for this purpose.

15.5.4.3 Preparation

Biobased polyurethanes are prepared by two different processes, namely, the prepolymer process and one-shot process. In both cases, polyurethanes are formed by a rearrangement reaction, which is not a condensation or addition polymerization process. In the one-shot process, all of the components including di/polyol and diisocyanate are reacted together at the desired ratio at 70—110 °C, depending on the reactivity and catalyst used, for 3—4 h. Urethane oils are also prepared by this process, whereas vegetable oils reacted first with glycerol or pentaerythritol followed by reaction of the resulting hydroxyl containing compounds with diisocyanates. On the other hand, in the prepolymer process, polyurethanes are prepared by a two-step method: in the first step, the reaction of di/polyols with diisocyanate at ratio of NCO/OH greater than 1 or at OH/NCO greater than 1 produced isocyanate or hydroxyl terminated prepolymers, respectively. In the second step, this prepolymer is reacted with a desired amount of chain extender or diisocyanate to obtain the desired ratio of NCO/OH in the final polyurethane, at 70—110 °C for 2—3 h. In the case of the two-pack system, one pack contains relatively low-molecular-weight isocyanate or hydroxyl terminated prepolymer, with the other container consisting of a hardener such as diol/diamine or diisocyanate depending on the terminal groups of the prepolymer in the first pack. The polyurethane obtained through this process is dried at a faster rate than that of the moisture-curable polyurethane of the one-shot process. Polyurethane can be prepared with or without using solvent in both the processes.

A large number of vegetable oil derivatives based on castor, soybean, sunflower, *M. ferrea*, olive, peanut, canola, corn, and safflower oils, among others, are used as naturally obtained bioresources to produce a wide variety of biobased polyurethanes with different structures and chemical compositions (Karak, 2012; Yakushin et al., 2014). Low-molecular-weight polyurethane is obtained by the reaction of soybean oil polyol, a product of methanolysis of epoxidized oil with toluene diisocyanate at 50 °C. Both poly(urethane ester) and poly(urethane amide) resins are produced from *M. ferrea* L. seed oil derivatives, such as monoglyceride and fatty amide diol, respectively, by the reaction with toluene diisocyanate in the presence of low-molecular-weight polyethylene glycol as a chain extender and dibutyl tin dilaurate as the catalyst using a one-shot process with varying NCO/OH ratios, as shown in Scheme 15.2 (Dutta and Karak, 2005, 2006). Biobased polyurethane is also prepared by interesterification of castor and linseed oils through a chemoenzymatic process using lipase as the catalyst and toluene diisocyanate as the isocyanate under ambient conditions (Athawale and Joshi, 2000). However, a toxic isocyanate-free process is also reported in the literature, although it has not been very successful. For example, linseed and soybean oil-based polyurethane is prepared in supercritical carbon dioxide by carbonation of fatty acid derivatives of the oil followed by the reaction with a primary amine such as ethylene diamine, hexamethylene diamine, or tris(aminoethyl) amine (Bähra and Mülhaupt, 2012). The study also showed

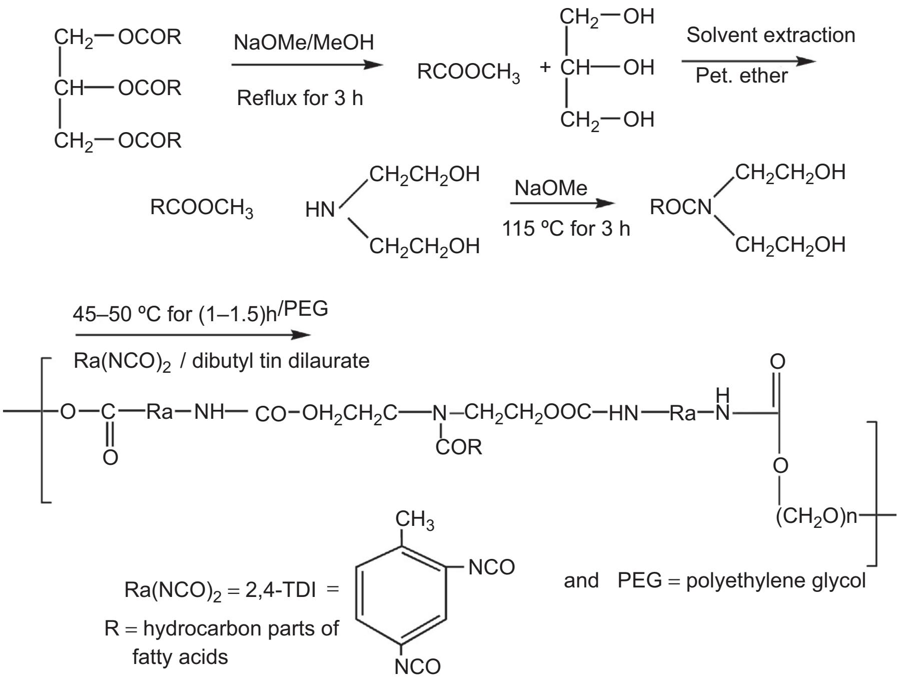

Scheme 15.2 Typical preparation protocol for polyurethane resin.
Reproduced with permission from Dutta and Karak (2005); Copyright Elsevier, 2005.

that the hyperbranched polyurethanes obtained from monoglyceride of castor oil showed better coating performance than the direct use of the oil.

15.5.4.4 Modification

A large number of modifications are reported in the literature for biobased polyurethanes. Different types of interpenetrating networks are produced by the polymerization of different vinyl, acrylic monomers in the presence of different vegetable oil-based polyurethanes using benzoyl peroxide as the catalyst at an elevated temperature. Similarly, boron-modified castor oil-based polyester polyurethane is obtained by the reaction of esterified polyester of the oil in the presence of boric acid, with toluene diisocyanate. *Mesua ferrea* L. seed oil-based polyurethanes are modified by partially butylated melamine-formaldehyde resin and bisphenol-A-based glycidyl ether epoxy, separately to improve the performance of the individual components (Dutta and Karak, 2007). Waterborne biobased polyurethanes are prepared from maleinized monoglyceride of vegetable oils, flexible hydrocarbon-based macroglycol, toluene diisocyanate, and ethylene diamine (Gündüz et al., 2005). By using the concept of ionogenic center in polymers, waterborne polyurethanes are also obtained. For this purpose, bis(hydroxyl methyl) propionic acid, butane diol, and isophorone diisocyanate are reacted together in a ratio, so that an isocyanate terminated prepolymer can be obtained, which subsequently is neutralized by using triethylamine to form the corresponding salt after a reaction with free carboxylic groups of the polyurethane chains. Waterborne hyperbranched polyurethane is also prepared from tannic acid as the biobased polyol, which exhibited good coating performance on modification with a combined system of vegetable oil-based glycerol-based glycidyl hyperbranched epoxy and dimer acid-based poly(amido amine) (Gogoi and Karak, 2014).

15.5.4.5 Curing

The resinous and some elastomeric polyurethanes are cured by a variety of hardener systems, including polyfunctional compounds such as di/polyol, di/polyamine, or di/polyisocyanate and resins such as epoxy, melamine-formaldehyde, and phenol-formaldehyde to obtain corresponding thermosets. They can also be cured by moisture under ambient conditions in the case of polyurethanes with sufficient free isocyanate groups (Chattopadhyay et al., 2006). In this process, the free isocyanate group is converted to amines by the reaction with water, which subsequently react with other isocyanate and urethane groups to form urea, biuret, and allophanate linkages and thereby forming a three-dimensional network structure. The drying oil-based polyurethane can also be cured by conventional free radical cross-linking reaction in the presence of an organic peroxide and organometallic catalyst.

15.5.4.6 Property

It was already stated that tailor-made properties are possible by the judicious choice of compositions and structures of the components of biobased polyurethanes. Thus, a lot of studies have been made on structure—property relationship, effect of NCO/OH ratio, effect of cross-linking, etc., on the ultimate properties of polyurethanes used in painting and coating applications. Table 15.4 shows the effect of the NCO/OH ratio on the performance of polyurethane-based coatings. The presence of strong intra/intermolecular attraction forces through H-bonding and other polar—polar and van der Waals interactions resulted in good performance of polyurethane. Furthermore, the presence of virtual or physical cross-linking through strong H-bonding of urethane linkages supports the performance.

It has been found that the effect of structure and composition of vegetable oils or fatty acids as well as their amount in polyurethane chains is significant on the ultimate properties of the polymers. For example, castor oil-based hyperbranched polyurethanes exhibited better mechanical strength than that of *M. ferrea* L. seed oil and sunflower oil based analogous polyurethanes (Kalita and Karak, 2014). Similarly, with the increase in amount of oil from 0 wt% to 10 wt%, flexibility increases but strength decreases for *M. ferrea* L. seed oil-based hyperbranched polyurethanes. The density of polyurethane generally increases from 1.01 to 1.12 g/mol with the increase of NCO/OH ratio, compactness in the structure, crystallinity, etc. The mechanical properties are also influenced by the same factors including molecular weight and physical as well as chemical (in case of thermoset) cross-link density. The adhesive strength and mechanical properties are generally increased with the increase of the above factors. Epoxidized linseed oil-based polyurethanes with 10 wt% toluene diisocyanate exhibited good physicomechanical and anticorrosive properties (Suresh and Kishanprasad, 2005). Similarly, chemoenzymatically synthesized polyurethanes of castor and linseed oils combination showed good hardness, adhesion, impact, and chemical resistance.

Although most of the vegetable oil-based polyurethanes exhibited non-Newtonian behaviors, a few such polyurethanes are also found to behave like Newtonian fluids. The thrixotopic behaviors of such biobased polyurethanes clearly indicate that high solid coatings can be used without much difficulty. Even though the chemical resistance of vegetable oil-based polyurethanes is relatively poor because of the presence of ester linkages, as well as the fact that urethane may also hydrolyze under high humid condition, properly designed polyurethane with shielding of such labile groups can result in good chemical resistance for the paints and coatings made by using these polyurethanes. These polyurethanes also have relatively high thermostability (190—210 °C) with a three-step degradation pattern in most cases. The incorporation metal, such as boron, in the polyurethane enhances thermostability (initial degradation increase to 220 °C). Again, polyurethanes are electrically insulating materials with volume resistivity 10^{14}—10^{15} Ωm. Thus, it is observed that vegetable oil-based polyurethanes exhibited higher permittivity, higher loss factor, lower dielectric, and higher resistivity compared to the epoxy thermoset under the same conditions.

A few hyperbranched polyurethanes of different vegetable oils are also reported in the literature and were found to possess good coating performance. Table 15.5 shows the coating performance of hyperbranched polyurethane obtained from different vegetable oils. Furthermore, a lot of studies have been reported for enhancement of performance, including achievement of smart coating material of biobased polyurethanes through nanocomposite formation with a number of nanomaterials (Liua et al., 2009; Thakur and Karak, 2014). Thus, biobased polyurethanes, including water-dispersible ones, have been extensively used in paint and coating applications.

Table 15.4 Coating performance of monoglyceride of vegetable oil-based polyurethane (PUE) and dihydroxy fatty amides-based polyurethane (PUA) thermosets with varying NCO/OH ratios

Property	PUE1.0[a]	PUE1.25[a]	PUE1.5[a]	PUE2.0[a]	PUA1.0[a]	PUA1.25[a]	PUA2.0[a]
Touch-free time (surface drying, min)	40–50	40–45	35–40	25–30	15–20	10–15	8–10
Hard drying time (30 °C, min)	80–90	70–80	60–70	50–60	40–50	30–40	25–30
Pencil hardness	HB	H	2H	3H	HB	H	2H
Gloss (at 60° for PUE and at 45° for PUA)	100–110	105–112	110–115	115–120	60–65	65–70	70–75
Impact strength (cm)	30–35	35–40	40–50	>50	25–30	35–40	40–45
Bending test (dia., cm)	<0.4	<0.3	<0.2	<0.2	<0.5	<0.4	<0.3
Adhesion (kN/m for PUE and % for PUA)	120–130	155–165	220–230	330–340	100	100	100

[a] Digit in the code indicates the NCO/OH ratio in the polymers.

Table 15.5 **Coating performance of biobased hyperbranched polyurethane with varying nature and amount of oils**

Property	**0 wt% Oil**	**10 wt% Castor oil**	**10 wt% Sunflower oil**	**5 wt% *M. ferrea* L.**	**10 wt% *M. ferrea* L.**	**15 wt% *M. ferrea* L.**
Tensile strength (MPa)	8−9	7.5−8	5−6	6.6−7.5	6−7	5.5−6.6
Elongation at break (%)	550−600	600−610	600−620	580−610	600−620	610−630
Scratch hardness (kg)	5−6	6−7	5−6	5.5−6	5.5−6.5	5−6
Impact resistance (m)	1−0.9	>1	>1	>1	>1	>1
Bending (m)	<0.001	<0.001	<0.001	<0.001	<0.001	<0.001
Gloss (60°)	85−90	88−90	85−88	86−92	85−87	80−85

15.6 Manufacturing of paints and coatings from biobased polymers

To manufacture biobased polymers contained in paints and coatings, a formulator must design the compound recipe, which consists of suitable biobased binder, pigment, solvent(s) and other desired additives. However, before formulating the recipe, the designer should consider the following points (Malshe and Sikchi, 2004):

1. Service requirements of the final product; i.e., the required performance including nonvolatile solid content, surface coverage, etc., of the formulated paint.
2. Processing and application methods to be employed.
3. Expected packing for storage and handling as well as pricing of the formulated paint.

Thus, the nature and amount of all components to be used in the formulation are based on the above criteria. Again, the main objective of paint preparation is to obtain a homogenous/uniform dispersion of all ingredients and their stabilization in the system. As a typical example, preparation of a highly branched, biobased, polyester-modified, epoxy-based, low-VOC, high-solid industrial paint is presented here (Konwar et al., 2012). This is a two-pack system, where one pack contains a biobased polyester modified epoxy as the base paint and the other pack consists of a catalyst or hardener, dimer acid-based poly(amido amine) (Table 15.6).

Table 15.6 **Formulation for a typical paint (Konwar et al., 2012)**

Ingredients	Amount (g)
(a) Pack I	
Pigment: Titanium oxide	10–12
Filler I: Barytes	12–14
Filler II: Silica	15–16
Binder I: Biopolyester	25–27
Solvent: Xylene	14–16
Cosolvent: *n*-Butanol	7–8
Flow promoter: Urea-formaldehyde resin (60% nonvolatile content in n-butanol)	1–1.5
Binder II: Epoxy resin (70% nonvolatile content in xylene)	16–18
(b) Pack II	
Curing agent: Poly(amido amine)	40–42
Solvent: Xylene	52–54
Cosolvent: *n*-Butanol	8–10

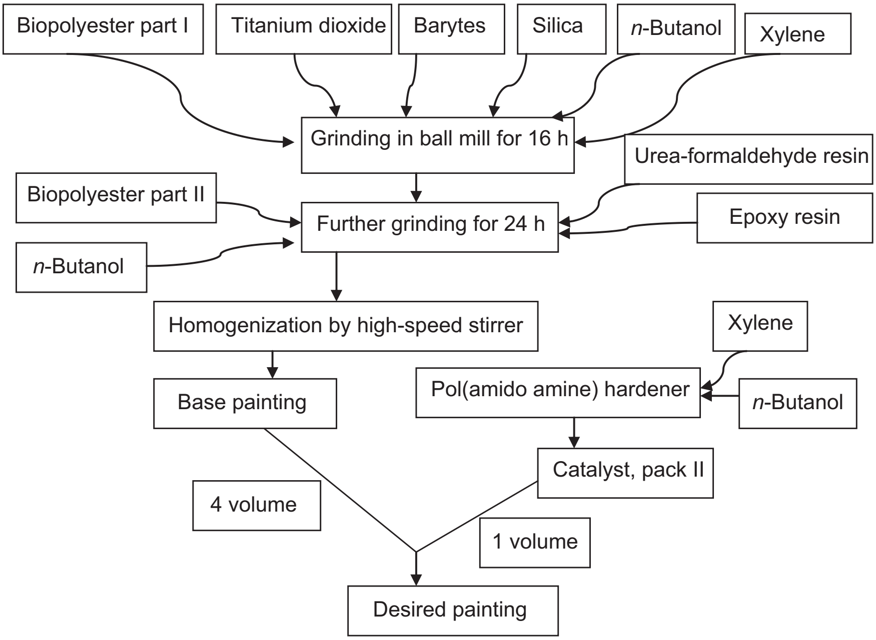

Scheme 15.3 Flow sheet diagram for the manufacturing process of a paint.

The flow diagram represents the preparative method in Scheme 15.3. The base paint (pack I) and the catalyst (pack II) formulation recipes along with their functions are also provided in Table 15.6. The base paint is prepared in a porcelain ball mill using *M. ferrea* L. seed oil modified highly branched polyester as one of the binders in the grinding stage. At first, the pigment titanium oxide, fillers, highly branched polyester and about 20% of solvent are charged in the ball mill. The grinding of the pigments and fillers is done for 15—18 h to make the particle size of 25—30 μm, as measured by Hegman gauge. After attaining the required grinding size, the materials are dropped into a separate container and mixed with epoxy resin and finally adjusted with the remaining amount of solvents and other additives to achieve the required amount of viscosity and solid content (nonvolatile content) of paint. Finally, the prepared paint has to be kept for at least 24 h for wetting before any application.

15.7 Conclusions and future trends

In a world of high-priced petroleum products, stringent rules and regulations, and concerns about the environment and ecology, scientists and industrialists have been prompted to investigate alternative naturally renewable resource-based polymers for paints and coatings. A large variety of biobased polymers with proper formulations are used as environmentally friendly products for paints and coatings. Through this chapter, it is clear that this approach not only uses the renewable and biodegradable polymers but it also leads to a sustainable development. Thus, such biobased polymers are the right choice as binders for todays' paints and coatings. Furthermore, improving their performance and imparting a new set of properties can be achieved by enriched scientific and technological knowledge of nanotechnology. Thus, a properly designed biopolymer and its nanocomposites with desirable multifunctional attributes are the future of materials in the painting and coating sectors.

References

Ahmad, S., Ashraf, S.M., Hasnat, A., Yadav, S., Jamal, A., 2001. Studies on urethane-modified alumina-filled polyesteramide anticorrosive coatings cured at ambient temperature. Journal of Applied Polymer Science 8, 1855−1865.

Ahmad, S., Ashraf, S.M., Hasnat, A., Sharmin, E., Kamal, A., 2005. Antimony acrylate modified polyesteramide anticorrosive coatings from a sustainable resource. Journal of Polymeric Materials 22, 377−384.

Ahmad, S., Ashraf, S.M., Naqvi, F., Yadav, S., Zafar, F., 2006a. Alumina-incorporated polyesteramide from non-edible seed oils. Journal of Macromolecular Science Part A: Pure and Applied Chemistry 43, 1409−1419.

Ahmad, S., Naqvi, F., Sharmin, E., Verma, K.L., 2006b. Development of amine−acid cured *Annona squamosa* oil epoxy anticorrosive polymeric coatings. Progress in Organic Coatings 55, 268−275.

Ansari, M.F., Goswami, D.N., 2006. Shellac-acrylic emulsion painting for cementations surfaces. Pigment and Resin Technology 35, 183−187.

Ashraf, S.M., Ahmad, S., Riaz, U., Alam, M., Sharma, H.O., 2007. Miscibility behavior of blend of polyesteramides of linseed oil and dehydrated castor oil with poly(methacrylic acid). Journal of Applied Polymer Science 103, 1367−1374.

Athawale, V.D., Joshi, K.R., 2000. Chemoenzymatic synthesis of PURs. European Coating Journal 6, 42−46.

Bähra, M., Mülhaupt, R., 2012. Linseed and soybean oil-based polyurethanes prepared via the non-isocyanate route and catalytic carbon dioxide conversion. Green Chemistry 14, 483−489.

Biemans, T., Thomas, A., 2014. The future of alkyd resins according to Worlée. Journal of Surface Coatings Australia 51, 16−32.

Cayli, G., Kusefoğlu, S., 2008. Biobased polyisocyanates from plant oil triglycerides: synthesis, polymerization, and characterization. Journal of Applied Polymer Science 109, 2948−2955.

Cecil, J.L., Kurnik, W.J., Babcock, D.E., 1988. High-solids coatings. US Patent US4786666 A.

Chandra, R., Rustgi, R., 1998. Biodegradable polymers. Progress in Polymer Science 23, 1273−1335.

Chattopadhyaya, D.K., Sreedharb, B., Raju, K.V.S.N., 2006. The phase mixing studies on moisture cured polyurethane-ureas during cure. Polymer 47, 3814−3825.

Chen, J., Soucek, M.D., Simonsick, W.J., Celikay, R.W., 2002. Synthesis and photopolymerization of norbornyl epoxidized linseed oil. Polymer 43, 5379−5389.

Das, G., Karak, N., 2010. Thermostable and flame retardant *Mesua ferrea* L. seed oil based non-halogenated epoxy resin/clay nanocomposites. Progress in Organic Coatings 69, 495−503.

Das, G., Karak, N., 2012. *Mesua ferrea* L. seed oil based amido-amine modified nanoclay/epoxy nanocomposites. Journal of Applied Polymer Science 124, 2403−2414.

Das, G., Kalita, R.D., Deka, H., Buragohain, A.K., Karak, N., 2013. Biodegradation, cytocompatability and performance studies of vegetable oil based hyperbranched polyurethane modified biocompatible sulfonated epoxy resin/clay nanocomposites. Progress in Organic Coatings 76, 1103−1111.

Das, G., Kalita, R.D., Gogoi, P., Buragohain, A.K., Karak, N., 2014. Antibacterial activities of copper nanoparticles decorated organically modified montmorillonite/epoxy nanocomposites. Applied Clay Science 90 C, 18−26.

Dredge, D.W., Knight, S.B., 2008. Method and composition for surface coating. World Patent WO2008102126 A1.

Dutta, N., Karak, N., Dolui, S.K., 2004. Synthesis and characterization of polyester resins based on Nahar seed oil. Progress in Organic Coatings 49, 146−152.

Dutta, S., Karak, N., 2005. Synthesis, characterization of poly(urethane amide) resins from Nahar seed oil for surface coating applications. Progress in Organic Coatings 53, 147−152.

Dutta, N., Karak, N., Dolui, S.K., 2007. Stoving painting from *Mesua ferrea* L. seed oil based short oil polyester and MF resins blend. Progress in Organic Coatings 58, 40−45.

Dutta, S., Karak, N., 2006. Effect of the NCO/OH ratio on the properties of *Mesua ferrea* L. seed oil-modified polyurethane resins. Polymer International 5, 549−556.

Dutta, S., Karak, N., 2007. Blends of *Mesua ferrea* L. seed oil based polyurethane with epoxy resin. Pigment Resin Technology 36, 74−82.

Eiri, 2008. Paint, Pigment, Solvent, Coating, Emulsion, Paint Additives and Formulations. EIRI Board, India.

Erhan, S.Z., 2005. Industrial Uses of Vegetable Oils. Taylor & Francis, London.

Ghosh, B., Urban, M.W., 2009. Self-repairing oxetane-substituted chitosan polyurethane networks. Science 323 (5920), 1458−1460.

Goud, V.V., Patwardhan, A.V., Dinda, S., Pradhan, N.C., 2007. Epoxidation of karanja (*Pongamia glabra*) oil catalysed by acidic ion exchange resin. European Journal of Lipid Science and Technology 109, 575−584.

Gogoi, S., Karak, N., 2014. Bio-based biodegradable waterborne hyperbranched polyurethane as an eco-friendly sustainable material. ACS Sustainable Chemistry and Engineering 2, 2730−2738.

Gündüz, G., Khalid, A.H., Mecidolu, A., Aras, L., 2005. Water-borne and air-drying oil-based resins. Progress in Organic Coatings 49, 259−269.

Hepburn, C., 1992. Polyurethane Elastomers. Springer, Netherlands.

Indeikin, E.A., Kulikova, O.A., Manerov, V.B., 2002. Physical-chemical conditions for production of alkyd-acrylic dispersion. Macromolecular Symposium 187, 563−571.

Jin, F.L., Park, S.J., 2008. Thermomechanical behavior of epoxy resins modified with epoxidized vegetable oils. Polymer International 57, 577−583.

Johannes, T.P., Derksen, F., Cuperus, P., Kolster, P., 1996. Renewable resources in coatings technology: a review. Progress in Organic Coatings 27, 45−53.

Kalita, H., Karak, N., 2014. Bio-based hyperbranched shape memory polyurethanes: effect of different vegetable oils. Journal of Applied Polymer Science 131, 39579 (1−8).

Karak, N., 2009. Fundamentals of Polymers-Raw Materials to Finish Products. PHI Learning Pvt. Ltd, New Delhi.

Karak, N., 2012. Vegetable Oil-Based Polymers: Properties, Processing and Applications. Woodhead Publishing Ltd, Oxford.

Konwar, U., Mandal, M., Karak, N., 2009. *Mesua ferrea* L. seed oil-based highly thermostable and biodegradable polyester/clay nanocomposites. Polymer Degradation and Stability 94, 2221−2230.

Konwar, U., Mandal, M., Karak, N., 2010. Vegetable oil based highly branched polyester/clay silver nanocomposites as antimicrobial surface coating materials. Progress in Organic Coatings 68, 265−273.

Konwar, U., Karak, N., 2011. Hyperbranched polyether core containing vegetable oil modified polyester and its clay nanocomposites. Polymer Journal 43, 565−576.

Konwar, U., Jana, T., Karak, N., 2012. Vegetable oil-based highly branched polyester modified epoxy based low VOC high solid industrial painting. Journal of Applied Polymer Science 125, E2−E9.

Liua, M., Petrovica, Z.S., Xu, Y., 2009. Bio-based polyurethane-clay nanocomposite foams: syntheses and properties. MRS Proceedings 1188. 1188-LL04-05.

Mahapatra, S.S., Karak, N., 2004. Synthesis and characterization of polyesteramide resins from Nahar seed oil for surface coating applications. Progress in Organic Coatings 51, 103−108.

Mahapatra, S.S., Karak, N., 2007. Hyperbranched polyamine: a promising curing agent for a vegetable oil-based poly(ester-amide) resin. Progress in Organic Coatings 60, 328−334.

Malshe, V.C., Sikchi, M., 2004. Basic of Painting Technology. UICT, Mumbai.

Morgans, W.M., 2000. Outlines of Paint Technology. CBS Publishers, Mumbai.

Nair, L.S., Laurencin, C.T., 2007. Biodegradable polymers as biomaterials. Progress in Polymer Science 32, 762−798.

Nishibori, S., 1992. Method for pulverizing gelatin and painting, coating layer, film and finished cloth. US patent US 5080292 A.

Park, S.J., Jin, F.L., Lee, J.R., 2004. Synthesis and thermal properties of epoxidized vegetable oil. Macromolecular Rapid Communication 25, 724−727.

Patel, H.S., Patel, S.J., 2010. Novel surface coating system based on maleated shellac. E-Journal of Chemistry 7 (S1), S55−S60.

Pramanik, S., Sagar, K., Konwar, B.K., Karak, N., 2012. Synthesis, characterization and properties of a castor oil modified biodegradable poly(ester amide) resin. Progress in Organic Coatings 75, 569−578.

Pramanik, S., Konwarh, R., Sagar, K., Konwar, B.K., Karak, N., 2013. Bio-degradable vegetable oil based hyperbranched poly(ester amide) as an advanced surface coating material. Progress in Organic Coatings 76, 689−697.

Pramanik, S., Hazarika, J., Kumar, A., Aidew, L., Buragohain, A.K., Karak, N., 2014. Green silver nanoparticles decorated multiwalled carbon nanotube—a precursor for fabrication of multifunctional bio-based sustainable nanocomposites. ACS Sustainable Chemistry and Engineering 2, 2510−2518.

Ratnayake, W.S., Hoover, R., Shahidi, F., Perera, C., Jane, J., 2001. Composition, molecular structure and physicochemical properties of starches from four filed pea cultivars. Food Chemistry 74, 189−202.

Sanderson, J.M., 1934. Rosin derivatives in painting products. Industrial Engineering and Chemistry 26, 711−715.

Saithai, P., Lecomte, J., Dubreucq, E., Tanrattanakul, V., 2013. Effects of different epoxidation methods of soybean oil on the characteristics of acrylated epoxidized soybean oil-co-poly(methyl methacrylate) copolymer. Express Polymer Letters 7, 910−924.

Shabeer, A., Garg, A., Sundararaman, S., Chandrashekhara, K., Flanigan, V., Kapila, S., 2005. Dynamic mechanical characterization of a soy based epoxy resin system. Journal of Applied Polymer Science 98, 1772−1780.

Sharmin, E., Ashraf, S.M., Ahmad, S., 2007. Epoxidation, hydroxylation, acrylation and urethanation of *Linum usitatissimum* seed oil and its derivatives. European Journal of Lipid Science and Technology 109, 134−146.

Shogren, R.L., Petrovic, Z., Liu, Z., Erhan, S.Z., 2004. Biodegradation behaviour of some vegetable oil-based polymers. Journal of Polymers and the Environment 12, 173–178.

Suresh, K.I., Kishanprasad, V.S., 2005. Synthesis, structure, and properties of novel polyols from cardanol and developed polyurethanes. Industrial and Engineering Chemistry Research 44, 4504–4512.

Talbert, R., 2008. Paint Technology Handbook. CRC Press, Boca Raton.

Thakur, S., Karak, N., 2014. Multi-stimuli responsive smart elastomeric hyperbranched polyurethane/reduced graphene oxide nanocomposites. Journal of Material Chemistry, A 2, 14867–14875.

Voit, B.I., Lederer, A., 2009. Hyperbranched and highly branched polymer architectures synthetic strategies and major characterization aspects. Chemical Reviews 109, 5924–5973.

Wang, C., Lin, G., Pae, J.H., Jones, F.N., Ye, H., Shen, W., 2000. Novel synthesis of carboxy-functional soybean acrylic-alkyd resins for water-reducible coatings. Journal of Coatings Technology 7255–7261.

Wang, R., Schuman, T.P., 2013. Vegetable oil-derived epoxy monomers and polymer blends: a comparative study with review. Express Polymer Letters 7, 272–292.

Wicks, Z.W., Frank, J., Jones, N., Pappas, S.P., 1999. Organic Coatings Science and Technology, second ed. John Wiley & Sons, New Jersy.

Wilson, A.D., Nicholson, J., Prosser, H. (Eds.), 1991. Waterborne Coatings, vol. 3. Springer, Netherlands.

Xu, M., 2012. Preparation process of low-cost environment-friendly inner wall coating. Chinese patent CN102382572 A.

Yakushin, V., Stirna, U., Bikovens, O., Misane, M., Sevastyanova, I., Vilsone, D., 2014. Synthesis and characterization of novel polyurethanes based on vegetable oils amide and ester polyols. Materials Science (Medžiagotyra) 20, 277–282.

Yebra, D.M., Kiil, S., Dam-Johansen, K., Weinell, C., 2005. Reaction rate estimation of controlled-release antifouling painting binders: rosin-based systems. Progress in Organic Coatings 53, 256–275.

Zafar, F., Ashraf, S.M., Ahmad, S., 2007. Studies on zinc-containing linseed oil based polyesteramide. Reactive Functional Polymers 67, 928–935.

Zafar, S., Zafar, F., Riaz, U., Ahmad, S., 2009. Synthesis, characterization, and anticorrosive coating properties of waterborne interpenetrating polymer network based on epoxy-acrylic-oleic acid with butylated melamine formaldehyde. Journal of Applied Polymer Science 113, 827–838.

Zafar, F., Zafar, H., Shah, M.Y., Sharmin, E., Ahmad, S., 2012. Vegetable seed oil based waterborne polyesteramide: a "Green" material. In: Khemani, L.D., Srivastava, M.M., Srivastava, S. (Eds.), Chemistry of Phytopotentials: Health, Energy and Environmental Perspectives. Springer Berlin Heidelberg, Berlin, pp. 127–130.

Bio-based adhesives

16

J.-D. Mathias[1], M. Grédiac[2,3], P. Michaud[2,3]
[1]IRSTEA, Laboratoire d'Ingénierie pour les Systèmes Complexes, Aubière, France; [2]Institut Pascal, Clermont Université, Université Blaise Pascal, Clermont-Ferrand, France; [3]CNRS, UMR, Institut Pascal, Aubière, France

16.1 Introduction

16.1.1 History of bioadhesives

Bonding components is one of the oldest engineering processes. The first uses of adhesive were highlighted by archaeologists and date back to the middle and upper Palaeolithic era (Carciumaru et al., 2012). Ochre was one of the natural resources used during this period (Wadley et al., 2004) essentially for practical reasons. From this period on, techniques continued to progress: adhesive applications became more and more used in daily life for both engineering purposes and artistic ones. We can especially cite the use of adhesive by the Egyptians, the Greeks, and the Romans who developed adhesive techniques for veneering and marquetry as well as for ceramics and wood materials. The origin of all these adhesives was natural (such as animal-, fish-, or plant-based glue). Turning points in the bioadhesive story were the Industrial Revolution and the arrival of plastics during the twentieth century. The production of plastic adhesives has continually increased during recent years due to economic incentive: adhesives are cheap and competitive in regard to other bonding techniques such as bolting techniques. One of the most significant markets of adhesives remains the building and construction sector. They are used for structural purposes as well as for flooring or wall covering. The main issue relies in the use of adhesive in timber buildings that is a growing market. Adhesives are used for bonding several layers of timber to design tailored components. Moreover, the development of the timber construction market (especially in the USA and Nordic countries) is on a par with the growing concern of public awareness of environment impacts of petrochemical-based products, because such products are based on depleting resources. Scholars are becoming more and more interested in the development of bioadhesives in industry and research. For instance, in 1990, only 30 research papers were devoted to bioadhesives versus 1200 in 2012 (source: scopus.com). This reflects the effective awareness of society to develop environmentally and health-friendly adhesives.

16.1.2 Bio-based versus synthetic adhesives

Comparing the pros and cons of bio-based and synthetic adhesives clearly depends on the engineering application and the associated purposes. However, bioadhesives

Biopolymers and Biotech Admixtures for Eco-Efficient Construction Materials. http://dx.doi.org/10.1016/B978-0-08-100214-8.00016-6
Copyright © 2016 Elsevier Ltd. All rights reserved.

definitively present benefits in terms of environmental and health properties: the components of the majority of synthetic adhesives such as poly(vinyl acetate), epoxy, phenol—formaldehyde, and polyurethane are based on toxic chemicals such as epichlorohydrin, methylene diphenyl diisocyanate (MDI), toluene diisocyanate (TDI), formaldehyde, and volatile organic compounds (VOCs). These are costly and harmful for both the health of living beings and the environment, including ecosystems. It particularly constitutes an issue in timber construction in which legislation is increasingly strict about the emission of VOCs. At the same time, the synthetic adhesive industry has been aware of the growing environmental concern of the public, and has developed synthetic adhesives that are less harmful to environment and health. This trend is increased by the depleting petrochemical feedstock and the rising oil prices that contribute to develop bio-based adhesive from a commercial interest. Indeed, green adhesives and sealant markets are projected to reach nearly $1.24 billion in 2017 (study done by IntertechPira) in a global market of US$ 48 billion in 2013. The issues rely on how to develop a competitive adhesive that addresses the following issues: (1) being environment and health friendly; (2) exhibiting suitable mechanical and chemical properties; (3) and showing competitive production costs. However, the transition from synthetic adhesives toward bio-based adhesives will be accelerated by international legislation (mainly US and EU legislation) that will contribute to reduce the use of adhesive exhibiting environmental and health impacts in the automotive and building industries.

16.2 Testing bioadhesives

16.2.1 Mechanical tests: single-lap and double-lap tests

Mechanical tests enable assessing the strength of bioadhesives. Different tests are reported to be used by scholars and engineers such as tension, compression, or shear tests (Patel et al., 2013a). However, the most popular mechanical tests remain the lap tests that rely on the assessment of the shear strength. Double- and single-lap tests were developed for measuring shear strength of adhesives. However, single-lap tests yield some bending moments, whereas double-lap tests avoid this effect. Besides, a double-lap test directly provides the shear strength of adhesives and avoids peel effects. The failure of double-lap tests is mainly due to the appearance of a shear stress peak near the free edge as depicted in Figure 16.1.

In this context, a key issue is the correct assessment of the shear stress of the adhesive.

16.2.2 Shear strength

During the test, the adhesive ensures a progressive load transfer from inner adherend to the outer one. To be sure to measure the shear strength, it is important to check that the failure occurs within this adhesive. In this case, the failure is called a cohesive failure. If the cohesive failure occurs within one of the adherends, the shear strength of the adhesive cannot be evaluated. Finally the failure may occur at the interface between the

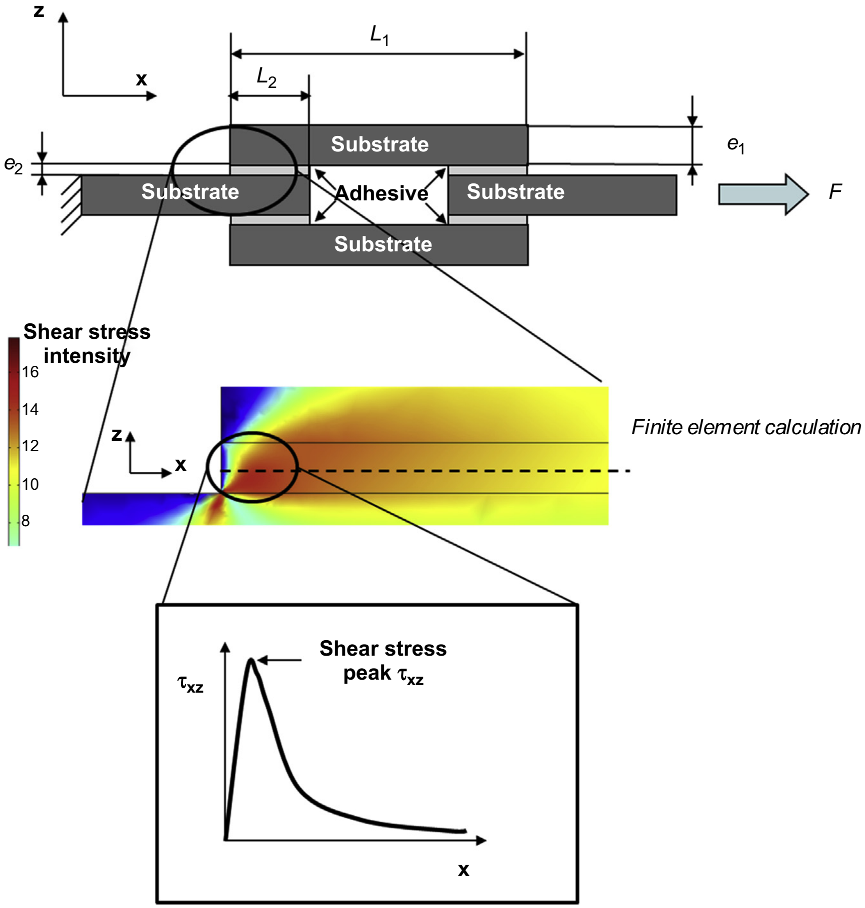

Figure 16.1 Example of shear of double-lap test: a shear stress peak occurs near the free edge yielding the failure of the specimen.

adhesive and the adherend. In this case, the failure is called adhesive failure. It clearly depends on the interface properties of the adherend (Figure 16.2).

Once the test has been performed, it is necessary to evaluate the shear strength from the experimental results. Standard methods (American Society for Testing and Materials (ASTM) D 5573-99 and ASTM D 1002) were developed for assessing the apparent shear strength (ASS) associated with the cohesive failure. ASS is defined as the average shear strength from which the specimen fails:

$$\mathrm{ASS} = F/(2A) \tag{16.1}$$

in which F is the applied force (N) when failure occurs and A the lap area (m^2). It is, however, well known that the ASS also depends on the thickness of the adhesive because the failure of the double-lap joint occurs near the free edge due to shear stress

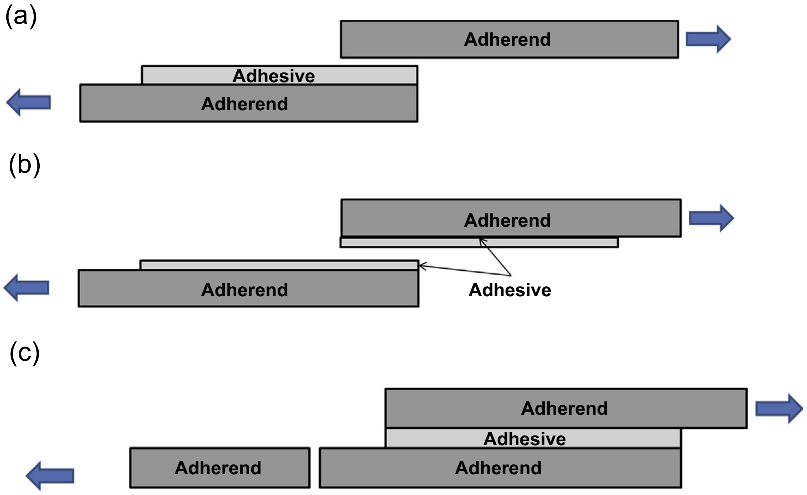

Figure 16.2 Different types of failure in the case of double-lap tests. (a) Adhesive failure (at the interface), (b) Cohesive failure within the adhesive layer, (c) Cohesive failure within the adherend layer.

concentration. Determining the stress distribution in bonded joints is a key issue in various industrial domains such as civil engineering and aeronautics (Adams and Wake, 1984; Baker and Jones, 1988). However, the shear stress in the adhesive depends on the thickness of the adhesive because of the shear stress peak occurring at the free ends (Mathias et al., 2006). Hence, this shear strength has meaning only if all the tested specimens have the same adhesive thickness. However, it was not possible to obtain the same thickness for all types of adhesives because significant changes in the viscosity were observed from one formulation to another (from nearly liquid to hydrogels). It was thus decided to consider this influence to compare consistent values of the shear strength for all adhesives. It is well known that the shear stress is not constant along a bonded joint (Volkersen, 1938). In particular, a shear stress peak occurs near the free boundaries. It is clear that this peak directly governs adhesive failure. This effect has, therefore, to be considered to correctly determine the shear strength, as proposed for instance in refined models (Chataigner et al., 2010; Mathias et al., 2006). The model proposed by Volkersen (1938) was used to account for this thickness variation in the strength calculation. With this model, the value of the shear stress peak is given by the following equations:

$$\tau(0) = \frac{G_2\sigma_0}{\sinh(\lambda L_2)e_2\lambda E_1}(1+\cosh(\lambda L_2)) \tag{16.2}$$

with

$$\lambda = \sqrt{\frac{2G_2}{e_2e_1E_1}} \tag{16.3}$$

in which σ_0 is the axial stress, equal to the ratio between the applied force F (N) and the cross-section S (m^2) of the adherend, e_2 (m) is the adhesive thickness. e_1 (m) is the thickness of the adherends, L_2 (m) is the lap length, and E_1 (Pa) is the Young's modulus of the adherends. G_2 (Pa) is the shear modulus of the adhesive: it must therefore be known if the shear strength is determined with Eqn (16.1). This model is sufficient for this first approach, although it does not, for example, consider some nonlinear phenomena.

16.2.3 Origin of adhesion

Many parameters affect the quality of bonding and therefore the value of the shear strength of the adhesive: it clearly depends on both the chemical and the mechanical properties of the bonding. In a mechanical point of view, the adhesive goes into small pores of the adherends. It depends on the ability of the adhesive to diffuse within the adherends before drying. Chemical bonding mechanism is essentially located at the interface at which primary and secondary chemical bonds may form. This chemical adhesion is more or less strong according to the nature of the chemical bonds (primary or secondary). However, it is well known that mainly two factors affect the quality of the bond: the wettability and the roughness.

The wettability is quantified by the interfacial tension between the adhesive and the adherend (Mittal, 1977). Indeed, the equilibrium of the different phases (e.g., air, adhesive, and adherend) depends on the interfacial tensions between the different phases (Figure 16.3(a)). Interfacial tensions are denoted as γ, and solid (for the adherend), liquid (for the adhesive), and gas (for the air) as s, l, and g, respectively. These interfacial tensions enable us to define the contact angle θ of the adhesive to the adherend in the presence of the air. Equilibrium phenomena allow assessment of the Young's equation (Eqn (16.4)):

$$\gamma_{lg} \cos\theta = \gamma_{sg} - \gamma_{sl} \tag{16.4}$$

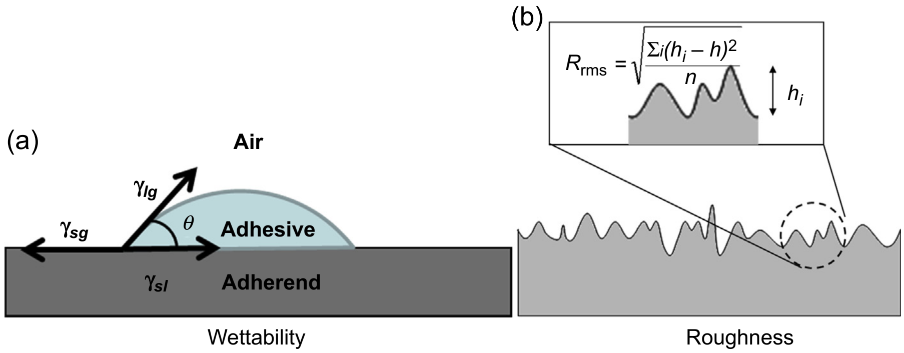

Figure 16.3 Adhesive–adherend interface: (a) wettability according to contact angle θ, (b) roughness of the adherend surface.

However, this equation is available in the "perfect" case, i.e., without any defect or other chemical molecules (surface must be clean). If the adhesive correctly wets the surface, it uniformly spreads in a thin film with a minimum of voids.

The roughness is linked to the "regularity" of the surface of the adherends. It contributes to the "mechanical" bonding between the adhesive and the adherends. A rough surface enables suitable conditions to ensure an efficient "anchorage," as shown in Figure 16.3(b). The roughness can be evaluated through the root mean square R_{rms} (see Figure 16.3(b)) value defined as:

$$R_{\mathrm{rms}} = \sqrt{\frac{\sum_i (h_i - h)^2}{n}} \tag{16.5}$$

in which h_i is the ith sampling point feature height value, h is the mean height value, and n is the number of data points. These sample points are measured using atomic force microscopy or indentation measurements (Kim et al., 2007).

16.2.4 Water resistance

Bioadhesives generally exhibit poor performance in terms of water resistance although adhesives are often used in cases in which moisture content affects their behavior. Assessing the shear strength of adhesives in such conditions is therefore essential. The main wet tests consist in immersing the specimen in water at different temperatures and during different periods. According to the temperature, the immersion time, and the resulting shear strength, each adhesive is classified according to ASTM standards. Note that water resistance of adhesive is associated with the nature of the adherend. For instance, the water resistance of bonded-wood specimens depends on the wood used. Each wood species exhibits its own moisture diffusion coefficient and moisture expansion coefficient of yielding. Microalgal proteins were recently used for improving the water resistance of plywood adhesive (*Acacia falcata*) (Roy et al., 2014). Chitosan-based adhesives were also tested. Umemura et al. (2010) found bond strength in wet conditions equal to 1.74 Mpa. Chitosan adhesives were also tested with glycerol and citric acid. This formulation was protected with oil coat yielding wet bond strength of 1.6 MPa, which is nearly 27% of its dry bond strength (Patel et al., 2013c). However, these values are difficult to compare: results clearly depend on the molecular weight of chitosan. Soy proteins were also studied for improving the water resistance, around 1–2 MPa (Liu and Li, 2007). Water resistance of bioadhesive has not been found competitive with the water resistance of synthetic adhesive and remains the main challenge of future developments.

16.2.5 Environmental impacts: life cycle assessment

Despite the natural origins of bioadhesive, it is important to assess the environmental impacts through a complete life cycle assessment (LCA), also referred to as "cradle to grave" analysis. Chemical processes are often used to purify the molecules and can provoke environmental or health impacts. The chemical substances responsible for these impacts are caustic soda and formic acid. It is also essential to consider agricultural production processing and feedstock. However, bio-based adhesives are expected to do less harm to the environment than synthetic adhesives. A recent study (McDevitt et al., 2014) reveals that such bioadhesives show a 22% lower cycle impact than the adhesive from petrochemical origin in fiberboard production. The midpoint method is generally used for the LCA: it calculates the impact through three categories: *human health*, *ecosystem quality*, and *resources*. Such an approach enables us to compare two products, in our case a bio-based adhesive and a synthetic adhesive. Bio-based adhesives are generally less impactive than synthetic adhesive except in *ecosystem quality* due to the impact on *land use*. It is mainly due to the fact that the bioadhesive comes from biological feedstock and the associated ecosystem degradation arises from that, whereas the petrochemical adhesive uses an extracted crude oil feedstock.

16.3 Bioadhesive species

Bioadhesives are natural polymers that act as adhesives. The term is sometimes used more loosely to describe glue formed synthetically from biological monomers such as sugars, or to mean a synthetic material designed to adhere to biological tissue. In these cases, the term bioinspired adhesive is more elegant.

Bioadhesives may consist of a variety of substances, but protein, tannin, and lignin derivatives and carbohydrates feature prominently for wood adhesive (Pizzi, 2006). Other adhesives found in nature are currently under investigation but not yet in widespread commercial use. For example, even if bioadhesives produced by barnacles and mussels have been found with excellent waterproof adhesive properties, their scale-up has proved difficult (Combie et al., 2004).

The biomass-based adhesives have been widely used throughout history. They have been replaced by petro-based adhesives during the last century because of their low bonding strengths and poor water resistances. Petro-based adhesives perform well, but their applications are restricted because they are based on nonrenewable raw materials (e.g., fossil fuel) and release toxic components (such as phenol and formaldehyde). Indeed, the development of environmentally friendly adhesives from renewable biomass, as a promising alternative to petro-based adhesives, has therefore attracted considerable attention in recent years. However, it is difficult to produce adhesives consisting of solely bio-based polymers, mostly due to their insufficient water resistance. Therefore, it might be necessary to add small amounts of additives derived from petroleum to obtain the necessary properties.

16.3.1 Bioadhesive polysaccharides

Polysaccharides are a chemically and structurally diverse class of natural products, some of which have adhesive properties (Patel et al., 2013b). Polysaccharides are biopolymers widely distributed in nature. Their occurrence is well documented in all organisms, *viz.* animals, plants, fungi, and bacteria. These are adequately implied in various biological functions such as storage of energy (starch), cell wall architecture (cellulose), and cellular communication (glycosaminoglycans). These macromolecules exhibit high molecular weight attaining sometimes several millions of Dalton. They are generally defined by the suffix “an” following the name of the sugar component for homopolysaccharide and/or by the same suffix, applied to define specificity of polymer (*viz.* curdlan for curdle, gellan for a bacterial gel-forming polysaccharide). All these polysaccharides can be homopolymers or heteropolymers of neutral sugars (pentoses and hexoses) or anionic sugars (hexoses). They may or may not be substituted by nonsugar compounds and attain linear or ramified final conformations. These features lead to exhibit specific behaviors in solutions correlated with different conformations such as spirals, sheets, or single, double, and triple helixes (Sutherland, 2007). The basic structural characteristics of polysaccharides for exhibiting adhesive properties mainly include high molecular weight and polar functional groups. The polysaccharides with polar and hydrogen bonding functional groups, *viz.* ethers, hydroxyls, and carboxylates, exhibit superior adhesion to wood and metals that are high surface energy adherends. The hydroxyl and carboxylate groups also serve as possible sites for chemical modification and cross-linking with the aim to improve adhesive property. These groups also support noncovalent inter- and intrachain interactions and promote adhesion. Note that the high molecular weight of these macromolecules improves their mechanical strength (Lazaridou et al., 2003). The most explored polysaccharides for adhesive development are starch, chitosan, pullulan, Arabic gum, and some bacterial exopolysaccharides. Figures 16.4 and 16.5 give some examples of chitosan uses for its adhesive properties.

Starch- and dextrin-based adhesives are almost exclusively water based and are widely used for bonding paper and cardboard. They are also popular as bookbinders’

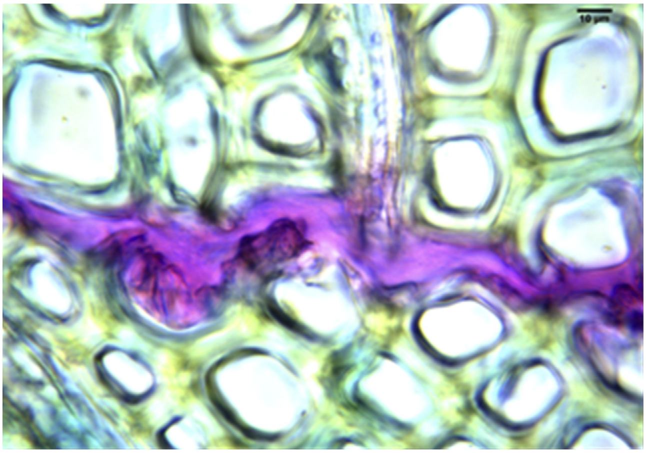

Figure 16.4 Pink-colored rhodamine-labeled chitosan layer adhering vertically both the left- and right-wood adherends.
From Patel et al. (2013c).

Figure 16.5 Composite chitosan/sunflower stalk used for designing thermal insulation panels for existing buildings.
Demether (2011).

adhesives. Starch used as adhesive on a large scale is dextrin based as it is more soluble in this form (Patel et al., 2013b). To limit the water solubility of starch adhesive, a bio-adhesive system based on solutions of chitosan and modified starch (oxidized maltodextrin) has been developed. Mixtures of these polysaccharides form either viscoelastic solutions or hydrogels, depending on various experimental parameters (chitosan concentration, starch degree of oxidation, molar ratio between amine and aldehyde functions, pH, etc.) (Serrero et al., 2011). Chitosan has been also used alone or in numerous polysaccharidic mixtures (with Konjac glucomannan, alginate, galactomannan such as guar) for its adhesive properties and also for its water resistance (Mati-Baouche et al., 2014a,b; Umemura et al., 2003). Indeed, this animal/fungal polysaccharide, which is the most abundant after cellulose, is the sole described cationic polysaccharide, which is due to its positive charges (NH_3^+) at acidic pH ($pH < 6.5$) (Barbosa et al., 2005). This cationic form is the sole in which chitosan is soluble. Starch has been also successfully modified to improve its adhesive properties. For example, starch and polyvinyl alcohol have been cross-linked with hexa(methoxymethyl)melamine, yielding an adhesive with promising results (Imam et al., 2001). Starch combined with tannins has also resulted in a wood adhesive with properties comparable to commercial wood adhesives, interesting for plywood applications (Moubarik et al., 2010). Furthermore, vinyl acetate has been grafted from starch using ammonium persulfate as initiator (Wang et al., 2011, 2012a) and further blended with silica nanoparticles (Wang et al., 2011) to improve bond strength and water resistance. Wheat flour, containing starch and proteins, has also been studied as a wood adhesive (D′amico et al., 2010). Numerous authors call into question the use of food resources as starch for energetic or material applications. In this context, as observed with second generation of biofuels, plant cell-wall derivatives could be an interesting alternative. The hemicellulose family is one of the most abundant classes of biopolymers present in hard wood and perennial plants such as grasses, cereals, and herbs. The most prevalently studied hemicellulose is xylan composed of a backbone of β-(1,4)-linked anhydroxylose units (Cunha and Gandini, 2010). Recently, xylan derivatives have gained increasing importance as new biopolymeric-based materials and functional polymers. In the pulp and milling industries, significant amounts of hemicelluloses and lignins are generated. Except combustion for energy recovery, they have not found real applications. Even xylan itself cannot be used as a wood adhesive due to its limited bonding performance, especially regarding water resistance. With the addition of dispersing agents, poly(vinyl alcohol) or poly(vinyl amine), and cross-linkers such as glyoxal or hexa(methoxymethyl) melamine, the xylan dispersions demonstrate promising results in the field of wood adhesives (Norström et al., 2014, 2015).

Seed gums are polysaccharides with a potential application in the adhesives area. Gum dispersions such as locust bean and guar gums (two galactomannans) and tamarind gum (a xyloglucan) are used in several types of adhesives such as pressure-sensitive tape, denture and medicinal adhesives, paper adhesives, pharmaceutical tablet binders, and label pastes (Conner, 1989). They show naturally interesting bond strength and heat resistance. Locust bean gum also exhibits very good water resistance. The bonding performance is comparable to a commercial poly(vinylacetate) D2 wood adhesive, and it is possible to perform the bonding with hot pressing as well as pressing at room temperature (Norström et al., 2014). In the same study, xanthan, a well-known anionic polysaccharide with a cellulosic backbone has been successfully tested as wood adhesive. Xanthan is a bacterial exopolysaccharide largely used in the food industry for its rheological properties. Bacterial exopolysaccharide synthesis is a prevalent and indispensible activity in many biological processes, including surface adhesion and biofilm formation. Adhesion of microorganisms to biological tissues is a challenge especially when the adhesive is in contact with physiological fluids. Microbial extracellular polysaccharides do not contain toxic compounds, and can be synthesized through fermentation of renewable resources including organic waste products. These microbiological products are also environmentally compatible and biodegradable. Moreover, efficient technology for large-scale production of microbial extracellular polysaccharides currently exists (Seviour et al., 2011). Except for xanthan, microbial polysaccharides that have been evaluated as commercial adhesives include pullulan (Prajapati et al., 2013), exopolysaccharide from periphytic marine bacteria (Labare et al., 1989), photocross-linkable dextran urethanes (Li et al., 2011), exopolysaccharide from *Bacillus megaterium* (Kumar and Shah, 2015), a microbial extracellular polysaccharide (MB adhesive) produced by a bacterium from the culture collection of Montana Biotech Corporation (Hagg et al., 2004), and others (Hagg et al., 2006). Some with successful results with dry bond strengths comparable to a poly(vinylacetate)-based adhesive (Haag et al., 2006).

16.3.2 Protein-based adhesives

Adhesives based on proteins have long been used to produce plywood, and their water resistances are better than those of carbohydrate-based adhesives (Frihart, 2010). As an example, casein has been used for more than a century (Pizzi and Lambuth, 1994). Another protein that has obtained significant interest in this context is wheat gluten. Wheat gluten (WG) is a by-product from starch production and is at present mainly used in the bakery industry and as animal feed. Wheat gluten is an elastomeric protein that possesses unique viscoelastic and cohesive properties, making it suitable for material applications, such as wood adhesives (Nordqvist et al., 2012).

Gelatin, a water-soluble natural protein derived from collagen, has become one of the most investigated materials for tissue adhesives due to its suitable natural properties. Gelatin is considered biocompatible, biodegradable, and nonimmunogenic (Kuijpers et al., 1999). Despite its promising qualities, the mechanical strength of physically cross-linked gelatin adhesives is not sufficient as an adhering substance on its own (Bae et al., 2002). A chemical cross-linking agent and a polymeric additive (with suitable available functional groups for the cross-linking reaction) were therefore usually added to the solution in a wide range of published attempts and notably in the field of soft-tissue adhesion (Otani et al., 1996; Bae et al., 2002; Matsuda et al., 1999). In the same way, novel tissue adhesives based on a combination of gelatin with an alginate polymeric additive and cross-linked by carbodiimide have recently been developed and studied (Cohen et al., 2013). Other adhesive formulations with gelatins but without cross-linking agents are possible as, for example, a two-component tissue adhesive based on oxidized urethane dextran and gelatin prepared and photocross-linked under ultraviolet irradiation (Wang et al., 2012b).

Marine adhesive proteins secreted from invertebrates, such as mussels and barnacles, insolubilize and adhere to the surfaces of a variety of substrates. These adhesive properties have been partially explained by the amino acid sequences of these proteins, as in the case of biological adhesion of sperm cells from a goby fish on a glass plate that exhibited marked adhesion activity due to the Lys residues in the precoated marine adhesive proteins (Yamamoto et al., 1999).

Soy protein is a plant protein with many potential applications due to its relatively low cost, wide availability, and complete biodegradability. Soy proteins have been used in many industrial products such as adhesive for wood and paper binders in coatings and paints and as emulsifiers in colloidal rubber products (Kumar et al., 2002). The adhesive performance of soybean proteins is dependent upon the particle size, nature of the surface, structure of the protein, its viscosity, and pH (Lambuth, 1977). Other factors that can affect their performance are the processing parameters (press temperature, pressure, and time) used to obtain them. Improvement of the adhesive properties of soy protein is possible by altering its molecular structure or conformation through physical, chemical, or enzymatic agents and has been well documented in the literature (Kumar et al., 2002). As described for gelatin, the potentialities of soy protein as adhesive have been increased after blending them with other proteins such as casein but also poly(vinyl acetate) or poly(vinyl alcohol) (Kumar et al., 2002).

16.3.3 Phenolic-acids based adhesives

The most common adhesives used in the plywood industry are phenol—formaldehyde (PF), urea—formaldehyde (UF), and melamine—urea—formaldehyde (MUF) adhesives (Danielson and Simonson, 1988; Olivares et al., 1988). Particularly, PF adhesive is more widely used due to its high weather and water resistance. However, rapidly rising oil prices have increased the cost of petrochemicals, and the high price of phenols has been the main reason for the restriction of PF adhesive for broad applications. Therefore, several attempts have been made to replace phenol by lignin (Khan et al., 2004) or tannin (Hong et al., 2011) based on the structural similarity. Lignin is an amorphous, polyphenolic material derived from three phenylpropanoid monomers: coniferyl, sinapyl, and *p*-coumaryl alcohols. These structures are linked by a multitude of interunit bonds that include several types of ether (β—O—4, α—O—4, 4—O—5) and carbon–carbon linkages. Lignin is a highly branched, three-dimensional polymer with a wide variety of functional groups providing active centers for chemical and biological modifications (Dence and Lin, 1992). In nature, lignin is covalently associated with hemicellulose and serves as cement to bond together cellulose fibers in woods. It also serves as a waterproofing and antimicrobial agent. The conventional technical lignin is the by-product of the pulping industry and the lignocellulosic biorefinery. The lignin from the pulping industry has drawbacks for adhesive developments as during the process many hydroxyl functions are oxidized by strong conditions (alkaline treatment and high temperatures). On the contrary, the lignocellulosic residue from the biorefinery of wood is rich in highly activated lignin. It can condense with phenol and formaldehyde under alkaline conditions (Maity, 2015). The lignin and phenol can undergo hydroxymethylation by reacting with excess formaldehyde in the presence of NaOH as catalyst, and the hydroxymethyl lignin and the PF prepolymer can then copolymerize to produce a lignin–phenol–formaldehyde copolymer to combine phenolic and lignin parts (Ibrahim et al., 2011; Zhang et al., 2013). It was found that the phenol could be replaced by lignocellulosic residue from the biorefinery of wood for 50% at most in PF adhesives. The performance of plywood bonded by these adhesives met the requirement of exterior grade according to the Chinese National Standard (Zhang et al., 2013). Several investigations have been targeted toward using lignin in formulation of formaldehyde-free wood adhesives (Li and Geng, 2005). However, the presence of abundant methyl groups makes lignin less reactive and poor in cross-linking (Okamoto et al., 1996). The reactivity of lignin can be improved by demethylating the lignin aromatic rings. Demethylation can be achieved chemically (Liu and Li, 2006) or enzymatically using laccase (a milder, cleaner, and safer treatment) (Ibrahim et al., 2011), and the activated lignin can react with molecules bearing nucleophilic groups to form cross-linked complexes. Therefore, laccase-treated and reduced lignin–soy protein adhesive exhibited more than half the strength of commercial polyurethane adhesive and retained 70% of its initial strength after two cycles of 1 h boiling and drying (Ibrahim et al., 2013).

16.4 Discussion and conclusions

16.4.1 "Mixed" adhesives: conciliating bio- and synthetic adhesives

The development of bioadhesives has slowed because of the mechanical properties, especially water resistance, that confer a disadvantage in many applications. A first step to improve these properties will rely on the development of mixed adhesives. A mixed adhesive is an adhesive exhibiting both bio-based compounds and synthetic compounds. Environmental and health impacts of synthetic adhesives can be reduced by exchanging a part of toxic compounds by bio-based compounds, whereas the mechanical behavior is slightly altered. This is the case of formaldehyde adhesives from which a more or lesser amount of synthetic compounds have been replaced by hydrolyzable tannins (Spina et al., 2013) or more recently by wheat protein (Lagel et al., 2015) to reduce formaldehyde emissions. The main studies have focused on the emission of formaldehyde, but we must be aware of the presence of other aldehydes (such as phenol or cyanate-based molecules). Another issue, seldom addressed in the literature, is the direct formulation of mixed adhesive: most studies deal with the replacement of toxic compounds in existing synthetic adhesives but few studies were carried out on the formulation of new mixed adhesives.

16.4.2 Market evolution

The global bioadhesive market is surging mainly due to the evolution of techniques and knowledge. Moreover, people are aware of the benefits involved by bioadhesives both in environmental and health terms. It makes the bioadhesives increasingly popular. The global bioadhesive market has been estimated at $3 billion in 2013 [marketsandmarkets.com] and is expected to reach $6 billion in 2019. The main market regions of bioadhesives are located in Europe, North America, and Asia–Pacific, which exhibit a high potential for development. The market evolution closely depends on both research advances and legislation. Research advances offer new possibilities of development of bioadhesives by providing new molecular extraction from biomass or new chemical formulation. In the same way, governments play a crucial role for the development of both the bioadhesive market and the associated technologies. Legislation may lead in accelerating the transition from synthetic adhesive to bioadhesive by regulating the presence of VOCs and the presence of recyclable materials, especially in the building industries, the main objective being the reduction of the emission of VOCs while keeping suitable mechanical properties for structural applications that require high mechanical strength.

16.4.3 Future trends

New generations of bio-based adhesives are progressing because of high concern to avoid environmental and health impacts and our dependence on depleting petroleum resources. The future of the development of bio-based adhesives relies on the capacity to improve some specific properties (such as wet strength) and on how they can be associated with synthetic adhesives. A new generation of bio-based adhesives is also under development: bio-inspired adhesives. Bio-inspired adhesives (Brubaker and Messersmith, 2012) are based on bioadhesives that can be found in nature. Among these bio-inspired adhesives, the main efforts have been done on the development of mussel-mimetic adhesives (Lee et al., 2011). We can also cite adhesives based on the mimetic of gecko, bacteria, frog, etc. However, these developments need to combine knowledge of chemical, biological, and engineering processes. These bio-inspired adhesives can be formulated with other compounds (bio-based or synthetic ones) for improving their properties. It will constitute a new and promising way for the development of the new generation of environmentally friendly and health-friendly adhesives especially for building applications that constitute the largest market area for adhesives.

References

Adams, R.D., Wake, W.C., 1984. Structural Adhesive Joints in Engineering. Elsevier.

Bae, S.K., Sung, T.H., Kim, J.D., 2002. A soft-tissue gelatin bioadhesive reinforced with a proteinoid. Journal of Adhesive Science and Technology 16, 361−372.

Baker, A.A., Jones, R., 1988. Bonded Repair of Aircraft Structures. Martinus Nijhoff Publishers.

Barbosa, M.A., Granja, P.L., Barrias, C.C., Amaral, I.F., 2005. Polysaccharides as scaf folds for bone regeneration. ITBM-RBM 26, 212−217.

Brubaker, C.E., Messersmith, P.B., 2012. The present and future of biologically inspired adhesive interfaces and materials. Langmuir 28 (4), 2200−2205.

Cârciumaru, M., Ion, R.M., Niţu, E.C., Ştefănescu, R., 2012. New evidence of adhesive as hafting material on middle and upper palaeolithic artefacts from Gura Cheii-Râşnov Cave (Romania). Journal of Archaeological Science 39 (7), 1942−1950.

Chataigner, S., Caron, J.F., Diaz-Diaz, A., Aubagnac, C., Benzarti, K., 2010. International Journal of Adhesion and Adhesives 2010 (30), 10.

Cohen, B., Pinkas, O., Foox, M., Zilberman, M., 2013. Gelatin-alginate novel tissue adhesives and their formulation-strength effect. Acta Biomaterialia 9, 9004−9011.

Combie, J., Steel, A., Sweitzer, R., 2004. Adhesive designed by nature (and tested at redstone arsenal). Clean Technology Environmental Policy 6, 258−262.

Conner, A.H., 1989. Carbohydrates in adhesives. Introduction and historical perspective. ACS Symposium Series 385, 271−288.

Cunha, A., Gandini, A., 2010. Turning polysaccharides into hydrophobic materials: a critical review. Part 2. Hemicelluloses, chitin/chitosan, starch, pectin and alginates. Cellulose 17, 1045−1065.

D'amico, S., Hrabalova, M., Mueller, U., Berghofer, E., 2010. Bonding of spruce wood with wheat flour glue − effect of press temperature on the adhesive bond strength. Industrial Crops and Products 31, 255−260.

Danielson, B., Simonson, R., 1988. Kraft lignin in phenol formaldehyde resin. Part 2. Evaluation of an industrial trial. Journal of Adhesion Science and Technology 12 (9), 941−946.

Demether, 2011. Development of Biomaterials from Agricultural Byproducts for the Thermal Insulation of Existing Buildings. French national project granted by the French National Research Agency (anr-10-ecot- 004 grant). http://demether.cemagref.fr.

Dence, C.W., Lin, S.Y., 1992. Introduction. In: Dence, C.W., Lin, S.Y. (Eds.), Methods in Lignin Chemistry. Springer-Verlag, Berlin, pp. 3−19.

Frihart, C.R., 2010. Soy Protein Adhesives, McGraw-Hill Yearbook of Science &Technology. The Mc Graw-Hill Companies, Inc., New York, pp. 354−356.

Haag, A.P., Geesey, G.G., Mittleman, M.W., 2006. Bacterially derived wood adhesive. International Journal of Adhesion and Adhesives 26, 177−183.

Haag, A.P., Maier, R.M., Combie, J., Geesey, G.G., 2004. Bacterially derived biopolymers as wood adhesives. International Journal of Adhesion and Adhesives 24, 495−502.

Hoong, Y.B., Paridah, M.T., Loh, Y.F., Jalaluddin, H., Chuah, L.A., 2011. A new source of natural adhesive: *Acacia mangium* bark extracts co-polymerized with phenol−formaldehyde (PF) for bonding Mempisang (*Annonaceae* spp.) veneers. International Journal of Adhesion and Adhesives 31, 164−167.

Ibrahim, M.N., Zakaria, N., Sipaut, C.S., Sulaiman, O., Hashim, R., 2011. Chemical and thermal properties of lignins from oil palm biomass as a substitute for phenol in a phenol formaldehyde resin production. Carbohydrate Polymers 86, 112−119.

Ibrahim, M.N., Mamo, G., Gustafsson, P.J., Hatti-Kaul, R., 2013. Production and properties of adhesives formulated from laccase modified Kraft lignin. Industrial Crops and Products 45, 343−348.

Imam, S.H., Gordon, S.H., Mao, L., Chen, L., 2001. Environmentally friendly wood adhesive from a renewable plant polymer: characteristics and optimization. Polymer Degradration and Stability 73, 529−533.

Khan, M.A., Ashraf, S.M., Malhotra, V.P., 2004. Development and characterization of a wood adhesive using bagasse lignin. International Journal of Adhesion and Adhesives 24, 485−493.

Kim, J.Y., Kang, S.K., Lee, J.J., Jang, J.I., Lee, Y.H., Kwon, D., 2007. Influence of surface-roughness on indentation size effect. Acta Materialia 55, 3555−3562.

Kuijpers, A.J., Engbers, G.H.M., Feijen, J., De Smedt, S.C., Meyvis, T.K.L., Demeester, J., Krijgsveld, J., Zaat, S.A.J., Dankert, J., 1999. Characterization of the network structure of carbodiimide cross-linked gelatin gels. Macromolecules 32, 3325−3333.

Kumar, R., Choudhary, V., Mishra, S., Varma, I.K., Mattiason, B., 2002. Adhesives and plastics based on soy protein products. Industrial Crops and Products 16, 155−172.

Kumar, S., Shah, A.K., 2015. Characterization of an adhesive molecule from *Bacillus megaterium*. Carbohydrate Polymers 117, 543−548.

Labare, M.P., Guthrie, K., Weiner, R.M., 1989. Polysaccharide exopolymer adhesives from periphytic marine bacteria. Journal of Adhesion Science and Technology 3, 213−223.

Lagel, M.C., Pizzi, A., Redl, A., Al-Marzouki, F.M., 2015. Phenol-wheat protein-formaldehyde thermoset wood adhesives. European Journal of Wood and Wood Products 1−10.

Lambuth, A.L., 1977. Blood glues-Chapter 11, Soybean Glues-Chapter 10. In Handbook of Adhesives. In: Skeist, I. (Ed.), 2nd ed. Van Nostrand Reinhold Co., New-York.

Lazaridou, A., Biliaderis, C.G., Kontogiorgos, V., 2003. Molecular weight effects on solution rheology of pullulan and mechanical properties of films. Carbohydrate Polymers 52, 151−166.

Lee, B.P., Messersmith, P.B., Israelachvili, J.N., Waite, J.H., 2011. Mussel-inspired adhesives and coatings. Annual Review of Materials Research 41, 99−132.

Li, H., Niu, R., Yang, J., Nie, J., 2011. Photocrosslinkable tissue adhesive based on dextran. Carbohydrate Polymers 86, 1578−1585.

Li, K.C., Geng, X.L., 2005. Formaldehyde-free wood adhesives from decayed wood. Macromolecular Rapid Communication 26, 529−532.

Liu, Y., Li, K., 2006. Preparation and characterization of demethylated lignin−polyethylenimine adhesives. Journal of Adhesion 82, 593−605.

Liu, Y., Li, K., 2007. Development and characterization of adhesives from soy protein for bonding wood. International Journal of Adhesion and Adhesives 27 (1), 59−67.

Maity, S.K., 2015. Opportunities, recent trends and challenges of integrated biorefinery: Part 1. Renewable and Sustainable Energy Reviews 43, 1427−1445.

Mathias, J.D., Grédiac, M., Balandraud, X., 2006. On the bidirectional stress distribution in rectangular bonded composite patches. International Journal of Solids and Structures 43 (22−23), 6921−6947.

Mati-Baouche, N., Elchinger, P.H., De-Baynast, H., Pierre, G., Delattre, C., Michaud, P., 2014a. Chitosan as an adhesive. European Polymer Journal 60, 198−212.

Mati-Baouche, N., De Baynast, H., Lebert, A., Sun, S., Lopez-Mingo, C.J.S., Leclaire, P., Michaud, P., 2014b. Mechanical, thermal and acoustical characterizations of an insulating bio-based composite made from sunflower stalks particles and chitosan. Industrial Crops and Products 58, 244−250.

Matsuda, S., Iwata, H., Se, N., Ikada, Y., 1999. Bioadhesion of gelatin films crosslinked with glutaraldehyde. Journal of Biomedical Materials Research 45, 20−27.

McDevitt, J.E., Warren, J., Grigsby, J., 2014. Life cycle assessment of bio- and petro-chemical adhesives used in fiberboard production. Journal of Polymers and Environment 22, 537−544.

Mittal, K.L., 1977. The role of the interface in adhesion phenomena. Polymer Engineering and Science 17, 467−473.

Moubarik, A., Charrier, B., Allal, A., Charrier, F., Pizzi, A., 2010. Development and optimization of a new formaldehyde-free corn starch and tannin wood adhesive. European Journal of Wood and Wood Products 68, 167−177.

Nordqvist, P., Lawther, M., Malmström, E., Khabbaz, F., 2012. Adhesive properties of wheat gluten after enzymatic hydrolysis or heat treatment − a comparative study. Industrial Crops and Products 38, 139−145.

Norström, E., Fogelström, L., Nordqvist, P., Khabbaz, F., Malmström, E., 2014. Gum dispersions as environmentally friendly wood adhesives. Industrial Crops and Products 52, 736−744.

Norström, E., Fogelström, L., Nordqvist, P., Khabbaz, F., Malmström, E. Xylan, June 2015. A green binder for wood adhesives. European Polymer Journal 67, 483−493.

Oilvares, M., Guzman, J.A., Natho, A., Saavedra, A., Santiago, C., 1988. Kraft lignin utilization in adhesives. Wood Science and Technology 22, 157−165.

Okamoto, T., Takeda, H., Funabiki, T., Takatani, M., Hamada, R., 1996. Fundamental studies on the development of lignin-based adhesives 1. Catalytic demethylation of anisole with molecular oxygen. Reaction and Kinetic Catalysis Letters 58, 237−242.

Otani, Y., Tabata, Y., Ikada, Y., 1996. Rapidly curable biological glue composed of gelatin and poly (-glutamic acid). Biomaterials 17, 1387−1391.

Patel, A.K., Michaud, P., De Baynast, H., Grédiac, M., Mathias, J.-D., 2013a. Preparation of chitosan-based adhesives and assessment of their mechanical properties. Journal of Applied Polymer Science 127 (5), 3869−3876.

Patel, A.K., Mathias, J.D., Michaud, P., 2013b. Recent advances and perspectives of polysaccharides as adhesives. Reviews of Adhesion and Adhesives 1 (3), 312−343.

Patel, A.K., Michaud, P., Petit, E., de Baynast, H., Grédiac, M., Mathias, J.D., 2013c. Properties of chitosan-based adhesive improved by glycerol. Application to wood bonding. Journal of Applied Polymer Science 127, 5014−5021.

Pizzi, A., 2006. Recent developments in eco-efficient bio-based adhesives for wood bonding: opportunities and issues. Journal of Adhesion Science and Technology 20, 829−846.

Pizzi, A.M., Lambuth, A.L., 1994. Handbook of Adhesive Technology. Marcel Dekker, New York, p. 259.

Prajati, V.D., Jani, G.K., Khanda, S.M., 2013. Pullulan: an exopolysaccharide and its various applications. Carbohydrate Polymers 95 (1), 540−549.

Roy, J.J., Sun, L., Ji, L., 2014. Microalgal proteins: a new source of raw material for production of plywood adhesive. Journal of Applied Phycology 26 (3), 1415−1422.

Serrero, A., Trombotto, S., Bayon, Y., Gravagna, P., Montanari, S., David, L., 2011. Polysaccharide-based adhesive for biomedical applications: correlation between rheological behavior and adhesion. Biomacromolecules 12, 1556−1566.

Seviour, R.J., McNeil, B., Fazenda, M.L., Harvey, L.M., 2011. Operating bioreactors for microbial exopolysaccharide production. Critical Reviews in Biotechnology 31, 170−185.

Spina, S., Zhou, X., Segovia, C., Pizzi, A., Romagnoli, M., Giovando, S., Pasch, H., Rode, K., Delmotte, L., 2013. Phenolic resin adhesives based on chestnut (*Castanea sativa*) hydrolysable tannins. Journal of Adhesion Science and Technology 27 (18−19), 2103−2111.

Sutherland, I.W., 2007. Bacterial exopolysaccharides. In: Kamerling, J.P. (Ed.), Comprehensive glycoscience. Elsevier, Amsterdam.

Umemura, K., Inoue, A., Kawai, S., 2003. Development of new natural polymer-based wood adhesives I: dry bond strength and water resistance of konjac glucomannan, chitosan, and their composites. Journal of Wood Science 49, 221−226.

Umemura, K., Mihara, A., Kawai, S.J., 2010. Journal of Wood Science 56, 387.

Volkersen, O., 1938. Luftfahrtforschung 15, 41.

Wadley, L., Williamson, B., Lombard, M., 2004. Ochre in hafting in middle stone age southern Africa: a practical role. Antiquity 78 (301), 661−675.

Wang, Z., Gu, Z., Hong, Y., Cheng, L., Li, Z., 2011. Bonding strength and water resistance of starch-based wood adhesive improved by silica nanoparticles. Carbohydrate Polymers 86, 72−76.

Wang, Z., Li, Z., Gu, Z., Hong, Y., Cheng, L., 2012a. Preparation, characterization and properties of starch-based wood adhesive. Carbohydrate Polymers 88, 699−706.

Wang, T., Nie, J., Yang, D., 2012b. Dextran and gelatin based photocrosslinkable tissue adhesive. Carbohydrate Polymers 90, 1428−1436.

Yamamoto, H., Nishida, A., Ohkawa, K., 1999. Wettability and adhesion of marine and related adhesive proteins. Colloids and surface A 149, 553−559.

Zhang, W., Ma, Y., Xu, Y., Wang, C., Chu, F., 2013. Lignocellulosic ethanol residue-based lignin-phenol-formaldehyde resin adhesive. International Journal of Adhesion and Adhesives 40, 11−18.

Biopolymers as biofilters and biobarriers

17

M.A. Ashraf[1,2,3], *S. Batool*[1], *M. Ahmad*[4], *M. Sarfraz*[5], *W.S.A.W.M. Noor*[6]
[1]University of Malaya, Kuala Lumpur, Malaysia; [2]Centre for Research in Biotechnology for Agriculture (CEBAR), University of Malaya, Kuala Lumpur, Malaysia; [3]Universiti Malaysia Sabah, Kota Kinabalu, Sabah, Malaysia; [4]Quaid-i-Azam University, Islamabad, Pakistan; [5]Institute of Pharmacy, Physiology & Pharmacology, University of Agriculture, Faisalabad, Pakistan; [6]School of Biosciences and Biotechnology, Faculty of Science and Technology, National University Malaysia (UKM), Bangi, Selangor, Malaysia

17.1 Introduction

Water treatment elements play an important role in public health and environmental quality. They are exploited to reduce contaminants in industrial wastewater, to eradicate toxins from municipal sanitary sewers, and to recover the quality of our raw drinking water. Generally, dozens of water treatment elements have been utilized; most of them are inorganic compounds or organic polymers such as alum (aluminum sulfate), ferric chloride, and polyacrylamides. Each of these polymers has benefits and drawbacks when their applicability and contaminant remediation efficacy is considered (Ashraf et al., 2013b). Comparatively, biopolymers illustrate greater performance where so many synthetic polymers are incapable. A biopolymer is a "polymer of natural origin" and can include such diverse materials as wood, cellulose, chitosan, and chitin (Chiellini et al., 2001). Biopolymers can work as a substance for enzyme and cell entrapment owing to their exceptional characteristics, such as nontoxicity, biocompatibility, mucus adhesion, and biodegradation (Krastanov and Yoshida, 2003). Cellulose, chitosan, and chitin are versatile polymers with applications in various types of biofilters for effluent treatment.

The social and health issues related to odors from waste management facilities has led to the implementation of particular biofiltration systems, which use microbes to break down putrid complexes to less putrid complexes. To decrease the prolonged startup procedure of a biofilter, such systems are often seeded with microbes of interest to expedite quick biofilm development. These microbes can be immobilized by trap within three-dimensional polymer mediums, such as alginate beads (Figure 17.1) (Low et al., 2014). The type of support matrix applied for anoxic biomass immobilization can disturb the effectiveness of a bioreactor; meanwhile, the number of cells sticking to the matrix may fluctuate from one medium to another. Quite a lot of natural substances (agar, agarose, collagen, alginates, and chitosan) have been utilized for the immobilization (Fang et al., 2004). These

Biopolymers and Biotech Admixtures for Eco-Efficient Construction Materials. http://dx.doi.org/10.1016/B978-0-08-100214-8.00017-8
Copyright © 2016 Elsevier Ltd. All rights reserved.

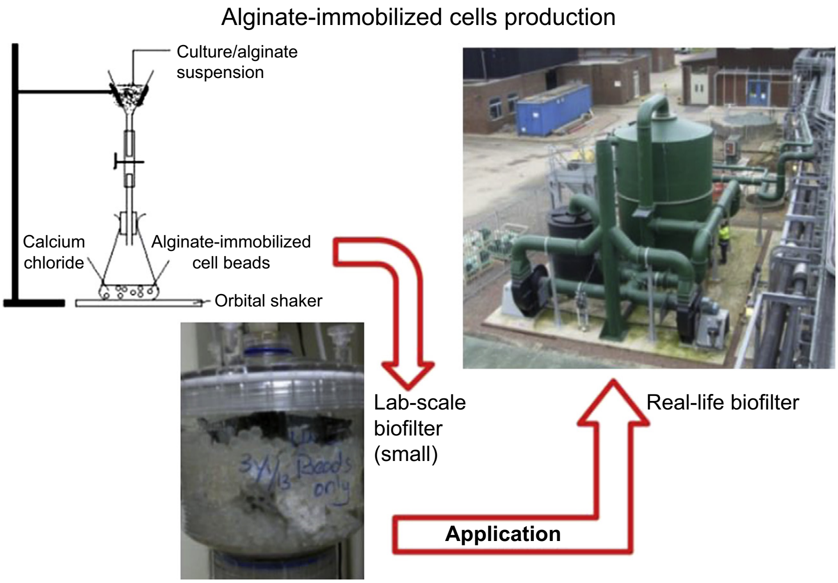

Figure 17.1 Seeding biofiltration system using alginate bead-immobilized cells (Low et al., 2014).

matrixes are accessible, easily applied, economically feasible, less harmful, and constancy (Rezaee et al., 2005; Son et al., 2003).

A permeable reactive barrier has been implemented for several organic complexes, both at the laboratory scale and full scale. Miller et al. (2001) also reported a full-scale biobarrier system that attained a treatment efficacy of more than 99.9% for dissolved benzene–toluene–ethylene–xylene (BTEX). Among several types of matrixes for employment in permeable reactive barriers, solid organic substances, such as organic mulch and peat moss, have normally been applied in bioremediation and bioretention systems to enhance the proficiency of the permeable reactive biobarriers (Yerushalmi et al., 1999). Organic mulch has many biopolymers; among them, lignin is recognized to have good efficiency and sorption capability for nonionic organic complexes (Garbarini and Lion, 1986); it can perform as complex additive fertilizer for hydrocarbon degradation as well (Kastner and Mahro, 1996). Nevertheless, besides the sorption capability of supporting substances in the biobarrier, microbial activity and biofilm development play significant roles in the working efficiency of the permeable reactive biobarrier.

The biofilter treated with immobilized nitrifying bacteria cells (INBC) can be used to remediate nitrogen oxides (NO_x) in low levels. The investigations revealed that immobilized nitrifying bacteria using sodium alginate and poly(vinyl alcohol) as trapped matrixes removed the NO_x up to 80.8%; at pH 7.3, sprinkling amount 0.0906 L/h, and empty bed residence time (EBRT) of 29.3 s. The microbial cellulose (MC) presented the high competence of the system for denitrification under different running conditions (Hussin et al., 2013). The attained biological denitrification of the artificial effluent was 100% at minimum hydraulic residence time (i.e., within 4 h) and maximum nitrate level (200 mg NO_3^--N/L). The bacterial immobilization on MC enhanced the adsorption efficiency, reduced the cell leakage from the beads, led to the maximum efficiency of the immobilized cells, and endorsed improved functioning control configuration (Rezaee et al., 2008a).

Chitin and chitosan have also been utilized with high efficiency for the remediation of pollutants from effluent of a petroleum refinery industry (Ashraf et al., 2012a). The chitin and chitosan showed an adsorption capacity of 1.96 and 1.26 mg/g, respectively. Similarly, chitin used in a fixed-bed reactor revealed the highest reduction of phenol, around 70–80% (flow rate: 1.5 mL/min, bed height: 18.5 cm, and 30 mg/L of phenol). For the chemical oxygen demand (COD) and oil and grease in wastewater, chitin and chitosan used in a fixed-bed system reduced around 52/92% and 65/67%, respectively. These outcomes illustrate the upgrading of the wastewater quality after treatment with chitin and chitosan (Milhome et al., 2009). Biopolymers offer a biodegradable alternative in biofiltration systems and are gaining popularity as an odor control system with the modernization of biotechnology (Nanda et al., 2011). Table 17.1 provides examples of effluents treated by biofilters using biopolymers.

Table 17.1 Examples of effluents treated by biofiltration using biopolymers (Renault et al., 2009)

Effluent	References
Ink-containing effluent	Roussy et al. (2005)
Food, seafood, and fish processing wastes	Savant and Torres (2000)
Wastewater from milk processing plants	Chi and Cheng (2006)
Brackish water	Divakaran and Pillai (2002)
Partially purified sewage	Zeng et al. (2008)
Effluent containing phenol derivatives	Wada et al. (1995)
Effluent containing metal ions	Wu et al. (2008)
Aquaculture wastewater	Chung (2006)
Oil-in-water emulsions	Bratskaya et al. (2006)
Olive oil wastewater	Meyssami and Kasaeian (2005)
Pulp and paper mill wastewater	Rodrigues et al. (2008)
Effluents containing dyes	Guibal and Roussy (2007)
Effluents containing humic substances	Bratskaya et al. (2004)
Bacterial suspensions	Strand et al. (2003)
Inorganic suspensions (bentonite, kaolinite)	Roussy et al. (2005)
Surimi wash water	Wibowo et al. (2007)
Brewery wastewater	Cheng et al. (2005)
Raw drinking water	Rizzo et al. (2008)

17.2 Mechanism

17.2.1 Mechanisms for biofiltration

A number of mechanisms, such as polymer bridging, polymer adsorption, charge neutralization (including electrostatic patch effects), coagulation/flocculation, and adsorption, have been suggested to describe the destabilization of colloids and suspensions by polymers.

17.2.1.1 Electrostatic patch

Chitosan is a weak base and its dissociation equilibrium is described by Eqn (17.1).

$$\text{Chitosan} - \text{NH}_3{}^+ + \text{H}_2\text{O} \leftrightarrows \text{Chitosan} - \text{NH}_2 + \text{H}_3\text{O}^+ \tag{17.1}$$

Its dissociation equilibrium constant is shown in Eqn (17.2).

$$K_\text{a} = \frac{[\text{Chitosan} - \text{NH}_2][\text{H}_3\text{O}^+]}{\left[\text{Chitosan} - \text{NH}_3{}^+\right]} \tag{17.2}$$

Protonation of amine functions is controlled by the pKa value of chitosan in acid solutions, and it is regulated by the charge density and extent of deacetylation (Guibal, 2004). Sorlier et al. (2001) detected that the pKa fluctuates directly with the deacetylation extent between 6.3 and 7.2 at complete dissociation. This feature is very imperative for an understanding of the electrostatic interactions of chitosan with cations and anions. Equation (17.1) considers the effect of pH on the generation of $-\text{NH}_3{}^+$ groups. The protonation of amino groups is high and the efficacy to adsorb metal anions is raised (Ashraf et al., 2012b). The most favorable pH is recurrently detected at about 2—4. This electrostatic attraction may take place by direct interference with free metal anions. This characteristic has been utilized for gelation of chitosan. Around 50% of the entire amino group persists protonated at neutral pH (Guibal, 2004). As the pH increases, the overall number of protonated amino groups decline by increasing the pH level, and they become accessible for the removal of metallic cations.

17.2.1.2 Adsorption

Adsorption is a phenomenon where one or more constituents (adsorbates) are attracted and bonded to the surface of a solid (adsorbent) with which they are in interaction. It is a surface phenomenon with common mechanism for organic and inorganic pollutant removal. The characteristics of the species involved contributes to the exact type of bonding (ionic, covalent, or metallic); however, the adsorbed particles are normally categorized as revealing physisorption (characteristic of weak van der Waals forces), chemisorption (characteristic of covalent bonding), or electrostatic sorption (Ashraf et al., 2013a) (Table 17.2). When a solution having absorbable solute comes into interaction with a solid with a highly porous surface

Table 17.2 **Common features of physisorption and chemisorption (Benavente, 2008)**

Physisorption	Chemisorption
• Low heat of adsorption (<2 or 3 times the latent heat of evaporation)	• High heat of adsorption (>2 or 3 times the latent heat of evaporation)
• Relatively low temperature, always under the critical temperature of the adsorbate	• High temperatures
• Nonspecific	• Type of interaction: strong covalent bond between adsorbate and surface
• Adsorption takes place in monolayer or multilayer	• Adsorption takes place only in a monolayer
• No dissociation of adsorbed species	• High activation energy
• Rapid, nonactivated, reversible	• Increase in electron density in the adsorbent–adsorbate interface
• Low activation energy	• Reversible only at high temperature
• No electron transfer, although polarization of sorbate may occur	

structure, liquid–solid intermolecular forces of attraction cause some of the solute molecules from the solution to be concentrated or deposited at the solid surface. This formation of an adsorbed phase containing a configuration different from that of the bulk fluid phase generates the basis of isolation by adsorption technology (Benavente, 2008).

As the adsorption proceeds, an equilibrium of adsorption of the solute between the solution and adsorbent is achieved (where the adsorption of solute from the bulk onto the adsorbent is minimum). The adsorbate concentration (qe, mmol/g) at the equilibrium step can be calculated according to Eqn (17.3):

$$\mathrm{qe} = V(\mathrm{Co} - \mathrm{Ce})/M \tag{17.3}$$

where V represents the solution volume (L); M represents the mass of monolithic adsorbents (g); and the initial and equilibrium adsorbate concentrations are symbolized by the Co and Ce, correspondingly.

17.2.1.3 Coagulation/flocculation

Coagulation by charge neutralization weakens colloidal contaminations and converts small elements into large aggregates (bridge formation) and adsorbs dissolved organic substances onto the aggregates by an adsorption mechanism, which can then be eliminated effortlessly by filtration and sedimentation. For instance, cationic chitosan derivatives can be simply adsorbed onto the colloid surface of

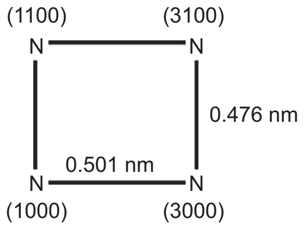

Figure 17.2 Coordination models of Cu(II)-chitosan complex: bridge model (Rhazi et al., 2002).

anionic inorganic (bentonite) suspensions because of electrostatic attraction. Adsorbed macromolecules have a tendency to make loops and prolong certain space from the particle surface into the aqueous phase (Ashraf et al., 2013b). Their culminations also suspend and get adsorbed by one more particle, creating a bridge between particles. For active bridging to occur, the length of the biopolymer chains should be adequate to prolong from one particle surface to another. Therefore, a polymer composed of longer chains should be more efficient than one with shorter chains.

17.2.1.4 Bridge formation

Formation of a polymer bridge takes place when long-chain polymers adsorb onto the surface of more than one particle, thereby forming strong aggregates of large flocks (Renault et al., 2009). The bridge model projected by Schlick (1985) proposes that a metal ion, such as cupric ion, is organized with four nitrogen atoms of intra- and interchitosan chains, developing a square-planar structure (Figure 17.2).

On the contrary, Rhazi et al. (2002) suggested two forms of complex for Cu(II)-chitosan, which are dependent on the pH of the medium. At a pH range from 5.3 to 5.8, the complex ($[Cu(-NH_2)]^{2+}$, $2OH^-$, H_2O) is proposed; above 5.8 pH, the complex ($[Cu(-NH_2)_2]^{2+}$, $2OH^-$) is deliberated (see Figure 17.3).

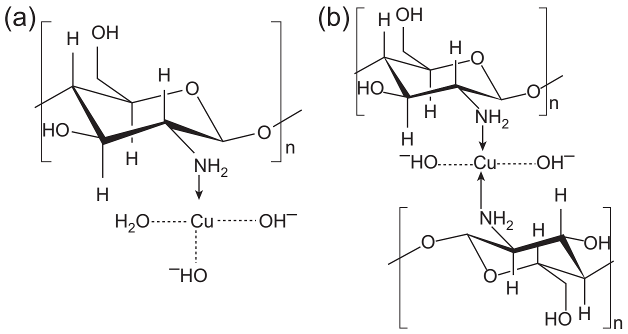

Figure 17.3 Projected structures of Cu-chitosan complex: (a) at various pH levels ranging from 5.3 to 5.8 and (b) at pH > 5.8. (Rhazi et al., 2002).

17.3 Schematic view of contaminant removal by biobarrier

A schematic view of contaminant removal by biobarrier is shown in Figure 17.4. (1) In the primary settling zone, a SaniTEE® device is used to prevent large solids from entering the treatment zone. (2) A remote, above-ground blower introduces air (oxygen) into the treatment module to facilitate a robust circulation of wastewater. (3) Once inside the treatment tank, suspended treatment occurs. Optional added components, such as the Lixor® System, can be used for extra aeration for higher than normal BOD (biological oxygen demand) concentrations. (4) Immersed in the treatment tank, the Bio-Barrier® modules and air grid create an upward flow between membrane plates, providing vigorous scouring action to reduce clogging. This ensures superior robust performance. (5) The membrane pore size is specifically designed to allow for *microfiltration* and *ultrafiltration* processes. (6) Clear, odorless, treated water is ready for standard or innovative dispersal.

17.4 Monitoring the performance of a biofilter/biobarrier

To optimize the immobilization conditions, the effects of chitosan characteristics, pH pretreatment, and the immobilization time on the nitrite removal rate of nitrite oxidizing bacteria (NOB) immobilized chitosan were explored by Lertsutthiwong et al. (2013).

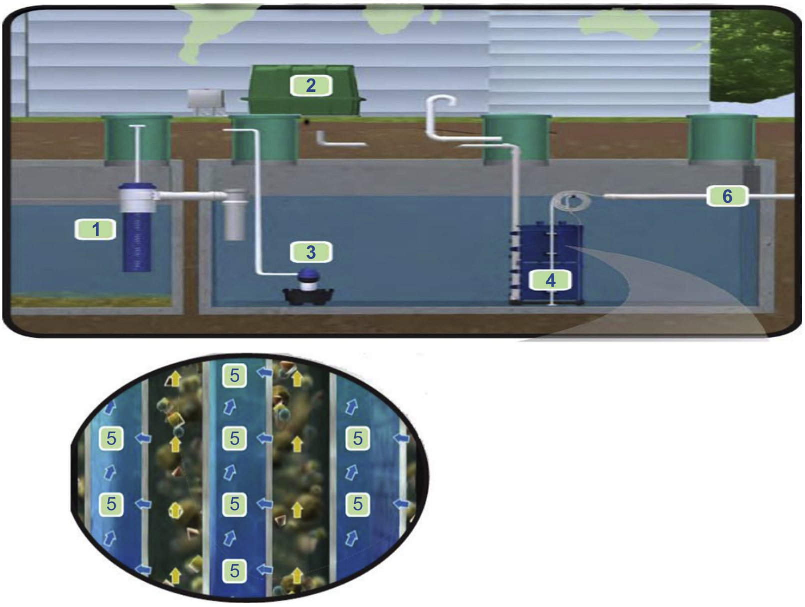

Figure 17.4 Schematic view of contaminant removal by biobarrier.

17.4.1 Sorption capacity of biopolymer

17.4.1.1 Effect of particle size of biopolymer

The ideal size of chitosan used for the immobilization of NOB should be less than 5 mm. Figure 17.5 demonstrates the removal of nitrite as a function of the particle size of chitosan. Immobilization of NOB on chitosan with a size of 1−2 mm and 3−5 mm can decrease nearly 100% of the nitrite level within 2.5 h with a nitrite removal rate of 1.18 ± 0.03 and 1.12 ± 0.05 mg-N/(g·day), correspondingly. Conversely, chitosan having a size of 8−10 mm requires around 3 h to eradicate nitrite with a rate of 0.84-0.03 mg-N/(g·day). Comparable outcomes were also perceived in the case of nitrifying bacteria immobilized on wood particles, as shown by Manju et al. (2009). Wood particles with a size of 0.3−1.5 mm gave excellent proficiency of nitrite reduction. No significant difference between chitosan with a size of 1−2 mm and 3−5 mm ($P > 0.05$) has been detected, but these two particle sizes revealed a significant difference from those sized 8−10 mm ($P < 0.05$) (Lertsutthiwong et al., 2013).

17.4.1.2 Effect of degree of deacetylation of biopolymer

Deacetylation of biopolymer escalates the NOB immobilization on the biopolymer surface. Figure 17.6 exhibits that NOB attached on chitosan with either degree of deacetylation (DD) 82% or DD 91% (molecular weight of 310,000−410,000 g/mol) showed a considerably higher nitrite reduction rate compared to that of chitin. For instance, NOB attached on chitosan with a DD of 91% can reduce nitrite level at a rate of 0.82 ± 0.05 mg-N/(g·day), while NOB attached on chitin simply accomplished 0.44 ± 0.03 mg-N/(g·day). Chitosan with DD of 82% and 91% does not have a substantial effect on nitrite reduction rate ($P > 0.05$). In other words, chitosan employed as a biofilter should have DD exceeding 80%. This fact can be clarified by charge density. After pretreatment of the surface of chitosan with a buffer at pH 6.5, chitosan having DD exceeding 80% comprises higher cationic charges than chitin, which has

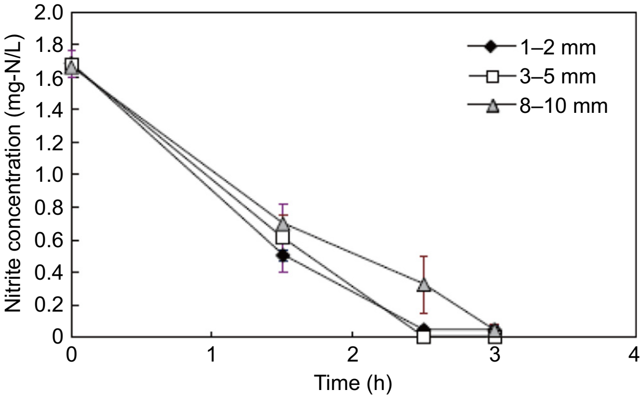

Figure 17.5 Effect of particle size of chitosan on nitrite removal rate (Lertsutthiwong et al., 2013).

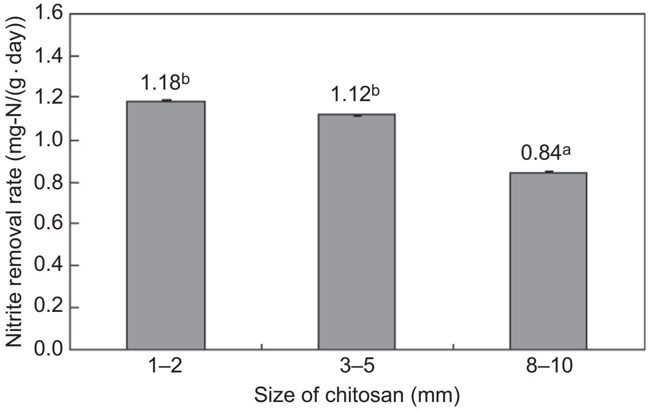

Figure 17.6 Effect of the degree of deacetylation of chitosan on the rate of nitrite reduction (Lertsutthiwong et al., 2013).

a DD of 10−15% (Lertsutthiwong et al., 2002). This leads to strong ionic bonding with the anionic surface of the bacterial cell wall (Lertsutthiwong et al., 2013).

17.4.1.3 Effect of molecular weight of biopolymer

A molecular weight of chitosan ranging from 200,000 to 600,000 g/mol (controlled DD of 85% ± 5%) gave a comparable rate of nitrite removal around 0.80 mg-N/(g·day) ($P > 0.05$) (Figure 17.7). It may be decided that the nitrite removal proficiency of NOB attached on chitosan is not affected by the molecular weight of chitosan, while the DD had a substantial effect on the nitrite removal rate (Lertsutthiwong et al., 2013).

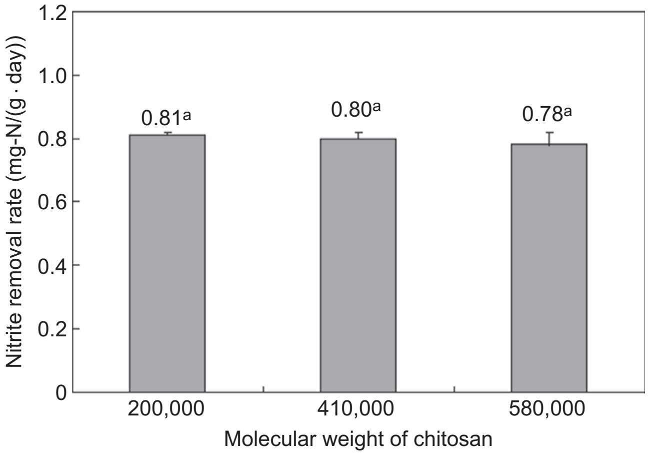

Figure 17.7 Effect of molecular weight of chitosan on nitrite removal rate. The letters in the graph represent no significant difference ($P > 0.05$) (Lertsutthiwong et al., 2013).

17.4.2 Concentration of biopolymers

Biopolymers have an ability to start the flocculation of the phytoplankton suspension from aquaculture tanks in slightly acidic, neutral, or alkaline conditions. As anticipated, the effect of biopolymer on flocculation depends on biopolymer concentration and pH level as well. As such, an overdose of chitosan in acidic medium brings out dense positive charges and converses the charges at the cell surface of phytoplankton, which normally has a negative charge (Grima et al., 2003). Consequently, restabilization occurs because of the repulsion of positively charged phytoplankton cells. Generally, the charge number plays a significant role in the flocculation mechanism. From a pilot study, it was found that to obtain 95% flocculation efficacy in alkaline medium (pH 8.5) consuming a 40 mg/L chitosan concentration, the pH of the chitosan−water mixture must be regulated to an isoelectric point (pH 6.5) after chitosan application and be monitored by a pH regulation to 8.5. However, this delinquency could be reduced when the equivalent quantity of chitosan is mixed into either neutral or alkaline medium (Figure 17.8) (Lertsutthiwong et al., 2009).

17.4.3 Extracellular polymeric substances

The potential foulant of biofilters—extracellular polymeric substances (EPS)—are generated by bacteria present in the biofilter. EPS can inhabit as much as 1000 times the filter media void space engaged by bacteria, thus having a far more important role than bacteria in media clogging, underdrain fouling, and filter head loss (Mauclaire et al., 2004). Nutrients play a significant role in the microbial generation and excretion of EPS (Liu et al., 2006), an adhesive medium comprising exopolysacharides and other polymers (Flemming and Wingender, 2001). Biofilm EPS also make available bacteria with fortification from xenobiotics, high/low pH, oxidants, shear (Wang et al., 2008),

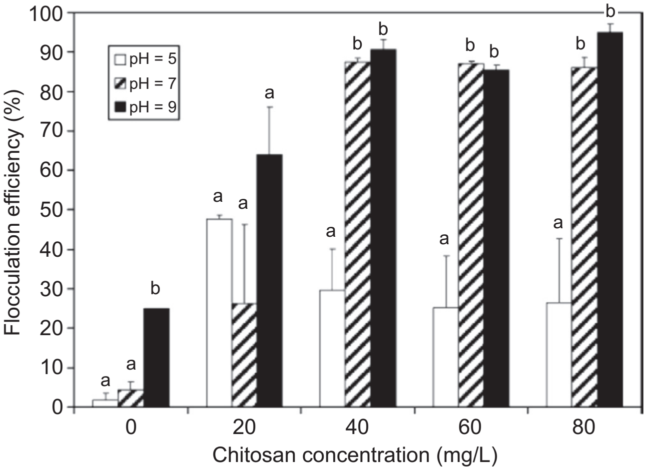

Figure 17.8 Effect of various chitosan concentrations on flocculation efficiency at various pH levels (Lertsutthiwong et al., 2009).

and other kinds of strain for the related microbial community (Mauclaire et al., 2004). Certainly, the incentive of EPS manifestation in biofilms is influenced by these environmental considerations and by the accessibility of nutrients (Fang et al., 2009). Interestingly, EPS may be the crucial supplier to biofilter clogging, either openly by filling filter spaces and binding media or secondarily by enhancing requisitioning of minerals into the biofilm, which also may stimulate filter fouling (Rinck-Pfeiffer et al., 2000).

Biofilter nutrient enrichment was attained by upholding a substrate-limited condition through directing a C:N:P ratio of 100:10:1. This scheme decreased the biofilter lethal head loss by just about 15%, which transformed to extensive filter run times. Microbial characterization data propose that nutrient enhancement can decline EPS levels (>30%) while growing media adenosine triphosphate (ATP) levels (>30%). The detected decline in EPS was the probable cause of the decline in biofilter head loss (Lauderdale et al., 2012)

17.4.4 Effect of dissolved oxygen

To assess the effect of dissolved oxygen (DO) on biofilter efficiency, the oxygen transport and flux in the biofilm were regulated, and oxygen contours inside the biofilm under various flow rate settings were determined using an oxygen microelectrode. Three-point oxygen calibrations were implemented consuming three DO levels (0, 10, and 21%) before and after measurements so as to regulate any response drift. The microelectrode was fixed on a motor-driven micromanipulator, and the oxygen profile in the biofilm on the mulch was determined at 10 or 50 l-m intervals under three various flow rate settings (5, 10, 15 m/d).

Along the length of the biotic column reactor, the naphthalene removal was carried out within the first 6 cm of the column from the influent port where oxygen was most plentiful (Ashraf et al., 2013c). Concentration profiles of pore water naphthalene and electron acceptors specified that DO was specially consumed as the electron acceptor, and the highest reduction carried at the inlet to the column reactor where DO was maximum. Nevertheless, when using nitrate as an alternative electron acceptor, both biofilm formation and continual degradation of naphthalene also occurred (Seo and Bishop, 2008).

17.4.5 Effect of additives

Acclimatization of biopolymers by adding four dissimilar salts (Na_2SO_4, $NaHSO_4$, $(NH_4)_2SO_4$, and $KHSO_4$) together with H_2SO_4 and optimized treatment conditions were examined to improve coagulating efficacy for bentonite suspension. Acclimatization of chitosan with different additives enhanced the coagulating proficiency, but to a different degree. The addition of sulfate ions in bentonite suspension increased the coagulating proficiency of coagulant (Roussy et al., 2005). Acclimatization of chitosan escalates the coagulating proficiency of chitosan because all of the additives comprise sulfate ions. Van Duin and Hermans (1959) postulated that chitosan generates larger aggregates when sulfate ions are present. Consequently, chitosan seems to have a higher molecular weight, and this might cause improvement of bentonite coagulation.

Among the five additives employed for chitosan acclimatization, $NaHSO_4$ and $KHSO_4$ have been detected to be more operative than the others, owing to protonation of the amine group of chitosan shown in Eqn (17.4):

$$RNH_2 \xrightarrow{NaHSO_4 \text{ or } KHSO_4 \text{ or } H_2SO_4} RNH_3^+ \qquad (17.4)$$

Generally, acclimatization of chitosan with $NaHSO_4$ and $KHSO_4$ improved its coagulating capability because the amine group of chitosan is protonated by H^+ generated from the detachment of $NaHSO_4$ or $KHSO_4$ in the chitosan solution throughout acclimatization. Acclimatization of chitosan solution with ammonium sulfate would possibly produce the $R{-}NH_3SO_4NH_4^-$, as suggested by Muzzarelli and Rocchetti (1974), which would boost the bentonite coagulation (Eqn (17.5)).

$$RNH_2 \xrightarrow{(NH_4)_2SO_4} RNH_3^+NH_4SO_4^- \qquad (17.5)$$

Conversely, the improvement of coagulating capability of chitosan after acclimatization with $(NH_4)_2SO_4$ was detected to be much less than with $NaHSO_4$ and $KHSO_4$, attributable to very high pKa value (9.25) for $(NH_4)_2SO_4$.

Protonation of chitosan solution was also increased by H_2SO_4 (pKa values of -3 and 1.92) throughout acclimatization, which enhanced its efficacy for bentonite coagulation. Nevertheless, $NaHSO_4$-acclimatized chitosan resulted in improved bentonite eradication than H_2SO_4-acclimatized chitosan caused by occurrence of alkaline cations, which eliminated the bentonite particles in the suspension (Figure 17.9) (Assaad et al., 2007).

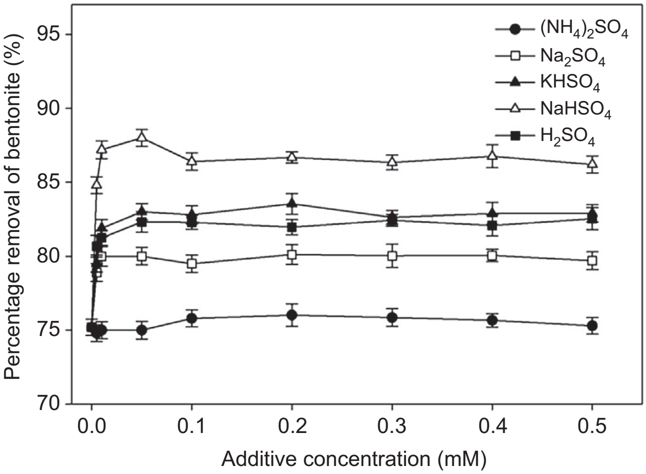

Figure 17.9 Effects of chitosan acclimatization, adding various additives at different levels, for the removal of bentonite (%) at pH 6 (Chatterjee et al., 2009).

17.4.6 Effect of NO_3^-

Magnetic Fe_3O_4 and chitosan microspheres are used in fluidized-bed reactor for the removal of Fe(III)EDTA. At high levels, the rate of the reduction of Fe(III)$EDTA^-$ is reduced, for which NO_3^- reductase substituted Fe(III)$EDTA^-$ reductase as the primary terminal electron transfer enzyme. Li et al. (2011) clarified the inhibition of Fe(III)Cit (citrate) reduction by NO_2^- as the higher standard redox potential of $NO_2^- = NO(+0.99\ V)$ than that of Fe(III)/Fe(II) (+0.34 V). The standard redox potential of NO_3^- is +0.433 V (Jenneman et al., 1986). This potential difference produced electrons to be transmitted to NO_3^- and NO_2^- (Zhang et al., 2009); subsequently, the inhibition of NO_2^- and NO_3^- on Fe(III)$EDTA^-$ reduction might be brought about from the variance in the rate of electron transportation to NO_2^-, NO_3^-, and Fe(III)$EDTA^-$ that had developed to permit special use of the utmost promising oxidant (Cooper et al., 2003).

To investigate the effects of NO_3^-on Fe(III)$EDTA^-$ reduction, different levels (0, 0.5, 1, 2, and 4 mM) of NO_3^- were applied correspondingly to the basal medium containing 10 mM Fe(III)$EDTA^-$. Figure 17.10 shows that the Fe(III)$EDTA^-$ reduction efficacy was 86.6%, 89.6%, 99.3%, 86.6%, and 29.3% for the immobilized bacteria, and the value of the free bacteria was 83.4%, 83.1%, 82.2%, 64.9%, and 33.9%, when 0, 0.5, 1, 2, and 4 mM NO_3^- was applied, correspondingly. One more motivating outcome was that the reduction of Fe(III)$EDTA^-$ was stimulated at low levels of NO_3^- and subdued at high NO_3^- levels, whether free or immobilized bacteria were used. Meanwhile, Fe(III) dissimilatory reduction was a sort of metabolism of microorganism under anaerobic condition; in this procedure, Fe(III), which functioned as the terminal electron acceptor, was reduced to Fe(II) and together with the oxidation of organo/abio electron donors. It is normally acknowledged that microorganisms produce

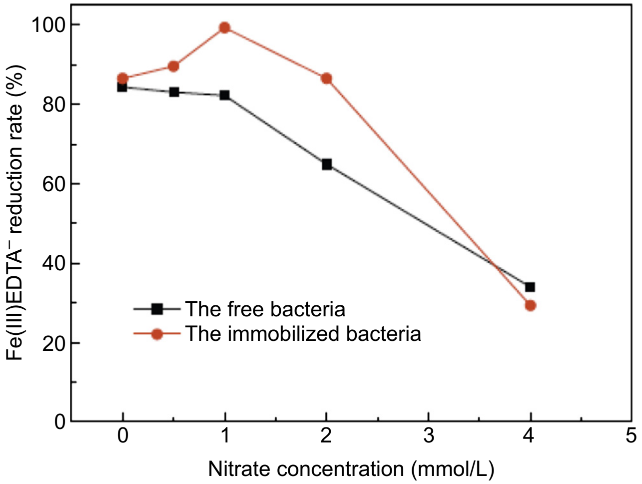

Figure 17.10 The rate of reduction of Fe(III)$EDTA^-$ using free and immobilized bacteria with various primary levels of NO_3^- (Jing et al., 2012).

more energy from the dissimilatory reduction NO_3^- than from the dissimilatory reduction of Fe(III). At the initial metabolic process, NO_3^- worked as electron acceptors and produced more energy, which was helpful to reduce the adaptation period of the bacteria. After NO_3^- was used up, the bacteria activated to catabolize $Fe(III)EDTA^-$ in large numbers (Jing et al., 2012).

17.4.7 Effect of pH pretreatment

The nitrite elimination proficiency of NOB immobilized on biopolymer is highly dependent on the pH level of the biopolymer surface (Figure 17.11). Compared with the chitosan (without pH pretreatment), pH amendment between 5.5 and 7.5 considerably affects the remediation of nitrite of the immobilized NOB on chitosan. This can be clarified by the fact that a large number of protons are generated at lower pH and bring about dense positive charges on $-NH_2$ on the chitosan molecules (Chatterjee et al., 2009). In other words, the charge density of chitosan is highly dependent on pH level (Kaseamchochoung et al., 2006). At pH of less than 7, chitosan comprises dense cationic charges, which permit the ionic bonding to the anionic cell wall of the bacteria. In practice, the chitosan surface should be treated with a buffer at pH 6.5 before the NOB immobilization process (Lertsutthiwong et al., 2013).

17.4.8 Effect of immobilization time

Figure 17.12 illustrates that the variation of immobilization time influenced the nitrite removal efficiency of the NOB immobilized chitosan. A longer immobilization time exhibited a faster nitrite removal rate. As expected, a greater immobilization time allowed more NOB cells to be attached to the surface of chitosan. This was confirmed by SEM analysis, as shown in Figure 17.13. It was clear that a higher number of NOB were found on the chitosan surface after 24 h immobilization time; hence, a higher

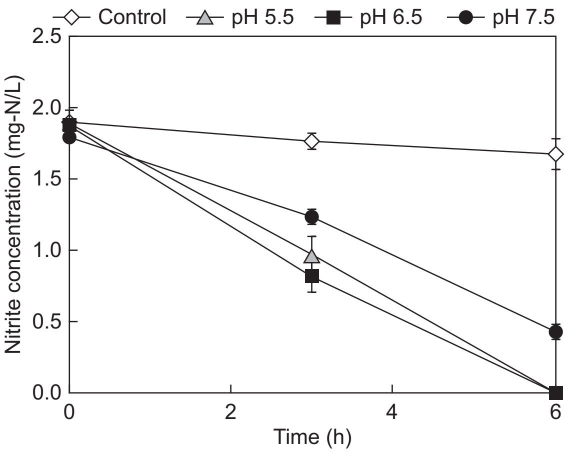

Figure 17.11 Effect of pH adjustment on rate of nitrite removal (Lertsutthiwong et al., 2013).

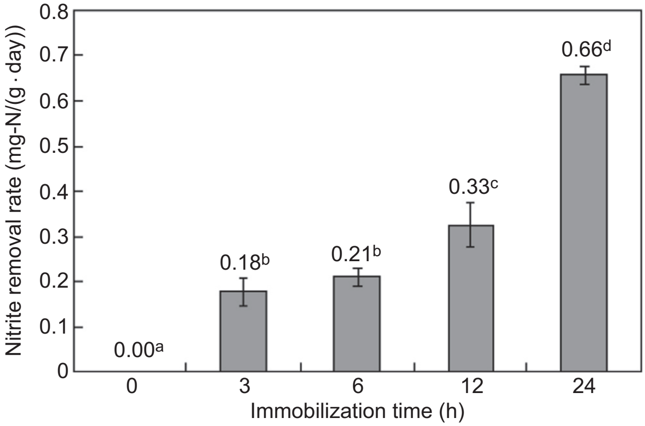

Figure 17.12 Effect of immobilization time on nitrite concentration and removal rate. The different letters in a graph under each immobilization time represent a significant difference ($P < 0.05$) (Lertsutthiwong et al., 2013).

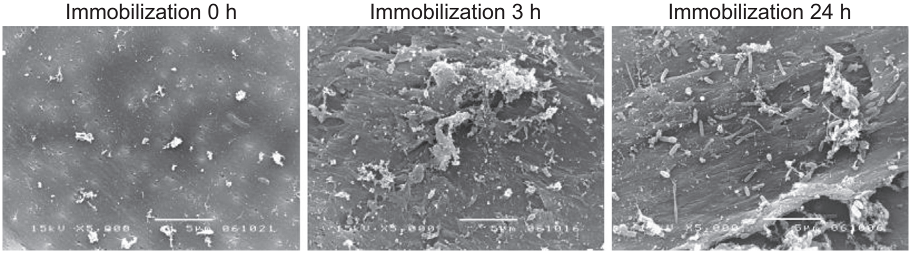

Figure 17.13 SEM images of bacteria immobilizing on chitosan after immobilization for 0, 3 and 24 h (Lertsutthiwong et al., 2013).

nitrite removal rate was the result of cell coverage on the chitosan surface. In general, the incubation period of NOB on conventional nitrification biofilter media takes about 30–45 days because of the limitation of NOB cells in natural waters and the substantially lower growth rate of the nitrifying bacteria (Ruiz et al., 2006). According to the results of this study, the use of chitosan as a biofilter media can reduce the immobilization time by the immediate transfer of NOB from a preacclimated stock of NOB into the chitosan flakes. This phenomenon might be explained by the cationic character of chitosan in slightly acidic conditions. In the beginning, sterilized chitosan modified its surface through soaking in buffer at pH 6.5, which resulted in high cationic charges on the chitosan surface. Consequently, this treated chitosan could interact with the anionic charges of the bacterial cell wall (Lertsutthiwong et al., 2009). On the other hand, conventional plastic biofilter media are nonionic polymers, so the attachment of NOB to plastic surfaces without electrostatic interaction requires a longer time with, probably, a lower adhesion strength.

17.5 Characterization of biopolymers as a supporter

17.5.1 Biopolymer-immobilizing microorganisms

Biofiltration or the transformation of ammonia to nitrate by nitrifying bacteria is one of the best competent methods for nitrogen management in our environment. Two groups of autotrophic bacteria—ammonia oxidizing bacteria (AOB) and nitrite oxidizing bacteria (NOB)—are involved in the nitrification process. Both consist of slow-growing species and are extremely subtle to the fluctuating environmental conditions. Introduction of a novel biofilter requires an extensive bacteria acclimation period, for instance, 3–4 weeks, until both the AOB and NOB are completely developed (Shan and Obbard, 2001). Devoid of full acclimation, a buildup of extremely lethal nitrite is largely set up, owing to the imperfect nitrification process. Biofiltration signifies an immobilization of AOB and NOB on a definite media so as to retain the water quality in an aquatic system (Dong et al., 2011; Manju et al., 2009). Henceforth, the application of nitrifying bacterial immobilizing on biopolymeric substrate is a substitute biofilter for large-scale applications.

17.5.1.1 Chitosan

Biopolymeric chitosan or poly [-(1,4)-2-amino-2-deoxy-D-glucopyranose] is generally obtained from shrimp biowaste (Lertsutthiwong et al., 2002). It comprises *N*-acetyl-D-glucosamine and D-glucosamine units linked by [-(1,4)-glycosidic bonds, as shown in Figure 17.14 Owing to its characteristics such as biodegradability, biocompatibility, cationic property, and nontoxicity, chitosan can be used in several applications comprising water and wastewater treatments (Franco and Peter, 2011). For example, chitosan can make multiplexes with microorganisms (Strand et al., 2003) owing to its cationic property. Hence, the use of chitosan-immobilizing nitrifying bacteria is an innovative practical technique for water quality control since it can be directly introduced into the water system to improve nitrification process; thus, the toxic ammonia and nitrite throughout the first month of the crop could be organized. Chitosan with a degree of deacetylation (DD) of 91% and molecular weight of 410,000 g/mol can be used for immobilization of NOB on chitosan.

Twenty pieces of plastic biofilter media (BCN-009) with active NOB biofilm were shifted into a container enclosing 40 mL of sterilized 30 PSU seawater with 2 mg-N/L nitrite and sonicated for 4 min to the isolated NOB cells. Subsequently, the biofilter media were exchanged with 0.60 g of sterilized chitosan flakes under

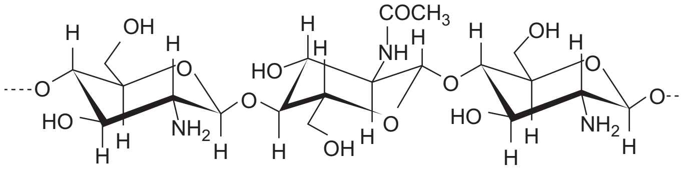

Figure 17.14 Chemical structure of chitosan.

Table 17.3 **Features of the nitrite broth used for assortment of nitrite-oxidizing bacteria (NOB) (Satoh et al., 2000)**

Parameter	Value
Alkalinity (mg/L)	113.33 ± 8.16
Salinity (PSU)	30.33 ± 0.52
Temperature (°C)	26.50 ± 0.15
Dissolved oxygen (mg/L)	5.43 ± 0.21
pH	7.34 ± 0.18

150 r/min agitation at 25 °C. With this immobilization process, a substantial number of bacterial cells can be shifted from the biofilter media to the chitosan flakes. The chitosan agitation period can be mottled at 3, 6, 12, and 24 h. The proficiency of NOB-immobilized chitosan on nitrite elimination was evaluated by insertion of 0.60 g of NOB-immobilized chitosan flakes in 40 mL seawater holding 2 mg N/L of nitrite. The decline in nitrite concentration was supervised by means of the standard method of seawater investigation (Strickland and Parson, 1972).

Mixed culture of nitrifying bacteria from biofilters was immobilized on plastic media after 45 days incubation. This was followed by NOB selection in nitrite broth under laboratory conditions. The desired condition for NOB assortment is shown in Table 17.3 (Satoh et al., 2000). The activity of assorted NOB on plastic media is shown in Figure 17.15. The nitrite level in the water was dropped up to 0.20 mg-N/L within 8 h and nitrite elimination rate was around 28.09−0.58 mg-N/(m^2·day). Therefore, the nitrate level in the test chamber amplified in fraction to the decline of nitrite; however, ammonia stayed persistent. This is designated as the comprehensive nitrite oxidation process (Lertsatthiwong et al., 2013).

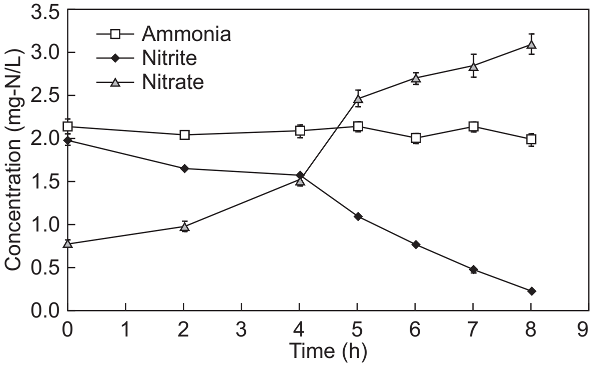

Figure 17.15 Activity of assorted NOB stock culture in terms of ammonia, nitrite, and nitrate concentrations (Lertsatthiwong et al., 2013).

17.5.1.2 Magnetic chitosan microspheres

Magnetic supports have been applied in enzyme immobilization and cell separation in recent years. Magnetic supports provide an easy way to recover immobilized microorganisms from a fluidized-bed reactor by applying an external magnetic field (Krastanov and Yoshida, 2003). An approach using two stages of microbial reduction with magnetic microsphere-immobilized denitrifying bacteria and iron-reducing bacteria were suggested by a group of scientists. Denitrifying bacteria are a group of facultative anaerobic microorganisms that can transform $NO_3^- \rightarrow NO_2^-$, and $NO \rightarrow N_2$ in a series of the subsequent reaction steps: $NO_3^- \rightarrow NO_2^- \rightarrow NO \rightarrow N_2O \rightarrow N_2$ (Zhou et al., 2010). Iron-reducing bacteria are rigorously anaerobic bacteria that can reduce Fe(III) to Fe(II). Consequently, in the first phase, Fe(II)EDTA-NO, in addition to a small amount of NO_2^- and NO_3^-, could be transformed into N_2 by the immobilized denitrification bacteria, which might subside the reticence of these constituents on Fe(III)EDTA$^-$ reduction by the immobilized iron-reduction bacteria in the second phase. Moreover, a minor volume of dissolved oxygen carried from the scrubber might be down in the first phase by oxidizing Fe(II) to Fe(III), which would be advantageous to the iron-reducing bacteria in the second phase. Furthermore, immobilization can be responsible for high cell density in the transporter and defend the bacteria from the destruction of hostile conditions (Kampf, 2002).

Magnetic chitosan microspheres can be developed by co-precipitating of Fe^{2+} and Fe^{3+} ions by NaOH in the presence of chitosan (Eqn (17.6)):

$$Fe^{2+} + 2Fe^{3+} + 8OH^- \rightarrow Fe_3O_4 + 4H_2O \tag{17.6}$$

An adsorption technique was applied to immobilize the mixed iron-reducing bacteria onto the magnetic Fe_3O_4 and chitosan microspheres, which was settled by Qiu et al. (2006). Reduction of Fe(III)EDTA$^-$ was accompanied at 40 °C with trembling at 140 rpm in 100 mL serum bottles, which enclosed 50 mL of basal medium, 0.5 g microspheres immobilized with bacteria (i.e., 1.0 mg dry weight bacteria), and 10 mM Fe(III)EDTA$^-$. The investigation was conducted under anaerobic condition by substituting the air above the solution surface with N_2 at pH 7.0 ± 0.1 adjusted by 0.1 M HCl or NaOH.

To evaluate the constancy of the immobilized bacteria, the reusability of the immobilized bacteria was conducted for five cycles and the Fe(III)EDTA$^-$ reduction efficiency was 92.0%, 93.5%, 99.0%, 99.9%, and 99.8%, respectively. Activity of the immobilized bacteria did not decline throughout the repetitive application. Iron-reducing bacteria immobilized by magnetic Fe_3O_4 and chitosan microspheres displayed efficient performance on Fe(III)EDTA$^-$ reduction. Figure 17.16 represents the comparison of Fe(III) EDTA$^-$ reduction by free and immobilized bacteria (Jing et al., 2012).

17.5.1.3 Peat moss, bentonite, and alginate

Peat moss, made up of lignin and cellulose, is a favorable choice to be a cell immobilization medium (Choi and cloud, 1992). It also has a high and fast contaminant elimination capability due to its inherent hydrophobic characteristics (Radetić et al., 2003).

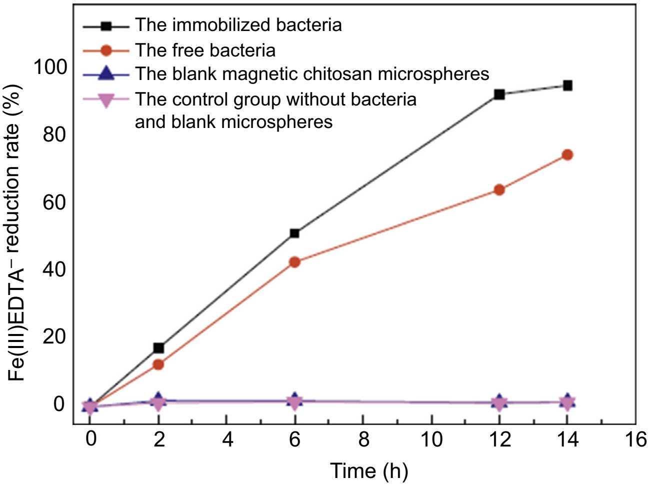

Figure 17.16 Contrast of the Fe(III)EDTA$^-$ reduction by free and immobilized bacteria (Jing et al., 2012).

Hybrid supports combine peat moss with additives to make available higher diesel adsorption, stimulate cell immobilization, and shield cells from detrimental diesel oil. The peat moss hybrid (PBA) is substantiated to be a valuable diesel adsorbent with the addition of bentonite and alginate, which convert the pH of the peat moss to neutral. PBA proved to have a good diesel adsorption and efficient cell immobilization capacity (Figure 17.17). Consequently, the percent biodegradation of diesel applying a consortium of three bacterial strains immobilized onto a hybrid support was comparable to that of free cells in batch experiments. The pilot and field experiments are in progress. Pores permit nutrients, oxygen, and diesel oils to reach cells locked in on the peat moss (Figure 17.18(a)).

As Figure 17.18(b) shows, the surface of bentonite is uneven, with many crests and trenches, and not encrusted. Above all, bentonite was excellently adsorbed to the peat moss surface, creating a crumpled uneven surface and considerably growing the surface area. This morphology may stimulate a good diesel elimination capability (Figure 17.18(c) and (d)). The diesel adsorption capabilities of hybrid supports were larger than tainted peat moss for the equivalent weight basis since additives have a sophisticated diesel adsorption capability. On the basis of diesel adsorption capability only, PBA could be a favorable choice. For enhancing diesel degradation (%), bentonite may be an ideal choice since bentonite (pH 9.29) can neutralize the overall pH to 6.58 and in that way expedite cell immobilization and development. Consequently, it is proposed that PBA is an appropriate supporting matrix for cell immobilization proceeding to diesel degradation (Lee et al., 2010).

17.5.1.4 Bacteria immobilized on microbial cellulose

Through constant operation, the efficacy and the constancy of attached growth reactors relies on the construction of the biofilm formed (Alves et al., 2002). The growth and

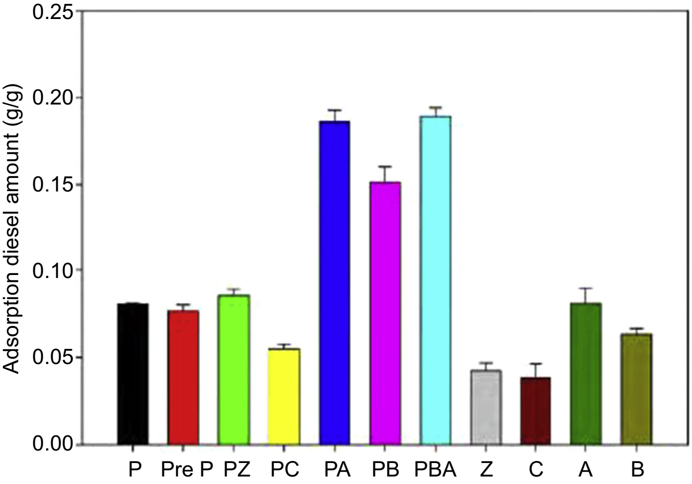

Figure 17.17 Diesel sorption capabilities of P (1 g), Pre P (1 g P autoclaved in DI water), PZ (0.5/0.5 g, w/w), PC (0.5/0.5 g, w/w), PA (0.5/0.5 g, w/w/), PB (0.5/0.5 g, w/w), PBA (0.5/0.48/0.02 g, w/w/w), Z (1 g), C (1 g), A (1 g), and B (1 g). Sorption capabilities are represented as mg of absorbed oil per g of sorbent. P: peat moss, Pre P: Presoaked P, PZ: peat moss/zeolite, PC: peatmoss/chitosan, PA: peat moss/alginate, PB: peat moss/bentonite, PBA: peat moss/bentonite/alginate, Z: zeolite, C: chitosan, A: alginate, and B: bentonite (Lee et al., 2010).

the conformation of the biofilm are affected by the substrate level in the influent. The bacterial development and activity can be intensified using the surplus carbon source; however, this also points to greater cell accretion. Demolition of the biofilm by the elevated velocity of the liquid phase (shear stress) is also recurrent (Chang et al., 1999). All of these influences can be avoided by solicitation of appropriate media for denitrifying immobilization. The microbial cellulose delivers an incessantly abundant cell growth in the bioreactor. A consortium of bacteria immobilized onto microbial cellulose (MC) packed-attached biofilm reactor can efficiently remove nitrate in wastewater.

An upflow packed bed reactor has been constructed to explore the technical viability of biological nitrate removal. Ethanol was applied as a carbon source for biological denitrification. This continuous flow bioreactor verified a competent denitrification system with comparatively less retention time. In an MC-packed bioreactor, a Plexiglas column has been implemented as a reactor monitored by a 5-L sedimentation tank. The tips of the column were enclosed with plastic screens to grip the biofilter media. The entire capacity of the reactor up to the top level was 3500 mL, with a height of 70 cm and diameter of 8 cm, of which merely 50 cm was occupied with MC. The MC particle dimensions were around 5—10 mm on a side and 5—7 mm in wideness. This artificial upflow packed bed reactor can perform well in total darkness for attaining the appropriate natural denitrification (Rezaee et al., 2008a). Darkness is compulsory for the denitrification process in this reactor because metabolic activity of the aquatic macrophyta took place in the dark and persuade higher in the presence of high light and in low oxygen concentration (Eriksson and Weisner, 1999).

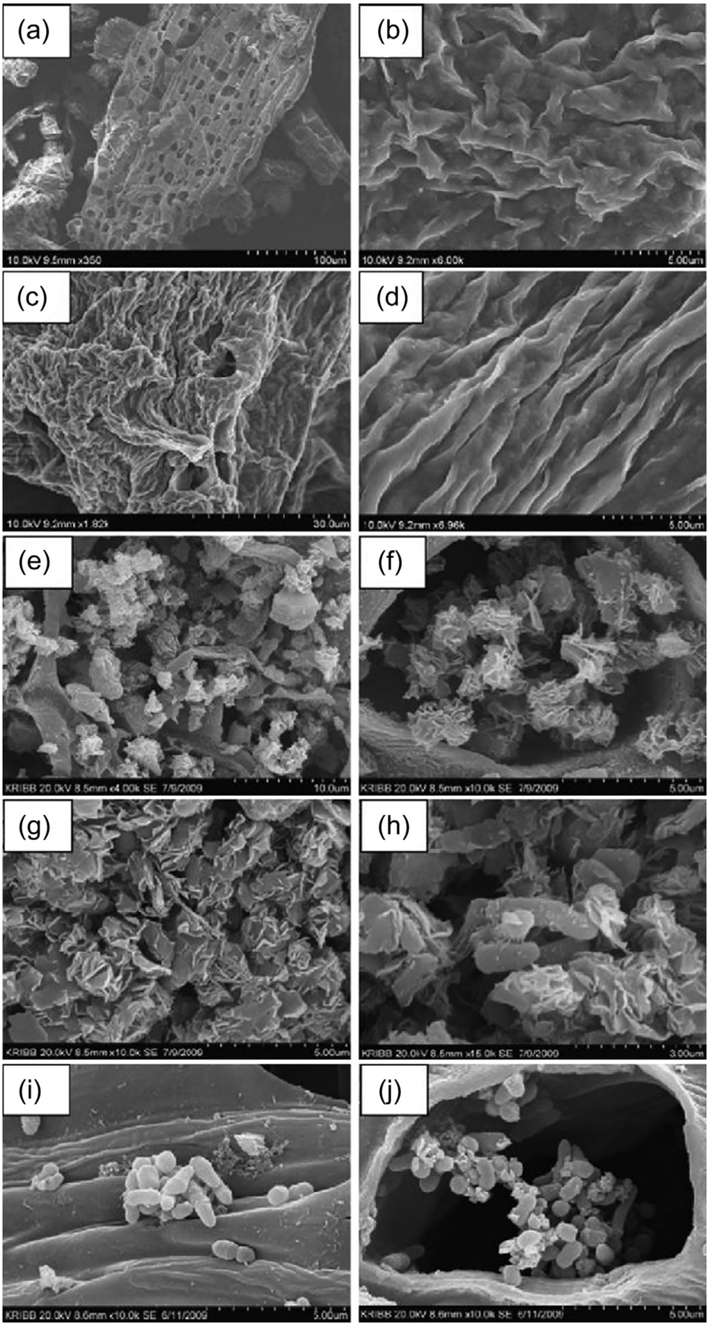

Figure 17.18 SEM images of P (a), B (b), low magnification (c) and high magnification (d) of PB (2/3 g, w/w) hybrid, mixed cells immobilized onto PBA (2/2.9/0.1 g) hybrid support (e and f) with diesel (g and h), and without diesel (only, i and j) at neutral pH. Scale bars represent (a) 100 m, (b) 5 m, (c) 30 m, (d) 5 m, (e) 10 m, (f and g) 5 m, (h) 3 m, and (i and j) 5 m. P: peat moss, B: bentonite, PB: peat moss/bentonite, PBA: peat moss/bentonite/alginate (Lee et al., 2010).

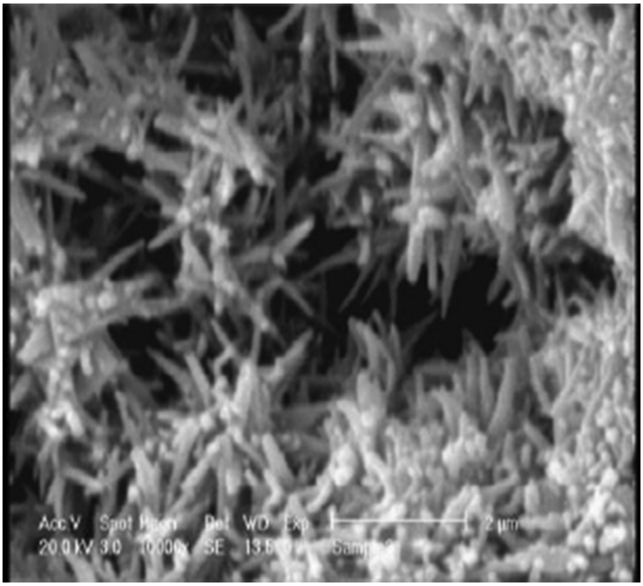

Figure 17.19 The SEM image of *Pseudomonas stutzeri* immobilizing onto the surface of the MC (original magnification, ×10,000) (Rezaee et al., 2008a).

The immobilization of the bacterium in MC improved the adsorption capacity, reduced the cell leakage from the beads, led to intensive activity of the immobilized cells, and endorsed improved operational control. The number of cells immobilized on the MC was measured as a function of optical density (OD 650) of the cell suspension used for immobilization. The number of cells immobilized on the substrate relies on the density of the bacterial cell suspension. The MC matrixes offer the superlative distinctive adhesion (3.39 mg biomass/g support). On the other hand, the reactors with MC offer the maximum absolute biomass retention in the reactor. This effect can be clarified by improved attraction of positive groups to negatively charged bacterial cells. The SEM images demonstrate the adhesion of the *Pseudomonas stutzeri* (quantified as biomass) on support material (Figure 17.19). The immobilization of viable cells is a multipurpose implement that functions to upsurge the constancy of a microbial system, letting its solicitation under extreme environmental conditions. Through the immobilization process, the denitrifying bacteria are provided with a very appropriate environment to carry out with maximum efficiency. This is significant when evaluating the solicitation of denitrification techniques for treatment plants because building expenses can be controlling factors (Rezaee et al., 2008a,b).

17.5.1.5 Alginate immobilization of cells

Alginate bead-immobilized cells can be a valuable technology for seeding biofilters. They permit a very fast rate of colonization and lessen the "wash-out" influence when irrigation (recirculatory or noncirculatory) is implemented to the system. Figure 17.20

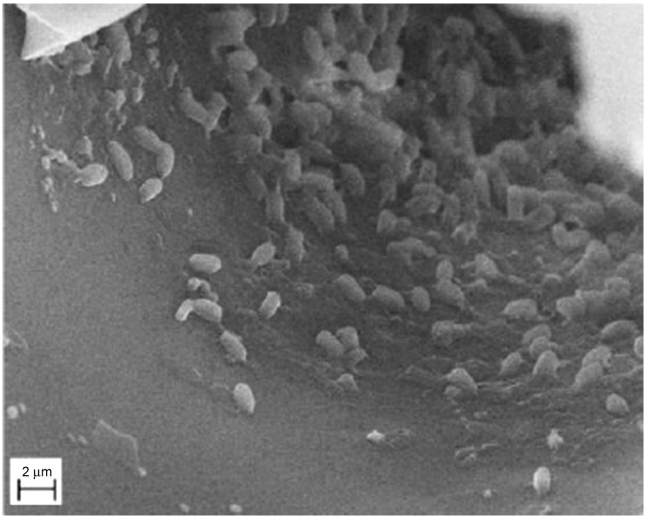

Figure 17.20 SEM photomicrograph of pumice surface after incubation in alginate bead-immobilized cells for 72 h (Low et al., 2014).

represents that the alginate bead-immobilized cells can immobilize and colonize the pumice surface excellently (Low et al., 2014). This characteristic of the alginate-immobilization of the cells permits the cells to be populated locally (Chen et al., 2013) and not easily "washed" away by the contiguous liquid media (Lin et al., 2010), therefore prolonging the capability for surface attachment. The efficacy of cell immobilization can be influenced by the weak attachment generated on the surface of the pumice, which escalates the possibilities of inoculums being washed off. Therefore, to sustain a constant immobilization on a surface, microbial cells need to generate and evacuate a nonspecific adhesive extra polysaccharide (EPS) substance for the development of biofilms. Furthermore, it is conceivable that earlier to biofilm generation, the surface chemistry of the pumice may be modified for its appropriateness for microbial colonization (Karunakaran and Biggs, 2011). Thus, the localized accessibility of nutrient leachate from the beads onto the surface of the pumice may participate in accelerating the rate of colonization.

17.5.2 Biopolymer supporting other polymers

17.5.2.1 Fusion protein/cellulose

Cellulose binding domains (CBDs) from several bacterial species provide a new class of affinity tags with appealing new biotechnological attributes, including effective immobilization of CBD fusion proteins to cellulose-based matrices without the need for covalent cross-linking, as well as a readily available, low-cost affinity matrix (cellulose) with inherent low nonspecific protein-binding characteristics. Moreover, after the construct has been overexpressed in a bacterial or fungal system, the construction of a biofilter is achieved in one easy step, such as breaking the cells or harvesting an excreted soluble enzyme and reacting the protein with the cellulose, which will later be used as a biofilter to remove atrazine from wastewater (Raffi et al., 1999).

17.6 Removal of contaminants from wastewater

17.6.1 Biofilter/biobarrier for the removal of inorganic contaminants

Bioremoving is an imperative substitute and favorable technology to disinfect waters. The bioremoving techniques can be categorized as biosorption, phytoremediation, bioremediation, and biofiltration. Chitosan, a biopolymer hauled out from the wastes of the seafood industries, was demonstrated for As(V) sorption (Gerente et al., 2010). Langmuir maximum monolayer capabilities were attained in the range 0.4—0.7 mg/g, at various temperatures (4—40 °C), pH about 6 and initial levels in the range 25—2000 mg/L. Spring water contaminated with arsenic was used as well to certify the elimination of arsenate and attain sorption isotherms. While the experimental data were not gained at similar pH levels, the contrast between deionized water and spring water displayed a decline in the adsorbed concentration for equilibrium concentrations up to 1000—1300 mg/L and an upsurge for higher levels. This biopolymer was employed in a semidynamic treatment process as well and its efficiency was assessed through the experimental breakthrough curves. A model has been projected on the basis of a mass balance equation as a prognostic tool.

Iron-chitosan composites (flakes and granules) were examined for the removal of arsenic from groundwater at pH 7 (Gupta et al., 2009). In the case of flakes, the maximum adsorbed concentrations were 22.47 mg/g for As(V) and 16.15 mg/g for As(III), considerably higher than for granules, 2.24 mg/g for As(V) and 2.32 mg/g for As(III). Sulfate, phosphate, and silicate, at concentrations existing in ground water, did not originate significant intrusions in the sorption performance of arsenate/arsenite. As(III) or As(V) contaminated groundwater samples (500 mg/L As) were treated in fixed beds of iron-chitosan sorbents, by two adsorption—desorption cycles, using NaOH 0.1 M for regeneration. Amounts surpassing 10 mg/L were attained in outlet water for 147 and 112 bed volumes, correspondingly in view of As(III) and As(V) (Ungureanu et al., 2015).

Biofilters comprising chitosan-metal composites can eliminate 12 g of P/kg of chito-M in a reversible order. More prominently, ~1 kg of chitosan-metal composite has the ability to constantly reduce P concentrations up to ~12 μM, even after an overall flow of ~40,000 L of wastewater originating from vegetable washing. Biofilters comprising chitosan flake also have the ability to eliminate copper from industrial wastewater with a capability of ~100 g of Cu/kg of chitosan (Mutus, 2014).

There are two identified dissimilar nitrate-reducing pathways: denitrification and the dissimilatory nitrate reduction to ammonium (DNRA). Elements defining the two nitrate-reducing processes comprise the nature of carbon source and the ratio of electron donors (i.e., organic substrate) and electron acceptors (i.e., nitrate and oxygen) (van Rijn et al., 2006). The reduction of nitrate to ammonium results in the improved ammonium concentration in the effluent. Low oxygen levels and high C/N ratios are hypothesized to favor DNRA organisms over denitrifiers (van Rijn and Barak, 1998).

A fixed-bed bioreactor occupied by biopolymer polycaprolactone (PCL) was constructed to eliminate nitrate from ground water through denitrification. PCL functions both as carbon source and biofilm carriers. Throughout a long-standing process of 561 days, the efficiency of the reactor in nitrogen elimination, properties of biofilm immobilized to biodegradable carriers, and the hydrolysis and consumption of solid carbon source have been explored. At temperatures above 24 °C, the average nitrate level in the discharge was less than 3.7 mg N/L, and TN exceeding 95% was reduced at hydraulic retention time of 3−6 h. Ammonium and nitrite persisted at low concentrations (less than 0.32 and 0.78 mg-N/L, correspondingly). The considered PCL concentration expended was found to be in the range of 1.6−3.7 g PCL/g $NO_3{}^-$−N. The FTIR spectrum of the utilized PCL specified the chain scission by hydrolytic degradation.

A pyrosequencing analysis of the biofilm determined that the genus *Diaphorobacter* belonging to the family Comamonadaceae contributed to most of the series. Bacteria of genera *Hydrogenophaga*, *Rhodocyclaceae* uncultured, and *Desulfovibrio* were highly augmented in the PCL biofilm. Microelectrode data showed that the biofilm had an average thickness of around 800 lm and the intensive denitrification activities happened in the area of 300−500 ml of biofilm, with values up to 400 μmol/cm^3 h. Table 17.4 summarizes the performance data of the fixed-bed reactor in nitrogen removal (Chu and Wang, 2013).

Wastewater contains the Hg, Cd, and Pb metals abundantly. One of the best methods for the removal of Hg, Cd, and Pb metals is an absorption method using chitosan solution, which is then monitored by a biofilter of mussels *Anodonta woodiana* and water hyacinth. Chitosan solution has an adsorption capacity of 46.6%, 78.64%, and 53.52% for Pb, Hg, and Cd, respectively. The application of a biofilter can decrease Pb, Hg, and Cd concentrations of wastewater up to 98.05%, 98.88%, and 97.86%. These biomaterials can be easily found in the environment, so they can be practiced more often in the progression of wastewater processing.

Dynamic and static adsorption experiments with mercury, chromium, and copper ions specified that chitosan can be efficiently utilized to adsorb these metals by creating their various interfaces with its amino and hydroxyl groups. To examine which group is accountable for adsorbing ions or even to upsurge the adsorption efficiency, it is conceivable to selectively and chemically amend the structure of this biopolymer, applying methods such as cross-linking with glutaraldehyde or epichlorohydrin (Ashraf et al., 2012c). The excellent recovery conditions can also be attained by fine-tuning the operational limitations that affect the adsorption process and also by monitoring the number of adsorption−desorption cycles. It defines the best practice to recuperate or isolate some metal species selectively from wastewater by utilizing this economical and renewable biopolymer (Rodrigo and Marisa, 2014).

Table 17.4 Summary of the performance data of the fixed-bed reactor in nitrogen removal (Chu and Wang, 2013)

Time (d)	Temperature (°C)	HRT (h)	N conc. in effluent (mg/L)			TN removal efficiency (%)	Volumetric rate (mg NL/h)
			NO_3–N	NO_2–N	NH_4–N		
49–188	30	5–6	2.8 ± 2.0	0.12 ± 0.32	0.31 ± 0.29	96 ± 3	10.8 ± 1.4
192–206	30	3–4	3.3 ± 1.4	0.19 ± 0.27	0.49 ± 0.33	96 ± 3	23.5 ± 5.9
207–277	24–28	4–6	3.7 ± 1.6	0.32 ± 0.34	0.78 ± 0.51	95 ± 2	15.3 ± 2.2
299–351	20	6–9	5.0 ± 2.9	1.0 ± 0.6	0.60 ± 0.40	92 ± 4	7.6 ± 1.8
356–399	10–15	13–17	10.7 ± 4.8	0.8 ± 0.2	0.26 ± 0.18	82 ± 9	3.2 ± 0.5
404–460	15–18	10–11	16.1 ± 7.9	2.6 ± 1.6	1.6 ± 0.7	76 ± 12	4.4 ± 1.0
473–561	24–29	6–8	6.5 ± 3.5	1.7 ± 0.9	1.2 ± 0.6	91 ± 7	8.0 ± 1.3

17.6.2 Biofilter/biobarrier for the removal of organic contaminants

Considering in situ bioremediation technologies, the application of permeable reactive barriers within contaminated aquifers has grown as a way to inhibit additional movement of dissolved hydrocarbons from polluted plumes with the least maintenance charges (Kao et al., 2001). The permeable reactive barrier has been verified for many organic compounds, at both laboratory scale and full scale. Lamarche et al. (2001) stated that the field testing of a funnel and gate system enclosing a coarse-medium silica sand contained 1% by volume of granular activated carbon. A field-scale system was verified on a naphthalene plume for over 2 years, and its removal efficiency was found to be up to 98%. It is also indicated by Miller et al. (2001) on a full-scale biobarrier system that attained a treatment efficiency of more than 99.9% for dissolved benzene—toluene—ethylene—xylene (BTEX).

Among several various kinds of support materials for use in permeable reactive barriers, solid organic materials, such as organic mulch and peat moss, have normally been used in bioremediation and bioretention systems to enhance the efficacy of the permeable reactive biobarrier (Yerushalmi et al., 1999). Organic mulch has several biopolymers; of them, lignin is recognized as having a high affinity and sorption capacity for nonionic organic compounds (Garbarini and Lion, 1986); they can also serves as complex additive fertilizer for hydrocarbon degradation (Kastner and Mahro, 1996). Along with the sorption ability of supporting material in the biobarrier, microbial processes and biofilm generation participate significantly in the functioning of the permeable reactive biobarrier. Higher amounts of biomass and the extracellular polymeric substance (EPS) fraction of the biofilm can also develop a strong attraction for the hydrophobic organic compounds (Ebihara and Bishop, 2002). The amplified mass of organic carbon adsorbed on the biofilm matrix, besides the organic mulch itself, can prompt intensification in the population of gradually developing hydrocarbon degraders, a maximum degradation rate, and more steady elimination (Tabassum et al., 2014).

A laboratory-scale mulch biofilm barrier was built up and established to assess the impact of biofilm generation on the working efficiency of the biobarrier. Naphthalene, a two-ring polycyclic aromatic hydrocarbon, was used as the model compound. Along the length of the biotic column reactor, the removal of naphthalene carried out within the first 6 cm of the column from the influent port where oxygen was found to be maximum along the length of the biotic column reactor (Seo and Bishop, 2008).

Biotrickling filter (BTF) systems and cell-immobilization techniques in an incorporated biofiltration system have been developed. They utilize BTF combined with cell-entrapped polyvinyl alcohol (PVA)-alginate beads to remove the isopropyl alcohol (IPA). The experimental findings indicate that the suggested biotrickling filter system efficiently decreases the inhibitory effects of raised IPA level on microbial development, thus resolving the delinquency of elevated IPA loading that normally comes across the electronic high-technology industries (Hussin et al., 2013). To assess the constancy and efficiency of this system under higher IPA shock, the influent IPA level was amplified to 1100 ± 47 ppm, 900 ± 11 ppm, and 1900 ± 43 ppm on various

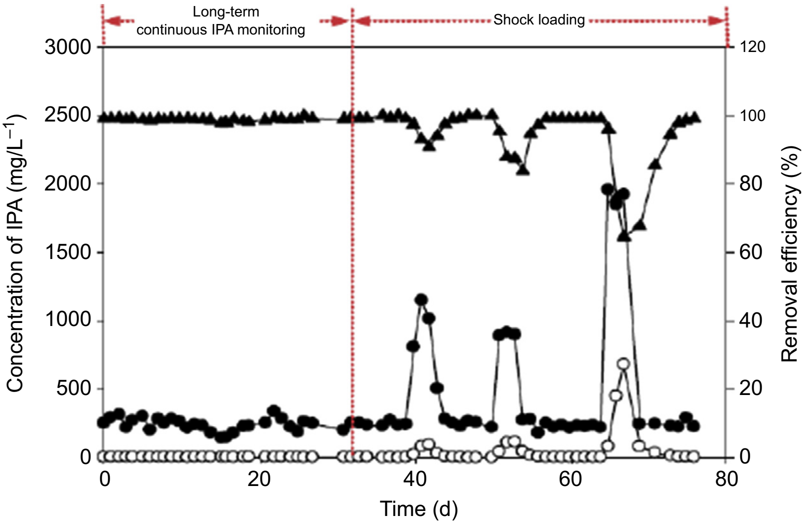

Figure 17.21 Removal summaries of a biotrickling filter functioning constantly with continual IPA loading and shock loading. (▲) Removal capacity; (•)BTF influent; (°) BTF effluent (Tsai et al., 2012).

days (40, 53, and 66 days). Figure 17.21 shows that removal capacity marginally declined from 95% to 90% when the first IPA shock took place, but the system reverted to equilibrium after 5 days. However, removal capacity considerably declined up to 80% after the next shock loading. This suggests that, after removal capacity was reestablished, the system microenvironment persisted as unstable after the first shock, even with a comparatively smaller load. As anticipated, an even larger reduction in removal capacity (up to 67%) took place at the third shock loading, when concentrations reached as high as 1900 ± 73 ppm (Tsai et al., 2012).

17.7 Future trends

Biopolymers have proven to be suitable for removal properties by adjusting the microbial entrapment and adsorption in biofiltration system. New applications will emerge in specific niches, but it seems likely that biopolymers may be an alternative to the large-scale uses of chemicals and synthetic polymers (due to their unavoidable higher prices). On the other hand, biopolymers are a very promising alternative to synthetic polymers with inherent environmental benefits. The development of these new biofilters and biobarriers for large-scale effluent treatment and use should also meet some key objectives: sludge formation in the biofiltration process needs to be as low as possible, as well as other by-products that have to be carefully controlled. Finally, biopolymers should be consistent with health and safety legislations where more research and work is needed.

Acknowledgment

The research was financially supported by Institute Research Management & Monitoring (IPPP) Postgraduate Research Grant (PG008-2013B, PG138-2014B, PG133-2014B), University Malaya Research Grant UMRG (RG257-13AFR), and Fundamental Research Grant FRGS (FP038-2013B).

References

Alves, C.F., Melo, L.F., Veiria, M.J., 2002. Influence of medium composition on the characteristics of a denitrifying biofilm formed by *Alcaligenes denitrificans* in a fluidized bed reactor. Process Biochemistry 37, 837−845.

Ashraf, M.A., Maah, M.J., Yusoff, I., 2012a. Poly vinyl acetate (PVA) as fill material for land reclamation. Chiang Mai Journal of Science 34 (9), 693−711.

Ashraf, M.A., Maah, M.J., Yusoff, I., 2012b. Development of new fill material technology for the ex-mining land reclamation for construction purposes. Fresenius Environmental Bulletin 21 (5a), 1334−1343.

Ashraf, M.A., Maah, M.J., Yusoff, I., 2012c. Poly vinyl acetate (PVA) as fill material for land reclamation. Chiang Mai Journal of Science 34 (9), 693−711.

Ashraf, M.A., Ullah, S., Ahmad, I., Qureshi, A.K., Balkhair, K.S., Rehman, M.A., 2013a. Green biocides, a promising technology: current and future applications. Journal of the Science of Food and Agriculture 94 (3), 388−403. http://dx.doi.org/10.1002/jsfa.6371.

Ashraf, M.A., Maah, M.J., Qureshi, A.K., Gharibreza, M., Yusoff, I., 2013b. Synthetic polymer composite membrane for the desalination of saline water. Desalination and Water Treatment 51 (16−18), 3650−3661. http://dx.doi.org/10.1080/19443994.2012.751152.

Ashraf, M.A., Qureshi, A.K., Gharibreza, M., Rehman, M.A., Ahmad, I., Yusoff, I., 2013c. Intercationic effect on biosorbent efficacy. Desalination and Water Treatment 52 (7−9), 1504−1513. http://dx.doi.org/10.1080/19443994.2013.788456.

Assaad, E., Azzouz, A., Nistor, D., Ursu, A.V., Sajin, T., Miron, D.N., Monette, F., Niquette, P., Hausler, R., 2007. Metal removal through synergic coagulation-flocculation using an optimized chitosan−montmorillonite system. Applied Clay Science 37, 258−274.

Benavente, M., 2008. Adsorption of Metallic Ions onto Chitosan: Equilibrium and Kinetic Studies. Licentiate Thesis Royal Institute of Technology Department of Chemical Engineering and Technology Division of Transport Phenomena Stockholm, Sweden.

Bratskaya, S.Y., Avramenko, V.A., Schwarz, S., Philippova, I., 2006. Enhanced flocculation of oil-in-water emulsions by hydrophobically modified chitosan derivatives. Colloids and Surface A: Physicochemical and Engineering Aspects 275, 168−176.

Bratskaya, S.Y., Schwarz, S., Chervonetsky, D., 2004. Comparative study of humic acids flocculation with chitosan hydrochloride and chitosan glutamate. Water Research 38, 2955−2961.

Chang, C.C., Tseng, S.Z.K., Huang, H.K., 1999. Hydrogenotrophic denitrification with immobilized *Alcaligenes eutrophus* for drinking water treatment. Bioresource Technology 69, 53−58.

Chen, D.Z., Fang, J.Y., Shao, Q., Ye, J.X., Ouyang, D.J., Chen, J.M., 2013. Biodegradation of tetrahydrofuran by *Pseudomonas oleovorans* DT4 immobilized in calcium alginate beads impregnated with activated carbon fiber: mass transfer effect and continuous treatment. Bioresource Technology 139, 87−93.

Chatterjee, T., Chatterjee, S., Woo, S.H., 2009. Enhanced coagulation of bentonite particles in water by a modified chitosan biopolymer. Chemical Engineering Journal 148, 414—419.

Cheng, W.P., Chi, F.H., Yu, R.F., Lee, Y.C., 2005. Using chitosan as a coagulant in recovery of organic matters from the mash and lauter wastewater of brewery. Journal of Polymers and the Environment 13, 383—388.

Chiellini, E., et al. (Eds.), 2001. Biorelated Polymers: Sustainable Polymer Science and Technology. Kluwer Academic/Plenum Publishers, New York.

Chi, F.H., Cheng, W.P., 2006. Use of chitosan as coagulant to treat wastewater from milk processing plant. Journal of Polymers and the Environment 14, 411—417.

Choi, H., Cloud, R.M., 1992. Natural sorbents in oil spill cleanup. Environmental Science and Technology 26, 772—776.

Chu, L., Wang, J., 2013. Denitrification performance and biofilm characteristics using biodegradable polymers PCL as carriers and carbon source. Chemosphere 91, 1310—1316.

Chung, Y.C., 2006. Improvement of aquaculture wastewater using chitosan of different degrees of deacetylation. Environmental Technology 27, 1199—1208.

Cooper, D.C., Picardal, F.W., Schimmelmann, A., Coby, A.J., 2003. Chemical and biological interactions during nitrate and goethite reduction by *Shewanella putrefaciens*. Applied and Environmental Microbiology 69, 3517—3525.

Divakaran, R., Pillai, V.N.S., 2002. Flocculation of river silt using chitosan. Water Research 36, 2414—2418.

Dong, Y.M., Zhang, Z.J., Jin, Y.W., Li, Z.R., Lu, J., 2011. Nitrification performance of nitrifying bacteria immobilized in waterborne polyurethane at low ammonia nitrogen concentrations. Journal of Environmental Sciences 23 (3), 366—371.

Ebihara, T., Bishop, P.L., 2002. Influence of supplemental acetate on bioremediation for dissolved polycyclic aromatic hydrocarbons. Journal of Environmental Engineering 129, 505—513.

Eriksson, P.G., Weisner, S.E.B., 1999. An experimental study on effects of submersed macrophytes on nitrification and denitrification in ammonium rich aquatic system. Limnology and Oceanography 44, 1993—1999.

Fang, H., Wenrong, H., Yuezhong, L., 2004. Investigation of isolation and immobilization of a microbial consortium for decoloring of azo dye 4BS. Water Research 38, 3596—3604.

Fang, W., Hu, J., Ong, S., 2009. Influence of phosphorus on biofilm formation in model drinking water distribution systems. Journal of Applied Microbiology 106, 1328.

Flemming, H.C., Wingender, J., 2001. Relevence of microbial polymeric substances (EPS)-Part I: structural and ecological aspects. Water Science and Technology 43, 1.

Franco, T.T., Peter, M.G., 2011. Advances in chitin and chitosan research. Polymer International 60 (6), 873—874.

Garbarini, D.R., Lion, L.W., 1986. Influence of the nature of soil organics on the sorption of toluene and trichloroethylene. Environmental Science and Technology 20, 1263—1269.

Gerente, C., Andres, Y., McKay, G., Le Cloirec, P., 2010. Removal of arsenic(V) onto chitosan: from sorption mechanism explanation to dynamic water treatment process. Chemical Engineering Journal 158 (3), 593—598.

Grima, E.M., Belarbi, E.H., Ferná ndez, F.G.A., Medina, A.R., Chisti, Y., 2003. Recovery of microalgal biomass and metabolites: process options and economics. Biotechnology Advances 20, 491—515.

Guibal, E., 2004. Interactions of metal ions with chitosan-based sorbents: a review. Separation and Purification Technology 38, 43—74.

Guibal, E., Roussy, J., 2007. Coagulation and flocculation of dye-containing solutions using a biopolymer (chitosan). Reactive and Functional Polymers 67, 33—42.

Gupta, A., Chauhan, V.S., Sankararamakrishnan, N., 2009. Preparation and evaluation of iron-chitosan composites for removal of As(III) and As(V) from arsenic contaminated real life groundwater. Water Research 43 (15), 3862−3870.

Hussin, N.H., Yusoff, I., Alias, Y., Mohamad, S., Rahim, N.Y., Ashraf, M.A., 2013. Ionic liquid as a medium to remove iron and other metal ions: a case study of the North Kelantan Aquifer, Malaysia. Environmental Earth Science 71 (5), 2105−2113. http://dx.doi.org/10.1007/s12665-013-2615-5.

Jenneman, G.E., McInerney, M.J., Knapp, R.M., 1986. Effect of nitrate on biogenic sulfide production. Applied and Environmental Microbiology 51, 1205−1211.

Jing, G., Zhou, J., Zhou, Z., Lin, T., 2012. Reduction of Fe(III)EDTA$^-$ in a NO_x scrubbing solution by magnetic Fe_3O_4−chitosan microspheres immobilized mixed culture of iron-reducing bacteria. Bioresource Technology 108, 169−175.

Kampf, N., 2002. The use of polymers for coating of cells. Polymers for Advanced Technologies 13, 895−904.

Karunakaran, E., Biggs, C.A., 2011. Mechanisms of *Bacillus cereus* biofilm formation: an investigation of the physicochemical characteristics of cell surfaces and extracellular proteins. Applied Microbiology and Biotechnology 89, 1161−1175.

Kao, C.M., Chen, S.C., Liu, J.K., 2001. Development of a biobarrier for the remediation of PCE-contaminated aquifer. Chemosphere 43, 1071−1078.

Kaseamchochoung, C., Lertsutthiwong, P., Phalakornkule, C., 2006. Influence of chitosan characteristics and environmental conditions on flocculation of anaerobic sludge. Water Environment Research 78 (11), 2210−2216.

Kastner, M., Mahro, B., 1996. Microbial degradation of polycyclic aromatic hydrocarbons in soils affected by the organic matrix of compost. Applied Microbiology and Biotechnology 44, 668−675.

Krastanov, A., Yoshida, T., 2003. Production of palatinose using *Serratia plymuthica* cells immobilized in chitosan. Journal of Industrial Microbiology & Biotechnology 30, 593−598.

Lamarche, P., Lauzon, F., Tetreault, M., Barker, J.F., 2001. Biodegradation of a naphthalene plume in a funnel-and-gate system. In: Bioaugmentation, Biobarriers, and Biogeochemistry, the Sixth International In situ and On-site Bioremediation Symposium, San Diego, pp. 95−103.

Lauderdale, C., Chadik, P., Kirisits, M.J., Brown, A.J., 2012. Engineered biofiltration: enhanced biofilter performance through nutrient and peroxide addition. Journal of American Water Works Association.

Lee, Y., Shinb, H., Ahnc, Y., Shind, M., Leed, M., Yanga, J., 2010. Biodegradation of diesel by mixed bacteria immobilized onto a hybrid support of peat moss and additives: a batch experiment. Journal of Hazardous Materials 183, 940−944.

Lertsutthiwong, P., Boonpuak, D., Pungrasmi, W., Powtongsook, S., 2013. Immobilization of nitrite oxidizing bacteria using biopolymeric chitosan media. Journal of Environmental Sciences 25 (2), 262−267.

Lertsutthiwong, P., How, N.C., Chandrkrachang, S., Stevens, W.F., 2002. Effect of chemical treatment on the characteristics of shrimp chitosan. Journal of Metals, Materials Minerals 12 (1), 11−18.

Lertsutthiwong, P., Sutti, S., Powtongsook, S., 2009. Optimization of chitosan flocculation for phytoplankton removal in shrimp culture ponds. Aquacultural Engineering 41, 188−193.

Li, W., Liu, N., Cai, L.L., Jiang, J.L., Chen, J.M., 2011. Reduction of Fe(III) chelated with citrate in an NO_x scrubber solution by *Enterococcus* sp. FR-3. Bioresource Technology 102, 3049−3054.

Liu, J., Liu, C., Edwards, E., Liss, S., 2006. Effect of phosphorus limitation on microbial flock structure and gene expression in activated sludge. Water Science and Technology 54 (1), 247.

Low, W.L., Leea, C., Wilkesa, M., Roberts, C., Hill, D.J., 2014. Development of a rapid, effective method for seeding biofiltration systems using alginate bead-immobilized cells. International Journal of Chemical & Environmental Engineering 5 (1).

Lin, Q., Wen, D., Wang, J., 2010. Biodegradation of pyridine by *Paracoccus* sp. KT-5 immobilized on bamboo-based activated carbon. Bioresource Technology 101, 5229–5234.

Manju, N.J., Deepesh, V., Achuthan, C., Rosamma, P., Bright Singh, I.S., 2009. Immobilization of nitrifying bacterial consortia on wood particles for bioaugmenting nitrification in shrimp culture systems. Aquacult 294 (1–2), 65–75.

Mauclaire, L., Schurmann, A., Thullner, M., Gammeter, S., Zeyer, J., 2004. Sand filtration in water treatment plant: biological parameters responsible for clogging. Journal of Water Supply Research & Technology – Aquaculture 53 (2), 93.

Meyssami, B., Kasaeian, A.B., 2005. Use of coagulants in treatment of olive oil wastewater model solutions by induced air flotation. Bioresource Technology 96, 303–307.

Milhome, M.A.L., de Keukeleire, D., Ribeiro, J.P., Nascimento, R.F., Carvalho, T.V., Queiroz, D.C., 2009. Removal of phenol and conventional pollutants from aquous effluents by chitosan and chitin. Quimica Nova 32 (8), 2122–2127.

Miller, K.D., Johnson, P.C., Bruce, C.L., 2001. Full-scale in-situ biobarrier demonstration for containment and treatment of MTBE. Remediation Journal 12, 25–36.

Mutus B., 2014. Biopolymer-based biofilters for the removal of nutrients from agriculture-generated wastewater. Presented in Seminar at University of Windsor.

Muzzarelli, R.A.A., Rocchetti, R., 1974. Enhanced capacity of chitosan for transition-metal ions in sulphate–sulphuric acid solutions. Talanta 21, 1137–1143.

Nanda, S., Sarangi, P.K., Abraham, J., 2011. Microbial biofiltration technology for odour abatement. International Research Journal of Microbiology 2, 415–422.

Qiu, G.L., Li, Y.L., Zhao, K., 2006. *Thiobacillus thioparus* immobilized by magnetic porous beads: preparation and characteristic. Enzyme and Microbial Technology 39, 770–777.

Radetić, M.M., Jocić, D.M., Jovančić, P.M., Petrović, Z., Thomas, H.F., 2003. Recycled wool-based nonwoven material as oil sorbent. Environmental Science and Technology 37, 1008–1012.

Raffi, F., FlashEner, Y., Reuveny, G., 1999. Novel approaches for bioremediation of organic pollution. In: Atrazine Degradation in Wastewater. Springer Science + Business Media, New York.

Renault, F., Sancey, B., Badot, P.M., Crini, G., 2009. Chitosan for coagulation/flocculation processes – an eco-friendly approach. European Polymer Journal 45, 1337–1348.

Rezaee, A., Drayat, J., Mortazavi, S.B., 2005. Removal of mercury from chlor-alkali industry wastewater using *Acetobacter xylinum* cellulose. American Journal Environmental Sciences 1, 102–105.

Rezaee, A., Godini, H., Bakhtou, H., 2008a. Microbial cellulose as support material for the immobilization of denitrifying bacteria. Environmental Engineering and Management Journal 7 (5), 589–594.

Rezaee, A., Godini, H., Naimi, N., Masobaigi, H., 2008b. High nitrate removal in a packed bed bioreactor using microbial cellulose. Research Journal of Environmental Science 2 (6), 424–434.

Rhazi, M., Desbrières, J., Tolaimate, A., Rinaudo, M., Vottero, P., Alagui, A., 2002. Contribution to the study of the complexation of copper by chitosan and oligomers. Polymer 43, 1267–1276.

van Rijn, J., Barak, Y., 1998. Denitrification in recirculating aquaculture systems: from biochemistry to biofilter. In: Proceeding of the Second International Conference on Recirculating Aquaculture, Virginia.

van Rijn, J., Tal, Y., Schreier, H.J., 2006. Denitrification in recirculating systems: theory and applications. Aquacultural Engineering 34, 364–376.

Rinck-Pfeiffer, S., Ragusa, S., Sztajnbok, P., Vandevelde, T., 2000. Interrelationship between biological, chemical and physical processes as an analog to clogging in aquifer storage and recovery (ASR) wells. Water Research 34 (7), 2110.

Rizzo, L., Di Gennaro, A., Gallo, M., Belgiorno, V., 2008. Coagulation/chlorination of surface water: a comparison between chitosan and metal salts. Separation and Purification Technology 62, 78–85.

Rodrigo, S.V., Marisa, M., 2014. Chitosan as Adsorbent for Heavy Metal Ions: Performance and Adsorption Mechanism, pp. 149–175.

Rodrigues, A.C., Boroski, M., Shimada, N.S., Garcia, J.C., Nozaki, J., Hioka, N., 2008. Treatment of paper pulp mill wastewater by coagulation–flocculation followed by heterogenous photocatalysis. Journal of Photochemistry Photobiology A: Chemistry 194, 1–10.

Roussy, J., Van Vooren, M., Dempsey, B.A., Guibal, E., 2005. Influence of chitosan characteristics on the coagulation and the flocculation of bentonite suspensions. Water Research 39, 3247–3258.

Ruiz, G., Jeison, D., Rubilar, O., Ciudad, G., Chamy, R., 2006. Nitrification-denitrification via nitrite accumulation for nitrogen removal from wastewaters. Bioresource Technology 97 (2), 330–335.

Satoh, H., Okabe, S., Norimatsu, N., Watanabe, Y., 2000. Significance of substrate C/N ratio on structure and activity of nitrifying biofilms determined by in situ hybridization and the use of microelectrodes. Water Science and Technology 41 (4–5), 317–321.

Savant, V.D., Torres, J.A., 2000. Chitosan-based coagulating agents for treatment of cheddar cheese whey. Biotechnology Progress 16, 1091–1097.

Schlick, S., 1985. Binding sites of Cu^{2+} in chitin and chitosan. An electron spin resonant study. Macromolecules 19, 192–195.

Seo, Y., Bishop, P.L., 2008. The monitoring of biofilm formation in a mulch biowall barrier and its effect on performance. Chemosphere 70, 480–488.

Shan, H., Obbard, J.P., 2001. Ammonia removal from prawn aquaculture water using immobilized nitrifying bacteria. Applied Microbiology and Biotechnology 57 (5–6), 791–798.

Son, H.J., Kim, H.G., Kim, K.K., 2003. Increased production of bacterial cellulose by *Acetobacter* sp. V6 in synthetic media under shaking culture conditions. Bioresource Technology 86, 215–219.

Sorlier, P., Denuzière, A., Viton, C., Domard, A., 2001. Relation between the degree of acetylation and the electrostatic properties of chitin and chitosan. Biomacromolecules 2, 765–772.

Strand, S.P., Vårum, K.M., Østgaard, K., 2003. Interactions between chitosans and bacterial suspensions: adsorption and flocculation. Colloids and Surfaces B: Biointerfaces 27 (1), 71–81.

Strickland, J.D.H., Parson, T.R., 1972. A Practical Handbook of Seawater Analysis, second ed. Fisheries Research Board of Cannada, Ottawa.

Tabassum, N., Rafique, U., Balkhair, K.S., Ashraf, M.A., 2014. Chemodynamics of methyl parathion and ethyl parathion: adsorption models for sustainable agriculture. Biomed. Res. Int. 2014, 1–8, 831989. http://dx.doi.org/10.1155/2014/831989.

Tsai, S., Lin, C., Wuc, C., Xind, B., 2012. Cell immobilization technique for biotrickle filtering of isopropyl alcohol waste vapor generated by high-technology industries. Journal of Chemical Technology & Biotechnology. http://dx.doi.org/10.1002/jctb.3836. wileyonlinelibrary.com.

Ungureanu, G., Santos, S., Boaventura, R., Botelho, C., 2015. Arsenic and antimony in water and wastewater: overview of removal techniques with special reference to latest advances in adsorption. Journal of Environmental Management 151, 326−342.

Van Duin, P.J., Hermans, J.J., 1959. Light scattering and viscosities of chitosan in aqueous solutions of sodium chloride. Journal of Polymer Science 36, 295−304.

Wada, S., Ichikawa, H., Tatsumi, K., 1995. Removal of phenols and aromatic amines from wastewater by a combination treatment with tyrosinase and a coagulant. Biotechnology and Bioengineering 45, 304−309.

Wang, Z., Wu, Z., Tang, S., 2008. Extracellular polymeric substances (EPS) properties and their effects on membrane fouling in a submerged membrane bioreactor. Water Research 43 (9), 2504.

Wibowo, S., Velazquez, G., Savant, V., Antonio, T.J., 2007. Effect of chitosan on protein and water recovery efficiency from surimi wash water treated with chitosan−alginate complexes. Bioresource Technology 98, 539−545.

Wu, Z.B., Ni, W.M., Guan, B.H., 2008. Application of chitosan as flocculant for coprecipitation of Mn(II) and suspended solids from dual-alkalin FGD regenerating process. Journal of Hazardous Materials 152, 757−764.

Yerushalmi, L., Manuel, M.F., Guiot, S.R., 1999. Biodegradation of gasoline and BTEX in a microaerophilic biobarrier. Biodegradation 10, 341−352.

Zeng, D., Wu, J., Kennedy, J.F., 2008. Application of a chitosan flocculant to water treatment. Carbohydrate Polymers 71, 135−139.

Zhang, S.H., Cai, L., Mi, X.H., Jiang, J.L., Li, W., 2009. NO_x removal from simulated flue gas by chemical absorption − biological reduction integrated approach in a biofilter. Environmental Science and Technology 42, 3814−3820.

Zhou, S.Q., Zhang, X.J., Feng, L.Y., 2010. Effect of different types of electron acceptors on the anoxic phosphorus uptake activity of denitrifying phosphorus removing bacteria. Bioresource Technology 101, 1603−1610.

Biopolymers for superhydrophobic photocatalytic coatings

18

A.Z.M. Rus
University Tun Hussein Onn Malaysia (UTHM), Batu Pahat, Johor, Malaysia

18.1 Introduction

Environmental pollution and destruction on a global scale has drawn attention to the vital need for new, safe and clean chemical technologies and processes, the most important challenge facing chemical scientists for the twenty-first century. Developments in organic chemistry and fundamental knowledge on the physics and chemistry of paints and coatings are providing solutions to these problems. This has resulted in the development of coating formulations with much improved performances that are based on renewable resources (Anika Zafiah et al., 2014). One useful application for biopolymer composites could be in the construction industry as applied in the coating field.

Polymeric materials are commonly used as long-lasting products in engineering applications that bring a significant contribution to sustainable development. This is also in view of the wider range of disposal options with minor environmental impact. Biopolymers and admixtures have been developed from natural oils like epoxidized palm oil that has been used as a monomer for production of resins. These vegetable oils have their own particular advantages; for example, they are renewable products derived from natural oils and fats. Hence, their impact on the environment is less.

Organic coatings are commonly employed to protect a large variety of materials against photo-ageing and corrosion, as well as to improve surface properties. Such varnishes, lacquers or paints are usually made of highly cross-linked polymers which must exhibit a great resistance to solar radiation, moisture, pollutants and chemicals to ensure long-lasting protection. By lowering the mobility of the polymer chains, the network structure reduces the extent of both the production of initiating species (cage effect) and the propagation step, thus making cross-linked polymers more resistant to photo-oxidation. The durability of organic coatings can be further enhanced by the addition of light stabilizers (Decker et al., 1994).

By incorporating stabilizers or other means, the biopolymer coating from renewable resources is more stable to heat or light; formulated to provide self-cleaning surfaces based on two principal ways: (1) the development of photocatalytic superhydrophilic properties, and (2) if such a superhydrophilic is illuminated by light, the grease, dirt and organic contaminants will be decomposed. The applications of metal oxide fillers as polymer additives include superhydrophobic photocatalysis as a self-cleaning

Biopolymers and Biotech Admixtures for Eco-Efficient Construction Materials. http://dx.doi.org/10.1016/B978-0-08-100214-8.00018-X
Copyright © 2016 Elsevier Ltd. All rights reserved.

coating and photovoltaic solar cell (Anika Zafiah et al., 2009; Anika and Kemp, 2008). Hence, the quality of the physical properties of the biopolymer can be upgraded as desired.

18.2 Survey of approaches to biopolymers from renewable resources

Realizing that the supply of fossil resources is inherently finite and the growing concern for environmental issues involving volatile organic solvent emission recycling or waste disposal problems at the end of a resin's economic lifetime, it is considered crucial to develop polymers from a more sustainable source. A favourable sustainable source would be from renewable materials.

Oils and fats (animal or vegetable in origin) have long been identified as possible substitutes for petrochemical derivatives in the production of polymers for many applications (Adhvaryu and Erhan, 2002; Blayo et al., 2001). This might result in a new order by placing agricultural industry amongst the largest wealth-generating sectors. These products are materials which are synthesized by sunlight. Natural products or crops such as sugar, starch, cellulose or proteins and natural fats and oils could act as the fundamental material to replace currently used plastics, as well as make new plastics with never-before-seen properties.

Oils and fats are triglycerides which are esters of glycerin and saturated and unsaturated fatty acids. These triglycerides offer two reactive sites, the double bond in the unsaturated fatty acid chain and the ester group. Ninety percent of the derivatization reactions are carried out at the carboxylic group. Only 10% of oleochemical reactions involve the alkyl chain or the double bond. For most other uses, oils and fats must be split into the so-called oleochemical base material: fatty acids, glycerol and, as hydrogenation products of the fatty acid methyl esters, fatty alcohols (Bauman et al., 1988). Oleochemicals are chemicals derived from biological oils or fats. Palm, soybean, rapeseed and sunflower oil, as well as animal fats such as tallow, contain mainly long-chain fatty acids (e.g. C-18, saturated and unsaturated) and are used as raw materials for polymer applications and lubricants (Kreienfeld and Stoll, 1997; Robbelen, 1994).

Most plastic products currently are made from petroleum-based synthetic polymers that do not degrade in a landfill or in a compost-like environment. Based on results from cycle analyses and ecological and toxicological studies for selected cases, one can assume that products based on renewable resources are usually much more ecologically compatible when compared with petrochemical-based substances; an important criterion in the development of a new product, just as significant as price performance (Steber, 1991; Patel et al., 1991). Therefore, because the disposal of petroleum-based products poses a serious long-term environmental problem, an environmentally conscious alternative is to design or synthesize biodegradable polymers.

Nowadays, plants could provide a renewable, biodegradable source of high-value specialty products such as nylon, glue, paints, cosmetics, lubricants and components of detergents or plastics. These could all be produced from plants rather than fossil or petroleum-based materials. The sustainability of this industrial sector is highly dependent in the long term on a fundamental shift in the way in which resources are used. This shift is from nonrenewables to renewables, from high levels of waste to those of reuse and recycling and from products based on lowest first cost to those based on life cycle costs and full cost accounting, especially as applied to waste and emissions from the industrial processes that support construction activity (Kibert and Sendzimir, 2002).

Over the next several decades, plant oils will become just as essential to everyday life as fossil fuels are today. This is due to the enthusiastic scientists who are interested in making plastics from plants because it can produce an amazing array of compounds that could be used for monomers in plastics. Monomers are the individual molecules that form the chains called plastic or polymer. Moreover, plant oils and fats have the same base chemical structure as petroleum. Both are made up of chains of chemicals known as hydrocarbons. A hydrocarbon is a carbon atom surrounded by hydrogen atoms. Methane is the simplest hydrocarbon in which a carbon atom is surrounded by four hydrogen atoms.

18.3 Development of biopolymer from renewable resources

The development of novel feedstocks of biopolymers derived from renewable materials has become important because the use of biopolymers is increasing at a rate of one million tonnes a year (Anika Zafiah et al., 2009). This level is unsustainable in the long term without the development of alternative sources. Oils from vegetable crops can be manipulated chemically to produce a variety of polymeric materials, including polyurethane products. The reaction of organic isocyanate with compounds containing OH (hydroxyl) groups is capable of wide application in polymer formation (Barnes et al., 2000). Thus, the urethane linkage, $-(\mathrm{NHCOO})-$ can be produced by reacting compounds containing active hydrogen atoms with isocyanate, in which polymer formation can take place if the reagents are di- or polyfunctional, according to the following reaction:

$$\underset{\text{isocyanate}}{\mathrm{RNCO}} + \underset{\text{hydroxyl group/(diols)}}{\mathrm{ROH}} \rightarrow \underset{\text{urethane}}{\mathrm{RNHCOOR}}$$

Although the unsaturated vegetable oils such as rapeseed or *Euphorbia* do not contain the necessary hydroxyl group as a chemical functionality for making polyurethane polymers, they contain oleic acid and vernolic acid, respectively (refer to Figure 18.1). These fatty acids can be manipulated by the introduction of Venturello's catalyst and hydrogen peroxide to give epoxides, followed by ring opening to form polyols. Thus, hydroxylated feedstocks are available for use in the polyurethane and polyester sector. Moreover, the epoxides can be used for making epoxy resins.

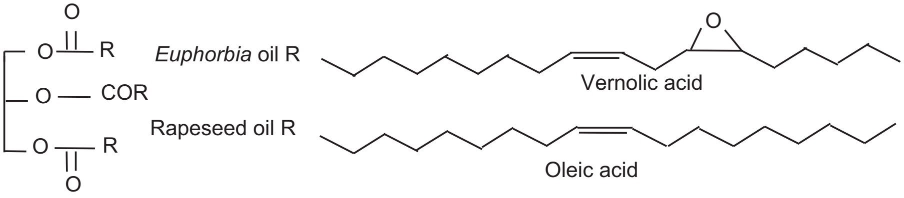

Figure 18.1 Renewable vegetable oils that are rich in fatty acids.

The only process currently used industrially for the epoxidation of unsaturated oils uses performic acid generated in situ from hydrogen peroxide and formic acid. This is currently used on the tonne scale for the production of epoxidized soybean oil (Anika Zafiah et al., 2009). However, there are several other methods for the generation of epoxides from unsaturated fatty compounds. These include the use of dioxiranes, hydrogen peroxide/methyl trioxorhenium and hydrogen peroxide/peroxyphosphotungstenates (Anika Zafiah et al., 2009).

The conversion of an unsaturated oil to the corresponding epoxide can be done by reacting Venturello's catalyst, $Q_3PO_4[W(O)(O)_2)_2]_4$ (in which Q is a phase-transfer catalyst, typically based on a quaternary nitrogen atom) (Venturello et al., 1983) in conjunction with hydrogen peroxide to convert the unsaturated group to the corresponding epoxide. The reaction can be accomplished without the use of a solvent because the active form of the catalyst is able to dissolve both in the aqueous phase and in the fatty acid phase of the reaction mixture, as long as the reaction mixture is properly emulsified (Barnes et al., 2000).

A phase-transfer catalyst such as Adogen 464 [methyltrialkyl (C_8—C_{10}) ammonium chloride] can be used and added to the tungsten powder, hydrogen peroxide and phosphoric acid to form this catalyst. However, Venturello's catalyst is normally added directly to the reaction mixture when the reaction time may vary from around an hour at 100 °C, to a few days at room temperature.

A second reaction is necessary whereby the polyepoxides are converted to the polyols by acid-catalyzed ring opening of the epoxides. Harsh conditions are required, namely 50% phosphoric acid (by weight with respect to the natural oil), 100 °C and vigorous stirring. The scheme of conversion of the unsaturated vegetable oils to the polyols (necessary to produce polyurethane polymer) is shown in Figure 18.2. The advantage of the *Euphorbia lagascae* oil, which is rich in vernolic acid, is that it only needs a single process to effect ring opening by using aqueous acid (phosphoric acid) to produce low hydroxylated monomer.

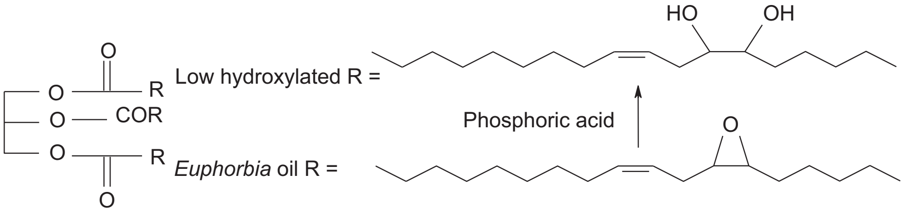

Figure 18.2 Preparation of low hydroxylated *Euphorbia*.

The chain extenders used are polyols or glycols and diamines (NH_2). The polyols can be ethylene glycol, diethylene glycol, propylene glycol, 1,4-butanediol etc. (Rasshofer et al., 1991). Cast polyurethanes are obtained at a ratio of isocyanate to −OH and/or NH_2 groups close to the stoichiometric value ($I_{NCO} \approx 1$) (Wirpsza, 1993). The final stoichiometry depends on the reaction conditions, namely time, temperature and concentration.

In this reaction the reaction centre has two neighbouring hydroxyl groups, If R (refer to Figure 18.3) is a short-chain segment, e.g. ethylene or butylenes, and diisocyanate is an aromatic unit, then the long and flexible polyethylene (PE) segments are connected by short and stiff blocks. For a given polyol−isocyanate system, the higher the OH content of the polyol, the greater the degree of cross-linking and hence the more rigid the polyurethane.

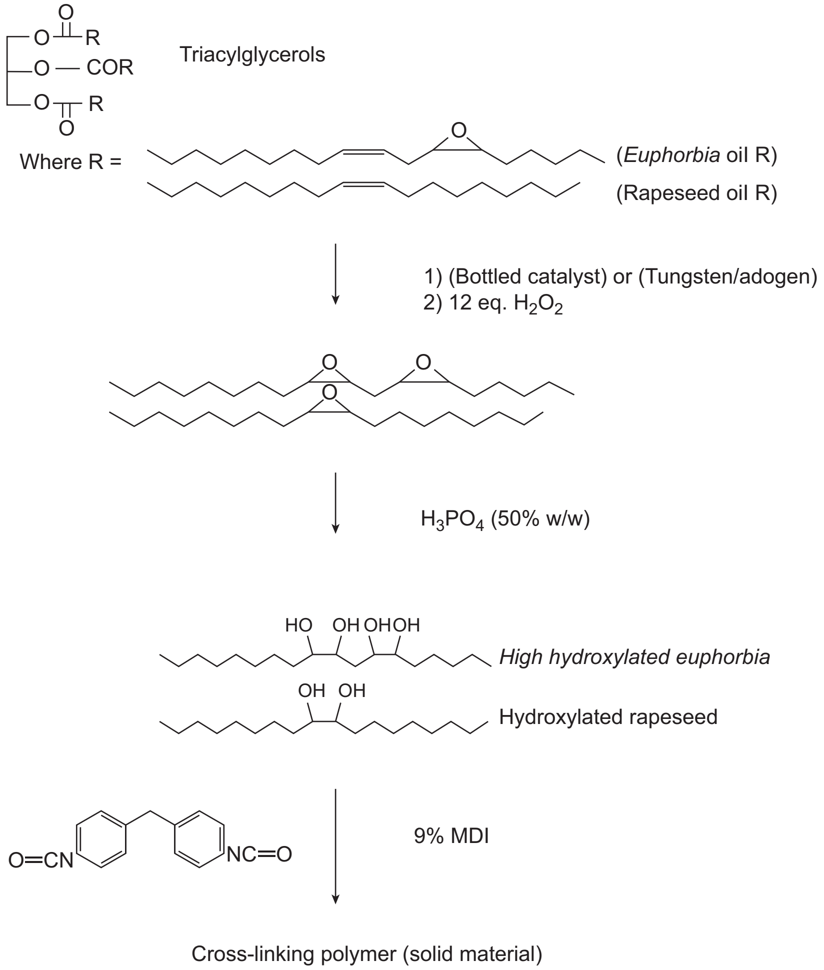

Figure 18.3 Preparation of hydroxylated vegetable monomers: Condensation method (Anika Zafiah et al., 2009).

Polyurethanes (PUs) are also one of the most important groups of polymers because of their versatility and because they can be manufactured in a wide range of grades, densities and stiffnesses.

18.4 Service life of biopolymers

All polymers undergo degradation, such as hydrolysis, photolysis, solvolysis, thermolysis, biologically induced environmental stress cracking, oxidation and microbial attack. The exposure of polymers to high temperatures or ultraviolet (UV) light over time generally leads to deterioration in their physical properties.

The evaluation of the resistance to weathering of materials can be done by direct outdoor weathering, but, for most purposes, it is more practical in economic and time consumption terms to assess the materials performance by exposing it to artificial light sources that accelerate the degradation. Degradation of polymeric materials by exposure to solar radiation or light is referred to as photo-oxidation. It is a free radical process, progressing even at low temperatures by the combined action of light and oxygen. Thermal oxidation is always superimposed on photo-oxidation.

Under the action of sunlight, polymer materials undergo a series of oxidative reactions that lead to chemical degradation, with consequences like brittleness, loss of brightness, colour change, opacity and formation of surface cracks. Besides the reduction in molecular weight, a number of changes take place in the molecules during photodegradation with the formation of chemical groups like carbonyl, carboxylic acids and hydroperoxides (Rabek, 1996). Henceforth, to ensure a long service life of the biopolymers, it is essential to understand and study the degradation processes which occur.

Generally, photochemical reactions, or those following photolysis, are (Brown, 1988):

1. photophysical processes, involving the transition of an electron from a bonding orbital to a nonbonding or antibonding orbital, and its subsequent return; and
2. those steps involved through a free-radical chain mechanism, starting with bond haemolysis.

Meanwhile, the irradiation of polyurethanes with UV light leads to many possible changes in their structures. The changes are (Rek and Bravar, 1983):

1. formation of quinoid structures (yellowing of polyurethane coating);
2. homolytic scission of bonds in the urethane groups on further irradiation leading to the formation of free radicals;
3. recombination and formation of new structures such as amino, azo- and carbodiimide;
4. addition of oxygen to the free radical yields hydroperoxide ($\bullet OOCH_2$), the decomposition of which leads to carbonyl-containing structures;
5. destruction of material during the formation of new structures, which causes further darkening of the irradiated samples; and
6. formation of gaseous products such as CO and CO_2. Also small amounts of formaldehyde and H_2O can be formed (Figure 18.4).

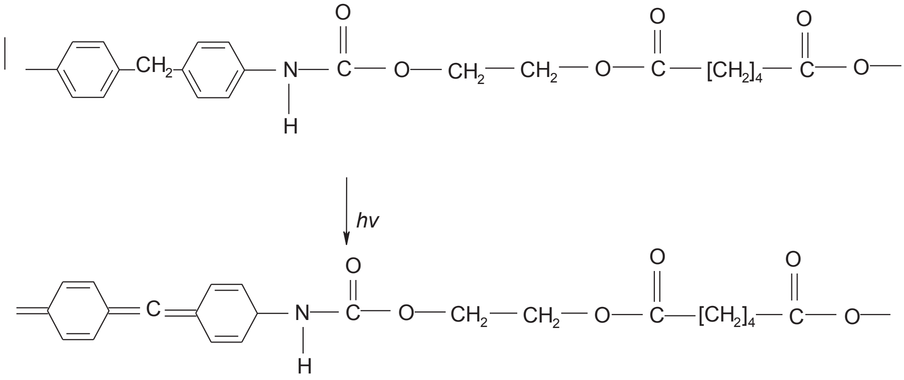

Figure 18.4 Formation of quinoid structures.

18.5 Modification of biopolymers using fillers

Fillers, either particulate or of fibrous nature, such as glass, metal oxides, natural fibres and metals, have been added to thermoplastics and thermosets for decades to form polymer composites. Fillers are used in polymers for a variety of reasons: cost reduction, improved processing (for example in curing with a cross-linking agent such as in sulphur vulcanization), density control, optical effects, thermal conductivity, control of thermal expansion; electrical properties; magnetic properties, flame retardancy and improved mechanical properties, such as hardness and tear resistance and many more reasons.

18.5.1 Benefit of fillers for biopolymers

The global demand for fillers or reinforcing fillers, including calcium carbonate, aluminium trihydrate, talc, kaolin, mica, wollastonite, glass fibre, aramid fibre, carbon fibre and carbon black for the plastics industry is estimated about 15 million tonnes (Xanthos, 2005). The primary end-use markets are construction, furniture, packaging and automotive industrial. Automotive interior and underhood parts and electrical connectors and microwaveable containers are examples of applications requiring high-temperature resistance (Mahajan, 2003).

The term ‘functional filler’ is often used to describe materials that do more than provide cost reduction. Examples of functional fillers include carbon black and precipitated silica reinforcements in tyre treads, the role of stabilizers to reduce in-process degradative effects, and many more miscellaneous additives for polymers such as blowing agents, impact modifiers, lubricants or antimicrobials. Increased polymer consumption over the past 20 years has not only stimulated developments in manufacturing plants, but has also led to a parallel growth in the usage of a large variety of liquid and solid modifiers, including fillers and reinforcements.

Fillers may be classified broadly as organic or inorganic substances, and further subdivided according to chemical family as tabulated in Table 18.1. In a recent review,

Table 18.1 Chemical families of fillers for plastics (Mahajan, 2003)

Chemical family	Examples
Inorganic	
Oxides	Glass (fibres, spheres, hollow spheres, flakes), MgO, SiO_2, Al_2O_3
Hydroxides	$Al(OH)_3$, $Mg(OH)_2$
Salts	$CaCO_3$, $BaSO_4$, $CaSO_4$, phosphates
Silicates	Talc, mica, kaolin, wollastonite, montmorillonite, nanoclays, feldspar, asbestos
Metals	Steel
Chemical elements	Boron
Organic	
Carbon, graphite	Carbon fibres, graphite fibres and flakes, carbon nanotubes, carbon black
Natural polymers	Cellulose fibres, wood flour and fibres, flax, cotton, sisal, starch
Synthetic polymers	Polyamides, polyesters, aramid, polyvinyl alcohol fibres

more than 70 types of particulates or flakes and more than 15 types of fibres of natural or synthetic origin have been used or evaluated as fillers in thermoplastics and thermosets (Bierman, 1983).

The classification of polymer additives is according to their primary function and a plethora of additional functions. The scheme adopted by Xanthos involves classification of fillers according to five primary functions as shown in Table 18.4. From the point of view of this research, TiO_2 should be added as an optical agent. TiO_2 has an important role as a (white) colourant in synthetic polymers such as poly(vinyl chloride) which is used as a building material (windows, doors, fascia boards) and polyethylene film (the familiar supermarket shopping bag material) (Kemp and McIntyre, 2006).

- Fibrous fillers

  A search has been made for plant fibres with optimal material properties for structural purposes in composite materials (Dahlke et al., 1998), and the most well-known example of the use of a fibrous filler is in glass fibre-reinforced plastic (GFRP) in which the synthetic polymer is most often a polyester or a poly(vinyl ester), but other plastics, like epoxy (glass-reinforced epoxy (GRE)), are also sometimes used. The use of natural fibres, such as flax, hemp, sisal or yucca, is of increasing interest for various applications, amongst them the automotive industries, in which the composites can be used in door pockets, covers, instrument panels and sound insulation.

  In addition, those fibres obtained from plants such as hemp, kenaf, sisal or flax, when combined with suitable resins, can give cost-effective materials for many applications. Physical methods include stretching, calendering, thermal treatment and electronic discharge. Meanwhile, chemical methods include alkali treatment, treatment with compatibilizers and other coupling agents. Plant fibres are known to have very high strength and can be effectively utilized for many load-bearing applications. A comparative study between different types of natural fibre–polyester resin composites on the basis of strength and cost has been reported (Bledzki and Gassan, 1999) and the addition of such fillers to composites is made for technical and economic reasons.

- Particulate fillers

  The most widely used mineral particulate fillers in polymer composites are calcium carbonate $CaCO_3$ (as chalk or limestone), china clay, mica, microspheres, silica and talc. New organic fillers have also entered commercial markets, including corn cobs, flour fillers etc. Similarly, newly developed ceramic microspheres and their metal-coated forms have recently found application in aerospace and conductive plastics (Ray et al., 2002).

  Inorganic materials are very attractive because they have the advantages of high mechanical strength, good chemical resistance, thermal stability or enhanced optical properties. As inorganic fillers, a range of different metal-oxide particles can be dispersed into the polymeric matrix (Schmidt et al., 2000). Examples of inorganic pigments include titanium dioxide, iron oxides and zinc chromate. As a practical matter, the particle size of the particulate materials should not be greater than 1 mm, and preferably from 0.1 to 500 μm (Cho et al., 2005).

- Nanocomposite fillers

  A growing interest in polymer material has been in polymer nanocomposites. Polymer nanocomposites are a mixture of organic polymer matrix and nanoscale fillers. The advantages in the application of these polymer nanocomposites in automotive parts are their greater stiffness, saving of weight, improved surface quality, less brittleness at low temperatures and being easily recyclable (Harris, 2003).

  For structural applications, composites have become very popular and are sold in billion pound quantities because these composites, compared to neat resins, show improved properties including tensile strength, heat distortion temperature and modulus. Clearly, the idea of adding fillers to thermoplastics and thermosets to improve properties, and in some cases to decrease costs, has been very successful for many years.

18.6 Titanium dioxide as polymer stabilization and photocatalysis agent

Titanium dioxide (titania, TiO_2) is a semiconductor, with a band gap of 3.1 eV for rutile (Diebold, 2000). The high refractive index ($n = 2.4$) and bright white colour of titanium dioxide makes it an effective opacifier for pigments. One of the major advantages of the material for applications in exposed conditions is its resistance to discolouration under UV light. Even in mildly reducing atmospheres, titania tends to lose oxygen and become sub-stoichiometric. In this form, the material becomes a semiconductor and the electrical resistivity of the material can be correlated to the oxygen content of the atmosphere to which it is exposed.

In photocatalytic purification of water, it is the •OH radical which plays the major role. OH• will react with nearby organic molecules causing them to become oxidized. For example, TiO_2 is also suitable for photocatalysis (Mayadevi et al., 2000) because it is nontoxic and chemically stable. TiO_2-based materials are widely applicable in many areas because of these properties. The applications of TiO_2 as polymer additives include inorganic membranes (Mayadevi et al., 2000), photovoltaics (Thelakkat et al., 2002), optics (Frindell et al., 2002), catalysis (Stark et al., 2001) and gas sensors (Ferroni et al., 2001; Morris et al., 2001).

In the past two decades, TiO_2 heterogeneous photocatalyst has been extensively investigated (Fujishima, 2000; Anpo, 2000). In addition to its low cost, biocompatibility and nontoxicity, the relatively high photo-efficiency of TiO_2 in decomposing some inorganic pollutants, have made this material one of the best candidates for environmental treatments and purification purposes. TiO_2 is used in heterogeneous catalysis (Diebold, 2002) and ways have been identified to make this catalyst more efficient and more applicable such as in thin and thick film coatings, powders and membranes (Arana, 2002).

Anpo (2000) found that thin TiO_2 films have been found to exhibit a unique and useful function (i.e. a superhydrophilic property). Usually, metal oxide surfaces such as TiO_2 become cloudy when water is dropped on them because the contact angle of the water droplet and the surface is 50°–80°. However, under UV light irradiation this contact angle becomes smaller, its extent depending on the irradiation time. Thus, under UV light irradiation, titanium oxide surfaces never become cloudy, even in the rain. In a similar study by Anika Zafiah et al. (2013), biopolymer doped with TiO_2 superhydrophobic photocatalysis can be a self-cleaning coating for lightweight composites.

Kobayashi and Kalriess (1997) studied the photocatalytic activity of TiO_2 and ZnO, and they concluded that TiO_2, especially the ultrafine grades supplied with inorganic coatings, such as Al_2O_3 and/or ZrO_2, can lower the photoreactivity, whereas ZnO does not require inorganic coatings to ensure good light stability. Another study by Mukherjee (2011) found that the characterization of TiO_2/polymeric film as photocatalyst acts in the photocatalytic degradation of methyl orange under UV light.

A review of the anatase-to-rutile phase transformation of TiO_2 by Hanaor and Sorrel (2011) mentioned that at all temperatures and pressures, rutile is the stable phase of TiO_2 whereas anatase is metastable. However, anatase can be considered to be kinetically stabilized at lower temperatures at which TiO_2 is an important photocatalytic material that exists as two main polymorphs, anatase and rutile. However, Gesenhues (2000) studied a nanocrystalline rutile powder, an anatase white pigment and a photoactive as well as a photostable rutile pigment to examine their influence of TiO_2 on the photodegradation of poly(vinyl chloride). Research on TiO_2 as photocatalyst is summarized in Table 18.2.

18.7 Biopolymers as superhydrophobic photocatalytic coatings

Uses of sustainable industrial products have been widely studied for suitability in construction. It has been possible to assess the feasibility of using filler in concrete construction and investigate means of exploiting the inherent strength, durability and physical characteristics. In the case of coatings such as surfaces of roofing tiles are often more exposed to climatic conditions than the other exterior elements of a

Table 18.2 **Various research on the TiO_2 photocatalyst**

Research study	Photocatalyst	Author
The effect of nano-particle TiO_2 fillers on structure and transport in polymer electrolytes	TiO_2 (Degussa P-25, 21 nm, dried at 250 °C for 24 h)	Forsyth et al. (2002)
Photocatalytic activity and biodegradation of polyhydroxybutyrate (PHB) films containing TiO_2	Nanosized TiO_2 photocatalysts (P-25, ca. 80% anatase, 20% rutile; BET area, ca. 50 $m^2\ g^{-1}$) provided by JJ Degussa Co., Malaysia	Saw et al. (2006)
Biopolymer doped with different percentages of superhydrophilic photocatalysis filler of TiO_2 superhydrophobic photocatalysis as self-cleaning coating for lightweight composite (LC)	Doped with different percentages of superhydrophilic photocatalysis fillers of TiO_2 named as TOP which were 1.0%, 1.5%, 2.0% and 2.5% equivalent to weight of monomer	Anika Zafiah et al. (2013)
Influence of N_2 and H_2O of UV-irradiated biopolymer composite	10% TiO_2 Kronos	Anika Zafiah et al. (2014)

building. With few exceptions, surfaces which are not protected by adjoining buildings are generally fully exposed to wind, precipitation, temperature variations and sunlight.

Biopolymers doped with superhydrophilic fillers provide self-cleaning and act as multifunctional coatings to prevent attack by algae and moss. Superhydrophilic fillers of titanium dioxide, particularly in the anatase form, is the most widely used photocatalyst. Besides the breakdown of organics, a second light-induced phenomenon called superhydrophilicity occurs in parallel on such a photocatalytic surface. Coatings are also designed to provide self-cleaning on the surfaces based on two principal ways of development of superhydrophobic or superhydrophilic materials.

When water droplets encounter a superhydrophobic surface (contact angle $>150°$ as refer to Figure 18.5 (a) meanwhile Figure 18.5 (b) is without superhydrophobic surface property) from nearly spherical beads, the contaminants, either inorganic or organic, on such surfaces are picked up by the water droplets or adhere to them and are removed from the surface when the water droplets roll off. Figure 18.6 shows the self-cleaning properties of surfaces with and without superhydrophilicity. The surfaces with superhydrophobic show that the self-cleaning mechanism has successfully been developed on the surfaces. The leaf of a lotus plant has a water-repellent wax cover which makes rain droplets fall off the surface without spreading. The reason for this is the minimal contact between the surface and a droplet of water. If a rain droplet

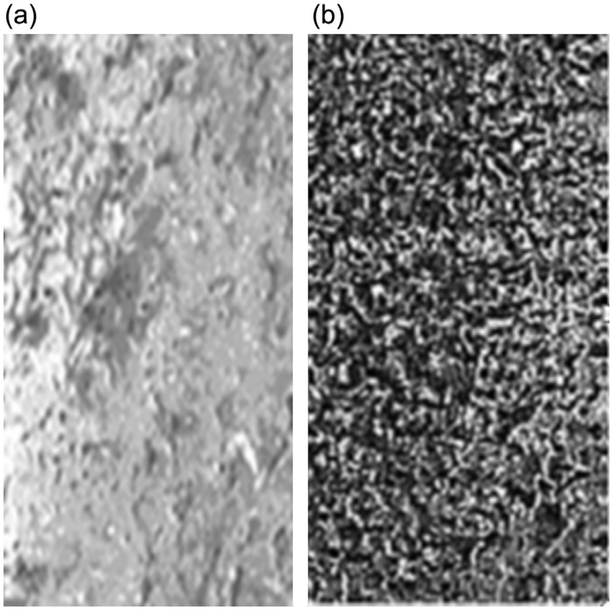

Figure 18.5 Biopolymer coating of (a) superhydrophobic surface and (b) without superhydrophobic surface.

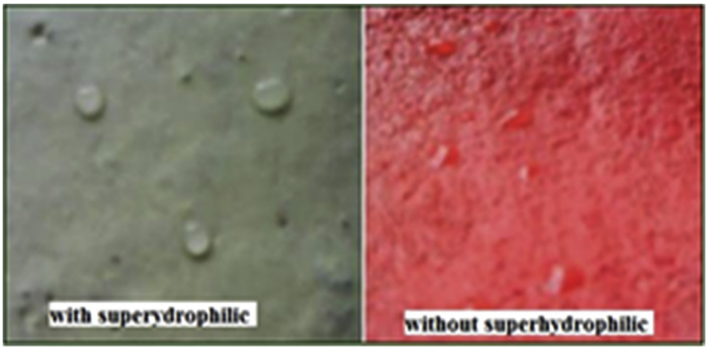

Figure 18.6 Biopolymer coating with superhydrophobic surface show self-cleaning property.

hits the leaf surface, it will immediately run off and will carry dirt deposits from the surface, thus leaving the leaf clean (Figure 18.6).

The ability of a coating on any type of surface to absorb water and wash the surface free of dirt or bacteria helps to retain the original surface structure that can be exposed to sunlight and humidity on the long term.

Photocatalysis is a technique whereby light is used to irradiate the surface of a semiconductor material to achieve the transformation of a molecule in contact with the surface, either in solution or in the gas phase.

When photons of light with energy of *hv* that exceeds the energy of the band gap, an electron (e^-) is promoted from the valence band (VB) to the conduction band leaving a hole, h^+ behind. The hole, h^+, can oxidize donor molecules such as H_2O or OH^- ion to create an OH• radical.

$$h^+{}_{VB} + OH^- \rightarrow OH\bullet$$

$$h^+{}_{VB} + H_2O \rightarrow H^+ + OH\bullet$$

When the high-energy electron returns to the electron hole in a 'recombination reaction', the energy is then released as heat. It can also transfer via the conduction band to a neighbouring oxygen molecule to produce an $O_2\bullet^-$ radical, known as superoxide ion.

$$e^-{}_{CB} + O_2 \rightarrow O_2\bullet^-$$

The $O_2\bullet^-$ radical quickly reacts with H_2O to form a hydroperoxyl radical, $HO_2\bullet$

$$O_2\bullet^- + H_2O \rightarrow HO_2\bullet + OH^-$$

The total reaction can be written:

$$\text{UV light} + O_2 + H_2O \rightarrow HO_2\bullet + OH\bullet$$

According to Hanaor and Sorrell (2011), the importance of TiO_2 addition as a filler or pigment has been investigated, and it is well accepted that the protective action of this compound depends on its crystal form, rutile or anatase. In the rutile form, the hydroxyl groups (OH) present on the filler surface are rather stable, whereas in the anatase crystal form they are very reactive and can initiate polymer degradation. They also state that, at all temperatures and pressures, rutile is the stable phase of TiO_2.

Anpo and Takeuchi (2001) have studied the design and development of second-generation TiO_2 photocatalysts which absorb UV—visible light. These work as efficient photocatalysts under irradiation in the UV—visible light regions and were successfully studied by applying advanced metal ion-implantation techniques.

Anika Zafiah et al. (2014) reported on the effect of UV light on the Fourier transform infrared (FTIR) spectra of biopolymer doped with 10% TiO_2 in a gas cell filled with nitrogen gas (N_2) and a droplet of water (H_2O). The TiO_2 as a catalyst was added into the bio-polymer to absorb UV radiation from sunlight, which accelerates the oxidation process in the atmosphere and decomposes any airborne toxic organic matter.

The high energy of TiO_2 would react directly with nitrogenous substances to form chemical adsorb unstable intermediate, and this intermediate could form nitrogen doping in the subsequent thermal treatment. The surface of biopolymer/TiO_2 resulting in the formation of the doped nitrogen may demonstrate chemical adsorption occurring between the Ti atom and the N atom. The nitrogen atom has unpaired electrons which may be easily adsorbed on Ti. The most probably existing bond in this system is O_2 Ti—N—H,

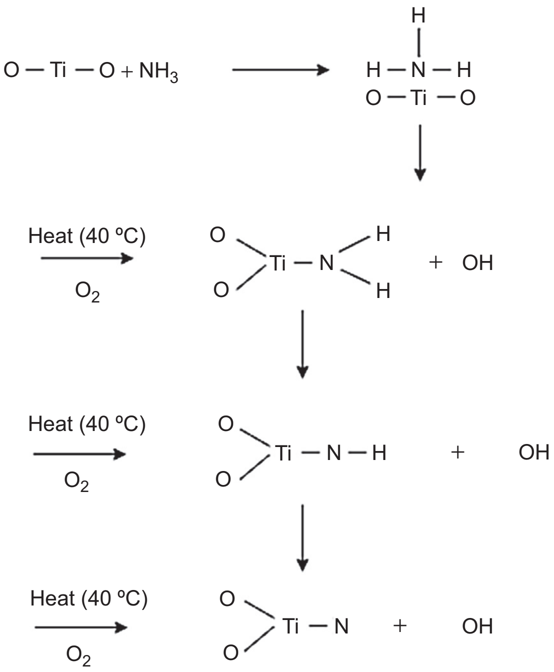

Figure 18.7 Doping mechanism of nitrogen on titanium dioxide (Yu et al., 2012).

and this indicates the chemical adsorption occurring between the Ti atom and the N atom as referred to in Figure 18.7 on the mechanism of nitrogen and titanium dioxide.

It has been reported that the nitrogen-doped TiO_2 could improve visible light absorption efficiency with the characterization of a catalyst (Yu et al., 2012).

18.7.1 Artificial weathering for determination of physical and mechanical properties of biopolymers

The terms ‘weathering’ may be used to describe changes developed by the action of the weather that add to the aesthetics of a building and give character to its materials. Although weathering is accurate description for the behaviour of building stone that is exposed to exterior environmental conditions, it is preferable that the term weathering include all those changes, desirable and undesirable, caused by the weather that can possibly lead to dangerous conditions.

According to Singh and Sharma (2007), weathering is a degradation process and as such is temperature dependent, i.e. it will occur more rapidly at higher temperatures. The general rule is that for every 10 °C increase in temperature the reaction rate will double. Tropical areas therefore suffer not only from an increase in UV exposure but also faster reaction rates because of the increased temperatures. Humidity also affects the degradation processes; most weathering processes are considerably slower in hot dry climates than in hot wet climates.

Performance during use is a key feature of any composite material, which decides the real fate of products during use in outdoor applications. Whatever the application, there is often a natural concern regarding the durability of polymeric materials partly because of their useful lifetime, maintenance and replacement. The deterioration of these materials depends on the duration and the extent of interaction with the environment (Pandey et al., 2005). The use of biopolymers as building products has resulted in concern about the durability of these products when exposed to outdoor environments. Outdoor durability may include thermal stability, moisture resistance, fungal resistance and ultraviolet (UV) stability. UV exposure, for example, can cause the composites to undergo photodegradation leading to undesirable effects, including a loss in mechanical properties and surface quality, i.e. surface micro-cracking and colour change (Mat Taib et al., 2010).

Pure laboratory testing involves using environmental chambers and artificial light sources to approximately replicate outdoor conditions but with a greatly reduced test time under highly controlled conditions. Laboratory testing can quickly assess the relative stability of plastics but has the major disadvantage that the quicker the tests the lower is the correlation to real behaviour in the field (Singh and Sharma, 2007). Meanwhile, Yousif et al. (2014) studied the photostabilization of poly(methyl methacrylate) films using QUV tester (Q-Panel Company, USA) for irradiation of polymers films. Each side contains a lamp (type Fluorescent Ultraviolet Lights) 40 W each. These lamps are of the type UV-B 313 giving a spectrum range between 290 and 360 nm with a maximum at wavelength 313 nm. The polymer film samples were vertically fixed parallel to the lamps to make sure that the UV incident radiation is perpendicular on the samples.

Artificial weathering methods are useful tools for studying the durability of polymer products. There are two common methods for accelerated UV testing of plastic parts which are (a) QUV Weatherometer and (b) Xenon Arc Weatherometer. The QUV simulates the effect of sunlight with fluorescent lamps and simulates rain and dew with constant humidity. The exposure conditions can be varied. The QUV is a good screening tool. Such weathering testing can accelerate the effects of natural weathering from 5 to 20 times depending on the exposure condition chosen. The tests are valuable tools because the conditions can be controlled and reproduced. Because all the modes of natural weathering degradation cannot be simulated collectively (such as degradation by UV light, wetting by liquid water and discolouration by mould and stain fungi), accelerated testing generally focuses on the effects of UV light, moisture and temperature.

Test methods specifying the QUV UV-340 lamp include American Society for Testing and Materials (ASTM) D4329 Standard Practice for Fluorescent UV Exposure of Plastics and ASTM D4587 Standard Practice for Fluorescent UV-Condensation Exposures of Paint and Related Coatings, International Organization for Standardization (ISO) 4892 Methods of exposure to laboratory light sources and SAE J2020 Accelerated Exposure of Automotive Exterior Materials using a Fluorescents UV and Condensation Apparatus (McKeen, 2013).

The solar spectrum covers a broad range of radiation including short-wavelengths UV, visible light, as well as infrared radiation. UV light, as presented in Figure 18.8

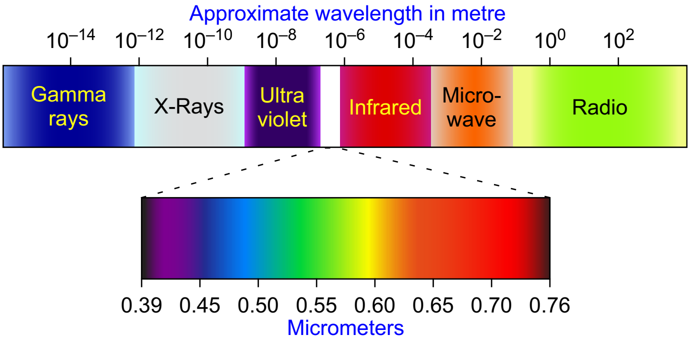

Figure 18.8 The UV light spectrum and solar radiation (Vazquez and Hanslmeier, 2006).

has a wavelength ranging from 100 to 400 nm. The energy from sunlight is mainly visible light and infrared. UV radiation makes up less than 5% of sunlight. However, UV light is the main cause of photodegradation of polymeric materials. The solar UV radiation spectrum is divided into three ranges as shown in Table 18.3, which will affect the polymers differently.

According to Wojciechowski et al. (2014), four types of polymers, including styrene-butyl acrylate (S-BA), vinyl acetate-butylacrylate (VA-BA), vinyl acetate (VA) and methyl methacrylate-ethyl-hexyl acrylate (MM-EHA) typically used in exterior wall paint formulations, were irradiated under UV lamp. The UV degradation under the same conditions of four polymer binders was probed by means of FTIR-attenuated total reflectance (ATR) and UV−Vis spectroscopy.

Nakamura et al. (2006) investigated photodegradation of poly(ether ether ketone) (PEEK) under tensile stress equivalent to a low Earth orbit environment using FTIR, X-ray photoemission spectroscopy (XPS), differential scanning colourimetry (DSC) and hardness and tensile tests. The results confirmed that both cross-linking and molecular scission is caused by UV radiation. The tensile properties of PEEK sheets after exposure indicate a tendency to embrittlement caused by cross-linking.

Table 18.3 Three ranges of solar UV radiation spectrum

Wavelength region of UV	
Class/Range	**Characteristics**
UV-A/315−400 nm	Always present in sunlight; 400 nm is the boundary between visible light and ultraviolet light; 315 nm begins to cause adverse effects to human skin and some polymers.
UV-B/290−315 nm	Includes the shortest wavelengths at the Earth's surface; responsible for severe polymer damage.
UV-C/100−290 nm	The UV-C boundary is a sharp cut-off of solar radiation at the Earth's surface due to complete absorption by ozone; found only in outer space.

Besides, applying tensile stress accelerates molecular scission during UV exposure, inhibiting the cross-linking effect on the tensile properties.

Al-Ani and Anabtawi (2012) studied the photostability of thin films of poly (fluorostyrene) isomers by irradiation with UV light, in presence of air at room temperature in which the irradiated polymer films were exposed to different intervals of time and the degradation process was investigated with absorption, fluorescence and FTIR spectroscopic methods.

Anpo (2000) reported that the TiO_2 photocatalyst have been successfully developed for the purification of the polluted atmosphere as well as toxic water using UV light of wavelength shorter than 380 nm (i.e. a larger energy than the band gap of the TiO_2 photocatalysts).

Various research studies on the sample preparation and UV irradiation for polymeric materials have been summarized and are tabulated in Table 18.4.

18.7.2 Spectroscopic analysis of biopolymer coating of UV-irradiated exposure

FTIR spectra recorded after UV irradiation of samples show noticeable changes in the intensities of characteristic bands in the case of pure chitosan and its blends with starch in which chitosan and starch belong to the group of biodegradable, natural polymers. An example of FTIR spectra of chitosan before and after 13 h UV irradiation is shown in Figure 18.9. Only small insignificant changes were found for a starch sample exposed separately at the same conditions (Bajer and Kaczmarek, 2010).

Examples of FTIR results on coating degradation are given to demonstrate the approach for measuring the material damage and calculating the spectral quantum efficiency in the samples. Figure 18.10 present typical FTIR spectra of the coating before and after ageing for two different times under the 300-nm cut-on filters (KG) at 50 °C/∼0% relative humidity (RH) condition. The major FTIR bands of interest in a cured, unaged acrylic—urethane coating based on an acrylic polyol and an aliphatic isocyanate are the bands at 3380 cm^{-1}, due to NH stretching, 1730 cm^{-1}, due to C=O stretching of the urethane linkage, 1520 cm^{-1}, due to amide II (NH bending and CN stretching), and 1250 cm^{-1}, due to amide III (NH bending and CN stretching).

The assignments are based on extensive IR data of polyurethanes. Although a comparison between spectra of the unaged and aged samples can give some information about the effects of exposure on a polymer film, the degradation behaviour is best studied from the difference spectra, in which the formation or depletion of a band and the appearance of a new species can be readily observed (Nguyen et al., 2002).

Furthermore, Anika Zafiah (2008) has studied UV—Vis spectrum for thin film of rapeseed—polyurethane (RS-PU) and sunflower—polyurethane (SF-PU). The UV—Vis spectra are shown in Figures 18.11 and 18.12. These spectra show no significant specific absorption band, apart from a small feature at ca. 330 nm, but rather an absorption increasing monotonically towards shorter wavelengths. The absorption in the visible region appears as a yellow colouration to the eye and is a universal feature of polyurethane polymers in which no special steps have been taken to eliminate the colourant. The chromophore responsible for the band at ca. 330 nm is considered the quinone

Table 18.4 Study on the sample preparation and UV irradiation for polymeric materials

Research study	Sample preparation	Irradiation experiments	Author
Photostabilization of organic coatings	A 40-mm-thick film was applied to a quartz plate and exposed to the UV radiation of a medium pressure mercury lamp (80 W cm^{-1})	QUV accelerated weatherometer operated at 40 °C, under continuous irradiation with fluorescent UVB-313 lamps	Decker et al. (1995)
Correlation of physicochemical changes in UV-exposed low-density polyethylene (LDPE) films containing various UV stabilizers	The polyethylene containing 0.3% w/w Hindered Amine Light Stabilizer (HALS) stabilizer was blown into films on the BK 32 Labline Equipment within the laboratories at Cabot Plastics Ltd, UK. Film thicknesses of 50, 100 and 200 μm were selected.	The QUV Tester (The Q-Panel Company, UK, Ref. ASTM G53-88) consists of an array of 8 UV-B fluorescent lamps, emitting light over the wavelength region from 280 to 315 nm with a UV-A tail extending to 400 nm in an alternating illuminated, dry and dark saturated atmosphere to simulate day—night exposure. The black body temperature of specimens was set at 60 °C during exposure	Liu et al. (1995)
Photo-oxidative stability of water-based acrylic and isocyanate-based acrylic coatings	The paint films coated on stainless steel plates for accelerated weathering and aluminium plates for natural exposures	QUV, Q-Panel Company, Farnworth, Bolton, UK., UV-340 nm fluorescent lamps for outdoor simulation	Norman et al. (2002)

Surface characterization of photodegraded poly(ethylene terephthalate) (PET): The effect of ultraviolet absorbers	Two types of films were prepared, (i) unstabilized PET and (ii) with a UV absorber. All films contained 0.06% SiO_2, used as an antiblocking agent	The exposure was conducted in a Comexin weathering chamber using Q-Panel UV-A fluorescent lamps that produce ultraviolet light that matches reasonably well with sunlight, with a cut-off at 290 nm. The weathering cycle was defined as follows: 4 h under UV light at 60 °C and 4 h in the dark under condensed water at 50 °C.	Fechine et al. (2004)
Effect of TiO_2 on material properties for renewable rapeseed and sunflower polyurethane	Thin films normally about 200 μm thickness of renewable rapeseed–polyurethane (RS-PU) were prepared by adding the hydroxylated rapeseed monomer (1 g; 0.2 g equivalent weight with polyol) with an appropriate amount of 4,4′-methylene-bis-(phenylisocyanate (MDI)).	The instrument used was a Q-Panel Accelerated Weatherometer. The device is a UV radiation tank with 8 fluorescent bulbs (300 W) selected at UV-B wavelength are fitted inside the apparatus.	Anika Zafiah (2008)

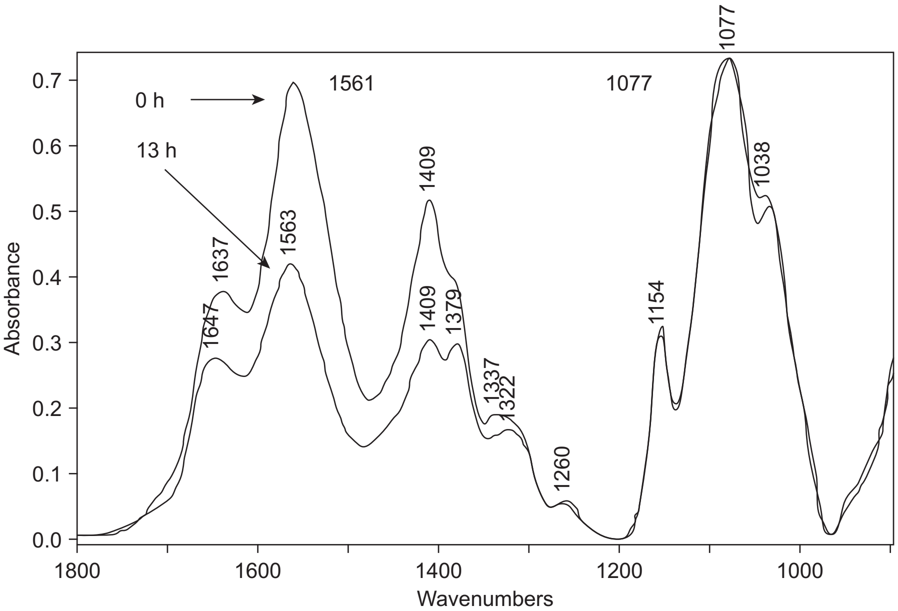

Figure 18.9 FTIR spectra of chitosan before and after 13 h of UV irradiation (Nguyen et al., 2002).

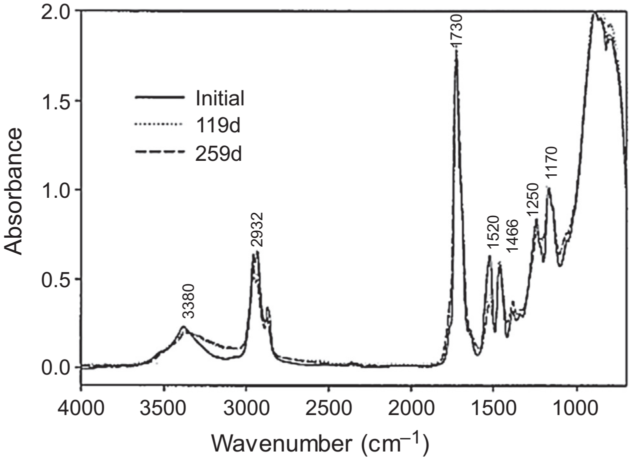

Figure 18.10 Typical FTIR spectra of PU coating before and after exposures for two different time intervals under the 300 nm cut-on filters in 50 °C/~0% relative humidity condition (Nguyen et al., 2002).

methide group and, the colouration is intensified on exposing the polymers to UV irradiation or heat (Anika Zafiah, 2008).

Meanwhile, advanced metal ion-implantation method has been successfully applied by Anpo et al. (2001) to modify the electronic properties of TiO_2 photocatalysts by bombarding them with high-energy metal ions and have found that this advanced physical

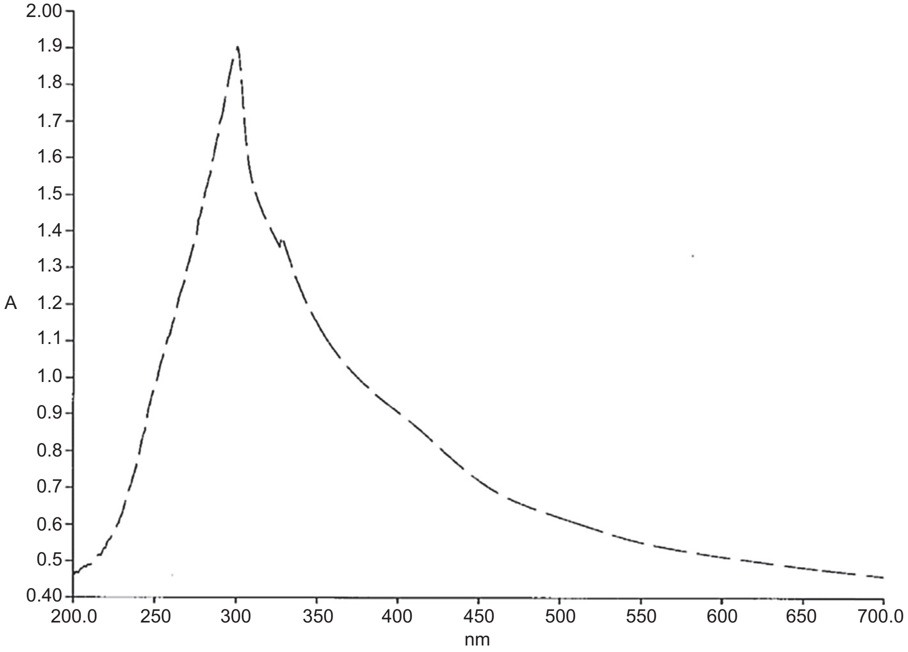

Figure 18.11 UV−Vis spectrum for thin film (150−200 μm) of RS-PU (Anika Zafiah, 2008).

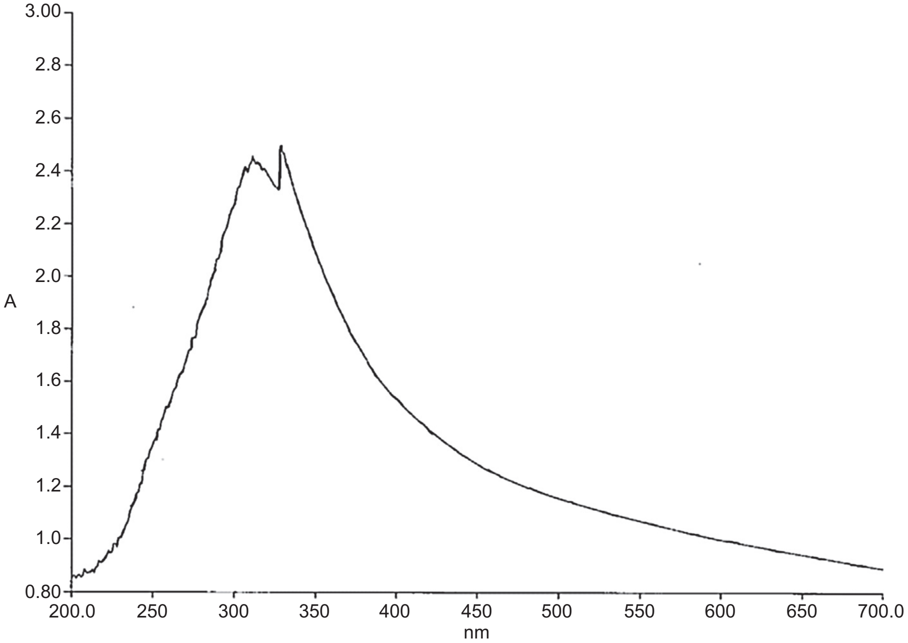

Figure 18.12 UV−Vis spectrum for thin film (150−200 μm) of SF-PU (Anika Zafiah, 2008).

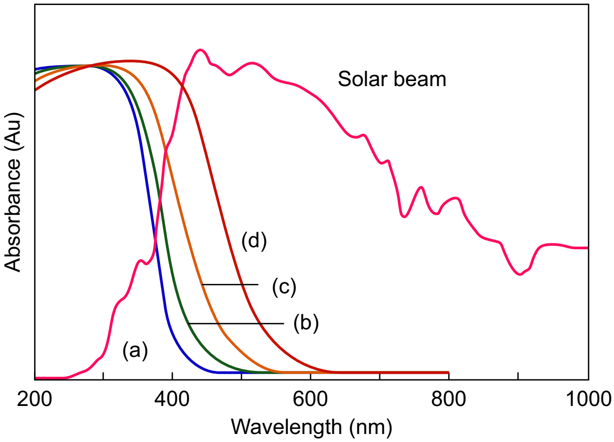

Figure 18.13 UV—Vis absorption spectra (diffuse reflectance) of the original unimplanted pure TiO_2 (a) and the Cr ion-implanted TiO_2 (b—d), and the solar spectrum which reaches the Earth (Anpo et al., 2001).

method is the most suitable and promising for the dramatic modification of the electronic state of the photocatalysts. Figure 18.13 shows the action spectrum for the reaction on the metal ion-implanted TiO_2 was in good agreement with the absorption spectrum of the catalyst, indicating that only metal ion-implanted catalysts were effective for the photocatalytic decomposition of NO. Thus, the metal ion-implanted catalysts enabled the absorption of visible light up to a wavelength of 400 to 600 nm and were able to operate effectively as photocatalysts under visible light irradiation, hence their name, "second-generation titanium oxide photocatalysts" (Anpo et al., 2001).

As can be seen in Figure 18.13(b—d), the absorption band of the metal ion-implanted titanium oxide was found to shift smoothly to visible light regions, the extent of the red shift depending on the amount and type of metal ions implanted with the absorbance maximum and minimum values always remaining constant. Such a shift allows the metal ion-implanted TiO_2 to use solar beams more effectively and efficiently, at up to 20% to 30%. As mentioned previously, with titanium oxide photocatalysts, the photo catalytic reaction does not proceed under visible light irradiation ($l > 450$ nm). However, the visible light irradiation of these metal ion-implanted titanium oxide photocatalysts led to various significant photocatalytic reactions. Thus, the metal ion-implanted catalysts enabled the absorption of visible light up to a wavelength of 400 to 600 nm and were able to operate effectively as photocatalysts under visible light irradiation, hence their name, "second-generation titanium oxide photocatalysts" (Anpo et al., 2001).

Duka (2008) introduced the mechanical properties of thin films, measurement of the mechanical properties of very thin coatings and creep performance of coatings. Thin-film mechanical properties can be measured by tensile testing of freestanding films and by the microbeam cantilever deflection technique. The mechanical properties of a coating/substrate system depend on the microstructure of the coating/substrate and interface region including composition, phases present, porosity, grain size, grain shape, defect types and density (Duka, 2008).

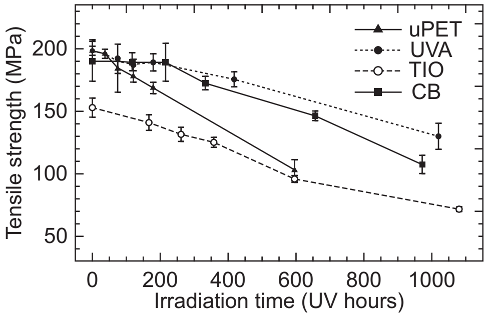

Figure 18.14 Tensile strength after different periods of weathering (Fechine et al., 2004).

Salem (2001) studied the effect of UV rays on the mechanical properties of low-density polyethylene (LDPE) films pigmented with carbon black and titanium dioxide (TiO_2) in different formulations. The results show that the use of pigments, carbon black and TiO_2 in appropriate concentration ratios gives a reliable improvement in the mechanical and physicochemical properties of LDPE films exposed to UV radiation (Salem, 2001).

Furthermore, Saleh and Shnean (2009) studied the effect of UV light on pigmented and unpigmented LDPE. After the exposure to UV light, all mechanical properties declined but pigmented LDPE still had higher mechanical properties such as tensile strength, tensile at break, modulus of elasticity and hardness, as compared to unpigmented LDPE. The same study by Saleh and Shnean (2009) found that the increasing exposure times decrease tensile strength, tensile strength at break, elongation at break and the higher exposure times seem to reduce the impact strength for all samples.

According to Fechine et al. (2004), the effects of various types of stabilizers on the photodegradation behaviour of PET films were analysed using a number of techniques. The unstabilized PET showed a large deterioration in mechanical properties, because of extensive chemical degradation that resulted in chain scission reactions and the formation of carboxyl end-groups. Tensile strength and percentage

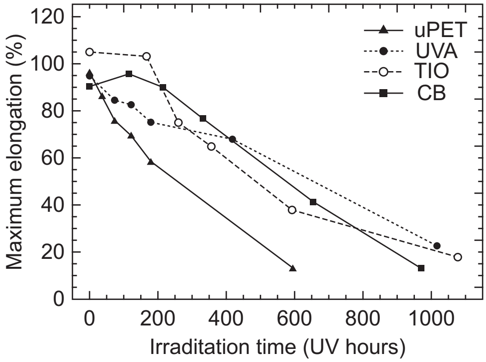

Figure 18.15 The effect of exposure time on maximum elongation (Fechine et al., 2004).

elongation showed a significant decrease with exposure time (Figures 18.14 and 18.15), results in a typical behaviour of a polymer that undergoes chain scission reactions during weathering. Samples stabilized with UV absorber had less deterioration in tensile properties due to a relatively low reduction in molecular sizes. Comparing the various types of samples, it is clear that those containing the UV stabilizer are more stable.

18.8 Conclusions and future trends

Materials can be classified as natural or synthetic, recycled or virgin, renewable or nonrenewable, degradable and nondegradable or biodegradable. No clear-cut answers are available on which is least environmentally damaging. However, new technologies and incorporation of appropriate advanced technology into products and processes should be safer, more effective and less costly. Furthermore, it can definitely make a significant contribution to improving their environment performance. Besides that, photo-oxidative degradation of these biopolymers when compared to other well-known polymers is significantly at an advantage. The undoped biopolymers show that treatment of the pigment critically affects its photoactivity towards biopolymers, whereas titanium dioxide pigment is invariably the most aggressive towards any of the polymers. Very interestingly, the presence of pigment stabilizes further the biopolymer of polyurethane coatings, instead of reducing the level of protection. This beyond doubt supports the use of biopolymers for superhydrophobic photocatalytic coatings.

References

Adhvaryu, A., Erhan, S.Z., 2002. Industrial Crops Production. Alexandaria, VA.

Al Ani, K.E., Anabtawi, M., 2012. UV-irradiation effect on the photodegradation of plasticized poly (*ortho*, *meta*, *and para*-fluorostyrene) isomers in solid films. International Journal of Chemistry 4 (5), 62–84.

Allen, N.S., Edge, M., Ortega, A., Liauw, C.H., Stratton, J., McIntyre, R.B., 2002. Polymer Degradation and Stability 78 (3), 467–478.

Anika Zafiah, M.R., Kemp, T.J., 2008. Progress in Reaction Kinetics and Mechanism 33, 363–391.

Anika Zafiah, M.R., Kemp, T.J., Clark, A.J., 2009. Progress in Reaction Kinetics and Mechanism 34 (1), 1–41.

Anika Zafiah, M.R., 2008. Degradation studies of polyurethanes based on vegetables oils. (part I) Photodegradation. Progress in Reaction Kinetics and Mechanism 33, 363–391.

Anika Zafiah, M., Rus, S.R., Nurulsaidatulsyida, Mohid, Marsi, N., 2013. Advances in Materials Science and Engineering, Hindawi 2013.

Anika Zafiah, M.R., Mohid, S.R., Shaiqah, M.R., 2014. Influence of N_2 and H_2O on UV irradiated bio polymer composite. International Review of Mechanical Engineering 8 (1), 271–276.

Anpo, M., 2000. Utilization of TiO_2 photocatalysts in green chemistry. Pure and Applied Chemistry 72 (7), 1265–1270.

Anpo, M., Kishiguchi, S., Ichihashi, Y., Takeuchi, M., Yamashita, H., Ikeue, K., Morin, B., Davidson, A., Che, M., 2001. Research on Chemical Intermediates 27 (4), 459–467.

Anpo, M., Takeuchi, M., 2001. Design and development of second-generation titanium oxide photocatalysts to better our environment—approaches in realizing the use of visible light. International Journal of Photoenergy 3, 89–94.

Arana, J., 2002. Catalysis Today 76, 279.

Bajer, D., Kaczmarek, H., 2010. Study of the influence on UV radiation on biodegradable blends based on chitosan and starch. Progress on Chemistry and Application of Chitin and Its Derivatives XV, 17–24.

Barnes, P.J., et al., 2000. Feature article in peer reviewed journal. Lipid Technology 12, 129–132.

Baumann, H., Buhler, M., Fochem, H., Hirsinger, F., Zoebelein, H., Falbe, J., 1988. Journal of Angewandte Chemie International Edition in England 100, 41.

Bierman, U., 1983. Journal of Organic Chemistry 48, 3831–3833.

Blayo, A., Gandini, A., Le Nest, J.-F., 2001. Industrial Crops Production 14, 155.

Bledzki, A.K., Gassan, J., 1999. Composites reinforced with cellulose fibers. Progress in Polymer Science 24, 221–224.

Brown, M.E., 1988. Introduction to Thermal Analysis. Chapman and Hall, London, p. 6,127.

Cho, J.D., Ju, H.T., Hong, J.W., 2005. Journal of Polymer Science Polymer Chemistry 63, 658.

Dahlke, B., Larbig, H., Scherzer, H.D., Poltrock, R., 1998. Journal of Cellular Plastics 34, 361.

Decker, C., Biry, S., Zahouily, K., 1994. Photostabilisation of Organic Coatings. Elsevier Science Limited.

Decker, C., Biry, S., Zahouily., K., 1995. Polymer Degradation and Stability 49 (1), 111–119.

Diebold, M.P., 2000. The Causes and Prevention of Titanium Dioxide Photodegradation of Paints. DuPont de Nemours and Company.

Duka, E., 2008. Mechanical Characterisation of Very Thin Films. Physics of Advanced Materials Winter School. Tirana University, Albania.

Fechine, G.J.M., Rabello, M.S., Souto Maior, R.M., Catalani, L.H., 2004. Surface characterization of photodegraded poly(ethylene terephthalate): the effect of ultraviolet absorbers. Polymer 45, 2303–2308.

Ferroni, M., Carotta, M.C., Guidi, V., Martinelli, G., Ronconi, F., Sacerdoti, M., Traversa, E., 2001. Sensors Actuators 77, 163.

Forsyth, M., MacFarlane, D.R., Best, A., Adebahr, J., Jacobsson, P., Hill, A.J., 2002. The effect of nano-particle TiO_2 fillers on structure and transport in polymer electrolytes,. Solid state ionics 147 (3–4), 203–211.

Frindell, K.L., Bartl, M.H., Popotsch, A., Stucky, G.D., 2002. Journal of Angewandte Chemie International Edition in England 41, 959.

Fujishima, A., 2000. Titanium dioxide photocatalysis. Journal of Photochemistry and Photobiology C: Photochemistry Reviews 1, 1.

Gesenhues, U., 2000. Influence of titanium dioxide pigments on the photodegradation of poly(vinyl chloride). Polymer Degradation and Stability 68, 185–196.

Hanaor, D.A.H., Sorrell, C.C., 2011. Review of the anatase to rutile phase transformation. Journal Material Science 46, 855–874.

Harris, T., 2003. Production of Functional Fillers for Plastics. Intertech Corporation, Atlanta, GA.

Kemp, T.J., McIntyre, R.A., 2006. Polymer Degradation and Stability 4979, 1–10.

Kibert, C.J., Sendzimir, J., Guy, G.B. (Eds.), 2002. Construction Ecology: Nature as a Basis for Green Buildings. Spon Press, London and New York, p. 7.

Kobayashi, M., Kalriess, W., 1997. Photocatalytic activity of titanium dioxide and zinc oxide: the effect of organic and inorganic surface treatments. Cosmetics and Toiletries Magazine 112, 83−85.

Kreienfeld, G., Stoll, G., 1997. In: Hill, K., Rybinski, W., Stoll, G. (Eds.), Alkyl Polyglycosides: Techn., Properties and Appl. VCH, Weinheim, p. 225.

McKeen, Laurence W., 2013. The effect of UV light and weather on plastics and elastomers. William Andrew.

Mahajan, S., 2003. Production of Functional Fillers for Plastics 2003. Intertech Corporation, Atlanta, GA.

Mat Taib, R., Ahmad Zauzi, N.S., Mohd Ishak, Z.A., Rozman, H.D., 2010. Effects of photo-stabilizers on the properties of recycled high-density polyethylene (HDPE)/ wood flour (WF) composites exposed to natural weathering. Malaysian Polymer Journal 5 (2), 193−203.

Mayadevi, S., Kulkarni, S.S., Patil, A.J., Shinde, M.H., Potdar, H.S., Deshpande, S.B., Date, S.K., 2000. Journal of Material Science 35, 3943.

Liu, M., Horrocks, A.R., Hall, M.E., 1995. Polymer Degradation and Stability 49 (1), 151−161.

Morris, D., Edgell, G., 2001. Journal of Material Chemistry 11, 3207.

Mukherjee, D., 2011. Development of a Novel TiO_2-Polymeric Film Photocatalyst for Water Purification Both under UV and Solar Illuminations (Ph.D. thesis). The University of Western Ontario.

Nakamura, H., Nakamura, T., Noguchi, T., Imagawa, K., 2006. Photodegradation of PEEK sheets under tensile stress. Polymer Degradation and Stability 91 (4), 740−746.

Nguyen, T., Martin, J.W., Byrd, E., Embree, E., 2002. Effects of spectral UV on degradation of acrylic-urethane coatings. In: Proceedings of the 80th Annual Meeting of the Program of the FSCT, Federation of Societies for Coatings Technology, October 30−November 1, 2002, New Orleans, LA, pp. 354−356.

Pandey, J.K., Reddy, K.R., Kumar, A.P., Singh, R.P., 2005. An overview on the degradability of polymer nanocomposites. Polymer Degradation and Stability 88, 234−250.

Patel, M.K., Theiβ, A., Worrell, E., 1991. Resources, Conservation and Recycling 25, 61.

Rabek, J.F., 1996. Photodegration of Polymers: Physical Characteristics and Applications. Springer-Verlag Berlin Heidelberg, New York.

Rasshofer, W., Liman, U., Wagner, J., 1991. Polyurethane World Congress, Nice, Proc., p. 636.

Ray, D., Sarkar, B.K., Bose, N.R., 2002. Composites 33 (A), 233−241.

Rek, V., Bravar, M., 1983. Journal of Elastomers & Plastics 15, 33.

Robbelen, G., 1994. Pflanzliche Ole als Rohstoffbasis − Potential und Veranderungen in der Verfugbarkeit. In: Tagungsband 3. Symposium Nachwachsende Rohstoffe − Perspektiven fur die Chemie, Schriftenreihen des Bundesministeriums fur Ernahrung, Munster, p. 115.

Saleh, N.J., Shnean, Z.Y., 2009. A study of the effect of UV light on pigmented and unpigmented LDPE. Engineering & Technology Journal 27 (4), 706−716.

Salem, M.A., 2001. Mechanical properties of UV-irradiated LDPE films formulated with carbon black and titanium dioxide. Egyptian Journal of Solids 24 (2), 141−150.

Saw-Peng, Yew, Tang, H.-Y., Kumar, S., Degradation, Polymer, 2006. Stability 91 (8), 1800−1807.

Schmidt, H., Jonschker, G., Goedicke, S., 2000. Journal of Sol-Gel Science and Technology 19−39.

Singh, B., Sharma, N., 2007. Mechanistic implications of plastic degradation. Polymer Degradation and Stability 93 (2008), 561−584.

Stark, W.J., Wegner, K., Pratsinis, S.E., Baiker, A., 2001. Journal of Catalysis 197, 182.

Steber, J., 1991. Textilveredlung 26, 348.

Thelakkat, M., Schmitz, C., Schmidt, H.-W., 2002. Advanced Materials 14, 577.

Vazquez, M., Hanslmeier, A., 2006. Ultraviolet Radiation in the Solar System. Springer, Netherlands.

Venturello, C., Alneri, E., Ricci, M., 1983. Journal of Organic Chemistry 48, 3831.

Wirpsza, Z., 1993. Polyurethanes: Chemistry, Technology and Applications. Ellis Horwood, New York, p. 31.

Wojciechowski, K., Skowera, E., Pietniewicz, E., Zukowska, G.Z., Van der Ven, L.G.J., Korczagin, I., Malanowski, P., 2014. UV stability of polymeric binder films used in waterborne facade paints. Progress in Organic Coatings 77, 298−304.

Xanthos, M., 2005. Polymers and Polymer Composites, Functional Fillers for Plastics. Wiley-VCH Verlag GmgH & Co KgaA.

Yousif, E., El-Hiti, G.A., Haddad, R., Balakit., A.A., 2015. Polymers 7 (6), 1005−1019.

Yu, C.T., Xian, H.H., Han, Q.Y., Li, H.T., 2012. Nitrogen-doped TiO_2 photocatalyst prepared by mechanochemical method: doping mechanism and visible photoactivity of pollutant degradation. International Journal of Photoenergy 10, 1155.

Index

'*Note*: Page numbers followed by "f" indicate figures and "t" indicate tables.'

A

Accelerators, 109
  accelerating admixtures, 110f
  calcium chloride accelerators, 110−111
  non-chloride accelerators, 111−112
  rapid-set accelerators, 110
  setting and hardening, 110
Acetic acid (CH_3COOH), 27, 157−158
Acidification potential (AP), 65, 257
Acidolysis process, 343−344
Acrylated epoxidised soybean oil, 281f
Active admixtures, 99
Active sites, 231−232
Additives, 196
  origin of, 373−374
Adhesive−adherend interface, 373f
Adhesives. *See also* Bioadhesives
  bio-and synthetic adhesives, 380−381
  bio-based, 369−370
  future trends, 381
  market evolution, 381
  phenolic-acids based, 379−380
  protein-based, 378−379
  synthetic, 369−370
Adsorption, 390−391
Air-entraining admixtures, 99−101, 100f
Alcoholysis, 343−344
Alginate(s), 243−244, 404−405
  bead-immobilized cells, 388f, 408−409
  immobilization of cells, 408−409
Alkylation, 230
American Society for Testing and Materials (ASTM), 371−373
American Type Culture Collection (ATCC), 37
Amines, 111
Ammonia oxidizing bacteria (AOB), 402
Ammonia transformation, 402
Ammonium borate oleate preservative, 309
Animal biomaterials, 17
Animal/fungal polysaccharide, 376−378
Anoxic heterotrophic bacteria, biocement based on, 47−48
Antibacterial action mechanisms, 310−311
Antibacterial activity, 310, 313
Antiwashout admixtures, 228
AOB. *See* Ammonia oxidizing bacteria (AOB)
AP. *See* Acidification potential (AP)
Apparent porosity (AP), 114
  PBL waste effect on, 115−117
Apparent shear strength (ASS), 371−373
Aquatic toxicity potential, 65
Araucária resin, concrete blocks with, 216
Artificial coral reefs, 23
Artificial weathering, 434−437
Ashby−Gibson model, 286−287
ASS. *See* Apparent shear strength (ASS)
ASTM. *See* American Society for Testing and Materials (ASTM)
ATCC. *See* American Type Culture Collection (ATCC)
ATR. *See* Attenuated total reflectance (ATR)
Attenuated total reflectance (ATR), 436−437

B

Bacillus subtilis (*B. subtilis*), 207f
Bacteria(l), 254
  bacteria-based healing agent, 263−264, 266
  exopolysaccharide synthesis, 378
  immobilization on microbial cellulose, 405−408
  production of limestone, 254−258
    heterotrophic bacterial limestone production, 257−258

- Bacteria(l) (*Continued*)
    - spore-forming alkaliphilic bacteria, 258f
    - ureolytic bacterial limestone production, 255–257
- Base accelerators, 111
- BD. *See* Bulk density (BD)
- Bending, 288
  - members, 292–293
- Bentonite, 404–405
- Benzene sulphonate formaldehyde (BSF), 106–107
- Benzene–toluene–ethylene–xylene (BTEX), 388, 413
- Bingham, 166
  - yield stress, 222
- Bio-admixtures, 81
- Bio-Barrier® modules, 393
- Bio-based adhesives, 369–370
- Bio-inspired adhesives, 381
- Bio-resins, 59–61, 60t
- Bioadhesives, 369, 375, 380–381. *See also* Adhesives
  - species, 375–380
    - bioadhesive polysaccharides, 375–378
    - phenolic-acids based adhesives, 379–380
    - protein-based adhesives, 378–379
  - testing
    - LCA, 374–375
    - mechanical tests, 370
    - origin of adhesion, 373–374
    - shear strength, 370–373
    - water resistance, 374
- Bioaggregation of soil, 14
- Biobarrier
  - additives effect, 397–398
  - concentration of biopolymers, 396
  - contaminant removal by, 393, 393f
  - DO effect, 397
  - extracellular polymeric substances, 396–397
  - future trends, 414
  - immobilization time effect, 400–401, 401f
  - for inorganic contaminants removal, 410–411
  - monitoring performance, 393–401
  - NO_3^- effect, 399–400
  - for organic contaminants removal, 413–414
  - pH pretreatment effect, 400, 400f
  - sorption capacity of biopolymer, 394–395
- Biobased epoxy resins, 325, 352f
- Biobased hyperbranched polyurethane, 362t
- Biobased linear polyester, 343f
- Biobased mortar systems, 263–267. *See also* Liquid bacteria-based system
  - fiber-based control and bacterial repair mortars composition, 264t
  - practical applications, 266–267
  - properties of biobased self-healing repair mortars, 264–266
- Biobased poly(ester amide)s, 348
- Biobased polymers, 334–335
  - background and importance, 340–341
  - for paintings and coatings, 341–360
  - paints and coatings manufacturing from, 363–364
- Biobased polyols, 280–283, 282t
- Biobased polyurethane resins, 324–325
- Biobased polyurethanes, 357
- Biobased resins
  - biobased epoxy resins, 325
  - biobased polyurethane resins, 324–325
  - natural oligomeric and polymeric resins, 325–326
- Biobased urethanes, 324f
- Biocementation, 22
  - biogas production in situ for soil liquefaction mitigation, 26–27
  - and biogrouts, 22
  - calcium bicarbonate
    - biocementation, 28
    - production, 48
  - calcium-and urea-dependent biocementation, 22–24
  - calcium-phosphate biocementation, 27
  - on carbonates production, 25–26
  - eco-efficient and composite biocement, 50–51
  - iron-based, 49–50
  - iron-based bioclogging and biocementation, 28
  - of soil, 15
  - spatial types of biocementation, 24f

Biocements and biogrouts biotechnological production, 46
  biocement based on anoxic heterotrophic bacteria, 47−48
  calcium bicarbonate production for bioclogging/biocementation, 48
  calcium-and urea-dependent biocement production, 46−47
  eco-efficient and composite biocement, 50−51
  iron-based bioclogging and biocementation, 49−50
Biocidal agents, 310
Bioclogging
  calcium bicarbonate production for, 48
  iron-based, 49−50
  using microbial polysaccharides in situ production, 19−21
  of soil, 15
Biocoating of solid surfaces, 15
Biocrusting, 14
Biodegradability, 203, 296
Bioderived polymers, 334−335
Biodesaturation of soil, 15
Bioencapsulation of clay/soil/particles, 15
Biofilm formation, 20−21
Biofilter, 388−389
  future trends, 414
  for inorganic contaminants removal, 410−411
  nutrient enrichment, 397
  for organic contaminants removal, 413−414
Biofiltration, 390, 402
  adsorption, 390−391
  bridge formation, 392
  coagulation/flocculation, 391−392
  electrostatic patch, 390
  monitoring performance, 393−401
  physisorption and chemisorption features, 391t
Biofoams, 277, 296
Biogas production in situ for soil liquefaction mitigation, 26−27
Biological additives for concrete, 151
Biological oxygen demand (BOD), 393
Biomass-based adhesives, 375
Bioplasticizer, 152
  proportions of SCCs, 161t
Bioplastics, biotechnological production for construction, 42−44
Biopolyethylene (PE), 2
Biopolymer wood preservatives, 308. *See also* Traditional wood preservatives
  antibacterial action mechanisms of biopolymers, 310−311
  biobased resins, 324−326
  biopolymer definition, 308−309
  chitin and chitosan, 311−316
  PLA, 323−324
  proteins in wood preservation, 316−323
  wood impregnation techniques with biopolymers, 309−310
Biopolymer-immobilizing microorganisms, 402
  alginate immobilization of cells, 408−409
  bacteria immobilization on microbial cellulose, 405−408
  chitosan, 402−403, 402f
  magnetic chitosan microspheres, 404
  magnification, 407f
  peat moss, bentonite, and alginate, 404−405
Biopolymer(s), 2, 57, 173−174, 196, 334−335, 387
  antibacterial action mechanisms of, 310−311
  application, 59−61
  artificial weathering, 434−437
  bio-derived resins, 60t
  characterization as supporter, 402−410
  concentration, 396
  in concrete, 216
    concrete blocks with Araucária resin, 216
    shotcrete with latex of rubber tree, 216−217
  effect of degree of deacetylation, 394−395, 395f
  development from renewable resources, 423−426
  for eco-efficient construction materials, 2−5
  effluents treated by biofiltration, 389t
  end of life, 61−63
  foams, 275
  future research trends, 74
  GHG emissions for, 68f

Biopolymer(s) (*Continued*)
  land use for, 69f
  LCA
    case studies, 73–74
    comparative cradle-to-manufacture impacts, 72t
    comparison of LCA of biopolymers, 67–71
    data for, 67
    end of life of biopolymers, 71–73
  modification using fillers, 427–429
  molecular weight effect, 395, 395f
  in paints and surface coatings, 334–335
  particle size effect, 394
  photocatalysis agent, 429–430
  sample preparation and UV irradiation, 438t–439t
  service life of, 426
  spectroscopic analysis of biopolymer coating of UV-irradiated exposure, 437–444
  state of development of thermoplastic, 58f
  as superhydrophobic photocatalytic coatings, 430–444
  with superplasticizer, 203–216
    B. subtilis, 207f
    concrete–chitosan–latex system, 205f
    latex–biopolymer system, 213f
    latex–concrete system, 212f–213f
    tensile strength for concrete–latex–chitosan system, 214f
  supporting other polymers, 409–410
  survey of approaches from renewable resources, 422–423
  SWOT analysis, 63t
  titanium dioxide as polymer stabilization, 429–430
  types, 58
  wood impregnation techniques with, 309–310
Biopolymers for eco-efficient construction materials
  biotechnological production
    biocements and biogrouts, 46–51
    bioplastics for construction, 42–44
    polysaccharide admixtures, 44–46
  biotechnology for construction materials production, 37–42
  construction biotechnology, 13–15
  microorganisms in construction processes, 14f
  physiological groups of chemotrophic prokaryotes, 40t
  principles of construction-related biotechnological processes, 16f
  types, 15–17
Bioproducts, 152
Bioremediation of soil, 15
Biotechnological admixtures for eco-efficient construction materials
  biotechnological production
    biocements and biogrouts, 46–51
    bioplastics for construction, 42–44
    polysaccharide admixtures, 44–46
  biotechnology for construction materials production, 37–42
  in building materials, 45t
  construction biotechnology, 13–15
  for eco-efficient construction materials, 2–5
  microbial plastics for civil engineering, 21–22
  microbial polysaccharides, 17, 18t
  microorganisms in construction processes, 14f
  physiological groups of chemotrophic prokaryotes, 40t
  principles of construction-related biotechnological processes, 16f
  viscosity modifiers, 88–91
  water reducers, 91–95
  water-retention agents, 83–88
Biotechnology for construction
  biocements and biogrouts, 46–51
  bioplastics for construction, 42–44
  materials production, 37–42
  polysaccharide admixtures, 44–46
  for production of calcium-and urea-based biocement, 38f
Biotrickling filter (BTF), 413–414
Black liquor waste, 112
  black liquor gasification plant, 113f
  compressive strength, 114
  Fourier transform infrared spectra, 119–120
  future trends, 126
  PBL waste effect

    - on bulk density and apparent porosity, 115−117
    - on combined water content, 117−118
    - on compressive strength, 118−119
    - on water of consistency and setting times, 115
  - pulping process, 112f
  - SEM microscopy, 120−121
  - water of consistency, 114
- Bleeding, 226−228, 235−237
- Blowing agents, 283
- BOD. *See* Biological oxygen demand (BOD)
- Bonding components, 369
- BP. *See* British Petroleum (BP)
- Bridge formation, 392
- British Petroleum (BP), 1
- BSF. *See* Benzene sulphonate formaldehyde (BSF)
- BTEX. *See* Benzene−toluene−ethylene−xylene (BTEX)
- BTF. *See* Biotrickling filter (BTF)
- Bulk density (BD), 114
  - PBL waste effect on, 115−117
- Butyl stearate, 126
- by weight of cement (bwoc), 137−138

C

- C2S. *See* Dicalcium silicate (C2S)
- C3A. *See* Tricalcium aluminate (C3A)
- C3S. *See* Tricalcium silicate (C3S)
- C4AF. *See* Tetracalcium aluminoferrite (C4AF)
- $(C_8H_{13}O_5N)_n$. *See* Chitin
- Ca-lignosulfonates (CL), 92−93, 104−105
- Cactus mucilage, 241−243
- CAH. *See* Calcium aluminate hydrate (CAH)
- Calcium aluminate hydrate (CAH), 119−120
- Calcium bicarbonate
  - biocementation, 28
  - production for bioclogging/biocementation, 48
- Calcium carbonate, 25
  - minerals, 262f
  - production, 258
- Calcium chloride accelerators, 110−111
- Calcium silicate hydrate (CSH), 82, 110, 163, 233, 257
- Calcium-and urea-dependent biocement production, 46−47
- Calcium-phosphate biocementation, 27
- Carbon dioxide (CO_2), 174−175
- Carbon fibre (CF), 63
- Carbon nanofibers (CNFs), 175
- Carbon nanotubes (CNTs), 175
- Carboxymethyl hydroxyethyl cellulose (CMHEC), 84
- Casein, 94−95
- CBDs. *See* Cellulose binding domains (CBDs)
- CCA-based preservatives. *See* Chromated copper arsenate-based preservatives (CCA-based preservatives)
- Cell metabolism, 15
- Cell wall bacteria, peptidoglycan from, 245−246
- Cellulose, 4, 85−87, 93−94, 203, 204f, 335−336, 387, 409−410
  - aerogel, 5
  - cellulose-based VMAs, 91
  - derivatives, 229−230
    - CEs, 230
    - HEC, 231−232, 231f
    - MHEC, 232−233, 232f
    - MHPC, 233−234, 234f
  - nanocrystals, 3−4
  - polymer, 87f
  - unit, 230f
- Cellulose binding domains (CBDs), 409−410
- Cellulose ethers (CEs), 83, 230
- Cement, 81
  - EM as plasticizer in, 155−160
  - hydration heat, 139
  - notation, 127
  - paste, 139, 235−237
    - setting time, 139−140
  - physical−mechanical properties, 155t
  - technology, 99
- CEs. *See* Cellulose ethers (CEs)
- CF. *See* Carbon fibre (CF)
- Chemical oxygen demand (COD), 389
- Chemisorption, 391t
- Chitin, 203, 246f, 311−316, 387, 389
- Chitin-impregnated wood, 315−316, 316f

Chitosan, 91, 203, 246–247, 246f, 311–316, 337, 376–378, 387, 389–390, 402–403, 402f
  in concrete, 210f
  FTIR spectra, 136f
  high-performance superplasticizer based on
    chitosan superplasticizer preparation, 134–135
    chitosan superplasticizer structure, 135–137
    SM contents, 136t
  modifying, 134f
  in paste, 210f
  properties, 133–134
  SEM of concrete with, 204f
  structure, 133, 133f
Chitosan superplasticizer
  dispersion capacity characterization, 137
    cement hydration heat, 139
    concrete slump, 138
    concrete slump retention time, 138–139
    setting time of cement paste, 139–140
    water-reducing capacity, 137–138
  preparation, 134–135
  SM contents, 136t
  structure, 135–137
Chitosan-based adhesives, 374
Chitosan-impregnated wood, 315–316, 316f
Chromated copper arsenate-based preservatives (CCA-based preservatives), 307–308
Civil engineering
  microbial plastics for, 21–22
  microbial polysaccharides applications in, 17
CL. *See* Ca-lignosulfonates (CL)
CMHEC. *See* Carboxymethyl hydroxyethyl cellulose (CMHEC)
CNFs. *See* Carbon nanofibers (CNFs)
CNTs. *See* Carbon nanotubes (CNTs)
Coagulation, 391–392
Coaxial cylinders, 223
COD. *See* Chemical oxygen demand (COD)
Cohesion, 224, 228–229
Collagen, 336
Combined loading, 294
Combined water content, PBL waste effect on, 117–118
Composite chitosan/sunflower stalk, 377f
Compression, 287–288
  members, 293–294
Compressive strength, 114, 167
  PBL waste effect on, 118–119
Concrete, 17, 173–174
  with cocktails of N-200 and MEF, 168t
  EM as plasticizer in, 160–163
  EM as viscosity modifier in, 166–167
  mixture, 161
  slump, 138
    retention time, 138–139
  technology, 99
Concrete repair with enhanced durability
  bacterial production of limestone in alkaline environments, 254–258
    heterotrophic bacterial limestone production, 257–258
    spore-forming alkaliphilic bacteria, 258f
    ureolytic bacterial limestone production, 255–257
  biobased mortar systems, 263–267
    fiber-based control and bacterial repair mortars composition, 264t
    practical applications, 266–267
    properties of biobased self-healing repair mortars, 264–266
  biotechnological strategies for durable repair, 253–254
  liquid bacteria-based system, 259–263
    bacteria-based two-component system composition, 259t
    improvement of frost damage resistance, 259–260
    practical applications, 261–263
    waterproofing of cracked-concrete structures, 260
Condensation method, 425f
Consistency test, 156
Construction
  biotechnology, 13–15
  biotechnology for materials production, 37–42
  material, 81
Contaminants removal from wastewater
  biofilter/biobarrier
    for inorganic contaminants removal, 410–411

    - for organic contaminants removal, 413–414
  - performance data of fixed-bed reactor, 412t
- Conventional polymers, 67–71
- Copper soaps, 308
- Core processes, 37
- Couette geometry, 223
- Cracked mortar disks, 260
- "Cradle to grave" analysis. *See* Life cycle assessment (LCA)
- Crude oil-related disasters, 2
- CSH. *See* Calcium silicate hydrate (CSH)
- Cu-chitosan complex, 392f
- *Cyamopsis tetragonolobus* (*C. tetragonolobus*), 244

D

- "Damage management" design, 254
- "Damage prevention" design, 253–254
- Damp proofers. *See* Water-resisting admixtures
- DD. *See* Degree of deacetylation (DD)
- Degradation in polymeric materials, 296
- Degree of deacetylation (DD), 402
- Degree of polymerization (DP), 230
- Degree of substitution (DS), 230
- Dendrimer polymer, 341f
- Density of foam, 285
- Depolymerization, 313
- Dextrin-based adhesive, 376–378
- Dicalcium silicate (C2S), 83
- Differential scanning colourimetry (DSC), 436–437
- Dihydroxy fatty amides-based polyurethane, 361t
- Dissimilatory nitrate reduction to ammonium (DNRA), 410–411
- Dissociation equilibrium constant, 390
- Dissolved oxygen (DO), 397
- Diutan gum, 237
- DNRA. *See* Dissimilatory nitrate reduction to ammonium (DNRA)
- DO. *See* Dissolved oxygen (DO)
- Dormant period, 82
- Double-lap tests, 370, 371f
- Downstream processes, 37, 69
- DP. *See* Degree of polymerization (DP)
- DS. *See* Degree of substitution (DS)
- DSC. *See* Differential scanning colourimetry (DSC)
- Durability of materials, 253
- Dynamic viscosity, 222

E

- EBRT. *See* Empty bed residence time (EBRT)
- Eco-efficient and composite biocement, 50–51
- Eco-efficient construction materials. *See also* Rigid foam composites
  - biopolymers and biotech admixtures for, 2–6
    - construction biotechnology, 13–15
    - microorganisms in construction processes, 14f
  - biopolymers and biotechnological admixtures for
    - biocements and biogrouts, biotechnological production of, 46–51
    - bioplastics for construction, biotechnological production of, 42–44
    - biotechnology for construction materials production, 37–42
    - physiological groups of chemotrophic prokaryotes, 40t
    - polysaccharide admixtures, biotechnological production of, 44–46
  - principles of construction-related biotechnological processes, 16f
- Ecosystem quality, 374–375
- Efficient microorganism (EM), 152
  - assessment of impact on concrete microstructure, 163–165
  - characterization, 152–153
  - as plasticizer
    - in cement, 155–160
    - in concrete, 160–163
  - repulsion forces between lactate ion and cement grains, 158f
  - as viscosity modifier in concrete, 166–167
- EG. *See* Epoxidised glycerol (EG)
- Electrostatic effect, 197
- Electrostatic patch, 390
- ELO. *See* Epoxidised linseed oil (ELO)

EM. *See* Efficient microorganism (EM)
EM-like bioplasticizer, 152
Empty bed residence time (EBRT), 388−389
End of life of biopolymers, 61−63, 71−73
Environmental impact
  assessment methods, 64−65
  classification factors, 65−67
Environmental pollution and destruction, 421
EP. *See* Eutrophication potential (EP)
EPBD. *See* European Energy Performance of Buildings Directive (EPBD)
Epoxidised glycerol (EG), 281−282
Epoxidised linseed oil (ELO), 281−282
Epoxidized *Annona squmosa* oil, 354−356
Epoxidized soybean oil, 353
Epoxy. *See also* Polyester; Poly(ester amide); Polyurethane (PU)
  biobased epoxy resin, 352f
  coating performance, 355t
  concept and importance, 351
  curing, 354
  modification, 353
  preparation, 353
  property, 354−356
  raw materials, 351
Epoxy-cured biobased polyester thermosets, 345
EPS. *See* Expanded polystyrene (EPS); Extra polysaccharide (EPS); Extracellular polymeric substance (EPS)
Ethanol (C_2H_5OH), 27
Ethylene chlorohydrin, 231
Ettringite (Aft), 83
EU. *See* European Union (EU)
Euphorbia, 423
Euphorbia lagascae oil, 424
  seed oils, 339−340
European Commission, 74
European Energy Performance of Buildings Directive (EPBD), 5
European Union (EU), 5
Eutrophication, 65
Eutrophication potential (EP), 65, 257
Expanded polystyrene (EPS), 5
Extra polysaccharide (EPS), 408−409
Extracellular polymeric substance (EPS), 396−397, 413
Extruded polystyrene (XPS), 5

F
False-set admixtures. *See* Rapid-set accelerators
Fats, 422
Fatty acid
  fatty acid-derived wood preservatives, 309f
  fatty acid-oil process, 343−344
  process, 343−344
FDN. *See* Formaldehyde condensates (FDN)
Fe(III)$EDTA^-$, 399−400, 404, 405f
Fiber form, 203
Fibre-reinforced soy foams, 297−298
Fibrous fillers, 428−429
Fillers
  biopolymers modification using, 427
    benefit for biopolymers, 427−429
  chemical families for plastics, 428t
Flame-retardant epoxy thermoset, 354−356
Flash-set admixtures. *See* Rapid-set accelerators
Flocculation, 391−392
Flow test, 156
Fly ash-based geopolymer, 176, 176f
  biopolymers, 173−174
  enhancement, 185−186
  experimental study
    FTIR spectroscopy analysis, 179
    materials, 177
    scanning electron microscopy characterization, 179
    specimen preparation, 177
    splitting tensile tests, 178
    unconfined compression tests, 177−178
  hydrogen bonds, 186f
  results
    FTIR characteristic bands, 184t
    FTIR spectra, 182−185
    prepeak toughness based on splitting tensile tests, 181
    SEM images, 182
    splitting tensile strength, 180−181
    UCS, 179−180
Foam chemistry, 278

Foam morphology and characterisation, 285–289. *See also* Rigid foam composites
  chemical characterization, 285–286
  mechanical characterization, 286–289
    bending, 288
    chemical structure as function of FTIR absorbance, 287t
    compression, 287–288
    shear, 289
    tension, 288
Foam processing, 283–285. *See also* Rigid foam composites
  RIM, 283–285
Formaldehyde condensates (FDN), 94
Fossil fuel industry, 1
Fourier transform infrared spectroscopy (FTIR spectroscopy), 119–120, 136–137, 176, 179, 182–185, 285, 433, 437, 440f
Fresh state, 202
Frost damage resistance improvement, 259–260
FTIR spectroscopy. *See* Fourier transform infrared spectroscopy (FTIR spectroscopy)
Functional filler, 427
Fusion protein, 409–410

G

GbfS. *See* Granulated blast furnace slag (GbfS)
Gelatin, 336, 378–379
Geopolymer, 174–175
GEs. *See* Glycidyl ethers (GEs)
GHG. *See* Greenhouse gas (GHG)
Global Warming Potential (GWP), 65
Glucose ($C_6H_{12}O_6$), 27
Glycerolysis, 343–344
Glycidyl ethers (GEs), 325
  epoxy, 351
Granulated blast furnace slag (GbfS), 122–123
Greenconcrete, 195
Greenhouse gas (GHG), 65
  emissions for biopolymers, 68f
Guaiac resin, 325
Guaiac resin-impregnated wood, 326f
Guaiacum. *See* Guaiac resin
Guar gum, 244–245
Gums, 241–247
  dispersions, 378
GWP. *See* Global Warming Potential (GWP)

H

Hardened cement paste micrsostructure characterization
  pore structure analysis, 144
  SEM image analysis, 144–145
Hardened state, 206–207
Hardness of foam, 285
HEC. *See* Hydroxyethyl cellulose (HEC)
HEMC. *See* Hydroxyethylmethyl cellulose (HEMC)
Herschel–Bulkley equation, 222–223
Herschel–Bulkley model, 228
Heterotrophic bacteria, biocementation by, 25–26
Heterotrophic bacterial limestone production, 257–258. *See also* Ureolytic bacterial limestone production
High range plasticizers, 92
High-performance
  concrete, 132
  liquid chromatography, 153
  thermal insulators, 5
High-performance superplasticizers, 132–133
  on chitosan
    chitosan superplasticizer preparation, 134–135
    chitosan superplasticizer structure, 135–137
    SM contents, 136t
  future research trends, 147–148
High-range water-reducing admixtures (HRWR admixtures), 105, 160–161, 223–224
HPG. *See* Hydroxypropyl guar (HPG)
HPMC. *See* Hydropropyl methylcellulose (HPMC)
HPMC2. *See* Hydroxypropyl methyl cellulose (HPMC2)
HRWR admixtures. *See* High-range water-reducing admixtures (HRWR admixtures)

HTP. *See* Human toxicity potential (HTP)
Human health, 374–375
Human toxicity potential (HTP), 65, 257
Hydrated cement, 81
Hydration delay, 88
Hydrocarbon, 423
Hydrogen peroxide (H_2O_2), 63
Hydrophobers, 123–126
Hydropropyl methylcellulose (HPMC), 91
Hydroxyethyl cellulose (HEC), 84, 231–232, 231f
Hydroxyethylmethyl cellulose (HEMC), 84
Hydroxylated feedstocks, 423
Hydroxylated vegetable monomers, 425f
Hydroxypropyl guar (HPG), 85, 244–245
Hydroxypropyl methyl cellulose (HPMC2), 85
Hyperbranched polyester, 343f
Hyperbranched polymer, 341f
Hyperbranched polyurethanes, 360

I
Immobilized nitrifying bacteria cells (INBC), 388–389
INBC. *See* Immobilized nitrifying bacteria cells (INBC)
Infrared spectroscopy (IR), 114
Inoculum, 37–39
Integral permeability reducers. *See* Water-resisting admixtures
International Organization for Standards (ISO), 64, 435
IPA. *See* Isopropyl alcohol (IPA)
IPDA. *See* Isophorone diamine (IPDA)
IPN. *See* Waterborne interpenetrating network (IPN)
IR. *See* Infrared spectroscopy (IR)
Iron-based bioclogging and biocementation, 28, 49–50
Iron-chitosan composites, 410
ISO. *See* International Organization for Standards (ISO)
ISO 14040 method, 295
Isocyanates, 278–279
Isophorone diamine (IPDA), 281–282
Isopropyl alcohol (IPA), 413–414

K
Kappa-carrageenan (KC), 176–177. *See also* Fly ash-based geopolymer
Kappacarrageenan biopolymer (KC biopolymer), 6–7

L
Lactic acid, 157–158
LCA. *See* Life cycle assessment (LCA)
LCI. *See* Life cycle inventory (LCI)
LCIA. *See* Life cycle impact assessment (LCIA)
LDPE. *See* Low-density polyethylene (LDPE)
Life cycle analysis. *See* Life cycle assessment (LCA)
Life cycle assessment (LCA), 63–64, 257, 294–295, 374–375
  biopolymers
    comparative cradle-to-manufacture impacts, 72t
    comparison of LCA of biopolymers, 67–71
    data for, 67
    end of life, 71–73
  environmental impact
    assessment methods, 64–65
    classification factors, 65–67
    petroleum-based epoxy resin, 66t
Life cycle impact assessment (LCIA), 64–65
Life cycle inventory (LCI), 64
Light-induced phenomenon, 431
Lignin, 337–338, 379–380
Lignocellulosic fibres, 291t
Lignocellulosic fillers, 289–290
Lignosulfonate (LS), 92–93, 104, 131, 132f
Limestone ($CaCO_3$), 254
  bacterial production in alkaline environments, 254–258
Limestone Portland cement (LPC), 113
Linear polymer, 341f
Liquid bacteria-based system, 259–263. *See also* Biobased mortar systems
  bacteria-based two-component system composition, 259t
  improvement of frost damage resistance, 259–260

- practical applications, 261–263
- waterproofing of cracked-concrete structures, 260

Liquid form of biopolymers, 203
Lixor® System, 393
Lorama Chemical Incorporation, 336
Low-density polyethylene (LDPE), 443
LPC. *See* Limestone Portland cement (LPC)
LPR™, 336
LS. *See* Lignosulfonate (LS)

M

Magnetic chitosan microspheres, 404
Maleic anhydride (MAH), 135
Marine adhesive proteins, 379
Mass transit bus flooring system, 297
MC. *See* Methyl cellulose (MC); Microbial cellulose (MC)
MCC. *See* Microcrystalline cellulose (MCC)
MDI. *See* Methylene diisocyanate (MDI); Methylene diphenyl diisocyanate (MDI)
Mechanical tests, 370
MEF, 152–153, 156–157
- chemical and physical properties, 153t
- elemental composition, 154t
- impact on cement, 155
- microbial consortium, 152–153
- plasticity index for polar fractions, 158f

Melamine sulphonate (MS), 107
Melamine–urea–formaldehyde adhesives (MUF adhesives), 379–380
Methane, 423
Methyl cellulose (MC), 86, 233–234
Methyl methacrylate-ethyl-hexyl acrylate (MM-EHA), 436–437
Methyl-hydroxy-ethyl-cellulose (MHEC), 84f, 232–233, 232f
Methyl-hydroxy-propyl-cellulose (MHPC), 233–234, 234f
Methylene diisocyanate (MDI), 278–279
Methylene diphenyl diisocyanate (MDI), 369–370
MHEC. *See* Methyl-hydroxy-ethyl-cellulose (MHEC)
MHPC. *See* Methyl-hydroxy-propyl-cellulose (MHPC)
MICCP. *See* Microbially induced calcium carbonate precipitation (MICCP)
MICP. *See* Microbially induced calcite precipitation (MICP)
Microbacterium arborescens (*M. arborescens*), 19–20
Microbial biotechnology, 13
Microbial cellulose (MC), 388–389, 405–406
- bacteria immobilization on, 405–408

Microbial exopolysaccharides, 234–235
- diutan gum, 237
- tetrasaccharide backbone structure, 236f
- welan gum, 235–237
- xanthan gum, 237–238, 239f

Microbial extracellular polysaccharides, 378
Microbial plastics for civil engineering, 21–22
Microbial polysaccharides, 378
- applications in civil engineering, 17, 18t
- bioclogging of soil using in situ production, 19–21

Microbially driven calcium carbonate precipitation, 256
Microbially induced calcite precipitation (MICP), 47
Microbially induced calcium carbonate precipitation (MICCP), 22–24
Microcrystalline cellulose (MCC), 86–87, 87f
Microfiltration, 393
Microorganisms, 37, 39
Minicone test, 156–157
“Mixed” adhesives, 380–381
MM-EHA. *See* Methyl methacrylate-ethyl-hexyl acrylate (MM-EHA)
Molar substitution (MS), 230
Monomers, 423
Mortar, 81
MS. *See* Melamine sulphonate (MS); Molar substitution (MS)
Mucilages, 241–247
MUF adhesives. *See* Melamine–urea–formaldehyde adhesives (MUF adhesives)

N

Na-lignosulfonates (NL), 92
Nanocomposite fillers, 429
NaOH. *See* Sodium hydroxide (NaOH)
β-naphthalene sulphonate (NS), 107

Naphthalene sulphonate formaldehyde (NSF), 106–107
Natural fibres, 290
Natural oligomeric and polymeric resins, 325–326
NCO/OH ratio, 356–360
–(NHCOO)–. *See* Urethane linkage (–(NHCOO)–)
Nitrite oxidizing bacteria (NOB), 393, 400–403
  features of the nitrite broth, 403t
NL. *See* Na-lignosulfonates (NL)
NOB. *See* Nitrite oxidizing bacteria (NOB)
Non-chloride accelerators, 111–112
Non-glycidyl ether type epoxy, 351
Nonconventional synthesis routes, 278
Nonrenewable energy use (NREU), 68f
Nonrenewable/abiotic resource depletion potential, 65
Normal water-reducing admixtures, 104
NREU. *See* Nonrenewable energy use (NREU)
NS. *See* β-naphthalene sulphonate (NS)
NSF. *See* Naphthalene sulphonate formaldehyde (NSF)

O
Ochre, 369
Oils, 422
Oleochemical base material, 422
Oligomers, 308
OPC. *See* Ordinary Portland Cement (OPC)
Optional added components, 393
Opunti ficus indica mucilage, 242f
Ordinary Portland Cement (OPC), 3, 104–105, 113, 124t, 174–175
Organic coatings, 421
Ozone depletion potential, 65

P
Paints and surface coatings, 333
  binders and film formers, 333–334
  biobased polymers for, 341–360
  biopolymers in, 334–335
  manufacturing from biobased polymers, 363–364
  pigment, 333–334
  polymers advantages, 334
PAN. *See* Polyacrylonitrile (PAN)
Paper industry, 112–113
Paracoccus denitrificans (*P. denitrificans*), 20
Particulate fillers, 429
Passive admixtures, 99
PBA. *See* Peat moss hybrid (PBA)
PBL. *See* Pulp black liquor (PBL)
PCL. *See* Polycaprolactone (PCL)
PCs. *See* Polycarboxylate superplasticizers (PCs)
PDI. *See* Polydispersity index (PDI)
PE. *See* Biopolyethylene (PE); Polyethylene (PE)
Peat moss, 404–405
Peat moss hybrid (PBA), 404–405
PEEK. *See* Poly(ether ether ketone) (PEEK)
Peptidoglycan
  from cell wall bacteria, 245–246
  molecular structure, 245f
Permeability reducers, 122–123
PET. *See* Polyethylene terephthalate (PET)
Petrochemical-based superplasticizers (PNS), 196f
Petroleum products, 126
Petroleum-based synthetic polymers, 422
PF adhesives. *See* Phenol–formaldehyde adhesives (PF adhesives)
Pfa. *See* Pulverized fuel ash (Pfa)
PHAs. *See* Polyhydroxyalkanoates (PHAs)
Phase-transfer catalyst, 424
PHB. *See* Polyhydroxybutyrate (PHB)
Phenol–formaldehyde adhesives (PF adhesives), 379–380
Phenolic-acids based adhesives, 379–380. *See also* Protein-based adhesives
Photo-oxidation, 426
Photocatalysis, 432
  agent, 429–430
Photochemical oxidants creation potential, 65
Photolysis, 426
Physisorption, 391t
Pink-colored rhodamine-labeled chitosan layer, 376f
PLA. *See* Poly(lactic acid) (PLA); Polylactic acid (PLA)
Plain fly ash-based geopolymer, 176f
Plant seed oil, 340–341
Plant-produced biopolymers, 334–335

Plasticizers, 102, 102f
  accelerating water-reducing admixtures, 104
  EM
    in cement, 155–160
    in concrete, 160–163
  normal water-reducing admixtures, 104
  retarding water-reducing admixtures, 104–105
PLLA. *See* Poly-L-lactic acid (PLLA)
PMDI. *See* Polymethylene polyphenyl diisocyanate (PMDI)
PNS. *See* Petrochemical-based superplasticizers (PNS)
Poly-L-lactic acid (PLLA), 22, 44
Poly-L-lactide. *See* Poly-L-lactic acid (PLLA)
Poly(ester amide). *See also* Epoxy
  coating performance, 350t
  concept and importance, 347
  curing, 348
  modification, 348
  preparation, 347
  properties, 348–349
  raw materials, 347
  3D network structure, 349f
Poly(ether ether ketone) (PEEK), 436–437
Poly(lactic acid) (PLA), 59–61
  production step of 1 kg, 62f
Polyacrylonitrile (PAN), 71–73
Polycaprolactone (PCL), 411
Polycarboxylate superplasticizers (PCs), 131, 132f
Polydispersity index (PDI), 135–136
Polyester. *See also* Epoxy
  coating performance, 346t
  concept and importance, 342
  curing, 344
  modification, 344
  preparation, 343–344
  properties, 344–347
  raw materials, 342–343
Polyethylene (PE), 61, 425
Polyethylene terephthalate (PET), 59–61
Polyhydroxyalkanoates (PHAs), 21, 42, 57
Polyhydroxybutyrate (PHB), 15, 21
Polylactic acid (PLA), 2, 22, 44, 323–324
Polylactides. *See* Polylactic acid (PLA)
Polymer industry, 1
Polymer stabilization, titanium dioxide as, 429–430
Polymer-based admixtures, 206
Polymeric materials, 421
Polymer–particle interaction, 225
Polymer–polymer interaction, 225
Polymer–water interaction, 225
Polymethylene polyphenyl diisocyanate (PMDI), 278–279
Polyol, 279–283
  biobased, 280–283, 282t
  synthetic, 280
Polypropylene (PP), 61
Polysaccharides, 93, 229, 334–335, 375–378
  biotechnological production of polysaccharide admixtures, 44–46
  derivatives, 94
Polyurethane (PU), 324, 426. *See also* Epoxy; Polyester
  coating performance, 361t–362t
  concept and importance, 356
  curing, 359
  foams, 275, 278
    chemical reaction schematic, 278f
    non-isocyanate route for the synthesis, 279f
    system production, 284f
  modification, 359
  preparation, 357–359
  property, 359–360
  raw materials, 357
Portland cement, 221
  concrete, 195
  hydration, 82–83
    cement heat evolution, 82f
  mortar, 195
  paste, 195
Powder form, 203
PP. *See* Polypropylene (PP)
Prepeak toughness, 181
Primary structure, 318
Protein-based adhesives, 378–379. *See also* Phenolic-acids based adhesives
Proteins, 336–337
  in wood preservation, 316–323
Pseudomonas stutzeri (*P. stutzeri*), 408f
PU. *See* Polyurethane (PU)

Pulp black liquor (PBL), 105, 113–114
  waste effect
    on bulk density and apparent porosity, 115–117
    on combined water content, 117–118
    on compressive strength, 118–119
    on water of consistency and setting times, 115
Pulverized fuel ash (Pfa), 122–123
Pumped concrete, 228
PUR. *See* Polyurethane (PU)
Pure lignin, 92

Q

$Q_3PO_4[W(O)(O)_2)_2]_4$. *See* Venturello's catalyst ($Q_3PO_4[W(O)(O)_2)_2]_4$)
Quasi-prepolymer technique, 277
Quaternary structure, 318
Quinoid structure formation, 427f
QUV tester, 435
QUV UV-340 lamp, 435

R

Rapeseed–polyurethane (RS-PU), 437–440
Reaction injection moulding (RIM), 283–285
Recovery of polymeric foams, 297
Recyclamines®, 63
Recycling of polymeric foams, 297
Relative density, 286–287
Relative humidity (RH), 437
Renewable resources
  biopolymers development from, 423–426
  survey of approaches to biopolymers from, 422–423
Renewable vegetable oils, 424f
Resins, 308
Retarders, 108–109
RH. *See* Relative humidity (RH)
Rheology, 155, 222–224
Rheometers, 223–224
Rigid biofoam composites, 275–276
Rigid foam composites, 289–294. *See also* Foam morphology and characterisation
  application case studies, 297–298
  environmental impact, 294–297
    degradation and biodegradability, 296
    recycling and recovery, 297
  SIP, 292–294
    bending members, 292–293
    combined loading, 294
    compression members, 293–294
Rigid foams, 277–283
  foam chemistry, 278
  isocyanates, 278–279
  polyol, 279–283
Rigid polyurethane foam, 282
RIM. *See* Reaction injection moulding (RIM)
Rosin, 325, 338
Rosin-sizing agents, 325
Roughness, 374
RS-PU. *See* Rapeseed–polyurethane (RS-PU)
Rubber tree (*Hevea brasiliensis*), 216
  shotcrete with latex, 216–217

S

S-BA. *See* Styrene-butyl acrylate (S-BA)
Salt-River Materials Group (SRMG), 177
Sandwich composites, 276, 289, 293, 297
SaniTEE® device, 393
SAP. *See* Superabsorbent Polymers (SAP)
SBR. *See* Styrene-butadiene rubber (SBR)
Scanning electron microscopy (SEM), 114, 120–121, 144, 173–174, 179, 182
SCC. *See* Self-compacting concrete (SCC); Self-consolidating concrete (SCC)
SCS. *See* Sulfonated chitosan superplasticizer (SCS)
SE. *See* Starch ether (SE)
Secondary structure, 318
Seed gums, 378
Seeding biofiltration system, 388f
Segregation, 227–228
Self-compacting concrete (SCC), 160–161
  experimental results for, 162t
  mechanical properties, 164t
Self-consolidating concrete (SCC), 222, 227–228
Self-healed crack, 265f
Self-healing bacteria-based repair mortar, 266f
SEM. *See* Scanning electron microscopy (SEM)
Service life of biopolymers, 426
SF. *See* Silica fume (SF); Slump Flow (SF)

SF-PU. *See* Sunflower−polyurethane (SF-PU)
Shear, 289
  shear-thinning, 226, 235−238, 241−243
  strength, 370−373
  stress peak, 371−373
Shellac, 338
Shotcrete with latex of rubber tree, 216−217
Silica fume (SF), 122−123
Single-lap tests, 370
SIPs. *See* Structural insulated panels (SIPs)
Slump Flow (SF), 161
SM. *See* Sodium metabisulfite (SM)
SNF. *See* Sulfonated naphthalene formaldehyde condensates (SNF)
Soaps, 124
Sodium hydroxide (NaOH), 177
Sodium metabisulfite (SM), 135
Soy protein, 379
Soy-based polyols, 292
Soybean oil-based polyisocyanate, 357
SPF. *See* Sulfanilic acidephenoleformaldehyde condensates (SPF)
Splitting tensile strength, 180−181
Splitting tensile tests, prepeak toughness based on, 181
Sprayed concrete, 228−229
SPs. *See* Superplasticizers (SPs)
SRMG. *See* Salt-River Materials Group (SRMG)
SS. *See* Starch sulfonate (SS)
Stabilizers, 421−422, 427, 443−444
Stabilizers. *See* Viscosity Modifying Admixtures (VMA)
Starch, 93−94, 238−240, 336
Starch ether (SE), 83
Starch sulfonate (SS), 93−94
Starch-based adhesive, 376−378
Stereo effect, 197
Strengths, Weaknesses, Opportunities and Threats analysis (SWOT analysis), 61, 63t
Structural insulated panels (SIPs), 292
  bending members, 292−293
  combined loading, 294
  compression members, 293−294
Styrene-butadiene rubber (SBR), 124t
Styrene-butyl acrylate (S-BA), 436−437
Sugars, 92
Sulfanilic acidephenoleformaldehyde condensates (SPF), 131, 132f
Sulfonated chitosan superplasticizer (SCS), 135
  adsorption properties on cement surface, 140
    behavior, 140−141
    zeta-potential of cement particles, 142
  application in concrete, 142−143
  working mechanism, 145−147, 145f
Sulfonated naphthalene formaldehyde condensates (SNF), 131, 132f
Sunflower−polyurethane (SF-PU), 437−440
Super plasticizers, 92
Superabsorbent Polymers (SAP), 202
Superhydrophobic photocatalytic coatings, biopolymers as, 430−444
Superplasticizers (SPs), 99, 105, 131, 137−138, 151
  biopolymers with, 203−216
    B. subtilis, 207f
    concrete−chitosan−latex system, 205f
    latex−biopolymer system, 213f
    latex−concrete system, 212f−213f
    tensile strength for concrete−latex−chitosan system, 214f
  chemical structure, 196
  classification, 105f
  compatibility, 202
  copolymer dispersions, 106−108
  dispersing mechanisms, 198f
  fresh properties of SCC mixtures, 199t−200t
  fresh self-compacting concrete, 201t
  hydroxylated polymers, 106−108
  modified lignosulphonate, 106
  network formation, 198f
  physicochemical effects, 196−197
  stereo effect, 197f
  sulphonated melamine formaldehyde condensates, 105−106
  sulphonated naphthalene formaldehyde condensates, 106
  sulphonated polystyrene, 106−108

Supporter, biopolymers characterization as
  biopolymer supporting other polymers, 409–410
  biopolymer-immobilizing microorganisms, 402–409
Sustainability, 257, 263–264
SWOT analysis. *See* Strengths, Weaknesses, Opportunities and Threats analysis (SWOT analysis)
Synthetic adhesives, 369–370, 380–381
Synthetic fibers, 22
Synthetic polyols, 280

T

Tannin moieties, 323f
Tannin–protein combination, 321–322
TDI. *See* Toluene diisocyanate (TDI)
Technical Committee 225-SAP, 202
Tensile strength, 173–175, 178, 214f
Tension, 288
Tertiary structure, 318
Tetracalcium aluminoferrite (C4AF), 93, 233
Thixotropy, 223
TiO_2. *See* Titanium dioxide (TiO_2)
Titania. *See* Titanium dioxide (TiO_2)
Titanium dioxide (TiO_2), 429–430
  doping mechanism of nitrogen, 434f
  research on photocatalyst, 431t
Toluene diisocyanate (TDI), 369–370
Traditional wood preservatives, 307–308. *See also* Biopolymer wood preservatives
Tricalcium aluminate (C3A), 82, 104, 206–207
Tricalcium silicate (C3S), 82, 159, 233
Triethanolamine, 111

U

UCS. *See* Unconfined compressive strength (UCS)
UF adhesives. *See* Urea–formaldehyde adhesives (UF adhesives)
Ultrafiltration, 393
Ultrahigh deacetylation degree of chitosan, 133–134
Ultraviolet light (UV light), 426, 436f
  ranges of solar UV radiation spectrum, 436t
  sample preparation and UV irradiation, 438t–439t
  spectroscopic analysis of biopolymer coating, 437–444
Unconfined compressive strength (UCS), 177–180
Underwater concrete, 228
UPB. *See* Urease-producing bacteria (UPB)
Upstream processes, 37
Urea–formaldehyde adhesives (UF adhesives), 379–380
Urease-producing bacteria (UPB), 22, 47
Ureolytic bacterial limestone production, 255–257. *See also* Heterotrophic bacterial limestone production
Urethane linkage (–(NHCOO)–), 423
UV light. *See* Ultraviolet light (UV light)
UV–Vis spectrum, 441f–442f

V

VA. *See* Vinyl acetate (VA)
VA-BA. *See* Vinyl acetate-butylacrylate (VA-BA)
Valence band (VB), 432–433
VB. *See* Valence band (VB)
VEAs. *See* Viscosity-enhancing admixtures (VEAs)
Vegetable oil-based epoxies, 351
Vegetable oil-based polyurethane, 361t
Vegetable oils, 276, 308, 338–340
Venturello's catalyst ($Q_3PO_4[W(O)(O)_2)_2]_4$), 424
Vernonia galamensis, 351
  seed oils, 339–340
Vernonia oil, 351
Vinyl acetate (VA), 436–437
Vinyl acetate-butylacrylate (VA-BA), 436–437
Viscosity, 161
Viscosity modifiers, 88
  cement-based material rheology, 89–90
  VMA, 90–91
  working mechanism, 88–89
Viscosity-enhancing admixtures (VEAs), 88, 90–91, 167, 221, 224–226
  applications, 227
    pumped concrete, 228
    SCC, 227–228

- sprayed concrete, 228–229
- underwater concrete, 228
- biopolymers in, 229
  - cellulose derivatives, 229–234
  - microbial exopolysaccharides, 234–238
  - with potential for future use, 240–247
  - starch, 238–240
- future trends, 247
- polymer-based, 225f
- rheology, 222–224
- stress–strain rate diagrams, 222f

Viscosity-modifying admixtures (VMAs). *See* Viscosity-enhancing admixtures (VEAs)
Volatile organic compounds (VOCs), 65, 369–370
- paints, 333

W

w/c ratio. *See* Water-to-cement ratio (w/c ratio)
Wastewater, contaminants removal from, 410–414
Water
- reducers, 91
  - casein, 94–95
  - cellulose, 93–94
  - lignosulfonates, 92–93
  - starch, 93–94
- repellents, 123–126
- resistance, 374
- treatment elements, 387
- water of consistency and setting times, PBL waste effect on, 115

Water-proofers. *See* Water-resisting admixtures
Water-reducible polyesters, 344
Water-reducing
- admixtures, 102
  - acceleration, 104
  - retardation, 104–105
- agent, 131
- capacity, 137–138
- ratio, 135, 137–138

Water-resisting admixtures, 121
- permeability reducers, 122–123
- water repellents, 123–126

Water-retention agents
- and hydration delay, 88
- microcrystalline cellulose and cellulose derivatives, 85–87
- polysaccharide–cement interaction, 86f
- water-soluble cellulose derivatives, 87f
- working mechanism, 83–85

Water-to-cement ratio (w/c ratio), 81, 99, 131, 151
Waterborne interpenetrating network (IPN), 353
Waterproofing
- admixtures, 124t
- of cracked-concrete structures, 260

Waxes, 308
Weathering, 434
Weight percent gain (WPG), 313–315
Welan gum, 90–91
Wettability, 373
Wheat gluten (WG), 378
Wood, 305, 306f
- quality, 305–307

Wood impregnation techniques, 309–310
Wood preservation mechanisms, 306–311
- biopolymer wood preservatives, 308–311
- factors affecting wood stability, 307f
- traditional wood preservatives, 307–308

World Health Organization (WHO), 3
WPG. *See* Weight percent gain (WPG)

X

X-ray diffraction (XRD), 88
X-ray photoemission spectroscopy (XPS), 436–437
Xanthan gum, 91, 237–238, 239f
XPS. *See* Extruded polystyrene (XPS)

Y

Yeast fermentation waste (YFW), 151
Yield stress, 166
Young's equation, 373

Z

Zein, 321
Zein-impregnated wood, 322f
Zeta-potential of cement particles, 142